Archaeological Investigations at Delta River Overlook, Central Alaska

September, 2018

Archaeology GIS Laboratory, Report #7

UNIVERSITY OF ALASKA FAIRBANKS
Department of Anthropology

Archaeological Investigations at Delta River Overlook, central Alaska

Edited by:

Ben A. Potter[1]

Authors:

Ben A. Potter[1], Julie A. Esdale[2], Joshua D. Reuther[1, 3], Holly J. McKinney[1], Charles E. Holmes[1], Caitlin R. Holloway[3], and Crystal L. Glassburn[4]

---

1. Department of Anthropology, University of Alaska Fairbanks
2. Colorado State University
3. University of Alaska Museum of the North
4. Bureau of Land Management, Fairbanks Office

EXECUTIVE SUMMARY

The primary objective of this project is to support the US Army Garrison Fort Wainwright with the excavation at the National Register Eligible sites 49-XMH-297, Delta River Overlook (DRO), and 49-XMH-838, Hurricane Bluff. This is in support of maintenance and erosion control activities at OP 9c under FW-MOA-1411. Funding was obtained through the U.S. Army Corps of Engineers. This report serves as the final submittal under two Fort Wainwright Scopes of Work: 15-18, Mitigation for FW-MOA-1411 OP9c Maintenance and Erosion Control; and 16-15, Mitigation for FW-MOA-1411 Submittals IIB and IIC. This project is intended to provide more comprehensive information on the nature and significance of cultural materials at DRO. Excavations at DRO and tests at Hurricane Bluff conducted during the 2015 and 2017 field seasons have demonstrated the sites to be unique in Alaska for its repeated use by people over many millennia.

Site Significance

We have collected and analyzed a substantial amount of data at DRO. The site is more significant than previously thought, and easily could be listed on the National Register of Historic Places (NRHP) under Criterion D. DRO was found eligible (NRE) on 8/30/1979 and Hurricane Bluff was found eligible (NRE) on 12/19/2013. We briefly summarize here the salient conclusions. Items 1, 2, 3, and 4 make DRO unique among archaeological sites in Alaska.

1) The most significant aspect of DRO is the *number of distinct cultural occupations*, fourteen (14) episodes of human occupation have occurred at the site over 13,000 years, including multiple occupations of individual traditions (Chindadn, Denali, and Northern Archaic). This is unprecedented in interior Alaska, allowing us for the first time to address variation *within* cultural traditions as well as *among* traditions, controlling for site location.

2) *Ancient animal and plant remains are very well preserved*, allowing us to directly evaluate human use of plants and animals from the last Ice Age to the recent past. This allows us a unique window to understand effects of climate change directly on exploited faunal resources accessible from the site. Significant new discoveries (so far) include very late human exploitation of bison (long after they disappeared in other regions) and the first evidence (through bison teeth geochemical analyses) of bison migration patterns.

3) *Stratigraphy at DRO (layering of sediments and soils) is very highly resolved*, and we have identified and dated 11 major paleosol complexes, representing at least 32 buried soils. This provides a significant window into tracking regional and local environmental changes for 13,000 years in very precise intervals. No other interior Alaskan site has a similar stratigraphic record allowing this quality of detailed analyses.

4) *New prehistoric Alaskan human behaviors* have been inferred at DRO, including (a) presence of multiple ochre-stained areas that probably served as hide processing areas and (b) the first known winter occupation in all of Beringia (east or west). There is also evidence of tent structures that would represent some of the earliest habitation structures in Alaska.

5) *Artifact density is much higher* than previously thought, and we have recovered 18,760 stone artifacts, including 283 stone tools, making this one of the most productive sites in the interior of Alaska (Potter 2008).

6) *DRO site extent is very large*; we estimate total area with preserved cultural remains to be 4,037 m^2. All excavations to date have sampled approximately 2.5% of the overall estimated site area.

Site Adverse Impacts

The major adverse impact currently is wind erosion (aeolian deflation) exacerbated by vehicle and foot traffic across the site and bison using the area for wallowing and for transit from the Delta River floodplain to grazing areas in the east. We have mapped the areas and routes bison have used and continue to use to move across the site (Chapter 3).

We also identified evidence of human disturbance (military personnel or local hunters), including use of the site over the 2015-2016 and 2016-2017 winters, as well as the potential for access and use of the site at other times.

It is important to note that while there is extensive evidence of wind erosion, and much of the upper sediments, representing the last 3000 years of human occupation history, have been destroyed, much of the lower sediments remain intact across the site. It is important that these areas be protected from further disturbance.

Recommendations

We have evaluated site extent and effects of natural (wind, bison) and cultural (vehicle disturbance) adverse impacts to the site, and have the following recommendations.

Recommendations for reducing further erosion

1) Make the DRO site environs (see map in Chapter 3) off-limits to off-duty personnel and to other individuals, as far as possible. The site is currently located behind locked gates. Foot and vehicle traffic will exacerbate ongoing wind erosion and more of the upper sediments and the cultural remains that are situated therein will be lost.

2) Fences should be installed at specific locations (see Figure 3.15) to help detour bison herd movement away from culturally sensitive areas.

3) Management strategies should include annual monitoring of the DRO site area.

4) We recommend that the military cultural resource management team consult with U.S. Army leadership if field operations near the DRO site are planned, to help aid in site avoidance.

5) If parts of the site are damaged, reassessment and mitigation through excavation should occur.

6) The west and east deflation bowls should be reseeded with grasses to help mitigate against further wind erosion (see Figure 3.15).

Recommendations for future development

1) We do not recommend use of the immediate DRO site area for observation posts or any other activity that will result in ground disturbing activities, in order to preserve the site.

2) If military use of the area is required, we recommend minimizing destruction of the site by restricting ground disturbance and traffic to areas outside those with intact cultural materials (see Figure 3.15).

Recommendations for future research

Because of the unique nature of the deposits, excellent faunal preservation, and unprecedented repeated use of the site since the end of the glacial era, we recommend that research continues at DRO.

1) We recommend future collaborations with University of Alaska Fairbanks with support of grant opportunities, access for archaeological field schools, and encouragement of student research.

2) We would encourage using DRO as an example of excellent cultural resource stewardships through presentations to soldiers, the community, and in academic venues.

TABLE OF CONTENTS

LIST OF FIGURES

LIST OF TABLES

CHAPTER 1. INTRODUCTION

Ben A. Potter and Julie A. Esdale

The primary objective of this project is to support the US Army Garrison Alaska (USAGAK) with the excavation at the National Register Eligible sites 49-XMH-297, Delta River Overlook (DRO), and 49-XMH-838, Hurricane Bluff. The sites are located in the middle Tanana River valley alongside the Delta River (Figure 1.1). This work is in support of maintenance and erosion control activities at OP 9c under FW-MOA-1411. Funding was obtained through the U.S. Army Corps of Engineers. This report serves as the final submittal under two Fort Wainwright Scopes of Work: 15-18, Mitigation for FW-MOA-1411 OP9c Maintenance and Erosion Control, and 16-54, Mitigation for FW-MOA-1411 Submittals IIB and IIC. This project is intended to provide more comprehensive information on the nature and significance of cultural materials at DRO.

Specific major requirements (Tasks) are:

1. Perform data recovery at the two sites
2. Conduct data analysis
3. Provide an educational opportunity for a university student.
4. Provide a report in support of consultation

Task 1 was completed during the summers of 2015 and 2017 (8/1/2015 to 8/31/2015 and 7/15/17 to 8/11/2017), and is summarized in this report, Chapter 3. At DRO, we excavated a total of 79 m^2 to sterile glacial till, and 85 m^2 excavated to below Paleosol 6a (below Component 7b) (Figure 1.2). This is far in excess of our expected excavation extent of approximately 60 m^2 (30 m^2 each year). Part of our success was due to the concentration of materials in C8b, which was eroded in the southern part of the excavation area, and below Paleosol 1 (Components 1, 2a, 2b, 2c) and relatively lack of cultural materials in intervening areas. All surface artifacts were mapped and collected. Testing was also conducted in the vegetated area north of the main erosion areas. At Hurricane Bluff, we excavated 4 square meters along the eroding bluff edge to document site stratigraphy and establish control chronology through sradiocarbon dating. We also correlated stratigraphic profiles between DRO and Hurricane Bluff (Chapters 4 and 5).

Task 2 was completed between August 2015 and May 2017, and the results are summarized in this report, Chapters 2-12. These analyses include standard archaeological analyses: site mapping (Chapter 3), spatial analyses (Chapter 13), lithic analyses (Chapter 7), faunal analyses (Chapter 8), and geoarchaeological analyses (Chapter 5), following the research design of FWA-MOA-1411. In addition, we conducted a wide range of additional analyses, integrating this research with ongoing research at regional sites, including Upward Sun River (Potter et al. 2011, 2014), Mead (Potter et al. 2008), XBD-167, and Quartz Lake sites (Reuther et al. 2010). These include archaeobotanical, tephra microprobe, and strontium isotope analyses (Chapters 5, 9, 11).

Task 3 was completed by supporting several undergraduate and graduate students. Five undergraduate students and four MA students were hired as archaeological

technicians in 2015 and 2017. Additionally, three undergraduate students received excavation training as volunteers in 2015. Seven archaeological technicians already held B.A./B.S. degrees but participated in the project prior to enrolling in a graduate program at UAF and other universities. Two PhD students received training as an assistant field director in 2015 (Justin Hays) and 2017 (Gerad Smith), and one Post-doc received training as a field director in 2017 (Dr. Holly McKinney). A number of undergraduate and graduate students worked as paid laboratory technicians in 2015 and 2017 (Kelly Meierotto, Anna Burchfield, Casey Jobe). Data have been provided to Bree Doering (U Michigan) for possible use in her dissertation on hearth sediment geochemistry. In addition, the lithic data are situated for another M.A. student to pursue in the near future.

Task 4 was completed in the form of this report. Consultation on the project has been ongoing each year, with the SHPO and our liaison with the U.S. Army, Dr. Julie Esdale (CEMML). Accession logs and analytical data for artifacts and faunal material have been provided in Microsoft Excel form to USAGAK's Cultural Resources manager and to the University of Alaska Museum of the North (UAMN) for curation. A GIS database containing artifact spatial data has also been given to USAGAK. Artifacts and faunal material has been accessioned and deposited at UAMN. Updated AHRS cards are provided in an appendix to this report and have been given to the SHPO (Appendix D).

UAF utilized personnel that meet the "Secretary of the Interior's Professional Qualifications Standards" defined in 36 CFR §61. Dr. Ben Potter (P.I.), Dr. Charles Holmes (consultant), Dr. Josh Reuther (geoarchaeologist), Dr. Holly McKinney (field director in 2017) have doctoral degrees in Anthropology. Justin Hays (assistant field director in 2015) holds a M.A. degree and is enrolled in a PhD program. Four of the field technicians in 2015 had M.A. degrees in Anthropology and one of the field technicians in 2017 had M.A. degrees. All (100%) of the field technicians in 2015 and 2017 had previous field experience, in some cases, over a decade of Alaskan field experience.

Other tasks related to the scope of work include dissemination of our research results. This report satisfies the final report requirements (well beyond the estimated 200 pages). We also presented our results at several international and regional meetings, where it has been very well received by the scientific community. These publications include:

(5) Potter, Ben A., et al. (2018) *Archaeological Investigations at Delta River Overlook*. Archaeology GIS Laboratory, University of Alaska Fairbanks. Report #7. (This report)

(4) Potter, Ben A., Julie Esdale, Charles E. Holmes, Joshua D. Reuther, and Holly J. McKinney (2018) New Discoveries at Delta River Overlook. Paper presented at the 83rd Annual Society for American Archaeology Meetings, Washington, D.C.

(3) Esdale, Julie and Ben A. Potter (2018) The Northern Archaic tradition revisited. Invited paper presented at the 45th Annual Alaska Anthropological Association Meetings, Anchorage, Alaska. *AAA Program* 45:pp. 49

(2) Potter, Ben A., Julie Esdale, Charles E. Holmes, Joshua D. Reuther, and Holly J. McKinney (2016) New Discoveries at Delta River Overlook, a terminal Pleistocene

– late Holocene multicomponent site in central Alaska. Paper presented at the 49th Annual Canadian Archaeological Association Meeting, Whitehorse, Yukon.

(1) Potter, Ben A, Julie Esdale, Charles E. Holmes, Joshua D. Reuther, and Holly J. McKinney (2016) Delta River Overlook, a terminal Pleistocene – late Holocene multicomponent site in central Alaska. Paper presented at the 43rd Annual Alaska Anthropological Association Meetings, Sitka, Alaska. *AAA Program* 43:54

1.1 Research Objectives

Per the research design, research objectives of this investigation are as follows:

(1) Recover artifacts, fauna, features, and explore spatial relationships among them to understand function, seasonality and social organization
(2) Securely date and characterize technology and subsistence from multiple components to evaluate changing land use
(3) Recover geoarchaeological samples to characterize the paleoenvironments and link with ongoing regional research; and
(4) Recover bison and associated activity areas to better understand bison hunting, processing, nutritional stress, regional extirpation, paleodiet, and genetic relationships

These research objectives were met, and the results were analyzed and presented in this report.

1.2 Report Organization

This report is organized as follows. Chapter 2 presents a history of research at DRO, from its initial discovery in 1978, through the 1979 testing and related analyses, and the aborted 1985 excavation. It also tracks multi-year evaluation of erosion control and ongoing erosion at the site.

Chapter 3 is an overview of this current (2015-2018) investigation at DRO, including excavation methods, analyses performed, and additional geoarchaeological, geological, isotopic, paleoecological, and genetic samples for ongoing and future work. It also includes estimation of DRO site extent and topographic mapping results.

Chapters 4 through 12 are data analysis chapters. Chapter 4 provides radiocarbon analyses and results relating to site chronology and occupation history. All significant cultural features were radiocarbon dated, and these data are used to help delineate components (site occupations).

Chapter 5 provides the results of geoarchaeological investigations at DRO and Hurricane Bluff including an assessment of site formation and site disturbance.

Chapter 6 presents results of analyses geared towards delineating components at the site. This includes stratigraphic analyses, radiocarbon dates, 3d backscatter plots, level analyses of screened materials, and ArcGIS analyses. These results are used to create lithic and faunal assemblages which are analyzed later.

Chapter 7 presents analyses of lithic materials at DRO. Questions relate to how were people using stone technology at the site, what stages of reduction occurred, how

can we infer lithic procurement, and are there observable trends in lithic behaviors through time? Detailed debitage analyses, tool analyses, and spatial analyses are presented to address these questions.

Chapter 8 presents analyses of faunal remains at DRO. Questions relate to assemblage composition, skeletal element presence/absence, and richness and diversity measures to understand economic strategies, site function, and specific butchery patterning.

Chapter 9 presents analyses of archaeobotanical remains, focusing on seasonality and floral use by site occupants. Flotation analyses and standard macrobotanical analyses were used to address these questions.

Chapter 10 provides geochemical analyses of obsidian artifacts from DRO to understand lithic procurement, lithic conveyance, and differences among components and cultural traditions.

Chapter 11 provides isotope analyses of bison teeth from Components 2b and 3, geared towards understanding bison mobility, especially evidence of seasonal migration. Multiple serial samples from each tooth were analyzed for strontium, carbon, and oxygen isotope variation.

Chapter 12 presents analyses of features and spatial analyses combining results from lithic and faunal analyses. These data are used to interpret activity areas and infer site function for each component, as well as evaluate changing human ecology through time at DRO.

Supplemental information is provided in the Appendices. Appendix A provides detailed data on lithic raw materials. Appendix B contains lithic artifact photographs. Appendix C provides results of our work at Hurricane Bluff. Appendix D contains updated AHRS site cards for both DRO and Hurricane Bluff.

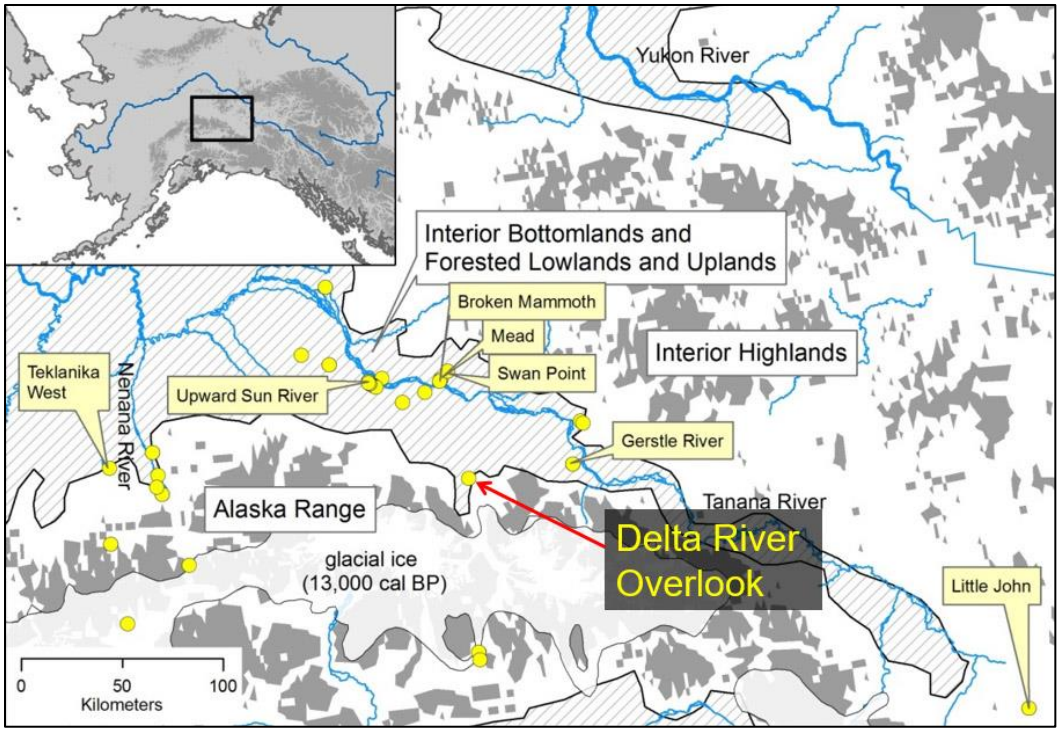

Figure 1.1 Location of Delta River Overlook. Ecoregions from Gallant et al. 1995.


Figure 1.2 Aerial photograph showing the area of our excavations (in yellow).

CHAPTER 2. HISTORY OF RESEARCH AT DELTA RIVER OVERLOOK

Charles E. Holmes

2.1 1978 Investigation

In 1978, the first systematic archaeological survey of U.S. Army lands was undertaken for Alaska. This was driven by the need to comply with national environmental laws and regulations and to implement Executive Order 11953, "Protection and Enhancement of the Cultural Environment" (36 FR 8921, 16 USC, 470) and Army regulation AR 200-1. Charles Holmes, a graduate student at Washington State University, was hired by the U.S. Army Corps of Engineers to conduct a reconnaissance level survey to identify, locate, and inventory archaeological sites on Forts Wainwright, Greely, and Richardson withdrawal lands in Alaska (Holmes 1979). Eight weeks in July and August were allocated for Holmes, with a three-person crew (Lizette Boyer, Bill Grey, and Kathy Leitgeb), to conduct the field survey for approximately 609,000 acres at Fort Greely. This small team recorded over 60 archaeological sites, on average over one per day.

The Delta River Overlook site (XMH-297) was discovered late in the 1978 season. On the last day of the survey the team found recently disturbed ground on a promontory overlooking the Delta River floodplain to the west. Two survey monuments stamped "O.P. 9c – July, 1978" indicated the disturbance had been done prior to the installation of the monuments. This Army activity and subsequent blowing winds resulted in more than 2m of stratified sand and organic layers being stripped away leaving lithic artifacts scattered about the exposed surface (Figure 2.1).

Figure 2.1 Two views (north) showing the site on day of discovery. Crew (L. Boyer, B. Grey, and K. Leitgeb) excavating test pit in the erosion zone at XMH-297 in 1978.

A single 1x1m test pit was excavated in the disturbed area (Figure 2.1) that revealed almost 2m of intact loess that contained a tephra, multiple paleosols, and *in situ* lithic artifacts 10cm beneath the deepest paleosol. The test did not reach the underlying gravel till surface. A radiocarbon date from the deepest paleosol showed the artifacts to be older than about 9600 cal yr BP. A preliminary granulometric analysis of sediments (Holmes 1979, Appendix B) indicated several episodes of aeolian activity: beginning with an early post-glacial accumulation of silt, coinciding with human occupation;

continuing silt increase with alternating paleosol development; and then a change in wind velocity resulting in sand accumulation with brief intervals of calm that allowed for vegetation growth. A shallow hearth (10cm beneath the sod) exposed on the western side of the hill was observed, but not tested (Figure 2.2).

Figure 2.2. L. Boyer pointing to a hearth exposed near the surface in 1978. Note: the displaced charcoal and thermally altered rock (bottom center) that has fallen down the slope.

Although limited in scope, the 1978 investigation showed XMH-297 to be a deeply buried, stratified site with the potential to contain a record of multiple human occupations throughout the Holocene. The undated tephra was thought to have potential as a time stratigraphic marker for the region, once its age was determined. It was recommended that XMH-297, along with three other sites, XBD-106, XBD-110, and XMH-280, be investigated further to assess its significance and for determination of eligibility for inclusion in the National Register of Historic Places. Also, there was concern that erosion would continue to impact the integrity of XMH-297.

2.2 1979 Investigation

In 1979 Alaskarctic, a cultural resources consulting group, under contract (DACA85-78-C-0045) to the Alaska District, Army Corps of Engineers, conducted archaeological survey and test excavations on the Fort Greely military reservation (Bacon and Holmes 1980). Charles Holmes was hired by Alaskarctic to direct field operations and supervise a three-person crew (Kevin Leehan, Daniel Rouse, and Lloyd Jones). The team worked at XMH-297 a total of 21 days in June, July, and August with a break between July 16 and August 11 to allow for frozen sediment to thaw. The site showed evidence of continued wind erosion and several artifacts were found on the surface that

had been exposed since 1978 (Figure 2.3). Three excavation blocks were laid out in a metric grid and a topographic map made with the aid of transit, compass, and tape over the land form (Figures 2.4, 2.5). Block A was a 2 x 2 m unit, Block B 1 x 3 m, and Block C 1 x 2 m. Frozen ground was encountered about 1.25 m deep in Block B between paleosols 3 and 2 on July 11.

Figure 2.3 C. Holmes pointing to artifact and bone in the disturbed area at XMH-297 at the beginning of the 1979 work. View is north.

Figure 2.4 C. Holmes at transit set up over "O.P 9c – July 1978" monument in 1979. Beginning the excavation of Blocks A and B, view is south.

Figure 2.5. Aerial photo showing the location of Blocks A, B, C, and X.

Block A (Figure 2.6) was located near to the 1978 test pit and Holmes found as expected, a sediment matrix consisting of loess under a shallow disturbed sandy surface. Excavation revealed five prominent paleosols, a faint tephra, a moose bone, and two cultural components. The upper .5m of the profile showed an unconformity, the top loess had been scoured away and replaced with sand. Two radiocarbon dates associated with the deepest paleosols, 1 and 2, were obtained that bracketed the tephra between c. 8000 cal yr BP and 7600 cal yr BP, indicating it could not be the Jarvis Creek/Hayes volcanic event that occurred circa 4000 cal yr BP.

Excavation Block B was located 7m northwest of Block A where the ground surface was at the loess and sand contact (Figure 2.7). Here the overlying sand had been almost completely removed leaving the underlying loess intact. Seven prominent paleosols were recorded with a distinct tephra occurring between paleosols 6 and 7, but no tephra was found between paleosols 1 and 2 as was the case in Block A. Radiocarbon dates suggested the age for the Block B tephra lies between c. 2250 cal yr BP (hearth above paleosol 7) and 4460 cal yr BP (paleosol 4). A bison tibia was recovered immediately above the tephra in loess below paleosol 7 (Figure 2.8). Four archaeological components, or five if the bison bone is included, were identified in Block B. Fauna represented include bird (cf. small duck), hare, and beaver from the late- Holocene component plus bison associated with the credible c. 4,000 year old Jarvis/Hayes tephra. Biface, burin, and microblade artifacts were found in situ in the loess below paleosol 1.

The Block C excavation began August 11 and was abandoned after reaching a depth of 1.12m entirely within laminated sand. No artifacts were found but skeletal elements of hare were recovered. Narrow surface trenches were dug to connect Blocks A and B with the intact recent Holocene sand sediment to draw a complete profile from the basal gravel to the modern vegetated surface (Figure 2.9). Sediment samples were collected from the upper sand and lower loess for granulometric analysis by Kevin Leehan (Bacon and Holmes 1979, Appendix B). Kevin expanded the sediments study into a master's degree thesis at Washington State University in 1981.

In September 1979, the Army took measures to alleviate the continuous erosion to XMH-297 by placing snow fences across the site. They also placed a large plywood sign "Archaeological site XMH-297 off limits to all personnel by order of the Commander" on the site (ref. Figure 2.10). This sign and the fence were in evidence in 1985, but the fence was mostly broken and pieces missing.

Figure 2.6. Location of 1979 excavation Blocks A and B, crew member D. Rouse, and north wall profile of Block A. Note: disturbed sand over intact stratified loess. View is north.

Figure 2.7. L. Jones at Block B excavation in 1979 (view is northeast), and C. Holmes at east wall profile showing tephra 2.

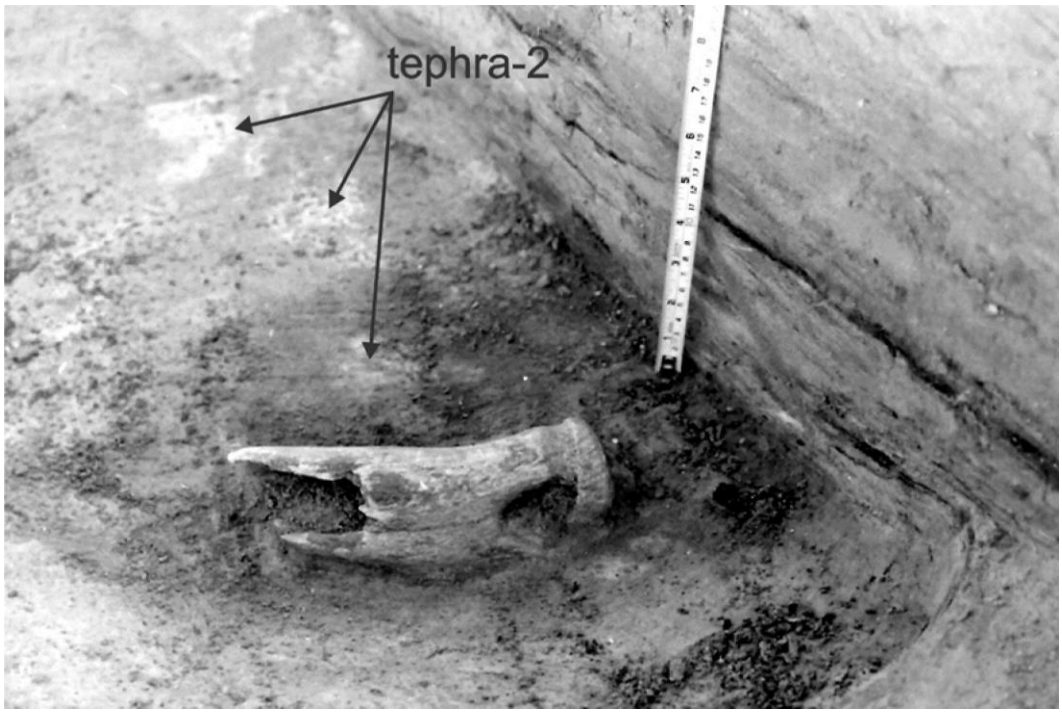

Figure 2.8. In situ bison tibia in Block B, 1979.

Figure 2.9. Profile in the upper sand strata showing sediment sampling in 1978. The upper sand profile was traced to the lower loess stratigraphy in Blocks A and B to reconstruct the complete depositional record prior to the disturbance at XMH-297. View is north.

Figure 2.10 C. Holmes points to a hearth in the lower bench, 1979. The site was investigated in 1998 and named Hurricane Bluff and given AHRS designation XMH-838.

2.3 1985 Investigation

Following the original fieldwork in 1978-79 Holmes continued dialogue with the Alaska District, Army Corps of Engineers, Ft. Greely, and Ft. Richardson personnel about conducting additional research. The project proposed in March 1984, by the University of Alaska Anchorage (Dr. Charles Holmes and Dr. William Workman) with the participation of the National Museum of Ethnology, Japan (Dr. Yoshinobu Kotani), focused on XMH-297 as the major interest, but also included investigations at XMH-280, XBD-106, and XBD-110. The field work was scheduled to begin in June 1985 and go through August 1985. An application for federal permit under the Archaeological Resource Protection Act (ARPA) was submitted in October 1984 to AFZT-EH-PSE, Ft. Richardson. Specific logistics for the project were discussed with AFZT-EH-PSE, Ft. Richardson and the Alaska District, Army Corps of Engineers. Concurrence was received from the Advisory Council on Historic Preservation for the project that was requested by the Army Corps of Engineers and approved by the Alaska State Historic Preservation Officer. In late June 1985 our crew reported to Ft. Greely for orientation and to undergo safety training by Ft. Greely Range Control. The Explosive Ordinance Disposal (EOD) group at Ft. Greely, Range Control conducted a sweep for unexploded ordinance at XMH-297, the site of our field camp, the access to and from the excavation area at XMH-297, and the area surrounding the immediate work area. They declared it safe to work per the field plan. The research team then commenced with mapping and excavations at XMH-297. Our field camp was located nearby on the flood plain below the site. During this time some mapping and testing was conducted at XMH-280 as well.

The first task was to establish an excavation grid and create another topographic map to track any changes due to site erosion (Figure 2.11). A 10 x 10 m excavation block was positioned to overlap previous excavations and encompassed the 1978 test pit and the 1978 Blocks A and B (Figure 2.12, 2.13). The day to day operation was under the direction of Drs. Kotani and Workman with a crew of 10 persons, while Holmes was away on other duties. This work proceeded with the intent of exposing the entire excavation block by natural levels beginning with the loess above paleosol 7. A hearth and associated flake concentration was discovered about 3m the northwest of Block A (1979), and another artifact cluster on north side of Block B (likely associated with the date of c. 2350 cal yr BP from 1979). The work was abruptly halted before reaching paleosol 7. Unexpectedly in July1985 the crew was told to stop work, take down the camp, and leave immediately. The order came through Ft. Richardson from the higher Army command at FORSCOM in Georgia. The reason given was that XMH-297 was in a bombing range and it was unsafe for civilians. The crew was gone within 24 hours. Attempts to show that Ft. Greely had cleared the area and declared it safe to work fell on deaf ears. No one was willing to take it back up the command tree. Nevertheless, Holmes tried to get the Army to reconsider the decision and Ft. Richardson told him they would take the request under advisement.

Figure 2.11. Plan view of XMH-297 showing the 10 x 10 m excavation grid and topographic map produced by the Japanese team in 1985.

Figure 2.12 A large 10 x 10 m excavation block was arranged over the previous excavations done in 1978 and 1979. Note: the 1978 test pit and Block A can be seen in the upper right, and Block B left-center. View is east.

Figure 2.13 Y. Kotani and C. Holmes confer about the work in 1985. The sign reads "Archaeological site XMH-297 off limits to all personnel by order of the Commander." View is south.

A formal request for permission to continue archaeological work at XMH-297 was made by Holmes in November 1985 through Headquarters 177th Infantry Brigade, A Ft. Richardson for the 1986 season. A new ARPA permit for the 1986 season was applied for. Also, the Army Corps of Engineers cultural resources officer, Dr. Constance Ramirez, DAEN-ZCF-M, Washington D.C., was kept informed. In January 1986 Holmes wrote to Headquarters 177th Infantry Brigade, Ft. Richardson concerning the decision by the Army to allow future work at XMH-297and suggested having a meeting to go over the matter.

By May 1986 no word had been received from the Army on the question of access to XMH-297 and the status of the ARPA permit request, so Holmes wrote to Senator Ted Stevens asking for help. By now the ability to do the field project for 1986 was lost, and given the budgeting schedules and procedures for the Japanese partners and the National Science Foundation, it was doubtful there would be time to obtain funding for the 1987 season as well. Holmes made it clear that, "We do, however, wish to obtain the permits that have been requested so that our work can continue, regardless of the funding level." Senator Stevens received a letter (dated June 13, 1986) from Maj. Gen. G. H. Bethke, Commanding, Ft. Richardson, stating that Holmes' request along with their recommendation was forwarded to Headquarters, U.S. Army Forces Command (FORSCOM). FORSCOM then forwarded the request to the Dept. of Army for approval on June 10, 1986. In short Ft. Richardson did not recommend access to XMH-297 because, "Funding and staffing constraints make it impossible to provide and on-site Explosive Ordnance Disposal (EOD) Team that could assure the continued safety of the survey team while conducting their excavations." It was, however, recommended that the archaeologists have access to the other sites that were requested. But there was not any direct communication from the Army, so Holmes again wrote a follow-up letter to Senator Stevens in July 1986 stating his concerns.

Senator Stevens informed Holmes in December 1986 that he had contacted the Dept. of the Army for an update and hoped that something could be worked out and the project could be resumed during the 1987 field season. Holmes thanked Senator Steven for his interest and help, but expressed frustration with what had happened and stressed that XMH-297 continued to suffer erosion which the Army had known about for 8 years, pointing out that this constituted demolition by neglect. Senator Stevens informed Holmes that he recognized and appreciated his continuing concerns about the importance of resuming work at XMH-297 (letter January 12, 1987). But, "…the Army has not responded to my most recent inquiry on your behalf." Finally, a response, dated January 14, 1987, from Ft. Richardson informed Holmes that his permit request made in November 1985 had all necessary approvals. "The permit request in now on file at the latter office and will be issued for a period of 120 days upon your request. Approval has been granted for sites XBD-106 and XBD-110, but not XMH-297. This site is still considered unsafe due to ordnance problems."

In subsequent years, it was determined that although XMH-297 is located adjacent to and overlooks the Washington Impact Area, the site location itself is not in a bombing range. Over the years since 1987 a number of archaeological survey and testing projects (CRM work for the Army) have been permitted to survey numerous locations very near to XMH-297. During this time no serious effort on the part of the Army to protect the site from damage, beyond the fencing and signage in 1979 has occurred. No further archaeological work was done at XMH-297 until the current project began in August 2015.

2.4 Artifact summaries from 1978 and 1979 testing

Artifact totals from the 50 x 50 cm test pit excavated in 1978 (located at N202.20-203.00, E499.20-499.90 in the 2015-2017 grid system, and identified as F2015-2) and the 4 units excavated to varying depths in 1979 (Blocks A, B, C, and X) are listed in Table 2.1. Blocks A (2 x 2 m) and B (1 x 3 m) were excavated to bedrock, and Block C (1 x 2 m) was excavated only a few cm deep. Block X was a narrow 50 cm wide trench to evaluate upper stratigraphy. The total area excavated in 1978 and 1979 was 9 m^2.

Table 2.1 Summary of artifacts recovered in 1978 and 1979.

Component	*N lithics*	*N tools*	*Density*	*Microblades*	*Proj. pt.*	*Tools*
C1	52	4	5.8	Yes	Yes	1 biface, 1 biface frag, 8 mb, burin spall
C2	4	0	0.4	Yes	No	1 mb, 3 flakes
C3	16	1	1.8	No	Yes	1 proj point base
C4	1	0	0.1	No	No	1 flake
C5	271	1	30.1	No	No	-
C6	0	1	0.0	No	No	Hammerstone

Six components were identified. Component 1 was identified at the base of Paleosol 1 and the upper half of Loess 1. Numerous large mammal bone fragments were recovered in association with the lithics. Component 2 was identified in Loess 2/3, consisting of 1 microblade, 3 flakes and possible hare. Component 3 was identified in Paleosol 4, and included a projectile point base, numerous flakes, and unidentified animal bones. Component 4 (a single flake) was found in Loess 5, with no associated fauna. Component

5 was found in Loess 6 and consisted of numerous flakes, a boulder spall scraper, 2 hammerstones, and associated fauna: small duck, hare, beaver, and bison. Component 6 was found above Component 5 in the upper sands and consisted of a single hammerstone. Correlations of these components with 2015-2017 excavations are provided in Chapters 4 and 6.

CHAPTER 3. CURRENT INVESTIGATION (2015-2017)

Ben A. Potter

3.1 Introduction

This chapter summarizes the methods of excavation used in the 2015-2017 investigations at Delta River Overlook, as well as other excavation details. Results of site mapping of DRO and Hurricane Bluff are also presented (Figure 3.1).

Research objectives were focused on understanding site context, paleoecological relationships of geology and archaeology, and human ecology of human occupants through time. Specific research objectives are as follows:

(1) Recover artifacts, fauna, features, and explore spatial relationships among them to understand function, seasonality and social organization,

(2) Securely date and characterize technology and subsistence from multiple components to evaluate changing land use,

(3) Recover geoarchaeological samples to characterize the paleoenvironments and link with ongoing regional research, and

(4) Recover bison and associated activity areas to better understand bison hunting, processing, nutritional stress, regional extirpation, paleodiet, and genetic relationships

3.2 Excavation Methods

Excavation methods generally follow those developed and utilized in excavations of other deeply buried well-stratified sites in the Tanana basin, including Gerstle River, Upward Sun River, Mead, and Swan Point (Potter 2005, Potter et al. 2008, 2011, 2014). In 2015, a site datum (Datum 1) was established in a protected area north of the site outside of the area of aeolian deflation (Figure 3.2). This is intended to be a permanent datum. From there, we established a baseline and Datum 2, located on a topographic rise to the south of the major area of interest, centered on the 1978-1979 and 1985 excavation areas in the east deflation bowl. A metric grid was established over the area of interest using a Leica total station (Figure 3.1).

Datum 1 (permanent datum and backsight for Datum 2) was given the coordinates:

N = 221.000 meters
E = 492.000 meters
Z = 503.185 m above mean sea level, derived from Garmin CX GPS device.

Datum 2 (day to day datum, southwest of main excavation area) was given the coordinates:

N= 197.000 meters
E = 492.000 meters
Z = 500.973 meters ASL

Excavation Blocks (2 x 2 m) were established and numbered incrementally (e.g., 1, 2, 3, etc.). We laid out Blocks 1-19 in 2015 and Blocks 20-26 in 2017 (Figure 3.3).

Subdatums were established for each block, labeled by Block (e.g., subdatum 1a, 1b, etc.). These were generally located at the highest elevation corner of the units. Additional subdatums were established to aid in control of levels due to the thickness of the loess deposit and the difficulty in taking vertical provenience when the distance grew more than 1.5 m. Each subdatum was noted on the field books (Table 3.1).

Excavation was conducted in arbitrary 5 cm levels below the ground surface until Paleosol 1 was reached. When the disturbed layer was removed, this was adjusted slightly to match the general slope. The arbitrary countered level approach was used because of the thinness of the upper paleosols (in some cases they were not continuous) and the general paucity of cultural materials in these strata, excepting for Component 8b. When Paleosol 1 was reached, the next level would be the top of Paleosol 1 to the bottom of the paleosol, generally about 5 cm. Once the bottom contact of Paleosol 1 and Loess 1 was reached, we excavated in 5 cm contoured arbitrary levels: e.g., 0-5 cm below P1, 5-10 cm below P1, etc. This allowed for consistent recording across the site, particularly important given the large amount of cultural material below P1 (Components 1, 2a, 2b, and 2c). Level controls were maintained by line-level measurements for each excavation unit (1 x 1 m).

Twenty cm wide baulks were maintained at the edges of most Blocks. The baulks were used to maintain vertical control and to assess changes in deposition or stratigraphy during the excavation. The baulk generally remained until Paleosol 1 was reached, or safety required it to be removed earlier. The baulks were profiled and excavated and screened in 50 cm quads.

Three-point provenience was used for all cultural material encountered while troweling, including debitage. All sediment was passed through 1/8-inch screens in 50 x 50 cm quads. 3-point controls were provided with a Leica total station with sub-centimeter accuracy. All artifacts were bagged with detailed provenience information on the bag and within the field books. Excavators used incremental FS (field specimen) numbers per Excavation Block, providing a unique identifier for each sample recovered (e.g., 17-234 is the 234th sample recovered from Block 17).

Faunal remains were 3-pointed and recovered carefully, focusing on minimal loss of integrity and structure. Organic probes and soft brushes were used to excavate around the bone to decrease the possibility of fragmentation prior to recovery. Larger faunal remains were pedastaled in order to assess the relationships among bone scatters, lithic debris, and features. Photographs were taken and bones were removed and placed in aluminum foil and within plastic bags. They would later be aired out gradually in the lab.

Features, both natural and cultural, were recorded individually upon encounter. Once a feature was identified, it was photographed and the following protocols were utilized. Different feature classes necessitated different recovery methods. Cobble concentration were recorded, photographed, and excavated. Each individual item was 3-point provenienced. Stains or lenses that were determined to be natural were

photographed, recorded, and samples may have been taken. Hearth features were the main class of feature encountered at Delta River Overlook, and we used the following methods of excavation:

Basic principles apply through all stages of the excavation protocol.

1) All feature matrix was collected
2) Photo-documentation and plan and cross-section drawings were detailed allowing for feature reconstruction,
3) All artifacts/ecofacts were 3-point provenienced as normal, enabling comparison with other parts of the site to facilitate density, refit analysis and fine-grained spatial analyses,
4) Pertinent controls were collected through systematic sample collection in 10 or 20 cm units,
5) Careful excavation (taking care to identify new problems or questions in the field and modify the sampling to accommodate them) was balanced expediency often needed in field conditions,
6) The excavation was iterative, with new findings (e.g., multiple overlapping features, unique activity areas) made interpretable through the earlier stages of the excavation, and
7) All measurements were made by total station.

Upon encountering a hearth (or prospective hearth), we exposed the surface to identify the maximum feature extent. During the entire process, all identifiable materials were piece-plotted. If the hearth surface was at the interface of arbitrary excavation levels, the screened collection protocols by level was followed, but those screen bags directly associated with the hearth were labeled as such. If the hearth surface dipped below the bottom of an arbitrary level, the excavation followed the hearth surface, not the level, in order to expose the angle and dimensions of the hearth surface and artifacts/ecofacts directly associated with the outer edge to at least 50 cm.

Once the entire hearth surface was exposed, the feature was mapped by total station (on a 5-10 cm grid) and in a field plan-view map and photographed from various angles. The field map included observations about the outer edge of the feature (blurred, clear/sharp boundary, etc.) to evaluate feature discreteness and possible disturbance. Charcoal flecks or oxidized patches that lie beyond the edge were also mapped, and the latter were collected in bulk. In general, all attempts were made to establish the surface of the activity area associated with the hearth at the time of excavation rather than at successive times. The level system was resumed once the feature had been totally excavated, and all screened items were still provenienced by level.

The hearth was excavated using a 50 cm quadrant grid, within the overall 1 meter^2 excavation unit. The excavation grid for the surrounding area was maintained (necessary particularly to link the hearth stratigraphically to the profiles drawn in adjacent areas). The hearths were generally quartered, but in all cases, all hearth matrix were collected in successive bags (digging levelly, e.g., Field specimen (FS) #1, bag 1, FS#1, bag 2, etc.). This enables future screening/floated material to be systematically collected by depth from hearth surface). We carefully excavated to identify and delineate hearth stratigraphy. Once unaltered matrix was reached, we photographed and continue

excavation below the bottom of the hearth to 5 cm or the end of the arbitrary level. The bottom of the hearth was also documented by total station (on a 5-10 cm grid) at each stage. Once the quarter cross-section was complete and cleaned, we photographed, measured, and drew the profile. This was quickly done by total station and mapping on graph paper using those measurements rather than horizontal line level-aided profile drawings.

Potential hearth stratigraphy was identified from the cross-section and this was used to excavate the remaining hearth. If possible, we expanded the quarter excavation to a half, in order to expose more of the cross-section and using the initial quarter stratigraphic profile to collect the remaining hearth (by 50 x 50 cm quadrant) by cultural hearth layers. We did not excavate by scraping the trowel, which tends to damage delicate macrofossils, etc., but rather to pry in very small chunks to loosen the material that will protect these for future ID and analysis. We continued to excavate each 50 x 50 cm quadrant in a way to maximize cross-sectional variability, if it is observable, throughout the feature.

Documentation followed general protocols following best-practices in archaeology, geared for consistency with other interior Alaskan excavations. Each excavator was responsible for a 1 x 2 meter unit, generally, and each 2 m^2 Excavation Block was excavated by two technicians. Each excavator filled out a field book, including daily activities, excavation levels, a field specimen log for those units assigned to the technician, and detailed notes about the excavation. The PI (Potter), the assistant field director (Hays, McKinney) kept separate log books documenting overall excavation progress. A project camera (high quality digital SLR with a Sigma lens) was used to document the excavation. A total of 804 photos from 2015 and 1006 photos from 2017 documented the excavation (for a total of 1810 digital photographs). Some video recordings were also produced. Stratigraphic profiles using metric grid paper were produced in both years. A total of 29 and 67 linear meters of stratigraphy were recorded in 2015 and 2017 respectively, for a total of 96 linear meters for both years of investigation. Generally stratigraphic profiles were 1.5 to 2.5 meters in depth from disturbed surface to glacial till.

Table 3.1 Site datum and subdata measurements

Station	*Year*	*Role*	*North*	*East*	*Elevation*
Datum 1*	2015	permanent offsite datum, backsight	220.995	491.999	503.185
Datum 2*	2015	primary operational datum	196.997	492.001	500.973
Datum 3	2015	topographic control	184.006	462.857	500.043
Datum 4	2015	topographic control	187.153	493.065	500.592
Datum 5	2015	topographic control	200.651	525.944	498.009
Datum 6	2015	topographic control (XMH-838)	151.034	633.760	485.081
Datum 7	2015	topographic control (XMH-838)	130.968	671.559	478.737
Datum 8	2015	topographic control	224.027	462.994	502.820
Datum 9	2015	topographic control	212.166	574.988	487.781
subdatum 1a	2015	excavation control	198.998	498.002	500.099
subdatum 2a	2015	excavation control	199.995	502.010	500.073
subdatum 3a	2015	excavation control	202.006	501.003	500.244
subdatum 4a	2015	excavation control	202.000	496.005	500.491

subdatum 5a	2015	excavation control	203.999	497.996	500.567
subdatum 6a	2015	excavation control	204.005	496.001	500.703
subdatum 7a	2015	excavation control	205.998	496.002	500.800
subdatum 8a, 13a	2015	excavation control	206.000	494.001	500.857
subdatum 9a	2015	excavation control	208.000	498.007	501.042
subdatum 10a	2015	excavation control	208.001	489.995	501.094
subdatum 10b	2017	excavation control	207.933	490.999	499.612
subdatum 11a	2015	excavation control	209.997	495.992	501.126
subdatum 11b	2015	excavation control	209.943	495.938	499.726
subdatum 12a	2015	excavation control	210.011	493.999	501.106
subdatum 13a	2015	excavation control	206.000	493.998	500.856
subdatum 14a	2015	excavation control	206.006	492.000	500.931
subdatum 15a	2017	excavation control	212.003	493.990	501.214
subdatum 15b	2017	excavation control	211.947	492.963	499.938
subdatum 16a	2015	excavation control	210.000	486.000	500.941
subdatum 17a	2015	excavation control	209.002	476.005	503.720
subdatum 17b	2015	excavation control	209.000	476.000	502.220
subdatum 18a	2015	excavation control	181.004	455.997	497.085
subdatum 19a	2015	excavation control	209.009	490.006	501.035
subdatum 19a	2017	excavation control	207.993	488.999	501.107
subdatum 20a	2017	excavation control	202.001	494.998	500.538
subdatum 20b	2017	excavation control	201.740	494.030	499.583
subdatum 21a	2017	excavation control	204.004	493.992	500.712
subdatum 21b	2017	excavation control	204.015	494.127	499.638
subdatum 22a	2017	excavation control	210.002	498.005	501.333
subdatum 22b	2017	excavation control	209.948	496.946	500.024
subdatum 23a	2017	excavation control	208.987	487.803	501.001
subdatum 24a	2017	excavation control	211.998	496.004	501.348
subdatum 24b	2017	excavation control	211.957	495.004	499.993
subdatum 25a	2017	excavation control	204.004	501.000	500.527
subdatum 26a	2017	excavation control	209.987	490.997	501.007

* Permanent datums

Figure 3.1 Delta River Overlook and Hurricane Bluff area map and aerial photograph showing areas of excavation (red).

Figure 3.2 Delta River Overlook site map showing areas of excavation (red).

3.3 Excavation Overview

This section describes the archaeological fieldwork conducted in 2015 and 2017. Figure 3.3 shows the history of excavation at DRO, created through location of older excavation edges (1978-1979) and comparison with photographs (1985). Figure 3.4 shows all 2015-2017 Excavation Block locations at DRO. Figures 3.5-3.9 show overview photographs of the 2015 and 2017 excavations.

3.3.1 2015 Excavation

The 2015 excavation occurred between August 1 and August 31, 2015 (23 working days). We worked Saturday through Wednesday, with Thursdays and Fridays off. Excavation personnel are listed in Table 3.2. The UAF crew consisted of Ben Potter (PI), Chuck Holmes (Consultant) Josh Reuther (geoarchaeologist), Justin Hays (assistant field director) and 17 archaeological technicians, most working for 23 days. Four volunteers worked at the site between 5-15 days.

Chuck Holmes and Ben Potter relocated the area of the 1979 and 1985 excavation based on photographs and tree locations (most of the area was revegetated). We could not directly relocate the old backfilled units. We started clearing brush off of the disturbed surface and began coring parts of the area to identify the depth of disturbance. We identified the corners of Blocks A and B. No corner nails/stakes from the 1979 or 1985 excavation were identified (they may have been removed). Using the Block A east wall, we established a metric grid over the site. Datum 2 was used almost exclusively for mapping and excavation, and we used Datum 1 as a backsight (due north, 360 degrees).

The 2015 Excavation Blocks 1-14 were located around and between Blocks A and B in order to maximize artifact recovery, association of cultural components and complex stratigraphy, and provide chronological control for cultural occupations and paleosols. Block 15 was mapped out but not excavated in 2015 (it would be later excavated in 2017). Blocks 16 and 17 were placed to provide an east-west transect to analyze site stratigraphy. Block 17 was placed on the edge of the deflation bowl, thus allowing for the uppermost stratigraphy to be connected to the main excavation area. Block 16 was placed intermediate between Block 17 and the main excavation (Blocks 12 and 14), allowing for a stratigraphic profile at the same north line (N 210) to connect the various parts of the site. Block 18 was a 1 x 2 m test in the west bowl, placed in an area of surface thermally altered rocks. Block 18 was excavated a few levels, but no cultural remains were noted, and the sediment consisted of loose aeolian sand. Block 19 was a small 1 x 1 m^2 unit placed along the North 210 line between Blocks 12 and 16. Cultural material was found in this unit and it was expanded in 2017.

During the 2015 excavation, we excavated 60 m^2 to varying depths. The majority (Blocks 1-9, 11-14 totaling 49 m^2) were excavated to (sterile) glacial till. Blocks 16 and 17 were too deep to safely excavate and were halted at appropriate levels (as their purpose was to link upper stratigraphy). No artifacts were found in Block 17. Blocks 10 and 19 were halted due to time constraints, but both were completely excavated to glacial till in 2017.

During the excavation we fully exposed several previous excavations, including the 1978 test pit, Blocks A and B from 1979, and a narrow 10 cm-wide and 25-35 cm

deep mini-trench connecting Blocks A and B, probably excavated (but not reported) in 1985.

Topographic mapping of the entire area, including Delta River Overlook and Hurricane Bluff and the areas between them, was conducted on 8/11 and 8/12/2015. Datums 3-9 were established to shoot topography of both DRO and Hurricane Bluff.

Table 3.2 2015 personnel, role, and days at site.

Name	*Initials*	*Role*	*Days*
Ben A. Potter	BAP	Principal Investigator	23
Charles E. Holmes	CEH	Consultant	23
Joshua D. Reuther	JDR	Geoarchaeologist	18
Justin Hays	JMH	Assistant Field Director	23
Jessica Ainslie	JAA	Archaeological technician	23
Kelsey Anderson	KJA	Archaeological technician	23
Kathryn Bobolinski	KLB	Archaeological technician	15
Cameron Brewer	CAB	Archaeological technician	23
Nicolette Edwards	NME	Archaeological technician	23
Robert Holstine	RJH	Archaeological technician	23
Justin Hopt	JRH	Archaeological technician	23
Kaitlyn Hosken	KNH	Archaeological technician	23
Nicki Hurley	NMH	Archaeological technician	23
Aleks Jimenez	APJ	Archaeological technician	23
Justin Junge	JAJ	Archaeological technician	21
Aaron Larsen	ADL	Archaeological technician	23
Georgina Podany	GLP	Archaeological technician	23
Cody Strathe	CJS	Archaeological technician	16
Michael Wendt	MLW	Archaeological technician	23
Dave Plaskett	DCP	Archaeological technician	23
Eric Carlson	EC	Archaeological technician	15
Rob Childers	RKC	Volunteer	5
Pierce Bateman	PAB	Volunteer	15
Casey Somerville		Volunteer	8
Kelly Meierotto		Volunteer	

3.3.2 2017 Excavation

The 2017 excavation occurred between July 15 to August 11, 2017 (22 working days). We worked Sunday through Thursday, with Fridays and Saturdays off. Excavation personnel are listed in Table 3.3. The UAF crew consisted of Ben Potter (PI), Chuck Holmes (Consultant), Holly McKinney (field director), Gerad Smith (assistant field director) and 9 archaeological technicians, most working for 22 days.

The 2017 excavation was intended to complete and expand on the original objectives given the large quantity of significant cultural materials encountered in 2015. Given the results of the 2015 research, the primary 2017 objectives (and associated excavation blocks) were to:

1. Explore Component 1 activity areas: Block 25, 21
2. Explore Component 2a activity areas: Blocks 20-21, 25, 22, 24
3. Confirm stratigraphic separation of C2a, C2b, and C2c: Block 21
4. Explore Component 2c activity areas: Blocks 20-21, 22, 24, 25, 15, 10
5. Connect E-W transect of strats: Blocks 23, 19, 26
6. Explore Component 8 activity areas: Blocks 22, 24, 15

7. Explore upper components: Blocks 19, also 26 and 23
8. Continue 2015 excavation to glacial till: Block 10

Blocks 20-26 were newly mapped and excavated to glacial till. Blocks 10, 15, and 19 from 2015 were continued and excavated to glacial till. Blocks 23 and 26 were excavated to below Component 7b. Totaling both 2015 and 2017 excavations, we excavated almost all blocks to (sterile) glacial till (Blocks 1-15, 19-22, 24-25), totaling 79 m^2. Blocks 23 and 26 (4 m^2) were excavated to Paleosol 6a (below C7b).

In terms of area of excavation relative to components, we excavated 79 m^2 through strata associated with all components, and 85 m^2 of area where Components 7b, C8a, C8b were potentially present.

Table 3.3 2017 personnel, role, and days at site.

Name	*Initials*	*Role*	*Days*
Ben A. Potter	BAP	Principal Investigator	21
Charles E. Holmes	CEH	Consultant	20
Holly McKinney	HJM	Associate Field Director	22
Gerad Smith	GMS	Assistant Field Director	22
Rob Bowman	RCB	Archaeological technician	22
Jill Baxter-McIntosh	JBM	Archaeological technician	22
Tom Allen	TCA	Archaeological technician	22
Cassidy Phillips	CHP	Archaeological technician	22
Casey Jobe	PCJ	Archaeological technician	22
Nell Bishop	NMB	Archaeological technician	22
Travis Shinabarger	TJS	Archaeological technician	22
Peter Schnurr	PFS	Archaeological technician	22
Lori Hansen	LRH	Archaeological technician	22

Dr. Nancy Bigelow (UAF) visited Delta River Overlook on July 16, 2017 to collect samples for sedimentary environmental DNA analysis, focusing on plant, animal, and fish taxa that would have been present in the sediments. In all, 35 samples were collected from both the natural (loess and paleosols) and cultural (hearths) stratigraphy at the site. The natural samples were collected from the north wall of Block 12 (spanning about 2500-13,000 cal yr BP), in order to document what sorts of plants and animals were present at the site. The cultural samples come from two hearths (F2015-5 and F2015-9) and adjacent sediments to assess DNA preservation and identify the taxa preserved in the hearths. All samples were collected with DNA protocols (gloves, bleached trowel, and sampling into a sterile bag) and have been stored at approximately -15º C since field collection.

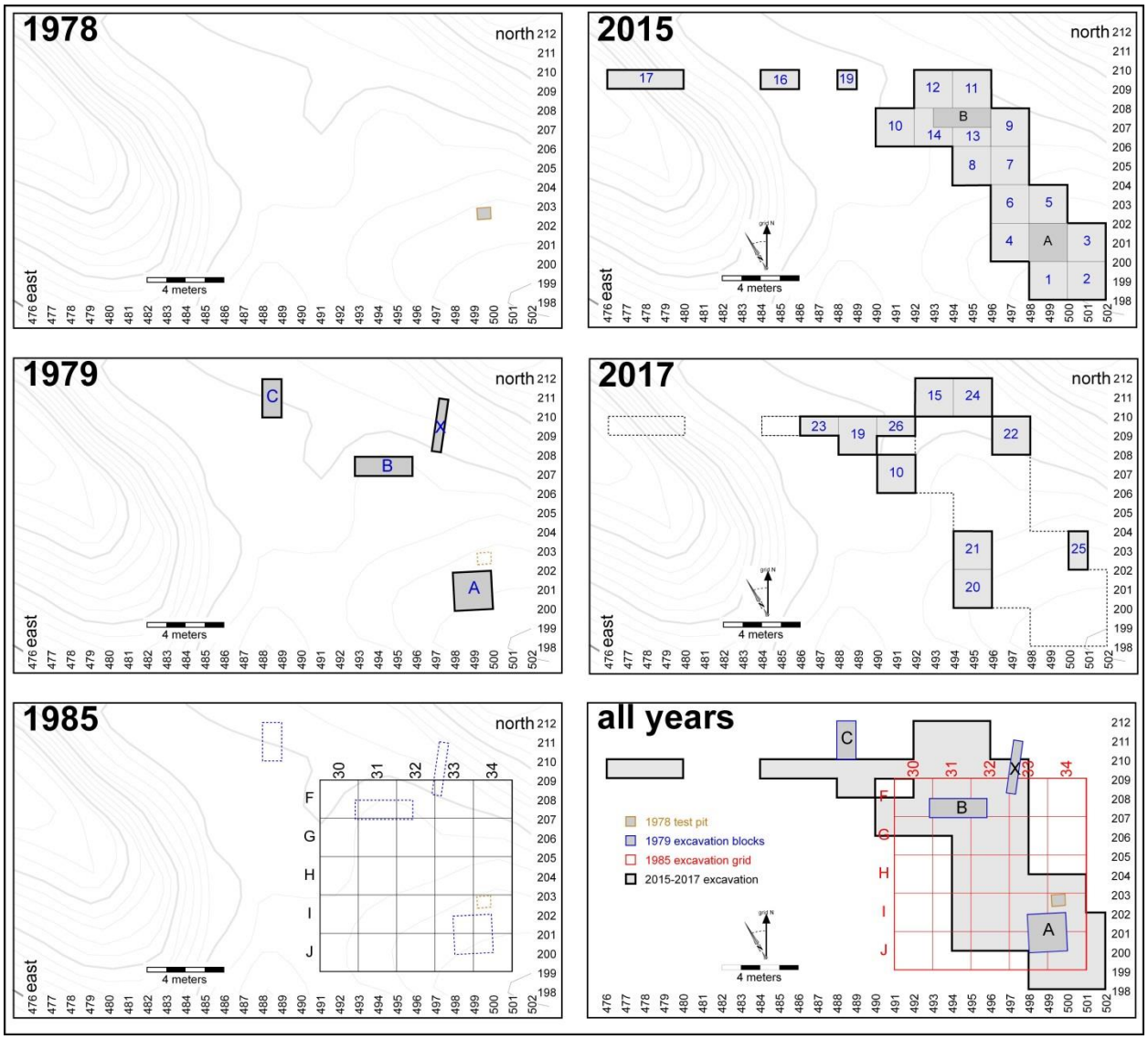

Figure 3.3 History of investigation at Delta River Overlook.

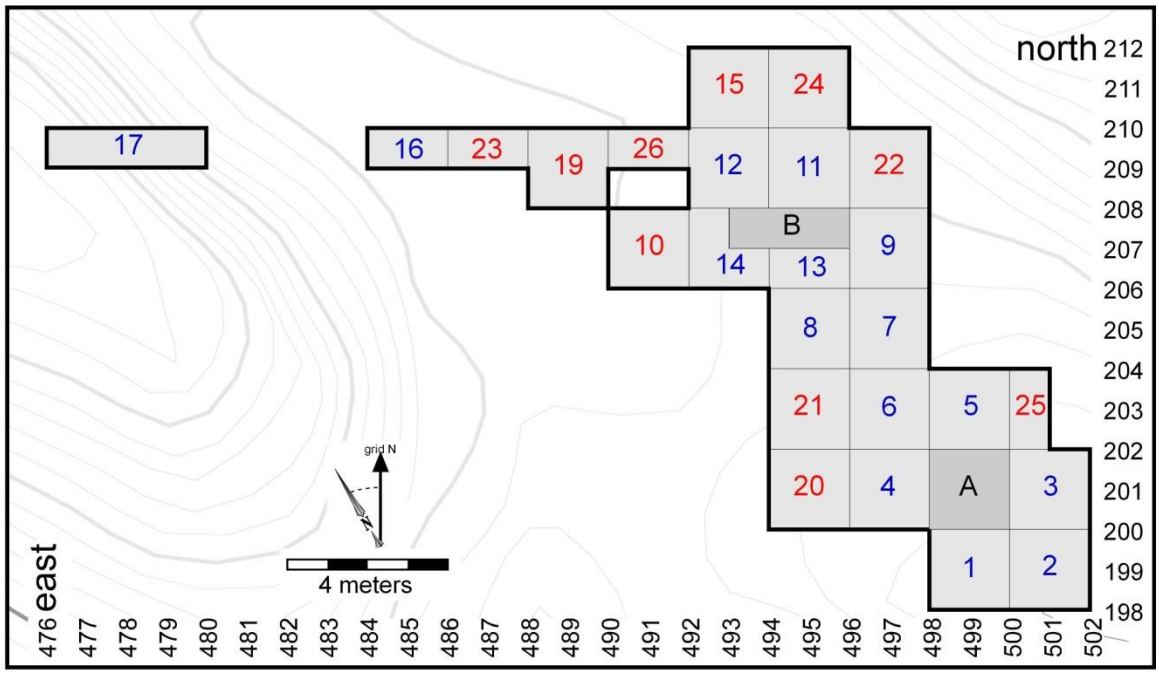

Figure 3.4 Delta River Overlook excavation grid and excavation blocks (1979 Blocks A and B, 2015 blocks in blue, 2017 blocks in red).


Figure 3.5 2015 Excavation overview, view southeast

Figure 3.6 2017 Excavation overview, view southeast.

Figure 3.7 2017 Excavation, view south

Figure 3.8 2017 Excavation overview, view northwest.

Figure 3.9 Excavation overview, view south. Clockwise from upper left: at beginning of 2015 excavation, after clearing underbrush in 2015, end of 2017 excavation, end of 2015 excavation.

3.4 Site Extent, Site Disturbance, and Management Recommendations

3.4.1 Site Mapping

XMH-297 is located at -145.9481 dd W, 63.8176 dd N, and XMH-838 is located at -145.9461 dd W, 63.8167 dd N (WGS_84 datum). We mapped the XMH-297 and XMH-838 sites and environs using a Leica Total Station in order to (1) assess locations and extent of erosion and other damage to the site through time, (2) evaluate site boundaries, and (3) evaluate local geomorphology, stratigraphy, and geochronology. We documented all surface artifacts through a close surface transect across the site. Datums 3 through 9 were established to generate 699 elevation measurements over the landforms associated with XMH-297 and XMH-838. These data were uploaded to Surfer 3d mapping software to generate a comprehensive high resolution topographic map for both sites (Figure 3.10). They were overlain with high resolution aerial imagery within ArcGIS. These data provide a baseline to aid in monitoring additional erosion at the site.

The data were also uploaded into ArcGIS and analyzed through the 3d Analyst extension. Figures 3.11 and 3.12 show selected elevation profiles through both sites and between the sites. Figure 3.11 shows two transects through both major erosional areas (west block and east block) showing relatively how much sediment was lost, about 2 meters in the west bowl and 2.7 meters in the east bowl. This is consistent with stratigraphic measurements from Block 17 along the western edge of the east bowl erosion area relative to the stratigraphy from the main site.

Figure 3.12 (top) shows a grid southeast – northwest transect across both sites showing the relative elevation. Figure 3.12 (bottom) shows a grid southwest to northeast transect across Hurricane Bluff, showing the steep natural slope to the grid southwestern part of the site and gradual (vegetated) slope across the top and grid northeastern part of the site. Aeolian and bison-related disturbance was identified throughout both sites, in particular multiple bison trails (with dung), tracks, and wallow areas. Two access points from the modern Delta River floodplain were identified, one following the break in slope from the western end of Delta River Overlook through to the top of that site, across to Hurricane Bluff and down the edge of the slope to the southern part of the site.

To aid in identifying preservation of undisturbed sediments in the area north of the erosional areas (West and East Blocks), eleven (11) 50 x 50 cm test units were excavated, labeled TU1-11 (Figure 3.13). Undisturbed stratified sediments were identified in all 11 tests. Only two test units were positive for cultural material, TU1 and TU2. TU1 contained 4 bone fragments at 25-30 cmbs. TU2 contained a few flakes at 15-20 cmbs above non-decomposed organics. This indicates later Holocene cultural materials preserved north of the erosional areas. The other 9 test units were unable to be excavated beyond about 1 meter due to size restrictions, and it is likely that additional cultural materials may extend north of the site.

Figures 3.14 and 3.15 are compiled from various datasets, including surface observations, test unit and main block excavations, exposed surface artifacts, and detailed topographic mapping. Estimated site extent of XMH-297 is shown in the blue dotted line (Figure 3.14). Erosional areas (both natural and cultural) are shown outlined in red. Road-related erosion, several bulldozer cuts, and apparent bulldozer berms were identified

across the site. The west bowl erosional cut is largely devegetated and actively eroding through aeolian deflation. The east bowl erosional cut was revegetated with grasses, shrubs, and small deciduous trees. The area of excavation was cleared, but the grasses and undergrowth were kept to help prevent additional erosion. The area south of the erosional cuts is characterized by steep slopes and sparse xeric flora (e.g., grasses). The break in slope extending to the west sloping downward to the active Delta River floodplain is largely denuded for about 40 meters, and then transitions to a denuded bison trail. An older bulldozer cut connecting the two erosional cuts is largely revegetated with shrubs, but the surface is clearly disturbed. Most of the area south of this older bulldozer cut between the two erosional cuts is vegetated with old growth (mostly large white spruce trees).

Surface artifacts (chert and quartz flakes) were observed eroding along the steep slope south of the site as well as in the west bowl (thermally altered rocks). Considering the overall landform topography and the area of recovered artifacts, we tentatively estimate total site area to be 4,037 square meters. All excavations (1978, 1979, 2015, 2017) and the 11 test units total 101.5 m^2, or 2.5% of the overall estimated site area. If we consider the site to comprise only those areas where artifacts have been recovered, this totals 1,213 square meters, with the excavations covering 8.4% of the site.

3.4.2 Assessment of Site Adverse Impacts and Recommendations

The major adverse impact currently is wind erosion (aeolian deflation) exacerbated by vehicle and foot traffic across the site and bison using the area wallowing and for transit from the Delta River floodplain to the glacial highlands to the east. We have mapped the areas and routes bison have used and continue to use to move across the site (Figure 3.15).

We also identified evidence of human disturbance (military personnel or local hunters), including use of the site over the 2015-2016 and 2016-2017 winters, as well as the potential for access and use of the site at other times.

It is important to note that while there is extensive evidence of wind erosion, and much of the upper sediments, representing the last 3000 years of human occupation history, have been destroyed, much of the lower sediments remain intact across the site. It is important that these areas be protected from further disturbance.

We have evaluated site extent and effects of natural (wind, bison) and cultural (vehicle disturbance) adverse impacts to the site, and have the following recommendations.

3.4.3.1 Management recommendations for reducing further erosion

1) Make the DRO site environs (see Figure 3.14) off-limits to off-duty personnel and to other individuals, as far as possible. The site is currently located behind locked gates. Foot and vehicle traffic will exacerbate ongoing wind erosion and more of the upper sediments and the cultural remains that are situated therein will be lost.

2) Fences should be installed at specific locations (see Figure 3.15) to help detour bison herd movement away from culturally sensitive areas.

3) Management strategies should include annual monitoring of the DRO site area.

4) We recommend that the military cultural resource management team consult with U.S. Army leadership if field operations near the DRO site are planned, to help aid in site avoidance.

5) If parts of the site are to be damaged, reassessment and mitigation through excavation should occur.

6) The west and east deflation bowls should be reseeded with grasses to help mitigate against further wind erosion (see Figure 3.15).

3.4.3.2 Management recommendations for future development

1) We do not recommend use of the immediate DRO site area for observation posts or any other activity that will result in ground disturbing activities, in order to preserve the site.

2) If military use of the area is required, we recommend minimizing destruction of the site by restricting ground disturbance and traffic to areas outside those with intact cultural materials (see Figure 3.15).

3.4.3.3 Management recommendations for future research

Because of the unique nature of the deposits, excellent faunal preservation, and unprecedented repeated use of the site since the end of the glacial era, we recommend that research continues at DRO.

1) We recommend future collaborations with University of Alaska Fairbanks with support of grant opportunities, access for archaeological field schools, and encouragement of student research.

2) We would encourage using DRO as an example of excellent cultural resource stewardships through presentations to soldiers, the community, and in academic venues.

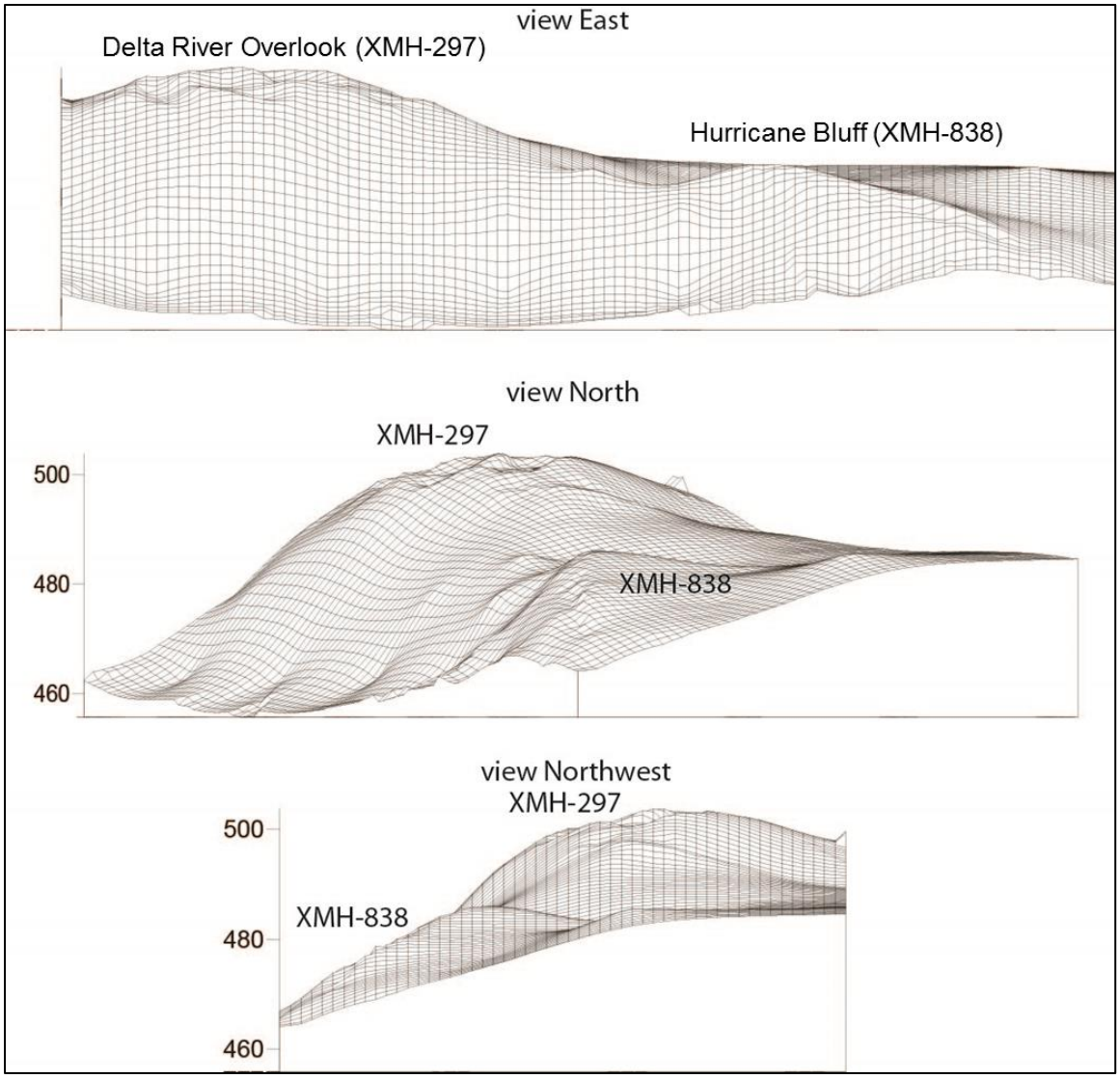

Figure 3.10 High resolution topographic mapping of Delta River Overlook and Hurricane Bluff.

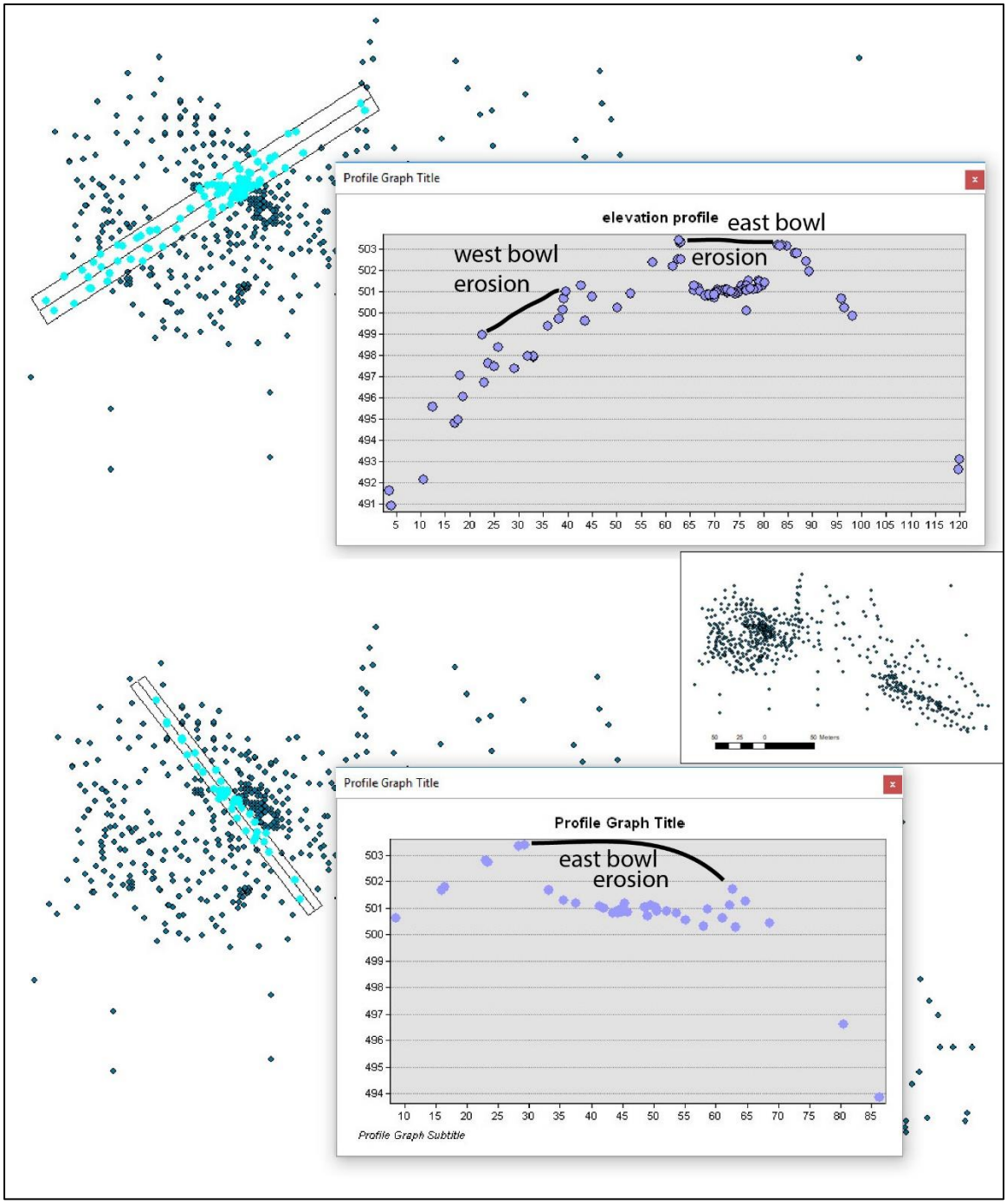

Figure 3.11 Delta River Overlook topographic points and elevation profiles. Top: southwest-northeast transect showing erosional areas. Bottom: southeast to northwest transect showing erosional areas (inset, scalebar).

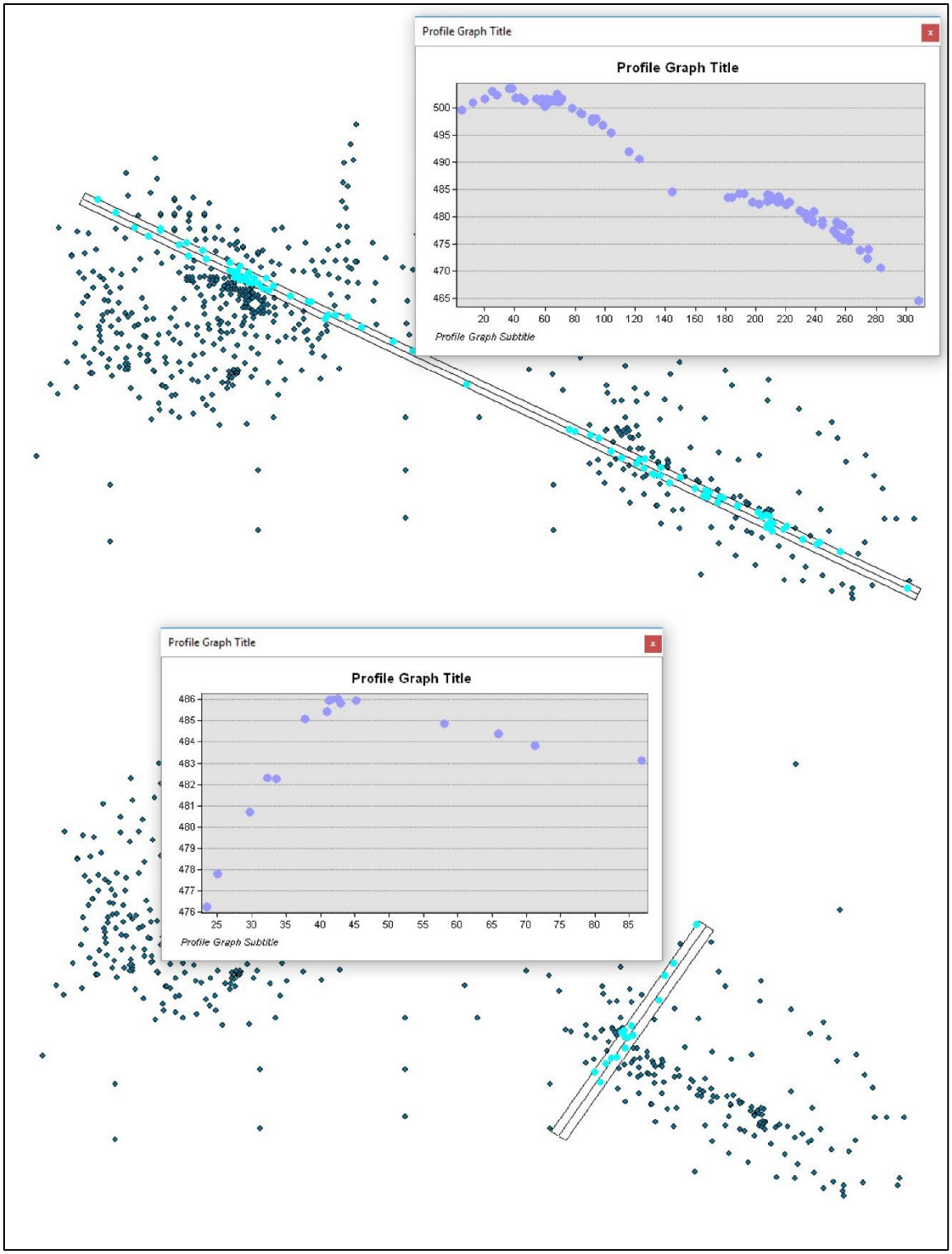

Figure 3.12 Topographic points and elevation profiles. Top: northwest to southeast transect through Delta River Overlook and Hurricane Bluff. Bottom: northeast to southwest transect through Hurricane Bluff.

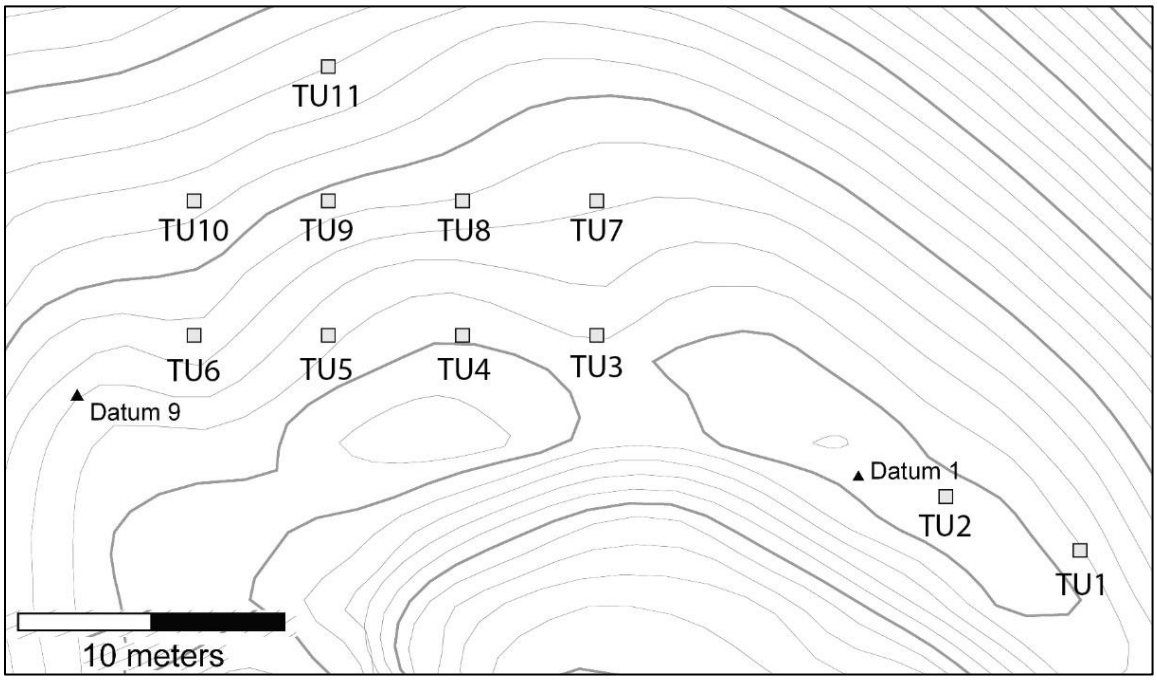

Figure 3.13 Test Unit (TU) locations. TU1 and TU2 were positive for cultural materials.

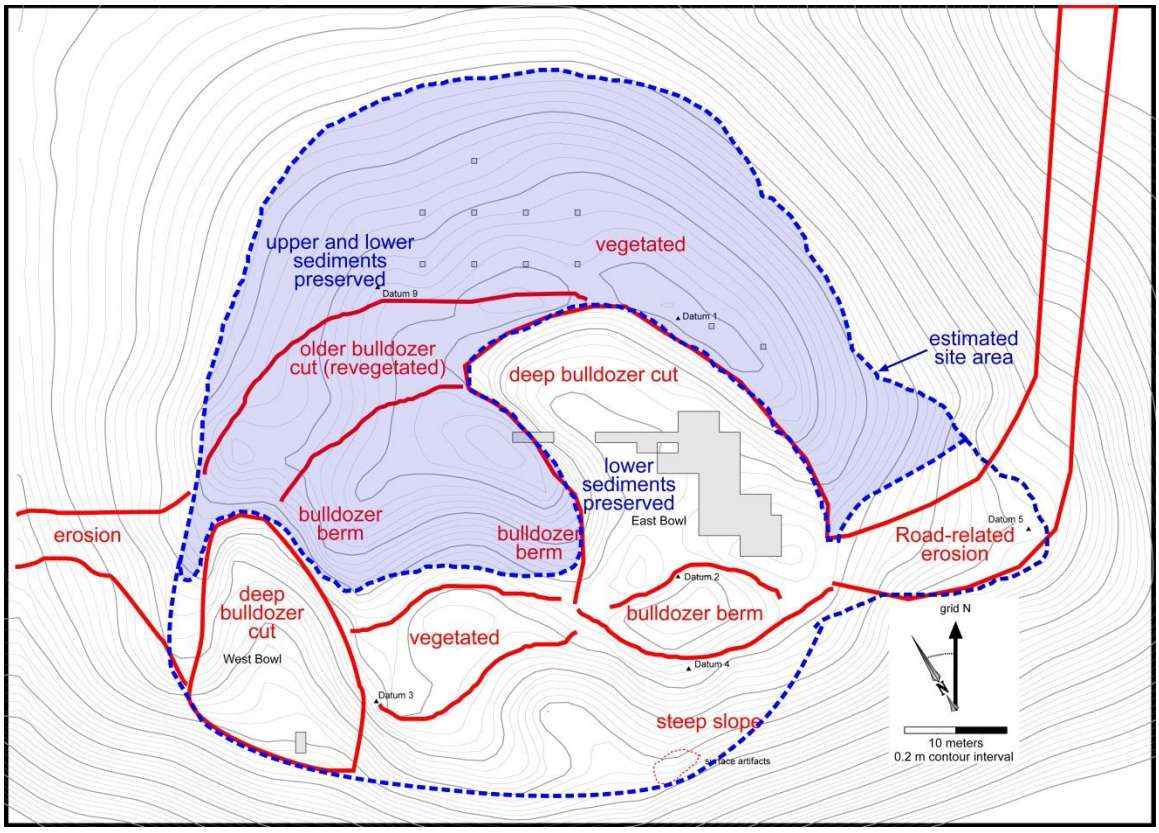

Figure 3.14 Delta River Overlook site extent and disturbance

Figure 3.15 GIS map of Delta River Overlook (XMH-297) and Hurricane Bluff (XMH-838) sites and environs. Yellow fonts indicate erosion, red and purple polygons indicate estimated site limits.

CHAPTER 4. SITE CHRONOLOGY

Ben A. Potter and Joshua D. Reuther

4.1 Introduction and Methods

This chapter describes the results of chronometric and relative dating strategies with respect to site chronology, activity area contemporaneity and site occupations. Along with an extensive radiocarbon dating program, other spatial and stratigraphic data are used to provide a sound base for spatial analyses (Chapter 12). Prior to this research, none of the cultural components were directly dated, and only some of the components had relative (bracketing) ages. The general stratigraphic sequence was outlined by earlier researchers (Bacon and Holmes 1980, Leehan 1981); however, ambiguities in associations of dates and strata remained from this work.

The primary objectives of establishing a site chronology and assessing occupation history (activity areas within components) require secure dating, particularly given the complex stratigraphic record at DRO. A limited number of stratigraphic dates (n=5) were available from Bacon and Holmes (1980), but these are early radiometric dates with large standard deviations (generally over 200 years). In the 2015-2017 project, we provided 13 additional C14 dates from DRO. Two dates were previously reported from XMH-838 (Potter et al. 2007), and we provided 9 additional C14 dates; these and all of the Hurricane Bluff radiocarbon ages are Accelerator Mass Spectrometry (AMS) assays. Through stratigraphic correlation between the two sites we have added 22 additional C14 dates to develop a secure site chronology. This record extends for the entire duration of sedimentation at the site, from the earliest paleosol (P0a) at ~13,000 cal yr BP to the most recent paleosol (P9) at 400 cal yr BP.

Our collection protocols included the strictest of provenience controls, focus on structurally well-preserved charcoal that could be identified to taxon, and focus on cultural features or stratigraphic samples that are clearly connected throughout the sites. Field treatment of the samples were similar – they were photographed *in situ* and collected with clean trowel and placed in archival 4 mil plastic bags within aluminum foil. Large, single fragments were preferred. We used AMS dating from two labs (Beta Analytic, U Georgia) to mitigate laboratory error. Calibrations were calculated in Calib 7 program using the Intcal13 calibration curve (Reimer et al. 2013). All charcoal identifications were made by Owen Davis, at the University of Arizona, except two samples that were identified by Marine Vanlandeghem, of the Université Paris 1 Panthéon Sorbonne.

4.2 Results

All radiocarbon assays for DRO and Hurricane Bluff are listed in Tables 4.1 and 4.2, respectively. Prior to this research, six stratigraphic dates and one cultural date were obtained from both sites. We produced an additional 22 dates, including seven from cultural features, one from C2a, one from C2b, two from C2c, one from C6, and one from C8b.

All of the new dates were in the predicted ranges given the earlier dating, and no obvious contamination is apparent in their distribution. All dates are stratigraphically consistent with each other and previous dates. All dates from XMH-838 are internally and stratigraphically consistent with no reversals, and all dates (except one) from DRO are internally and stratigraphically consistent with no reversals (except Gx-6752, see below). Table 4.3 shows correlations in ages and stratigraphy between DRO and Hurricane Bluff. We discuss results in terms of overall site chronology and occupation history.

4.2.1 Site Chronology

A generalized stratigraphy at DRO is shown in Figure 4.1, utilizing the north wall of Block 12, which captures almost all of the stratigraphic units, except the upper sands which are eroded from most of the excavation areas. Hurricane Bluff stratigraphy is shown in Figure 4.2. Figures 4.3 and 4.4 illustrate all calibrated ages from DRO and Hurricane Bluff (respectively) radiocarbon samples ordered by depth below surface. Figure 4.5 illustrates all calibrated ages from DRO and Hurricane Bluff, enhancing the precision of the site chronology presented below. Figure 4.6 illustrates all calibrated ages from both sites from this project (thus removing the early standard radiometric dates with high standard deviations).

The lowest sediments at DRO remain undated. No charcoal, wood, or bone samples were present within the glacial deposits (till and outwash) (Unit 1) or with the lowest aeolian sand layers (Unit 2).

Unit 3 is the loess that dominates the cultural occupations at the site. This loess contains numerous paleosols and paleosol complexes, labeled P0 through P8 and sometimes further subdivided (e.g., P0a, P6b). These will be discussed separately.

Loess 1 denotes the sediments between the lower sands (Unit 2) and Paleosol 1. It is generally 35-50 cm thick, and contains Pedocomplex 0. Pedocomplex 0 comprises a series of two thin generally discontinuous Ab horizons (10 YR 5/4 to 10 YR 3/3). P0a comprises two thicker paleosols within an 8 cm thick vertical span. The lower paleosol (P0a1) is about 1.5 cm thick, and the upper paleosol P0a2 (10 YR 3/3) is 0.7 cm thick, and is associated with the lowest cultural component, C1. A single date on charcoal from within this paleosol dates the soil and cultural occupation to 10,990±50 BP (Beta-422155, 12,995-12,729 cal yr BP, *Betula* sp.).

P0b complex, within Loess 1 contains at least four discontinuous thin Ab horizons (10 YR 5/4 to 10 YR 3/3) within a 12 cm vertical span that are stratigraphically associated with cultural components C2a and C2b. Two radiocarbon dates are associated with P0b, but are not directly taken from paleosol charcoal, but rather from cultural features that appear to anthropogenically enhance these sediments. The lowest is Beta-422157 (10,000±40 BP, 11,700-11,274 cal yr BP, *Alnus* sp.) taken at about 27 cm below P1, and directly associated with hearth feature F2015-8 (Component 2a). The second date is Beta-422156 (10,060±40 BP, 11,803-11,355 cal yr BP, *Betula* sp.) taken at 17 cm below P1, and directly associated with hearth feature F2015-7 (Component 2b). Given the overlap in ages, this indicates the P0b paleosols were forming during the latter half of the Younger Dryas.

The uppermost dates within Loess 1 are not directly associated with paleosols, but derive from two cultural hearths, F2015-9 and F2015-5, both associated with Component 2c. They overlap at one standard deviation and suggest contemporaneity for C2c across the site. Both of the dates were on *Betula* sp. charcoal. F2015-9 is dated to 9470±30 BP (Beta-422154, 11,047-10,588 cal yr BP) and F2015-5 is dated to 9510±30 BP (Beta-422158, 11,069-10,685 cal yr BP. Both of these features are about 5 cm below P1. Overall, the Loess 1 was deposited over the course of at least 4,000 calendar years.

Pedocomplex 1 complex is around 9 cm thick, and comprised of a 5 cm thick reddened, organic rich Bwb horizon (7.5 YR 4/3 to 7.5 YR 3/2) and four thin Ab horizons. Two dates were obtained by Holmes (Bacon and Holmes 1980) at the lower and upper parts of P1. The lower date was 8555±380 BP (Gx-5998, 10,512-8591 cal yr BP) and the upper date was 7190±200 BP (Gx-6751, 8387-7661 cal yr BP). Two dates from Hurricane Bluff on this paleosol complex provided a tighter window, at 8590±30 BP (Beta-420651, 9602-9505 cal yr BP) and 8810±60 BP (Beta-123339, 10,157-9632 cal yr BP). These latter two dates more accurately constrain Component 3, which was found within P1.

The remaining numbered Loess deposits (L2 through L8) relate to stratigraphic markers, loess deposition episodes, contrasting with the soil formation episodes, denoted by Pedocomplex/Paleosol numbers.

Loess 2 is situated between Pedocomplexes 1 and Tephra 1a. A single date was obtained from Loess 2 from a *Picea* sp. charcoal (the earliest spruce at the site), at 7 cm above P1 and 4 cm below Tephra 1a, Beta-447773 (7630±30 BP, 8512-8379 cal yr BP). This stratigraphically dates Component 4, which is associated with Loess 2. Tephra 1a is undated, but is bracketed between 7630±30 BP and 6675±175 BP; however, the timing is similar to the deposition of the Oshetna tephra in the Susitna River Valley between 7930-6570 cal yr BP (Mulliken 2016). Unfortunately, due to the limited extent, we were unable to conduct geochemical analysis on this tephra to correlate it with other distal and proximal ash beds and any relationship to distal tephras, such as the Oshetna, remain uncertain (see Chapter 5).

Pedocomplex 2 comprises two distinct Bwb and ABwb horizons, both reddish brown (7.5 YR 4/2) in Loess 3. Total thickness is around 8 to 9 cm thick, though this varies across the site. The upper Bwb horizon is ~3 cm thick and the lower ABwb is about 4 cm thick with a 2-3 cm thick C horizon between. A single date on this horizon at DRO dates to 6675±175 BP (Gx-6749, 7924-7255 cal yr BP). At Hurricane Bluff, two paleosols correlating to P2 date to 6990+/30 BP (Beta-389635, 7930-7736 cal yr BP) for the lower and 6230+30 BP (Beta-396693, 7251-7019 cal yr BP) for the upper. These three assays stratigraphically dates Component 5, which is associated with Loess 2.

Loess 3, between Tephra 1a and P3, remains undated. Pedocomplex 3 complex comprises four very thin Ab horizons (10 YR 4/2) over a vertical span of 6 cm. One date was obtained from a cultural hearth feature directly associated with P3, 50-55 cm below surface in Blocks 20-21. This hearth, F2017-2, associated with Component 6, dates to 5980±30 BP (UGAMS-34297, 6894-6737 cal yr BP).

Pedocomplex 4 complex comprises four paleosols, an uppermost dark Ab with some Bwb characteristics (7.5 YR 4/2) and lower three ABwb horizons, totaling 7 cm thickness. No cultural materials are associated with P4. A single assay on charcoal in P4 dates to 3980±150 BP (Gx-6752, 4840-3997 cal yr BP). This date appears to be the only

outlier, and appears to be slightly too young for its stratigraphic position. Three older ages are associated with upper strata, P5 and P6a (5029-4299 cal yr BP, see below).

Pedocomplex 5 complex is comprised of three discontinuous horizons, a lower 2 cm thick Ab horizon underlying a 4 cm thick ABwb horizon (7.5 YR 3/2) underlying a 1 cm thick Ab horizon, with a total vertical span of 7 cm. In some areas, the only one of the Ab horizons is present. A single assay is directly associated with P5 at DRO, Beta-447774 (4350±30 BP, 5029-4850 cal yr BP). No cultural materials are associated with P5. At Hurricane Bluff, another date of 3980±30 BP (Beta-38634, 4526-4406 cal yr BP), which does not overlap at two standard deviations with the Beta-447774 date. It is possible these ages represent the two Ab horizons in Paleosol 5.

Paleosol 6a is comprised of an Ab horizon that overlies an ABwb horizon (7.5 YR 4/4), both about 2 cm thick separated by a 1 cm thick C horizon, with a total vertical span of 5 cm. Two assays are directly associated with P6a and both overlap at one standard deviation. The dates are Beta-447775 (4010±30 BP, 4565-4418 cal yr BP) and Beta-447778 (3970±30 BP, 4523-4299 cal yr BP). These two assays stratigraphically date Component 7a, which is associated with P6a.

Paleosol 6b is comprised of two Ab horizons, the lower one is 1 cm thick and the upper one is 1.5 cm thick (both 7.5 YR 3/2), separated by a 1.5 cm thick C horizon, with a total vertical span of 4 cm. It remains undated but is bracketed between 3970±30 BP and 3220±125 BP assays. Component 7b is associated with P6b. At Hurricane Bluff, a single assay on P6 (undifferentiated) dates to 3670±30 BP (Beta-386246, 4087-3907 cal yr BP). Given this age, it may relate to either P6a or P6b.

Tephra 2 (upper tephra) is situated between P6b and P7a. Microprobe analyses (Chapter 5) shows significant correlations of this tephra to the Watana tephras in the Susitna River Valley (Dixon and Smith 1990; Mulliken 2016), and a weaker correlation to Tephra D of Unit III at the proximal Hayes Volcano tephra sets described by Wallace et al. (2014). The timing of the DRO Tephra 2 fall is similar to that of the middle Holocene aged Hayes Volcano proximal tephra sets, and more distally correlated ash deposits such as the Watana tephras, Jarvis Creek Ash and Cantwell Ash (Riehle et al. 1990; Beget et al. 1991; Wallace et al. 2014; Mulliken 2016). Beget et al. (1991) provide estimated age of deposition of the Jarvis Creek and Cantwell Ashes and the Hayes Volcano sets at 3660±125 BP (4404-3647 cal yr BP); Mulliken (2016) quotes a similar timing for deposition of the Watana tephras between 4400-3360 cal yr BP.

Paleosol 7a lies directly above Tephra 2, and is comprised of two Ab horizons, the lower one 0.8 cm thick and the upper one 1.5 cm thick, separated by a 1 cm thick C horizon, with a total vertical span of 3 cm. One assay is directly associated with P7a, Beta-447776 (3330±30 BP, 3637-3477 cal yr BP). This assay stratigraphically dates Component 8a, which is associated with P7a.

Paleosol 7b is comprised of a thin Ab horizon (1 cm thick) that overlies a thicker ABwb horizon (7.5 YR 3/3), about 2 cm thick. One assay is directly associated with P7b, Beta-447777 (2870±30 BP, 3136-2879 cal yr BP). No cultural materials appear associated with P7b. A single assay from Hurricane Bluff is correlated with P7 (undifferentiated) was obtained, Beta-386245 (3210±30 BP, 3543-3368 cal yr BP).

Loess 6 is situated between P7b and the upper sands, and contains a discontinuous Paleosol 8, a Bwb horizon about 3 cm thick (10 YR 3/4). Two cultural features were dated, and both overlap at two standard deviations. One hearth feature was dated to

2280+/145 BP (Gx-6750, 2724-1952 cal yr BP), and the other hearth feature (F2017-1) dated to 2210±20 BP (UGAMS-34298, 2310-2153 cal yr BP). Both features are associated with Component 8b.

Strata above Loess 6 are truncated at the excavation area at DRO, but are present at Hurricane Bluff. Two paleosols were dated at Hurricane Bluff that are difficult to correlate with DRO, but appear to be younger than P8, which should date to between 2870±30 BP and 2280±145 BP. Two dates at Hurricane Bluff are from the same paleosol, dating to 1780±40 BP (Beta-123338, 1819-1574 cal yr BP) and 1800±30 BP (Beta-386244, 1894-1548 cal yr BP), which overlap at two standard deviations. We have tentatively identified this paleosol at Hurricane Bluff as P8, but could relate to a number of unnamed paleosols above P7b and below the upper sands at DRO. A higher paleosol, labeled P9 at Hurricane Bluff was dated with a single assay (Beta-386243, 340±30 BP, 480-311 cal yr BP).

Table 4.1. XMH-297 radiocarbon results.

Lab#	*Material*	*Stratum*	*$\delta^{13}C/^{12}C$*	*RCYBP*	*Cal yr BP (2σ)*	*Comp.*
Beta-422155	charcoal (*Betula* sp.)	L1	N/A.	10,990±50	12995-12729	C1
Beta-422157	hearth charcoal (*Alnus* sp.)	L1	-24.8	10,000±40	11700-11274	C2a
Beta-422156	hearth charcoal (*Betula* sp.)	L1	-25.6	10,060±40	11803-11355	C2b
Beta-422154	hearth charcoal (*Betula* sp.)	L1	-26.3	9470±30	11057-10588	C2c
Beta-422158	hearth charcoal (*Betula* sp.)	L1	-25	9510±30	11069-10685	C2c
Gx-5998	charcoal	P1 (bot.)	NR	8555±380	10512-8591	C3
Gx-6751	charcoal	P1 (top)	NR	7190±200	8387-7661	C3
Beta-447773	charcoal (*Picea* sp.)	L2	-23.8	7630±30	8512-8379	C4
Gx-6749	charcoal	P2	NR	6675±175	7924-7255	C5
UGAMS-34297	hearth charcoal (*Picea* sp.) (F2017-2)	P3	-25.4	5980±30	6894-6737	C6
Gx-6752	charcoal	P4	NR	3980±150	4840-3997	
Beta-447774	charcoal (*Betula* sp.)	P5	-24	4350±30	5029-4850	
Beta-447775	charcoal (unid.)	P6a	-23.5	4010±30	4565-4418	C7a
Beta-447778	charcoal (*Picea* sp.)	P6a	-24.2	3970±30	4523-4299	C7a
Beta-447776	charcoal (*Picea* sp.)	P7a	-23	3330±30	3637-3477	C8a
Beta-447777	charcoal (*Picea* sp.)	P7b	-24.4	2870±30	3136-2879	
Gx-6750	hearth charcoal	L6	NR	2280±145	2724-1952	C8b
UGAMS-34298	hearth charcoal (*Picea* sp.) (F2017-1)	L6	-24.5	2210±20	2310-2153	C8b

Table 4.2. XMH-838 radiocarbon results.

Lab#	*Material*	*Stratum*	*$\delta^{13}C/^{12}C$*	*RCYBP*	*Cal yr BP (2σ)*	*Comp.*
Beta-386243	charcoal	P9	-24	340±30	480-311	C2
Beta-123338	charcoal	P8	-23.3	1780±40	1819-1574	C1
Beta-386244	charcoal	P8	-26.4	1800±30	1894-1548	C1
Beta-386245	charcoal	P7	-24.4	3210±30	3543-3368	
Beta-386246	charcoal	P6	-24.2	3670±30	4087-3907	
Beta-389634	charcoal	P5	-24.1	3980±30	4526-4406	
UGAMS-22799	gastropod shell	Unit 2 above T1	-9	6040±25	6950-6797	
Beta-396693	charcoal	P2	-23.2	6230±30	7251-7019	
Beta-389635	charcoal	P2	-24.3	6990±30	7930-7736	
Beta-420651	charcoal	P1	-24.8	8590±30	9602-9505	
Beta-123339	charcoal	P1	-25.3	8810±60	10157-9632	

Table 4.3 Stratigraphic and chronological correlations between XMH-297 and XMH-838 (uncalibrated yr BP).

Strata	*XMH-297*	*XMH-838*	*Components*
P0a	10,990		C1
P0b			
L1	10,000 10,060 9500 9470		C2a C2b C2c
P1	8560 7190	8810 8590	C3
L2	7630		C4
T1			
P2	6680	6990 6230	C5
L3		6040	
P3	5980		C6a
L4			
P4			C6b
L4			
P5	4350	3980	
L5			
P6a	4010 3980 3970	3670 3210	C7a
P6b			C7b
T2	3660		
P7a	3330	3210	C8a
P7b	2870		
P8/L6	2280 2210	1800 1750	C8b
P10		340	

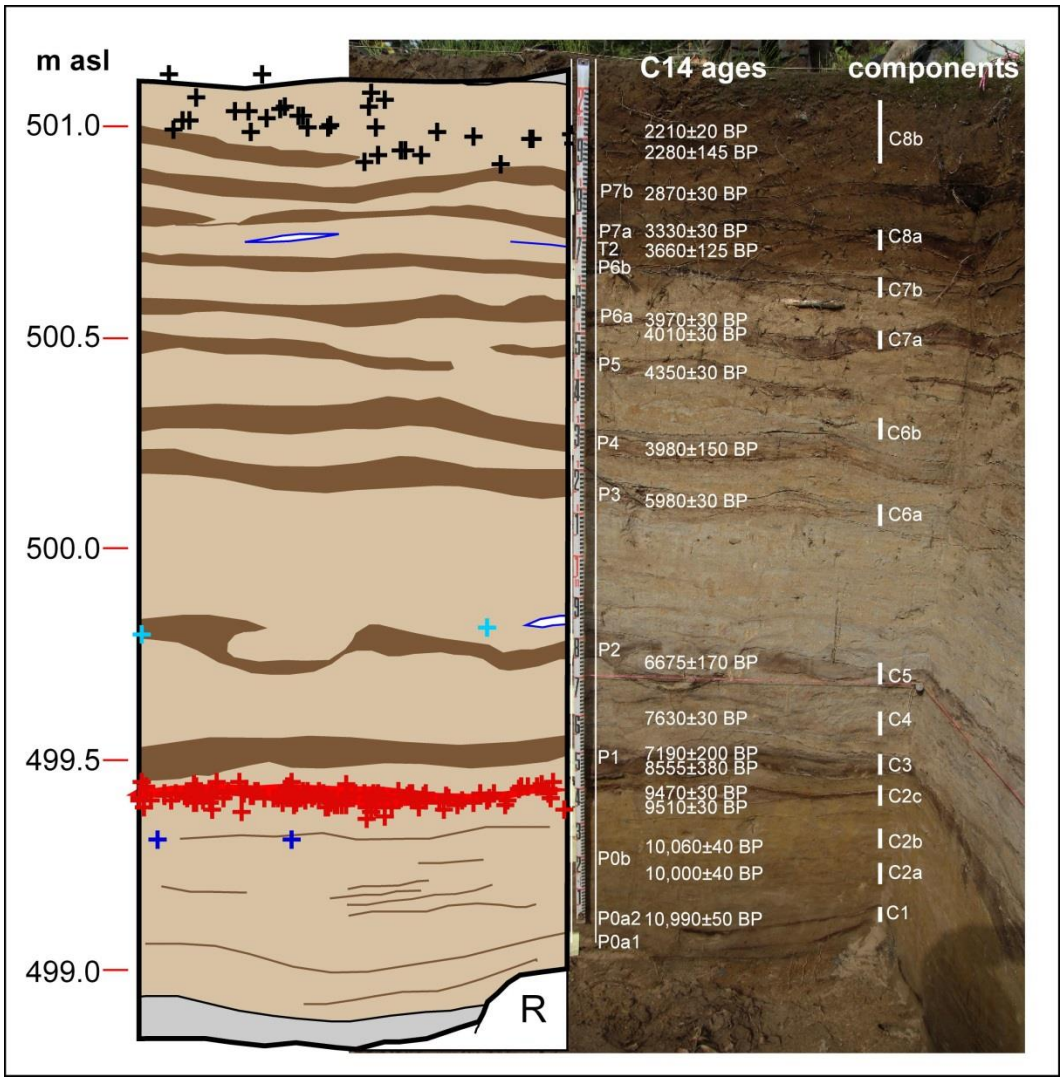

Figure 4.1. DRO stratigraphy and radiocarbon dates (Block 12 North Wall)

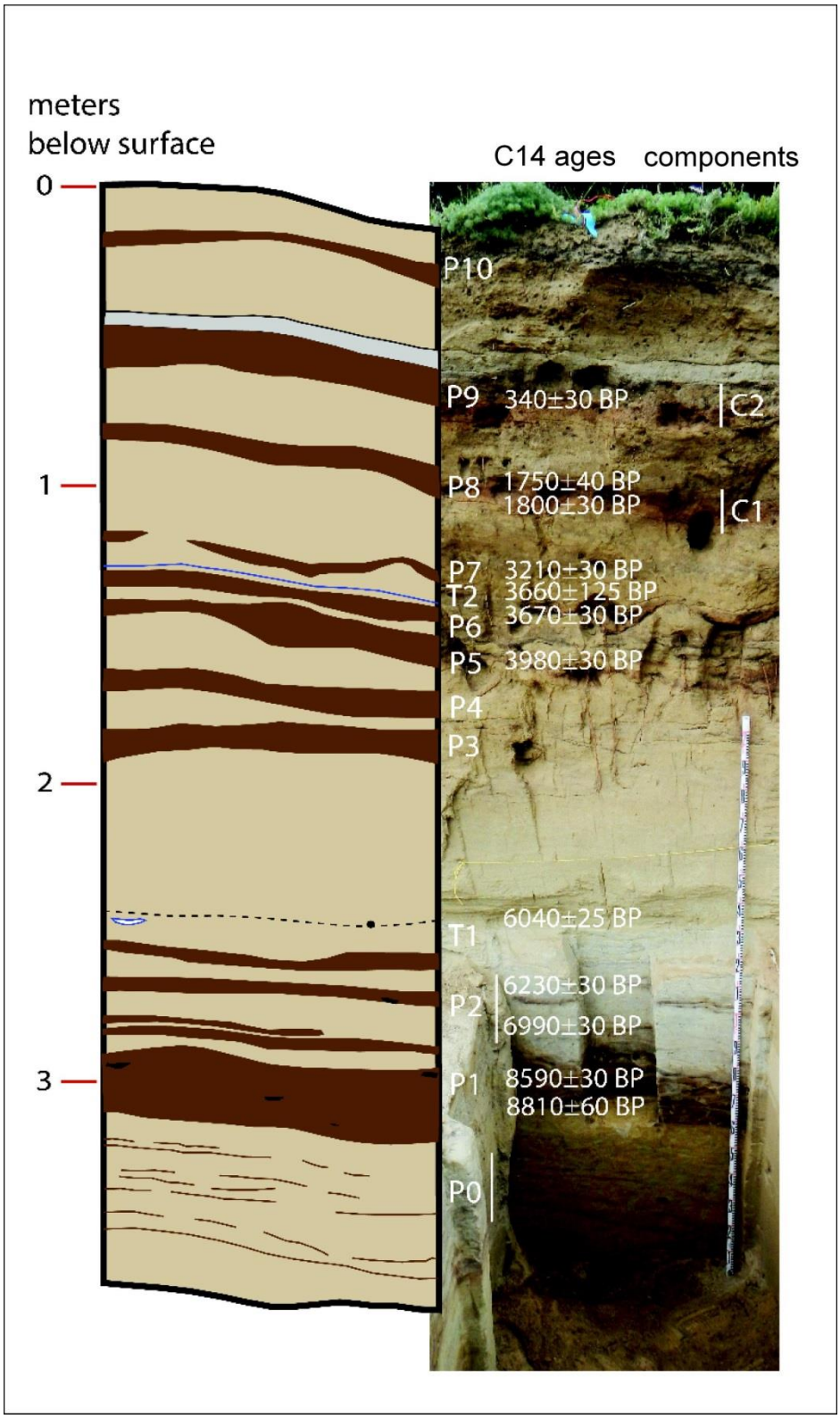

Figure 4.2. XMH-838 stratigraphy and radiocarbon dates

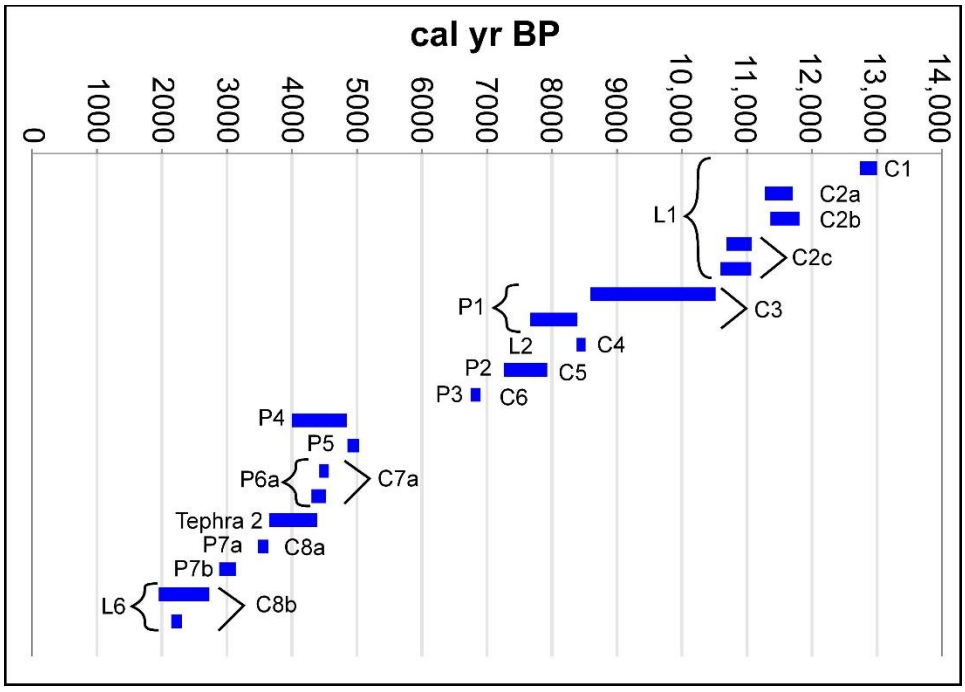

Figure 4.3. Delta River Overlook calibrated radiocarbon dates by depth (2 standard deviations). Strata denoted to the left of dates and associated cultural components denoted to the right of dates.

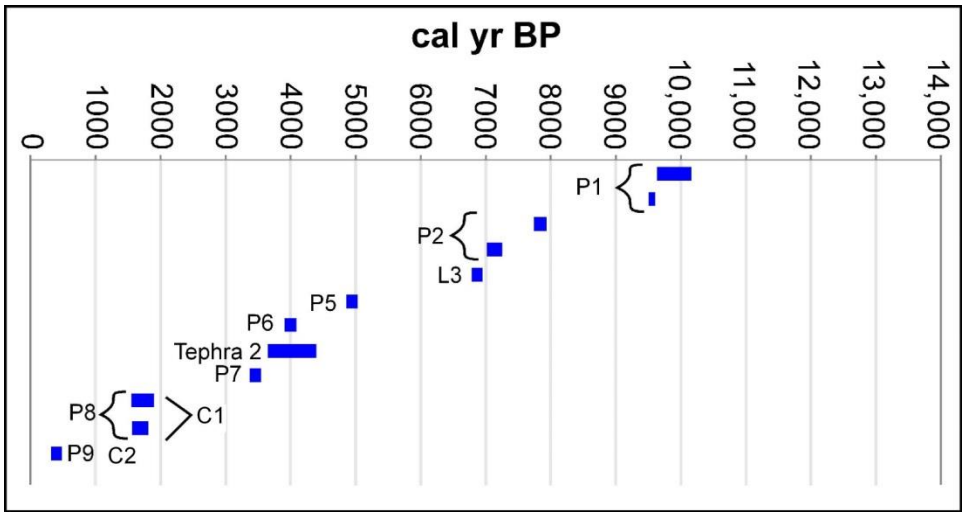

Figure 4.4. Hurricane Bluff calibrated radiocarbon dates by depth (2 standard deviations). Strata denoted to the left of dates and associated cultural components denoted to the right of dates.

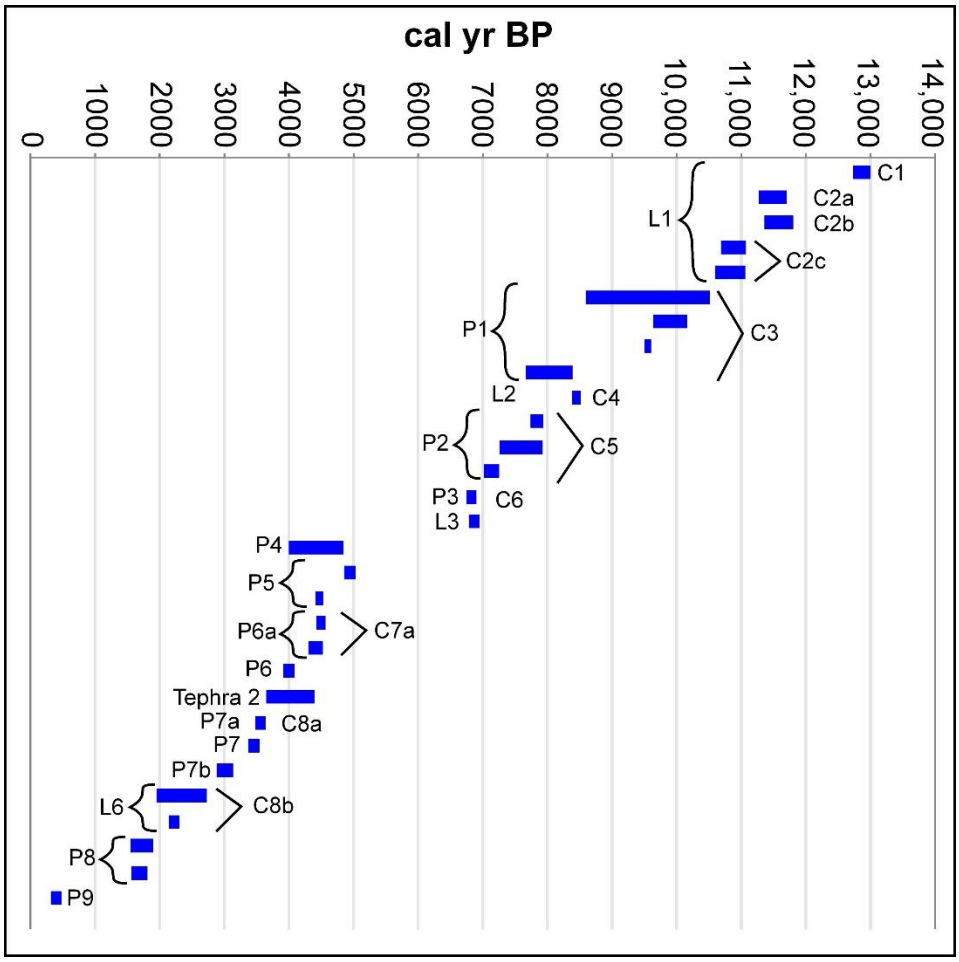

Figure 4.5. All radiocarbon dates from Delta River Overlook and Hurricane Bluff, ordered by depth below surface and associated strata.

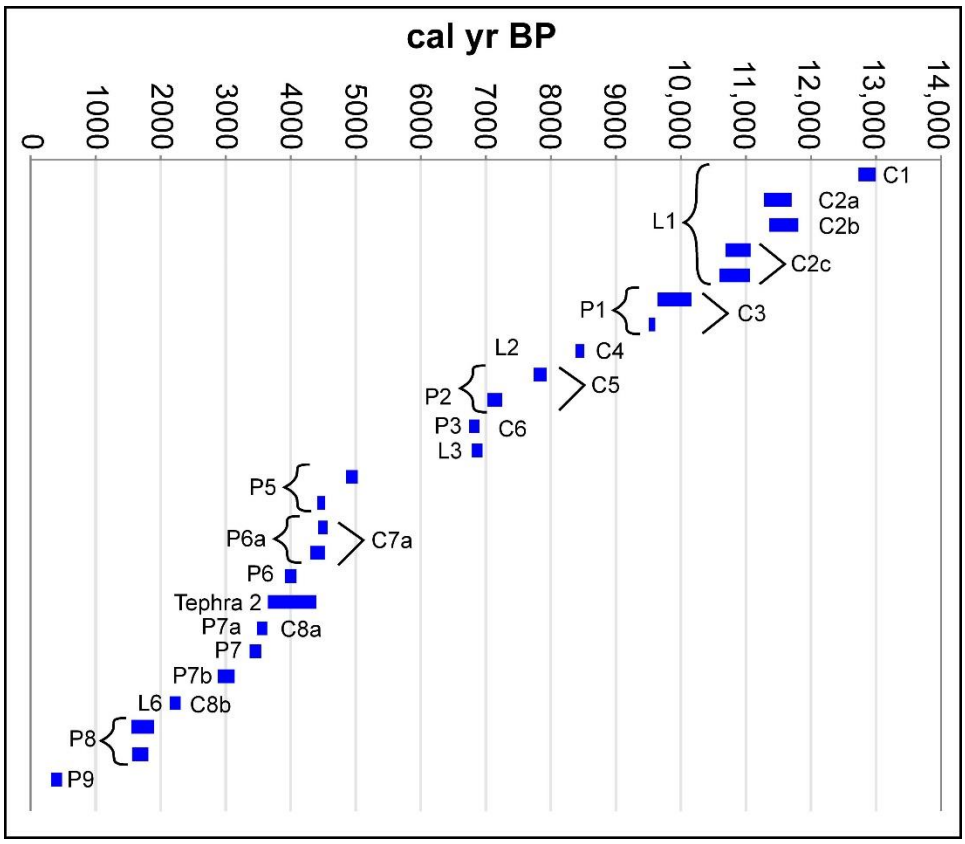

Figure 4.6. All radiocarbon dates from this project from Delta River Overlook and Hurricane Bluff, ordered by depth below surface and associated strata.

4.2.2 Occupation History

Chronological resolution at DRO is very fine, similar to the high resolution record at Gerstle River (Potter 2005, Potter and Reuther 2012). Table 4.4 shows the ages associated with each cultural component at DRO. Twelve cultural components were identified at DRO, and all have associated or estimated absolute ages. Of the twelve, five are directly dated through hearth features and six are dated through directly associated stratigraphic ages. One component (C7b) has age estimates based on bracketing ages that tightly constrain its age. The internal coherence and stratigraphic relationships are robust and very clear, allowing for each age estimate to be supported by multiple ages of underlying and overlying strata.

Multiple age estimates are available for four components: C2c, C3, C7a, and C8b. Tests of contemporaneity follow Ward and Wilson 1978 (see also Shott 1992). Component 2c contains two hearths that are potentially contemporaneous (overlap at 2 standard deviations). The average of these two hearths is 9490±21 BP (11,060-10,670 cal yr BP). Component 3 is associated with Paleosol 1 which has two age estimates that are not potentially contemporaneous (10,157-9632 and 9602-9505 cal yr BP). Since we cannot assign them to one or the other ages, we estimate the age as the average of these two dates, yielding an estimate of 8634±27 BP (9662-9536 cal yr BP), consistent with Hurricane Bluff age estimates of Paleosol 1. Component 7a is associated with Paleosol

6a, which has two age estimates that are potentially contemporaneous. The average of these two dates is 3990±21 BP (4519-4418 cal yr BP). Component 8b contains two hearths that are potentially contemporaneous. The average of these two hearths is 2211±20 BP (2311-2153 cal yr BP).

Table 4.4. Cultural component ages at DRO.

Component	*Stratum*	*Type*	*Age (RC yr BP)*	*Cal yr BP*
C1	L1	Stratigraphic	10,990±50	12995-12729
C2a	L1	Hearth Feature F2015-8	10,000±40	11700-11274
C2b	L1	Hearth Feature F2015-7	10,060±40	11803-11355
C2c	L1	Average (2 hearth dates)	9490±21	11060-10670
C3	P1	Average (2 stratigraphic dates)	8634±27	9662-9536
C4	L2	Stratigraphic date	7630±30	8512-8379
C5	P2	Stratigraphic date	6675±175	7924-7255
C6	P3	Hearth Feature F2017-2	5980±30	6894-6737
C7a	P6a	Average (2 stratigraphic dates)	3990±21	4519-4418
C7b	P6b	No direct dates	~3770	~4100
C8a	P7a	Stratigraphic date	3330±30	3637-3477
C8b	L6/P8	Average (2 hearth dates)	2211±20	2311-2153

4.2.3 Charcoal macrofossils

A total of 12 charcoal samples were identified to taxon at both DRO and Hurricane Bluff (Figure 4.7). A clear pattern emerges that may be proxies for overall environment, both in terms of forest taxa incorporated as charcoal into paleosols and taxa selected for burning in hearths. Birch dominates the cultural record prior to ~7600 BP (Loess 2), after which time spruce dominates the record until the late Holocene. Alder appears once in the early Holocene and a later occurrence of birch is evident at 4350 BP (Paleosol 5).

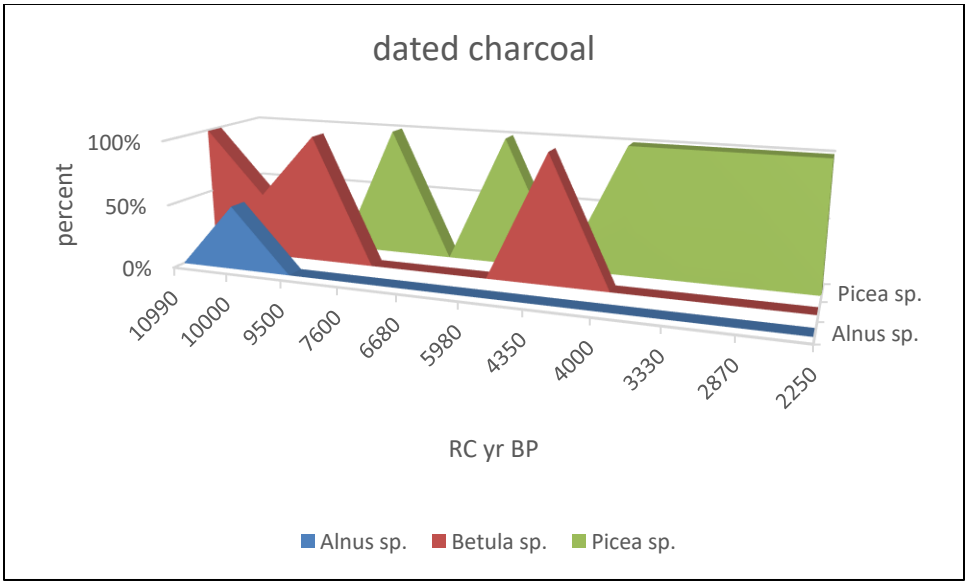

Figure 4.7 Dated hearth charcoal (n=12).

CHAPTER 5. GEOARCHAEOLOGY – DELTA RIVER OVERLOOK AND HURRICANE BLUFF SITES

Joshua D. Reuther, Ben A. Potter, Katherine M. Mulliken, Julie A. Esdale, and Jennifer R. Kielhofer

5.1 Introduction and Methods

This section provides a detailed description of the stratigraphy for Delta River Overlook and Hurricane Bluff sites. As mention above, the two sites are situated on a terrace that overlooks the Delta River. The terraced landform was created from glacial outwash and covered by a 3-6 m thick blanket of windblown (aeolian) sand and silt (loess) deposits. We report on the sedimentological and geochemical results on sediments and soils from both sites. Our results are integrated with Bacon and Holmes' (1980) and Leehan's (1981) previous stratigraphic and sedimentological analyses at the Delta River Overlook site, as well as the stratigraphic work of Higgs et al. 1999, also presented in Potter et al. 2007) at the Hurricane Bluff site.

5.1.1 Field Methods

The lithostratigraphy and pedostratigraphy (sediment and soil stratigraphy, respectively) were described across several columns at the excavation of the DRO site. A total of 96 m of columns were profiled at the DRO excavation. The stratigraphy for Block's A and B from the original excavations by Bacon and Holmes (1980) were redescribed and profiled for this project. We described a profile along the erosional cut at the Hurricane Bluff site within 4 m of the trench described by Higgs et al. (1999). These observations allow for potential stratigraphic correlations across a site area and between sites, to place an archaeological component in a stratigraphic context, and to understand periods of aeolian aggradation and erosion and landform stability across the terrace that both sites are situated on. Soil and lithological descriptions follow national conventions (USDA 1993) with modifications suggested by Holliday (2004). The soil subsurface horizon designations follow USDA (1993) and NRCS (2010; see also Soil Survey Staff 2015) conventions.

Sediment sampling was conducted at both sites to recover geochronological, paleoecological, and sedimentological samples. Samples were taken from Block's A and B of the Delta River Overlook site, and from the described column at erosional bluff edge of Hurricane Bluff site. Several types of samples were taken for sedimentological analyses. Larger bulk samples consisting of 0.5 to 1 quart of loose sediment were taken from distinct lithological units and soil horizons and complexes within a stratigraphic column. Smaller samples were taken continuously from a vertical transect of a column with 8 cc (2 x 2 x 2 cm) plastic boxes.

Munsell coloration of sediments and soils were taken in the field in dry to moist conditions, and in the laboratory in dry and wet conditions.

5.1.2 Laboratory Methods

Sedimentological and soil analytical techniques were used to supplement and complement field stratigraphic observations to understand changes in the composition of sand, silt and clay and the development of soils at stratigraphic sections in study areas (Holliday 2004, Muhs et al. 2000). The DRO site Block B sediment samples were the only samples analyzed because it provided the best overall representation of the site's litho- and pedostratigraphy. Particle size analysis (PSA) was used here to assess changes in the percentages of sand, silt, and clay throughout selected stratigraphic sections to compare across sections at the DRO and Hurricane Bluff sites. The percentages of sand, silt and clay were used to define the texture (e.g., silt, silt loam, loam) of the sediments and soils based on USDA (1993) and NRCS (2002) conventions.

Potential differences in particle sizes within a stratigraphic section or across sections also helped to correlate between stratigraphic sequences, and yield information on shifts in the type and energy of agents that created a deposit, post-depositional disturbances, and the environment of deposition.

Organic and inorganic carbon contents (%OC and %$CaCO_3$, respectively) were measured using the loss-on-ignition (LOI) and gasometric (chittick apparatus) techniques. Carbon and PSA clay content were used to help classify different soil types, identify weakly developed soils (entisols) that may otherwise remain unidentified solely through field observations, and assess taphonomic factors in the chemistry of deposits that may promote or inhibit the preservation of archaeological organic materials (e.g., osseous and plant materials).

Tephra samples were collected at both sites to geochemically and petrographically characterize them in order to: (1) compare between ash beds to correlate between sites; and (2) compare to data on reference tephra samples from proximal settings at source volcanoes, including the Hayes Volcano (Wallace et al. 2014), and regional distal tephra deposits, in particular those from the middle Susitna River valley (mSRV; Devil, Watana, and Oshetna tephras; Dilley 1988, Dixon and Smith 1990, Mulliken 2016), just to the south of the DRO and Hurricane Bluff sites.

Radiocarbon dating on charcoal and terrestrial shell carbonate were used as estimates to establish periods of landform stabilization and soil formation and episodes of aeolian deposition or deflation. Details specific to individual radiocarbon dates and the method used to calibrate them are outlined in Chapter 4 on site chronology.

5.1.2.1 Particle Size Analysis (PSA)

As noted above, bulk sediment samples for PSA were collected from lithostratigraphic units and distinct soil horizons throughout the stratigraphic columns at the DRO and Hurricane Bluff sites. The PSA was conducted at Environmental Archaeology Lab at the Department of Anthropology at the UAF using protocols for the pipette method modified from Janitzky (1986).

PSA protocols were as follows:

1) Around 50-100 g of sediment was subsampled with the fractions coarser than 2.0 mm (very coarse sand) removed with a sieve;
2) Large pieces of undecomposed organic matter (roots, woody particles) were picked out of the <2.0 mm fraction;
3) The ~25 g of the <2.0 mm fraction was placed into a 250 mL centrifuge tube, and ~200 mL of 0.5 N HCl was added to centrifuge tubes;
4) The centrifuge tubes were placed into a 400 mL glass beaker filled with deionized water until the centrifuge tubes floated, and then were placed on hot plates at a temperature ~60ºC for at least 24 hrs or until effervescence is negligible;
5) Samples were decanted of the HCl solution and washed (centrifuged and decanted) with deionized water;
6) Between 10-20 mL of hydrogen peroxide (H_2O_2; reagent grade [29-32%]) was added to the samples to remove the organic matter, and allowed to react for 12-24 hrs;
7) The samples were then placed on a hot plate at 60ºC for 1-2 hrs to finish the reaction;
8) Once the oxidation process was completed, the samples were washed with washed (centrifuged and decanted) with deionized water;
9) Exactly 25 mL of dispersant (sodium pyrophosphate [$Na_4O_7P_2$]) and 100-150 mL deionized water were added to the samples to aid in the dispersal sediments;
10) The samples were placed in a malt mixer and mixed at a low setting for about 7 minutes to disaggregate the sediments;
11) Samples were then wet sieved using a 63 µm sieve and deionized water with the < 63 µm fraction (clay and silt) funneled into a 1000 mL graduated cylinder, and the > 63 µm (sand) fraction washed from the mesh sieve into a tared beaker and placed in an oven to dry at 110ºC;
12) Sand beakers were placed in a desiccator to cool, and then weighed in total (weight of beaker + sand fraction), and subsequently sieved and weighed by selected grain sizes;
13) The < 63 µm fraction (clay and silt) was extracted from 1000 mL graduated cylinders, based on settling velocity of particle sizes, by pipetting the fractions into glass vials;
14) The clay and silt glass vials were placed in an oven at 110ºC overnight until dry, desiccated until cool, and weighed;
15) Percentages of sand, silt and clay fractions were calculated, and adjusted for the weight of the dispersant.

The PSA analyses were input into the Gradistat.v8 program (Blott and Pye 2001, Kenneth Pye Associates Ltd 2010) for statistical analysis for average size, sorting, skewness, and kurtosis. We present both in metric and phi units (ϕ). We follow the Folk and Ward (1957) methods for measuring and defining sorting, skewness, and kurtosis. *Sorting* refers to measurement of the distribution (or deviation) of grain sizes around a mean. Lower values indicate better sorted materials (<1.00), while higher values (>1.00) reflect more poorly sorted matrices.

Skewness refers to the asymmetry of grain size distribution from the average. A distribution that is normal is referred to as *symmetrical* lacking a dominant size or skewing. Symmetrical distributions have values between -0.1 to 0.1. An asymmetrical distribution with a tail that trends to the left is consider to be *fine* and *very fine* skewed. Fine and very fine skewed sediments have values between -0.1 to -0.3 and -0.3 and -1.0, respectively. Distribution with tail weighted to the right are considered *coarse* and *very coarse* skewed. Coarse and very coarse skewed sediments have values between 0.1 to 0.3 and 0.3 to 1.0, respectively.

In terms of sediment analyses, kurtosis is defined by the shape of the tails, or the degree of concentration from a mean, and the peakedness of a probability distribution curve (Blott and Pye 2001, Folk and Ward 1957). *Mesokurtic* distributions have outliers that are contained within 3-standard deviations of a mean and a normal distributional curve. Mesokurtic distributions have a kurtosis value around 1 (between 0.90 and 1.11). *Leptokurtic* distributions are more peaked with fatter tails that are closer to the central mean and kurtosis values between 1.11 and >3.00. *Platykurtic* have broader, flatter distributional curves and are more sorted toward the tails with kurtosis values between 0.90 to <067.

5.1.2.2 Tephra Geochemistry

A total of 5 samples of tephra were collected from the DRO and Hurricane Bluff site for potential geochemical and petrographic characterization as part of this study. Tephra samples were processed in the Environmental Laboratory at the UAF Anthropology Department. Raw bulk tephra samples were wet sieved using tap water to remove fine sediment and separate the samples into three size fractions to allow for microscopic analyses. Plastic frames and 64, 125, and 250-micron nylon mesh were used to prevent contamination between samples. All samples had very sparse material in the greater than 250-micron size fraction and microscopic analyses revealed that the size fractions between 250–125 and 125–64 microns were predominantly comprised of minerals and lithics. Therefore, tephra samples were processed utilizing heavy liquid separation to isolate glass shards smaller than 64 microns. Tephra samples were processed using heavy-liquid separation techniques in the UAF Geology Department Pollen Laboratory, following the techniques of Pinney (1991). Material isolated via heavy liquid separation was visually confirmed to consist of glass shards using a binocular microscope at 100X and 500X magnification.

Glass shards isolated via heavy-liquid separation were mounted and polished for electron probe microanalysis (EPMA) in the UAF Geology Department. Polished mounts were coated with carbon prior to EPMA, to create a conductive surface for analysis. Tephra samples were analyzed on the UAF Advanced Instrumentation Laboratory JEOL JXA-8530X electron microprobe from April 7–9, 2017. Analytical conditions utilized were an accelerating voltage of 15 kilovolts, a beam current of five nanoamps, and beam size of five microns. Standards with published compositions were used to calibrate the instrument. Multiple points of analysis (5–10) were collected routinely on secondary working standards KN18 volcanic glass and Rhyolitic Glass 216 (USNM 72854 VG-568) to monitor instrument drift. As many points of analysis were collected on each tephra sample as possible; however, samples consisted of such small volcanic glass shards that it

complicated efforts to locate shards large enough for analysis. The Probe for EPMA program (version 10.8.1; Donovan 2015) was used to quantify X-rays characteristic of each element into percent oxide compositions, using the CIT-ZAF correction.

The SIMAN similarity coefficient with the weighting option of Brochardt (1974) was used to evaluate how the glass geochemistry of the samples compares with mSRV tephra geochemical groups and glass geochemistry of Hayes River Outcrop (site 11HYKLW001 of Wallace et al. 2014) tephra samples from the Hayes Volcano (both previously reported in Mulliken 2016). The SIMAN coefficient considers the relative analytical deviation and allows for the error level to be manipulated. Specific oxides were considered in calculation of the coefficient, which prevents oxides with high relative errors from being considered in the correlation, and which could result in erroneous correlations. Following Begét et al. (1991), similarity coefficients greater than 0.90 are interpreted as representing correlation between tephra layers (i.e. same volcanic source, different eruption), while values greater than 0.95 are considered indicative of the same volcanic event or members of the same set. Unfortunately, only one sample from the DRO site has sizable populations of glass to provide a geochemical signature on the deposit. The results and ages of the tephras at DRO and Hurricane Bluff are discussed in more detail below.

5.1.2.3 Inorganic and Organic Carbon Measurement

The percentage of inorganic carbon (%$CaCO_3$) in a sample was measured using two methods, gas displacement and loss of weight through ignition, at the Environmental Archaeology Lab at the Department of Anthropology at the UAF. Gasometric analysis of the inorganic content of sediment samples was conducted through the use of a chittick apparatus (Machette 1986).

Chittick apparatus measurement protocols:

1) A subsample of sediment weighed between 1-10 mg, but generally ranged between 8-11 mg;
2) Subsample placed in 250 mL flask;
3) The temperature and atmospheric pressure within the lab were recorded;
4) Add 10 mL of 6N HCl from Chittick apparatus burette was slowly added into flask with sediment;
5) The volume of the displaced CO_2 was measured;
6) The percentage of $CaCO_3$ was calculated based on the sample weight and the volume of displaced CO_2, and corrected for the temperature and atmospheric pressure at the time of measurement.

The loss-on-ignition (LOI) method was also used to calculate the approximate amount of organic and inorganic carbon (%OC_{LOI} and %$CaCO_{3LOI}$) based on the loss of sample weight (percent weight [%wt]) after being combusted at different temperatures in an oven and muffled furnace. Organic carbon in samples tends to combust at temperatures between 200°C and 550°C without significant loss of the inorganic carbon component, which combusts into CO_2 at temperatures between 800°C and 1000°C (Ball

1964, Davies 1974). The combustion of CO_2 at 800°C and 1000°C is assumed to originate from $CaCO_3$, or calcium carbonate.

LOI protocols used for this study were modified from Ball (1964), Dean (1974) and Stein (1984).

1) Crucibles were dried for 24 hours in an oven at 100 °C prior to use, cooled in a dessicator until room temperature was reached, and weighed before samples were placed in them. An Ohaus Adventurer Pro analytical balance with a readability of 0.0001 g and repeatability of ± 0.1 mg was used to weigh the crucibles and samples.
2) Samples were placed in a freezer right from the field to prevent moisture loss or mold growth, and thawed at least 1 day prior to performing LOI. Thawed samples were picked of roots and larger organics and powderized in a mortar and pestle. Samples were then placed into crucibles and weighed. The difference between the original weight of the crucible and the combined weight of the crucible and sediment sample constitutes the sediment sample weight.
3) Sediment samples were dried in an oven for at least 24 hours at 100°C, and subsequently cooled in a dessicator until room temperature was reached. Once dry, the sample was reweighed. The difference between the wet and dry sediment weights divided by the wet weight multiplied by 100 constitutes the minimum amount of moisture (%wt H_2O) in the sample at the time of sample acquisition.
4) Samples were combusted at 500°C for 1 hour in a muffled furnace, cooled in a dessicator until room temperature was reached, and weighed. Organic carbon content (%wt) is the difference in weight between the original dry sediment and the post-550°C weights divided by the original dry sediment multiplied by 100.
5) Samples were combusted at 1000°C for 1 hour in the furnace, cooled in a dessicator until room temperature was reached, and weighed. The difference in weight of the evolved CO_2 content (%wt CO_2) is the difference between the post-550°C and the post-1000°C weights divided by the original dry sediment weight multiplied by 100. The weight percentage of inorganic carbon (assumed to be calcium carbonate) is calculated by dividing the %wt CO_2 by 0.44, the known fraction of CO_2 in $CaCO_3$.

LOI tends to provide higher estimates for organic and inorganic carbon components when compared to other analytical techniques, such as gasometric (i.e., chittick) and wet-oxidation (e.g., Walkley-Black) methods (Davies 1974, Dean 1974, Holliday and Stein 1989). LOI value overestimates can be due to variances in clay content and mineralogy, high structural water content in clays, and presence of sources of elemental carbon such as bituminous coal. The largest source of LOI over-estimation can be sediments with higher clay content and an increased amount of structural water content. The structural water in clay can be released between 550°C and 1000°C. Between these temperatures, Dean (1974) observed a 1-1.8% weight loss in a within a sediment with 33% clay content and that lacked carbonates, and Stein (1984) also notes loss up to 5%. The weight difference was presumed to be the loss of structural water in the clay (Dean 1974:243-244).

5.1.2.4 pH Measurement

The alkalinity and acidity (pH scale) for sediments and soils were measured for any change throughout the lithostratigraphic units and pedostratigraphic horizons. The pH measurements were made using an Oakton® pH 6 Acorn Series meter with the following protocols:

1) The electrodes were rinsed with distilled water, and rehydrated by soaking them for 1 hr in tap water;
2) The pH meter was calibrated using 4.01, 7.00, and 10.00 buffer solutions;
3) Between 15 to 50 g of sediment was placed into a beaker, distilled water was added to make a slurry, stirred, and allowed to sit for 20-30 minutes;
4) The electrodes were placed in the slurry and allowed to sit for 20-30 minutes, after such a pH measurement was taken with the Oakton meter;
5) Room temperature and the temperature of each slurry (taken by the instrument) were recorded;
6) The pH measurement was corrected for variations in temperature;
7) pH measurements were taken three times per sample, the instrument being checked with the calibration solutions between measurements;
8) The average of the three pH measurements for each sample was calculated.

5.2 DRO Results

5.2.1 Lithostratigraphy

Lithostratigraphy is the classification of stratigraphic units based on the properties of the physical and petrographic characteristics of sediments. The dominant process (e.g., wind, water, ice, and gravity movement) that led to a deposit's deposition can also be used to distinguish between different lithostratigraphic units. The stratigraphy at the Delta River Overlook site generally consists of around 630 cm of unconsolidated aeolian sands and silts that overlay glaciofluvial sands, gravels, cobbles, and boulders (Figures 5.1-5.3). Bacon and Holmes (1980) originally designated several units as Loess (L) and Sand (S). We have modified Bacon and Holmes' Loess and Sand sequence in this report. The lithostratigraphy of the Delta River Overlook site is summarized below and detailed in Table 5.1.

Unit 1 is the very poorly-sorted mixture of sand, gravels, cobbles and boulders that comprise the matrix of the terraced landform. The matrix is glaciofluvial in origin (i.e., glacial outwash or drift); what Péwé and Holmes (1964) defined as "younger deposits" (Qf2) of Donnelly Glaciation glaciofluvial deposits. The location of the DRO site is between two deposits of Donnelly-aged lateral moraines, and approximately 3.5 miles south of the outer edge of the end moraine. The "younger" glaciofluvial deposits are likely a mixture of deposits when the area was covered by the glaciers and deposited materials as outwash sediments after glacial recession.

Matmon et al. (2010) report on the Beryllium 10 (^{10}Be) exposure dating of boulders and gravels at the surface and adjacent to Donnelly-aged morainal materials in the Delta River Valley and Donnelly Dome area. Matmon et al. (2010) suggest that the Donnelly-aged end moraine with the greatest extent at the Last Glacial Maximum in the

Delta River Valley stabilized before 17 ka, after which it became exposed and ^{10}Be isotopes began accumulating at the surface. Briner et al. (2017), based on a recalculation of Matmon et al.'s ^{10}Be data, suggest that the terminal moraine was exposed by 19.4 +/- 0.9 ka. The glaciofluvial deposition for Péwé and Holmes' (1964) "younger deposits" (Qf2) of Donnelly Glaciation glaciofluvial deposits appears to have occurred around 19.4 ka, or shortly after the recession of the glacier into the upper reaches of the valley above the DRO site terraced landform. The escarpment of the landform was established after LGM glacial recession and deposition of the "younger" glaciofluvial materials, and as the river began to down cut into its modern position.

Some of the surfaces of the gravels in Unit 1 are ventifacted indicating at least some exposure of the upper portion of these deposits to wind abrasion after glaciofluvial deposition, possibly after downcutting of the river began and before aeolian accumulation on terrace's surface occurred. This period of exposure would have at least occurred between ~19.4 +/- 0.9 ka and 13,000 cal yr BP (the age of earliest human occupation of the landform - Component 1).

Unit 2 consists of a 3-7 cm thick, discontinuous grayish brown massive aeolian fine sandy loam. Unit 2's contact is broken and smooth or wavy depending on the topography of the underlying glaciofluvial deposits. The discontinuity of the Unit 2 aeolian sands likely reflects differential deflation of these deposits across the site. Timing of the Unit 2 aeolian sand deposition is after 19.4 +/- 0.9 ka (the deposition and exposure of the Unit 1 gravels) and before 13,000 cal yr BP (the deposition of the overlying Unit 3 loess and the time of the Component 1 human occupation). We have designated this deposit as Sand 1.

Unit 3 is the thickest package of aeolian sediments across the site area. Unit 3 consists of a ~250 cm thick massive silt to sandy loam that represents a loess deposit (aeolian silt deposition). Unit 3 directly overlies Unit 2 sands in areas where Unit 2 is present, otherwise Unit 3 directly overlies Units 1 outwash where the Unit 2 sands have been eroded and are missing from the stratigraphy. The contact of Unit 3 with Units 1 and 2 is very abrupt. The majority of the archaeology at the DRO site is contained within Unit 3. Unit 3 loess generally consists of greater than 50% silt (51 to 76%) content (see below for more details on the Particle Size Analysis results). Unit 3 particles are very angular to angular (97 to 99%) in shape, and lack sphericity (Leehan 1981), which indicates that distance from the original source rock in the watershed, and to the spot of the source for aeolian transport to the DRO site, was relatively short, as the longer the distance of the transport of a particle within a watershed the more the particle becomes rounded. Redoximorphic features were observed throughout the Unit 3 loess. Redoximorphic features consist of masses and circular to ovular shaped iron accumulations and are common (2 to <20% surface coverage) in the sediment matrices. Unit 3 includes Loess 1 through Loess 6.

Unit 3 loess accumulation commenced before 13,000 cal yr BP, based on the age of Component 1. It continued to accumulate throughout the Holocene and at least to 2310-2150 cal yrs BP, the age of Component 8b; however, a more specific age estimate when Unit 3 loess accumulation ceased is unknown because of erosion to the upper portion of these deposits throughout the site area. Eight buried soils or complexes of buried soils (Pedocomplexes 0 through 7 and Paleosol 8) are contained within the Unit 8 loess deposits, and are described in more detail below.

Three volcanic ash deposits (tephras) were observed within Unit 3 (Figure 5.1). Tephra 1a is the deepest tephra currently recognized (Figure 5.4), situated at 556 cmBS and 9-10 cm above Pedocomplex 1 (described below). Tephra 1a is a 1-2 cm thick, discontinuous whitish to very pale brown silt loam. This tephra deposit was first recognized by Bacon and Holmes (1980) and defined as "Tephra 1." Tephra 1b is the second deepest tephra situated at 537-538 cmBS. This volcanic ash deposit is a 1-2 cm thick, discontinuous whitish to very pale brown silt loam. This tephra was not recognized by Bacon and Holmes (1980). Tephra 1b overlies Pedocomplex 2 (described below) by 4 cm.

Tephra 2 is the highest tephra in the DRO stratigraphy situated between 442-443 cmBS (Figure 5.4). Tephra 2 was reported by Bacon and Holmes (1980) as "Tephra 2." This ash is a 0.5 to 2 cm thick, mostly continuous whitish to very pale brown silt loam. Tephra 2 is situated above Pedocomplex 6 and below Pedocomplex 7 (described below). The timing of these ash falls and their potential correlation to proximal and distal tephras are discussed below in this chapter in the section on tephra characterization.

Units 4 through 10 are encompassed in what Leehan (1981) termed the "Upper Sand." Unit 4 consists of an 8 to 10 cm thick loamy fine sand (aeolian deposit) that overlies Unit 3 loess. There is a sharp disconformity between Units 4 and 3 that is represented by an episode of deflation of the upper portion of the Unit 3 loess, sometime after 2310-2150 cal yrs BP. Bacon and Holmes (1980) and Leehan (1981) referred to this unit as "Sand 1 (S1)"; however, both did not recognize the Unit 2 aeolian sand in their Sand designations. In this report, we have referred to Unit 4 as Sand 2, and Unit 2 as Sand 1. Unit 4 marks the basal sediments of Leehan's (1981) Upper Sand.

Unit 5 is an 8 cm thick massive silt loam that is designated Loess 7. This aeolian silt bed was deposited on top of Unit 4 sand having an abrupt contact with the lower unit, marking a stark shift in the accumulation of aeolian particle sizes. Unit 6 is a 200 cm thick aeolian sand (sand to loamy sand) that is designated as Sand 3. These sands are bedded with horizontal laminations of coarse to fine sands. Unit 7 is a 7 to 12 cm thick massive silt loam bed that is designated as Loess 8 that overlies Unit 6 sands. Unit 8 is an 80 cm thick loamy sand designated as Sand 4. It has a very abrupt contact with the underlying Unit 7 loess, and has medium to fine sands and silt beds and laminations. Unit 9 is a 10-15 cm thick massive silt loam designated as Loess 9. Unit 10 is a 115 cm thick fine sand to sandy loam deposit designated as Sand 5 that is the highest unit in the Upper Sand sequence.

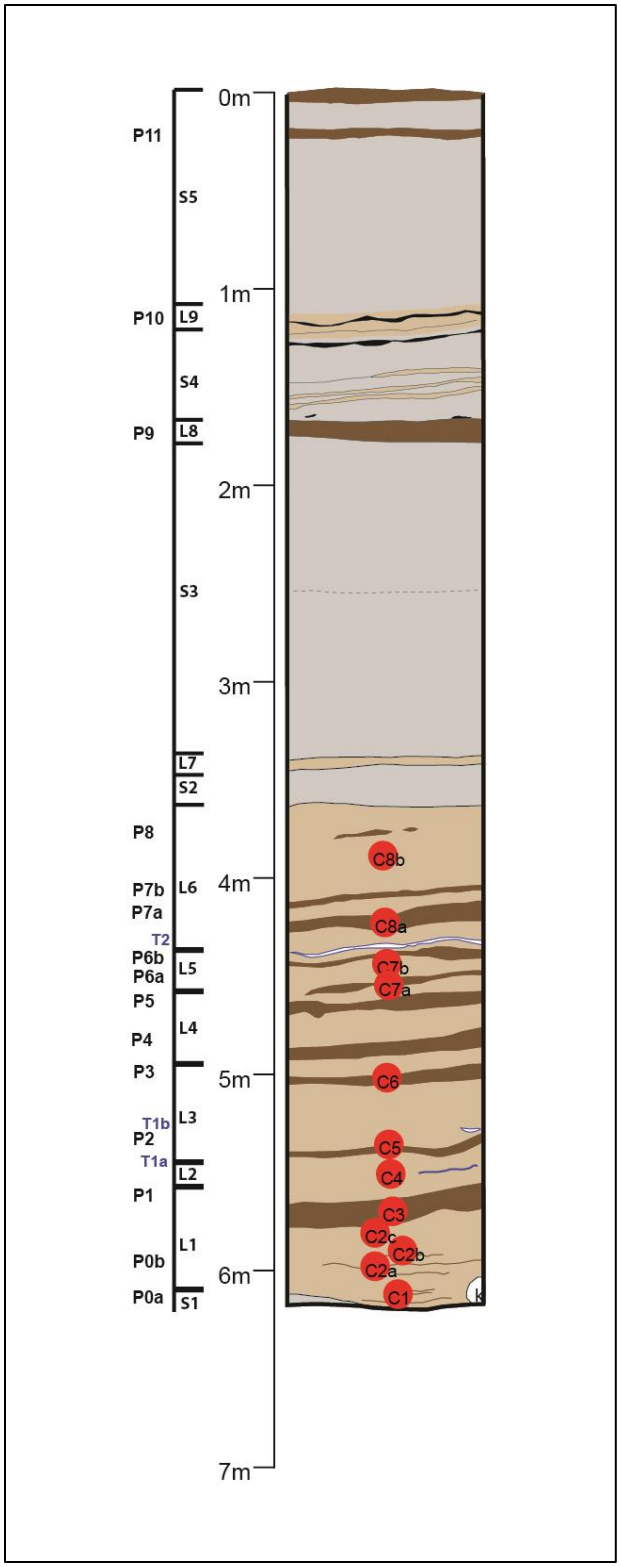

Figure 5.1. Generalized stratigraphic profile at the Delta River Overlook site. "P" refers to paleosols and pedocomplexes; "L" and "S" refer to loess and sand designations; red dots with "C" refer to archaeological components.

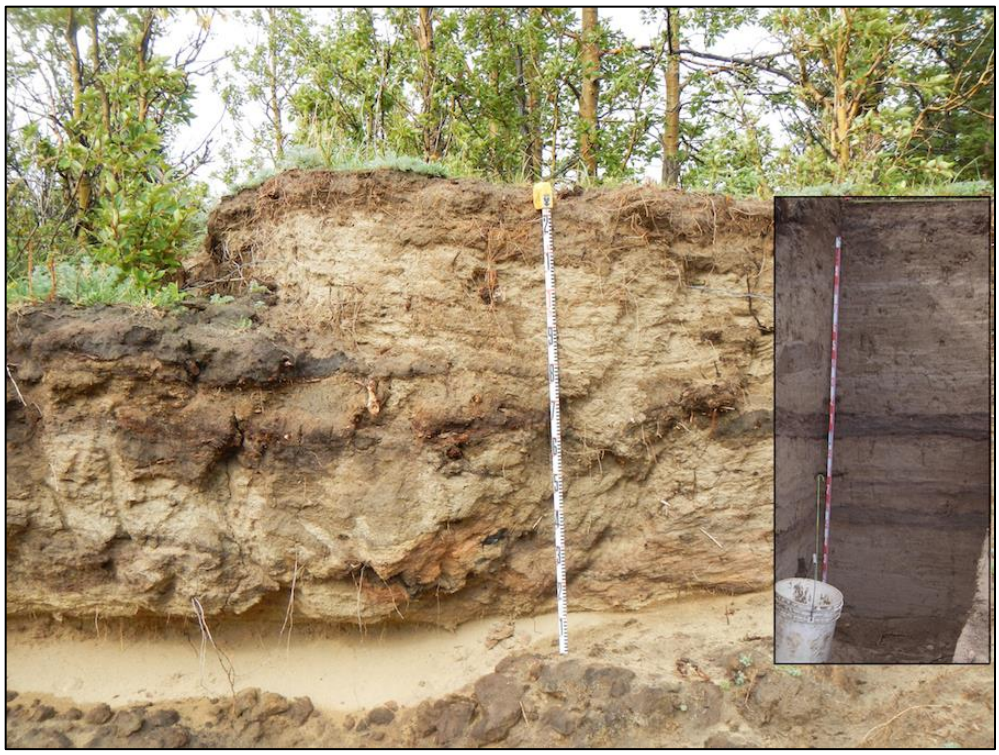

Figure 5.2. The Upper Sand at the Delta River Overlook site. Inset photo: the upper 2 m of the stratigraphic column of the Upper Sand.

Figure 5.3. Delta River Overlook Block B South Wall stratigraphic column (Units 1-3).

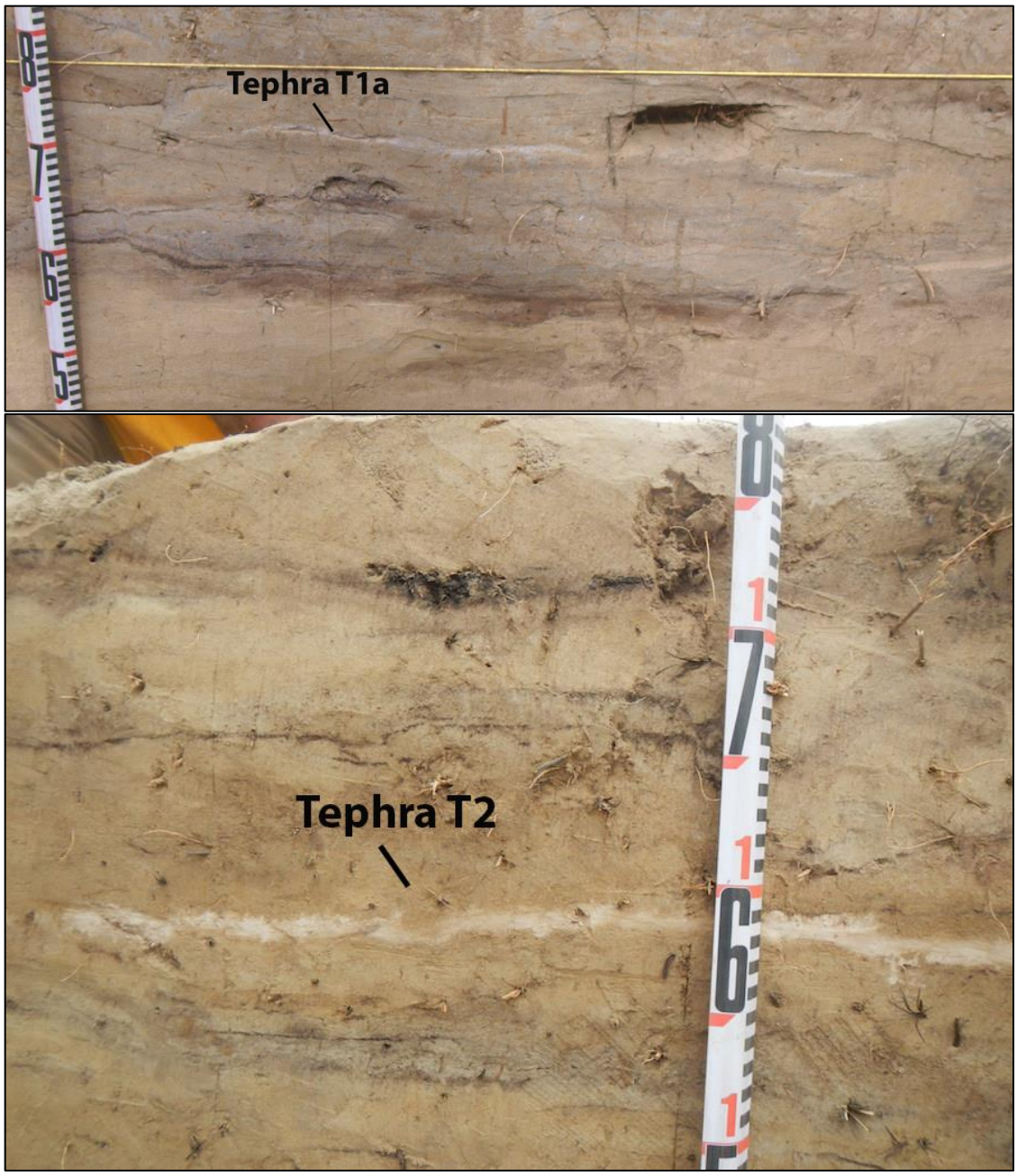

Figure 5.4. Tephras T1a (above) and T2 (below) in Unit 3 at the Delta River Overlook site.

Table 5.1. Descriptions of the Delta River Overlook site stratigraphy.

Unit (Soil Horizon) – This Study	*Unit (Soil Horizon) – Bacon and Holmes (1980)*	*General Depth (cmBS)*	*Thickness (cm) Range*	*Description*
10 (OA horizon)	-	0-5	3-5	Modern vegetative growth and litter; loam; partially to moderately decomposed organics; slightly moist to dry; abrupt and smooth boundary. OA horizon developed on the surface of Sand 4.
10 (C) Sand 5	Sand 3	3-118	115	Fine sand to sandy loam; bedded; dry; well sorted; abrupt and smooth boundary. Beds are horizontally oriented (0-4 degrees in slope). The lowest 50 cm of Sand 5 is the coarsest fractions being poorly sorted sands with nearly 1.5% gravel present (Leehan 1981). The middle and upper sections of Sand 5 contain fine fractions being fine sands and sandy loams.
10 (Ab horizon) Paleosol 11	-	3-15	4-5	Paleosol 11 (Ab horizon) - light gray sandy loam; massive; slightly moist; continuous; abrupt to clear and smooth boundary. Buried soil horizon exhibits more characteristics of an A horizon, but retains some partially to moderately decomposed organics in the upper part of the horizon. Paleosol 11 developed on a finer silty sand deposit in Sand 5.
9 (C) Loess 9	Loess 8	90-130	10-15	Silt loam; massive; slightly moist; continuous; abrupt, smooth boundary. Silt loam deposit is mostly massive but does contain a single discontinuous bed of fine sand overlying the lowest Ab horizon of Pedocomplex 10.
9 (Ab horizons) Pedocomplex 10	Paleosol 9	90-130	10-15	Pedocomplex 10 (Ab horizons) – dark brown silt loams; massive; dry to slightly moist. Pedocomplex 10 is composed of at least four continuous Ab horizons generally ranging in 2 cm or less in thickness. Each Ab horizon is separated by 3-5 cm of unweathered loess and fine sand. The boundaries of the Ab horizons are abrupt and smooth to slightly wavy. Pedocomplex 10 is contained within Loess 9. Charcoal fragments are present in the Ab horizons of Pedocomplex 10.
8 (C) Sand 4	Sand 2	90-170	80	Loamy sands; bedded; dry to slightly moist; continuous; very abrupt, smooth boundary. Bed and lamination orientations are horizontal (0-2 degrees in slope). Beds and laminations are composed of medium to fine sands and silts. This sand deposit is the upper portion of Sand 2 in Bacon and Holmes (1980) stratigraphic units. Leehan (1981) notes the abundance of charcoal and woody fragments in this sand deposit.
7 (C) Loess 8	Sand 2	170-192	7-12	Silt loam; massive; slightly moist; continuous; abrupt, smooth boundary.

7 (Ab horizons) Pedocomplex 9	-	170-192	7-12	Pedocomplex 9 (Ab horizons) – dark brown silt loams; massive; dry to slightly moist. Pedocomplex 9 is composed of a series of thin organic stringers (Ab horizons) generally ranging in 1-2 cm or less in thickness. The boundaries of the stringers are usually abrupt and smooth and broken (discontinuous). Pedocomplex 9 is contained within Loess 8.
6 (C) Sand 3	Sand 2 (S2)	170-350	200	Sand to loamy sands; bedded; dry; continuous; very abrupt, smooth boundary. Bed and lamination orientations are mostly horizontal (0-8 degrees in slope). Leehan (1981) notes that laminations are composed of coarse, medium and fine sands. This sand deposit is the lower portion of Sand 2 in Bacon and Holmes' (1980) stratigraphic units.
5 (C) Loess 7	Loess 7 (L7); Paleosol 8 (P8)	347-355	8	Silt loam; massive; slightly moist; continuous; abrupt, smooth boundary. Bacon and Holmes (1980) place their Paleosol 8 in Loess 7.
4 (C) Sand 2	Sand 1 (S1)	350-365	8-10	Yellowish brown loamy fine sand; loose structure (singular grained)**;** dry; continuous; very abrupt, smooth boundary. Leehan (1981) places this sand as the base of the "Upper Sand" unit.
3 (Bwb horizon) Paleosol 8	-	367-375	3	Paleosol 8 (Bwb horizon) – dark yellowish brown (10YR 3/4) silt loam; massive; slightly moist; discontinuous; abrupt, smooth and broken boundary. Discontinuous Bwb horizon that was truncated in several areas of the excavation area by deflation or mechanical disturbance. Radiocarbon dates on charcoal recovered cultural features in Component 8b in Paleosol 8: 2210+/-20 B.P. (UGAMS#34298) and 2280+/-145 B.P. (Gx-6750). Paleosol 8 is contained in Loess 6.
3 (C) Loess 6	Loess 6 (L6)	375-443	68	Brown to dark yellowish brown (10YR 5/3 to 4/3) silt loam; massive; slightly moist; discontinuous; abrupt, smooth boundary. Redoximorphic features are common (2 to <20% surface area) in the upper portion of Loess 6 and consist of irregular masses of iron accumulation with a few (2% surface area) light gray circular shaped reduction patches. Redoximorphic features are more abundant (or many; >20% surface area) in the lower 10 cm of Loess 6 and consist of irregular masses of iron accumulation that extends into the upper portion of Loess 5. Minor amounts of scattered charcoal are present. In the majority of the excavation area, the upper portions of Loess 6 are eroded by deflation. Bacon and Holmes (1980:Figure 17) define the boundaries of Loess 6 as between Tephra 2 and an erosional surface and/or unconformity with Sand 1. Due to the ephemeral nature and discontinuity of Tephra 2 in some areas of the site, the lower boundary of Loess 5 with the upper boundary of Loess 6 is not always well-defined. Pedocomplex 7 is contained within Loess 6.

3 (Ab and ABwb horizons) Pedocomplex 7	Paleosol 7 (P7)	413-433	10-20	Pedocomplex 7 (Ab and ABwb horizons) – brown to dark brown (7.5YR 4/3 to 3/2) silt loams; massive; dry to slightly moist; discontinuous; abrupt, slightly wavy and broken boundaries. Pedocomplex 7 consists of two soil couplets (P7a and P7b) separated by around 5-7 cm of yellowish brown (10YR 5/4) to light yellowish brown (10YR 6/4) unweathered silt loam (C horizon). The lower soil couplet P7a consists of two thin (1-2 cm thick) Ab horizons (brown loams; 7.5YR 4/3 to 4/2) separated by 1-3 cm of unweathered silt. In some areas of the excavation, the expression of the lower soil in couplet P7a is an ABwb horizon (reddish dark brown loam; 7.5YR 3/3 to 3/2) as more soil leaching of oxides is evident. The upper soil couplet P7b consists of a thin Ab horizon overlying and separated from an ABwb horizon by 1-2 cm of unweathered silt. The lower ABwb horizon of soil couplet P7b displays much more oxidization than the horizons in soil couplet P7a. Charcoal is abundant in both soil couplets. Component 8a is associated with soil couple P7a. Radiocarbon date on charcoal recovered from soil couplet P7a: 3330+/-30 B.P. (Beta-447776). Radiocarbon date on charcoal recovered from soil couplet P7b: 2870+/-30 B.P. (Beta-447777).
Tephra 2	Tephra 2 (T2)	442-443	0.5-2	Tephra 2 (T2) – whitish to very pale brown (10YR 8/1 to 10YR 8/3) silt loam; dry to slightly moist; massive; abrupt, smooth boundary. T2 is very thin (0.5-2 cm in thickness) and mostly continuous across the site. Tephra particles were very fine (5 microns or less in size) and moderately weathered. Geochemical analysis of T2 shows a similarity to the Watana tephra deposits in the Susitna River Valley and to the Hayes volcano (Unit D) in the Cook Inlet region, both deposited around 3600 B.P. Bracketing radiocarbon ages in P7a and P6b place the ashfall between 3330+/-30 B.P. and 3970+/-30 B.P. The bracketing ages of Tephra 2 place its deposition within the time frame of the regional deposition of a Hayes Volcano ashfall around 3660 +/- 125 B.P. (Begét et al. 1991).
3 (C) Loess 5	Loess 5	443-468	25	Yellowish brown (10YR 5/4) to light yellowish brown (10YR 6/4) silt loam to sandy loam; massive; dry to slightly moist; continuous; abrupt, smooth boundary. Above and below Paleosols 6a and 6b, the texture is a very well sorted silt loam. The particle sizes show an increase in fine and very fine sands, from a very well sorted silt loam to a well sorted sandy loam texture, between Paleosols 6a and 6b. Redoximorphic features are abundant (or many; >20% surface area) in upper 5-7 cm of Loess 5 and consist of irregular masses of iron accumulation. Redoximorphic features are common (2 to <20% surface area) in lower portion of Loess 5 and consist of irregular masses of iron accumulation with a few (2% surface area) light gray circular shaped reduction patches. Little to no charcoal is present. Bacon and Holmes (1980:Figure 17) define the boundaries of Loess 5 as between Tephra 2 and Pedocomplex 5; however, due to the ephemeral nature and discontinuity of Tephra 2 in some areas of the site, the lower boundary of Loess 5 with the upper boundary of Loess 6 is not always well-defined. Pedocomplex 6 is contained within Loess 5.

3 (Ab and ABwb horizons) Pedocomplex 6	Paleosol 6 (P6)	447-460	10-20	Pedocomplex 6 (Ab and ABwb horizons) – brown to dark brown (7.5YR 4/4 to 3/2) and grayish brown to brown (10YR 5/2 to 5/3) silt loams; massive; slightly moist; continuous; abrupt to clear, smooth to slightly wavy boundaries. Pedocomplex 6 consists of two soil couplets (P6a and P6b) that are separated by 5-7 cm of yellowish brown (10YR 5/4) to light yellowish brown (10YR 6/4) unweathered sandy loam. The lowest soil couplet (P6a) is represented by an Ab horizon (dark brown silt loam) overlying an ABwb horizon (dark brown to reddish dark brown silt loam). These Ab and ABwb horizons are separated by less than 2 cm of unweathered yellowish brown (10YR 5/4) silt loam (C horizon), however, in some areas of the site these horizons are mixed due to turbation of the sediments or the upper Ab horizon welded onto the lower ABwb horizon. The boundaries for the soil couplet P6a are abrupt and smooth with the exception of areas of turbation. The upper soil couplet (P6b) consists of two 1-3 cm thick Ab horizons (dark brown silt loam) that are separated by less than 2 cm of unweathered yellowish brown (10YR 5/4) silt loam (C horizon). The boundaries of the soil couplet P6b horizons are abrupt and slightly wavy. Soil couplet P6a is abundant in charcoal, while soil couplet P6b has very little charcoal present. Radiocarbon dates on charcoal recovered from a soil couplet P6a in Pedocomplex 6: 3970+/-30 B.P. (Beta-447778) and 4010+/-30 B.P. (Beta-447775). Component 7a is associated with soil couplet P6a, while Component 7b is associated with soil couplet P6b.
3 (Ab and ABwb horizons) Pedocomplex 5	Paleosol 5 (P5)	468-474	4-9	Pedocomplex 5 (Ab and ABwb horizons) – brown to very dark brown (7.5YR 4/2 to 2.5/3) silt loams; massive; slightly moist; discontinuous; abrupt, slightly wavy boundaries. Pedocomplex 5 consists of at least two periods of soil development. A reddish brown to dark brown (7.5YR 4/2 to 3/2) silt loam represents an ABwb horizon (4-6 cm thick). The A horizon portion of this soil horizon is missing in some of the excavation area and likely indicates some differential erosion across the site at the surface of this soil after its development. A very dark brown (7.5YR 2.5/3) silt loam represents a thinner Ab horizon (1-2 cm thick) that is separated from the overlying ABwb horizon by 2-3 cm yellowish brown (10YR 5/4) to light yellowish brown (10YR 6/4) relatively unweathered silt loam. The Ab horizon is blackened displaying charring in many areas of the site, and contains an abundance of charcoal. Radiocarbon date on charcoal recovered from Pedocomplex 5: 4350+/-30 B.P. (Beta-447774).
3 (C) Loess 4	Loess 4 (L4)	468-505	15-25	Brown (10YR 5/3) to light yellowish brown (10YR 6/4) silt loam; massive; slightly moist; continuous; abrupt, smooth boundary. Redoximorphic features are common (2 to <20% surface area) throughout Loess 4 and consist of irregular masses of iron accumulation. Little to no charcoal is present. Bacon and Holmes (1980:Figure 17) define the boundaries of Loess 4 between Pedocomplex 5 and Pedocomplex 3. Pedocomplex 4 is contained within Loess 4.
3 (Ab and Bwb horizons) Pedocomplex 4	Paleosol 4 (P4)	486-496	7-10	Pedocomplex 4 (Ab and ABwb horizons) – brown to very dark brown (7.5YR 4/2 to 3/3) silt loams; massive; slightly moist; continuous; very abrupt, smooth and slightly wavy boundaries. Pedocomplex 4 consists of at least 4 buried soils with the upper most soil being a thinner very dark brown silt loam (Ab horizon; 1-2 cm thick) that overlies three ABwb horizons. ABwb horizons are each 2-3 cm in thickness. The A horizons in the upper Ab horizon and in some of the ABwb horizons have discontinuous layers of root casts and compact, partially decomposed plant materials present. The ABwb horizons show nearly equal expressions of A and weakly expressed B horizons. Minor amounts of charcoal present. Radiocarbon date on charcoal from Pedocomplex 4: 3980+/-150 B.P. (Gx-6752).

3 (Ab horizons) Pedocomplex 3	Paleosol 3 (P3)	505-512	5-8	Pedocomplex 3 (Ab horizons) – grayish brown to brown (10YR 5/2 to 5/3) silt loams; massive; slightly moist; discontinuous; abrupt, smooth boundaries. Pedocomplex 3 consists of at least 4 very weakly developed Ab horizons; each horizon is 1-2 cm thick. Some of the horizons contain root casts that consist of partially decomposed fibrous organic materials. Pedocomplex 3 developed at the surface of Loess 3. Little to no charcoal is present in the soils; however, a radiocarbon date was obtained on charcoal from a hearth from Component 6 in Loess 3: 5980+/-30 B.P. (UGAMS#34297).
3 (Ck) Loess 3	Loess 3 (L3)	505-556	6-28	Gray to brown (10YR 5/1 to 5/3) silt loam; continuous; abrupt, smooth boundary. The deposit has visible carbonates. Root casts are 2-5 cm thick horizontally oriented reddish brown fibrous organic materials with some carbonate coating adhering to the outside of the casts. Redoximorphic features are few (<2% in surface area) in Loess 3 and consist of irregular masses of iron accumulation and scattered circular to ovular shaped bright reddish orange iron accumulations. Bacon and Holmes (1980:Figure 17) define the boundaries of Loess 3 as between Pedocomplex 3 and Tephra 1; however, due to the ephemeral nature and discontinuity of Tephra 1b in many areas of the site, the lower boundary of Loess 3 with the upper boundary of Loess 2 is not well-defined. Loess 3 contains Pedocomplex 2. Little to no charcoal is present.
Tephra 1b (T1b)	-	537-538	1-2	Tephra 1b (T1b) – whitish to very pale brown (10YR 8/1 to 10YR 8/3) loam; slightly moist; massive; abrupt, smooth and broken boundary. T1b is very thin (2 cm or less in thickness) recognized in limited areas and pockets across the site. T1b overlies Pedocomplex 2 soils by 4 cm. A slightly darker brown silt loam is present directly underneath T1b and may represent a very weakly developed soil that was present when the T1b ash fall occurred. Tephra particles are very fine (5 microns or less in size) and highly weathered. Geochemical analysis of T1b was not conducted due to the fineness and degradation of the tephra. The geological origin of the tephra remains uncertain.
3 (Bwb and ABwb horizons) Pedocomplex 2	Paleosol 2 (P2)	541-545	3-8	Pedcomplex 2 (Bwb and ABwb horizons) – dark gray to dark brown (7.5YR 4/1 to 3/2) silt loams; continuous; moist; massive; abrupt, smooth to slightly wavy boundaries. Pedocomplex 2 consists of at least two distinct episodes of soil development. An upper soil is a reddish brown silt loam (Bwb horizon), while the lower soil is an ABwb horizon that shows nearly equal expressions of A and weakly expressed B horizons. In some areas of the site, the two soils are separated by 2-3 cm of pale brown to brown (10YR 6/3 to 10YR 5/3) silt. In other areas of the site, welded of the upper Bwb horizon over the upper portions of the ABwb has occurred. Pedocomplex 2 is contained within Loess 3. Charcoal is present throughout horizons. Radiocarbon date on charcoal from Pedocomplex 2: 6675+/-175 B.P. (Gx-6749). Component 5 is associated with Pedocomplex 2.
Tephra 1a	Tephra 1 (T1)	556	1-2	Tephra 1a (T1a) – whitish to very pale brown (10YR 8/1 to 10YR 8/3) loam; slightly moist; massive; abrupt, smooth and broken boundary. T1a is very thin (2 cm or less in thickness) recognized in limited areas and pockets across the site. Tephra particles are very fine (5 microns or less in size) and highly weathered. Geochemical analysis of T1a was not conducted due to the fineness and degradation of the tephra. The geological origin of the tephra remains uncertain. Bracketing radiocarbon ages in P2 and Loess 2 place the ashfall between 6675+/-175 B.P. and 7630+/-30 B.P.

3 (Ck) Loess 2	Loess 2 (2)	556-565	14-20	Pale brown to brown (10YR 6/3 to 10YR 5/3) silt loam; slightly moist; massive; abrupt, smooth boundary. Very weak soil development (Ab horizons, or stingers, 1 cm thick or less) is present in the middle 3-5 cm of silt in Loess 2. Root casts consisting of moderately decomposed fibrous organics are also present in the middle of Loess 2. The silts immediately surrounding the root casts are highly oxidized (orange reddish brown mottling), while redoximorphic features in the upper 5-10 cm and lower 3-5 cm of silts are few (<2% in surface area) in Loess 2 and consist of irregular masses of iron accumulation and scattered circular to ovular shaped bright reddish orange iron accumulations. Horizontal and vertical pockets of carbonates, likely pedogenic carbonates and carbonate root casts, are also present in Loess 2 in some areas of the site. Component 4 is present in Loess 2 and is radiocarbon dated (*Picea* sp. charcoal) to 7630+/-30 B.P. (Beta-447773). Bacon and Holmes (1980: Figure 17) place the boundaries of Loess 2 between Tephra 1a and Pedocomplex 1; however, due to the ephemeral nature and discontinuity of Tephra 1a in many areas of the site, the upper boundary of Loess 2 with the lower boundary of Loess 3 is not well-defined.
3 (Ab and ABwb horizons) Pedocomplex 1	Paleosol 1 (P1)	565-582	9-17	Pedocomplex 1 (Ab and ABwb horizons) – brown to dark brown (7.5YR 4/3 to 7.5YR 3/2) silt loam; massive; moist; continuous; dark brown to reddish brown mottling; abrupt to gradual, wavy to irregular boundaries. Pedocomplex 1 is composed of at least 3-4 distinct Ab horizons and an ABwb horizon. Three to four thin brown silt loams in the upper 3-5 cm of Pedocomplex 1 represent the Ab horizons. Ab horizons are 2-3 cm thick and separated by yellowish to pale brown (10YR 5/4 to 10YR 6/3) unweathered silt. The lowest soil of Pedocomplex 1 is an ABwb horizon represented by reddish dark brown silt loam. The ABwb horizon is generally 5 cm thick and shows nearly equal expressions of A and weakly expressed B horizons. Bright reddish to orangish red mottling is present in the lower portion of the ABwb horizon in some area of the profile. Limited mixing or involuting of the Ab and ABwb horizons occurs likely due to cryoturbation or solifluction. Limited microfaulting is also evident in Pedocomplex 1. Wood charcoal is abundant throughout Pedocomplex 1. Radiocarbon dates on charcoal recovered from upper and lower portions of Pedocomplex 1: 7190+/-200 B.P. (Gx-6751) (upper portion) and 8555+/-380 B.P. (Gx-5998) (lower portion). Component 3 is associated with Pedocomplex 1. Pedocomplex 1 developed at the surface of Loess 1.
3 (C) Loess 1	Loess 1 (L1)	565-623	35-55	Loess 1 (C horizon) – yellowish to pale brown silt loam (10YR 5/4 to 10YR 6/3); massive; moist; continuous; abrupt, smooth to slightly wavy boundary. Redoximorphic features are few (<2% in surface area) in the upper 10 cm of Loess 1, while the lower 40-45 cm of the deposit redoximorphic features are common (2 to <20% in surface coverage). Redoximorphic features Loess 1 consist of irregular masses of iron accumulation and scattered circular to ovular shaped bright reddish orange iron accumulations. Pedocomplex 0 is contained in Loess 1. Components C2a and C2b are associated with Ab horizons in Pedocomplex 0. Component C2c is associated with the upper 10 cm of Loess 1, but not paleosols. Radiocarbon dates on Component 2c from Loess 1: 9470+/-30 B.P. (Beta-422154) and 9510+/-30 B.P. (Beta-422158).

3 (Ab horizons) Pedocomplex 0	-	600-623	2-0.5	Pedocomplex 0 (thin Ab horizons in C horizons) – brown to yellowish brown (10YR 5/3 to 5/4) and brown to dark brown (7.5YR 4/2 to 3/2); massive; moist; discontinuous; abrupt, smooth and broken boundaries. Pedocomplex 0 consists of at least 6 thin dark yellowish brown (10YR 4/6) silt loams (Ab horizons). Ab horizons vary in thickness between 2 and 0.5 cm; generally separated by 2-5 cm of yellowish to pale brown (10YR 5/4 to 10YR 6/3) unweathered silt. The two thickest Ab horizons (Paleosols P0a1 and P0a2; 1.5 to 0.7 cm in thickness; brown to dark brown silt loams) are situated in the lowest 10-15 cm of Loess 1 right above the lower sand and gravels of Unit 1. Three to four thinner, more weakly expressed Ab horizons (or stringers; Paleosols P0b; 0.5 cm or less in thickness) developed in the upper 20 cm of Loess 1. Component 1 is associated with P0a2, while Components C2a and C2b are associated with Ab horizons in P0b. Radiocarbon date on charcoal recovered from paleosol P0a2: 10,990+/-50 B.P. (Beta-422155). Radiocarbon dates on charcoal recovered from paleosol P0b: 10,000+/-40 B.P. (Beta-422157) and 10,060+/-40 B.P. (Beta-422156).
2 (C) Sand 1	-	623-627	3-7	Grayish brown (2.5Y 5/2) fine sandy loam; massive; slightly moist; no oxidization; discontinuous; abrupt and smooth to wavy boundary. The Unit 2 lower aeolian fine sands are not present everywhere throughout the excavation area, and likely were differentially eroded across the landform.
1 (C)	Outwash	627+	-	Yellowish brown to dark yellowish brown (10YR 5/4 to 44) glaciofluvial sand, gravels, cobbles and boulders; massive; slightly moist; continuous. Unit 1 is the glaciofluvial sand, gravels, cobbles and boulders that compose the terraces basal sediments. Boulders are present in some locations. Gravels and cobbles are sub-rounded to sub-angular with high sphericity; some have waterlain weathering rinds. Sands are from very coarse to very fine sizes with the majority of particles falling in the coarse to fine sand ranges. Some gravels appear polished and ventifacted.

5.2.2 Pedostratigraphy

Pedostratigraphy is the "study of the stratigraphy spatial relationships and implications of surface and buried soils" (Palmer 2007). The prefix "pedo-" refers to soil. A "paleosol" is used to refer to ancient soils, or soils that have "formed on landscapes in the geologic past" (Nettleton et al. 2000). The Delta River Overlook pedostratigraphy uses both informal designations for coherent soil groups, and standard nomenclature for soil horizons within those soil groups. As noted above, the standard soil horizon nomenclature follows the U.S. Department of Agriculture (USDA1993) and the National Resources Conservation Service (NRCS 2010) conventions. The pedostratigraphy of the Delta River Overlook site is summarized below and detailed in Table 5.1.

The informal designations for soil groups within the DRO pedostratigraphy were originally established by Bacon and Holmes (1980), and are used here with slight modifications. Bacon and Holmes (1980) referred to distinct soil groups within the stratigraphy as Paleosols and number them sequentially, the lowest being "Paleoso1 1" and the highest being "Paleosol 9" (Figure 5.1). The majority of the soil groups at DRO show multiple episodes of distinct soil development, therefore we have instituted the term "Pedocomplex" to refer to these types of soil groups (e.g., multiple A horizons or B horizons within one group). The general designation of Paleosol to a soil group is used to refer to a group that appears to have a single episode of soil formation and a clear linear relationship between the development of horizons (e.g., A to E to B horizonation). In some cases, we have also used the term "Paleosol" to refer to a distinct episodes of soil formation within a Pedocomplex, such as Paleosol 0a within Pedocomplex 0.

Thirteen soil groups have been defined at the DRO site: 10 Pedocomplexes, 2 Paleosols, and the surface soil (detailed below). The DRO pedostratigraphy consists of weakly and moderately developed soils (entisols and inceptisols, respectively). Pedocomplexes 1 through 7 and Paleosol 8 were recognized in the area of the immediate excavation. Pedocomplexes 9 and 10 and Paleosol 11 were solely observed within the outer margins of the excavation area in Blocks 16 and 17 where Leehan's "Upper Sand" is present.

Pedocomplex 0 is lowest group of buried soils in the DRO site pedostratigraphy and the Unit 3 loess. This complex consists of at least 6 discontinuous entisols (dark yellowish brown silt loams; Ab horizons) between 600 to 623 cmBS within Loess 1 of Unit 3. The two thickest Ab horizons (Paleosols 0a1 and 0a2; 1.5 to 0.7 cm thick) of Pedocomplex 0 are situated within the lower 10-15 cm of Loess 1 just above the contact with Unit 2 sand and Unit 1 gravels. The upper Ab horizons (Paleosol 0b) of Pedocomplex 0 are thinner (≤0.5 cm in thickness) and weaker in their expression than the lower Paleosols 0a1 and 0a2. Radiocarbon dating on Pedocomplex 0 ranges between 12,995 to 12,730 cal yrs BP (Paleosol 0a2) and 11,800 to 11,270 cal yrs BP (Paleosol 0b) (Table 5.1), and the late Pleistocene to early Holocene transition.

Pedocomplex 1 consists of at least 3-4 distinct episodes of soil development at the surface of Loess 1 in Unit 3 between 565 and 582 cmBS. The lowest soil in Pedocomplex 1 is a reddish dark brown silt loam (ABwb horizon). This 5 cm thick inceptisol shows equal expressions of an A horizon and humic accumulation at the soil's surface, and an underlying zone of illuviated sesquioxides and weakly expressed B horizon. The highest

soils in Pedocomplex 1 consist of 3-4 brown silt loams (Ab horizons) in the upper 3 to 5 cm of Loess 1. These entisols are 2-3 cm thick and separated by 1-2 cm yellowish brown silt. The ABwb horizon is separated from the upper Ab horizons by 3-5 cm of yellowish brown silt. The ABwb and Ab horizons display wavy and irregular boundaries and slight mixing in some areas likely due to cryoturbation or solifluction. Radiocarbon dating on Pedocomplex 1 ranges between 10,510 to 8590 cal yrs BP at the bottom, and 8390 and 7660 cal yrs BP at the top (Table 5.1), and the later stages of the early Holocene.

Pedocomplex 2 is made up of dark gray to brown silt loams (Bwb and ABwb horizons) that indicate two distinct periods of soil formation in Loess 3 of Unit 3 between 541 and 545 cmBS. The upper inceptisol of this pedocomplex consists of a 3 cm thick weakly oxidized brown silt (Bwb horizon). The lower soil is a 5-6 cm thick inceptisol (ABwb horizon) that shows equal expressions of an A horizon and humic accumulation at the soil's surface, and an underlying zone of illuviated sesquioxides and weakly expressed B horizon. The Bwb and ABwb horizons are separated by 2-3 cm pale brown silt. Both soil horizons show continuity across the site area; however, the expression of the horizons is variable being more strongly expressed in the north part of the site and more diffuse in the southern areas. In some areas of the excavation the Bwb horizon has welded over the ABwb horizon. Radiocarbon dating on charcoal from Pedocomplex 2 indicates that these soils were in development by 7920 to 7255 cal yrs BP (Table 5.1).

Pedocomplex 3 consists of at least 4 very weakly developed entisols that developed at the surface of Loess 3 in Unit 3 between 505-512 cmBS. These entisols are grayish brown to brown silt loams (Ab horizons) that are 1-2 cm thick and separated by 1-2 cm of yellowish brown silt. Root casts consisting of partially decomposed fibrous organic materials are present in Pedocomplex 3. Radiocarbon dating on charcoal from Pedocomplex 3 indicates that these soils were in development by 6890-6740 cal yrs BP (Table 5.1).

Pedocomplex 4 is composed of at least 4 brown to very dark brown silt loams in Loess 4 of Unit 3 between 486-496 cmBS. The lowest three soils of Pedocomplex 4 are inceptisols that are 2-3 cm thick and have thin layers of humic development (A horizon) and weak sesquioxide accumulation (Bw horizon). They show equal amounts of expressions of A and Bw horizons; we have designated them as ABwb horizons. The upper most soil is an entisol that is a thin layer (<1-2 cm thick) of a very dark brown silt loam (Ab horizon). Roots casts and discontinuous thin and compact layers of partially decomposed plant materials are present in the Ab horizon and some of the lower ABwb horizons. Radiocarbon dating on charcoal from Pedocomplex 4 indicates that these soils were in development by 4840-4000 cal yrs BP (Table 5.1), although this appears to be an age reversal in the stratigraphy's chronology.

Pedocomplex 5 consists of at least two brown to very dark brown silt loams that developed at the surface of Loess 4 in Unit 3. The lowest entisol is a thin (1-2 cm thick) very dark brown silt loam (Ab horizon) that is blackened and contains charcoal in many areas of the site excavation area. A thicker (4-6 cm thick) inceptisol overlies this lower entisol being separated by 2-3 cm of yellowish brown silt. The inceptisol is a reddish brown silt loam (ABwb horizon) that has equal expressions of A and Bw horizons. In some areas of the excavation, this ABwb horizon is only represented by the Bw horizon portion and likely indicates that some differential erosion and removal of the A horizon of this inceptisol occurred across the site area. Radiocarbon dating on charcoal from

Pedocomplex 5 indicates that these soils were in development by 5030-4850 cal yrs BP (Table 5.1).

Pedocomplex 6 is a set of two soil couplets that are contained within Loess 5 of Unit 3 between 447-460 cmBS. The lowest couplet (P6a) consists of a dark brown silt loam (Ab horizon; entisol) that overlies a reddish dark brown silt loam (ABwb; inceptisol) being separated by 2 cm of yellowish brown silt. In some areas of the site, these soils are mixed due to turbation of the sediments or the upper Ab horizon welded onto the lower ABwb horizon. The upper couplet (P6b) consists of two dark brown silt loam (Ab horizons; entisols) separated by 2 cm of yellowish brown silt. The upper couplet is separated from the lower couplet by 5-7 cm of yellowish brown silt. Radiocarbon dating on charcoal from the lower couplet of Pedocomplex 6 indicates that these soils were in development by 4656-4418 to 4520-4300 cal yrs BP (Table 5.1).

Pedocomplex 7 is a set of two soil couplets that are contained within Loess 6 of Unit 3 between 413-433 cmBS. The lowest couplet (P7a) consists of two thin dark brown silt loam (Ab horizons; entisols) separated by 1-3 cm of yellowish brown silt. In some areas of the excavation, the lowest entisol in the P7a couplet shows limited amounts of leaching and accumulation of sesquioxides giving a differential expression of this soil from an Ab horizon to an ABwb horizon. However, the dominant expression of this lower entisol is as an Ab horizon. The upper couplet (P7b) consists of a dark brown silt loam (Ab horizon; entisol) that overlies a reddish dark brown silt loam (ABwb; inceptisol) being separated by 1-2 cm of yellowish brown silt. In some areas of the site, these soils are mixed due to turbation of the sediments or the upper Ab horizon welded onto the lower ABwb horizon.

The upper couplet is separated from the lower couplet by 5-7 cm of yellowish brown silt. Radiocarbon dating on charcoal from the lower couplet of Pedocomplex 7 indicates that these soils were in development by 3640-3480 cal yrs BP, while dating on the upper couplet is 3140-2880 cal yrs BP (Table 5.1).

Paleosol 8 is a 3 cm thick dark yellowish brown silt loam (Bwb horizon) in Loess 6. The inceptisol shows weak illuviation of sesquioxides. The buried soil is discontinuous across the immediate excavation area due to disturbance and deflation of the upper portions of Loess 6. Radiocarbon dates on Paleosol 8 are 2720-1950 and 2310-2150 cal yrs BP (Table 5.1).

Pedocomplexes 9 and 10 and Paleosol 11 are contained in Leehan's "Upper Sand" sequence at the edge of the main excavation area. The soils developed on finer particles in the sequence including silt loams and fine silty sands. The ages of development of these soils are not known, however based on the underlying radiocarbon ages in Paleosol 8, their development occurred after 2720 to 1950 cal yrs BP. Pedocomplexes 9 and 10, Paleosol 11, and the surface soil have been truncated by more recent disturbance and erosion at several places surrounding the excavation area.

Pedocomplex 9 is a series of very thin dark brown silt loams (Ab horizons) in Loess 8 in Unit 7. These entisols are 1-2 cm in thickness and discontinuous across the Upper Sand. Pedocomplex 10 consists of at least 4 dark brown silt loams (Ab Horizons) that formed in Loess 9. These entisols are 2 cm or less in thickness being separated by 3-5 cm of loess and fine sand, and mostly continuous across the Upper Sand. Paleosol 11 consists of a light gray sandy loam (Ab horizon) that developed within Sand 5 in Unit 10. This entisol is 4-5 cm in thickness and is truncated at the western edge of the Upper Sand

column where disturbance and erosion has exposed or exhumed this paleosol. The surface soil is a weakly developed loam (entisol) that developed at the surface of the Unit 4 sand. The surface soil shows OA horizonation with partially to moderately decomposed organics at the surface with an underlying thin layer (2-3 cm thick) humus development. The surface OA horizon has welded onto Paleosol 11 where the older soil is closer to the surface due to its exhumation.

5.2.3 Sediment and Soil Analyses

5.2.3.1 Tephra Characterization

Several distal tephra beds recognized in central Alaska include the late Holocene (1625-1825 cal yrs BP) aged Devil tephra, the middle Holocene (3650-4400 cal yrs BP) aged Jarvis Creek, Cantwell, and Tangle Lakes ashes, the middle Holocene (3360-4400 cal yrs BP) aged Watana tephras, and the early to middle Holocene aged Oshetna tephra (6570-7930 cal yrs BP). These distal tephra beds relate to Hayes Volcano proximal deposits (Mulliken 2016).

Three tephras were recognized in the stratigraphic columns at the DRO site (Table 5.1; Figures 5.1). The upper most tephra, T2, was the only volcanic ash sample that yielded geochemical results. The major oxide composition of the T2 sample is presented in Table 5.2. Similarity coefficients demonstrate that T2 at DRO is significantly correlated with the Devil and Watana tephras. The DRO T2 tephra shows a slightly weaker correlation with the Unit D tephra from the Hayes Volcano. The DRO T2 tephra has bracketing ages of 3970±30 BP (4520-4300 cal yrs BP; median probability: 4440 cal yr BP) and 3330±30 BP (3640-3480 cal yrs BP; median probability: 3570 cal yr BP).

The lower DRO tephras (T1b and T1a) were too fine grained and weathered, and a small in sample size of glass, to acquire reliable geochemical data to correlate with other tephras. Much of these tephra samples showed mixing of the ash with silt grains from loess deposits. A radiocarbon age of 6675±175 BP (7920-7255 cal yrs BP; median probability: 7550 cal yr BP) from Pedocomplex 2 directly underlies the DRO T1b tephra, while a radiocarbon age of 5980±30 BP (6890-6740 cal yrs BP; median probability: 6820 cal yr BP) from Pedocomplex 3. Radiocarbon ages of 7630±30 BP (8510-8380 cal yrs BP; median probability: 8420 cal yr BP) and 6675±175 BP (7920-7250 cal yrs BP; median probability: 7550 cal yr BP) bracket the DRO T1a tephra. Given the median probabilities of the bracketing cal yr BP ages, the DRO T2 deposition occurred between 4440 and 3570 cal yrs BP, the T1b accumulated between 7550 and 6820 cal yrs BP, and the T1a between 8240 and 7520 cal yrs BP. The timing and potential correlations between the DRO tephras will be explored further below.

Table 5.2. Major-oxide glass composition of DRO T2 tephra and and similarity coefficients to mSRV and Hayes River Outcrop tephras.

Major Oxides														
Sample		**SiO_2**	**TiO_2**	**Al_2O_3**	**FeO_T**	**MnO**	**MgO**	**CaO**	**Na_2O**	**K_2O**	**P_2O_5**	**Cl**	**TOTAL (raw)**	**n[1]**
DRO T2	mean	72.57	0.23	15.56	1.63	0.05	0.52	2.41	4.00	2.56	0.11	0.35	97.94	6
	1 δ	*1.15*	*0.02*	*1.08*	*0.17*	*0.03*	*0.03*	*0.58*	*0.12*	*0.24*	*0.05*	*0.05*	*1.74*	
Similarity Coefficients														
Tephras	Devil [2]	Watana (oxidized) [2]	Watana (unoxidized) [2]	Watana (bulk) [2]	Oshetna[2]	Unit H1[3]	Unit H2[3]	Unit G[3]	Unit F1[3]	Unit F2[3]	Unit E[3]	Unit D[3]	Unit B[3]	Unit A[3]
DRO T2	**0.95**	**0.97**	**0.96**	**0.95**	-	-	-	-	-	-	-	0.93	-	-

[1]Reported compositions are weight percent averages of n points, normalized to 100 percent, total gives original sum.
[2]Distal tephras from the middle Susitna River Valley (Dilley 1988; Dixon and Smith 1990; Mulliken 2016).
[3]Proximal tephras from the Hayes River Outcrop near the Hayes Volcano (Wallace et al. 2014).
Note: bold similarity coefficients, values ≥0.95, indicate the same eruptive event. Similarity coefficients >0.95 and 0.90 indicate weaker correlations. Similarity coefficients <0.90 indicate no statistical correlation and therefore not reported.

5.2.3.2 Particle Size Analysis (PSA)

Particle size analysis results for the DRO sediments and soils in Units 1 and 3 are present in Tables 5.3 and 5.4 and graphically in Figure 5.5. Unit 1 outwash sediment particles less than 2000 microns consist coarse to very fine sands, with more than 70% sand composition. The texture is a sandy loam. The particles are very poorly sorted with a polymodal distribution, symmetrical skewness, and mesokurtic (normal) in distribution. Unit 2 sand samples were not subject to PSA.

Unit 3 loess texture is primarily a silt loam with 76.6 to 51.3% silt content. Sand content within Unit 3 loess is dominated by fine to very fine sands. Clay content ranges between 15.6 and 4.0%. There is no apparent relationship between depth and silt and clay content. Unit 3 loess sorting ranges between very poorly to moderately well sorted with polymodal to unimodal distributions. The deepest Unit 3 sediments have a polymodal distribution and are very poorly sorted, while the distribution becomes increasingly unimodal and sorted higher in the column. Unit 3 skewness ranges between symmetrical to very finely skewed. Kurtosis ranges between mesokurtic to extremely leptokurtic (tails very close to the central mean). An increase in very fine sand deposition (51.4% content) is present in Unit 3 between Ab horizons in Loess 5 creating a sandy loam texture.

Tephra 2 was the only tephra with a sample size large enough for us to run PSA on. Tephra 2 has 76.6% silt, 20.9% sand (dominated by very fine sand fractions), and 2.5% clay contents.

Soils and soil groups in Unit 3 are primarily associated with siltier deposits, having silt content averages of 63.38±4.93% in entisols and 60.53±4.85% in inceptisols, while C horizons contain 55.43±11.23%. Sand average content for entisols is 27.36±5.20% and inceptisols is 31.62±6.03%, while C horizons have 38.87±11.69%. Clay content is higher in entisols and inceptisols with 9.26±2.70% and 7.84±1.78%, respectively, while C horizons display 5.70±1.93%.

Leehan (1981) conducted particle sizes analysis on sediment samples from the Upper Sands using a hydrometer method for the silt and clay fractions. Unit 10 (Sand 3) sand content ranges from 63.37 to 95.14%, silt ranges from 3.48 to 32.63%, and clay between 0 and 4%. Loess 9 has a sand content of 25.09%, silt content of 71.91%. and clay content of 3%. Unit 8 (Sand 4), Unit 7 (Loess 8) and Unit 6 (Sand 3) have between 74.34 and 96.15% sand, 3.53 and 25.08% silt, and 0% clay content. Unit 5 (Loess 9) has 17.89% sand, 77.53% silt, and 4.58% clay content. Unit 4 (Sand 2) has 83.04% sand, 16.94% silt, and 0% clay content.

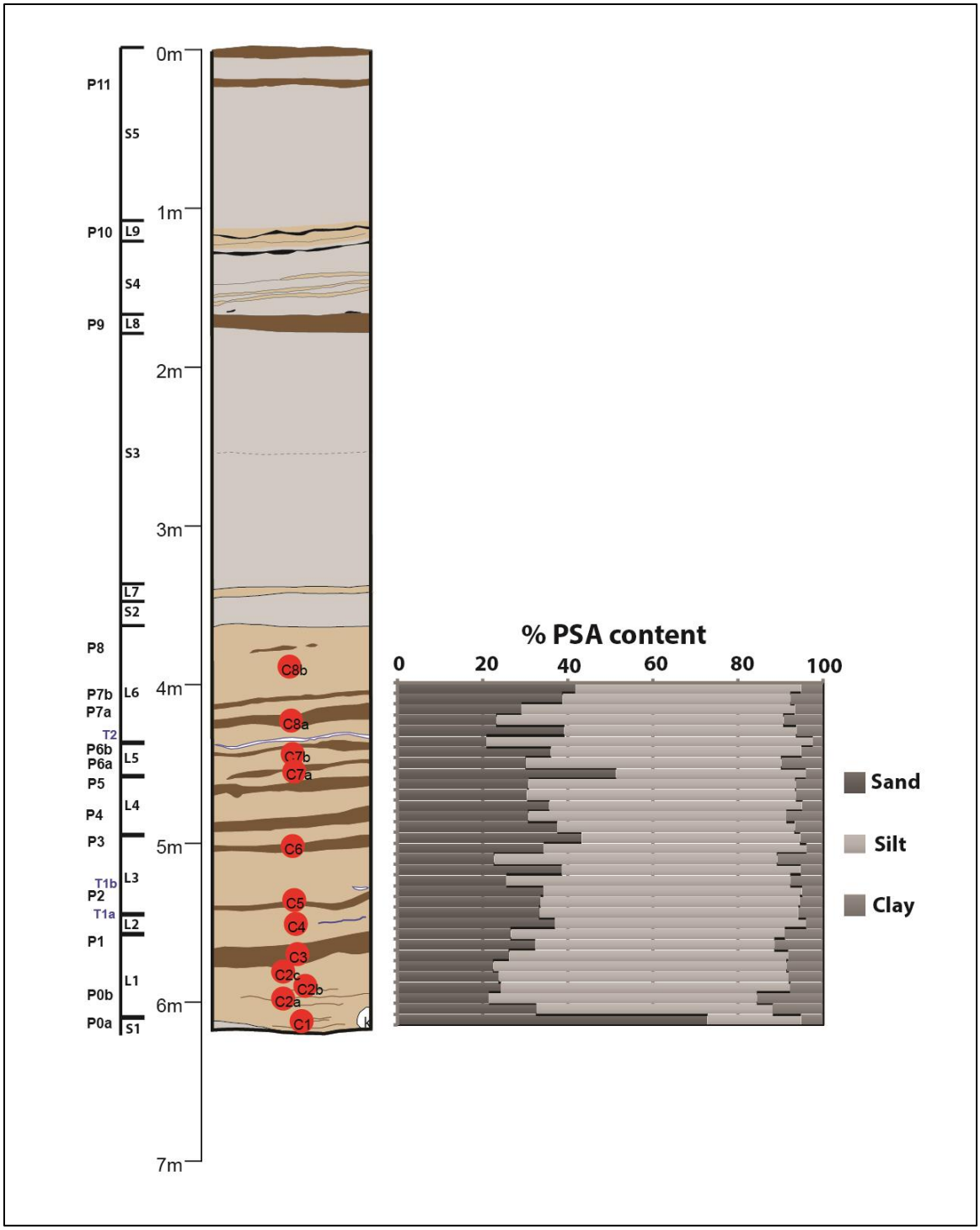

Figure 5.5. Generalized stratigraphic profile for the Delta River Overlook site with sand, silt and clay percentages in Units 1 and 3 by depth.

Table 5.3. Particle size analysis results on Delta River Overlook sediments and soils from Block B.

Unit (Soil horizon)	*Depth (cmBS)*[1]	*VCOS*[2]	*COS*[2]	*MS*[2]	*FS*[2]	*VFS*[2]	*% SAND*	*% SILT*	*% CLAY*	*TEXTURE*	*Site/Sample ID*
3 (C) - Loess 6	2.5	0.06	0.34	0.88	4.53	35.91	41.7	53.0	5.3	Silt loam	B-PSA-01
3 (Ab and ABwb) - Pedocomplex 7	5	0.08	0.38	0.73	2.30	35.25	38.7	53.6	7.6	Silt loam	B-PSA-02
3 (C) - Loess 6	6.5	0.00	0.13	0.49	2.33	26.11	29.1	64.3	6.7	Silt loam	B-PSA-03
3 (Ab) - Pedocomplex 7	11	0.02	0.13	0.21	0.98	21.90	23.2	67.4	9.3	Silt loam	B-PSA-04
3 (ABwb) - Pedocomplex 7	18.5	0.04	0.29	0.99	4.32	33.50	39.1	54.5	6.3	Silt loam	B-PSA-05
Tephra 2 (T2)	19	0.00	0.07	0.34	1.43	19.07	20.9	76.6	2.5	Silt loam	B-PSA-06
3 (C) - Loess 5	22	0.01	0.29	0.90	3.61	31.23	36.0	58.8	5.2	Silt loam	B-PSA-07
3 (Ab) - Pedocomplex 6	24	0.01	0.22	0.44	2.28	27.21	30.2	59.9	9.9	Silt loam	B-PSA-08
3 (C) - Loess 5	34	0.01	0.10	0.32	3.61	47.31	51.4	44.5	4.1	Sandy loam	B-PSA-09
3 (Ab) - Pedocomplex 6	36.5	0.00	0.09	0.23	1.67	28.79	30.8	62.7	6.6	Silt loam	B-PSA-10
3 (ABwb) - Pedocomplex 6	40	0.00	0.11	0.27	1.47	28.54	30.4	63.1	6.5	Silt loam	B-PSA-11
3 (C) - Loess 5	43.5	0.01	0.18	0.46	2.91	32.10	35.7	59.4	5.0	Silt loam	B-PSA-12
3 (ABwb) - Pedocomplex 5	50	0.00	0.07	0.15	1.07	29.35	30.6	60.6	8.7	Silt loam	B-PSA-13
3 (Ab) - Pedocomplex 5	52.5	0.03	0.05	0.14	1.36	35.95	37.5	55.7	6.8	Silt loam	B-PSA-14
3 (C) - Loess 4	53	0.00	0.13	0.20	2.24	40.64	43.2	51.3	5.5	Silt loam	B-PSA-15
3 (C) - Loess 4	64	0.00	0.04	0.20	3.01	31.09	34.3	61.8	3.9	Silt loam	B-PSA-16
3 (Ab and ABwb) - Pedocomplex 4	69.5	0.00	0.28	0.60	1.26	20.54	22.7	66.5	10.8	Silt loam	B-PSA-17
3 (C) - Loess 4	75	0.00	0.06	0.14	1.93	36.54	38.7	56.0	5.4	Silt loam	B-PSA-18
3 (Ab) - Pedocomplex 3	82	0.02	0.06	0.13	1.08	24.22	25.5	66.9	7.6	Silt loam	B-PSA-19
3 (Ck) - Loess 3	91	0.00	0.07	0.12	2.25	31.75	34.2	60.9	5.0	Silt loam	B-PSA-20
3 (Ck) - Loess 3	99.5	0.00	0.03	0.12	2.11	31.33	33.6	60.9	5.5	Silt loam	B-PSA-21
3 (Bwb and ABwb) - Pedocomplex 2	103	0.03	0.12	0.45	2.93	29.71	33.2	60.9	5.9	Silt loam	B-PSA-22
3 (Ck) - Loess 2	119.5	0.00	0.02	0.11	2.38	34.39	36.9	59.1	4.0	Silt loam	B-PSA-23
3 (Ab and ABwb) - Pedocomplex 1	130.5	0.04	0.14	0.48	1.78	24.09	26.5	64.4	9.0	Silt loam	B-PSA-24
3 (C) - Loess 1	137.5	0.04	0.27	0.67	2.17	29.18	32.3	56.3	11.4	Silt loam	B-PSA-25
3 (Ab) - Pedocomplex 0	149	0.01	0.15	0.23	1.21	24.60	26.2	65.5	8.3	Silt loam	B-PSA-26

3 (Ab) - Pedocomplex 0	155	0.01	0.11	0.20	0.99	21.13	22.4	69.0	8.6	Silt loam	B-PSA-27
3 (Ab) - Pedocomplex 0	167.5	0.01	0.13	0.25	1.07	22.29	23.8	68.1	8.2	Silt loam	B-PSA-28
3 (C) - Loess 1	181.5	0.01	0.14	0.34	1.40	22.38	24.3	67.9	7.8	Silt loam	B-PSA-29
3 (Ab) - Pedocomplex 0	189	0.14	1.07	1.95	1.83	16.47	21.4	63.0	15.6	Silt loam	B-PSA-30
3 (Ab) - Pedocomplex 0	194.5	1.01	4.20	6.68	4.62	16.04	32.5	55.6	11.8	Silt loam	B-PSA-31
1 (C)	206	6.68	14.02	20.59	17.68	13.82	72.8	21.9	5.3	Sandy loam	B-PSA-32

[1]Depth below the surface of Block B.
[2]VCOS= very coarse sand; COS= coarse sand; MS= medium sand; FS= fine sand; VFS= very fine sand.

Table 5.4. Particle size mean, sorting, skewness, and kurtosis analyses on Delta River Overlook sediments and soils from Block B.

		FOLK AND WARD METHOD (mm)				*FOLK AND WARD METHOD (ϕ)*				*FOLK AND WARD METHOD (Description)*			
sample	**sample type**	**mean**	**sorting**	**skewness**	**kurtosis**	**mean**	**sorting**	**skewness**	**kurtosis**	**mean**	**sorting**	**skewness**	**kurtosis**
B-PSA-01	Unimodal, Poorly Sorted	40.95	2.70	-0.64	1.06	4.61	1.43	0.64	1.06	Very Coarse Silt	Poorly Sorted	Very Fine Skewed	Mesokurtic
B-PSA-02	Unimodal, Poorly Sorted	45.96	2.43	-0.66	1.60	4.44	1.28	0.66	1.60	Very Coarse Silt	Poorly Sorted	Very Fine Skewed	Very Leptokurtic
B-PSA-03	Unimodal, Poorly Sorted	34.52	2.68	-0.65	0.72	4.86	1.42	0.65	0.72	Very Coarse Silt	Poorly Sorted	Very Fine Skewed	Platykurtic
B-PSA-04	Unimodal, Poorly Sorted	32.91	2.68	-0.59	0.70	4.93	1.42	0.59	0.70	Very Coarse Silt	Poorly Sorted	Very Fine Skewed	Platykurtic
B-PSA-05	Unimodal, Poorly Sorted	45.11	2.54	-0.63	1.45	4.47	1.34	0.63	1.45	Very Coarse Silt	Poorly Sorted	Very Fine Skewed	Leptokurtic
B-PSA-06	Unimodal, Poorly Sorted	38.31	2.58	-0.77	0.79	4.71	1.37	0.77	0.79	Very Coarse Silt	Poorly Sorted	Very Fine Skewed	Platykurtic
B-PSA-07	Unimodal, Poorly Sorted	36.22	2.85	-0.60	0.84	4.79	1.51	0.60	0.84	Very Coarse Silt	Poorly Sorted	Very Fine Skewed	Platykurtic
B-PSA-08	Unimodal, Poorly Sorted	36.00	2.65	-0.72	0.73	4.80	1.41	0.72	0.73	Very Coarse Silt	Poorly Sorted	Very Fine Skewed	Platykurtic
B-PSA-09	Unimodal, Poorly Sorted	44.75	2.44	-0.69	1.40	4.48	1.29	0.69	1.40	Very Coarse Silt	Poorly Sorted	Very Fine Skewed	Leptokurtic
B-PSA-10	Unimodal, Poorly Sorted	37.10	2.62	-0.76	0.75	4.75	1.39	0.76	0.75	Very Coarse Silt	Poorly Sorted	Very Fine Skewed	Platykurtic
B-PSA-11	Unimodal, Poorly Sorted	37.31	2.61	-0.77	0.76	4.74	1.38	0.77	0.76	Very Coarse Silt	Poorly Sorted	Very Fine Skewed	Platykurtic
B-PSA-12	Unimodal, Poorly Sorted	36.92	2.78	-0.66	0.83	4.76	1.47	0.66	0.83	Very Coarse Silt	Poorly Sorted	Very Fine Skewed	Platykurtic

B-PSA-13	Unimodal, Poorly Sorted	39.14	2.53	-0.78	0.84	4.68	1.34	0.78	0.84	Very Coarse Silt	Poorly Sorted	Very Fine Skewed	Platykurtic
B-PSA-14	Unimodal, Poorly Sorted	44.36	2.31	-0.80	1.22	4.49	1.21	0.80	1.22	Very Coarse Silt	Poorly Sorted	Very Fine Skewed	Leptokurtic
B-PSA-15	Unimodal, Poorly Sorted	40.93	2.46	-0.79	0.93	4.61	1.30	0.79	0.93	Very Coarse Silt	Poorly Sorted	Very Fine Skewed	Mesokurtic
B-PSA-16	Unimodal, Poorly Sorted	42.19	2.57	-0.67	1.13	4.57	1.36	0.67	1.13	Very Coarse Silt	Poorly Sorted	Very Fine Skewed	Leptokurtic
B-PSA-17	Unimodal, Poorly Sorted	33.23	2.69	-0.59	0.70	4.91	1.43	0.59	0.70	Very Coarse Silt	Poorly Sorted	Very Fine Skewed	Platykurtic
B-PSA-18	Unimodal, Poorly Sorted	39.37	2.52	-0.78	0.85	4.67	1.33	0.78	0.85	Very Coarse Silt	Poorly Sorted	Very Fine Skewed	Platykurtic
B-PSA-19	Unimodal, Poorly Sorted	31.88	2.69	-0.54	0.69	4.97	1.43	0.54	0.69	Very Coarse Silt	Poorly Sorted	Very Fine Skewed	Platykurtic
B-PSA-20	Unimodal, Poorly Sorted	36.96	2.62	-0.76	0.75	4.76	1.39	0.76	0.75	Very Coarse Silt	Poorly Sorted	Very Fine Skewed	Platykurtic
B-PSA-21	Unimodal, Poorly Sorted	53.10	2.12	-0.67	4.71	4.24	1.08	0.67	4.71	Very Coarse Silt	Poorly Sorted	Very Fine Skewed	Extremely Leptokurtic
B-PSA-22	Unimodal, Poorly Sorted	42.88	2.57	-0.66	1.20	4.54	1.36	0.66	1.20	Very Coarse Silt	Poorly Sorted	Very Fine Skewed	Leptokurtic
B-PSA-23	Unimodal, Moderately Well Sorted	73.82	1.59	-0.27	4.70	3.76	0.67	0.27	4.70	Very Fine Sand	Moderately Well Sorted	Fine Skewed	Extremely Leptokurtic
B-PSA-24	Unimodal, Moderately Well Sorted	74.96	1.53	-0.19	4.34	3.74	0.61	0.19	4.34	Very Fine Sand	Moderately Well Sorted	Fine Skewed	Extremely Leptokurtic
B-PSA-25	Unimodal, Poorly Sorted	37.45	2.76	-0.67	0.85	4.74	1.46	0.67	0.85	Very Coarse Silt	Poorly Sorted	Very Fine Skewed	Platykurtic
B-PSA-26	Unimodal, Poorly Sorted	32.35	2.69	-0.56	0.69	4.95	1.43	0.56	0.69	Very Coarse Silt	Poorly Sorted	Very Fine Skewed	Platykurtic
B-PSA-27	Unimodal, Poorly Sorted	27.47	2.75	-0.32	0.65	5.19	1.46	0.32	0.65	Coarse Silt	Poorly Sorted	Very Fine Skewed	Very Platykurtic

B-PSA-28	Unimodal, Poorly Sorted	29.14	2.73	-0.40	0.67	5.10	1.45	0.40	0.67	Coarse Silt	Poorly Sorted	Very Fine Skewed	Very Platykurtic
B-PSA-29	Unimodal, Poorly Sorted	34.26	2.67	-0.65	0.71	4.87	1.42	0.65	0.71	Very Coarse Silt	Poorly Sorted	Very Fine Skewed	Platykurtic
B-PSA-30	Unimodal, Poorly Sorted	39.24	3.15	-0.48	1.12	4.67	1.65	0.48	1.12	Very Coarse Silt	Poorly Sorted	Very Fine Skewed	Leptokurtic
B-PSA-31	Polymodal, Very Poorly Sorted	74.78	4.74	0.00	1.06	3.74	2.25	0.00	1.06	Very Fine Sand	Very Poorly Sorted	Symmetrical	Mesokurtic
B-PSA-32	Polymodal, Very Poorly Sorted	367.48	4.29	0.10	1.06	1.44	2.10	-0.10	1.06	Medium Sand	Very Poorly Sorted	Symmetrical	Mesokurtic

5.2.3.3 Soil Organic Carbon

Soil organic carbon ($\%OC_{LOI}$) on DRO Units 1 and 3 sediments and soils ranges from 9.90 to 0.82% with an average of 2.72±1.82%. Unit 1 outwash exhibits the lowest value with 0.82%. Unweathered loess horizons (C horizons) has a range of $\%OC_{LOI}$ values between 2.67 and 1.26% with an average of 1.80±0.42%. Immature entisols (Ab horizons) show a range of values between 7.26 and 1.51% with an average of 3.27±1.74% std. The pedocomplexes with more mature inceptisols (ABwb and Bwb horizons) shows a range of values between 9.90 and 2.15% with an average of 3.88±2.77%. There appears to be no relationship between depth and $\%OC_{LOI}$ values. Soil organic carbon ($\%OC_{LOI}$) measurements on DRO sediment and soil samples are presented in Table 5.5 and graphically represented in Figure 5.6.

5.2.3.4 Inorganic Carbon

The presence of carbonates ($\%CaCO_3$) are relatively low throughout Unit 1 and 3 sediments (Table 5.5). Results based on LOI, $\%CaCO_{3LOI}$ ranges between 1.81 and 5.39% with an average of 4.16±0.73%. There is no apparent relationship with depth (Figure 5.6). The lowest values appear in Unit 1 and Tephra 2 (2.59 and 1.81 $\%CaCO_{3LOI}$, respectively). In the Unit 3 loess, unweathered silt (C horizons) values range between 3.65 and 4.74% with an average of 4.22±0.37%. Entisols (Ab horizons) range between 3.37 and 5.39% with an average of 4.35±0.74%. Inceptisols (ABwb and Bwb horizons) have similar values between 3.44 and 4.76% with an average of 4.32±0.48%.

Results based on gasometry (chittick) show similar patterns to those produced by LOI. $\%CaCO_{3gas}$ for all sediments and soil samples range from 0.00 and 0.37% with an average of 0.07±0.09 $\%CaCO_{3gas}$. $\%CaCO_{3gas}$ for C horizons ranges between 0.00 and 0.37% with an average of 0.07±0.10 $\%CaCO_{3gas.}$ $\%CaCO_{3gas}$ for entisol horizons ranges between 0.00 and 0.14% with an average of 0.05±0.05 $\%CaCO_{3gas}$. $\%CaCO_{3gas}$ for inceptisol horizons ranges between 0.00 and 0.34% with an average of 0.10±0.13 $\%CaCO_{3gas}$.

As mentioned above, LOI tends to provide higher estimates for organic and inorganic carbon components than gasometric (i.e., chittick) methods. LOI value overestimates can be due to variances in clay content and mineralogy, high structural water content in clays, and presence of sources of elemental carbon such as bituminous coal. The largest source of over-estimation can be sediments with higher clay content and an increased amount of structural water content. LOI can produce overestimates between 1 to 5% (Dean 1974; Stein 1984) depending on the amount of clay in a given sample. Given that many of these samples range between 1 to 5% for both $\%OC_{LOI}$ and $\%CaCO_{3LOI}$ there appears to be very little of both within the sediments and soils with the exception of the samples from soils that range >5%.

Table 5.5. Organic (%OC) and inorganic (%$CaCO_3$) carbon and pH data on sediments and soils from DRO Block B.

Depth (cmBS)[1]	*Unit (Soil Horizons)*	*%OC_{LOI} (550 ℃)*	*%$CaCO_{3LOI}$ (1000 ℃)*	*%$CaCO_{3qas}$ (chittick)*	*pH value*	*Munsell - wet*	*Munsell - dry*	*Sample No.*
2.5	3 (C) Loess 6	1.70	4.25	0.00	7.36	10YR 3/2	10YR 5/4	B-PSA-01
5	3 (Ab and ABwb) Pedocomplex 7	3.97	4.73	0.20	7.19	7.5YR 3/2 to 2.5/2	7.5YR 4/2	B-PSA-02
6.5	3 (C) Loess 6	1.40	4.56	0.10	7.29	10YR 4/2 to 3/2	10YR 5/3 to 4/3	B-PSA-03
11	3 (Ab) Pedocomplex 7	4.78	5.23	0.05	7.42	7.5YR 3/1 to 3/2	7.5YR 4/2 to 4/3	B-PSA-04
18.5	3 (ABwb) Pedocomplex 7	2.15	4.42	0.00	7.38	7.5YR 2.5/2	7.5YR 3/2 to 3/3	B-PSA-05
19	Tephra 2 (T2)	2.89	1.81	0.05	7.73	10YR 7/1 to 6/1	10YR 8/1 to 8/3	B-PSA-06
22	3 (C) Loess 5	2.30	3.69	0.09	7.79	10YR 4/2 to 3/2	10YR 5/4 to 6/4	B-PSA-07
24	3 (Ab) Pedocomplex 6	3.25	3.69	0.04	7.87	7.5YR 3/2 to 3/3	7.5YR 4/4 to 3/2	B-PSA-08
34	3 (C) Loess 5	1.26	4.53	0.10	7.95	10YR 4/2 to 4/3	10YR 5/3 to 5/4	B-PSA-09
36.5	3 (Ab) Pedocomplex 6	1.51	4.49	0.10	7.77	10YR 3/1 to 3/2	10YR 5/2 to 5/3	B-PSA-10
40	3 (ABwb) Pedocomplex 6	2.53	4.76	0.10	7.82	7.5YR 2.5/2 to 2.5/3	7.5YR 4/4 to 4/2	B-PSA-11
43.5	3 (C) Loess 5	1.80	3.92	-0.04	7.96	10YR 4/2 to 4/3	10YR 5/3 to 5/4	B-PSA-12
50	3 (ABwb) Pedocomplex 5	2.28	3.44	0.00	7.83	7.5YR 2.5/3	7.5YR 4/2 to 3/2	B-PSA-13
52.5	3 (Ab) Pedocomplex 5	4.01	4.03	0.04	7.88	7.5YR 2.5/2	7.5YR 3/2 to 2.5/3	B-PSA-14
53	3 (C) Loess 4	2.67	4.23	0.00	7.81	10YR 4/2 to 4/3	10YR 6/4 to 5/4	B-PSA-15
64	3 (C) Loess 4	1.72	4.11	0.00	7.85	10YR 4/3 to 4/4	10YR 5/4	B-PSA-16
69.5	3 (Ab and ABwb) Pedocomplex 4	9.90	4.40	0.34	7.82	7.5YR 3/2 to 2.5/2	7.5YR 4/2 to 3/3	B-PSA-17
75	3 (C) Loess 4	2.35	4.03	0.19	7.91	10YR 4/3	10YR 5/3 to 5/4	B-PSA-18
82	3 (Ab) Pedocomplex 3	7.26	4.05	0.14	7.76	10YR 4/1 to 4/2	10YR 5/2 to 5/3	B-PSA-19
91	3 (Ck) Loess 3	1.91	3.94	0.05	7.89	10YR 4/2 to 3/2	10YR 5/2 to 5/3	B-PSA-20

99.5	3 (Ck) Loess 3	1.87	4.74	0.37	8.04	10YR 4/1 to 4/2	10YR 5/1 to 5/2	B-PSA-21
103	3 (Bwb and ABwb) Pedocomplex 2	2.37	3.88	0.00	7.96	10YR 3/1 to 3/2	7.5YR 4/1 to 3/2	B-PSA-22
119.5	3 (Ck) Loess 2	1.50	3.65	0.00	7.99	10YR 4/2 to 3/2	10YR 6/3 to 5/3	B-PSA-23
130.5	3 (Ab and ABwb) Pedocomplex 1	3.99	4.58	0.09	7.85	7.5YR 2.5/2	7.5YR 4/3 to 3/2	B-PSA-24
137.5	3 (C) Loess 1	1.65	4.72	0.05	8.01	10YR 4/2 to 4/3	10YR 5/3 to 6/3	B-PSA-25
149	3 (Ab) Pedocomplex 0	1.56	4.57	0.00	8.01	10YR 4/3 to 4/4	10YR 5/3	B-PSA-26
155	3 (Ab) Pedocomplex 0	2.14	3.50	0.00	7.98	10YR 4/2 to 4/3	10YR 5/3 to 5/4	B-PSA-27
167.5	3 (Ab) Pedocomplex 0	2.29	3.37	0.00	8.09	10YR 4/2 to 4/3	10YR 5/3 to 5/4	B-PSA-28
181.5	3 (C) Loess 1	1.34	4.50	0.10	8.13	10YR 4/2 to 4/3	10YR 5/3 to 5/4	B-PSA-29
189	3 (Ab) Pedocomplex 0	3.15	5.15	0.05	7.91	7.5YR 3/1 to 3/2	7.5YR 4/2 to 3/2	B-PSA-30
194.5	3 (Ab) Pedocomplex 0	2.77	5.39	0.05	-	-	-	B-PSA-31
206	1 (C)	0.82	2.59	0.00	7.94	10YR 4/2 to 3/2	10YR 5/4 to 4/4	B-PSA-32

[1]Depth below the surface of Block B.

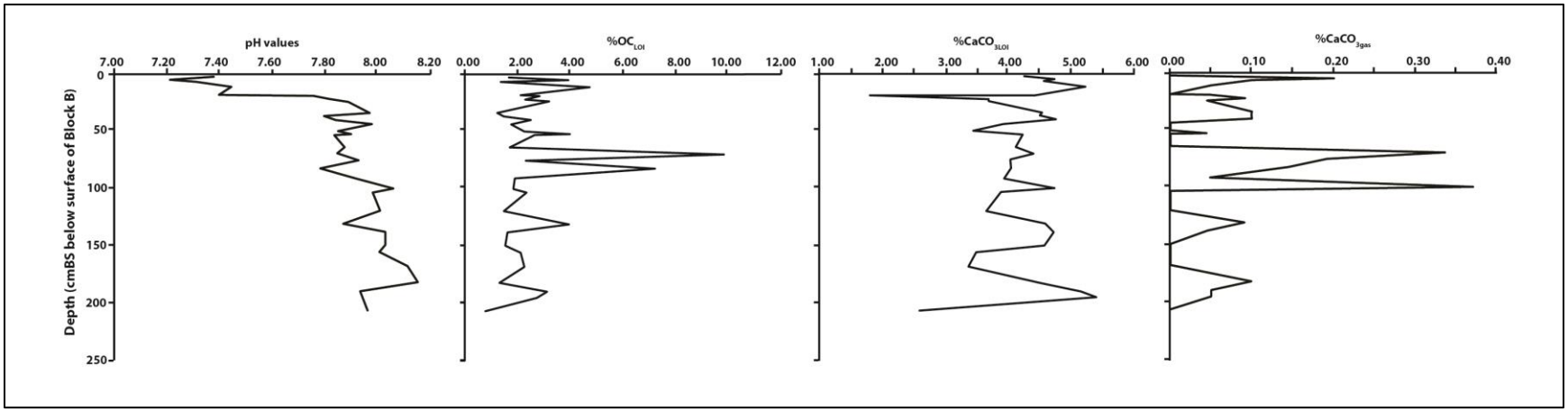

Figure 5.6. Delta River Overlook sediment and soils pH and organic (%OC) and inorganic ($\%CaCO_3$) carbon data by depth.

5.2.3.5 pH Scale Measurement

The DRO sediments and soils are neutral to alkaline throughout section (Table 5.5). The range is between 7.19 and 8.13 with an average of 7.81±0.24. There is a general trend of sediments being more alkaline with greater depth (Figure 5.6). Pedocomplexes with more mature inceptisols (ABwb and Bwb horizons) have slightly more neutral pH average values (7.69±0.29) than pedocomplexes with solely immature entisols (Ab horizons; 7.85±0.19) and relatively unweathered loess horizons (C horizons; 7.85±0.24). Pedocomplexes with solely Ab horizons have similar average pH values to C horizons. Both have slightly more alkaline values than the overall average pH values for DRO sediments and soils that likely a reflection of the lack of maturity in the development time of the Ab horizons. There is no evident relationship between pH values and $\%OC_{LOI}$ and $\%CaCO_{3LOI}$ values (Figure 5.7).

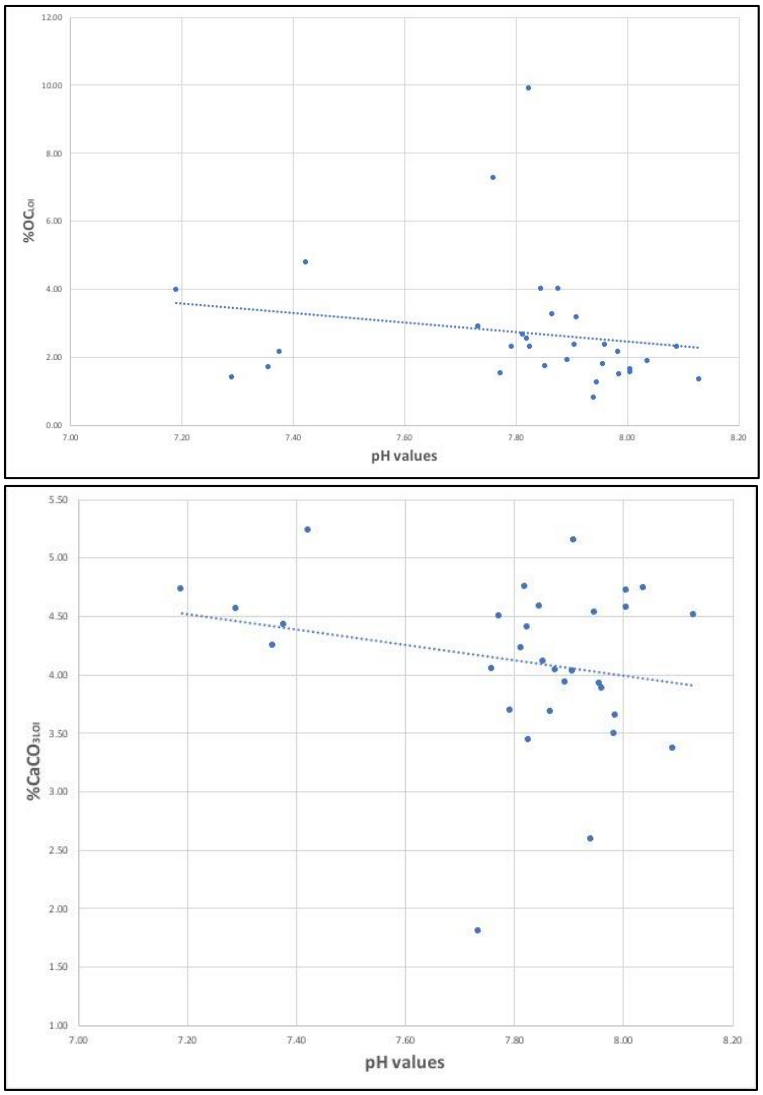

Figure 5.7. pH values vs. percent organic (%OC; above) and inorganic (%CaCO3; below) carbon data in Delta River Overlook sediments and soils.

5.3 Hurricane Bluff Results

The stratigraphy at the Hurricane Bluff site generally consists of around 360 cm of unconsolidated aeolian sands and silts that overlay glaciofluvial sands, gravels, cobbles, and boulders (Figure 5.8). The lithostratigraphy of the Hurricane Bluff site is summarized below and detailed in Table 5.6.

Higgs et al. (1999) originally designated the Hurricane Bluff site units into a sand sequence (Sand 1 though 8). We did not use Higgs et al.'s sand sequence designation in this study, although we have referenced it in Table 5.6.

5.3.1 Lithostratigraphy

Unit 1 is the very poorly-sorted mixture of sand, gravels, cobbles and boulders that comprise the matrix of the terraced landform. The matrix is glaciofluvial in origin (i.e., glacial outwash or drift), and the description and ages of these deposits are the same as Unit 1 in the Delta River Overlook site lithostratigraphy described above.

Unit 2 is the thickest package of aeolian sediments in the Hurricane Bluff stratigraphic column. The archaeology at the Hurricane Bluff site is contained within Unit 2 (Higgs et al. 1999, Potter et al. 2007). Unit 2 consists of ~320 cm thick silt to sandy loam deposits that represent loess accumulation. Unit 2 silt loams range in silt content between 67 and 50%, with 44 to 22% sand and 12 to 4% clay. Unit 2 sandy loams have sand contents between 69 and 46%, with 49 to 25% silt and 8 to 3% clay. Unit 2 loams have 42 to 40% sand, ~49% silt, and 11 to 7% clay content (see below for more details on the Particle Size Analysis results). Most of the Unit 2 deposits are massive in their structure, with the exception of a horizontally bedded sandy loam between 185-235 cmBS.

Unit 2 loess accumulation commenced well before 10,000 cal yr BP, based on the ages of Pedocomplex 1. It continued to accumulate intermittently throughout the Holocene to ~1800-1500 cal yrs BP, the age of based on the radiocarbon ages from Paleosol 9 (Table 5.6). Nine buried soils or complexes of buried soils (Pedocomplexes 0-2 and 5-6, Paleosols 3,4, and 7-9) are contained with the Unit 2 loess deposits, and are described in more detail below. The sandy loam and silt loam between 247.5 and 265 cm in Unit 2 are carbonate-rich (between 0.77 and 1.30% in $\%CaCO_3$ content) with visible carbonate accumulations within the sediment matrix. Redoximorphic features were only observed in Unit 2 loess between 185 and 360 cmBS. Redoximorphic features consist of masses and circular to ovular shaped iron accumulations in the sediment matrices. These features are common (2 to <20% surface coverage) in several portions of the sediments at this depth. A radiocarbon date of 6950-6800 cal yrs BP was obtained on a terrestrial snail shell recovered from the silt loam to sandy loam transition between 185-250 cmBS in Unit 2 (Table 5.6).

Two volcanic ash deposits (tephras) were observed within Unit 2 (Table 5.6 and Figure 5.8). Tephra 1 is the deepest tephra currently recognized at Hurricane Bluff, situated ~240 cmBS, between Pedocomplex 2 and Paleosol 3 (described below). Tephra 1 is a ≤1 cm thick, discontinuous whitish gray silt loam. This tephra deposit was first recognized by Higgs et al. (1999).

Tephra 2 is the highest tephra in the DRO stratigraphy situated between 122.5-135 cmBS. Tephra 2 was not reported in Higgs et al. (1999). This ash is a ≤0.5 cm thick, discontinuous whitish to very pale brown silt loam. Tephra 2 glass is very fine silt to clay. Tephra 2 is situated directly above a 1-2 cm thick O/Ab horizon, and between Pedocomplex 6 and Paleosol 7. The timing of these volcanic ash falls and their potential correlation to proximal and distal tephras are discussed below in this chapter in the section on tephra characterization.

Unit 3 consists of an 4-5 cm thick sandy loam (aeolian deposit) that overlies Unit 2 loess. The contacts between Units 3 and 2 is very abrupt. Higgs et al. (1999), and subsequently Potter et al. (2007), referred to this unit as a tephra ("Tephra 1"); however, this sandy loam does not show signs of pyroclastic contents. Unit 3 particles are loose in structure and show very little signs of weathering or illuvial accumulation. Unit 4 is a 15 cm thick massive sandy loam to loam. The sandy loam is carbonate-rich (>1% in $\%CaCO_{3gas}$ content). This aeolian silt bed was deposited on top of Unit 3 and shows more signs of soil development and weathering. This loam has very little carbonate content (0.20% in $\%CaCO_{3gas}$) compared to the underlying sandy loam.

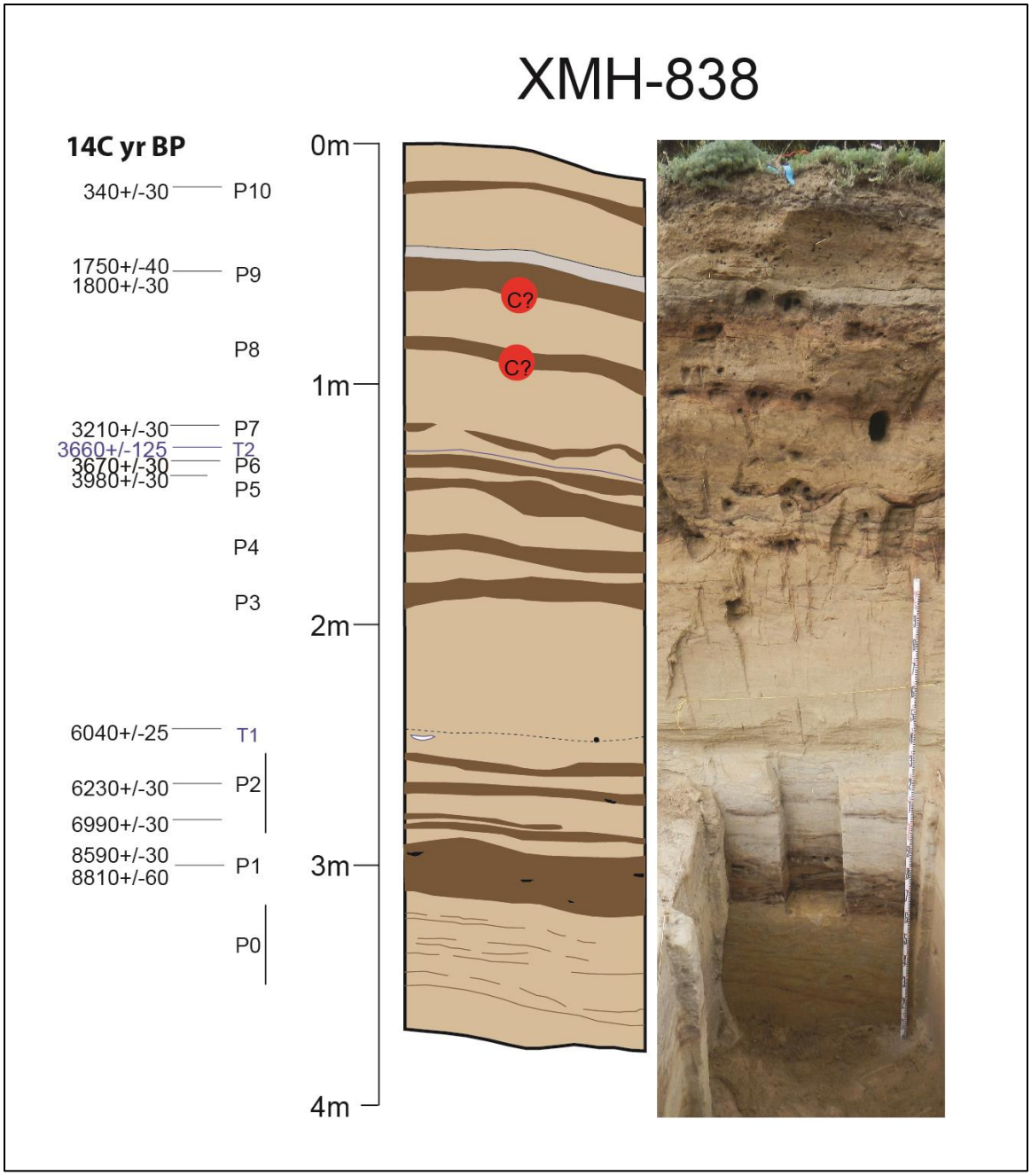

Figure 5.8. Generalized stratigraphic profile at the Hurricane Bluff site. "P" refers to paleosols and pedocomplexes; red dots with "C" refer to archaeological components in Higgs et al. (1999) and Potter et al. (2007).

Table 5.6. Descriptions of the Hurricane Bluff site stratigraphy.

Unit (Soil Horizon) – This Study	*Unit (Soil Horizon) – Higgs et al. 1999*	*General Depth (cmBS)*	*Thickness (cm) Range*	*Description*
4 (OA)	-	0-3	2-3	Modern vegetative growth and litter; loam; partially to moderately decomposed organics; slightly moist to dry; abrupt and smooth to slightly wavy boundary.
4 (C)	Sand 1 (S1)	3-15	9-12	Gray (10 YR 5/1) sandy loam; bedded; dry; abrupt and smooth boundary. Horizontal laminations (1-2 mm) consist of sand bound in grass that has grown at the top of each lamination.
4 (A/Ob) Paleosol 10	Paleosol 1 (P1)	15-22	2.5-7	Paleosol 10 (A/Ob horizon) – brown to dark brown (7.5YR 4/2 to 3/2) loam; massive; dry to slightly moist; continuous; clear to smooth boundary. Buried soil horizon exhibits more characteristics of an A horizon, but retains some partially to moderately decomposed organics in the upper part of the horizon. This soil developed on a finer sandy silt deposit.
4 (Ck)	Sand 2 (S2)	17.5-42.5	15-25	Light brownish gray to gray (10YR 6/2 to 6/1) sandy loam; massive; slightly moist; continuous; very abrupt to abrupt, smooth boundary. Deposit contains more fine and very fine sand particles than the coarser underlying sand deposit. This deposit fines upward into the loam that Paleosol 1 developed on. This C horizon has higher values of carbonates ($CaCO_3$).
3 (C)	Tephra 1 (T1)	40-45	4-5	Brown to grayish brown (10YR 5/3 to 5/2) sandy loam; loose structure (singular grained)**;** dry; continuous; very abrupt, smooth boundary. Deposit contains more very coarse and coarse sand particles than the overlying and underlying deposits. There is very little to no weathering evident in this deposit. Higgs et al. (1999) originally identified this as a tephra deposit, however pyroclastic materials was not observed among particles in bulk samples.
2 (Ab and Bwb) Paleosol 9	Paleosol 2 (P2)	42.5-60	12.5-15	Paleosol 9 (Ab and Bwb horizons) – brown (7.5YR 4/4 to 4/2) silt loam; massive to platy structure; dry; continuous; abrupt to clear, smooth to slightly wavy boundary. The upper 5-7 cm of this buried soil is a brown organic-rich silt loam (Ab horizon). This Ab horizon has a platy structure that will separate into flat, tabular-like units. The lower 8-10 cm of this buried soil is an oxidized brown silt loam (Bwb horizon) that is more reddish in coloration, massive in structure, and has less organic content that the upper Ab horizon. Radiocarbon date on charcoal recovered from the Bwb horizon: 340+/-40 B.P. (Beta-386243).
2 (C)	Sand 3 (S3)	60-85	17.5-22.5	Yellowish brown to brown (10YR 5/4 to 5/3) sandy loam; massive; dry; continuous; abrupt to clear, smooth to slightly wavy boundary. This deposit has an increase in medium and fine sand fractions when compared to the underlying and overlying deposits.

2 (Ab and Bwb) Paleosol 8	Paleosol 3 (P3)	75-97.5	5-10	Paleosol 8 (Ab and Bwb horizons) – brown to dark brown silt loam (7.5 YR 4/2 to 3/2); massive; dry; discontinuous; clear, broken and slightly wavy boundary. The upper 3-5 cm of this buried soil is a brown organic-rich silt loam (Ab horizon). The lower 3-4 cm of this buried soil is an oxidized brown silt loam (Bwb horizon) that is more reddish in coloration and has less organic content than the upper Ab horizon. Radiocarbon dates on charcoal recovered from the Bwb horizon: 1750+/-40 B.P. (Beta-123338) and 1800+/-30 B.P. (Beta-386244).
2 (C and Ab)	Sand 4 (S4)	80-120	27.5-35	Dark yellowish brown to brown (10YR 4/4 to 4/3) silt loam; massive; dry; continuous; abrupt, smooth to slightly wavy boundary. The upper 10 cm of this horizon is a brown silt loam with minor amounts of weathering and oxidization. Within the middle 10 cm of this horizon is a darker brown silt loam that is likely a very weakly expressed soil (Ab horizon). The darker brown silt loam is between 3-5 cm thick and has slightly more organic content than the underlying and overlying brown silts. The lower 7-9 cm of this horizon consists of brown silt that displays the lowest organic content in the horizon and shows little signs of weathering and oxidization.
2 (Ab and Bwb) Paleosol 7	Paleosol 4 (P4)	112-121	3-4	Paleosol 7 (Ab and Bwb horizons) – brown to dark brown (7.5YR 4/2 to 3/2) and grayish brown (10YR 5/2) silt loam; massive; dry; discontinuous; abrupt, smooth to wavy and broken boundary. Buried soil shows differential expressions of horizonation across the erosional edge. In most areas, the soil is expressed as darker brown silt (Ab horizon) with little oxidization evident. To a more limited extent, this soil is also expressed as reddish grayish brown silt (possible Bwb horizon) that displays oxidization. Wood charcoal is evident in both the darker brown and reddish dark brown silts. Radiocarbon date on charcoal recovered from the Bwb horizon: 3210+/-30 B.P. (Beta-386245).
2 (C)	Sand 5 (S5)	115-135	4-10	Yellowish brown to brown (10YR 5/4 to 5/3) silt loam; massive; dry; continuous; abrupt, smooth boundary.
Tephra 2 (T2); O/Ab horizon	-	122.5-135	1-2	Tephra 2 (T2) – brown (10YR 5/3) tephra was deposited within this silt loam. The tephra is discontinuous, 0.5 cm or less in thickness, and very fine glass particles (very fine silt to clay sized). A very weakly developed buried soil (O/Ab horizon) underlies Tephra 2. This soil is 1-2 cm thick and discontinuous with very abrupt and smooth boundaries. This soil has partially to moderately decayed and platy organics present, along with some wood charcoal. Radiocarbon date on charcoal recovered from the O/Ab horizon: 3670+/-30 B.P. (Beta-386246). The bracketing ages of Tephra 2 place its deposition within the time frame of the regional deposition of a Hayes Volcano ashfall around 3660 +/- 125 B.P. (Begét et al. 1991).
2 (Ab horizons) Pedocomplex 6	Paleosol 5 (P5)	125-140	5-6	Pedocomplex 6 (Ab horizons) – brown (7.5YR 4/4) silt loams; massive; dry; discontinuous; abrupt, smooth and broken boundaries. Pedocomplex 6 consists of at least a couplet of dark brown silt loams (Ab horizons) that are 2-3 cm thick and separated by 2-3 cm of unweathered yellowish brown (10YR 5/4) silt loam. The Ab horizon couplets merge in some areas of the bluff edge and show very slight and limited oxidization. Patches of platy, partially to moderately decomposed woody and plant materials are present in some areas of the Ab horizons.

2 (C)	-	130-145	2-5	Yellowish brown (10YR 5/4) silt loam; massive; dry; continuous; abrupt, smooth to slightly wavy boundary.
2 (Bwb horizons) Pedocomplex 5	Paleosol (P5)	135-155	5-15	Pedocomplex 5 (Bwb horizons) – brown (7.5YR 4/4 to 4/3) loams; massive; dry; continuous; clear, smooth to slightly wavy boundaries. Pedocomplex 5 consists of at least two Bwb horizons separated by yellowish brown (10YR 5/4) silt loam that is less weathered. The Bwb horizons are 2-6 cm thick when separated. The horizons coalesce in several areas into a thicker Bwb horizon (13-14 cm thick). Some larger pieces of wood and wood charcoal are present in horizons. Radiocarbon date on charcoal recovered from a Bwb horizon: 3980+/-30 B.P. (Beta-386247).
2 (C)	Sand 6 (S6)	140-160	8-20	Pale brown (10YR 6/3) silt loam; massive; dry; continuous; abrupt, smooth to slightly wavy boundary.
2 (Ab horizon) Paleosol 4	Sand 6 (S6)	158-175	5-7	Paleosol 4 (Ab horizon) – brown (7.5YR 5/3 to 5/2) silt loam; massive; dry; continuous; clear to gradual, smooth and slightly wavy boundary. Paleosol 4 is a very weakly developed Ab horizon that has discontinuous layers of root casts and compact, partially decomposed plant materials present.
2 (C)	Sand 6 (S6)	165-180	4-12	Pale brown to yellowish brown (10YR 6/3 to 5/4) silt loam; massive; dry; continuous; abrupt, smooth to slightly wavy boundary.
2 (Ab horizon) Paleosol 3	Sand 6 (S6)	178-185	7-10	Paleosol 3 (Ab horizon) – yellowish brown to brown (10YR 5/4 to 5/3) sandy loam; massive; dry; discontinuous; clear to gradual, smooth and slightly wavy boundary. Paleosol 3 is a very weakly developed Ab horizon that has discontinuous layers of root casts and compact, partially decomposed plant materials present.
2 (Ck); Tephra 1 (T1)	Sand 6 (S6)	185-250	60-65	Yellowish brown (10YR 5/4) sandy loam to light yellowish brown to pale brown (10YR 6/4 to 6/3) silt loam; continuous; abrupt, smooth boundary. The upper 55 cm of the deposit is a dry, bedded sandy loam that has more medium, fine and very fine sands than the silt loams above and below. The lower 12 cm of the deposit is a massive silt loam. The contact between the sandy and silt loams is abrupt and smooth. These deposits have visible carbonates and carbonate-rich roots casts. Terrestrial snail shells (Succineidae sp.) are present in the sandy loam. Redoximorphic features of reddish masses (iron accumulations) of sediment are common (2 to <20% surface coverage) in the silt loam, while iron accumulation masses are few or more infrequent (<2% surface coverage) within the upper sandy loam. Radiocarbon date on terrestrial snail shell near the contact of sandy and silt loams: 6040+/-25 B.P. (UGAMS#22799). Tephra 1 (T1) is a whitish gray tephra deposit; discontinuous; massive; 1 cm or less thick. Tephra 1 was observed only in a single horizontally oriented patch around 240 cmBS in the massive silt loam, approximately 3 cm below its contact with the sandy loam.

2 (Ab, Abk, and Ck horizons) Pedocomplex 2	Paleosol 6 (P6)	247.5-280	27-35	Pedcomplex 2 (Ab and Abk horizons) – gray to yellowish brown (10YR 6/1 to 5/4) and gray (7.5YR 6/1 to 5/1) silt loams; moist; massive to platy structure; abrupt, smooth to slightly wavy boundaries. Pedocomplex 2 consists of two couplets of Ab horizons separated by 10 cm of yellowish brown silt loam. The upper couplet consists of a discontinuous, very weakly developed light dark brown silt loam that overlies a more developed and continuous darker brown silt loam. The lower Abk horizon in the upper couplet bifurcates into two thinner Abk horizons (1-2 cm thick) in some areas; in other areas, it consists of one thicker Abk horizon (3-4 cm) that shows minor oxidization and reddish hues. The Abk horizons in the upper couplet are 2-4 cm in thickness and separated by 5-7 cm of yellowish brown silt (Ck horizon). Pedocomplex 2 Abk horizons have platy structures that separate in flat, tabular-like units. The Ck and Abk horizons have higher values of carbonates ($CaCO_3$). Circular redoximorphic features occur in the yellowish brown silts (C horizons) in this pedocomplex. Radiocarbon date on charcoal from the lower Abk horizon of the upper couplet: 6230+/-30 B.P. (Beta-396693). The lower couplet of Pedocomplex 2 consists of two dark brown silt loams separated by 2-3 cm of yellowish brown silt. The upper horizon of this couplet is a gray silt loam (weakly developed Ab horizon) that is 1-2 cm thick and fairly discontinuous. The lower Ab horizon is a more developed gray silt loam and more continuous in its extent that the upper Ab horizon. Radiocarbon date on charcoal the lowest Ab horizon couplet: 6990+/-30 B.P. (Beta-386249).
2 (C)	Sand 7 (S7)	275-285	5-7	Light brownish gray to gray (10YR 6/2 to 6/1) silt loam; slightly moist; massive; abrupt, smooth boundary. Circular redoximorphic features are present in this sandy loam.
2 (ABwb horizons) Pedocomplex 1	Paleosol 7 (P7)	278-305	20-25	Pedocomplex 1 (ABwb horizons) – dark grayish brown to dark gray (7.5YR 4/2 to 4/1) silt loam; massive; moist; continuous; dark brown to reddish brown mottling; abrupt, smooth to slightly wavy boundary. Pedocomplex 1 is composed of at least two distinct ABwb horizons. Very dark brown silt in the upper 3-5 cm of each soil marks the A horizons; dark reddish brown silts at the lower 3-5 cm of the soils represent the development of weakly expressed B horizons. Horizons show nearly equal expressions of A horizons and weakly expressed B horizons. Wood charcoal is present throughout Pedocomplex 1. The ABwb horizons are separated in some areas by yellowish brown silt, and in other areas the horizons are welded to each other. Redoximorphic features are present in Pedocomplex 1 consisting of irregular masses and circular to ovular shaped iron accumulations (brightly red oxidized sediment) that may have accumulated during the period of the soil complex formation, or superimposed during later periods. Radiocarbon dates on charcoal recovered from the lowest ABwb horizon: 8590+/-30 B.P. (Beta-420651) and 8810+/-60 B.P. (Beta-123339).
2 (C and Ab horizons) Pedocomplex 0	Sand 8 (S8)	300-360	57-60	Pedocomplex 0 (thin Ab horizons in C horizons) – very pale brown to light yellowish brown loam to sandy loam (10YR 7/3 to 6/4); massive; moist; continuous; clear, smooth boundary. Particle sizes fine upward from a sandy loam in the lower 20 cm of the C horizon, to a silty loam in the middle 20 cm, and to a loam in the upper 10 cm. Pedocomplex 0 consists of at least 5 thin and discontinuous dark yellowish brown [10YR 6/4] silt loams (Ab horizons); Ab horizons are 1 cm or less thick; generally separated by 2-10 cm of very pale brown (10YR 7/3 to 7/43) unaltered silt. The Ab horizons have very abrupt, smooth and broken boundaries. Redoximorphic features are abundant (or many; >20% surface area) in this silt loam and consist of irregular masses and scattered circular to ovular shaped iron accumulations (oxidized sediments).
1 (C)	Outwash	360+	-	Yellowish brown to brown (10YR 5/4 to 5/3) - glaciofluvial sand, gravels, cobbles and boulders; massive; slightly moist; continuous. Unit 1 is the glaciofluvial sand, gravels, cobbles and boulders that compose the terraces basal sediments. Boulders are present in some locations. Gravels and cobbles are sub-rounded to sub-angular with high sphericity; some have waterlain weathering rinds. Sands are from very coarse to very fine sizes with the majority of particles falling in the coarse to fine sand

				ranges. Some gravels appear polished and ventifacted.

5.3.2 Pedostratigraphy

The pedostratigraphy of the Hurricane Bluff site is summarized below and detailed in Table 5.6, and shown in Figure 5.8. The informal designations for soil groups within the Hurricane Bluff site pedostratigraphy were originally defined by Higgs et al. (1999). Similar to Holmes and Bacon, Higgs et al. (1999) referred to distinct soil groups within the stratigraphy as Paleosols and number them sequentially, the lowest being "Paleoso1 7" and the highest being "Paleosol 1." However, we have significantly modified their scheme here to incorporate previously unrecognized buried soils and number the paleosols and pedocomplexes from the lowest to the highest. Twelve soil groups have been defined at the Hurricane Bluff site: 5 Pedocomplexes, 6 Paleosols, and the surface soil (detailed below). Similar to the DRO soils, Hurricane Bluff site pedostratigraphy consists of entisols and inceptisols.

Pedocomplex 0 is lowest group of buried soils in the Hurricane Bluff site pedostratigraphy. The complex consists of at least 5 discontinuous entisols (very pale brown to light yellowish brown loam to sandy loams; Ab horizons) between 300 to 360 cmBS within Unit 2. The thin Ab horizons are separated by 2-10 cm of unweathered very pale brown silt. The Ab horizons have abrupt, smooth and broken boundaries. These lowest soils have not been directly dated; however, they are older than 10,000 cal yrs BP based on radiocarbon ages from overlying Pedocomplex 1.

Pedocomplex 1 consists of at least two inceptisols (ABwb horizons) between 278-305 cmBS in Unit 2. The upper 3-5 cm of each soil is a very dark brown silt loam that marks humic accumulation (A horizons). The lower 3-5 cm of each soil are dark reddish brown silt loams that show illuvial accumulations of sesquioxides (Bw horizons). Horizons show nearly equal expressions of A horizons and weakly expressed B horizons. The ABwb horizons of Pedocomplex 1 are separated in some areas by 2-3 cm of unweathered yellowish brown silt, although in other areas the upper ABwb horizon welded onto the lower ABwb horizon. Radiocarbon dating on charcoal from Pedocomplex 1 indicates that these soils were in development by 10160-9630 and 9600-9500 cal yrs BP (Table 5.6).

Pedocomplex 2 consists of two couplets of entisols between 247.5-280 cmBS in Unit 2. The upper couplet consists of carbonate-rich entisols (Abk horizons). The upper Abk horizon is a discontinuous, very weakly developed light dark brown silt loam. The lower Abk horizon is a more developed and continuous darker brown silt loam. The more developed Abk horizon bifurcates into two thinner horizons (1-2 cm thick) in some areas. The horizons in the upper couplet are 2-4 cm in thickness and separated by 5-7 cm of carbonate-rich yellowish brown silt (Ck horizon).

The lower couplet of Pedocomplex 2 consists of two dark brown silt loams (Ab horizons) separated by 2-3 cm of yellowish brown silt. The upper Ab horizon is a weakly developed gray silt loam that is 1-2 cm thick and fairly discontinuous. The lower Ab horizon is a more developed gray silt loam and more continuous in its extent that the upper Ab horizon. The lower couplet has less carbonate than the upper couplet horizons. The upper and lower couplets are separated by 10 cm of an unweathered yellowish brown

silt loam (C horizon). Radiocarbon ages on the lower couplet dated to 7930-7740 cal yrs BP and on the upper couplet to 7250-7020 cal yrs BP (Table 5.6).

Paleosol 3 consists of a 7-10 cm thick, discontinuous yellowish brown to brown sandy loam (Ab horizon) between 178-185 cmBS. This entisol has discontinuous layers of root casts and compact, partially decomposed plant materials. The soil's boundary is clear to gradual and smooth to slightly wavy.

Paleosol 4 is a 5-7 cm thick, continuous brown silt loam (Ab horizon) between 165-180 cmBS. Similar to Paleosol 3, this entisol has discontinuous layers of root casts and compact, partially decomposed plant materials. The soil's boundary is clear to gradual and smooth to slightly wavy.

Pedocomplex 5 consists of two inceptisols (Bwb horizons) between 134-155 cmBS in Unit 2. These continuous dark brown silt loams show reddish coloration and signs of illuvial accumulation of sesquioxides. The Bwb horizons are 2-6 cm thick when separated by yellowish brown silt. The horizons coalesce in several areas into a single, thicker Bwb horizon (13-14 cm thick). The boundaries of the Bwb horizons are clear, smooth to slightly wavy. A radiocarbon age on charcoal recovered from Pedocomplex 5 is 4530-4410 cal yrs BP (Table 5.6).

Pedocomplex 6 consists of a couplet of entisols (Ab horizons) between 125-140 cmBS in Unit 2. The discontinuous brown silt loams are 2-3 cm thick and separated by a relatively unweathered yellowish brown silt loam. The Ab horizons merge in some areas of the excavation area and show limited amounts of oxidization (reddish mottling). The Ab horizons have abrupt and smooth and broken boundaries. A radiocarbon age on charcoal recovered from Pedocomplex 6 is 4090-3910 cal yrs BP.

Paleosol 7 is a 3-4 cm thick, discontinuous entisol between 112-121 cmBS in Unit 2. This soil has differing expressions of Ab and Bwb horizons across the erosional edge. This dark brown to grayish brown silt loam has a massive structure with abrupt and smooth to wavy, broken boundaries. The soil is primarily expressed as a darker brown silt loam with little oxidization evident. To a more limited extent, this soil is also expressed as reddish grayish brown silt (possible Bwb horizon) that displays oxidization. A radiocarbon age on charcoal from Paleosol 7 indicates this soil was in development by 3540-3370 cal yrs BP (Table 5.6).

Paleosol 8 is a 5-10 cm thick inceptisol between 75-97.5 cmBS in Unit 2. The upper 3-5 cm of this soil is a very dark brown silt loam that marks humic accumulation (Ab horizons). The lower 3-4 cm of this soil is dark reddish brown silt loams that show illuvial accumulations of sesquioxides (Bwb horizons). Radiocarbon ages on Paleosol 8 indicate the soil was in development by 1890-1550 cal yrs BP (Table 5.6).

Paleosol 9 is a 4-5 cm thick inceptisol between 40-45 cmBS in Unit 2. The upper 5-7 cm of the soil is a brown organic-rich silt loam (Ab horizon). The lower 8-10 cm of this soil is a reddish brown silt loam (Bwb horizon) that displays illuviation of sesquioxides. The Ab horizon is platy in structure, while the Bwb horizon is massive. A radiocarbon age on charcoal indicates that this soil was in development by 480-310 cal yrs BP (Table 5.6).

Paleosol 10 is a 2.5-7 cm thick entisol (A/Ob horizon) between 15-22 cmBS on a Unit 4 sandy loam. This brown to dark brown loam is continuous with a clear and smooth boundary. The upper part of this soil retains some partially to moderately decomposed

organics (O horizon); however, the humus accumulation zone (A horizon) is the dominant characteristic of this soil. This soil developed after 300 cal yr BP.

The surface soil is a weakly developed loam (entisol) that developed at the surface of the Unit 4 sand. The surface soil shows OA horizonation with partially to moderately decomposed organics at the surface with an underlying thin layer (2-3 cm thick) humus development.

5.3.3 Sediment Analyses

5.3.3.1 Tephra Characterization

Two tephras, T1 and T2, were recognized in the stratigraphic column at the Hurricane Bluff site (Figure 5.8). Samples from both tephra beds were too fine grained and weathered, and a small in sample size of glass, to acquire reliable geochemical data to correlate with other tephras. These tephra samples showed mixing of the ash with silt grains from loess deposits. The upper most Hurricane Bluff tephra, T2 (Figure 5.9), has bracketing ages of 3980±30 BP (4410-4530 cal yrs BP; median probability: 4470 cal yr BP) and 3670±30 BP (3910-4090 cal yrs BP; median probability: 4000 cal yr BP). The lower tephra, T1, has bracketing ages of 6230±30 BP (7020-7250 cal yrs BP; median probability: 7170 cal yr BP) and 6040±25 BP (6800-6950 cal yrs BP; median probability: 6890 cal yr BP). Given the median probabilities, Hurricane Bluff T1 deposition dates between 4470 and 4000 cal yrs BP, while T2 dates between 7170 and 6890 cal yrs BP. The potential correlations of the Hurricane Bluff tephras to the DRO and other regional tephras based on stratigraphic and age of deposition is explored below.

Figure 5.9. Tephra T2 at the Hurricane Bluff site.

5.3.3.2 Particle Size Analysis (PSA)

Particle size analysis results for the Hurricane Bluff sediments and soils are present in Tables 5.7 and 5.8. Unit 1 outwash sediment particles less than 2000 microns consist very coarse to very fine sands, with 65% sand composition and loamy sand

texture. The particles are poorly sorted with a polymodal distribution, symmetrical skewness, and very platykurtic in distribution.

Unit 2 loess texture ranges from sandy loam to loam. Sand content ranges between 69.37 and 22.24%, silt between 67.77 and 25.35%, and clay between 12.83 to 2.82%. Particle distributions are unimodal to trimodal with poor sorting. Skewness ranges between coarse skewed to symmetrical to very fine skewed. Kurtosis spans very leptokurtic to very platykurtic.

Tephra 2 was the only tephra with a sample size large enough for us to run PSA on. Tephra 2 has 61.98% silt, 26.60% sand (dominated by fine and very fine sand fractions), and 11.42% clay contents.

Unit 3 has a sandy loam texture with 49.94% sand, 46.29% silt, and 3.77% clay content. Unit 3 distribution is bimodal and poorly sorted. It is very finely skewed and mesokurtic in distributional shape.

Unit 4 has a sandy loam to loam texture between 55.69 and 43.51% sand, 46.87 and 41.98% silt, and 9.62 and 2.33% clay content. Unit 4 is poorly sorted with distribution that is bimodal, finely skewed, and mesokurtic to leptokurtic in distributional shape.

Soils and soil groups are primarily associated with siltier deposits, having silt content averages of 55.34±13.52% in entisols and 61.48±7.36% in inceptisols, while C horizons contain 43.29±14.32%. Sand average content for entisols is 37.02±14.07% and inceptisols is 30.42±7.54%, while C horizons have 51.19±15.25%. Clay content is higher in entisols and inceptisols with 7.64±1.99% and 8.10±2.56%, respectively, while C horizons display 5.52±1.63%.

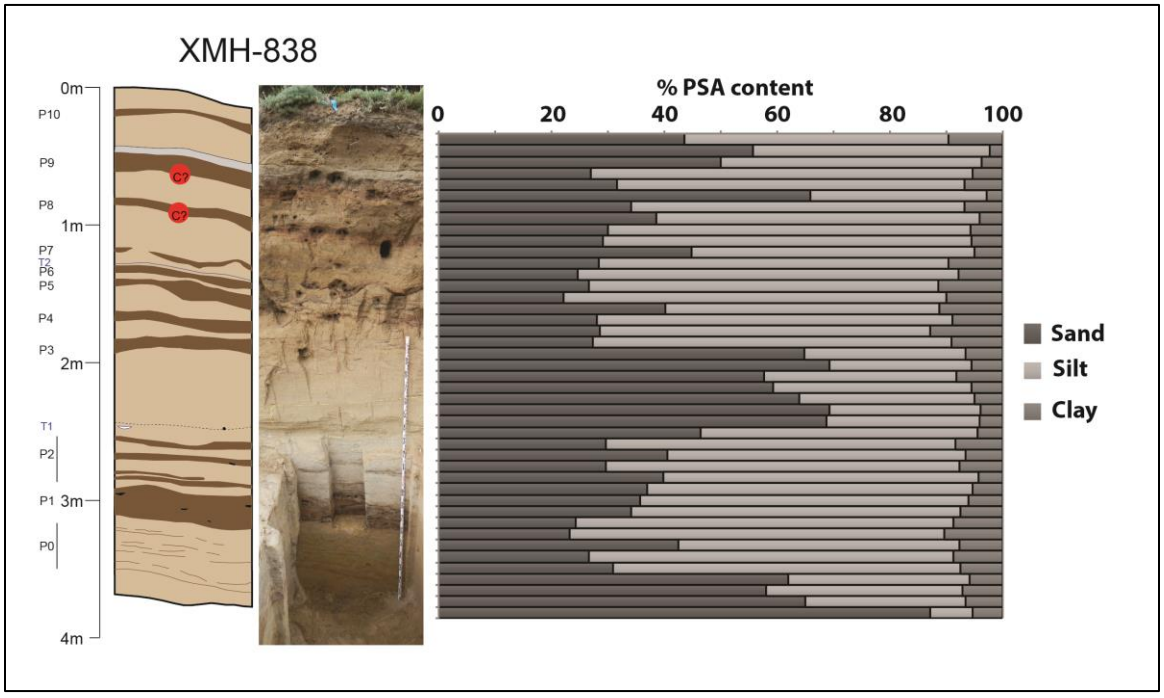

Figure 5.10. Generalized stratigraphic profile for the Delta River Overlook site with sand, silt and clay percentages by depth.

Table 5.7. Particle size analysis results on Hurricane Bluff sediments and soils.

Unit (Soil horizon)	*Depth (cmBS)*	*VCOS*[1]	*COS*[1]	*MS*[1]	*FS*[1]	*VFS*[1]	*% SAND*	*% SILT*	*% CLAY*	*TEXTURE*	*Site/Sample ID*
4 (A/Ob) Paleosol 10	16.5	0.07	0.83	1.67	8.01	32.94	43.51	46.87	9.62	loam	HB-PSA-15-01
4 (Ck)	27.5	0.02	0.29	2.35	15.08	37.95	55.69	41.98	2.33	sandy loam	HB-PSA-15-02
3 (C)	43	0.11	0.56	2.31	11.20	35.77	49.94	46.29	3.77	sandy loam	HB-PSA-15-03
2 (Ab) Paleosol 9	52.5	0.08	0.49	1.22	4.55	20.67	27.00	67.70	5.29	silt loam	HB-PSA-15-04
2 (Bwb) Paleosol 9	57.5	0.02	0.23	1.23	5.12	25.08	31.67	61.63	6.69	silt loam	HB-PSA-15-05
2 (C)	62.5	0.09	1.10	5.82	20.88	38.03	65.92	31.26	2.82	sandy loam	HB-PSA-15-06
2 (Ab) Paleosol 8	87.5	0.12	0.20	0.30	1.92	31.63	34.17	59.01	6.81	silt loam	HB-PSA-15-07
2 (Bwb) Paleosol 8	90	0.00	0.00	0.12	3.02	35.41	38.55	57.44	4.01	silt loam	HB-PSA-15-08
2 (C)	97.5	0.02	0.16	1.38	5.68	22.70	29.93	64.42	5.65	silt loam	HB-PSA-15-09
2 (C and Ab)	107.5	0.02	0.23	1.09	3.60	24.17	29.10	65.41	5.49	silt loam	HB-PSA-15-10
2 (C)	117.5	0.02	0.23	2.02	9.20	33.41	44.88	50.13	4.98	silt loam	HB-PSA-15-11
2 (Ab) Paleosol 7	122.5	0.08	0.17	1.15	3.98	23.05	28.44	62.01	9.55	silt loam	HB-PSA-15-12
2 (Bwb) Paleosol 7	124	0.00	0.13	0.73	2.62	21.17	24.65	67.47	7.87	silt loam	HB-PSA-15-13
Tephra 2	127.5	0.03	0.18	1.16	4.48	20.74	26.60	61.98	11.42	silt loam	HB-PSA-15-14
2 (Ab horizons) Pedocomplex 6	135	0.01	0.30	0.65	1.97	19.31	22.24	67.77	9.99	silt loam	HB-PSA-15-15
2 (Bwb horizons) Pedocomplex 5	142.5	0.01	0.23	2.32	8.53	29.04	40.14	48.75	11.12	loam	HB-PSA-15-16
2 (C)	157.5	0.03	0.04	0.27	2.25	25.41	27.99	63.10	8.90	silt loam	HB-PSA-15-17
2 (Ab) Paleosol 4	167.5	0.03	0.05	0.26	2.32	25.98	28.64	58.53	12.83	silt loam	HB-PSA-15-18
2 (Ab) Paleosol 4	170	0.04	0.03	0.23	2.04	24.95	27.30	63.70	9.00	silt loam	HB-PSA-15-19
2 (C)	172.5	0.01	0.28	4.69	20.86	39.07	64.90	28.63	6.47	sandy loam	HB-PSA-15-20
2 (C)	177.5	0.01	0.35	5.37	21.31	42.20	69.24	25.35	5.41	sandy loam	HB-PSA-15-21
2 (Ab) Paleosol 3	185	0.01	0.23	3.39	14.80	39.30	57.74	34.16	8.11	sandy loam	HB-PSA-15-22
2 (C)	192.5	0.00	0.28	3.74	14.54	40.77	59.34	35.10	5.57	sandy loam	HB-PSA-15-23
2 (C)	202.5	0.03	0.33	3.91	15.49	44.15	63.92	31.17	4.91	sandy loam	HB-PSA-15-24
2 (C)	217.5	0.07	0.79	6.40	20.47	41.63	69.37	26.72	3.92	sandy loam	HB-PSA-15-25
2 (C)	227.5	0.05	0.74	7.60	23.75	36.59	68.73	27.26	4.01	sandy loam	HB-PSA-15-26
2 (Ck)	247.5	0.00	0.01	0.09	3.29	43.08	46.46	49.14	4.40	sandy loam	HB-PSA-15-27
2 (Abk horizons) Pedocomplex 2	257.5	0.03	0.08	0.25	2.22	27.12	29.69	61.96	8.35	silt loam	HB-PSA-15-28

2 (Ck)	262.5	0.00	0.11	0.18	3.57	36.69	40.56	52.93	6.50	silt loam	HB-PSA-15-29
2 (Abk horizons) Pedocomplex 2	265	0.03	0.16	0.34	2.23	26.90	29.65	62.78	7.57	silt loam	HB-PSA-15-30
2 (C)	272.5	0.00	0.05	0.09	2.49	37.20	39.82	55.90	4.27	silt loam	HB-PSA-15-31
2 (Ab horizons) Pedocomplex 2	280	0.00	0.07	0.10	2.64	34.17	36.97	57.71	5.32	silt loam	HB-PSA-15-32
2 (Ab horizons) Pedocomplex 2	285	0.00	0.09	0.18	2.39	33.10	35.76	58.25	5.99	silt loam	HB-PSA-15-33
2 (C)	290	0.00	0.08	0.13	1.70	32.25	34.16	58.42	7.42	silt loam	HB-PSA-15-34
2 (ABwb) Pedocomplex 1	297.5	0.00	0.14	0.25	1.27	22.59	24.25	67.06	8.69	silt loam	HB-PSA-15-35
2 (ABwb) Pedocomplex 1	307.5	0.00	0.09	0.27	1.39	21.52	23.27	66.51	10.22	silt loam	HB-PSA-15-36
2 (C)	317.5	0.02	0.10	0.23	2.70	39.50	42.56	49.81	7.63	loam	HB-PSA-15-37
2 (C and Ab horizons) Pedocomplex 0	327.5	0.11	0.34	1.19	3.39	21.52	26.55	64.84	8.61	silt loam	HB-PSA-15-38
2 (C and Ab horizons) Pedocomplex 0	337.5	0.05	0.28	1.12	3.48	25.99	30.92	61.61	7.47	silt loam	HB-PSA-15-39
2 (C and Ab horizons) Pedocomplex 0	347.5	0.64	2.76	11.24	24.05	23.40	62.09	32.00	5.91	sandy loam	HB-PSA-15-40
2 (C and Ab horizons) Pedocomplex 0	357.5	0.33	1.59	6.67	20.81	28.59	57.98	34.85	7.17	sandy loam	HB-PSA-15-41
2 (C and Ab horizons) Pedocomplex 0	367.5	1.22	3.47	9.44	21.84	29.06	65.03	28.48	6.48	sandy loam	HB-PSA-15-42
1 (C)	377.5	13.27	18.51	24.72	18.65	12.11	87.26	7.49	5.25	loamy sand	HB-PSA-15-43

[1]VCOS= very coarse sand; COS= coarse sand; MS= medium sand; FS= fine sand; VFS= very fine sand.

Table 5.8. Particle size mean, sorting, skewness, and kurtosis analyses on Hurricane Bluff sediments and soils.

		FOLK AND WARD METHOD (mm)				*FOLK AND WARD METHOD (ϕ)*				*FOLK AND WARD METHOD (Description)*			
sample	**sample type**	**mean**	**sorting**	**skewness**	**kurtosis**	**mean**	**sorting**	**skewness**	**kurtosis**	**mean**	**sorting**	**skewness**	**kurtosis**
HB-PSA-15-01	Bimodal, Poorly Sorted	42.23	2.76	-0.60	1.11	4.57	1.46	0.60	1.11	Very Coarse Silt	Poorly Sorted	Very Fine Skewed	Mesokurtic
HB-PSA-15-02	Bimodal, Poorly Sorted	49.59	3.03	-0.45	1.13	4.33	1.60	0.45	1.13	Very Coarse Silt	Poorly Sorted	Very Fine Skewed	Leptokurtic
HB-PSA-15-03	Bimodal, Poorly Sorted	45.81	3.09	-0.47	1.00	4.45	1.63	0.47	1.00	Very Coarse Silt	Poorly Sorted	Very Fine Skewed	Mesokurtic
HB-PSA-15-04	Bimodal, Poorly Sorted	26.62	3.03	-0.14	0.76	5.23	1.60	0.14	0.76	Coarse Silt	Poorly Sorted	Fine Skewed	Platykurtic
HB-PSA-15-05	Bimodal, Poorly Sorted	30.64	2.99	-0.32	0.79	5.03	1.58	0.32	0.79	Coarse Silt	Poorly Sorted	Very Fine Skewed	Platykurtic
HB-PSA-15-06	Trimodal, Poorly Sorted	63.39	2.94	-0.29	1.66	3.98	1.56	0.29	1.66	Very Fine Sand	Poorly Sorted	Fine Skewed	Very Leptokurtic
HB-PSA-15-07	Unimodal, Poorly Sorted	38.90	2.55	-0.78	0.82	4.68	1.35	0.78	0.82	Very Coarse Silt	Poorly Sorted	Very Fine Skewed	Platykurtic
HB-PSA-15-08	Unimodal, Poorly Sorted	33.27	2.68	-0.60	0.70	4.91	1.42	0.60	0.70	Very Coarse Silt	Poorly Sorted	Very Fine Skewed	Platykurtic
HB-PSA-15-09	Bimodal, Poorly Sorted	31.27	3.01	-0.33	0.80	5.00	1.59	0.33	0.80	Very Coarse Silt	Poorly Sorted	Very Fine Skewed	Platykurtic
HB-PSA-15-10	Unimodal, Poorly Sorted	26.42	2.96	-0.17	0.73	5.24	1.57	0.17	0.73	Coarse Silt	Poorly Sorted	Fine Skewed	Platykurtic
HB-PSA-15-11	Bimodal, Poorly Sorted	38.22	2.92	-0.58	0.90	4.71	1.54	0.58	0.90	Very Coarse Silt	Poorly Sorted	Very Fine Skewed	Platykurtic
HB-PSA-15-12	Bimodal, Poorly Sorted	31.78	2.96	-0.38	0.80	4.98	1.57	0.38	0.80	Very Coarse Silt	Poorly Sorted	Very Fine Skewed	Platykurtic

HB-PSA-15-13	Unimodal, Poorly Sorted	27.19	2.78	-0.28	0.65	5.20	1.48	0.28	0.65	Coarse Silt	Poorly Sorted	Fine Skewed	Very Platykurtic
HB-PSA-15-14	Bimodal, Poorly Sorted	36.60	2.93	-0.56	0.86	4.77	1.55	0.56	0.86	Very Coarse Silt	Poorly Sorted	Very Fine Skewed	Platykurtic
HB-PSA-15-15	Unimodal, Poorly Sorted	28.96	2.90	-0.30	0.74	5.11	1.54	0.30	0.74	Coarse Silt	Poorly Sorted	Fine Skewed	Platykurtic
HB-PSA-15-16	Bimodal, Poorly Sorted	47.41	3.04	-0.47	1.09	4.40	1.60	0.47	1.09	Very Coarse Silt	Poorly Sorted	Very Fine Skewed	Mesokurtic
HB-PSA-15-17	Unimodal, Poorly Sorted	35.09	2.66	-0.68	0.72	4.83	1.41	0.68	0.72	Very Coarse Silt	Poorly Sorted	Very Fine Skewed	Platykurtic
HB-PSA-15-18	Unimodal, Poorly Sorted	36.78	2.64	-0.75	0.74	4.76	1.40	0.75	0.74	Very Coarse Silt	Poorly Sorted	Very Fine Skewed	Platykurtic
HB-PSA-15-19	Unimodal, Poorly Sorted	36.69	2.64	-0.75	0.74	4.77	1.40	0.75	0.74	Very Coarse Silt	Poorly Sorted	Very Fine Skewed	Platykurtic
HB-PSA-15-20	Bimodal, Poorly Sorted	87.34	2.21	-0.02	1.90	3.52	1.14	0.02	1.90	Very Fine Sand	Poorly Sorted	Symmetrical	Very Leptokurtic
HB-PSA-15-21	Bimodal, Poorly Sorted	93.49	2.07	0.13	1.85	3.42	1.05	-0.13	1.85	Very Fine Sand	Poorly Sorted	Coarse Skewed	Very Leptokurtic
HB-PSA-15-22	Bimodal, Poorly Sorted	74.22	2.41	-0.19	2.15	3.75	1.27	0.19	2.15	Very Fine Sand	Poorly Sorted	Fine Skewed	Very Leptokurtic
HB-PSA-15-23	Bimodal, Poorly Sorted	84.05	2.18	-0.03	2.13	3.57	1.13	0.03	2.13	Very Fine Sand	Poorly Sorted	Symmetrical	Very Leptokurtic
HB-PSA-15-24	Bimodal, Poorly Sorted	89.45	2.07	0.10	2.11	3.48	1.05	-0.10	2.11	Very Fine Sand	Poorly Sorted	Coarse Skewed	Very Leptokurtic
HB-PSA-15-25	Trimodal, Poorly Sorted	94.65	2.08	0.15	1.82	3.40	1.06	-0.15	1.82	Very Fine Sand	Poorly Sorted	Coarse Skewed	Very Leptokurtic
HB-PSA-15-26	Trimodal, Poorly Sorted	78.21	2.56	-0.17	1.86	3.68	1.35	0.17	1.86	Very Fine Sand	Poorly Sorted	Fine Skewed	Very Leptokurtic
HB-PSA-15-27	Unimodal, Poorly Sorted	44.14	2.34	-0.79	1.18	4.50	1.22	0.79	1.18	Very Coarse Silt	Poorly Sorted	Very Fine Skewed	Leptokurtic

HB-PSA-15-28	Unimodal, Poorly Sorted	39.18	2.55	-0.77	0.83	4.67	1.35	0.77	0.83	Very Coarse Silt	Poorly Sorted	Very Fine Skewed	Platykurtic
HB-PSA-15-29	Unimodal, Poorly Sorted	39.57	2.68	-0.67	0.95	4.66	1.42	0.67	0.95	Very Coarse Silt	Poorly Sorted	Very Fine Skewed	Mesokurtic
HB-PSA-15-30	Unimodal, Poorly Sorted	36.56	2.65	-0.75	0.74	4.77	1.40	0.75	0.74	Very Coarse Silt	Poorly Sorted	Very Fine Skewed	Platykurtic
HB-PSA-15-31	Unimodal, Poorly Sorted	38.85	2.55	-0.78	0.82	4.69	1.35	0.78	0.82	Very Coarse Silt	Poorly Sorted	Very Fine Skewed	Platykurtic
HB-PSA-15-32	Unimodal, Poorly Sorted	39.12	2.54	-0.78	0.83	4.68	1.35	0.78	0.83	Very Coarse Silt	Poorly Sorted	Very Fine Skewed	Platykurtic
HB-PSA-15-33	Unimodal, Poorly Sorted	38.34	2.57	-0.77	0.80	4.71	1.36	0.77	0.80	Very Coarse Silt	Poorly Sorted	Very Fine Skewed	Platykurtic
HB-PSA-15-34	Unimodal, Poorly Sorted	39.32	2.53	-0.78	0.84	4.67	1.34	0.78	0.84	Very Coarse Silt	Poorly Sorted	Very Fine Skewed	Platykurtic
HB-PSA-15-35	Unimodal, Poorly Sorted	28.32	2.74	-0.36	0.66	5.14	1.46	0.36	0.66	Coarse Silt	Poorly Sorted	Very Fine Skewed	Very Platykurtic
HB-PSA-15-36	Unimodal, Poorly Sorted	30.64	2.72	-0.47	0.68	5.03	1.44	0.47	0.68	Coarse Silt	Poorly Sorted	Very Fine Skewed	Platykurtic
HB-PSA-15-37	Unimodal, Poorly Sorted	40.18	2.50	-0.78	0.88	4.64	1.32	0.78	0.88	Very Coarse Silt	Poorly Sorted	Very Fine Skewed	Platykurtic
HB-PSA-15-38	Bimodal, Poorly Sorted	30.46	2.98	-0.32	0.79	5.04	1.58	0.32	0.79	Coarse Silt	Poorly Sorted	Very Fine Skewed	Platykurtic
HB-PSA-15-39	Unimodal, Poorly Sorted	37.24	2.87	-0.61	0.88	4.75	1.52	0.61	0.88	Very Coarse Silt	Poorly Sorted	Very Fine Skewed	Platykurtic
HB-PSA-15-40	Trimodal, Poorly Sorted	88.78	3.10	-0.14	1.69	3.49	1.63	0.14	1.69	Very Fine Sand	Poorly Sorted	Fine Skewed	Very Leptokurtic
HB-PSA-15-41	Trimodal, Poorly Sorted	72.69	2.88	-0.22	1.83	3.78	1.52	0.22	1.83	Very Fine Sand	Poorly Sorted	Fine Skewed	Very Leptokurtic
HB-PSA-15-42	Trimodal, Poorly Sorted	135.52	2.56	0.02	1.77	2.88	1.36	-0.02	1.77	Fine Sand	Poorly Sorted	Symmetrical	Very Leptokurtic

HB-PSA-15-43	Polymodal, Poorly Sorted	557.03	3.43	-0.03	0.60	0.84	1.78	0.03	0.60	Coarse Sand	Poorly Sorted	Symmetrical	Very Platykurtic

5.3.3.3 Soil Organic Carbon

Soil organic carbon ($\%OC_{LOI}$) measurements on DRO sediment and soil samples are presented in Table 5.9, and graphically represented by depth in Figure 5.11. Soil organic carbon ($\%OC_{LOI}$) on Hurricane Bluff sediments and soils ranges from 9.75 to 1.08% with an average of 3.17±1.90%. Unit 1 outwash exhibits a relatively low value with 1.40%. Unweathered loess and aeolian sands (C horizons) display ranges between 1.08 and 3.34% with an average of 2.09±0.70%. Immature entisols (Ab horizons) show a range of values between 9.75 and 1.27% with an average of 3.92±2.44%. The pedocomplexes with more mature inceptisols (ABwb and Bwb horizons) shows a range of values between 4.99 and 2.27% with an average of 3.87±1.15%. There appears to be slight trend towards decreasing $\%OC_{LOI}$ values with depth. Based on average values, the C horizons show less organic content than horizons that show traits of pedogensis. Entisols and inceptisols show similar values; however, entisols display a wider range of values likely because these mostly represent the breakdown of surface organics and humus development in A horizons, while the inceptisols reflect more illuviation horizons of sesquioxides.

Table 5.9. Organic (%OC) and inorganic (%$CaCO_3$) carbon and pH data on sediments and soils from the Hurricane Bluff site.

Depth (cmBS)	*Unit (Soil Horizons)*	*%SOM (LOI 550℃)*	*%CaCO3 (LOI 1000℃)*	*%CaCO3 (chittick)*	*pH value*	*Munsell - wet*	*Munsell - dry*	*Sample No.*
16.5	4 (A/Ob) Paleosol 10	9.75	3.50	0.20	7.51	7.5YR 2.5/2 to 2.5/1	7.5YR 4/2 to 3/2	HB-PSA-15-01
27.5	4 (Ck)	2.09	3.97	1.04	7.80	10YR 4/1 to 4/2	10YR 6/1 to 6/2	HB-PSA-15-02
43	3 (C)	3.17	3.28	0.08	7.30	10YR 4/2 to 3/2	10YR 5/2 to 5/3	HB-PSA-15-03
52.5	2 (Ab) Paleosol 9	7.23	4.40	0.36	7.78	7.5YR 3/1 to 3/2	7.5YR 4/2	HB-PSA-15-04
57.5	2 (Bwb) Paleosol 9	4.96	3.58	0.12	6.97	7.5YR 3/3 to 2.5/3	7.5YR 4/3 to 4/4	HB-PSA-15-05
62.5	2 (C)	2.08	2.74	0.12	7.30	10YR 4/2	10YR 5/3 to 5/4	HB-PSA-15-06
87.5	2 (Ab) Paleosol 8	4.57	4.15	0.16	7.32	7.5YR 2.5/2	7.5YR 4/2 to 3/2	HB-PSA-15-07
90	2 (Bwb) Paleosol 8	2.27	3.85	0.12	7.71	7.5YR 3/3 to 2.5/3	7.5YR 4/3 to 4/4	HB-PSA-15-08
97.5	2 (C)	3.04	3.83	0.16	7.82	10YR 4/2 to 3/2	10YR 5/3 to 5/4	HB-PSA-15-09
107.5	2 (C and Ab)	4.64	4.20	0.16	7.47	10YR 3/2 to 3/3	10YR 4/3 to 4/4	HB-PSA-15-10
117.5	2 (C)	2.81	3.58	0.12	7.59	10YR 4/3 to 4/4	10YR 5/3 to 5/4	HB-PSA-15-11
122.5	2 (Ab) Paleosol 7	6.72	4.00	0.20	7.60	7.5YR 2.5/2	7.5YR 4/2 to 3/2	HB-PSA-15-12
124	2 (Bwb) Paleosol 7	4.99	4.59	0.16	7.44	10YR 4/2 to 3/2	10YR 5/2	HB-PSA-15-13
127.5	Tephra 2	4.72	3.66	0.08	7.35	10YR 3/3	10YR 5/3	HB-PSA-15-14
135	2 (Ab horizons) Pedocomplex 6	6.25	4.55	0.16	7.71	7.5YR 3/2 to 2.5/2	7.5YR 4/4	HB-PSA-15-15
142.5	2 (Bwb horizons) Pedocomplex 5	2.82	4.25	0.12	7.71	7.5YR 2.5/3	7.5YR 4/3 to 4/4	HB-PSA-15-16
157.5	2 (C)	2.56	4.62	0.16	7.87	10YR 4/3 to 4/4	10YR 6/3	HB-PSA-15-17
167.5	2 (Ab) Paleosol 4	6.15	5.06	0.12	8.01	7.5YR 3/1 to 3/2	7.5YR 5/2 to 5/3	HB-PSA-15-18
170	2 (Ab) Paleosol 4	4.08	4.61	0.20	7.99	7.5YR 3/1 to 3/2	7.5YR 5/2 to 5/3	HB-PSA-15-19
172.5	2 (C)	2.59	3.19	0.20	7.78	10YR 4/3	10YR 6/3 to 5/3	HB-PSA-15-20
177.5	2 (C)	2.07	3.19	0.16	7.80	10YR 4/2 to 4/3	10YR 5/3 to 5/4	HB-PSA-15-21
185	2 (Ab) Paleosol 3	3.10	3.76	0.24	7.72	10YR 4/2	10YR 5/3 to 5/4	HB-PSA-15-22
192.5	2 (C)	2.16	3.53	0.08	7.86	10YR 4/3	10YR 6/3 to 5/3	HB-PSA-15-23
202.5	2 (C)	1.42	3.42	0.12	7.95	10YR 4/2 to 4/3	10YR 5/3 to 5/4	HB-PSA-15-24
217.5	2 (C)	1.08	3.49	0.24	8.06	10YR 5/3 to 4/3	10YR 6/3 to 6/4	HB-PSA-15-25

227.5	2 (C)	1.08	3.58	0.48	8.01	10YR 4/2 to 4/3	10YR 6/2 to 6/3	HB-PSA-15-26
247.5	2 (Ck)	1.51	5.42	0.81	8.02	10YR 5/1 to 5/2	10YR 6/1 to 6/2	HB-PSA-15-27
257.5	2 (Abk horizons) Pedocomplex 2	2.89	6.16	1.30	8.01	10YR 4/1 to 4/2	10YR 5/1 to 5/2	HB-PSA-15-28
262.5	2 (Ck)	1.96	5.46	1.14	7.99	10YR 5/1 to 5/2	10YR 6/1	HB-PSA-15-29
265	2 (Abk horizons) Pedocomplex 2	2.60	5.31	0.77	7.98	10YR 5/1 to 4/1	10YR 6/1 to 6/2	HB-PSA-15-30
272.5	2 (C)	1.59	4.68	0.48	8.13	10YR 5/1 to 5/2	10YR 6/1 to 6/2	HB-PSA-15-31
280	2 (Ab horizons) Pedocomplex 2	1.89	4.58	0.65	8.20	7.5YR 4/1 to 4/2	7.5YR 6/1 to 5/1	HB-PSA-15-32
285	2 (Ab horizons) Pedocomplex 2	2.92	4.75	0.65	8.15	7.5YR 4/1 to 4/2	7.5YR 6/1 to 5/1	HB-PSA-15-33
290	2 (C)	3.34	5.27	0.65	8.19	10YR 4/1 to 4/2	10YR 6/1 to 5/1	HB-PSA-15-34
297.5	2 (ABwb) Pedocomplex 1	3.63	5.51	0.52	8.07	7.5YR 3/1 to 3/2	7.5YR 4/2	HB-PSA-15-35
307.5	2 (ABwb) Pedocomplex 1	4.52	5.58	0.45	8.11	7.5YR 3/1 to 2.5/1	7.5YR 4/1 to 4/2	HB-PSA-15-36
317.5	2 (C)	1.72	5.53	0.32	8.08	10YR 5/3	10YR 7/2	HB-PSA-15-37
327.5	2 (C and Ab horizons) Pedocomplex 0	2.07	4.61	0.28	8.10	10YR 5/3 to 4/3	10YR 7/2 to 7/3	HB-PSA-15-38
337.5	2 (C and Ab horizons) Pedocomplex 0	1.53	4.34	0.12	8.06	10YR 5/3	10YR 7/3 to 6/3	HB-PSA-15-39
347.5	2 (C and Ab horizons) Pedocomplex 0	1.27	2.81	0.16	8.06	10YR 5/3	10YR 7/3 to 6/3	HB-PSA-15-40
357.5	2 (C and Ab horizons) Pedocomplex 0	1.56	3.02	0.12	8.07	10YR 5/3 to 5/4	10YR 6/3 to 6/4	HB-PSA-15-41
367.5	2 (C and Ab horizons) Pedocomplex 0	1.40	2.81	0.08	8.07	10YR 5/3 to 5/4	10YR 6/3	HB-PSA-15-42
377.5	1 (C)	1.40	2.79	0.28	8.14	10YR 4/4	10YR 5/3 to 5/4	HB-PSA-15-43

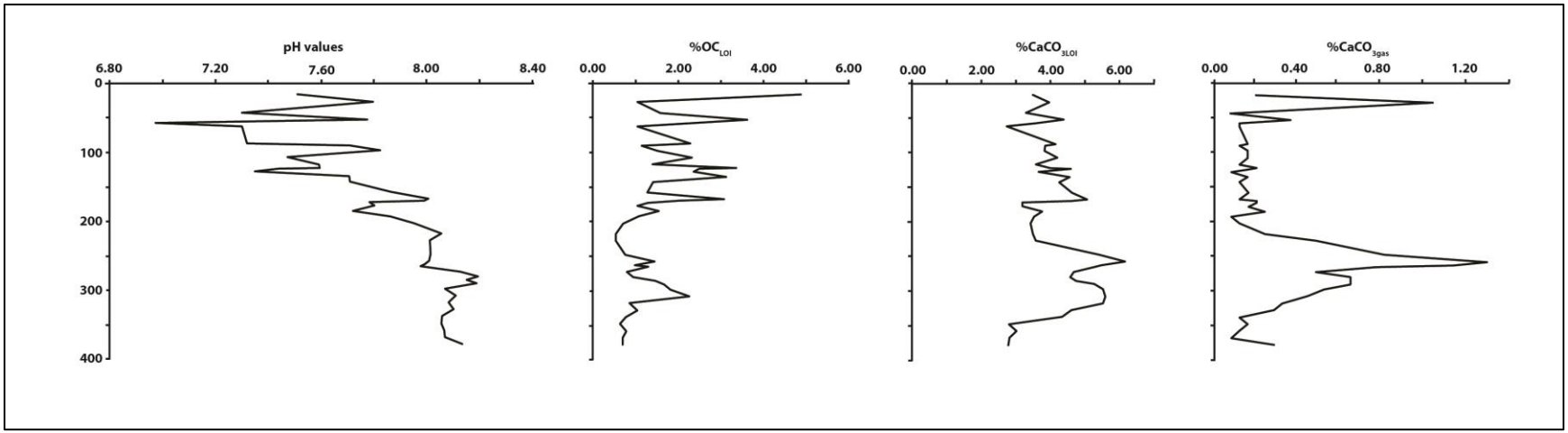

Figure 5.11. Hurricane Bluff sediment and soils pH and organic (%OC) and inorganic (%$CaCO_3$) carbon data by depth.

5.3.3.4 Inorganic Carbon

The presence of carbonates (%$CaCO_3$) are relatively low throughout the Hurricane Bluff sediments (Table 5.9, Figure 5.11). Results based on LOI, %$CaCO_{3LOI}$ ranges between 2.81 and 6.16% with an average of 4.18±0.90%. There is no apparent relationship with depth, other than some of the highest values appear in the lower 2 m of the section. The lowest values are associated with C horizons and entisols. C horizon values range between 2.74 and 5.53% with an average of 3.98±0.94%. Entisols range between 2.81 and 6.16% with an average of 4.26±0.86%. Inceptisols range between 3.58 and 5.58% with an average of 4.56±0.84%.

Results based on gasometry (chittick) show similar patterns to those produced by LOI. %$CaCO_{3gas}$ for all sediments and soil samples range from 0.08 and 1.30% with an average of 0.33±0.30%. %$CaCO_{3gas}$ for C horizons ranges between 0.08 and 1.14% with an average of 0.37±0.33%. %$CaCO_{3gas}$ for entisol horizons ranges between 1.30 and 0.08% with an average of 0.33±0.32%. %$CaCO_{3gas}$ for inceptisol horizons ranges between 0.12 and 0.52% with an average of 0.25±0.19%.

Again, LOI provides higher estimates for organic and inorganic carbon components than gasometric (i.e., chittick) methods, and given that many of these samples range between 1 to 5% for both %OC_{LOI} and %$CaCO_{3LOI}$ there appears to be very little of both within the sediments and soils with the exception of the samples from soils that range >5%.

5.3.3.5 pH Scale Measurement

In general, the pH values on Hurricane Bluff sediments are increasingly basic with depth (Table 5.9, Figure 5.11). pH values for the Hurricane Bluff sediments range from 6.97 and 8.20 with an average of 7.83±0.30 being mostly alkaline. C horizon pH values range between 7.30 and 8.19 with an average of 7.87±0.26. Ab horizon pH values range between 7.32 and 8.20 with an average of 7.88±0.26. More mature soils, Bwb and ABwb horizons, have pH values that range between 6.97 and 8.11 with an average of 7.67±0.42. Hurricane Bluff sediments and soils with higher organic carbon (%OC_{LOI}) values tend to have pH values that trend to the neutral to slightly acidic side of the scale (Figure 5.12); sediments and soils with low organic carbon content tend to have alkaline pH values. Hurricane Bluff sediments and soils with higher inorganic carbon (%$CaCO_{3LOI}$) values tend to have pH values are more alkaline (Figure 5.12, while sediments and soils with lower %$CaCO_{3LOI}$ content tend to more neutral to slightly acidic pH.

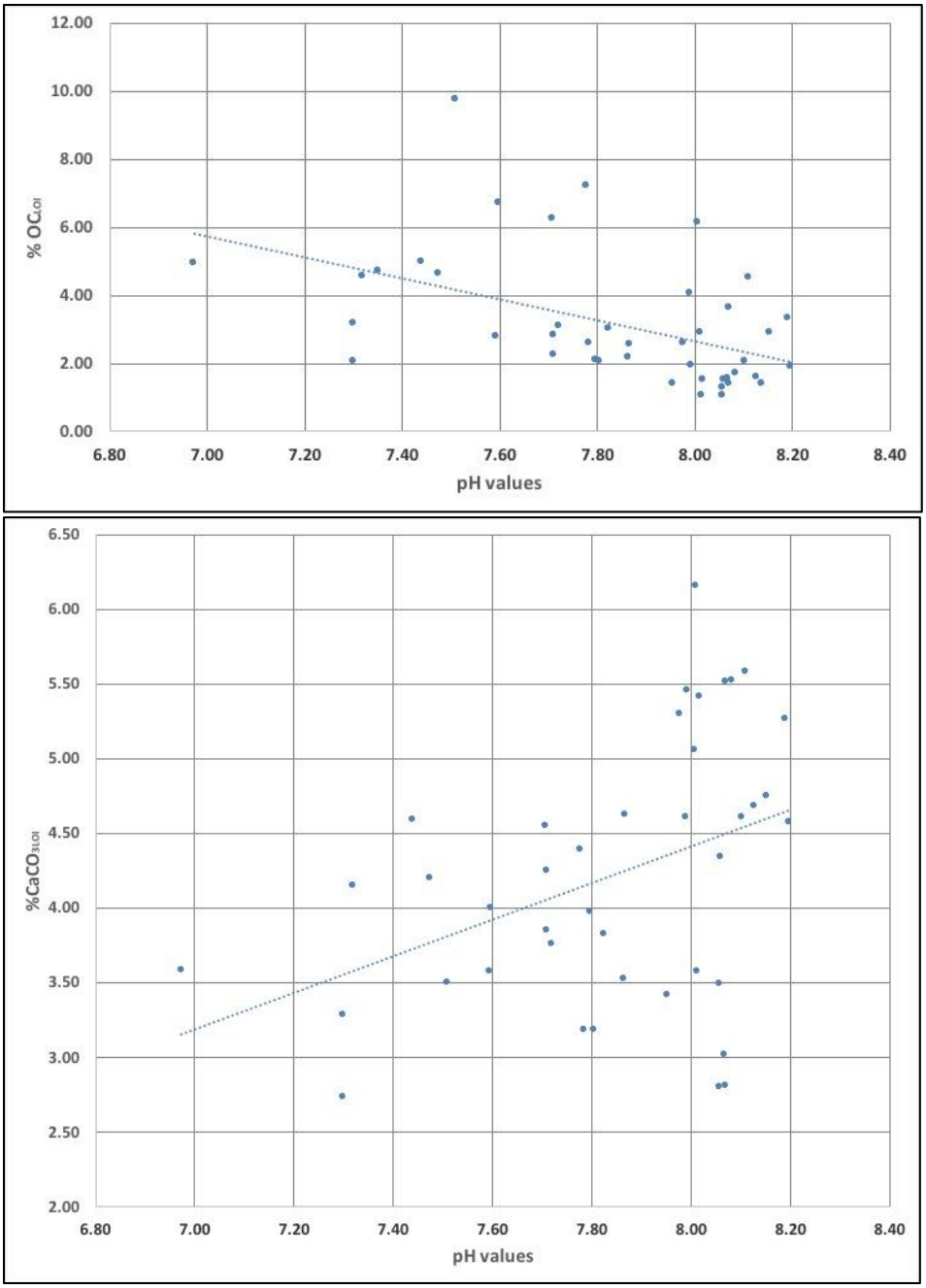

Figure 5.12. pH values vs. percent organic (%OC; above) and inorganic (%CaCO3; below) carbon data in Hurricane Bluff sediments and soils.

5.4 DRO and Hurricane Bluff Stratigraphic Considerations and Correlations

The DRO and Hurricane Bluff sites are situated on the same terrace system, only within 200 meters distance of each other. The lithostratigraphy and pedostratigraphy from each site shows similarities and variation across the terrace. The DRO stratigraphic column is over 6 m high, while the Hurricane Bluff column is around 3.6 m high. Much of this height difference

between the two sites' stratigraphies is due to the thickness of the Upper Sand at the DRO site, which is discussed more below. Figure 5.13 shows correlations across the stratigraphic profiles of the two sites.

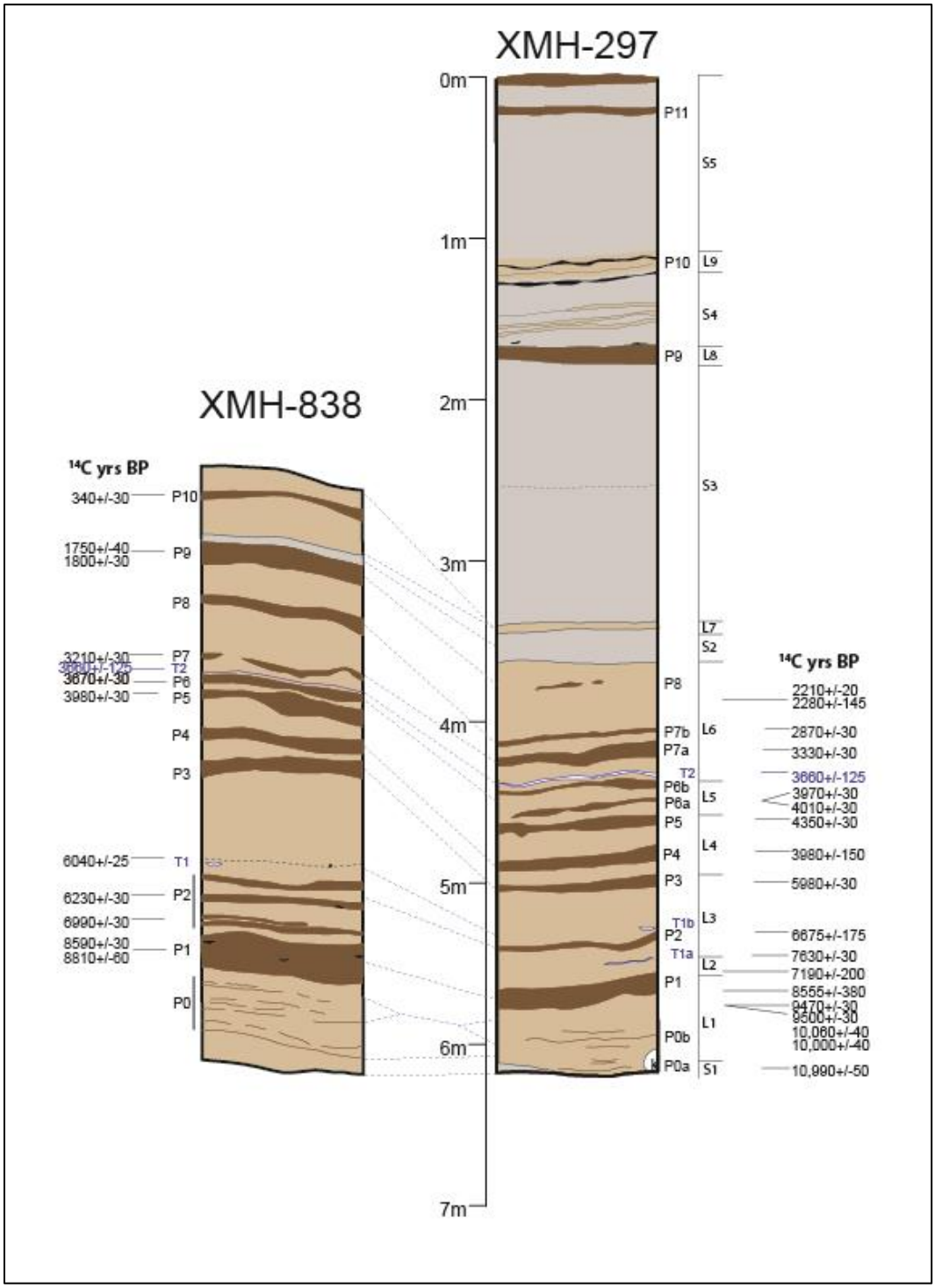

Figure 5.13. Generalized stratigraphic profiles of the Delta River Overlook and Hurricane Bluff sites showing correlations (blue lines) between sediment units and paleosols and pedocomplexes.

The basal outwash Unit 1 is the same across the sites The DRO Unit 2 aeolian sand was not recognized at the Hurricane Bluff stratigraphic column by either Higgs et al. (1999) nor the present study. This sand could have been removed from the Hurricane Bluff site area, as the Unit 2 sand was discontinuous in the DRO excavations likely due to deflation across the site area. Another explanation for the lack of recognition of this lower aeolian sand at Hurricane Bluff is that the Higgs et al. (1999) and the present study took stratigraphic observations from trenches very nearby each other and from limited area (<4 m wide area) along the erosional edge. The Unit 2 DRO aeolian sands may be present at the Hurricane Bluff site but they just have not been recognized yet due to this limited area of trenching.

The lower lithostratigraphic loess units of the sites displays some similarities. Unit 2 loess at the Hurricane Bluff site and Unit 3 loess at the DRO site accumulated at the same time given the ages on the soils from each stratigraphic column. The texture of loess from each lower loess unit is roughly similar with a dominance of silt loams, although the Hurricane Bluff site has coarser materials throughout its column. DRO Unit 3 loess is skewed toward very fine particle sizes, although particles sizes between 447 and 460 cmBS show a slight increase in sand content and are fine skewed. The Unit 2 loess at Hurricane Bluff fluctuated between very fine and fine to symmetrical and coarse skewing. Sorting at DRO is primarily unimodal, while at Hurricane Bluff soring ranges from unimodal to trimodal. The differences in skewness and sorting of particle sizes likely reflects slightly different distances from and elevations above the floodplain and the aeolian sediment sources. The DRO site excavation area is between 19-32 m higher than the Hurricane Bluff site from the floodplain.

The DRO site Upper Sands, Units 4 through 10, do not show distinctive correlations with the upper units, Units 3 and 4, at the Hurricane Bluff site. Unit 4 aeolian sand and Unit 5 loess deposition may correlate with Unit 3 aeolian sand and Unit 4 loess accumulation at Hurricane Bluff. Hurricane Bluff Units 3 and 4 accumulation occurred after 1500 cal yr BP and before 480-310 cal yr BP. We do not have ages estimates on the deposition of Units 4 and 5 at DRO other than that they began to accumulate after 2000-1900 cal yr BP. DRO Units 6 through 10 in the Upper Sand have no apparent correlations with units at Hurricane Bluff, possibly because the upper sands and silts at DRO were redeposited from disturbed local sources within the immediate vicinity of the excavation area.

The pedostratigraphy at both sites shows similar periods of soil development; however, paleosols and pedocomplexes show differing developmental expressions. DRO Pedocomplexes 0 through 7 and Paleosol 8 correlate with Pedocomplexes 0 through 2, 5 and 6 and Paleosols 3, 4, and 7-9 based on age and their position with each stratigraphic column. Pedocomplexes 0 at both sites are thin entisols (Ab horizons). Pedocomplex 1 at DRO has 3-4 thin entisols (Ab horizons) that overlay a single inceptisol (ABwb horizon), while Pedocomplex 1 at Hurricane Bluff has two inceptisols (ABwb horizons). Pedocomplex 2 at DRO has two inceptisols (Bwb and ABwb horizons); Pedocomplex 2 at Hurricane Bluff has two distinct couplets of thin entisols (Ab and Abk horizons). At DRO Pedocomplex 3 is a group of four thin entisols (Ab horizons), while the correlative buried soil, Paleosol 3, at Hurricane Bluff is a single entisol (Ab horizon). Pedocomplex 4 at DRO consists of a group of two thin entisols (Ab horizons) that overlay three inceptisols (ABwb horizons), while the correlative buried soil, Paleosol 4, at Hurricane Bluff is a single entisol (Ab horizon).

Pedocomplexes 5 from the DRO and Hurricane Bluff sites correlate across the terrace. Pedocomplex 5 at the DRO site is expressed as an inceptisol (ABwb horizon) overlying an

entisol (Ab horizon). At the Hurricane Bluff site, this complex is expressed as two distinct inceptisols (Bwb horizons).

Pedocomplexes 6 from the DRO and Hurricane Bluff sites also correlate across the terrace. Pedocomplex 6 at the DRO site is expressed as two soil couplets; the lower couplet is an entisol (Ab horizon) that overlies an inceptisol (ABwb horizon) and the upper couplet consists of two entisols (Ab horizons). Pedocomplex 6 at the Hurricane Bluff site solely consists of two entisols (Ab horizons).

The DRO site Pedocomplex 7 correlates with Paleosols 7 and 8 at the Hurricane Bluff site. The DRO Pedocomplex 7 has two soils couplets; the upper has two thin entisols (Ab horizons), while the lower has an entisol (Ab horizon) that overlays an inceptisol (ABwb horizon). The Hurricane Bluff site Paleosols 7 and 8 are inceptisols that have distinct A and Bwb horizons. Paleosol 8 from the DRO site correlates with Paleosol 9 from the Hurricane Bluff site; both are inceptisols but the Hurricane Bluff site Paleosol 9 has distinct A and Bwb horizons while the DRO site Paleosol 8 has only a Bwb horizon. The upper paleosols from DRO, Pedocomplexes 9 and 10 and Paleosol 11, have no apparent correlative soils at Hurricane Bluff. Paleosol 10 at the Hurricane Bluff site has no correlative soil in the DRO pedostratigraphy. The variation of the paleosols and pedocomplexes between the sites and across the terrace localized differences in topography, accumulation of aeolian sediments, erosion of soils and sediments, hydrology within the lithologic units, and changes in soil temperature.

The timing of tephra deposition at both sections appear similar. At DRO, three tephras (T1a, T1b, and T2) were recognized, while at Hurricane Bluff only two tephras (T1 and T2) have been documented thus far. Each of these tephra beds is very thin being 2 cm thick at the thickest extent but on average <1 cm in thickness. The particle sizes of the beds are mostly fine to very fine silts. The very thin and fine characteristics of the tephra beds indicates that the original volcanic sources of the pyroclastic materials is located some distance from the sites, likely on the order of hundreds of miles away.

T1a at DRO is situated between Pedocomplexes 1 and 2 with an estimated age of accumulation between 8240 and 7250 cal yrs BP. At Hurricane Bluff, a tephra between Pedocomplexes 1 and 2 has yet to be recognized. T1b at DRO is situated just above Pedocomplex 2 and several cm below Pedocomplex 3. T1b has an estimated age between 7550 and 6820 cal yrs BP based on radiocarbon ages from Pedocomplexes 2 and 3; however, the age is mostly likely closer to the older end of this age estimation based on its closer proximity to Pedocomplex 2. T1 at Hurricane Bluff is situated between Pedocomplex 2 and Paleosol 3 with an estimated age of accumulation between 7170 and 6890 cal yr BP. The positions of DRO T1b and Hurricane Bluff T1 within the pedostratigraphy of the terrace are similar, and the age estimations overlap (Figure 5.14). While we were unable to acquire geochemical data from DRO T1b and Hurricane Bluff T1 to verify these intersite correlations, the timing and stratigraphic placement of these tephras suggest that these are from the same eruptive event.

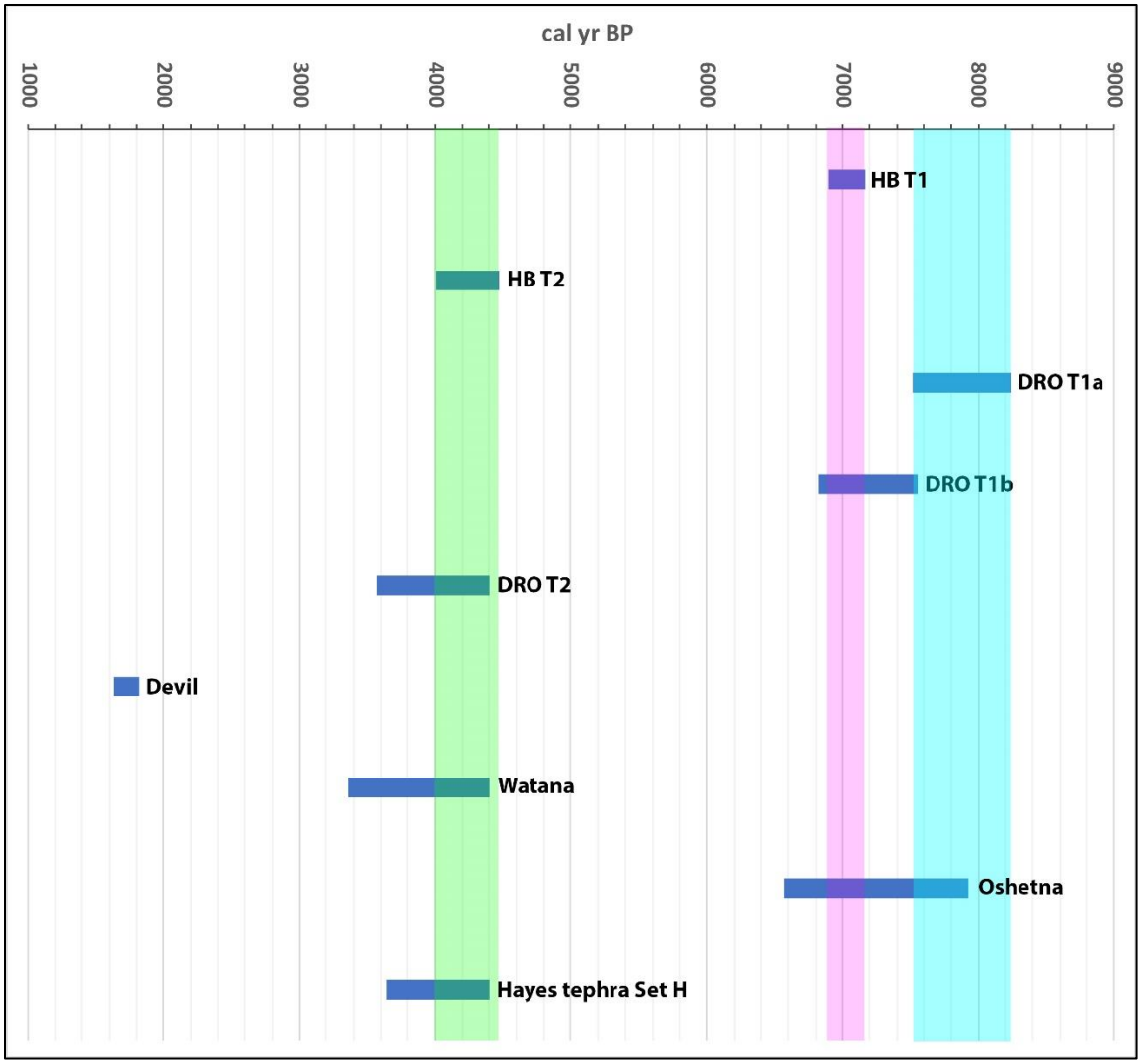

Figure 5.14. The age distribution of the Delta River Overlook (DRO) and Hurricane Bluff (HB) tephras, Hayes tephra set H, and the Devil, Watana and Oshetna tephras in the middle Susitna River Valley. Blue, purple and green shading indicates age distribution overlap.

DRO T2 is situated between Pedocomplexes 6 and 7; Hurricane Bluff T2 is situated between Pedocomplex 6 and Paleosol 7. The age estimate of DRO T2 accumulation is 4400 to 3570 cal yrs BP, while Hurricane Bluff T2 is between 4470 to 4000 cal yr BP. The similar positions in the pedostratigraphy and overlapping age estimates suggest the DRO T2 and Hurricane Bluff T2 tephras are from the same eruptive event (Figure 5.14). We were only to acquire geochemical data on a sample from DRO T2 to make absolutely certain the intersite correlation between the two T2 tephras is correct.

As mentioned above, the geochemical results on the DRO T2 suggest significant similarities to the Devil and Watana proximal tephra beds found primarily in mSRV (Table 5.2), south of the Delta River Overlook site area. The geochemical results also suggest that the DRO T2 tephra is weakly correlated with the Hayes Unit D tephra from the Hayes River Outcrop at the Hayes Volcano (Table 5.2). The Devil tephra accumulation in the mSRV is estimated between 1825 and 1625 cal yrs BP, and couple thousand years later than the DRO T2 deposition.

Watana tephra deposition in the mSRV is estimated between 4400 and 3360 cal yrs BP; the geochemistry of the Watana tephra was found to be similar to Hayes Units D, E, F2, H1 and H2, which were deposited after 4100 to 4000 cal yr BP. The Watana tephra was found to geochemically correlate with the Jarvis, Cantwell, and Tangle Lakes Ash beds that were found in the Delta and Nenana River valleys and Tangle Lakes region (Begét et al. 1991, Reihle 1994, Reihle et al. 1990). Begét et al. (1991) provided an age estimate of 4400 and 3650 cal yrs BP for the deposition of these proximal tephras. The timing of the DRO T2 and Hurricane Bluff T2 tephras overlaps with the Jarvis, Cantwell, and Tangle Lakes Ash beds, Watana tephra, and the Hayes River Outcrop units (Figure 5.14). The Jarvis, Cantwell, and Tangles Lakes Ash Beds, and the Watana tephra have all been found to correlate to proximal volcanic ashes near the Hayes Volcano (Begét et al. 1991, Mulliken 2016, Reihle 1994, Reihle et al. 1990, Wallace et al. 2014). We follow Reihle's (1994) suggestion of lumping the Jarvis, Cantwell, and Tangle Lakes Ash beds, and Watana tephra under the nomenclature "Hayes tephra set H."

Proximal tephra beds in central Alaska that date into greater than 6000 cal yrs BP are few with the Oshetna tephra as the most significant regional deposit of this tine period. The age estimation for the deposition of the Oshetna tephra in the mSRV is between 7930 and 6570 cal yrs BP. The DRO T1a age (8240 and 7250 cal yrs BP) overlaps with the early part of the age estimate for the Oshetna ash fall. The DRO T1b and Hurricane Bluff T1 tephras (7550 and 6280 cal yrs BP and 7170 and 6890 cal yrs BP, respectively) have overlapping age ranges with the later portion of the Oshetna ash fall age estimation. The Oshetna tephra in the mSRV has been shown to have geochemically different populations of glass that likely indicates multiple eruptive histories that have contributed to this regional proximal tephra bed (Mulliken 2016). The DRO T1a and T1b and Hurricane Bluff T1 tephras most likely correlate with the Oshetna tephra, given that it is the most significant proximal tephra bed in central Alaska that dates before 6000 cal yrs BP. Again, the ages of the DRO T1a and T1b and Hurricane Bluff T1 tephras overlap with the Oshetna's age distribution (Figure 5.14). The DRO T1a and T1b tephras may represent multiple eruptive events in the history of the Oshetna tephra deposition. However, geochemical analyses on the DRO and Hurricane Bluff tephras to confirm this hypothetical correlation.

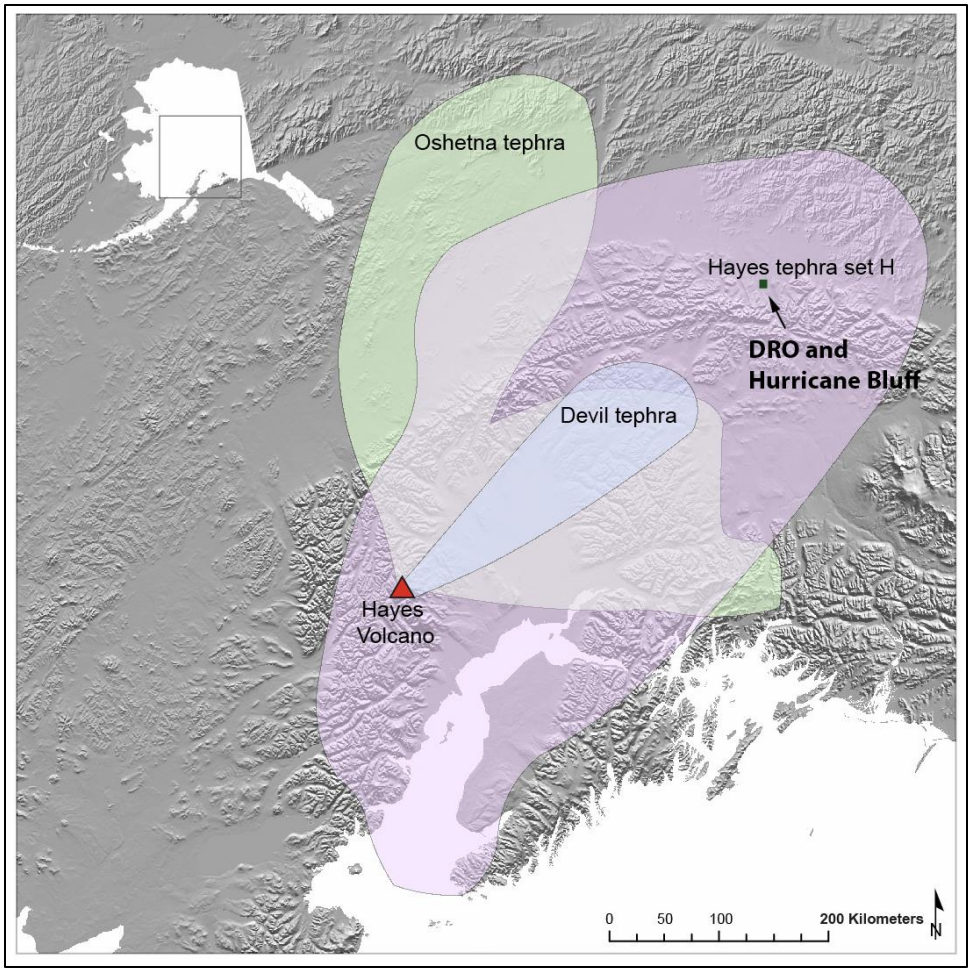

Figure 5.15. Map showing the location of the Delta River Overlook and Hurricane Bluff Sites and the distributions of the Hayes set H, Devil and Oshetna tephras.

5.5 Site Formation and Post-Disturbance Histories

The DRO and Hurricane Bluff site stratigraphic columns show histories of loess and aeolian sand accumulation, localized erosion, and periods of landform stabilization and soil development. Once loess accumulation commenced around 13,000 cal yr BP, accumulation appears to have remained relatively constant with high accumulations rates (Table 5.10) compared to other loessic depositional sequences in the middle Tanana Valley (Dilley 1998; Reuther 2013).

Table 5.10. Deposition rates of sediments calculated from depths of radiocarbon ages at the Delta River Overlook and Hurricane Bluff sites.

Time Period (cal yrs BP)	*Deposition Rate (cm/100 years)*[1]
Delta River Overlook	
2230-0	16.64
2990-2230	5.53
3570-2990	3.45
4000-3570	2.09
4480-4000	3.75
4915-4480	2.53
6820-4915	1.99
7550-6820	4.66
8420-7550	2.07
9580-8420	1.03
10730-9580	0.61
11470-10730	4.05
11590-11470	0.00
12850-11590	1.83
Hurricane Bluff	
390-0	11.28
1720-390	2.33
3420-1720	2.35
4000-3420	1.72
4470-4000	2.13
6890-4470	3.51
7170-6890	10.83
7830-7170	3.32
9580-7830	1.88

[1]Deposition rate calculation based on Stein et al. (2003).

When comparing to other loessic sequences in the middle Tanana Valley (the Bachner, Broken Mammoth, Mead, and Swan Point sites), loess accumulation rates in the middle to late Holocene at DRO are higher than most sequences (Figure 5.16). The closest accumulation rates at these middle Tanana Valley sections are in the late Pleistocene to early Holocene between 14,000 to 11,000 cal yrs BP. Péwé (1968) and Muhs et al. (2003) also noted higher accumulations of loess during the middle to late Holocene (after 6,000 cal yr BP) in Delta River sections.

The presence of multiple immature and weakly developed soils (entisols and inceptisols) throughout both DRO and Hurricane Bluff columns represent periods of landform stability across the terrace, even in the midst of the relatively constant and high accumulations of loess. The immaturity of the soils likely reflects disruptions to the vegetative and organic accumulation by excessive loess accumulation; in essence, loess deposition likely outcompeted more mature soil development across the terrace's edge.

Carbonate ($CaCO_3$) accumulation in Holocene occurred at both sites between 8500 and 6700 cal yrs BP. At the DRO site, carbonate accumulations are present in Unit 3 in Loess 2 and 3 between 505 and 556 cmBS. The DRO carbonate accumulation occurred between 8510 and 6730 cal yrs BP. At the Hurricane Bluff site, carbonate accumulations are in Unit 2 loess between 185-280 cmBS. An age of carbonate accumulation at Hurricane Bluff occurred between 7740 and 6800 cal yrs BP. Dilley (1998) has noted that periods of carbonate (assumed to be pedogenic carbonates) development in loess in the Tanana Valley likely occurred during more arid periods in the past.

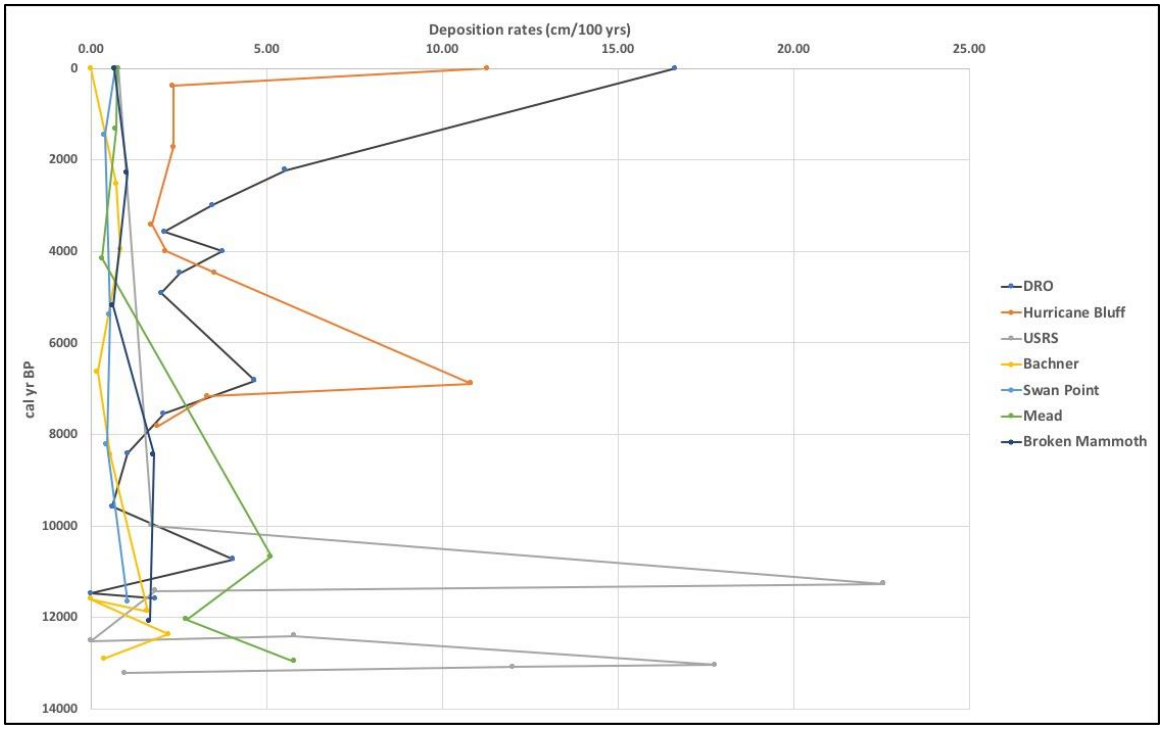

Figure 5.16. Deposition rates from the Delta River Overlook and Hurricane Bluff sites compared to the Bachner, Broken Mammoth, Mead, Swan Point and Upward Sun River (USRS) sites in the middle Tanana Valley (data from Reuther 2013).

At the DRO site, post-depositional disturbances include faulting and limited cryoturbation. Faults are evident in the DRO stratigraphic columns and cross-cut all of the soils and loess deposits in Unit 3 (Figure 5.17). In one area of the excavation area, a boulder in Unit 1 was separated in half by a fault. Soil horizon offsets by faulting are between 5-7.5 cm at their greatest extremes. All soil horizons were easily followed throughout the excavation area regardless of displacement by faults. Faults were not observed in the Upper Sand.

Post-deposition and post-soil formation disturbances on a macroscale to sediments and soils in Pedocomplex 5 and below at the DRO site are limited across the site area. Cryoturbation and solifluction were evident in Pedocomplexes 1 and 6 where some mixture of sediments and soil horizons has occurred (Figure 5.18). In Pedocomplexes 6 and 7 and Paleosol 8 at the DRO site, deflation and disturbance to the upper reaches of the Unit 3 loess has created truncations and discontinuity of these horizons across the entire excavation area.

As noted above, periodic localized erosion is indicated given within the DRO pedostratigraphy by missing Ab horizons from portions of paleosols that are otherwise ABwb horizons throughout most of the excavation area. In addition, the presence of an erosional disconformity between DRO's Units 3 and 4.

Figure 5.17. Faulting in Block B of the Delta River Overlook site.

Figure 5.18. Turbation is Pedocomplex 1 at the Delta River Overlook site.

5.6 Delta River Overlook Site Preservation Conditions

We provide a brief consideration of sediment condition at both of sites that may or may not promote the preservation of organic materials, including plant remains and osseous materials (i.e., bone and antler). There have been animal bones recovered from 11 out of the 14 components at the DRO site (see Chapter 8 Faunal Analysis). Sediment pH values for the sediments at both sites are primarily neutral to alkaline. The DRO sediments range is between 7.19 and 8.13 with an average of 7.81±0.24. pH values for the Hurricane Bluff sediments range from 6.97 and 8.20 with an average of 7.83±0.30.

Carbonate presence is high in some portions of the column and low to none existent in others, but pH remained neutral to low alkaline values which helps to slow the breakdown of bone. Entisols and inceptisols at DRO have relatively immature or weakly developed humic horizons and leaching zones that would create more acidic conditions and microbial activity conducive to breaking down bone. High accumulation rates of loess and aeolian sand may have quickly covered bones and moved them further away from leaching zones.

Colder environments that have lower soil temperatures through much of the year tend to have very slow microbial activity that works to break down bones in sediments and soils. The excellent bone preservation at the DRO site is likely due to all of the factors mentioned above.

CHAPTER 6. COMPONENT DELINEATION

Ben A. Potter

6.1 Introduction and Methods

The DRO site consists of 7+ meters of aeolian silt and sand overlying a poorly sorted glacial deposits. About 4 meters of the uppermost sediments, largely aeolian sand, has been deflated in the excavation area. Sediments within which Components 9 and 10 are situated have thus been removed from the excavation area, and will not be reported on. The extant cultural components are all situated in the lower aeolian loess (C horizons) and associated with numerous Ab and Bwb paleosol horizons and two tephras. Because of the rapid deposition of the loess and the clear horizonation of the paleosols and little evidence for cryoturbation and other homogenization factors, it is possible to clearly delineate multiple cultural components.

Several independent but connected methods were used to delineate components at DRO. First, stratigraphic analyses (presented in Chapters 4 and 5) linked each area of the main excavation to a unified comprehensive stratigraphic sequence. Each major paleosol (P0 through P8) were identified for each Excavation Block. Second, radiocarbon analyses independently supported the paleosol linkages (Chapter 4). Radiocarbon dates also delineated occupations within single strata, namely Loess 1 (Components 1, 2a, 2b, and 2c) through non-contemporaneity of assays and depth below Paleosol 1. Third, backscatter plots of 3-pointed items (Section 6.2 below) were used to visually identify cultural materials by strata and evaluate vertical displacement. Fourth, screened material was excavated to 5 cm level, and these level summaries are used to further constrain and delineate cultural components (Section 6.3 below). Tables 6.1 through 6.27 have lithic debitage and tool counts and fauna weights (in grams). Fifth, ArcGIS was used to visually analyze in ArcScene the 3 pointed items to confirm the patterning observed in Sections 6.2 and 6.3.

6.2 Backscatter Plots

Backscatter plots are 2-dimensional representations of 3-point provenienced artifacts displayed against a stratigraphic profile. All 3-pointed cultural items within 25 cm of a stratigraphic profile were added to each graph. Sixty-six linear meters of stratigraphy are illustrated in Figures 6.1 through 6.3. These profiles are chosen because (1) they are long, unbroken profiles showing variation in thickness, number, and expression of multiple paleosols, and (2) they are within the densest concentrations of cultural material.

In the E494 line, C2a (dark blue) and C2c (red) are clearly vertically separated (Figure 6.1). C2b (green) are generally well separated from both C2a and C2c. Dots illustrated as C5/6? are C5a. C8a and C8b are clearly separated in the northern part of the profile. In the E496 line, C2a and C2c are again clearly separated, as well as C8a and C8b. Several microfaults are obvious, particularly in the middle part of this unit. The group of C3 in Block 9 may be associated with C2c; however, these materials are more closely associated with P1 than the typical C2c position, about 5-10 cm below P1 within L1. So, provisionally, these are assigned to Component 3. In the E498 line, C2 a, C2b, and C2c are clearly distinguished. C8a and C8b are also clearly separated.

In the N212 line, C8b is clearly delineated, above P7b and below another unnumbered paleosol (Figure 6.2). C2a and C2c are separated within L1. In the N210 line, the general east-west slope is apparent. C8b is present as a tight cluster above P7b. C5 is directly associated with P2. C2a and C2c are again clearly separated.

In the N206 line, C2a, C2c, and C3 are shown superimposed in their appropriate stratigraphic order and C5 is associated with P2 (Figure 6.3). In the N204 line, C2a, C2b, and C2c are clearly separated. C1 is present right above the glacial deposits. C4 is between P1 and P2.

Component integrity is very high. The horizonation of the sediments are clearly relatively undisturbed. The primary post-depositional disturbance to the deposits is limited displacement by localized microfaulting. Because there is clear horizonation and limited vertical spreads of associated cultural materials, high resolution analyses to delineate multiple components is relatively straightforward.

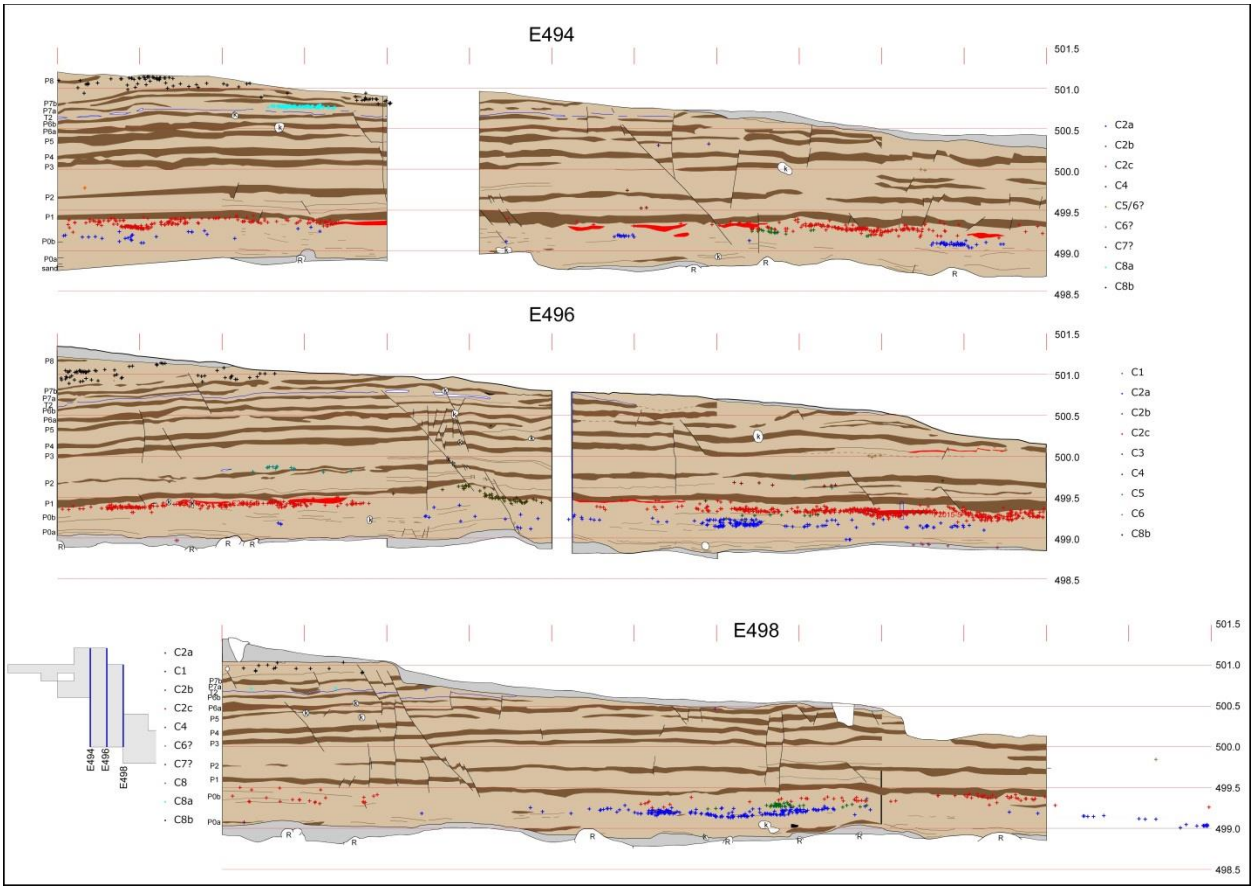

Figure 6.1 Backscatter plots along North-South stratigraphic profiles

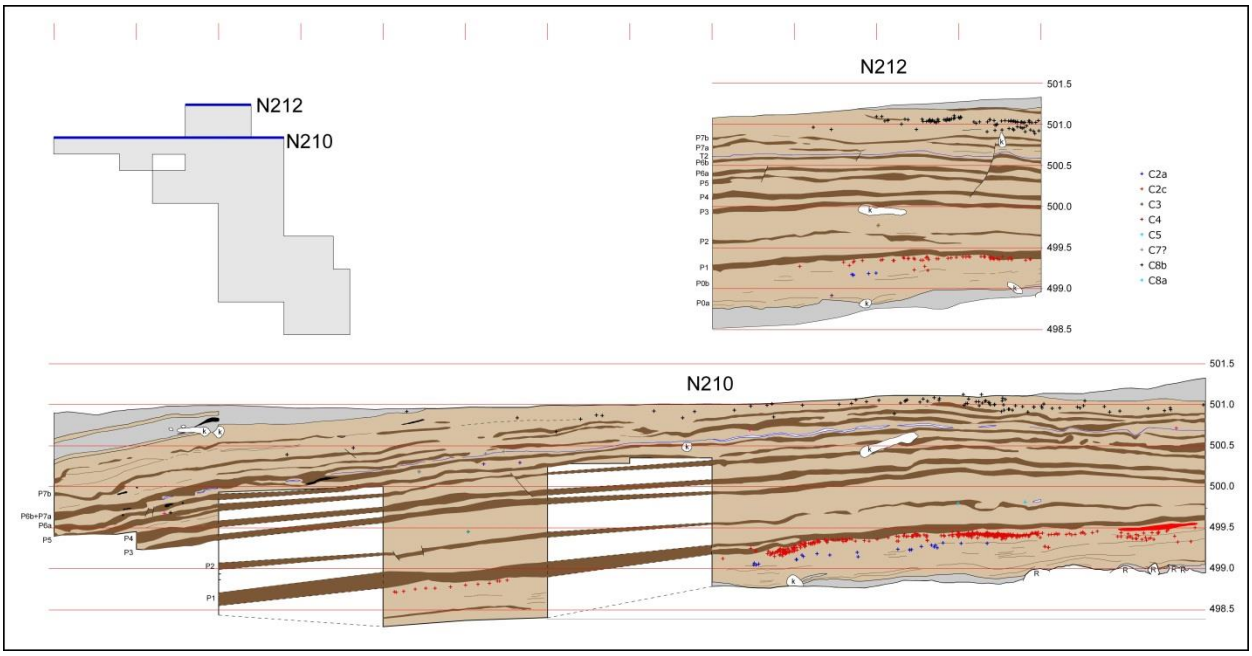

Figure 6.2 Backscatter plots along East-West stratigraphic profiles (N210, N212)

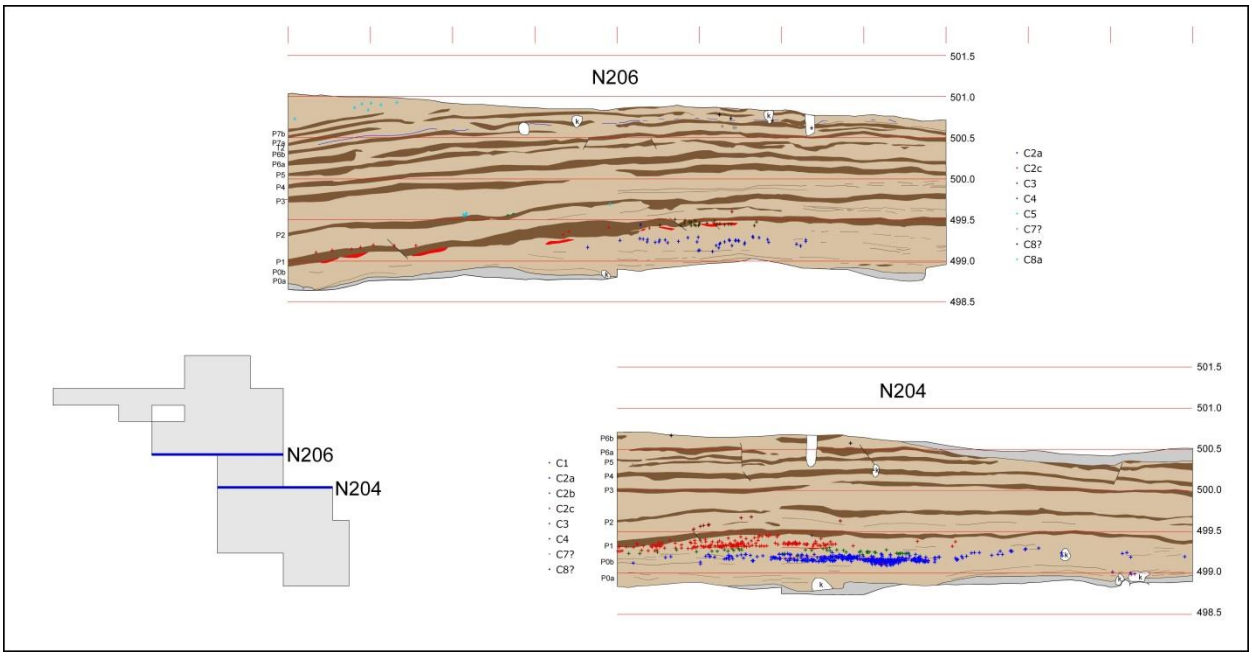

Figure 6.3 Backscatter plots along East-West stratigraphic profiles (N204, N206)

6.3 Excavation Block Analysis

Level data on lithics (debitage), lithic tools, and fauna (in grams) are provided for each 5 cm level below surface for all excavation blocks (Tables 6.1 through 6.26), including 1979 excavation Blocks A and B (Table 6.27). These data are graphically illustrated in bar charts along with position of Paleosols 1 and 2 and component designators (Figures 6.4 through 6.27).

6.3.1 Block 1 Analysis

Block 1 was excavated from the erosional surface to glacial deposits, between ~499.940 m elev to ~498.820 m elev, about 1.12 meters. A total of 318 pieces of lithic debitage and 5 tools were recovered (Table 6.1, Figure 6.4). Paleosols 1 and 2 were well expressed. The uppermost extant stratum was the Loess above P4. A clear separation between C2c at 0-10 cm below P1 and C2a at 20-30 cm below P1 is evident. Three components are present in Block 1: C2a, C2c, and C6a.

Table 6.1 Block 1 component data

Component	*Lithics*	*Tools*	*Fauna*
C8b			
C8a			
C7b			
C7a			
C6b			
C6a	21	1	
C5b			
C5a			
C4			
C3			
C2c	11	4	15.60
C2b			
C2a	286		33.03
C1			
Total	318	5	48.63

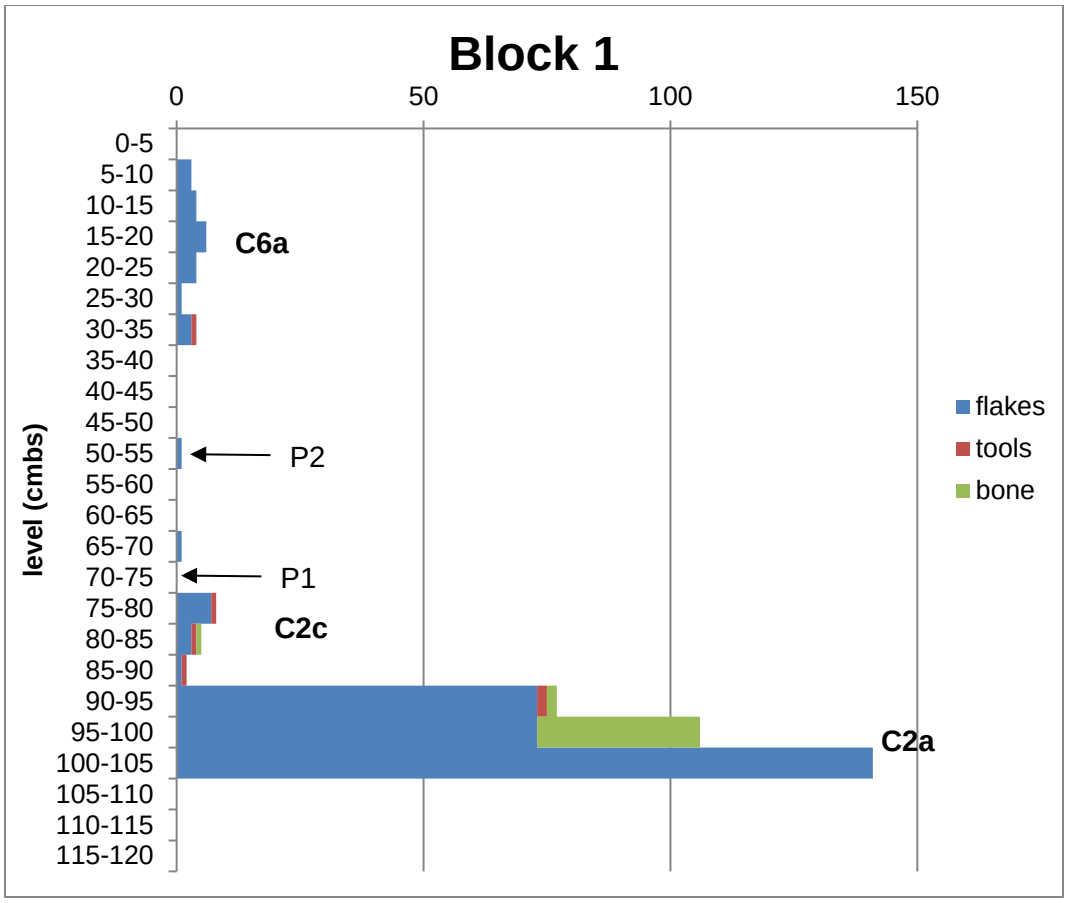

Figure 6.4 Block 1 level summary data

6.3.2 Block 2 Analysis

Block 2 was excavated from the erosional surface to glacial deposits, between ~500.084 m elev to ~498.765 m elev, about 1.319 meters. A total of 79 pieces of lithic debitage and 2 tools were recovered (Table 6.2, Figure 6.5). Paleosols 1 and 2 were well expressed. The uppermost extant stratum was the Loess above P4. Three major components were isolated based on lithics in Block 2, C3 and C4, along with C6a. Additionally, a bison mandible was found within Paleosol 2, and assigned to C5a. Four components are present in Block 2: C2c, C3, C4, and C6a.

Table 6.2 Block 2 component data

Component	*Lithics*	*Tools*	*Fauna*
C8b			
C8a			
C7b			
C7a			
C6b			
C6a	17		0.01
C5b			
C5a			109.07
C4	28		39.58
C3	33	1	12.08
C2c	1	1	
C2b			
C2a			
C1			
Total	79	2	160.74

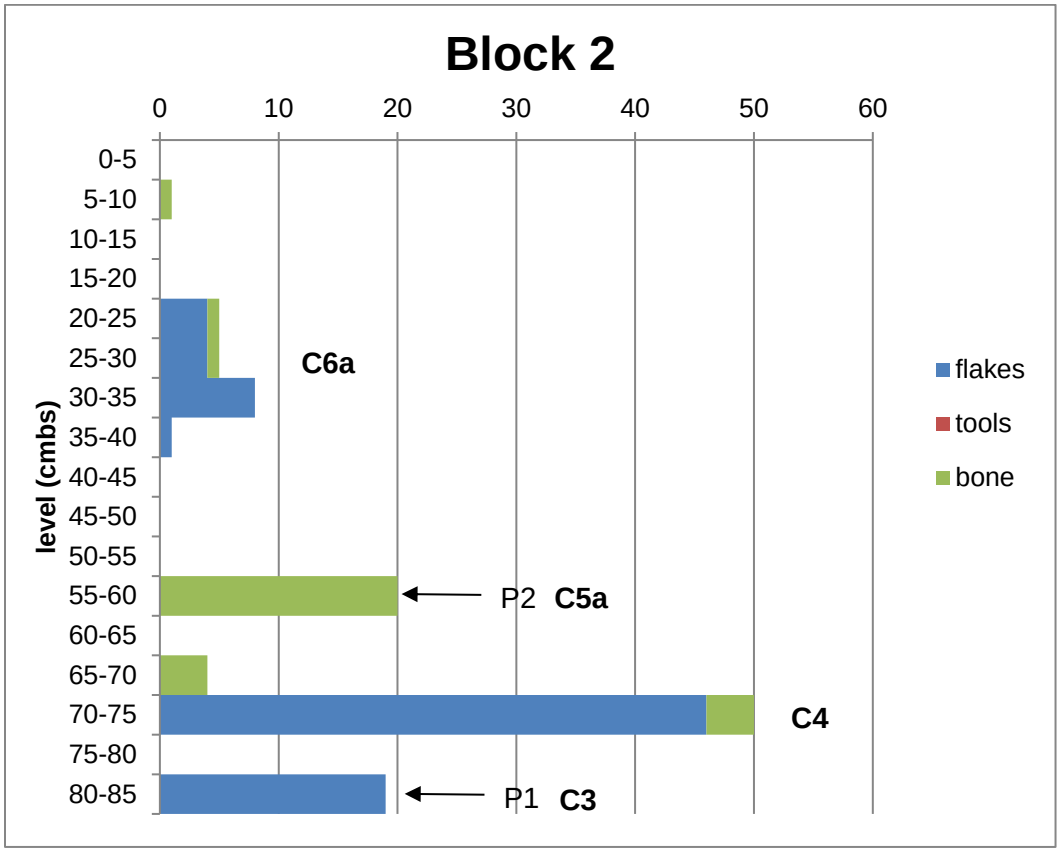

Figure 6.5 Block 2 level summary data

6.3.3 Block 3 Analysis

Block 3 was excavated from the erosional surface to glacial deposits, between ~500.183 m elev to ~498.838 m elev, about 1.345 meters. Three components are clearly delineated with respect to P1 and P2, C2c, C4, and C6a (Table 6.3, Figure 6.6). Additionally, a lithic cobble was recovered within C2c.

Table 6.3 Block 3 component data

Component	*Lithics*	*Tools*	*Fauna*
C8b			
C8a			
C7b			
C7a			
C6b			
C6a	83	2	3.83
C5b			
C5a			
C4	4	2	
C3			
C2c	66	1	
C2b			
C2a			
C1			
Total	153	5	3.83

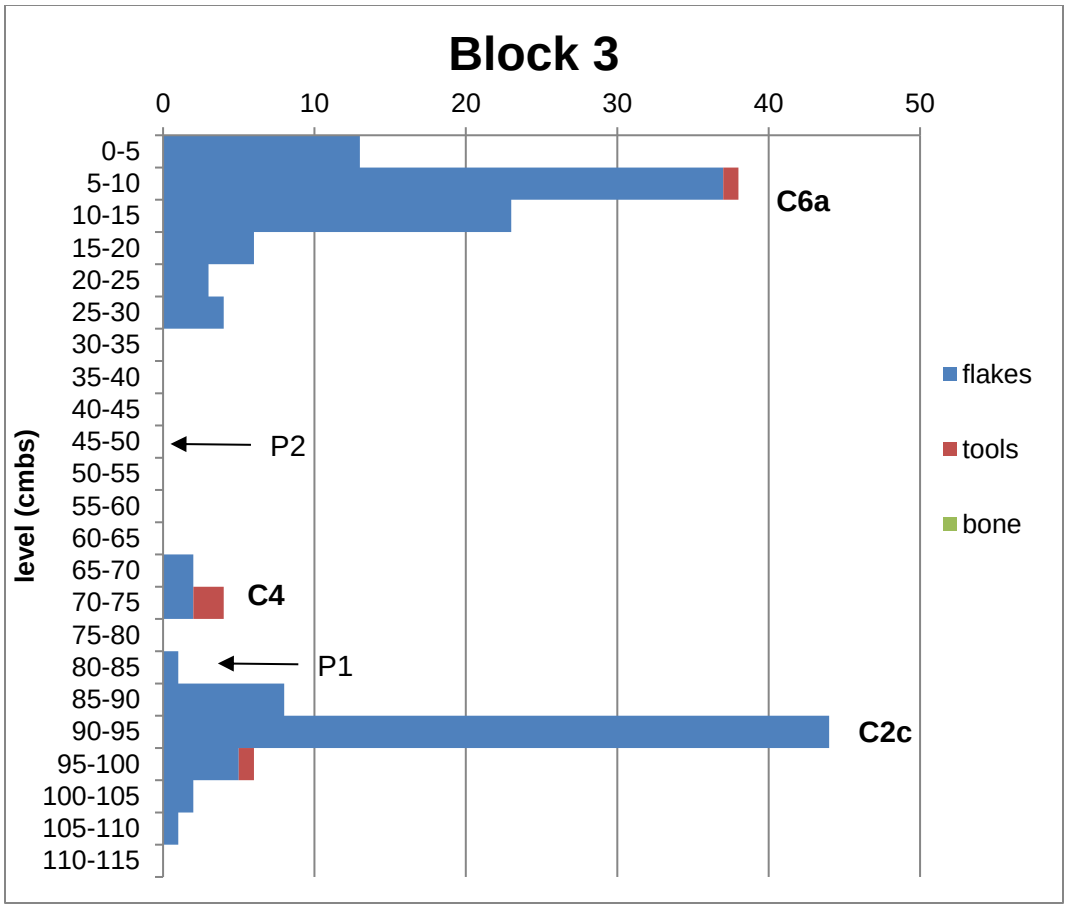

Figure 6.6 Block 3 level summary data

6.3.4 Block 4 Analysis

Block 4 was excavated from the erosional surface to glacial deposits, between ~500.288 m elev to ~498.843 m elev, about 1.445 meters. A total of 891 pieces of debitage and 12 tools were recovered (Table 6.4, Figure 6.7). In addition to the materials in Table 6.4, a lithic cobble was found in C2c. Six components are found in Block 4: C1, C2a, C2c, C3, and C6a.

Table 6.4 Block 4 component data

Component	*Lithics*	*Tools*	*Fauna*
C8b			
C8a			
C7b			
C7a			
C6b			
C6a	26		
C5b			
C5a			
C4	1	1	
C3			352.71
C2c	622	10	2.60
C2b			
C2a	240	1	14.09
C1	2		
total	891	12	369.40

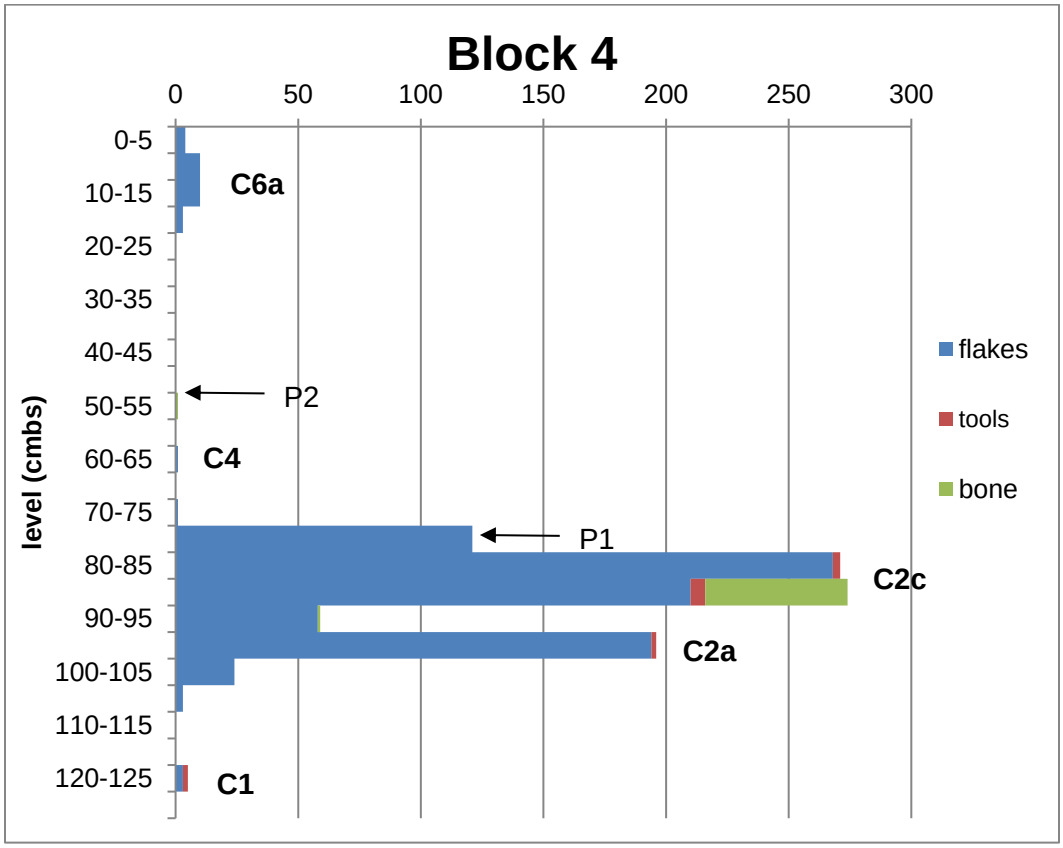

Figure 6.7 Block 4 level summary data

6.3.5 Block 5 Analysis

Block 5 was excavated from the erosional surface to glacial deposits, between ~500.348 m elev to ~498.869 m elev, about 1.479 meters. A total of 753 pieces of debitage and 5 tools and 2.72 g of fauna were recovered (Table 6.5, Figure 6.8). In addition, 3 lithic cobbles were found in C2a. Five components were found in Block 5: C1, C2a, C2c, C3, C6a.

Table 6.5 Block 5 component data

Component		*Lithics*	*Tools*	*Fauna*
C8b				
C8a				
C7b				
C7a				
C6b				
C6a		7		2.72
C5b				
C5a				
C4				
C3		1		
C2c		70		
C2b				
C2a		314	1	
C1		361	4	
Total		753	5	2.72

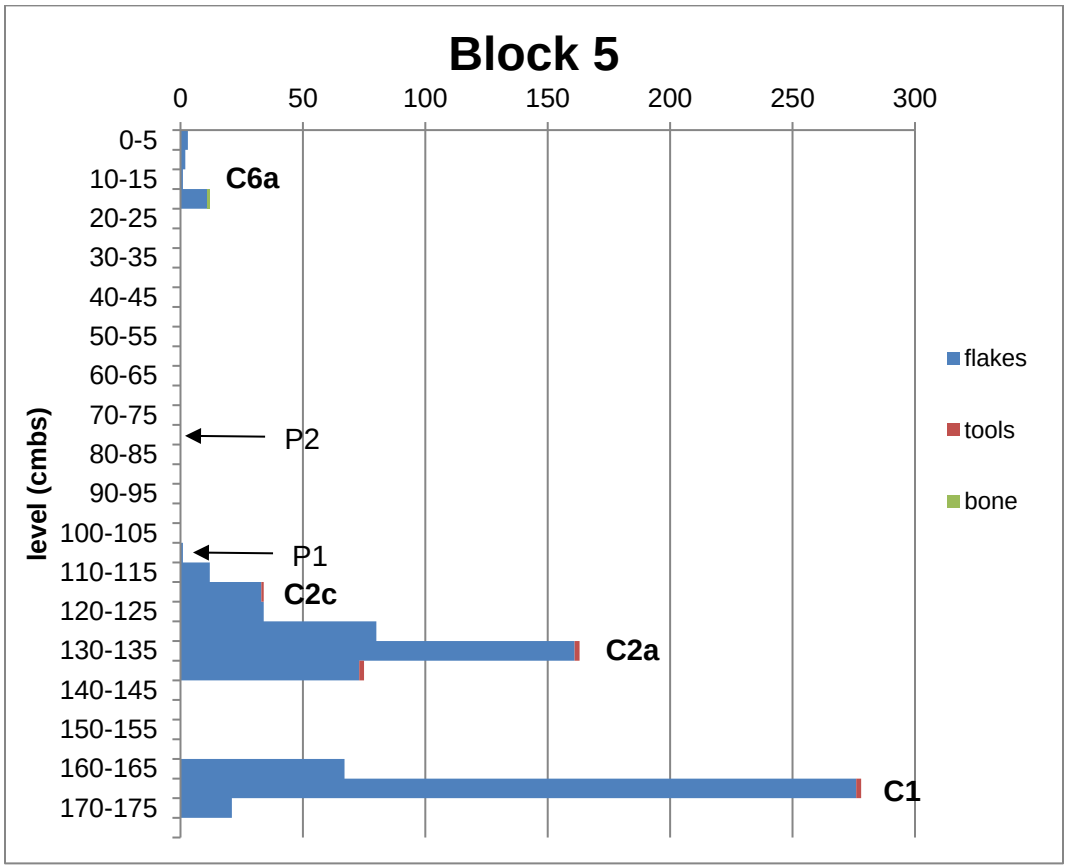

Figure 6.8 Block 5 level summary data

6.3.6 Block 6 Analysis

Block 6 was excavated from the erosional surface to glacial deposits, between ~500.561 m elev to ~498.876 m elev, about 1.685 meters. A total of 3904 pieces of debitage and 12 tools and 101.72 g of fauna were recovered in Block 6 (Table 6.6, Figure 6.9). In addition, two lithic cobbles were found in C6a and C7b respectively. Eight components were found in Block 6: C1, C2a, C2b, C2c, C4, C5a, C6a, and C7b.

Table 6.6 Block 6 component data

Component	*Lithics*	*Tools*	*Fauna*
C8b			
C8a			
C7b	6	1	3.00
C7a			
C6b			
C6a			
C5b			
C5a	11		
C4	6		
C3			
C2c	792	3	0.73
C2b	342	1	88.70
C2a	2745	6	9.29
C1	2		
Total	3904	12	101.72

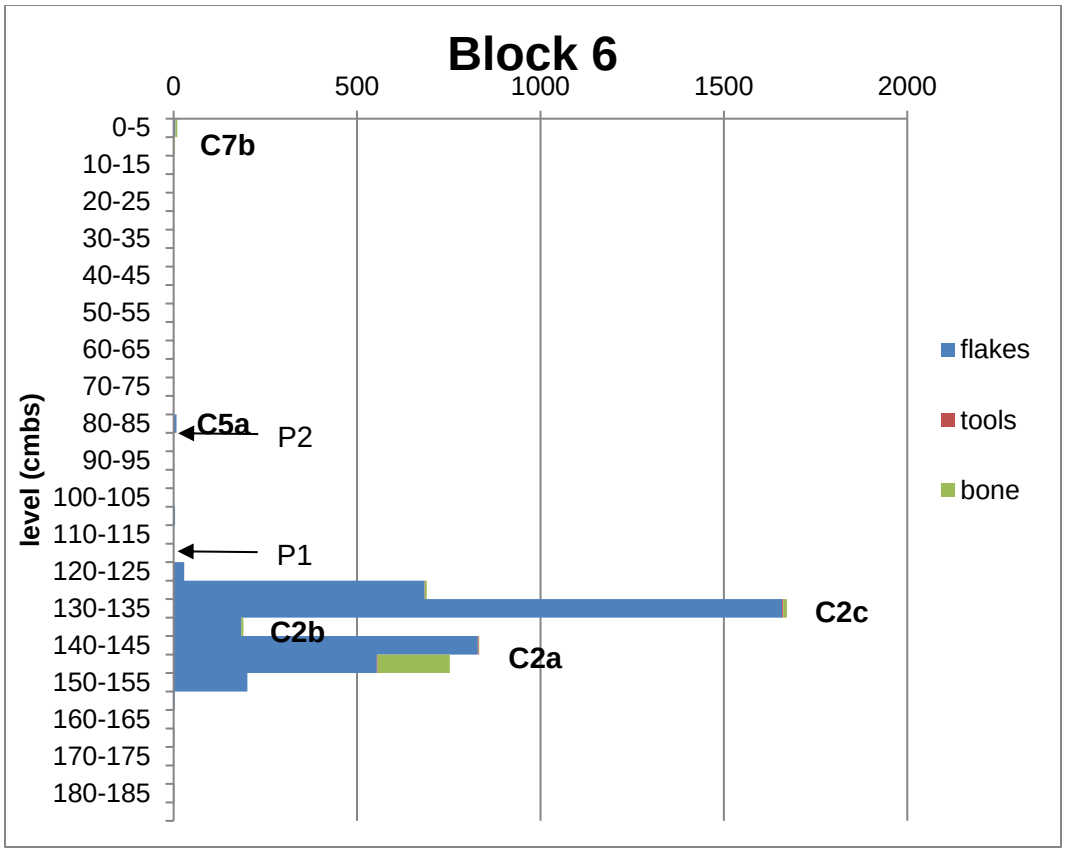

Figure 6.9 Block 6 level summary data

6.3.7 Block 7 Analysis

Block 7 was excavated from the erosional surface to glacial deposits, between ~500.764 m elev to ~498.846 m elev, about 1.828 meters. A total of 2598 pieces of debitage and 17 tools and 28.34 g of fauna were recovered in Block 7 (Table 6.7, Figure 6.10). In addition, 2 lithic cobbles were found in C2a and 1 lithic cobble was found in C2c. Eight components were found in Block 7: C1, C2a, C2c, C3, C5a, C6a, C7b, and C8b.

Table 6.7 Block 7 component data

Component	*Lithics*	*Tools*	*Fauna*
C8b	14		
C8a			
C7b	11	3	
C7a			
C6b			
C6a			1.27
C5b			
C5a	13	1	
C4			
C3	7		
C2c	171	1	0.32
C2b			
C2a	2382	11	26.75
C1		1	
Total	2598	17	28.34

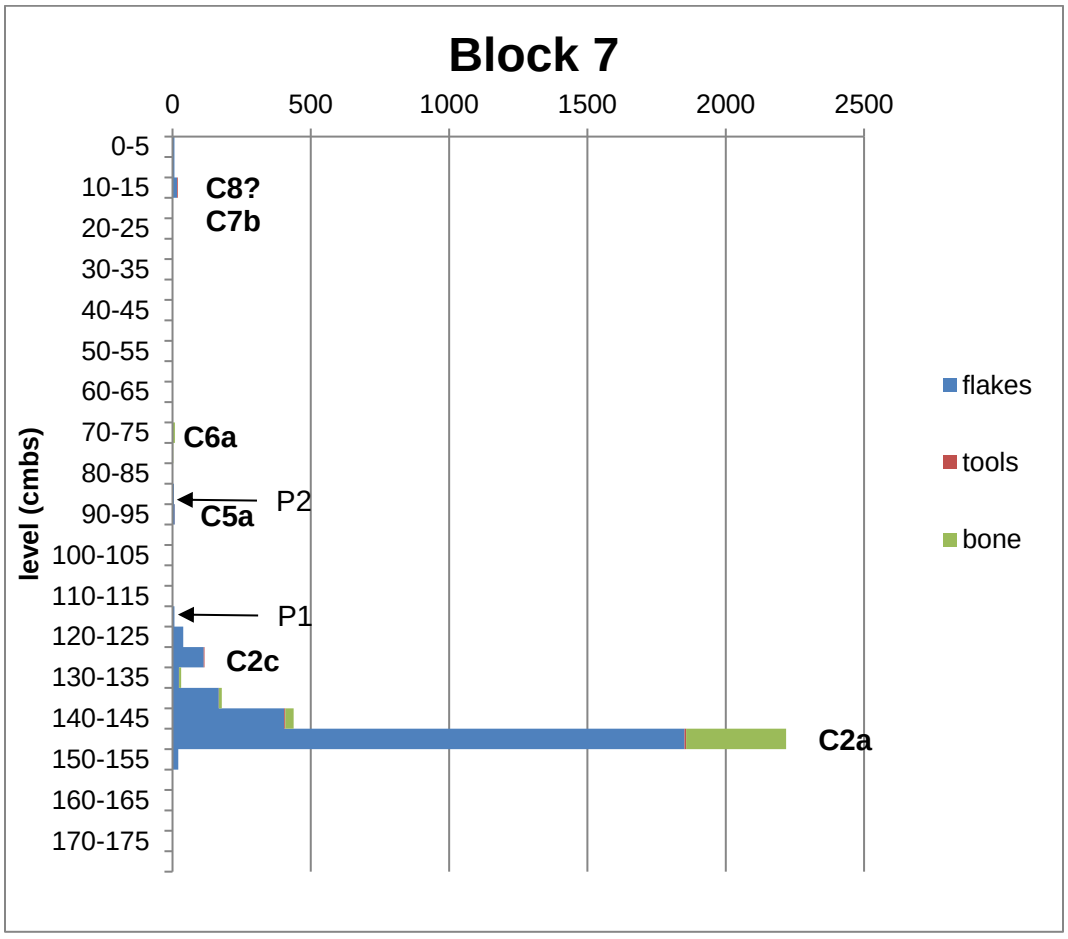

Figure 6.10 Block 7 level summary data

6.3.8 Block 8 Analysis

Block 8 was excavated from the erosional surface to glacial deposits, between ~500.739 m elev to ~498.831 m elev, about 1.908 meters. A total of 334 pieces of debitage and 5 tools and 15.63 g of fauna were recovered from Block 8 (Table 6.8, Figure 6.11). In addition, a lithic cobble was found in C2c. Six components were found in Block 8: C2a, C2c, C4, C5a, C7b, and C8b.

Table 6.8 Block 8 component data

Component	*Lithics*	*Tools*	*Fauna*
C8b	6		
C8a			
C7b	13	1	
C7a			
C6b			
C6a			
C5b			
C5a			2.51
C4	75	1	11.36
C3			
C2c	138	2	0.45
C2b			
C2a	102	1	1.31
C1			
Total	334	5	15.63

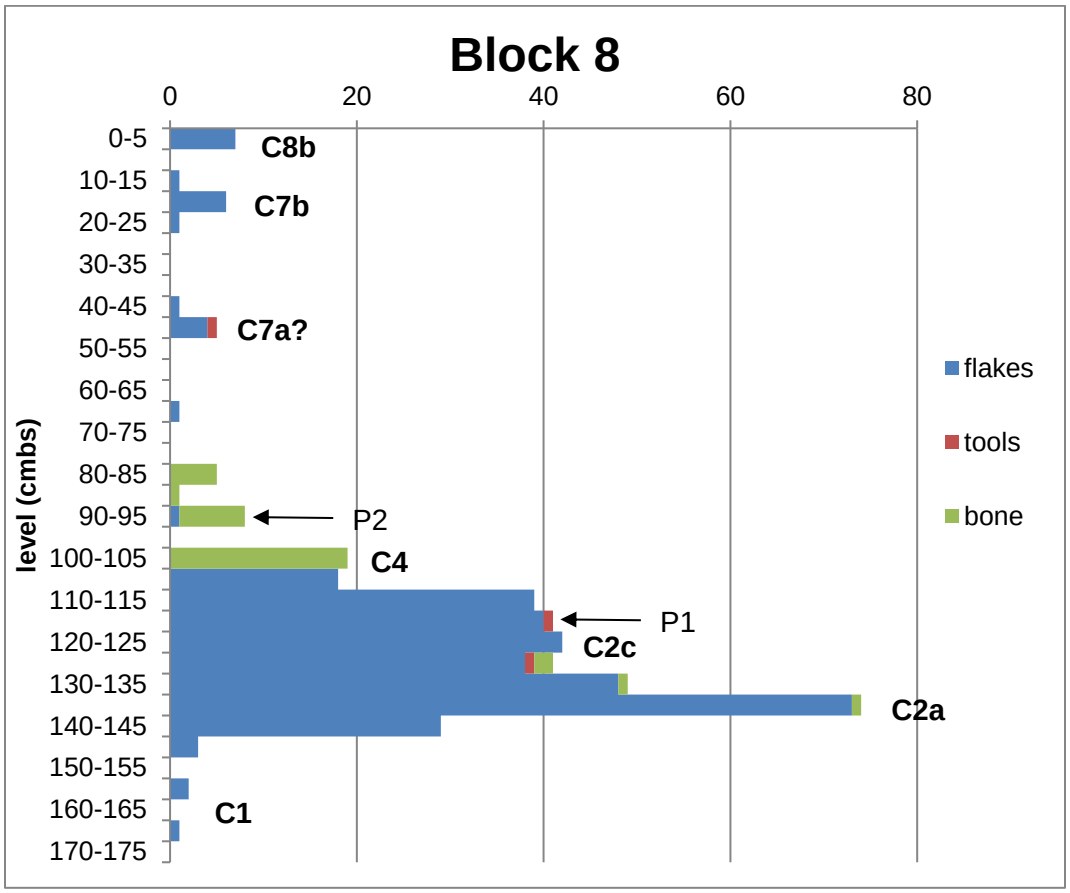

Figure 6.11 Block 8 level summary data

6.3.9 Block 9 Analysis

Block 9 was excavated from the erosional surface to glacial deposits, between ~500.877 m elev to ~498.934 m elev, about 1.943 meters. A total of 544 pieces of debitage and 8 tools and 71.56 g of fauna were recovered in Block 9 (Table 6.9, Figure 6.12). In addition, 2 lithic cobbles were found in C2a. Six components were found in Block 9: C2a, C2c, C3, C4, C6b, and C8b.

Table 6.9 Block 9 component data

Component	*Lithics*	*Tools*	*Fauna*
C8b	62	2	50.76
C8a			
C7b			
C7a			
C6b	1		
C6a			
C5b			
C5a			
C4	18		
C3	167	4	17.40
C2c	28		
C2b			
C2a	268	2	3.40
C1			
Total	544	8	71.56

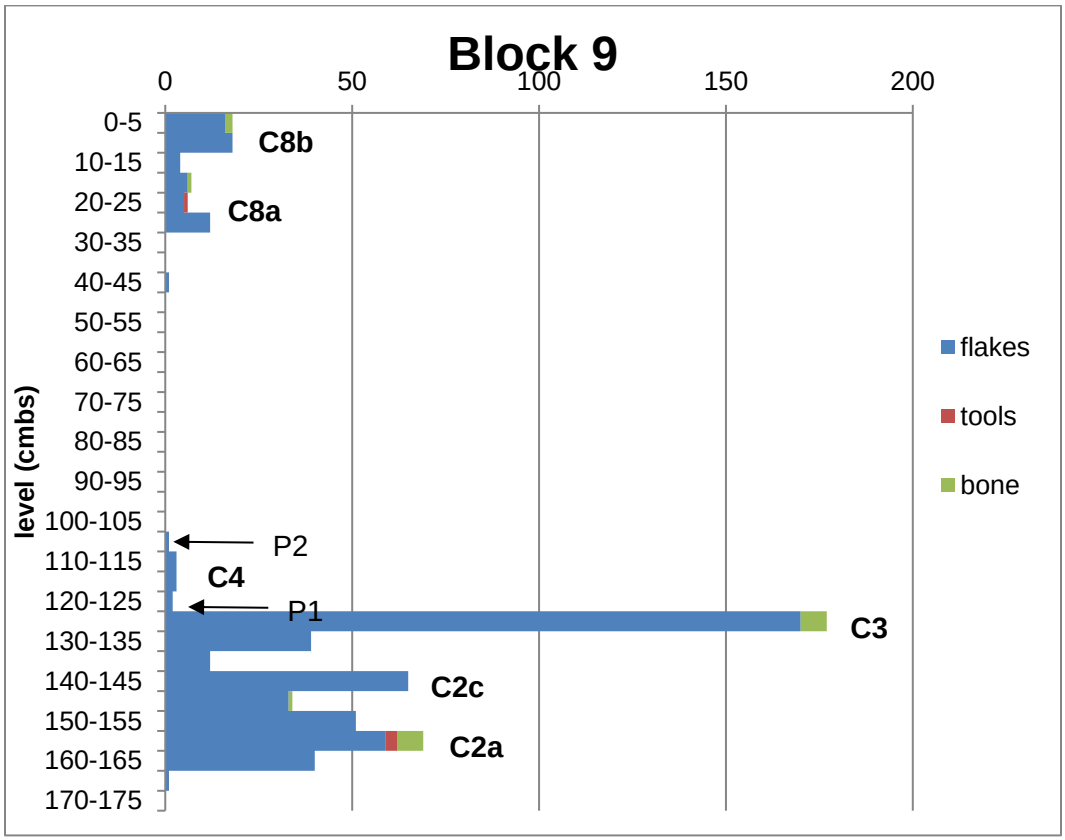

Figure 6.12 Block 9 level summary data

6.3.10 Block 10 Analysis

Block 10 was excavated from the erosional surface to glacial deposits, between ~501.006 m elev to ~498.749 m elev, about 2.257 meters. A total of 57 pieces of debitage and 2 tools and 5.45 g of fauna were recovered from Block 10 (Table 6.10, Figure 6.13). In addition, a lithic cobble was found in C8a. Seven components were found in Block 10: C2c, C3, C4, C5a, C6b, C8a, and C8b.

Table 6.10 Block 10 component data

Component	*Lithics*	*Tools*	*Fauna*
C8b	9		0.05
C8a	39	2	0.92
C7b			
C7a			
C6b	1		
C6a			
C5b			
C5a	3		4.48
C4	3		
C3	1		
C2c	1		
C2b			
C2a			
C1			
Total	57	2	5.45

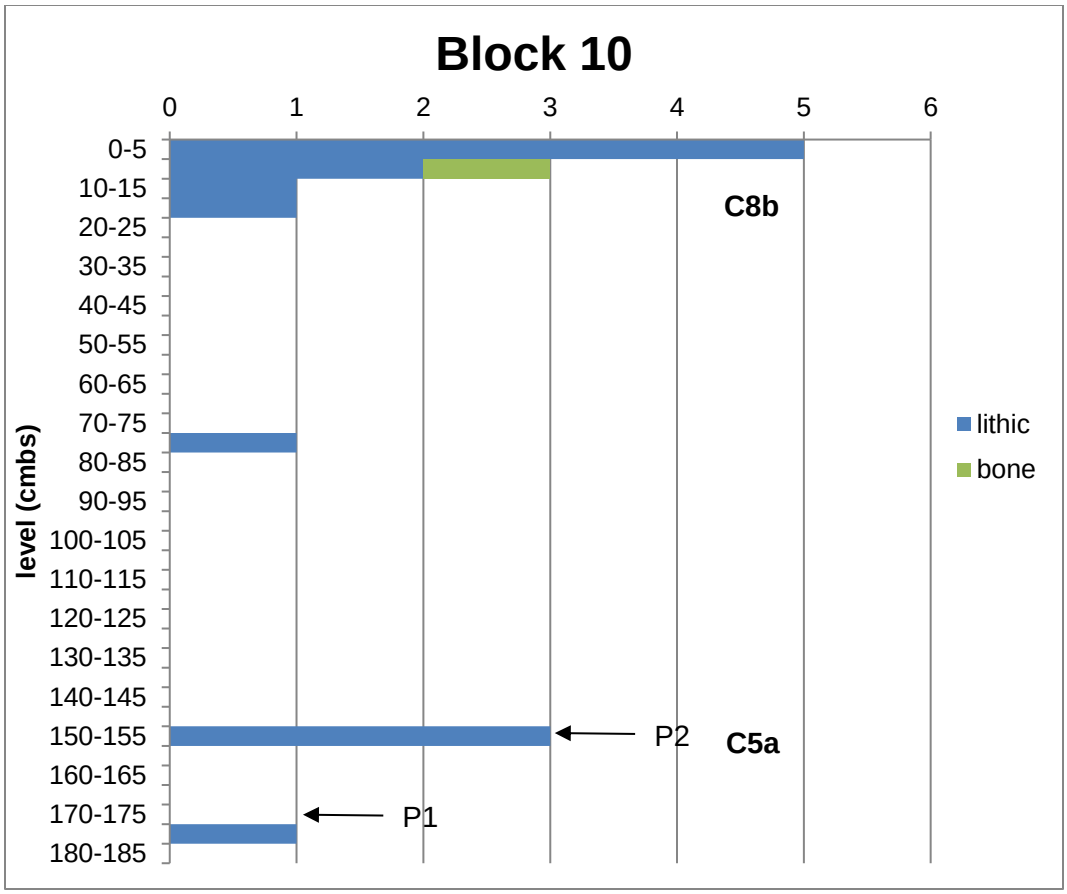

Figure 6.13 Block 10 level summary data

6.3.11 Block 11 Analysis

Block 11 was excavated from the erosional surface to glacial deposits, between ~501.033 m elev to ~498.908 m elev, about 2.125 meters. A total of 1827 pieces of debitage and 10 tools and 6.96 g of fauna were found in Block 11 (Table 6.11, Figure 6.14). Six components were found in Block 11: C2a, C2c, C4, C5b, C8a, and C8b.

Table 6.11 Block 11 component data

Component	*Lithics*	*Tools*	*Fauna*
C8b	68		0.1
C8a	314	1	
C7b			
C7a			
C6b			
C6a			
C5b	35	1	0.96
C5a			
C4	2		
C3			
C2c	1322	4	5.90
C2b			
C2a	86	4	
C1			
Total	1827	10	6.96

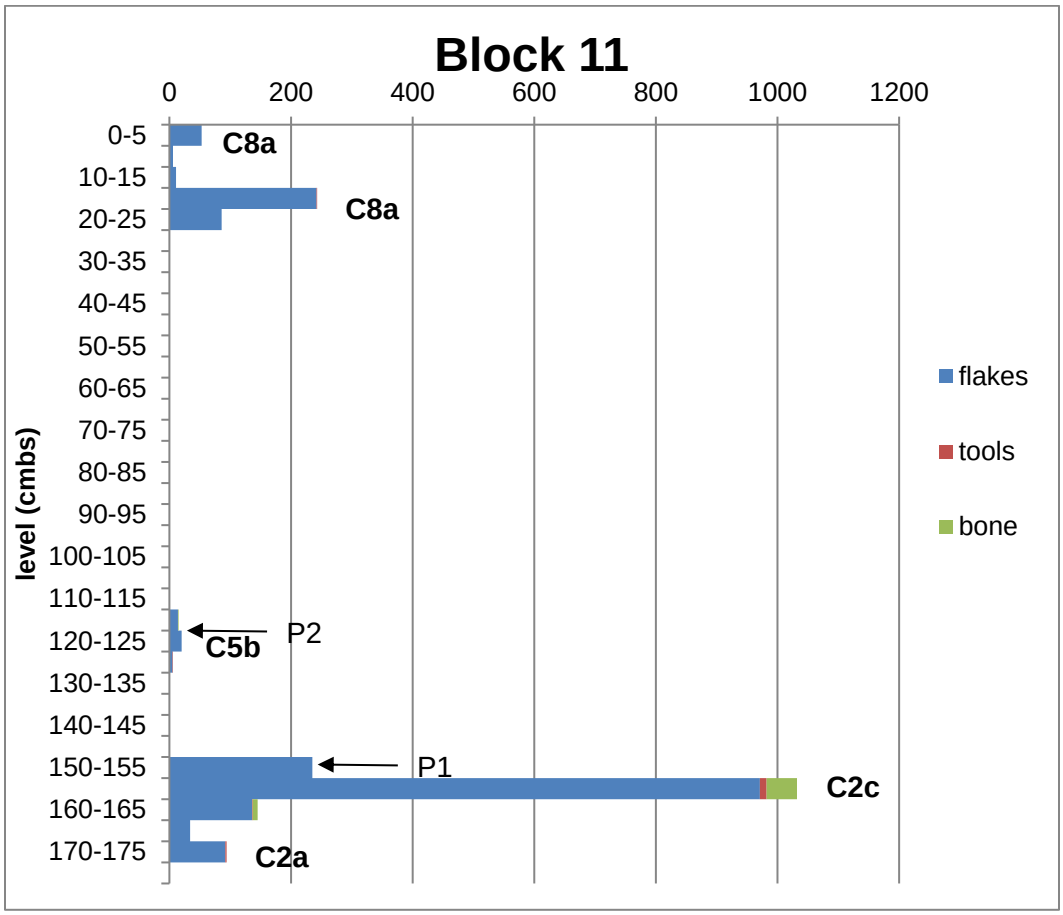

Figure 6.14 Block 11 level summary data

6.3.12 Block 12 Analysis

Block 12 was excavated from the erosional surface to glacial deposits, between ~500.997 m elev to ~498.711 m elev, about 2.286 meters. A total of 1514 pieces of debitage and 12 tools and 21.95 g of fauna were recovered from Block 11 (Table 6.12, Figure 6.15). Five components were found in Block 11: C2c, C4, C5a, C8a, and C8b.

Table 6.12 Block 12 component data

Component	*Lithics*	*Tools*	*Fauna*
C8b	94		3.92
C8a	697	1	
C7b			
C7a			
C6b			
C6a			
C5b			
C5a	1	1	
C4	8		
C3			
C2c	714	10	18.03
C2b			
C2a			
C1			
Total	1514	12	21.95

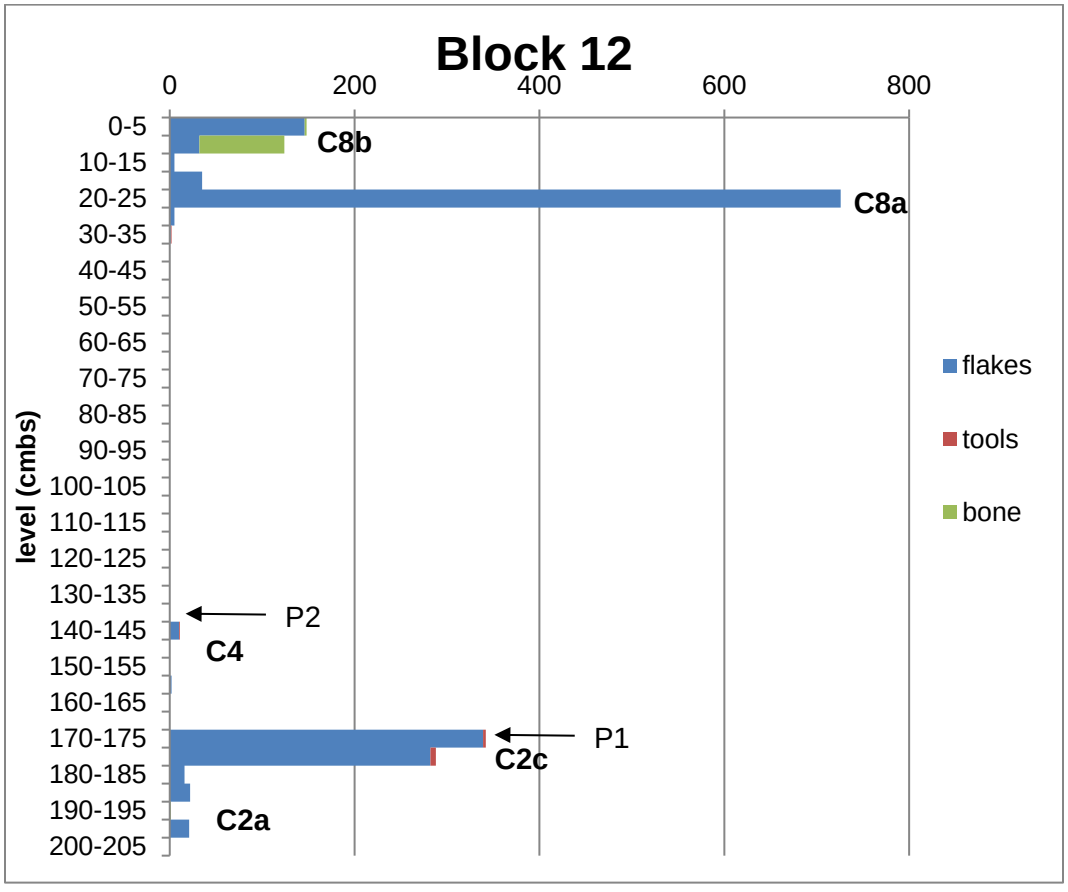

Figure 6.15 Block 12 level summary data

6.3.13 Block 13 Analysis

Block 13 was excavated from the erosional surface to glacial deposits, between ~500.873 m elev to ~498.904 m elev, about 1.969 meters. A total of 153 pieces of debitage, 2 tools and 6.74 g of fauna were recovered from Block 13 (Table 6.13, Figure 6.16). Four components were found in Block 13: C2a, C3, C7b, and C8b.

Table 6.13 Block 13 component data

Component	*Lithics*	*Tools*	*Fauna*
C8b	1		
C8a			
C7b	87		
C7a			
C6b			
C6a			
C5b			
C5a			
C4			
C3	48	1	1.44
C2c			
C2b			
C2a	17	1	5.30
C1			
Total	153	2	6.74

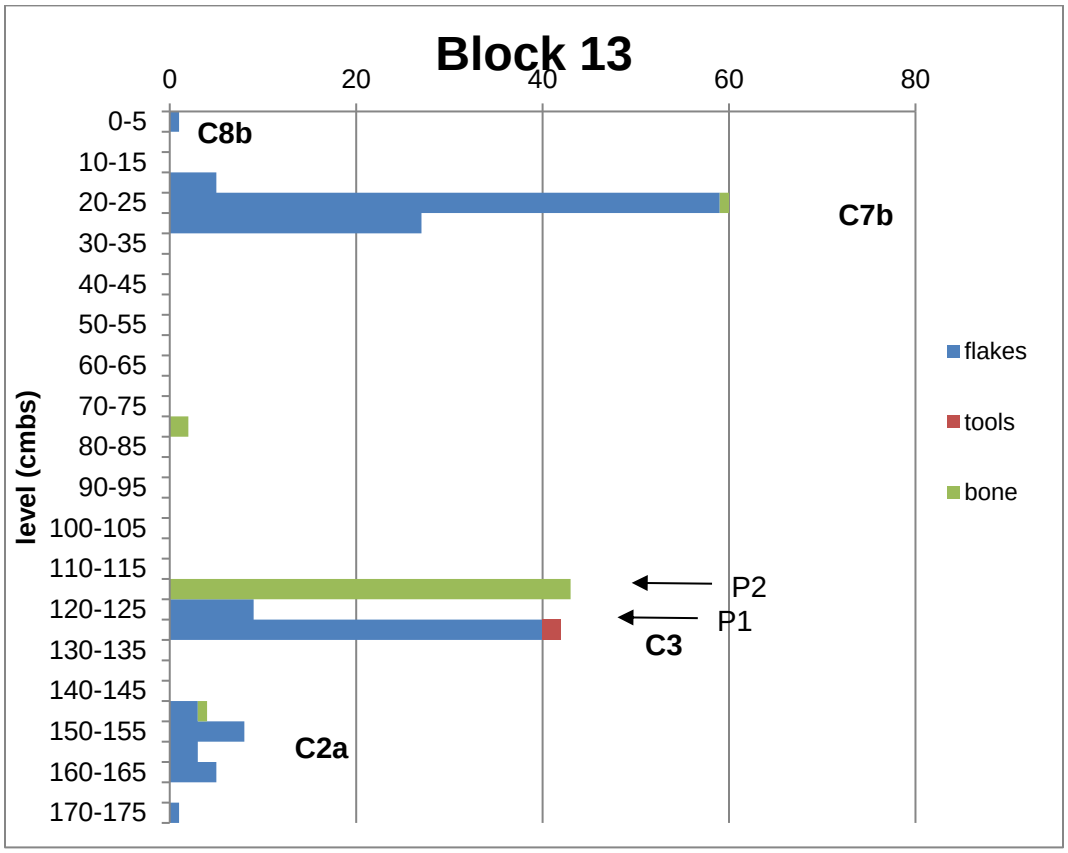

Figure 6.16 Block 13 level summary data

6.3.14 Block 14 Analysis

Block 14 was excavated from the erosional surface to glacial deposits, between ~500.912 m elev to ~498.806 m elev, about 2.106 meters. A total of 34 pieces of debitage and 2 tools and 6.82 g of fauna were recovered (Table 6.14, Figure 6.17). Five components were found in Block 14: C2a, C3, C4, C5a, and C8a.

Table 6.14 Block 14 component data

Component	*Lithics*	*Tools*	*Fauna*
C8b			
C8a	18	1	
C7b			
C7a			
C6b			
C6a			
C5b			
C5a			5.77
C4	2	1	
C3	9		1.05
C2c			
C2b			
C2a	5		
C1			
Total	34	2	6.82

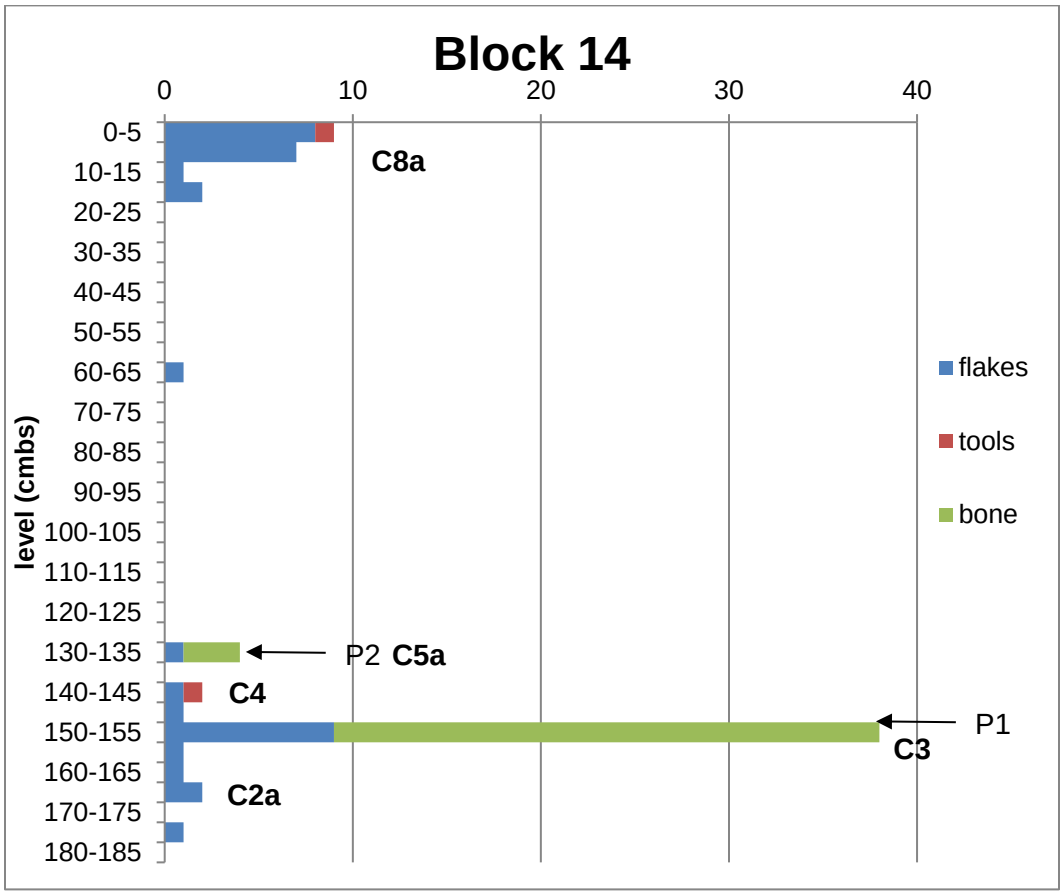

Figure 6.17 Block 14 level summary data

6.3.15 Block 15 Analysis

Block 15 was excavated from the erosional surface to glacial deposits, between ~501.099 m elev to ~498.570 m elev, about 2.529 meters. A total of 871 pieces of debitage and 3 tools and 288.09 g of fauna were recovered (Table 6.15, Figure 6.18). In addition, a lithic cobble was found in C2a. Eight components were found in Block 15: C1, C2a, C2c, C3, C6a, C7a, C7b, and C8b.

Table 6.15 Block 15 component data

Component	*Lithics*	*Tools*	*Fauna*
C8b	66		0.03
C8a			
C7b	2		
C7a	5		
C6b			
C6a	1		
C5b			
C5a			
C4			
C3	3		288.06
C2c	674	3	
C2b			
C2a	117		
C1	3		
Total	871	3	288.09

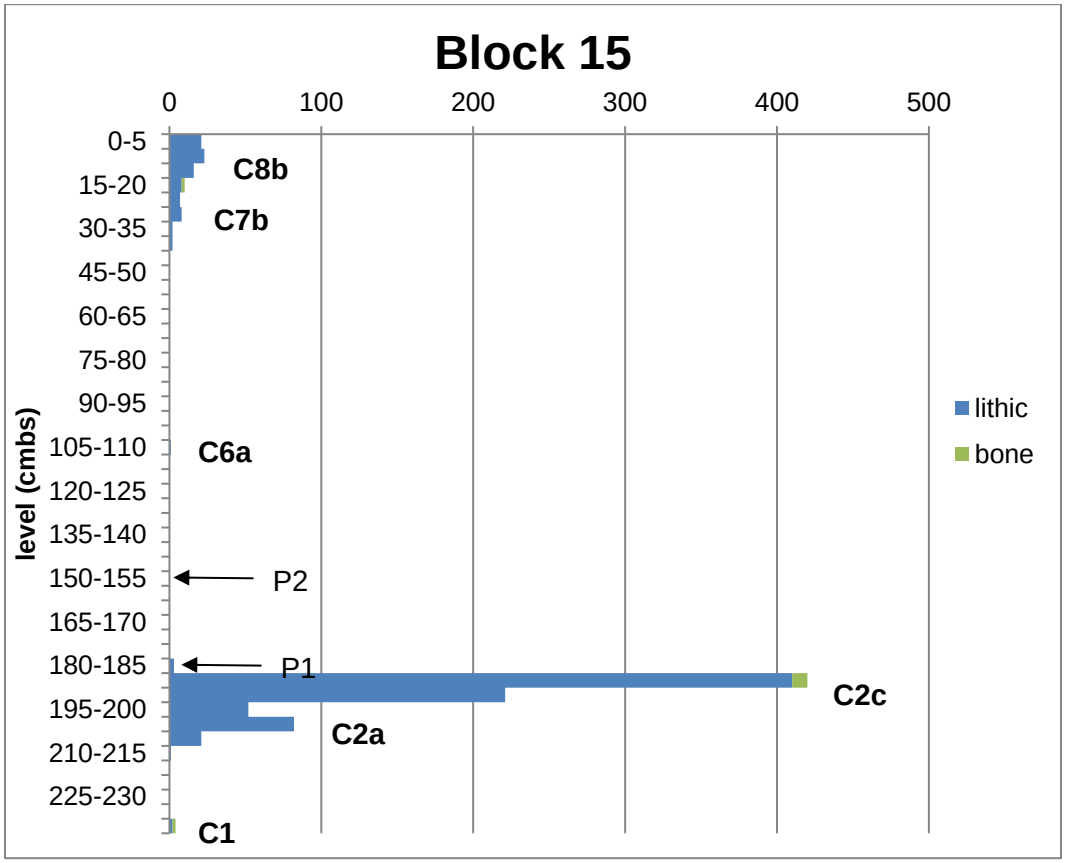

Figure 6.18 Block 15 level summary data

6.3.16 Block 16 Analysis

Block 16 was excavated from the erosional surface to a depth of 1.500 meters, from ~500.908 m elev to ~499.408, where it was stopped. A small area of the eastern unit of Block 16 was excavated to glacial deposits, about 2.52 meters below eroded surface, ~498.388 m elev. A total of 10 pieces of debitage and 73.59 g of fauna were recovered in Block 16 (Table 6.16, Figure 6.19). Two components are found in Block 16: C6a and C8b.

Table 6.16 Block 16 component data

Component	*Lithics*	*Tools*	*Fauna*
C8b	9		0.91
C8a			
C7b			
C7a			
C6b			
C6a	1		72.68
C5b			
C5a			
C4			
C3			
C2c			
C2b			
C2a			
C1			
Total	10	0	73.59

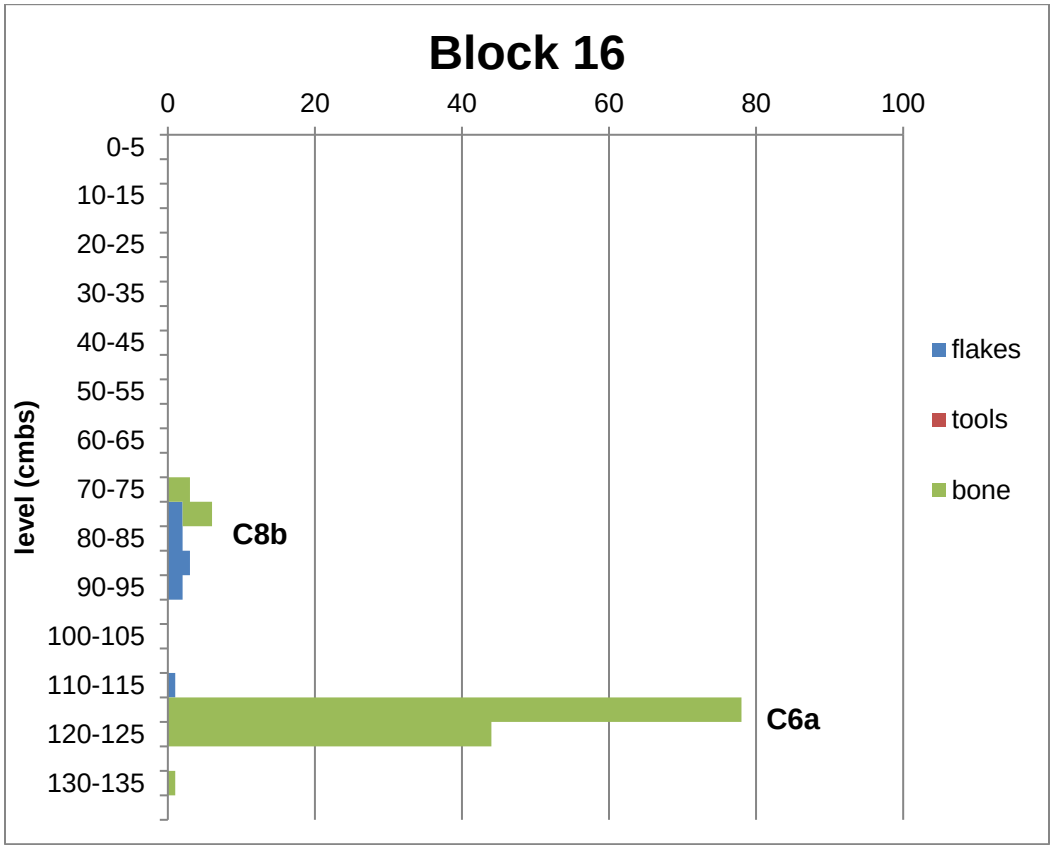

Figure 6.19 Block 16 level summary data

6.3.19 Block 19 Analysis

Block 19 was excavated from the erosional surface to glacial deposits, between ~500.974 m elev to ~498.264 m elev, about 2.520 meters. A total of 281 pieces of debitage and 11 tools and 66.39 g of fauna were recovered (Table 6.17, Figure 6.20). In addition, lithic cobbles were found in C2a (n=1, C7a (n=1) and C7b (n=3). Eight components were found in Block 19: C1, C2c, C3, C5a, C7a, C7b, C8a, and C8b.

Table 6.17 Block 19 component data

Component	*Lithics*	*Tools*	*Fauna*
C8b	8	1	22.18
C8a	41		1.47
C7b	219	8	0.53
C7a	1	1	
C6b			
C6a			
C5b			
C5a			34.27
C4			
C3	2		
C2c	10		7.94
C2b			
C2a			
C1		1	
Total	281	11	66.39

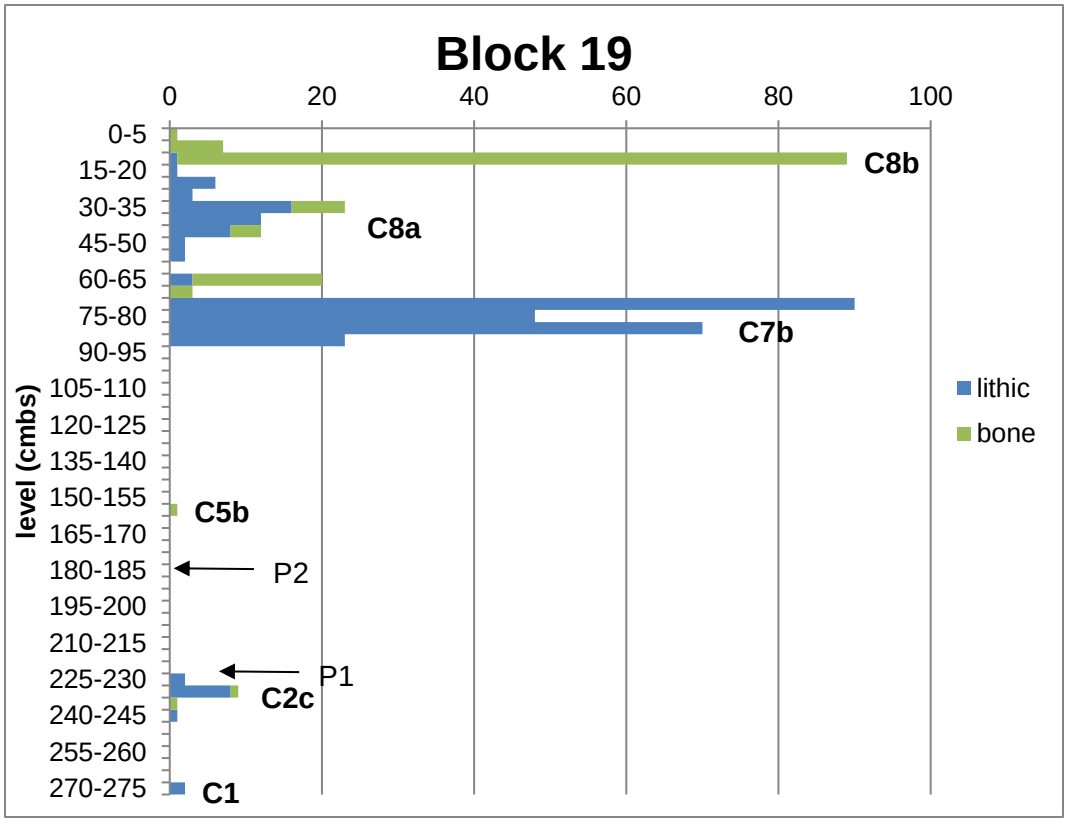

Figure 6.20 Block 19 level summary data

6.3.20 Block 20 Analysis

Block 20 was excavated from the erosional surface to glacial deposits, between ~500.365 m elev to ~498.812 m elev, about 1.553 meters. A total of 883 pieces of debitage and 10 tools and 21.67 g of fauna were recovered (Table 6.17, Figure 6.21). Seven components were found in Block 20: C1, C2a, C2c, C5a, C6a, C6b, and C7b.

Table 6.17 Block 20 component data

Component	*Lithics*	*Tools*	*Fauna*
C8b			
C8a			
C7b	1		
C7a			
C6b	2		
C6a	18		1.11
C5b			
C5a	8		4.26
C4			
C3			
C2c	566	8	16.27
C2b			
C2a	283	1	0.03
C1	5	1	
Total	883	10	21.67

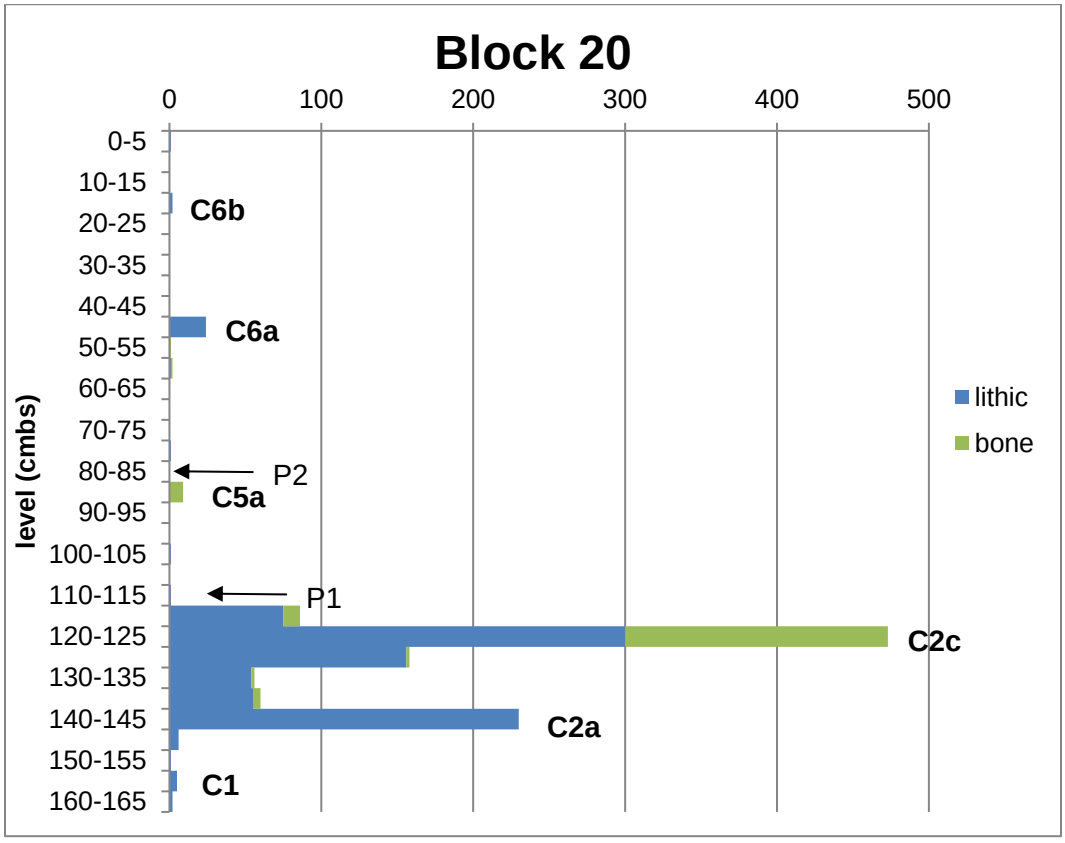

Figure 6.21 Block 20 level summary data

6.3.21 Block 21 Analysis

Block 21 was excavated from the erosional surface to glacial deposits, between ~500.600 m elev to ~498.812 m elev, about 1.788 meters. A total of 1271 pieces of debitage and 13 tools and 62.01 g of fauna were recovered (Table 6.18, Figure 6.22). In addition, 1 lithic cobble was found in C2a. Seven components were found in Block 21: C2a, C2b, C2c, C4, C6a, C6b, and C8b.

Table 6.18 Block 21 component data

Component	*Lithics*	*Tools*	*Fauna*
C8b	1		
C8a			
C7b			
C7a			
C6b	3		
C6a	5	2	0.48
C5b			
C5a			
C4	9	4	
C3			
C2c	1094	5	14.92
C2b	42	1	39.19
C2a	117	1	7.42
C1			
Total	1271	13	62.01

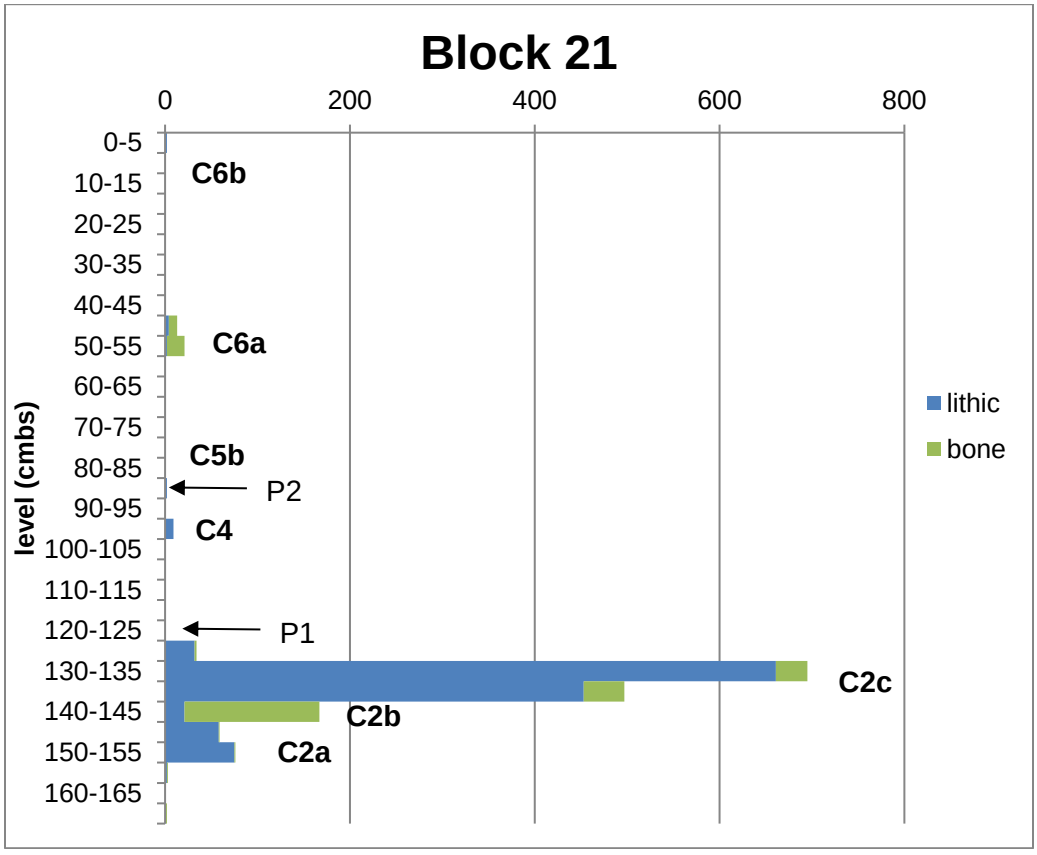

Figure 6.22 Block 21 level summary data

6.3.22 Block 22 Analysis

Block 22 was excavated from the erosional surface to glacial deposits, between ~501.096 m elev to ~498.902 m elev, about 2.194 meters. A total of 468 pieces of debitage and 51 tools and 18.64 g of fauna were recovered (Table 6.19, Figure 6.23). In addition, 2 lithic cobbles were found in C2c. Seven components were found in Block 22: C1, C2a, C2c, C5a, C7b, C8a, and C8b.

Table 6.19 Block 22 component data

Component	*Lithics*	*Tools*	*Fauna*
C8b	116		
C8a	34	48	
C7b	5		
C7a			
C6b			
C6a			
C5b			
C5a	10		0.48
C4			
C3			
C2c	300	3	5.06
C2b			
C2a			13.10
C1	3		
Total	468	51	18.64

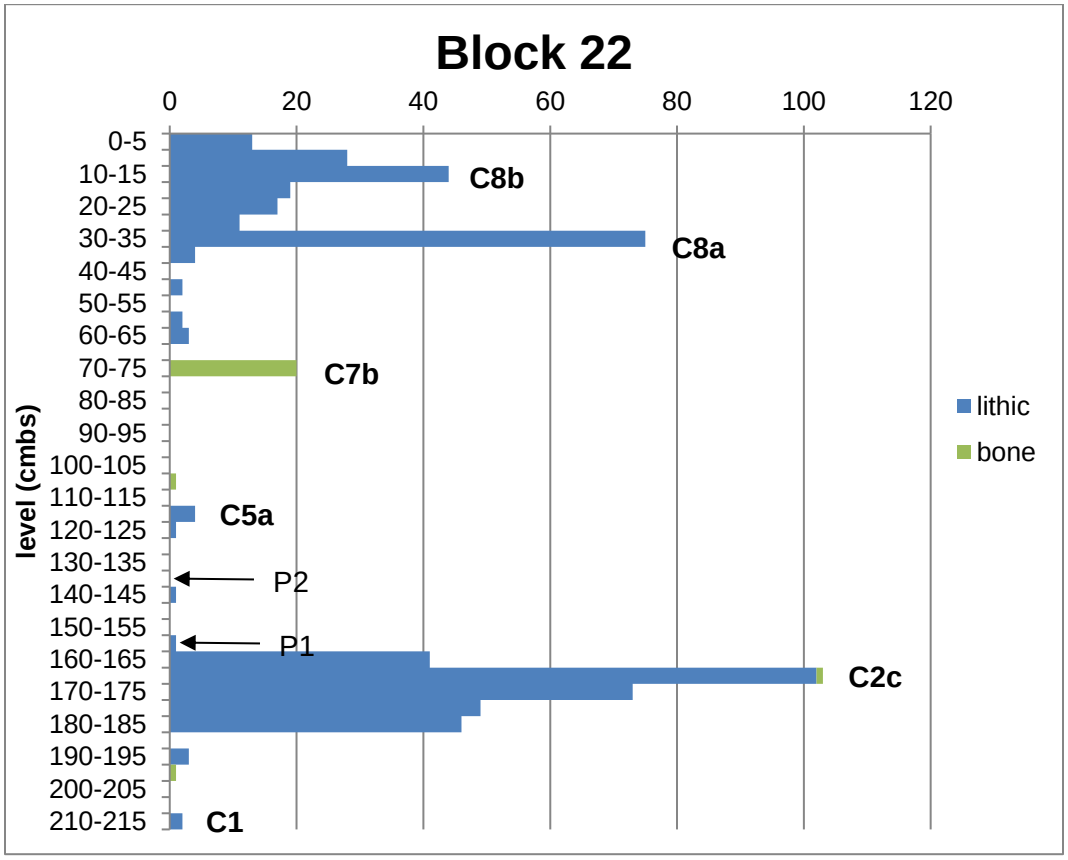

Figure 6.23 Block 22 level summary data

6.3.23 Block 23 Analysis

Block 23 was excavated from the erosional surface (~500.937 m elev) to a depth of 1.000 m below surface, about 499.937 m elev. A total of 35 pieces of debitage and 2 tools and 1.14 g of fauna were recovered from Block 23 (Table 6.20, Figure 6.24). Two components were found in Block 23: C7b and C8b.

Table 6.20 Block 23 component data

Component	*Lithics*	*Tools*	*Fauna*
C8b	23	1	1.14
C8a			
C7b	12	1	
C7a			
C6b			
C6a			
C5b			
C5a			
C4			
C3			
C2c			
C2b			
C2a			
C1			
Total	35	2	1.14

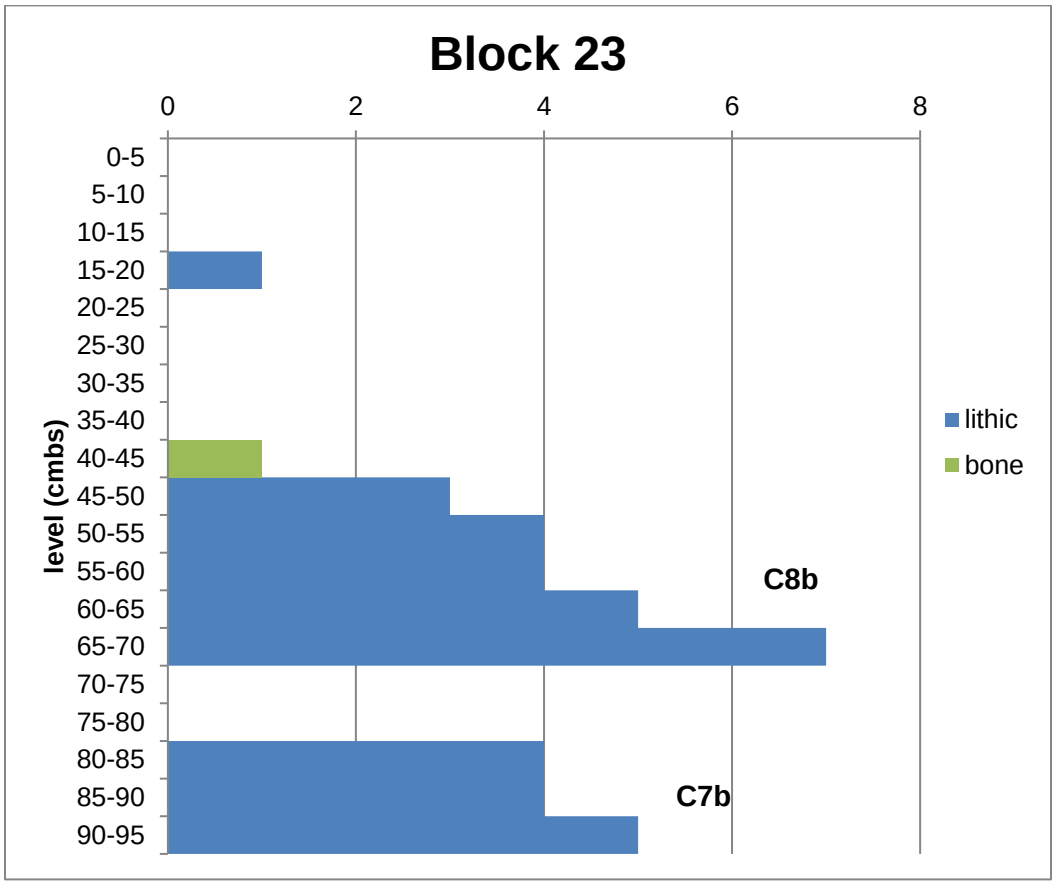

Figure 6.24 Block 23 level summary data

6.3.24 Block 24 Analysis

Block 24 was excavated from the erosional surface to glacial deposits, between ~501.190 m elev to ~498.835 m elev, about 2.355 meters. A total of 1400 pieces of debitage and 15 tools and 26.19 g of fauna were recovered from Block 24 (Table 6.21, Figure 6.25). In addition, 3 lithic cobbles were found in C8b. Eight components were found in Block 24: C1, C2a, C2c, C3, C5a, C7a, C7b, and C8.

Table 6.21 Block 24 component data

Component	*Lithics*	*Tools*	*Fauna*
C8b	303	6	22.35
C8a			
C7b			0.22
C7a		1	
C6b			
C6a			
C5b			
C5a	2		
C4			
C3	1		
C2c	1089	4	2.48
C2b			
C2a	5	4	0.26
C1			0.88
Total	1400	15	26.19

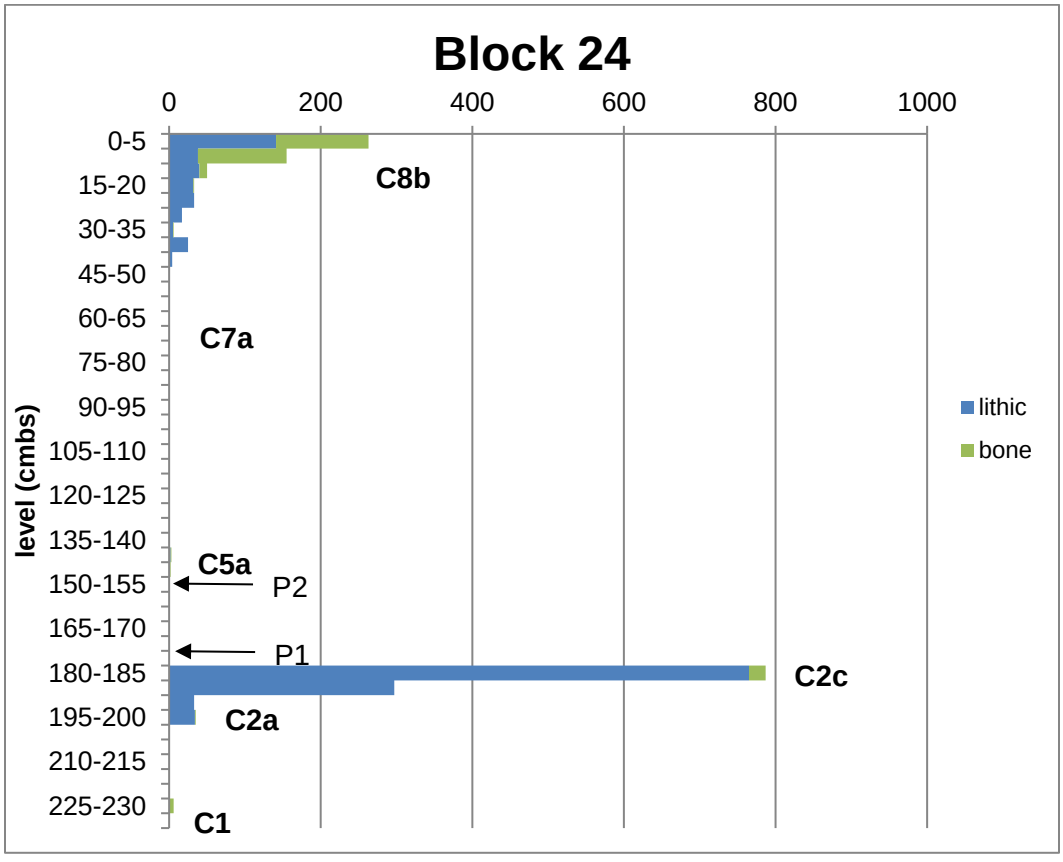

Figure 6.25 Block 24 level summary data

6.3.25 Block 25 Analysis

Block 25 was excavated from the erosional surface to glacial deposits, between ~500.3223 m elev to ~498.879 m elev, about 1.444 meters. A total of 116 pieces of debitage and 2 tools and 2.02 g of fauna were recovered from Block 25 (Table 6.22, Figure 6.26). Six components were found in Block 25: C1, C2a, C2c, C3, C5a, and C6a.

Table 6.22 Block 25 component data

Component	*Lithics*	*Tools*	*Fauna*
C8b			
C8a			
C7b			
C7a			
C6b			
C6a	7		
C5b			
C5a	1		2.02
C4			
C3	1		
C2c	8		
C2b			
C2a	10	1	
C1	89	1	
Total	116	2	2.02

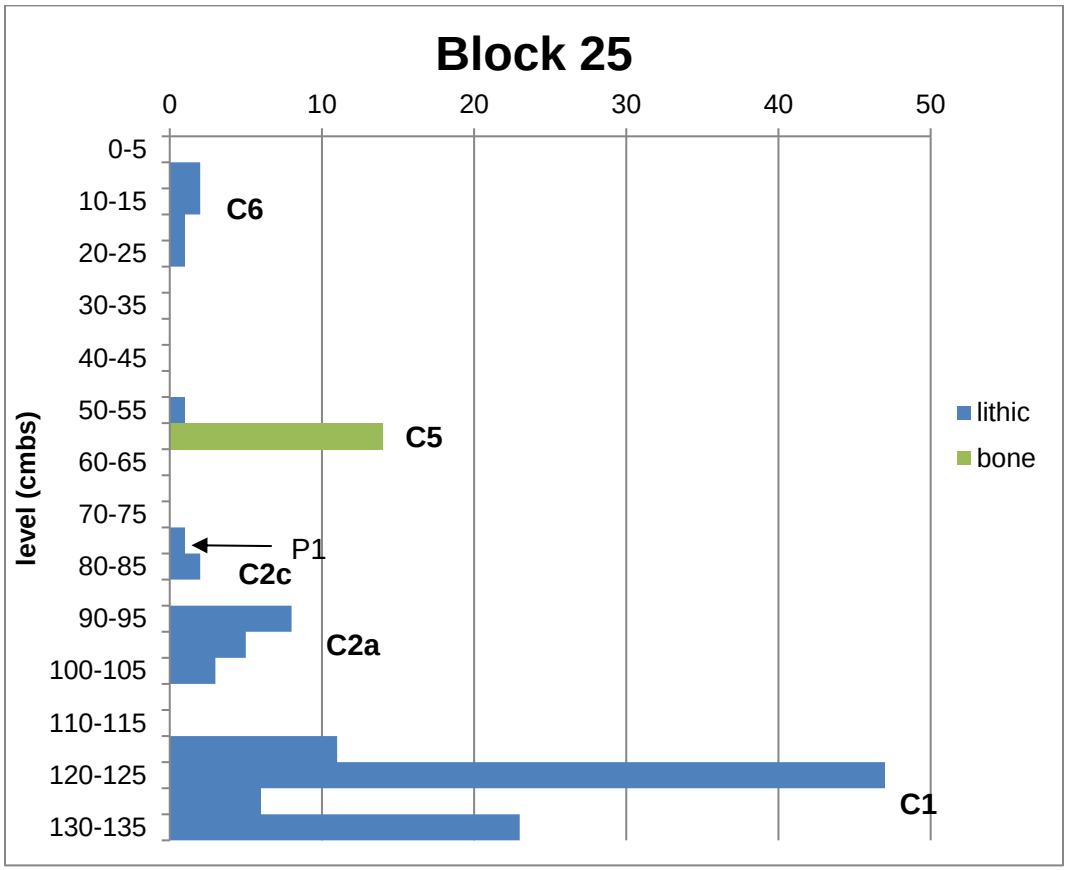

Figure 6.26 Block 25 level summary data

6.3.26 Block 26 Analysis

Block 26 was excavated from the erosional surface (~500.983 m elev) to a depth of 0.700 m below surface, about 500.283 m elev. A total of 70 pieces of debitage and 1 tool and 0.09 g of fauna were recovered in Block 26 (Table 6.23, Figure 6.27).

Table 6.23 Block 26 component data

Component	*Lithics*	*Tools*	*Fauna*
C8b	70	1	0.09
C8a			
C7b			
C7a			
C6b			
C6a			
C5b			
C5a			
C4			
C3			
C2c			
C2b			
C2a			
C1			
Total	70	1	0.09

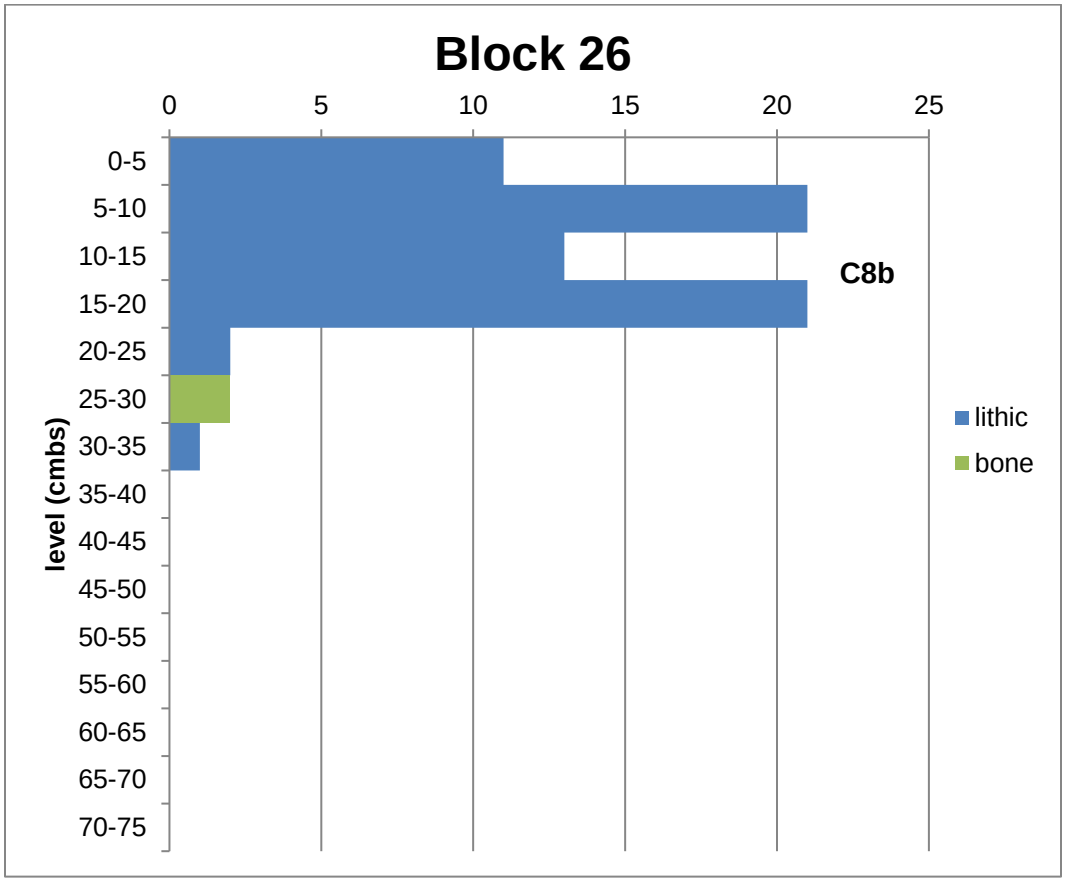

Figure 6.27 Block 26 level summary data

6.3.27 Blocks A and B Analyses (1979)

Blocks A and B were excavated in 1979 (Bacon and Holmes 1980). Stratigraphically, Block A is most similar to Block 5 from the 2015 excavation and Block B is most similar to Blocks 11 and 12 from the 2015 excavation. A total of 40 lithics were recovered from Block A and 147 lithics and 5 fauna were recovered from Block B (Table 6.24, Figures 6.28-29). Three components are found in Block A: C6a, C8b, and C2. The C2 materials (n=36 debitage) could refer to C2a or C2c, and given the surrounding materials, probably relate to both components. Four components are found in Block B: C6a, C7a, C8b, and C2. The C2 materials (n=34 debitage) could refer to C2a or C2c, and given the surrounding materials, they probably relate to C2c. The bison tibia is assigned to C7a on the basis of depth below surface and the associated stratigraphy (north wall of Block B).

Table 6.27 Blocks A and B component data

Component	*Block A lithics*	*Block A bone*	*Block B lithics*	*Block B bone*
C8b	1		112	4
C8a				
C7b				1*
C7a				1*
C6b				
C6a	3		1	
C5b				
C5a				
C4				
C3				
C2c	36		34	
C2b				
C2a				
C1				
Total	40		147	5

* bison tibia could be from either C7a or C7b.

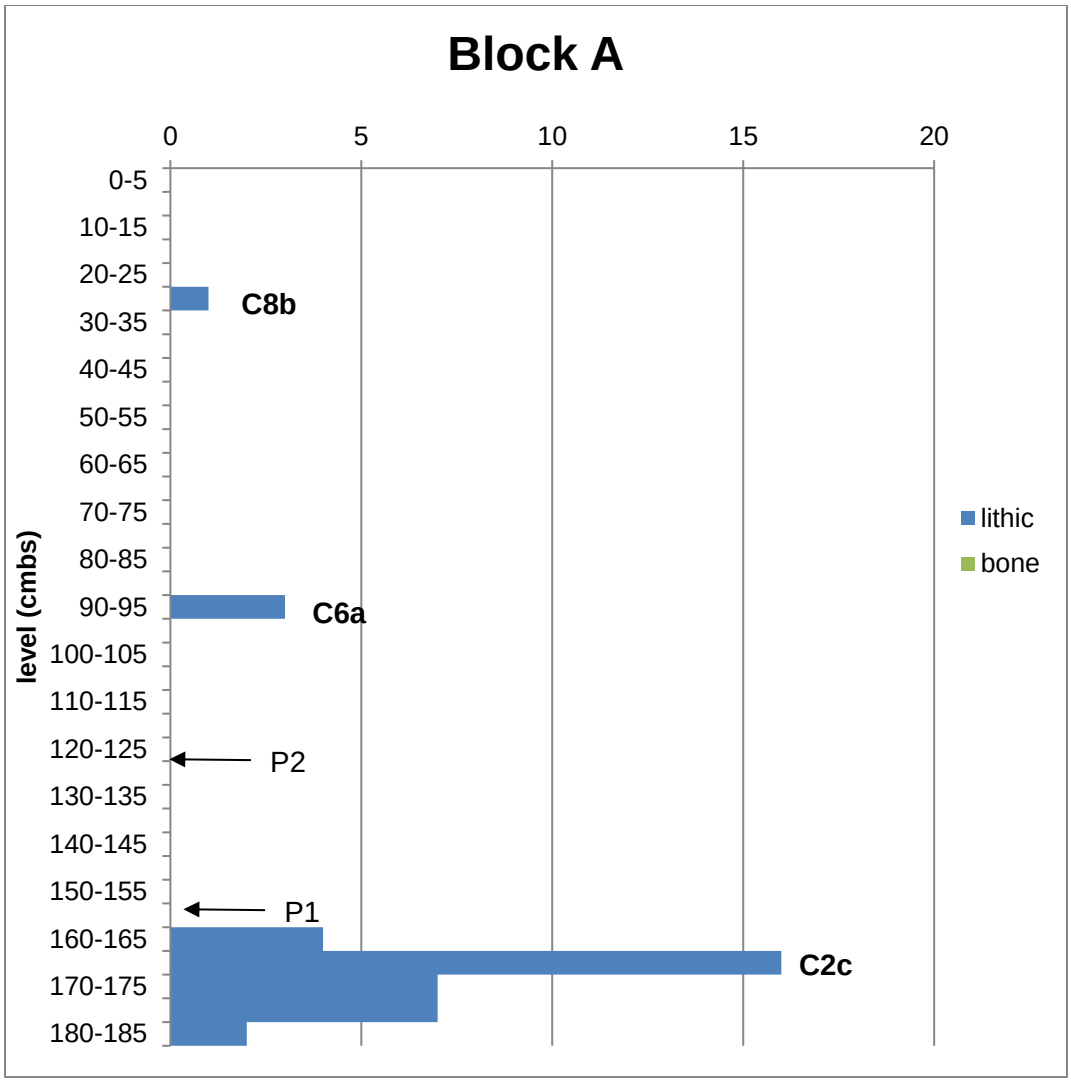

Figure 6.28 Block A level summary data

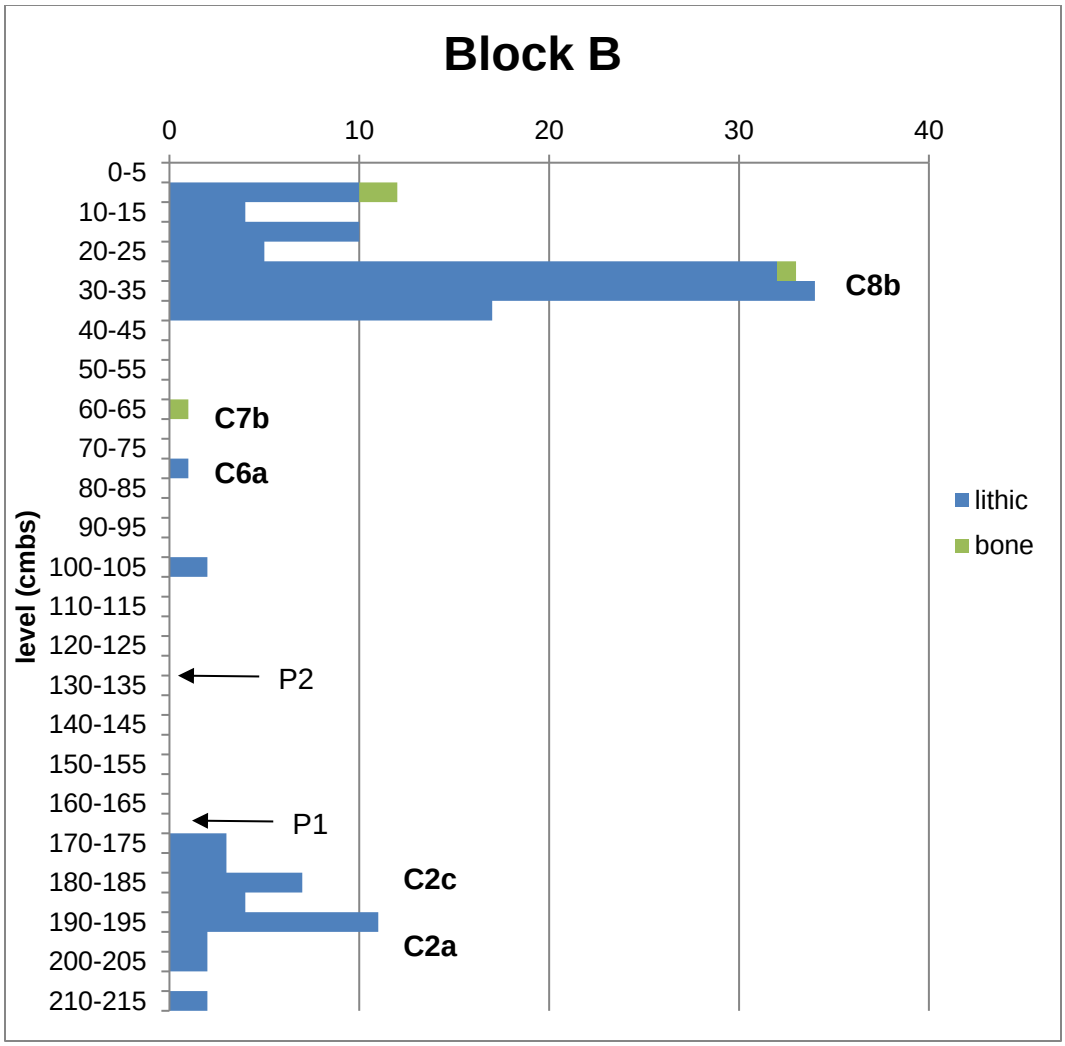

Figure 6.29 Block B level summary data

6.4 Loss of Upper Strata through Erosion

Given the stratigraphic, radiocarbon, and geological analyses presented in Chapters 4 and 5, it is evident that upper sediments containing upper components (C7a, C7b, C8a, and C8b) are differentially removed across the site. Figure 6.30 shows how aeolian erosion (deflation) has removed upper sediments associated with these components. Thus, only sediments associated with C1 through C6 are found at the southern part of the site. All components are potentially found north of about N208.

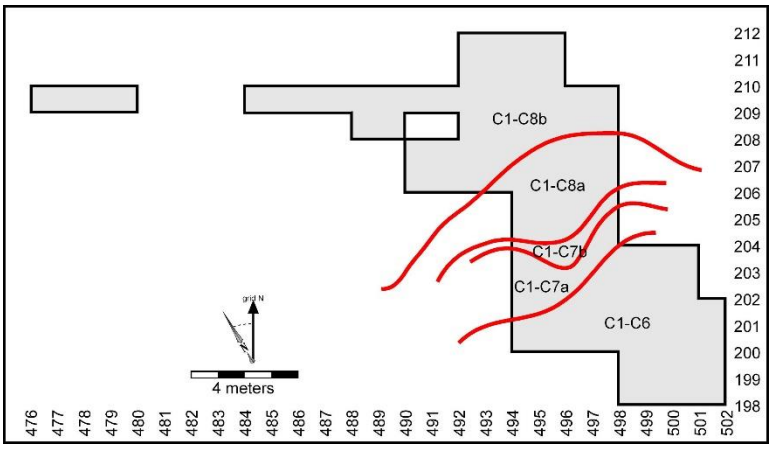

Figure 6.30 Distribution of components as a function of erosion

6.5 Comparison of 1978-1979 Components and 2015-2017 Components

In the 1978-1979 field testing, five cultural components were delineated (Bacon and Holmes 1980). With the larger spatial extent afforded by the 2015-2017 excavations, this initial estimate has been expanded. Component equivalencies are illustrated in Table 6.28. The lowest component in 1978-1979 was termed "Component 1", and it lay below the lowest (at that time) paleosol "Paleosol 1." This component in Block A likely correlates with Components 2a and 2c. The 1978/9 component 2 is associated with Paleosol 3 and is equivalent to Component 3. The 1978/9 component 3 is associated with Paleosol 4 and is equivalent to Component 6a. The 1978/9 component 4 is associated with Paleosol 6 and is equivalent to Component 6b. The major 1978/9 component 5 is equivalent to Component 8b.

Table 6.28 Comparison of 1978/1979 and current components.

Component	*Stratum*	*Depth below surface* (cm)*	*Age (cal yr BP)*	*1978-1979 component equivalent*
C9**	P9	Not present	<2340	C6
C8b	above P7b	0-17	2340	C5
C8a	P7a	25-31	3560	
C7b	P6b	35-39	4150	
C7a	P6a	43-48	4772	C4
C6b	P4	64-69	5940	C3
C6a	P3	80-87	6824	
C5b	L3	100-110	7250	
C5a	P2	119-125	7670	
C4	L2	132-139	8400	
C3	P1	145-151	9580	C2
C2c	L1	155-161	10,740	C1
C2b	L1/P0b	165-168	11,500	
C2a	L1/P0b	170-178	11,600	
C1	L1/P0a1	200-210	12,900	

* based on generalized stratigraphic profile (Block 11 North wall)
** C9 is present only in the 1978-1979 upper excavation; these upper strata have already been eroded from the 2015-2017 excavation area.

CHAPTER 7. LITHIC ANALYSIS

Ben A. Potter and Julie A. Esdale

Lithic artifact attributes recorded by:
Kelly Meierotto, Michael Wendt, Holly J. McKinney, Casey Jobe, Ben A. Potter, Julie A. Esdale

7.1 Introduction

Lithics form the majority of cultural materials at DRO, totaling nearly 20,000 items, including 283 tools, 12 cores, and 18,465 unmodified pieces. All materials are chipped stone; there is no ground stone industry. This chapter provides standard and more detailed analyses on debitage, tools and cores. Because microblade technology is a prominent part of the assemblages, these are given special attention. This chapter considers raw material, including material type delineation, descriptions, estimation of local and nonlocal materials, and raw material comparisons among components and traditions (Section 7.3). Lithic technological analyses include assemblage composition, density analyses, comparisons of tools and debitage with respect to raw material, and flake size distributions (Section 7.4). Spatial analyses of debitage at the level of component and lithic cluster are provided in Section 7.5. Tool and core analyses at the level of component and cultural tradition are provided in Section 7.6, as well as intersite comparisons at the level of activity area, component, and cultural tradition. Specific analysis of the Component 8a lithic cache is given in Section 7.7.

7.1.1 Lithic Landscape

Every site is situated within a lithic landscape, with potential sources of toolstone from primary and/or secondary deposits. Our knowledge of the local lithic landscape surrounding Delta River Overlook is very nascent. No bedrock exposures are present within several km, excepting that related to Donnelly Dome, a metamorphosed granitic rock (Augen gneiss) unsuitable for knapping (Nokleberg et al. 1982, 1992, Wilson et al. 2015). Most of the area to the west is active and abandoned floodplain deposits, in some cases overlain by sand dune fields. These deposits overlay Donnelly moraine from the last glacial maximum. Most of the area to the east is many meters of glacial till (Donnelly moraine) (Matmon et al. 2010, Pewe and Holmes 1964, Reger et al. 2008). The lithic materials within the glacial gravels that we examined onsite were very coarse grained and not suitable for knapping. Given this, we expect no high quality locally available toolstone in primary deposits. Most of the vegetated areas, and those areas covered by vegetated sand dunes yield no access to potential toolstone. However, stream transported cobbles in highly variable secondary deposits may have offered prehistoric occupants of the DRO area many choices in effectively local toolstone. The difficulty with this situation is that given the drainage area of the Delta River, many different kinds of raw materials could be introduced near the site along the braided river, and this potentially could change through time.

7.1.2 Research problems

Research questions relating to chipped stone technology at the DRO site include the following. All questions were explored at the level of activity area (or lithic cluster), component, and cultural tradition.

- How were people using stone tools at the site?
- What stages of reduction occurred in the assemblage?
- Are there different stages of reduction that vary by material type suggesting different procurement?
- Are the debitage variables consistent for expectations of early vs. later stages of reduction. And if not, what could explain the differences?
- Do we see evidence of core reduction, tool production/manufacture, and/or tool maintenance/resharpening?
- Are there raw material differences in lithic reduction activities (material, quality, heat treatment, etc.)?
- Are the materials primarily local or non-local. Are there different treatments for each?
- Did raw material conservation or maximization occur? Was there lithic resource stress?
- Are there observable trends in lithic behaviors from Chindadn through Denali through Northern Archaic components?

7.2 Methods

7.2.1 Introduction

Detailed analyses of the lithic component from DRO included raw material identification, debitage and tool description and classification, technological, and spatial analyses. Assemblages were defined by stratigraphic position and spatial association (see Chapter 6). Given the spatial locations of the few items denoted as "C7" and "C8" and uncertainty of connection with C7a, C7b, C8a, or C8b, these are isolated as distinct assemblages at the level of raw material analyses. For later technological analyses, "C7" is included in C7b and "C8" is included in C8b.

7.2.2 Raw Material Analysis

Numerous lithic toolstone materials were identified at DRO, grouped into 77 types based on visual examination (and low-power magnification [10-30x]) of grain size, lithology, surface texture, light transmittance, Munsell color, cortex, color texture and variation (e.g., banding), and inclusions. Materials were dominated by microcrystalline and cryptocrystalline stone, mostly sedimentary, including 55 varieties of chert (C) and 5 varieties of chalcedony (Ch). Igneous materials include obsidian (O) and 7 varieties of rhyolite (R). Six varieties of quartz or quartzite (Q) were and 3 varieties of macrocrystalline (M) materials were also identified. pXRF analysis was conducted on the obsidian (see Chapter 10).

7.2.3 Lithic Analysis

Descriptive, classificatory, and analytical methods generally follow Andrefsky (2008). The following classes are defined: *debitage* is unmodified material removed from cores, *cores*

are objective pieces showing detachment scars, and *tools* are secondarily modified flakes or cores (i.e., showing retouch or usewear). Within the debitage category, various subcategories are employed, following Sullivan and Rosen (1985) as modified by Prentiss (1998) and others, and using typical analytical categories by Andrefsky (2008) and others, e.g. bifacial thinning flake, decortication flake, bipolar flake. Cores at DRO are classed as flake cores or microblade cores. Tool classes include bifaces, unifaces, and flake tools like burins, burin spalls, and modified flakes and microblades.

The research questions above lead to specific types of analyses. More intensive reduction can be inferred from increased platform preparation (e.g., complex, abraded), greater percentages of smaller flakes, lack of cortex, and decreasing (more acute) exterior platform edge angles.

Maximization of raw materials can be indicated through higher frequencies of platform preparation, low frequencies of cortical flakes, and non-local materials used as formal tools.

Lithic tool maintenance and tool production can be distinguished by relatively lower weight density for the former and higher weight density for the latter. Tool production is associated with high percentages of complete and broken flakes while core reduction is associated with higher percentages of complete flakes and shatter (angular debris), and more simple platforms and less acute exterior platform edge angle. Bifacial tool manufacture and maintenance are associated with increasingly acute edge angles as the biface is thinned.

Percussor type can also be inferred from debitage characteristics. Soft-hammer percussion is associated with smaller flakes, platform lipping, and fewer complete flakes while hard-hammer percussion is associated with larger flakes, larger platforms, salient bulbs of force, eraillure scars, and more complete flakes. Pressure flakes are associated with very small flakes, tiny platforms, and more complete flakes. Allen (2018) estimated platform measurement cutoffs for these technologies using experimentation. Hard hammer percussion was defined by 15-50+ mm platform widths and 7-12+ mm platform thickness and means of 22 mm and 9 mm respectively. Soft hammer percussion was defined by 8-15 mm platform width and 2-7 mm platform thickness, with means of 10 mm and 2 mm respectively. Pressure flaking was defined by <8 mm platform width and <2 mm platform thickness, with means of 4 and 1 mm respectively.

Variation in flake size (length, width, thickness, and weight) may indicate a variety of behaviors. Under-representation of larger flakes may indicate preferential removal of blanks. Larger sizes relate to earlier stages of reduction while smaller sizes relate to later stages. Thicker flakes tend to relate to core reduction while thinner flakes tend to relate to tool production, all things being equal.

Microblade technology analyses at Gerstle River using multiple independent lines of evidence yield some expectations regarding bifacial tool maintenance vs. microblade production and use (Potter 2005). Microblade production is associated with 23-36% complete flakes, 20-26% broken flakes, 23-44% flake fragments, and 10-23% shatter. Biface tool maintenance is associated with 20-33% complete flakes, 16-17% broken flakes, 44-60% flake fragments, and 4-6% shatter. Microblade production is also associated with 66-72% simple platforms, 2-3% complex platforms, and 25-32% abraded, retouched, or crushed platforms (Potter 2005). Dorsal scar counts for microblade production areas are 8-15% 1 scar, 29-33% 2 scars, 31-35% 3 scars, and 22-27% 4+ scars.

Later stages of bifacial and unifacial reduction is associated with bifacial thinning and unifacial thinning flakes respectively. Early stages of reduction are associated with decortication

flakes. Microblade core reduction is associated with microblades, microblade cores, microblade core tablets (platform rejuvenation flakes), and microblade core facet rejuvenation flakes.

Bifacial reduction can be inferred from percentages of bifacial thinning flakes, thin, wide flakes, and relatively more dorsal flake scars on smaller flakes. Complex platforms, larger sizes, and more dorsal scars indicate biface thinning and edging (earlier stages).

Variation in cortex among raw materials may relate to proximity to material source. Differential use of certain raw materials or material flaking quality (high, moderate, low) may indicate specific preferences for specific tool types.

Termination types also can be useful guides to lithic behaviors. Feathered terminations indicate smooth/gradual force, and is generally preferred (as they do not leave obstructions on the core or tool) removals. Hinge terminations indicate the force rolling outward, and tend to be more common on flatter surfaces (they cannot be created through pressure flaking). Overshot or plunging flakes indicate the force rolling inward and are generally considered mistakes in flaking. Step or snap fractures is where the force stops in the core or tool and indicates breakage upon removal.

Heat damage may result from accidental heating (e.g., dumping in a hearth) but may also result from specific heating intended to extend the quality of the raw material. This may indicate lithic resource stress, as would the presence of bipolar technique. Both technologies are used when lithic raw material quality is poor.

Parent lithic nodule size may be inferred from smaller flakes retaining cortex. Larger nodules are associated with larger flakes with cortex and simple platforms. Larger nodules also may reflect closer proximity to source and earlier reduction.

Taphonomy can be evaluated through percentages of flake fragments across material types – if they are similar and high, then post-depositional breakage through trampling, etc., may be a factor in assemblage formation.

Relationships among different raw materials can be informative about broader behaviors. Residential sites and longer-term occupations should reflect ad hoc tool maintenance and overall lower raw material quality. Logistical and shorter-term task-specific sites should reflect gearing up maintenance, multiple lithic sources (with material obtained at different times) and higher quality raw material. Tool formality, particularly standardized complex technologies like bifacial and microblade industries are considered to be efficient, and may reflect higher overall mobility (Rasic 2011).

Locally obtained materials should have larger cortex, larger flake sizes, fewer dorsal scars, less acute platform angles, simple platforms, more flake cores and fragments, shatter, and more hard hammer percussion. Non-local materials should have no cortex, smaller flake sizes, more dorsal scars, more acute platform angles, more prepared platforms, less flake core parts, and more soft hammer percussion, and pressure flaking. Non-local debitage should consist mainly of discarded tools and maintenance flakes. The entire production sequence may be represented for local raw materials while only late stages (tool production and maintenance) may be represented for nonlocal raw materials.

7.2.4 Variable Coding

7.2.4.1 Debitage and Flake Attributes

The following variable attributes were recorded on all chipped stone debitage recovered at DRO, including flakes, flake fragments, shatter, and microblades.

Raw material. Lithic toolstone was categorized by visual characteristics (e.g., grain size, lithology, surface texture, light transmittance, Munsell color, cortex, etc.). pXRF analyses were undertaken for obsidian (see Chapter 10).

Analytical flake type follows Andrefsky (2001). The following flake types were recorded.

-bifacial thinning flake
-unifacial thinning flake
-decortication flake
-microblade
-microblade core tablet
-bipolar flake
-simple flake
-shatter (non-orientable fragments)

MSRT (Modified Sullivan-Rozen Typology) follows Prentiss (1998). Differing portions of MSR types have been argued to reflect core reduction vs. tool production.

-complete flake
-broken flake (proximal/platform present)
-flake fragment (proximal/platform absent)
-shatter (angular debris)
-split flake

Segment. This was recorded using the following categories:

-complete
-proximal
-medial
-distal
-shatter

Cortex percent. This was recorded using the following categories, and further combined in the analyses as presence/absence of cortex.

0 = 0% (tertiary)
1 = 1-49% (secondary)
2 = 50-99% (secondary)
3 = 100% (primary)

Cortex type

Cobble – rounded weathered surface with pitting or small percussion cones
Geological – flat weathered surface without evidence of rolling

Dorsal scar count. This was recorded as 0, 1, 2, 3, and 4+. Generally, dorsal scar count increases during reduction.

Weight. This variable was recorded in grams to the nearest 0.01 g.

Size class. This variable was recorded in increments of 5 mm maximum dimension, SC1 = 0-5 mm, SC2 = 5-10 mm, etc.). Size class was recorded for all debitage.

Length, Width, and Thickness values were recorded for most debitage (81.5%), but given time constraints, some debitage had size class (maximum dimension) recorded alone (n = 3331, or 18.5%).

Maximum length. Length is maximum distance from proximal to distal end of the flake in mm (to the closest 0.01 mm).

Maximum width. Width is the maximum distance perpendicular to the maximum length in mm (to the closest 0.01 mm).

Maximum thickness. Thickness is measured at the thickest portion of the artifact.

Thermal alteration. Thermal alteration was identified through evidence of heating, including pot-lid fractures, crazing, color changes, etc.). It was recorded as 1 = present, 0 = absent.

The following attributes were measured on platform-remnant-bearing flakes.

Eraillure scar. These are scars on the bulb of force, relating to hard hammer percussion. It was recorded as 1 = presence, 0 = absence.

Lipping. Lips on ventral platform edges reflect bending fractures associated with soft hammer reduction. It was recorded as 1 = presence, 0 = absence.

Bulb of force. Bulbs of force were recorded as *salient*, generally reflecting more force application, or *diffuse,* generally reflecting less application of force.

Platform preparation. Platform preparation relates to modification of the platform prior to flake removal. More prepared platforms are reflective of more intensive reduction. The categories used are:

-cortical (cortex on platform)
-abraded
-complex (multifaceted)
-crushed (damaged and partially/completely removed)
-simple (single facet)

Exterior platform exterior edge angle. The angle formed by the intersection of striking platform surface and the dorsal surface planes by a goniometer to the nearest degree. Later stage tool

manufacture and maintenance exhibit more acute exterior platform angles than core reduction and early stage reduction.

Termination. This variable records the termination of flakes. Feathered terminations generally do not obstruct further reduction while hinge and step terminations potentially can.

-feathered
-hinge
-overshot
-step

Platform width and thickness. Platform metrics are useful in predictions of flake types and position in reduction sequence. These are measured in mm to the nearest 0.01 mm. Allen (2018) through experimental work estimated platform width differences relating to hard hammer, percussion (platform width of >15 mm), soft hammer percussion (platform width of 8-15 mm), and pressure flaking (platform width of <8 mm). An additional variable of Flake Percussor Type was calculated on this basis.

7.2.4.2 Microblade Technology Attributes

Within the analytical flake type category (above), the following diagnostic types were identified: microblade core tablet (platform rejuvenation flake) and microblade facet rejuvenation flakes.

Microblades were recorded with all flake attributes, with these additional variables:

Arris. This was the number of parallel dorsal ridges were visible from previous microblade detachment.

Damage notes. This was a category to describe modification to specific portions of the microblade. (examples: 1 lateral edge retouch, 2 lateral edge damage). If the microblades were secondarily modified through retouch or damage, they were classes as tools, and labeled *modified microblades*.

Microblade core tablets were recorded with all flake attributes, with these additional variables:

Damage. This includes location and description of secondary working.

Number of (microblade) flutes. This is the number of previous microblade detachments.

Average (microblade) flute width. This is the average width of flutes in mm to the nearest 0.01 mm.

Platform notes. This is for observations about the flake platform (not the microblade core platform).

Microblade cores were recorded with the following variables, following descriptions above: raw material, weight, number of (microblade) flutes, and average flute width.

Maximum length. Measured from front to back of the core (fluting face is the front).

Maximum width. Measured perpendicular from maximum length.

Maximum height. Measured from base to platform of the core.

Core circumference. This measures the length (in mm) of microblade removals along the platform.

Core diameter. This measures the maximum length (in mm) of microblade removal from one side of the core to the other, essentially equivalent to platform width.

7.2.4.3 Burin Technology Attributes

Burins were recorded with all flake attributes, with these additional variables.

Burin facet length. This is the length of the burin scar in mm.

Burin facet width. This is the width of the burin scar in mm.

Damage edge angle. This is the angle of the two planes comprising the working edge of the burin, in degrees.

Burin depth of damage. This is the length (in mm) of damage/retouch perpendicular to the edge of the burin facet.

Edge damage type. This is a description of the type of observed damage on the burin (e.g., grinding, polish).

Burin spalls were recorded with all flake attributes, with these additional variables:

Burin spall type.

-primary (triangular cross section, generally with dorsal damage)
-secondary (quadrilateral cross section, with evidence of previous burin spall removals)

Burin spall damage type (e.g., grinding) and Damage location (e.g., medial dorsal, dorsal and lateral).

Burin spall depth of damage. Equivalent to burin depth of damage (above)

Burin spall length of damage (in mm).

Burin spall damage edge angle. Equivalent to burin damage edge angle (above).

7.2.4.4 Biface Technology Attributes

Variables for bifaces and biface fragments include these variables described above: raw material, raw material quality (high, medium, low), cortex, and weight. In addition, the following variables were recorded:

Flaking pattern.
- -comedial (flake scars meet at the midline of the biface)
- -parallel (flake scars are parallel of similar dimension or angle)
- -random (flake scars are random in size and orientation)

Dorsal flake scar extent.
- -< half way across the biface (does not reach the midline)
- -> half way across the biface (reaches beyond the midline)

Hafted. Based on shape, and secondary working (e.g., edge grinding), and recorded as yes, no, and indeterminate.

Modification. This includes edge grinding, burination, reworking, etc.

Maximum Length. Measured from the base to the tip, to the nearest 0.01 mm.

Maximum Length. Measured perpendicular to length, to the nearest 0.01 mm.

Maximum thickness. Measured at the point of maximum thickness of the piece, to the nearest 0.01 mm.

In addition, several ratios were calculated, including L/W, W/T, and Area (L x W).

Edge angle. This was the range of maximum and minimum edge angles along the bifacial edges. Generally, edge angles decrease with later stages of reduction.

Blade length, Haft length, Blade width, and Base width were also recorded.

Stage. This reflects stage of manufacture of bifacial implements, following Andrefsky (2001).
- -Stage 1 = blank
- -Stage 2 = edged biface with W/T ratio of 2-4 and edge angles of 50-80 degrees.
- -Stage 3 = thinned biface with W/T ratio of 3-4 and edge angles of 40-50 degrees.
- -Stage 4 = preform with W/T ratio of 4.1-6, edge angles of 25-45 degrees
- -Stage 5 = finished bifaces with W/T ratio of 4.1-6, edge angle of 25-45 degrees and refined trimming of edges.

7.2.4.5 Uniface Technology Attributes

Unifaces were defined as artifacts with unifacial retouch, generally more pronounced than modified flakes, where one or more edges were shaped through unifacial retouch. Typically

these were items typically referred to as end scrapers and side scrapers. Uniface attributes follow debitage attributes described above. Additional uniface variables include:

Blank type (flake, blade, blade-like flake, cobble).

Modification type (e.g., microflaking, retouch, damage, burination, polish)

Edge angle (for each retouched position).

Retouch length (for each retouched position)

Edge shape
- -point
- -convex
- -straight
- -concave
- -notch

Number of retouched margins and Percent of retouched margins (e.g., 1 of 4, 25%).

Position of retouch (left, right, proximal, distal) and (dorsal, ventral, edge, alternating)

Modification intensity (light, moderate, heavy)

Sum of retouched length, to the nearest 0.01 mm.

Sum of edge shape (point, convex, straight, concave, notch, or multiple).

Edge length. Maximum length of retouch or damage.

Edge diameter. Maximum length across the piece of retouch or damage (i.e., endscraper width at the working edge).

Edge thickness. Maximum thickness at the working edge(s) of the uniface.

Uniface type (End scraper, side scraper, double side scraper, etc.)

7.2.4.6 Modified Flake Technology Attributes

Modified flakes were defined as flakes or shatter with secondary retouch or damage. Modified flake attributes follow debitage attributes (above). Additionally, they were recorded with uniface attributes (above) except for edge length, edge diameter, edge thickness and uniface type.

7.2.4.7 Flake Core Technology Attributes

Flake core attributes include raw material, maximum length, width, thickness, weight (described above), and includes the following additional attributes.

Number of flake scars. Only those > 5 mm were counted.

Average scar width, to the nearest 0.01 mm.

Damage type, Damage location, and Damage length. These attributes record any observed retouch or usewear.

Flake Core Type.

-unidirectional. Flakes removed generally from single platform.
-multidrectional. Flakes removed from multiple dimensions.

7.2.4.8 Cobble Tools Technology Attributes

Cobble tool (unflaked) attributes include raw material (generally macrocrystalline, coarse grained materials not described for the core, flake, microblade and bifacial industries at DRO), maximum length (or largest dimension), maximum width (or second largest dimension), and maximum thickness (or third largest dimension), weight, and notes, including discussion of damage and/or heating.

Cobble spall tool (flaked) attributes include raw material, maximum length, width, and thickness (described above under debitage), weight, retouch/damage, and edge angle of use

7.2.5 Spatial Analysis

All artifacts were coded (see next section) and entered into an Excel spreadsheet. This was imported into SPSS for statistical analysis and ArcGIS for spatial analysis. Summed 3-pointed and screened materials for each 50 x 50 cm quadrant were entered into Surfer 3d to create density isopleths. Artifact clusters representing localized concentrations of lithic materials spatially separated from other occurrences of lithics were delineated to represent activity areas. These clusters were then analyzed using methods described above. These analyses are designed to be primarily heuristic in nature, exploratory data analyses, but statistical analyses included χ-square, t-tests, and ANOVA.

7.3 Lithic Raw Materials

7.3.1 Introduction

This section describes lithic raw materials, classifies local and nonlocal raw materials, and compares raw material use among components and traditions.

7.3.2 Lithic Raw Material Descriptions

A total of 77 different raw material types were identified in the DRO assemblages representing 77 minimum analytical units (Larson 2004, Larson and Kornfeld 1997). Lithic toolstone summary data are provided in Table 7.1 sorted by raw material. Detailed raw material descriptions and lithic toolstone summary data by component are found in Appendix A (Tables A1-A17).

A total of 55 varieties of chert were identified. These varied in color (black, gray, brown, greenish, and redish shades), texture (fine to coarse grained, with and without inclusions), and had varying amounts of cortex present). The cherts most frequently found in components (9 or more) were C5, fine-grained black chert, C11, fine-grained yellowish brown chert, and C19, fine grained dark gray chert. These were among the most abundant cherts in regards to weight and total artifact count, and all had a small portion of cortical flakes. Chert makes up 70.49% of the total assemblage. Five different varieties of chalcedony were delineated, making up 0.71% of the total flakes. All were fine grained, translucent, and none had any cortex. They were found in small numbers in 1 to 6 components each, most frequently in the Denali components. Three poor quality, unidentified, macrocrystalline materials comprising 0.04% of the assemblage were found in 3 components in low quantities. Obsidian was grouped together for analysis but pXRF analysis (see Chapter 10) discriminated at least three different sources. This material was found in 4 different Denali and Northern Archaic components and equates to 0.42% of the total assemblage. Six varieties of quartzite were used on site. All were found in low frequencies, with Quartzite 1 found in the highest frequency and across the largest number of components. Quartzite totals 0.80% of the assemblage. Seven varieties of rhyolite were defined based on observable characteristics. It is mainly found in the Denali components at DRO, but was also found in low frequencies in the Chindadn and Northern Archaic components. Rhyolite makes up 27.54% of the total artifacts.

7.3.3 Estimation of Local vs. Non-Local Raw Materials

For the purposes of elucidating raw material use and procurement strategies among components, we estimated local vs. non-local raw materials on the basis of several measures. We are aware of the potential problems in estimating local vs. non-local materials without clear geochemical identification. We justify this exploratory analysis for heuristic purposes for several reasons: (1) Very few raw materials have been geochemically identified in Alaska to date where source locations are known. These are limited to seven obsidian sources. Obsidian comprises 78 out of 18,768 chipped stone artifacts at DRO (0.4%). Rhyolite and basalt have seen some preliminary work (Coffman and Rasic 2015), but no sources of either are known. (2) We expect toolstone nodules to be potentially locally available in the nearby exposed Delta River, a large braided river with numerous observable cobbles of various sources. (3) The presence of 14 cultural components spanning three cultural traditions and many different climate regimes provides a significant opportunity to understand lithic procurement while holding site location constant. (4) These hypotheses provide frameworks for future testing with advanced geochemical sourcing techniques, such as pXRF or wave-dispersive XRF.

Five independent lines of evidence are used here to classify materials as provisionally local or non-local. We note that any measure by itself (excepting the first) is not demonstrative proof of local or non-local origin, but a cumulative case can be constructed.

First, DRO obsidian derives from two known obsidian sources, Wiki Peak and Batza Tena lie in 320 and 460 km straightline distance from DRO respectively, and are considered non-local. No other obsidian source is known or expected in the DRO area, so the remaining few unassigned obsidian are considered to be non-local.

Second, all things being equal, local sources should be exploited preferentially (in terms of overall abundance and proportionality of lithics at a site) over non-local sources. Materials acquired from local sources should be present in high proportions among different components at a single site. Material types present in only one or two components, no matter how high in quantity, may be introduced to the site as cores or tools which were reduced onsite. Material types present in many (or all) components are more likely to be local in origin, particularly if multiple different cultural traditions used the same toolstone.

Third, all things being equal, cortex should be preserved differentially on materials acquired close to the source at early stages of reduction. This is particularly expected if secondary cobbles adjacent to the site along the Delta River were utilized. Thus, relatively high proportions of primary and secondary (cortex-bearing) flakes are more expected for materials acquired nearby than for those that have undergone more curation and reworking.

Fourth, material from local sources should yield higher amounts of larger debitage (here defined as > 2.5 cm) than materials from nonlocal sources. Many studies note a positive relationship between long-distance movement of raw materials and flaking quality (Andrefsky 2008), with non-local pieces exhibiting more curation. In contrast locally acquired materials can be discarded without reworking (e.g. into blanks or expedient tools), because of its ease in procurement.

Fifth, all things being equal, we should expect relatively fewer tools made on local toolstone to be discarded after use (unless broken during manufacture) than tools made on non-local toolstone. Tools from non-local toolstone should be discarded in distant sites due to exhaustion while tools from local toolstone should be manufactured onsite or nearby and have relatively shorter portions of their uselife expended while onsite. Thus, we should see a higher tool:debitage ratio for nonlocal toolstone.

Complicating these assumptions are two issues. The first is potential package size differences, i.e., cortex could have been removed earlier or later in the reduction sequence. The second issue is that many materials could have been derived from locally available cobbles, i.e. from secondary deposits along the Delta River or among glacial till in surrounding area. Thus, while they may have been "local" they may not have been available in the same diversity or proportions through time. However, robust patterning in the five sets of variables described above could provide useful estimates to provisionally classify materials as local or nonlocal.

Several materials stand-out in relatively high proportions within and among assemblages, higher levels of cortex and larger debitage (Table 7.2). C33 is present in 8 components (57%) in large numbers (n=859), 13% have cortex and 5.2% are larger unretouched flakes, and the tool:debitage ratio is very low (0.23). C7 is present in 5 components (36%), 18% have cortex, 11% are larger unretouched flakes, and tool:debitage ratio is relatively low (1.45). Q1 is present in 8 components (57%), 17% have cortex, 4% are larger unretouched flakes, and tool:debitage ratio is relatively low (1.72). Four other materials (C5, C19, C30 and C36) have very high absolute and proportional abundances (n=3029, 1941, 1798, 893), are present in most components (93%, 86%, 36%, 57%), all three have cortex and larger unretouched flakes and very low tool:debitage ratios (0.30, 0.31, 0.11, 0.11). Thus, we provisionally classify C5, C7, C19, C30, C33, C36, and Q1 as local.

Rhyolites R1 and R2 meet some of the criteria discussed above. They are very common (over 2000 artifacts each) and are present in 10 and 9 components (71%, 64%), with relatively high amounts of cortical pieces (2.8-2.9%) and larger unretouched flakes (2.1-0.5%) as well as low tool:debitage ratios (0.21-0.10). However, the rhyolite is nearly absent in Northern Archaic and Chindadn components, suggesting these toolstone sources may be nonlocal. In addition, similar materials from Gerstle River (Potter 2005), Mead, and Healy Lake (Cook 1969) are widespread in the middle Tanana valley as well as the neighboring Nenana valley (Pearson 1999) also suggesting the source might be attractive and non-local, leading to the wide dispersal of these materials in the region. For these reasons, we are not considering R1 and R2 to be local.

Tool:debitage (*100) ratios among material types vary from 0 (no tools) to 50 (half as many tools as debitage). Two raw material types comprise single tools (Ch6, M2). Elevated tool:debitage ratios suggests tools were coming into the site from some distance near the end of their uselives and were thus discarded, perhaps with some flaking debris. These material types include those with tool:debitage (*100) ratios exceeding 2. These materials include C2, C4, C10, C21, C35, C49, C62, C67, C68, C72, Ch4, Ch6, M2, O, and Q2. Additionally, all of these materials are present in relatively small quantities (averaging 21.3 artifacts, ranging from 1 to 78). We provisionally classify these materials as non-local.

Thus, 15 materials are classified as non-local and 7 as local, with the remaining 56 as unknown (Table 7.2). These classifications comprise 9,117 artifacts, 48.6% of the total 18,771 artifacts at DRO.

7.3.4 Raw Material Comparisons Among Components and Traditions

Lithic raw material types present in DRO components provide an important window to explore lithic raw material use strategies among components and cultural traditions. The extent to which lithic raw materials are shared among components and traditions can be informative, potentially, as a proxy of how similar their raw material procurement strategies were, at least as recorded at DRO. Components and traditions that share many raw materials and assuming they were obtained from a single source, could be inferred to have similar lithic procurement strategies. All things being equal, components and traditions that do not share raw materials could reflect different procurement strategies. Other measures of raw material use similarities and dissimilarities are raw material richness, evenness, and diversity measures. Evenness is here defined as diversity/ln richness, where diversity is derived from Shannon-Wiener H'. Richness and evenness are both affected by sample size (Figures 7.1 and 7.2). To help overcome this, two additional diversity measures were calculated: Simpson's D and Shannon-Wiener H'. These diversity indices increase as both richness and evenness of the assemblage increases. Simpson's D ranges between 0 (uneven) and 1 (even), while Shannon-Wiener H' is unbounded with larger values reflective of more even assemblages.

In terms of overall lithic raw material use, there is greater diversity in Denali components than in Northern Archaic components (Table 7.3). Material type richness (number of raw material types per component) is generally higher in Denali components (averaging 27±21 types, ranging from 9-66) than in Northern Archaic components (averaging 16±14 types, ranging from 4-43) or Chindadn (17 types). For example, various rhyolite types are common in Denali components (32%), but nearly absent in Chindadn (0.04%) and Northern Archaic (2.3%) components. Obsidian is also present in small numbers in Denali (n = 67), but fewer in Northern Archaic (n = 11) and absent in Chindadn.

Figure 7.3 compares Chindadn, Denali, and Northern Archaic components by lithic raw material proportions. An "equal proportions" line in each graph shows expected values if each comparandum exhibited identical distributions of raw materials. Figure 7.3a shows that Chindadn and Denali traditions are quite dissimilar with almost all raw materials common among Denali components completely or nearly absent in the Chindadn component, and vice versa. This includes the nine most common Denali material types. Only two materials are appreciably shared between these components (C30 and C36). Notably C30 is absent and C36 is relatively rare in Northern Archaic assemblages. Figure 7.3b shows a different pattern between Denali and Northern Archaic assemblages. Two materials fall near the equal proportions line, C5 and C11, both of which are found in nearly all assemblages (93% and 79% respectively). This suggests these latter two may be local materials. A single material type, C12 is very common in one Northern Archaic component (C8a) and is absent in every other component.

Figure 7.4 compares the components with the largest sample sizes within cultural traditions. Figure 7.4a compares Denali components C2a and C2c. Many materials, including those with relatively large sample sizes are shared between the components. In contrast, Northern Archaic components C8a and C8b share almost no materials (Figure 7.4b). These patterns suggest that different procurement strategies operated within Denali and Northern Archaic traditions, and furthermore, that Denali components shared some procurement strategies at DRO, while Northern Archaic components were individually different, suggesting different use of the site by Northern Archaic populations.

When considering raw materials where total n > 30 (n = 38), 17 materials (45%) are exclusively or nearly exclusively shared among Denali components (and not Northern Archaic), and 4 (11%) exclusively or nearly exclusively shared among Northern Archaic (and not Denali), and 17 (45%) that are shared between Denali and Northern Archaic components (Figure 7.5). When considering raw materials where total n > 100 (n = 20), 6 materials (30%) exclusively shared among Denali components (and not Northern Archaic), 1 (5%) shared among Northern Archaic components (and not Denali), and 13 (65%) shared between Denali and northern Archaic components (Figure 7.6). Most are asymmetrically shared, with only 2 (10%) shared in any quantity: C5 (16% Denali, 25% Northern Archaic) and C11 (4%, 11%) [though possibly C19 (12%, 3%), R1 (15%, 2%).]. Broadly, this suggests different strategies and locations of raw material procurement.

Number of lithics divided by number of raw material types (assuming similar lithic use per material type) average 91±65 for Denali assemblages and 23±20 for Northern Archaic assemblages, suggesting overall different lithic behaviors, perhaps higher mobility or shorter site occupation for Northern Archaic populations. The Chindadn value (28) is more similar to Northern Archaic than Denali. These patterns are consistent with density values (n artifacts/excavation area) where Chindadn = 6 artifacts/m^2, Denali averages 40±50 artifacts/m^2, and Northern Archaic averages 6±6 artifacts/m^2. Individual Denali component density values are 89, 5, 99, 4, and 2. Individual Northern Archaic component density values are 2, 2, 3, 14, 10, and 6. The largest value of 14 artifacts/ m^2 is from C8a, where the dense lithic cache skews the overall averages. Without C8a, Northern Archaic density values average 4±4 artifacts/m^2.

Evenness and diversity measures are different between the groups (Table 7.3) and trends are illustrated in Figures 7.7 -7.9. Considering evenness (Figure 7.7), Chindadn = 0.521, Denali components average 0.593±0.125 and Northern Archaic components average 0.510±0.185, suggesting Denali components exhibit more even distributions of material types than Northern Archaic components. Diversity measures of raw material use are also different (Table 7.3,

Figures 7.8, 7.9). Considering those assemblages with n > 100 total artifacts, the Simpson's D value for the Chindadn component is 0.685, five Denali components average 0.753±0.153, and five Northern Archaic components average 0.591±0.247. Shannon-Wiener H' values are also different (with 1.475, and averages of 2.005±0.516 and 1.481±0.693 for Chindadn, Denali and Northern Archaic respectively). These data collectively suggest Denali assemblages exhibit both more evenness and diversity in raw material types than Northern Archaic assemblages. When considering these richness, evenness, and diversity patterns together, this suggests more similar lithic procurement and perhaps recurrent seasonal uses of the location by Denali populations and multiple and/or different lithic procurement and/or seasonal use of the location by Northern Archaic populations. Chindadn values are intermediate, and more difficult to evaluate given the sample size of one.

Within the seven Denali components, some differences can be teased out. Most earlier Denali components share many more raw materials (C2a, C2b, C2c), whereas the later Denali components (after 8600 cal yr BP, C3, C4, C5a, C5b) have slightly higher diversity measures between components, though nowhere near as much as Northern Archaic tradition components (C6-C8b).

These differences in diversity measures suggests more embedded procurement in early Denali components, and less embedded procurement in later Denali components. Northern Archaic components have more uneven distributions, suggesting more direct procurement and/or reduced mobility in relation to Denali.

Raw material quality varies by component (Table 7.4), but overall most assemblages are dominated by high flaking quality materials (overall average of 93% for Denali, 96% for Northern Archaic, and 91% for Chindadn). Low and moderate quality materials are present in C2a (11.3%), C4 (24.3%) and C7b (12.1%), the first two consistent with other data suggesting earlier stage manufacture of local raw materials in specific clusters (see below).

Tables A1-A17 show raw material summaries per component and lithic type (flake, microblade, core, and tool and are discussed by component below). Table 7.5 summarizes local and nonlocal raw materials by component. Figure 7.10 shows local:nonlocal ratios (excluding unassigned) and Figure 7.11 shows local toolstone as a percent of total (including unassigned materials). A general trend of decreasing use of nonlocal raw materials through time is evident. The earliest component, C1, exhibits a very high local:nonlocal ratio (147:1). Denali components vary in local:nonlocal ratios, but the early Denali components (C2a, C2b, and C2c) are relatively high (82:1, 75:1, and 12:1). Later Denali components (C3, C4, C5, C5b) have lower ratios (N/A (no non-local), 5:1, 2:1, 0.57:1). Northern Archaic components have generally low ratios throughout (5:1, 3:1, 4:1, 4:1, 8:1, 10:1, except for C6 (28:1). This general trend is independent of overall assemblage size. This provides additional data that separates earlier and later Denali components. When considering local toolstone as a percentage of total artifacts (including unassigned) (Figure 7.11), a general decreasing trend is still seen, but there is more variation, though the distinction between earlier and later Denali components is still evident.

Table 7.1. Raw material summary data.

material	*Chindadn*	*Denali*	*Northern Archaic*	*Total wt (g)*	*N (%) components*	*N cortex (%)*	*N >2.5 cm (%)*
C1	0	330	36	62.42	6 (43%)	5 (1.4%)	9 (2.5%)
C2	0	10	20	2.02	4 (29%)		
C3	0	1	27	7.79	5 (36%)		
C4	0	2	1	0.19	2 (14%)		1 (33.3%)
C5	4	2412	622	366.58	13 (93%)	20 (0.7%)	64 (2.1%)
C6	0	0	1	0.15	1 (7%)		
C7	0	139	1	76.92	5 (36%)	25 (17.9%)	15 (10.7%)
C8	0	5	3	0.4	3 (21%)		
C10	1	29	0	157.65	3 (21%)	3 (10.0%)	7 (23.3%)
C11	20	574	271	91.72	11 (79%)	2 (0.2%)	9 (1.0%)
C12	0	0	1038	43.13	1 (7%)		
C13	0	52	1	3.81	3 (21%)		
C14	0	38	1	15.62	3 (21%)		3 (7.7%)
C15	0	7	44	1.76	4 (29%)		
C17	0	116	4	8.64	5 (36%)		
C18	0	1	0	0.02	1 (7%)		
C19	35	1847	65	147.62	12 (86%)	8 (0.4%)	11 (0.6%)
C21	0	15	1	0.76	3 (21%)		
C22	0	60	1	8.96	4 (29%)		2 (3.3%)
C24	0	154	27	15.42	8 (57%)	2 (1.1%)	2 (1.1%)
C28	0	214	3	42.85	9 (64%)		5 (2.3%)
C29	0	117	25	13.98	7 (50%)		
C30	215	1585	0	263.68	5 (36%)	2 (0.1%)	24 (1.3%)
C31	0	0	56	2.22	2 (14%)		
C32	1	3	5	3.38	3 (21%)	2 (22.2%)	
C33	38	801	22	315.29	8 (57%)	112 (13.0%)	45 (5.2%)
C35	0	1	2	13.72	2 (14%)		1 (33.3%)
C36	142	723	29	116.62	8 (57%)	4 (0.4%)	15 (1.7%)
C38	0	16	0	0.22	4 (29%)		
C39	0	166	14	13.79	7 (50%)	1 (0.6%)	2 (1.1%)
C41	0	112	1	12.99	3 (21%)		3 (2.7%)
C42	0	10	0	1.51	3 (21%)		
C45	1	9	0	1.62	3 (21%)		
C46	0	80	0	6.06	2 (14%)		
C47	0	170	1	5.73	2 (14%)		1 (0.6%)
C48	0	53	0	3.67	1 (7%)		
C49	0	11	13	4.6	6 (43%)	1 (4.2%)	4 (16.7%)
C51	0	3	32	1.61	4 (29%)		
C52	0	4	0	2.69	2 (14%)		
C53	1	1	3	0.18	4 (29%)		
C55	1	98	0	6.63	4 (29%)	2 (2.0%)	
C56	0	46	2	2.14	5 (36%)		
C57	0	12	1	1	2 (14%)	7 (53.8%)	
C58	0	8	0	2.38	1 (7%)		1 (12.5%)
C59	0	2	3	1.39	3 (21%)	2 (40.0%)	
C62	0	23	0	1.75	3 (21%)	1 (4.3%)	4 (17.4%)
C63	0	5	0	2.62	2 (14%)		2 (40.0%)
C64	0	0	1	0.46	1 (7%)		
C65	0	12	0	0.87	2 (14%)		
C66	0	1	0	0.03	1 (7%)		
C67	0	1	48	3.28	3 (21%)		1 (2.0%)
C68	1	36	1	16.19	6 (43%)	1 (2.6%)	1 (2.6%)
C69	0	20	2	3.01	2 (14%)		
C70	0	54	1	3.7	3 (21%)		2 (3.6%)
C72	0	7	0	0.13	1 (7%)		1 (14.3%)
Ch1	1	27	2	0.66	6 (43%)		

Ch3	0	85	2	4.55	5 (36%)		1 (1.1%)
Ch4	0	5	3	1.45	4 (29%)		7 (87.5%)
Ch5	0	6	0	0.74	3 (21%)		
Ch6	0	0	1	0.01	1 (7%)		
M1	0	2	1	0.18	3 (21%)		
M2	0	0	0	0.09	1 (7%)		
M4	0	3	1	2.93	3 (21%)		1 (25.0%)
O	0	67	11	12.89	4 (29%)	4 (5.3%)	1 (1.3%)
Q1	0	99	19	30.76	8 (57%)	20 (16.9%)	5 (4.2%)
Q2	1	6	1	0.24	4 (29%)		
Q3	1	8	4	3.24	6 (43%)	1 (7.7%)	2 (15.4%)
Q4	0	0	4	0.13	2 (14%)		
Q5	0	0	4	4.46	2 (14%)		
Q6	0	1	1	3.67	2 (14%)		
R1	2	2297	39	254.51	10 (71%)	68 (2.9%)	49 (2.1%)
R2	0	2100	6	160.77	9 (64%)	59 (2.8%)	10 (0.5%)
R4	0	54	9	5.39	6 (43%)	1 (1.6%)	
R7	0	77	0	5.32	2 (14%)		1 (1.3%)
R8	0	3	0	0.45	1 (7%)		
R9	0	516	6	38.76	7 (50%)	4 (0.8%)	9 (1.7%)
R10	0	3	0	0.27	1 (7%)		

Table 7.2 Local vs. nonlocal material type estimation

Material	*Tools*	*debitage*	*percent components*	*N with cortex*	*N > 2.5 cm*	*Tool:debitage (*100)*	*Classification*
C5	9	3029	93	20	64	0.30	Local
C7	2	138	36	25	15	1.45	Local
C19	6	1941	86	8	11	0.31	Local
C30	2	1798	36	2	24	0.11	Local
C33	2	859	57	112	45	0.23	Local
C36	1	893	57	4	15	0.11	Local
C10	1	29	21	3	7	3.45	Nonlocal
C2	1	29	29	0	0	3.45	Nonlocal
C21	1	15	21	0	0	6.67	Nonlocal
C35	1	2	14	0	1	50.00	Nonlocal
C4	1	2	14	0	1	50.00	Nonlocal
C49	1	23	43	1	4	4.35	Nonlocal
C62	2	21	21	1	4	9.52	Nonlocal
C67	1	48	21	0	1	2.08	Nonlocal
C68	3	35	43	1	1	8.57	Nonlocal
C72	1	6	7	0	1	16.67	Nonlocal
Ch4	1	7	29	0	7	14.29	Nonlocal
Ch6	1	0	7	0	0	N/A	Nonlocal
M2	1	0	7	0	0	N/A	Nonlocal
O	3	75	29	4	1	4.00	Nonlocal
Q2	1	7	29	0	0	14.29	Nonlocal

Table 7.3 Diversity indices (flakes, microblades, tools, cores)

Component	*N artifacts*	*Material type richness (S)*	*Evenness (H'/ln(S))*	*Simpson's D*	*Shannon-Wiener H'*
C1	472	17	0.521	0.685	1.475
C2a	7009	48	0.598	0.847	2.314
C2b	385	18	0.614	0.712	1.776
C2c	7795	66	0.575	0.836	2.407
C3	279	18	0.415	0.501	1.199
C4	162	21	0.765	0.867	2.330
C5	51	12	0.672	0.671	1.671
C5b	36	9	0.865	0.819	1.900
C6	191	24	0.673	0.801	2.138
C6b	8	4	0.875	0.656	1.213
C7	128	16	0.643	0.743	1.783
C7a	7	4	0.921	0.694	1.277
C7b	244	5	0.493	0.417	0.794
C8	13	6	0.848	0.734	1.519
C8a	1196	27	0.206	0.243	0.679
C8b	840	43	0.535	0.750	2.011

Table 7.4 Material quality per component.

	low	*moderate*	*high*
C1		8.8%	91.2%
C2a	0.1%	11.2%	88.7%
C2b	0.3%	8.6%	91.1%
C2c	0.3%	3.8%	95.9%
C3		0.4%	99.6%
C4	0.6%	23.7%	75.6%
C5a			100.0%
C5b			100.0%
C6a	0.5%	6.5%	93.0%
C6b			100.0%
C7a			100.0%
C7b	0.3%	11.8%	87.9%
C8a			100.0%
C8b	0.6%	1.5%	97.9%

Table 7.5 Local and nonlocal summary by component.

Component	*total artifacts*	*Local*	*Nonlocal*	*Unassigned*	*Local:nonlocal*
C1	472	440	3	29	147:1
C2a	7007	5481	67	1461	82:1
C2b	387	299	4	82	75:1
C2c	7729	1565	135	6030	12:1
C3	279	232	0	47	N/A
C4	163	47	9	106	5:1
C5a	51	10	5	36	2:1
C5b	35	8	14	14	0.57:1
C6a	189	110	4	77	28:1
C6b	8	5	0	3	N/A
C7a	7	3	1	3	3:1
C7b	368	203	52	111	4:1
C8a	1196	71	9	1116	8:1
C8b	860	410	41	402	10:1

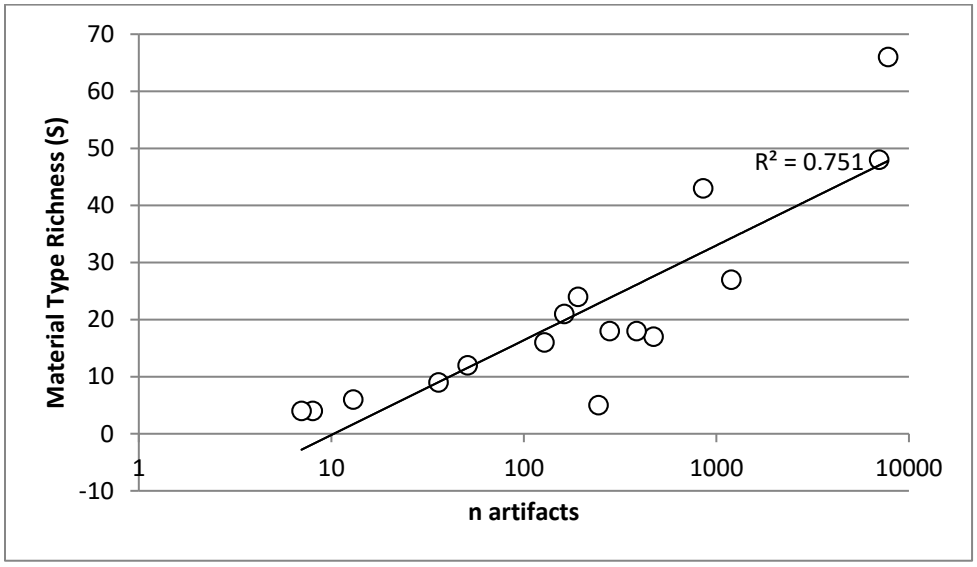

Figure 7.1. Material type richness by n artifacts per component.

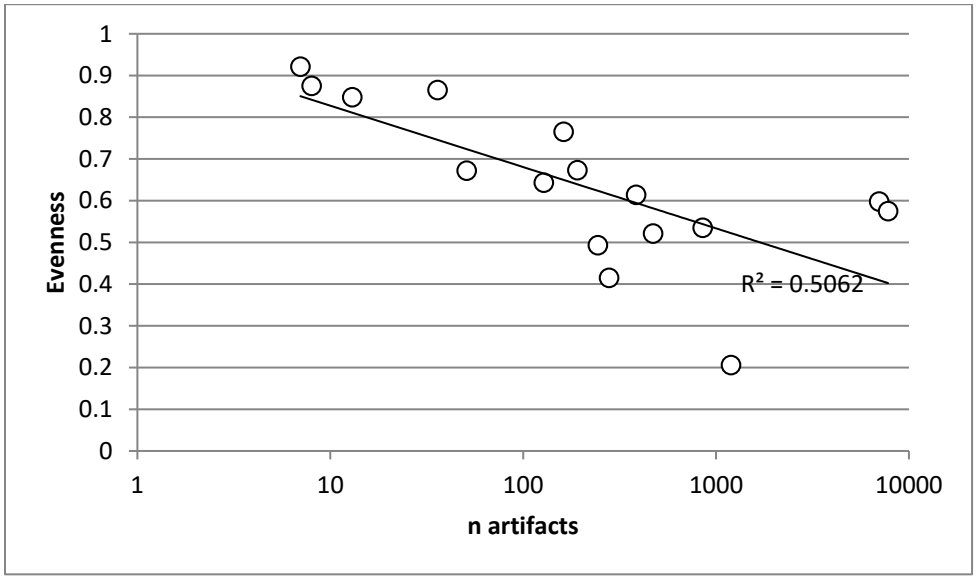

Figure 7.2 Material type evenness by n artifacts per component

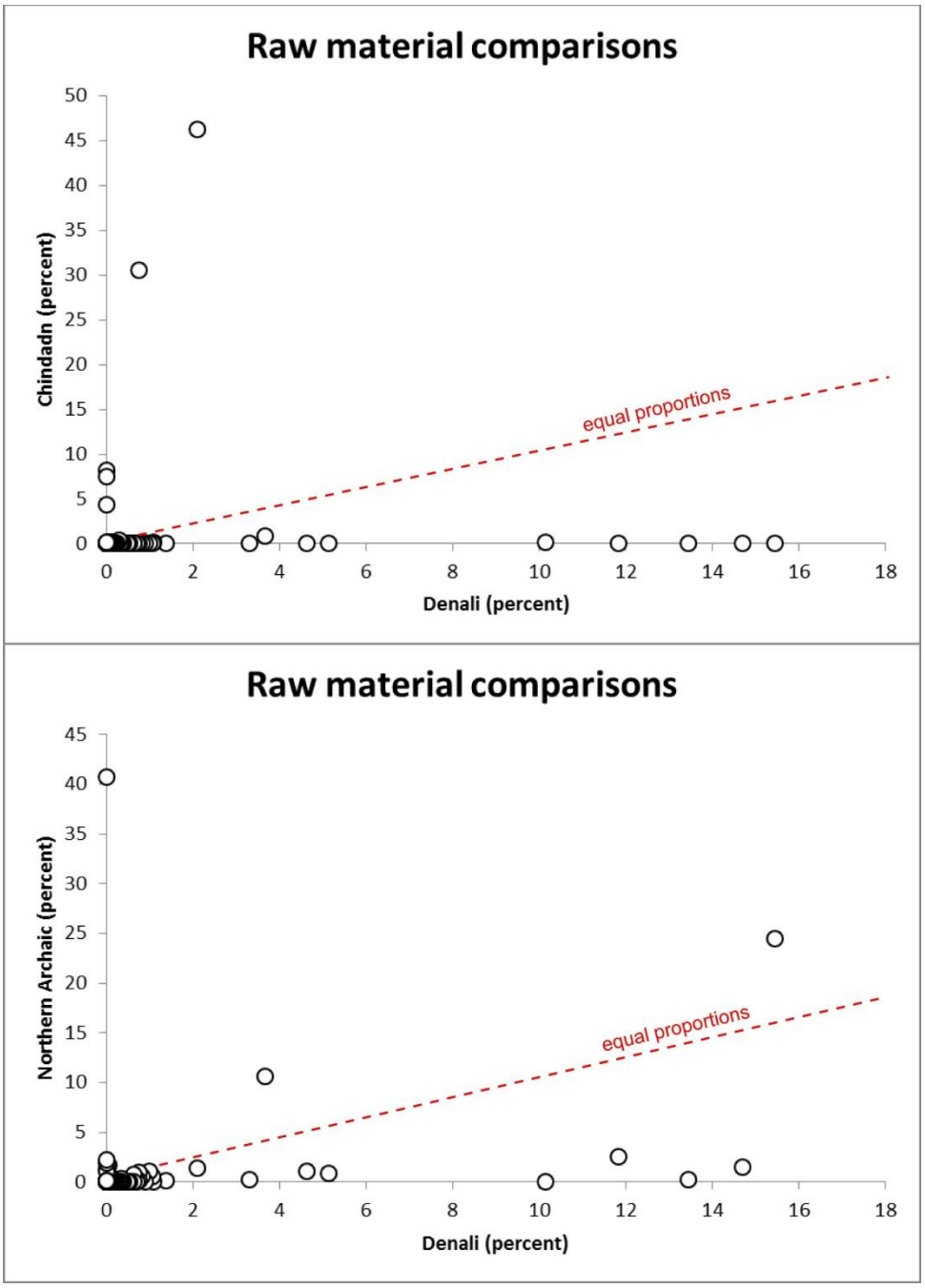

Figure 7.3 Comparison of raw materials, Chindadn and Denali (top) and Denali and Northern Archaic (bottom).

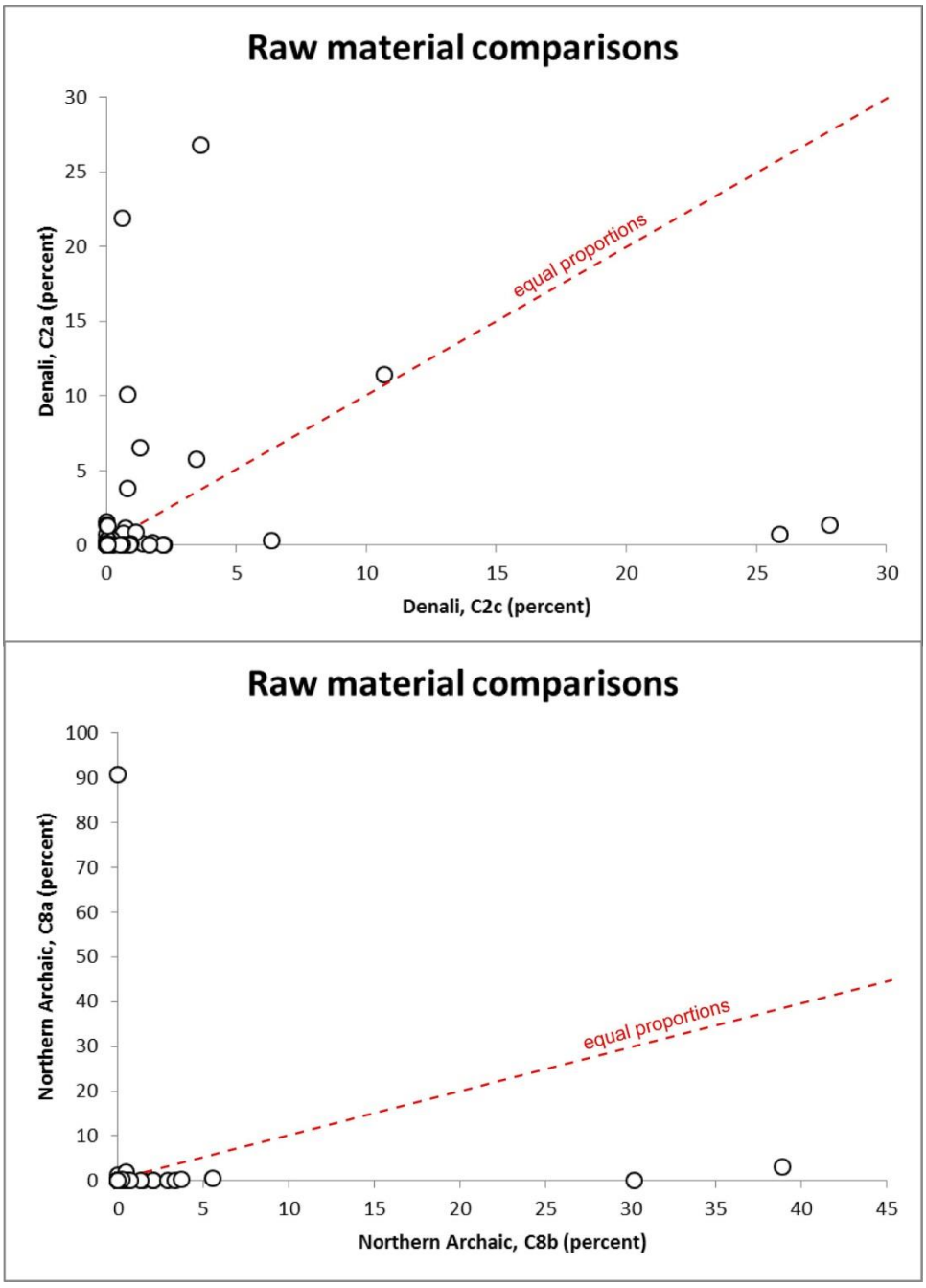

Figure 7.4 Comparison of raw materials within traditions; Denali (C2a and C2c top), Northern Archaic (C8a and C8b bottom).

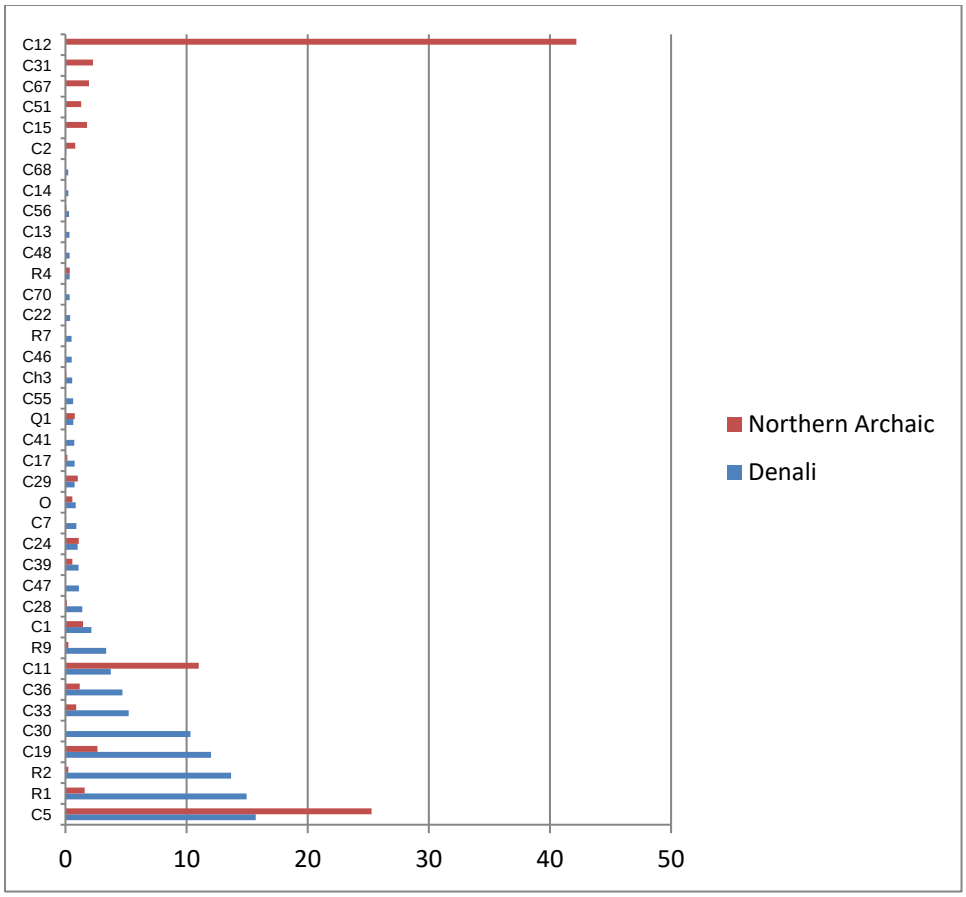

Figure 7.5 Raw material comparisons, Denali and Northern Archaic, where total sample size is >30 (n=38 materials).

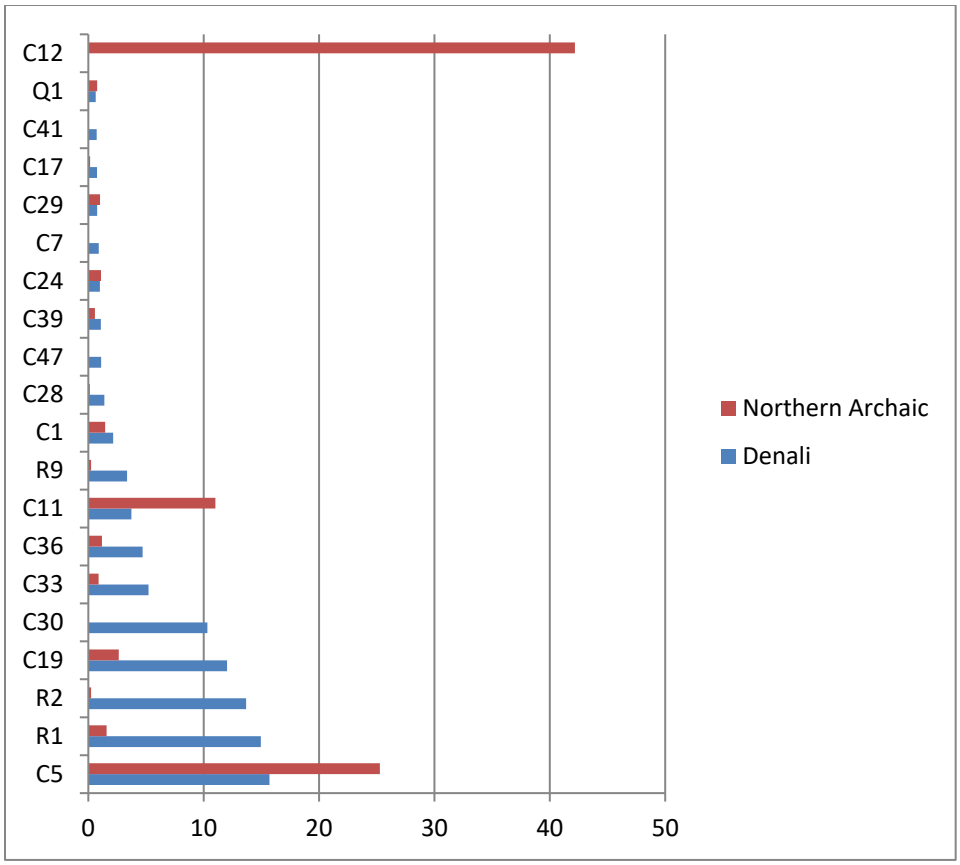

Figure 7.6 Raw material comparisons, Denali and Northern Archaic, where total sample size is >100 (n=20 materials)

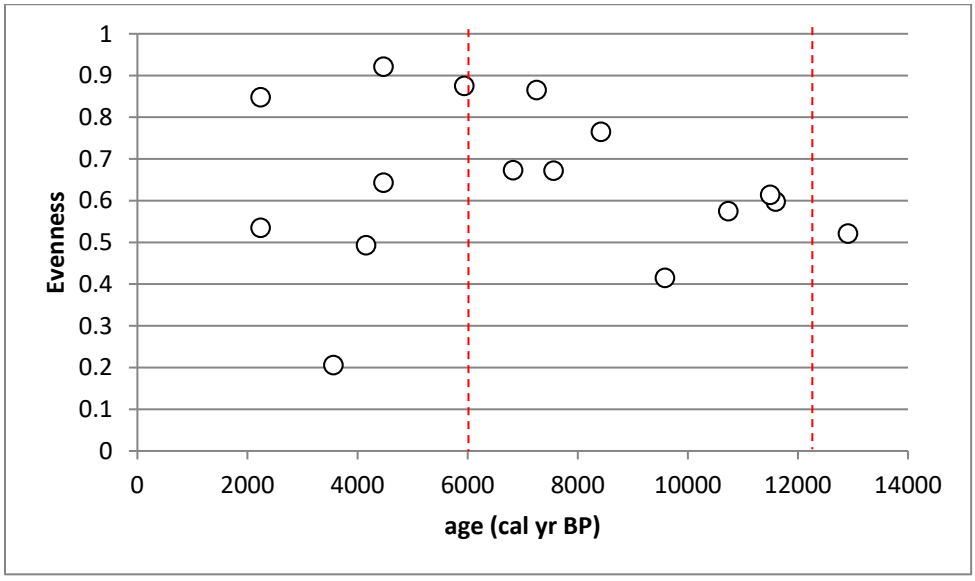

Figure 7.7 Evenness values per component through time.

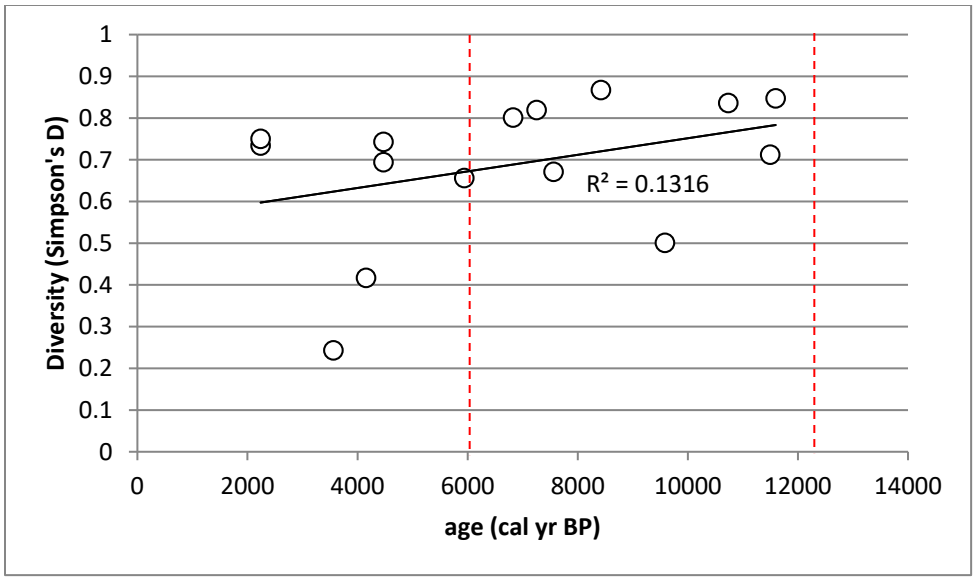

Figure 7.8 Diversity (Simpson's D) values per component through time (excluding C1).

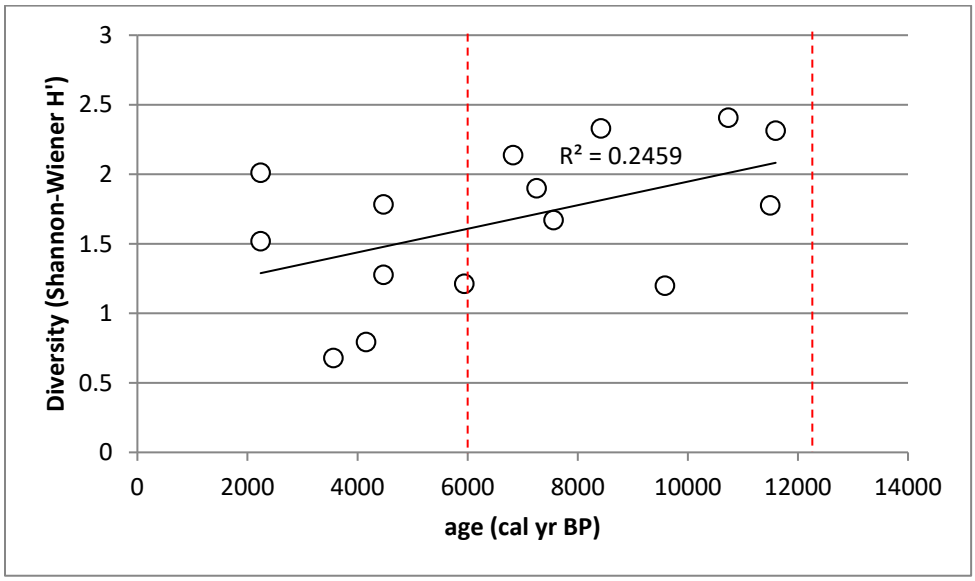

Figure 7.9 Diversity (Shannon-Wiener's H') values per component through time (excluding C1).

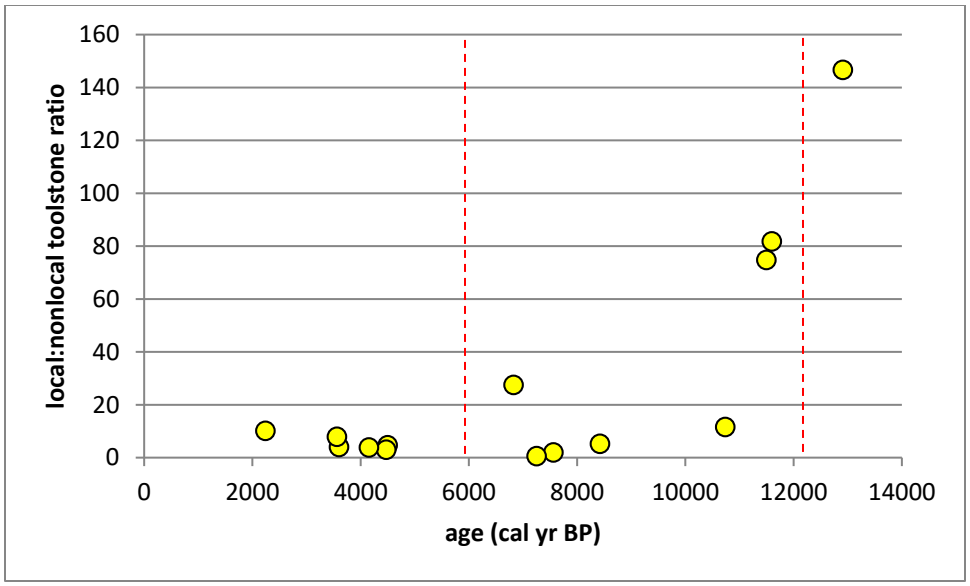

Figure 7.10 Local:nonlocal toolstone ratio by component.

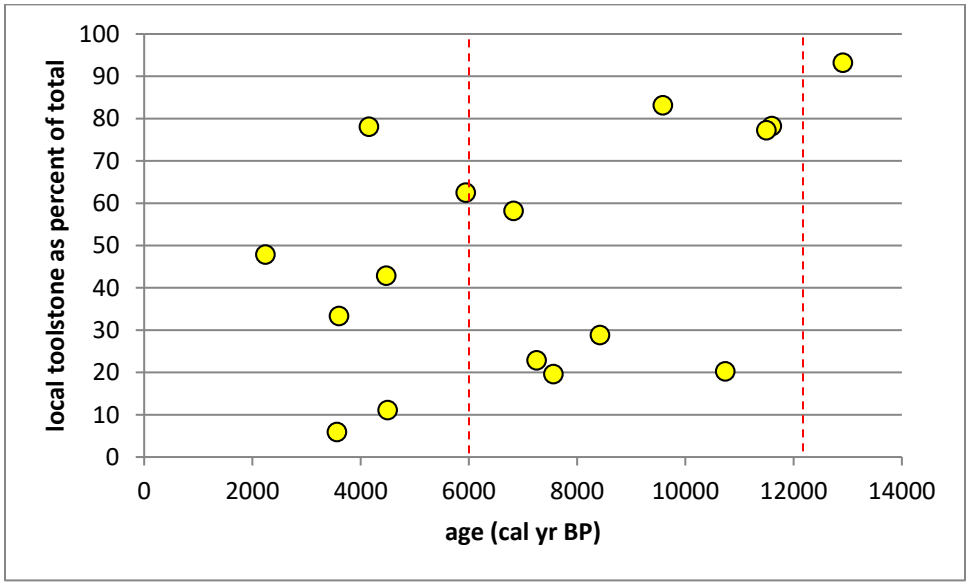

Figure 7.11 Local toolstone as a percent of total artifacts by component (includes unassigned)

7.4 Lithic Technological Analyses

This section examines technological and economic aspects of the lithic assemblages from DRO. Research questions include delineation of classes and types comprising the assemblage and characterization of the reduction strategies and major industries.

7.4.1 Assemblage composition

Assemblage summaries for each component are provided in Table 7.6 Overall quantity of debitage, microblades, and (non-microblade) tools are shown in Figure 7.12. Denali Components 2a and 2c are very large, while C2b, C3, and C4 are roughly similar, around 200-400 lithic items. The Chindadn Component 1 and Northern Archaic components C6a and C7b are also similar, between 200-500 lithic items. Denali Components 5a, 5b and Northern Archaic components 6a and 6b are much smaller (7-50 items).

Because of the abundance and stratigraphic isolation of components, we can explore occupation patterns at DRO through time and by cultural tradition (Figure 7.13). Denali occurs between ~12,500 and 6000 cal yr BP (6500 years) and Northern Archaic occurs between 6000-1000 cal yr BP (5000 years). Overall, component density between Denali and Northern Archaic are similar, with 0.11 Denali components and 0.12 Northern Archaic components per 100 years, suggesting similar overall occupation recurrence at the DRO overlook position. However, the period between 11,600-9500 cal yr BP exhibited the most lithic reduction, followed by a sharp decrease between 9000-4000y ears ago, present in both Denali and Northern Archaic components. An increase in Northern Archaic components between 4000-2000 cal yr BP is present. Thus, Denali use of the site is intensive in the early Holocene which declines in the middle Holocene while Northern Archaic use of the site is fairly spotty at low levels for thousands of years before increased use of the site is present in the middle-late Holocee after 4000 years ago. There is little evidence of post-2000 year occupations at the site. It is difficult to extrapolate from the single Chindadn occupation at the site, but its presence with the earliest paleoesol complex (P0) suggests occupation soon after the site became vegetated. There is a notable gap in occupations during the Younger Dryas period (12,800-11,500 cal yr BP), consistent with regional declines in site occupations.

Microblade technology is much more common in Denali than Northern Archaic components, though this does vary considerably within Denali (Figure 7.14). Microblade technology is present in low levels at Chindadn Component 1 and Denali Components 2a, 2b, and 3 and Northern Archaic Component C6a, less than 5%. Microblade industries are prevalent in Denali Components 2c, 4, 5a, and 5b, between 6-28% of total artifacts.

Tools as a percent of total artifacts also vary between Denali and Northern Archaic components (Figure 7.15). Generally, Denali components have relatively few tools per total artifacts, averaging 1.6%±1.7% while Northern Archaic components have higher percentages of tools, averaging 5.6%±6.4%. Interestingly, the later Denali occupations, while having fewer overall artifacts, generally have higher tool proportions (3.1%±1.6%) than earlier Denali occupations (averaging 0.6±0.1%), suggesting more reduction activities in the earlier Denali occupations.

Tool classes per component are shown in Figure 7.16. Tool classes richness is larger in the earlier Denali components (averaging 5) than in the later Denali (1.7) and Northern Archaic (2.8) components. Even when considering sample size, this holds, as the larger Northern Archaic

C8a and C8b components have relatively fewer tool classes, generally modified flakes, unifaces and bifaces. Modified flakes are common in all components except C7a, C2b, and C2c. Unifaces vary between cultural traditions (Figure 7.17). Denali unifaces are evenly divided between side scrapers and end scrapers, while Northern Archaic unifaces are almost entirely represented by end scrapers, which occur in every later occupation (C7a, C7b, C8a, C8b). The later Denali components (C3, C4, C5a, C5b) are almost entirely devoid of unifaces.

Bifaces are relatively common in all three cultural traditions, but with different stages of reduction (Figure 7.18). Chindadn Component 1 contain 1 stage 3 (thinned) and 3 stage 5 (finished) bifaces, generally projectile points. Denali components contain more earlier stages, including stage 2 (edged), stage 3 (thinned), and stage 4 (preform) types. Only 2 finished bifaces are found, both from Component 2c. In contrast, Northern Archaic components with bifaces (n=3) all contain finished bifaces (projectile points), and generally lack earlier stages. The exception is Component 8a, which is a blank cache with five edged bifaces (stage 2).

Mobile toolkits are thought to be composed of generally curated tools. Relatively high tool formality (i.e., low expedient tools) suggests higher levels of curation. Figure 7.19 shows formal:expedient tool ratios per component. Component 1 and early Denali component (2a) have relatively high tool formality, though with inclusion of microblade tools, C2c and C4 have relatively high tool formality. In contrast, later Denali components (C3, C4, C5a, and C5b) have similar low tool formality indices. In contrast, Northern Archaic components generally have low-moderate tool formality that increases through time. When adding modified microblades as part of a formal technological process, the formal:expedient tool ratio is greatly increased, particularly in C2c and C4.

Decortication and early stage reduction is present at low levels throughout the DRO record (Figure 7.20). This generally decreases through time throughout the Denali components, highest in C2a (2%), lowest in C4 (~1%), followed by relatively high levels in C5a (6%). Northern Archaic components C6a and C8b have similar levels (~3-4%) while the other Northern Archaic components have much less. The relatively similar low levels (1-4%) of decortication and early stage reduction throughout all periods (except Chindadn C1) suggests local acquisition of some raw materials along the Delta River (or glacial till) through time, but that there is no clear onsite or nearby single raw material source, given the variation in use (but see discussion of local and nonlocal classification below). Percentages of soft and hard hammer percussion flakes, estimated from platform measurements (Allen 2018), yield similar results (Figure 7.21).

Table 7.6 Lithic Assemblage Summaries by component

*Type**	*C1*	*C2a*	*C2b*	*C2c*	*C3*	*C4*	*C5a*	*C5b*	*C6a*	*C6b*	*C7a*	*C7b*	*C8a*	*C8b*
Debitage	**464**	**6974**	**384**	**7588**	**273**	**149**	**49**	**35**	**186**	**7**	**6**	**356**	**1143**	**850**
flakes	462	6955	381	7200	271	121	46	30	185	7	6	356	1143	850
mb	2	19	3	388	2	28	3	5	1	-	-	-	-	-
Cores	**1**	**2**	**-**	**5**	**-**	**1**	**1**	**1**	**1**	**-**	**-**	**-**	**-**	**-**
mb core	-	-	-	2	-	-	1	1	-	-	-	-	-	-
mb core part	-	-	-	3	-	1	-	-	-	-	-	-	-	-
flake core	1	2	-	-	-	-	-	-	1	-	-	-	-	-
tools	**8**	**33**	**2**	**140**	**6**	**13**	**1**	**-**	**3**	**-**	**1**	**13**	**53**	**10**
mod. mb	1	2	-	89	-	7	-	-	-	-	-	-	-	-
mod. flake	2	13	1	17	5	6	-	-	2	-	-	7	43	4
biface	4	13	-	6	1	-	-	-	1	-	-	-	6	2
uniface	-	4	-	9	-	-	1	-	-	-	1	6	4	4
burin	-	-	-	2	-	-	-	-	-	-	-	-	-	-
burin spall	-	1	1	17	-	-	-	-	-	-	-	-	-	-
cobble tools	**-**	**1**	**-**	**5**	**-**	**-**	**-**	**-**	**1**	**-**	**2**	**-**	**-**	**2**
Total	**472**	**7010**	**386**	**7738**	**279**	**163**	**51**	**36**	**191**	**7**	**9**	**369**	**1196**	**862**

*mb = microblade

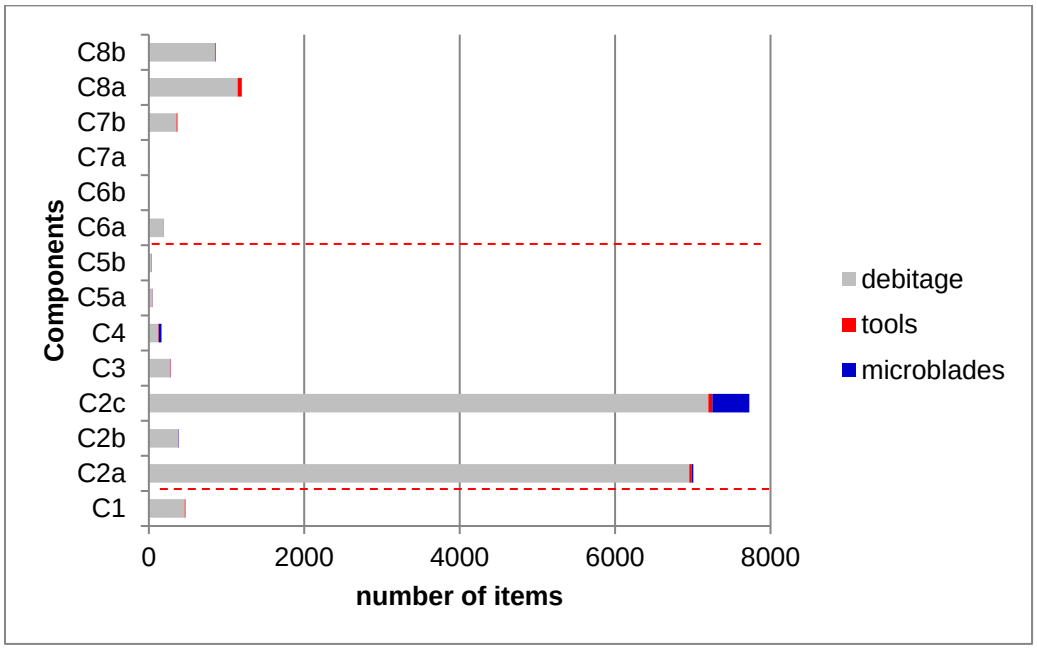

Figure 7.12 Lithic assemblage sizes (microblades include modified and unmodified and tools comprise non-microblade tools)

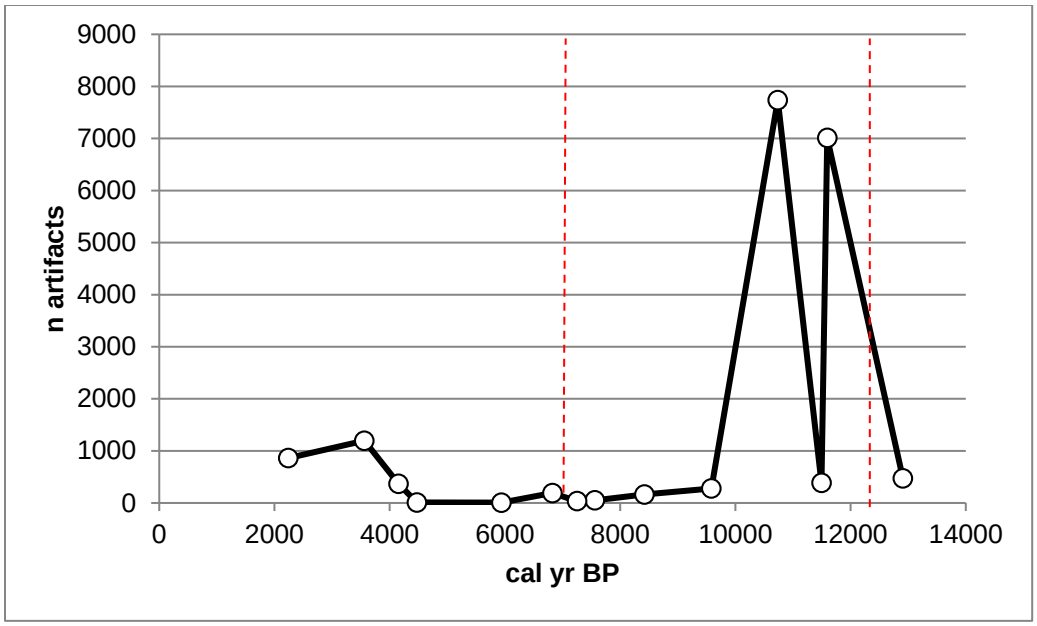

Figure 7.13 Lithic assemblage sizes through time

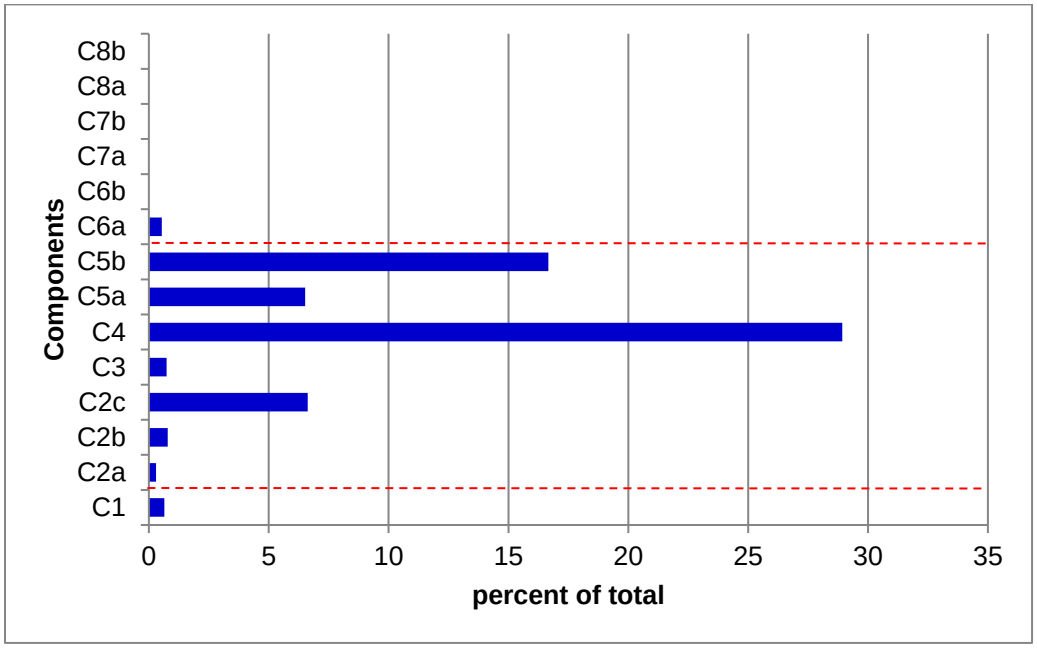

Figure 7.14 Microblade technology as a percent of total (microblades, core tablets, and cores)

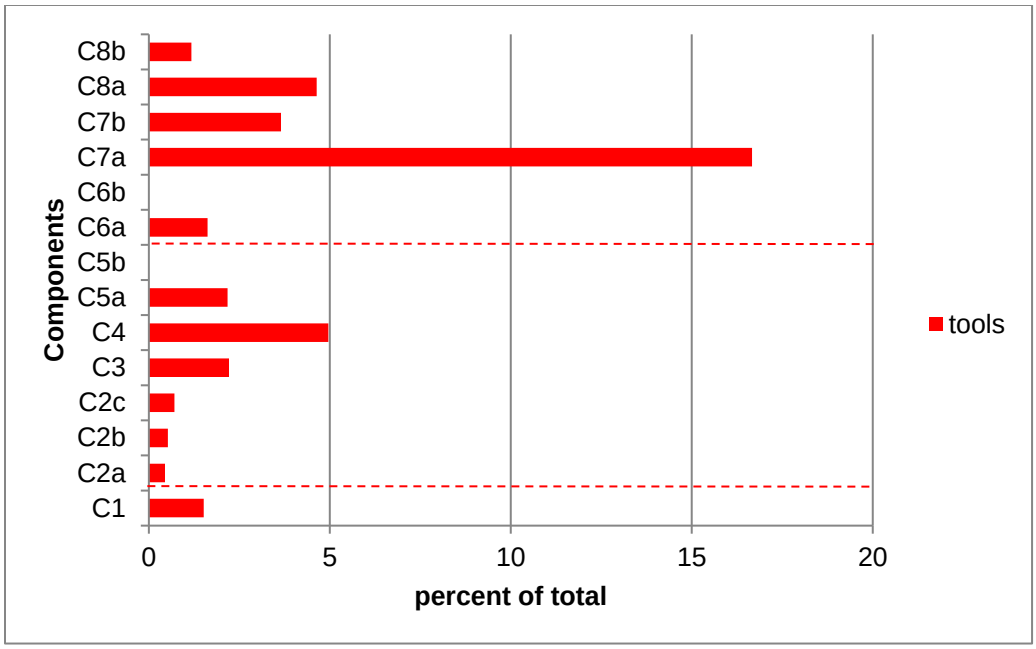

Figure 7.15 Tools as a percent of total artifacts

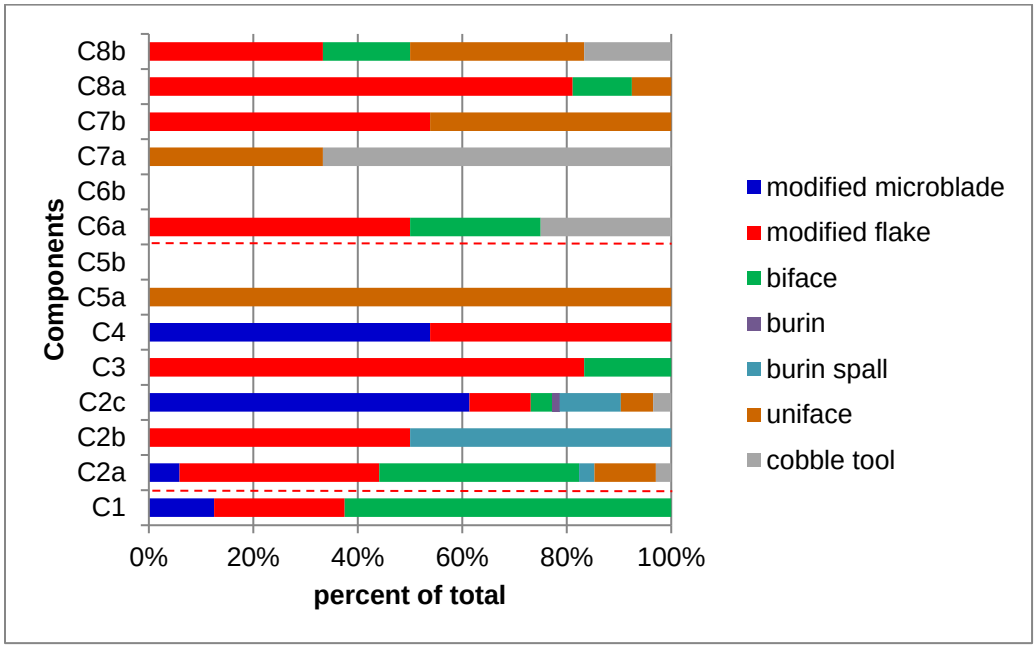

Figure 7.16a Tool type distributions (by percent)

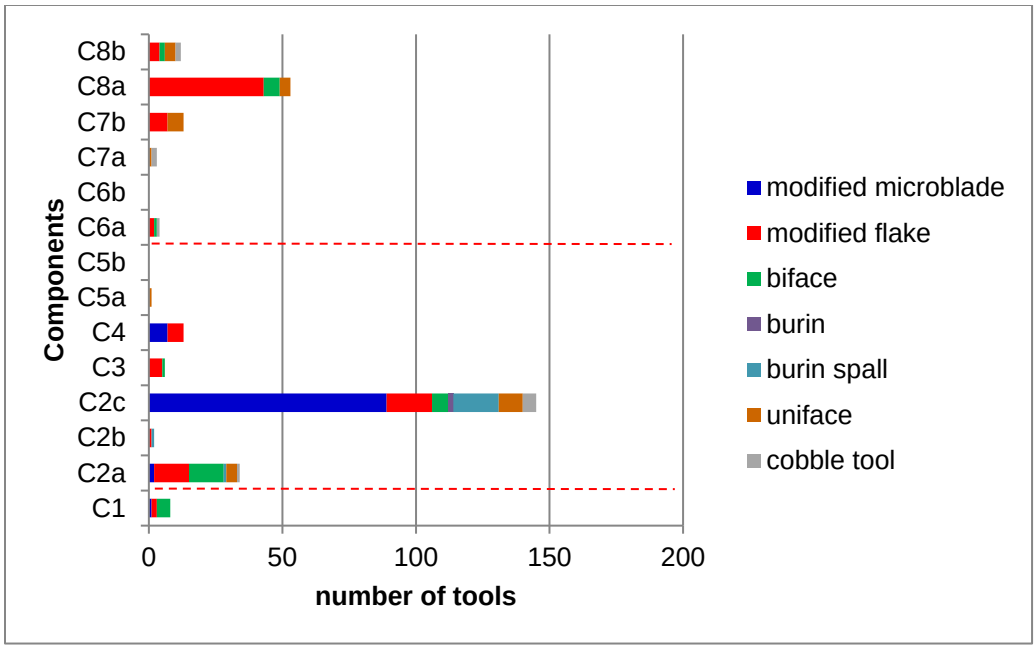

Figure 7.16b Tool type distributions (by count)

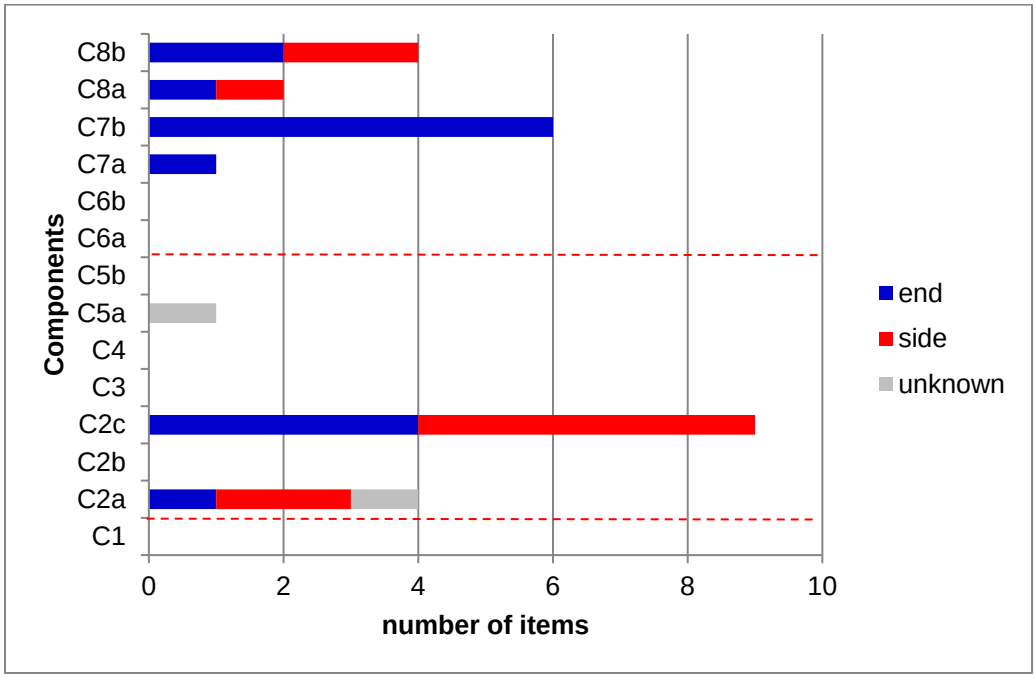

Figure 7.17 Uniface variation

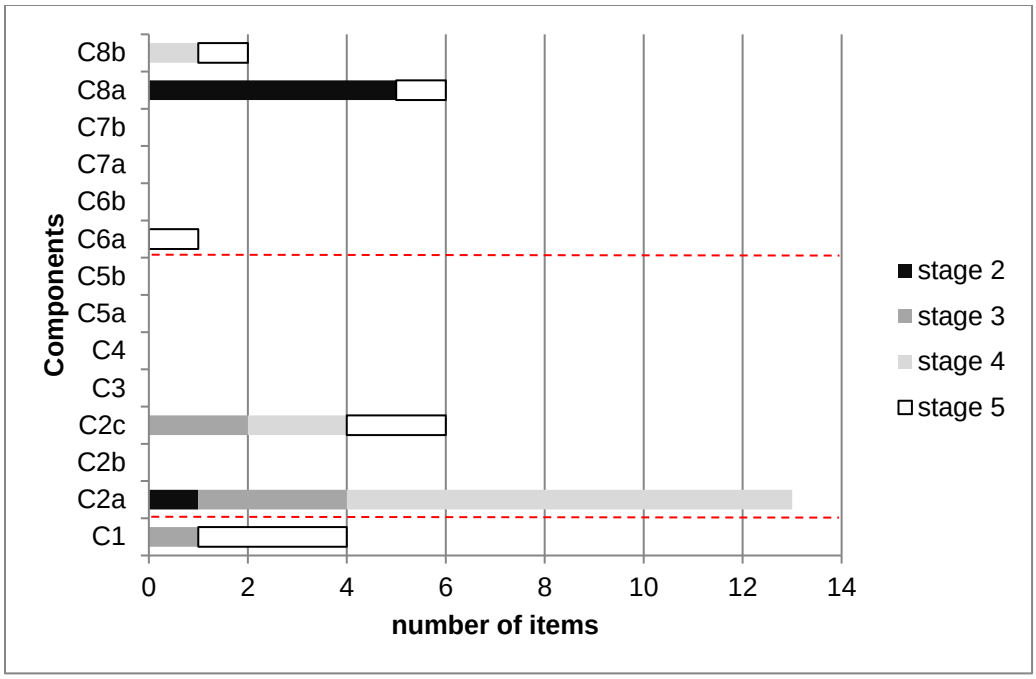

Figure 7.18 Biface variation (stages: 2 edged, 3 thinned, 4 preform, 5 finished)

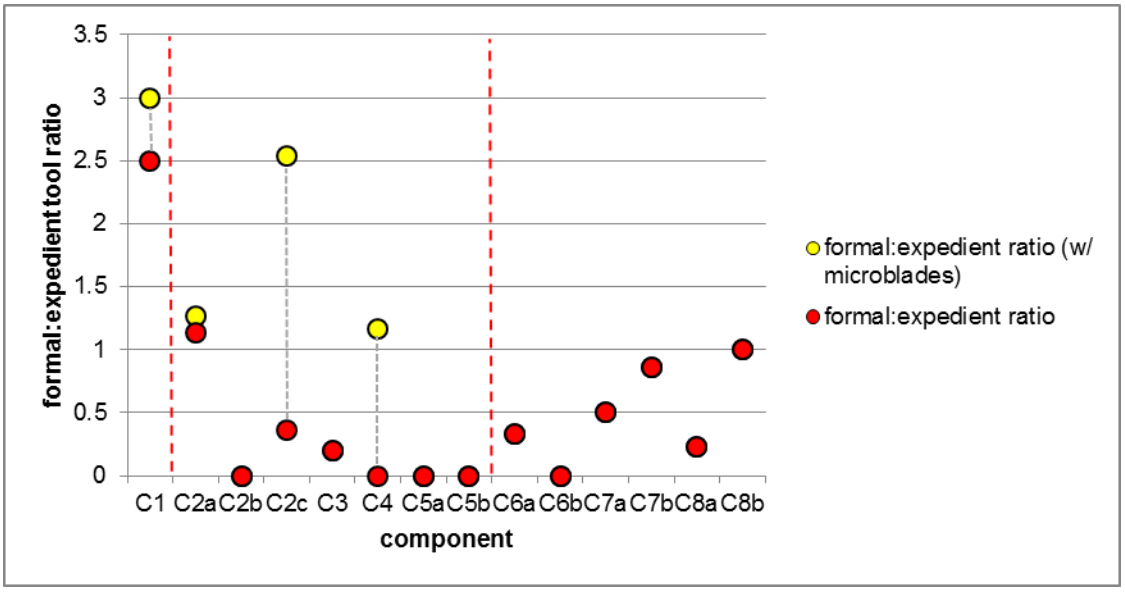

Figure 7.19 Formal:expedient tool ratios (including and excluding microblades).

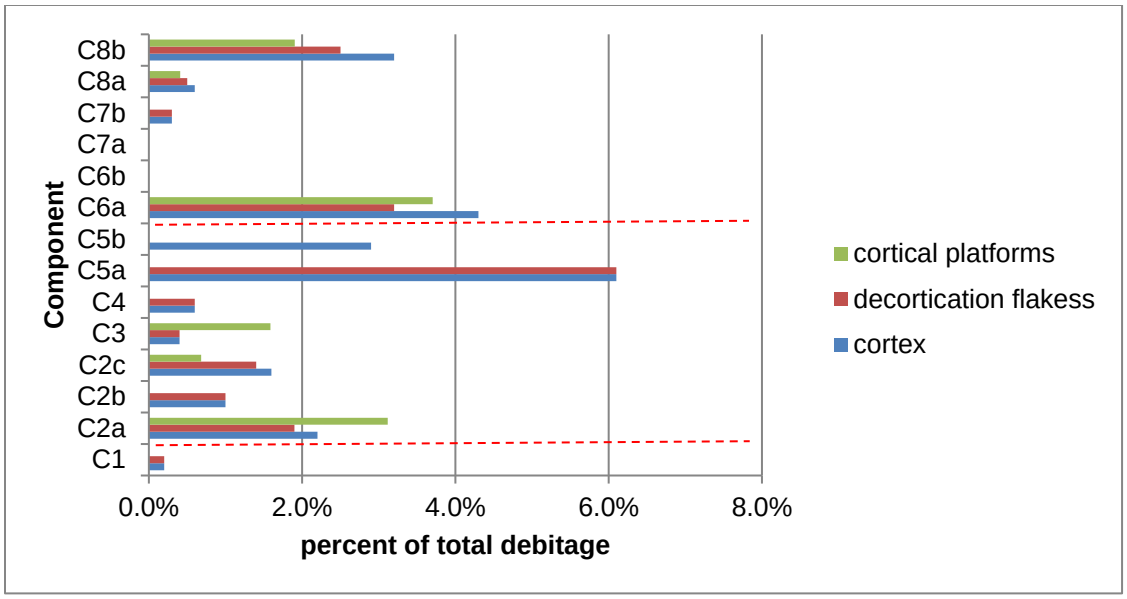

Figure 7.20 Evidence of early stage reduction

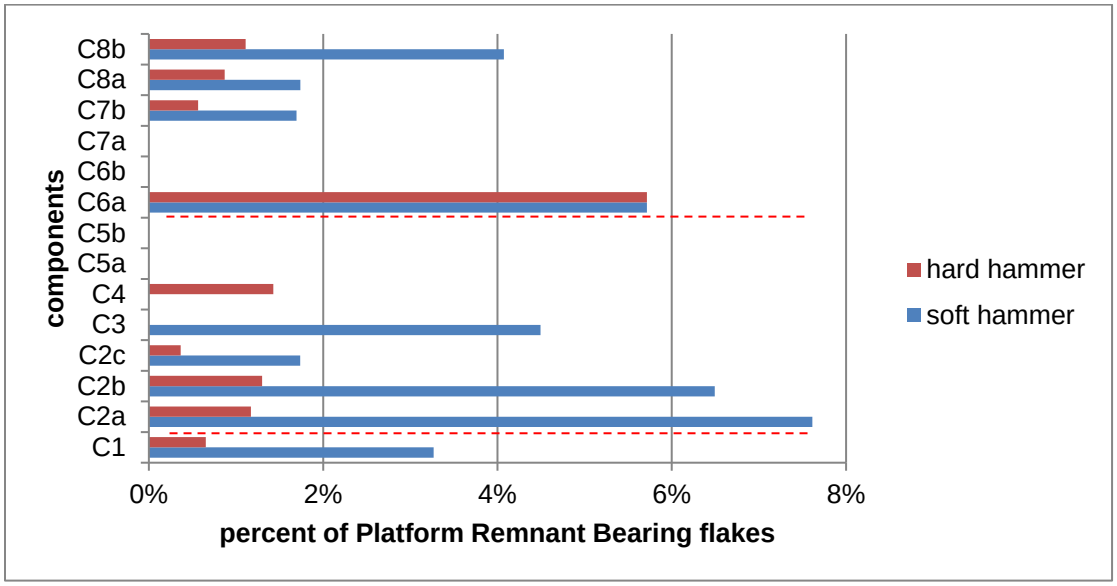

Figure 7.21 Hard and soft-hammer reduction, based on platform width and thickness.

7.4.2 Debitage Number and Weight Density

Number of debitage and total debitage weight, along with related density measures can be used to assess lithic reduction intensity among components. Table 7.7 lists analytical area (excavation area with at least one 3-pointed item from the component), number of debitage (flakes and microblades), total weight, debitage density and weight density (see Figures 7.22-7.23). Components C2a and C2c have by far higher density values than others (120-140 items/ m^2 and 20-14 g/m^2), Components C1, C2b, C7b, C8a, and C8b have moderately high density values (27-64 items/ m^2 and 4-6 g/ m^2), and Components C3, C4, C5a, C5b, C6a, C6b, and C7a have low density values (0.4-17 items/ m^2 and 0.05-2 g/ m^2). Debitage densities are generally linearly related to n debitage, except for C8a, which has higher density relative to the general

trend, likely related to the cache. Weight density is generally linearly related to n debitage, but C2a and C2c exhibit higher and lower weight density respectively. Figure 7.24 illustrates the relationship of item and weight density. All components fall along a general trendline, but C2b and C8a are slightly different (that is, more flakes of less weight) and C2a conversely comprises fewer flakes of heavier weight.

Since assemblage diversity is substantially different among components, these density values could reflect general lithic reduction intensity of the occupations. Given these data, five of the eight Denali components C3, C4, C5a, C5b) represent lower lithic reduction intensity (and perhaps shorter-term occupations), where few lithic items were maintained or refurbished, and the other three Denali components (C2a, C2b, C2c) reflect higher lithic reduction intensity (and perhaps longer-term occupations, independently supported by the presence of the only Denali hearth features). Again, these data distinguish the three earlier Denali components from the five later Denali components. The single Chindadn component also reflects relatively more intensive lithic reduction episodes. Three of the five Northern Archaic components (C6a, C6b, C7a, C7b) reflect lower lithic reduction intensity and the other two (C8a, C8b) reflect higher lithic reduction intensity (and perhaps longer-term occupations in C8b, again supported by the presence of hearth features in C8b. The cache feature in C8a might skew the data, and it reflects very different lithic behaviors (see below).

Table 7.7 Debitage (flakes and microblades) frequency, weight, and density

Component	*analytical area (m2)*	*debitage N*	*debitage wt*	*debitage density (items/m2)*	*weight density (g/m2)*
C1	11	464	64.93	42.18	5.90
C2a	58	6974	1172.52	120.24	20.22
C2b	8	384	51.18	48.00	6.40
C2c	54	7588	746.11	140.52	13.82
C3	16	273	31.24	17.06	1.95
C4	15	149	23.57	9.93	1.57
C5a	12	49	3.71	4.08	0.31
C5b	12	35	2.72	2.92	0.23
C6a	19	186	45.84	9.79	2.41
C6b	19	7	4.13	0.37	0.22
C7a	9	6	0.45	0.67	0.05
C7b	9	356	33.15	39.56	3.68
C8a	18	1143	71.15	63.50	3.95
C8b	31	850	127.91	27.42	4.13
Cultural tradition					
Chindadn		464	64.93	42	5.90
Denali		2207±3473	290±474	49±57	6±8
Northern Archaic		423±471	47±48	24±25	2±2

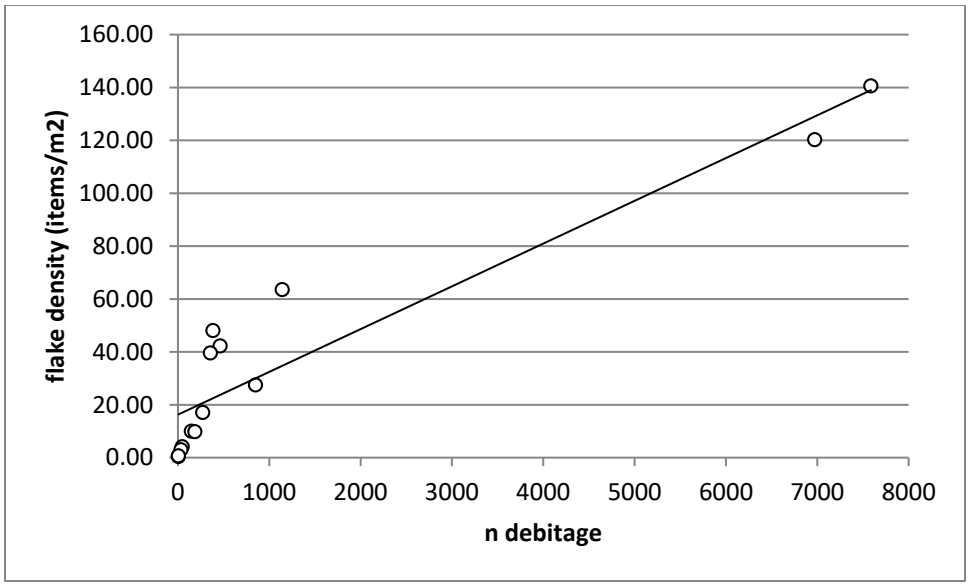

Figure 7.22 Debitage totals and item density.

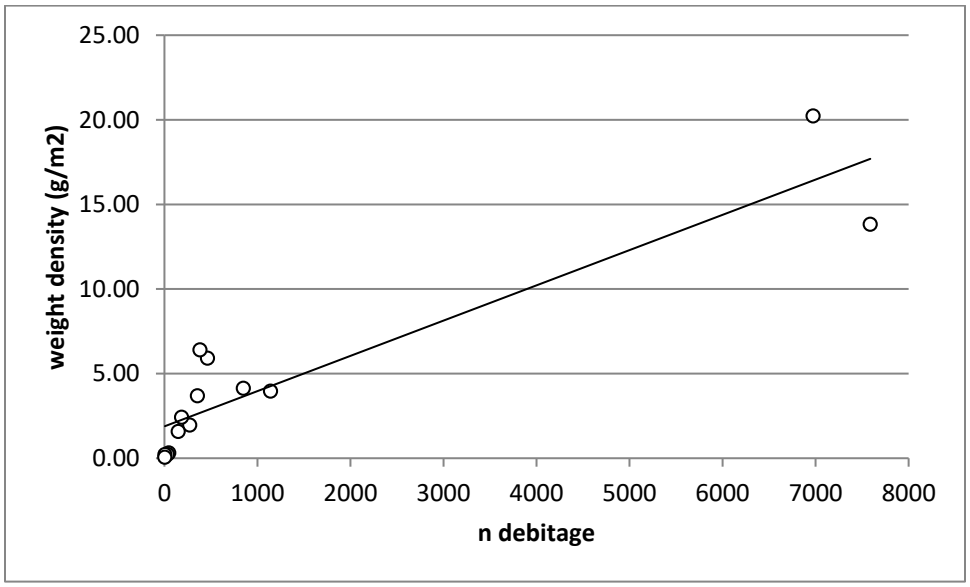

Figure 7.23 Debitage totals and weight density.

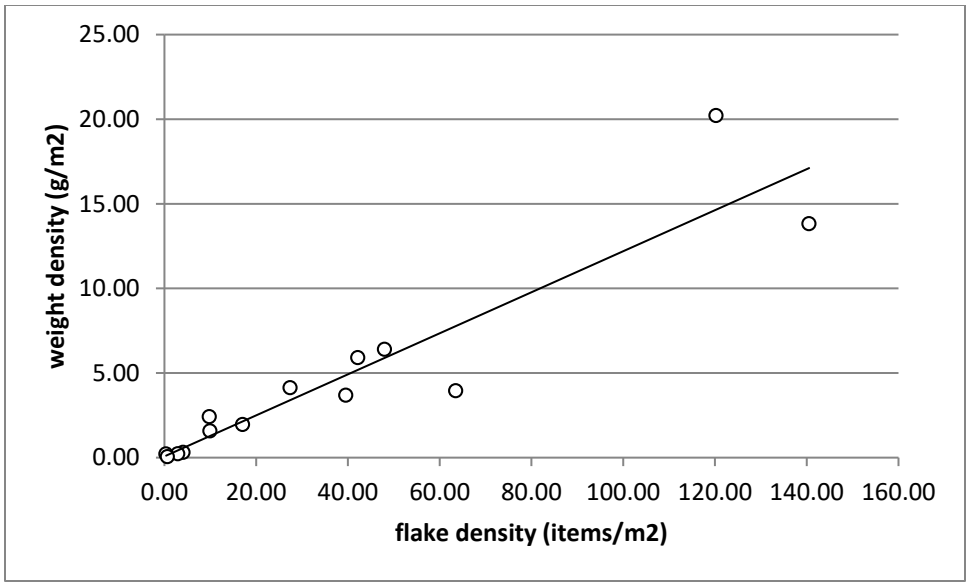

Figure 7.24 Debitage (item) and weight density.

7.4.3 Comparison of Tool and Debitage by Raw Material Proportions

Figures 7.25 to 7.36 illustrate proportions of tools, microblades, and debitage for each material type by component. Similarities between tools and microblades and debitage distributions suggest they were modified (and possibly manufactured) onsite while dissimilarities in their distributions suggests that the tools and microblades were modified (and possibly manufactured) offsite and discarded onsite.

Component 1 tool proportions (Figure 7.25) for the most common debitage materials (C30 and C36) are similar, and both of these materials are classified as local, suggesting manufacture onsite. In contrast, C7, R1, and C68 have little or no debitage, suggesting manufacture offsite and tool discard onsite. The three microblades are not from materials with debitage, suggesting they too were manufactured elsewhere and discarded onsite.

Component 2a tool proportions (Figure 7.26) are only similar to two raw materials with respect to debitage proportions, the most common, C5 and C33. Both of these material types are classified as local, suggesting these tools were manufactured onsite. In contrast, a wider range of tools come from materials with little or no debitage (C10, Q3, C61, C67, C71, and M2), suggesting they were manufactured elsewhere and discarded onsite. With respect to C2a microblades, C5, C19, C11, and C1 are associated with appreciable debitage quantities, suggesting some onsite microblade manufacture. The remaining microblades are associated with materials with relatively little debitage.

Component 2b tool proportions (Figure 7.27) are highly dissimilar to debitage distributions, as the most common raw materials by debitage (C5, C36, C33, R2, R1, C11) have no tools. In contrast, all of the tools and microblades are from materials with relatively few/no debitage. This suggests onsite manufacture/modifications of tools that were transported offsite, as well as discard of tools and microblades made elsewhere. In sum, these patterns (along with the relatively small assemblage size within one small activity area) suggest a very short term occupation.

Component 2c tool proportions (Figure 7.28) generally correspond to debitage proportions, particularly the most common materials in C2c (R1, R2, C19, R9, C5, and C33). Three of these materials (C5, C19, C33) are classified as local suggesting onsite manufacture of non-microblade tools. In contrast, microblades are associated with both materials with relatively high debitage (R1, R2, C19, C5, C36, C17) but also with materials with low debitage (particularly C30, C39, C46, C13, C70, C69) suggesting microblades manufactured onsite to replace nonlocal discards.

Component 3 tool and microblade proportions (Figure 7.29) tend to follow debitage proportions, given the small tool sample size. Microblades particularly are all made from the most common debitage material (C19), which is classified as local. This suggests onsite manufacture of microblades.

Component 4 tools distributions (Figure 7.30) are dissimilar to debitage, except possibly C5 and C19, suggesting generally offsite tool manufacture (Ch4, C62, C49) with some onsite manufacture (C5, C19). Most microblades (67%) are from R1, which has no debitage, suggesting offsite manufacture of the microblade core.

Component 5a tool distributions (Figure 7.31) are similar to debitage, with all tools and 60% of debitage from C28. Microblades, in contrast are from raw materials with little/no debitage (Ch3 and Ch4), suggesting they were manufactured offsite from nonlocal materials. The relatively low number of material types and close correspondence of tool and debitage proportions suggests a very short term occupation.

Component 5b (Figure 7.32) contains no tools, but microblades are generally from materials with little/no debitage (R4, C28).

Component 6a tool and debitage distributions (Figure 7.33) suggest onsite manufacture of the C5 tool and offsite manufacture of the C11 and C39 tools.

Component 7b tool and debitage distributions (Figure 7.34) generally correspond, suggesting onsite manufacture/maintenance of C5 tools, classified as a local toolstone. C39 and Ch4 tools were likely manufactured offsite.

Component 8a tool and debitage distributions (Figure 7.35) are very dissimilar, with the tools (C5, R1, R9) made from materials with relatively little debitage. In contrast, the most common debitage raw material (C11) is associated with no tools, suggesting onsite manufacture and removal offsite of C11 tools.

Component 8b tool and debitage distributions (Figure 7.36) are generally similar, with C5 (classified as a local material) comprising both the highest debitage and tool proportions. This suggests C5 tools were made, used, and discarded onsite. High numbers of C11 and C19 debitage were produced onsite, but with no tools, suggesting onsite manufacture of tools using local raw material, and then transport offsite. In contrast, C24, O, C28, and Ch3 tools were likely manufactured offsite and discarded onsite.

The debitage leaves a record of tools or cores manufactured, reduced, and/or maintained on site. The differences between raw material richness of tools and debitage are direct proxies for minimum number of tools/cores worked onsite vs. discarded (Table 7.8). Considerable numbers of tools/cores were worked onsite and transported offsite, assuming all unmodified debitage were not brought onsite as flakes, a reasonable assumption given the generally tiny sizes of the debitage. Figure 7.37 illustrates missing tools as a percentage of total (non-microblade) tools. Larger values denote more missing tools and smaller values denote fewer missing tools. These data show low percentages of missing tools in the Chindadn component (40% of total expected tools given debitage diversity were recovered), followed by greater portions of missing tools in

Denali components. This increases to the later Denali components which have fewer discarded tools. The situation is reversed in the Northern Archaic where more tools are discarded onsite to a peak in C8a (61% of total expected tools are extant), followed by an increase in C8b. These data are proxies for what portion of lithic reduction (production/maintenance and discard or just one or the other) occurred onsite. Figure 7.38 shows the opposite, isolated tools (with no associated debitage) discarded as a percentage of total non microblade tools. Here we see relatively low levels of isolated tools with a large increase in C2b (50% of the tools have no debitage). The decrease in C2c is consistent with other data suggesting logistical organization. C6a has a higher portion of exotic tools, followed by lesser values for C7b and C8a. C8b contains only tools with associated debitage. These data could also suggest C2b and C6a are shorter-term occupations.

Table 7.8 Raw materials and extant/missing tools and cores

Comp.	*materials (debitage)*	*materials (tools)*	*materials (debitage only, missing tools)*	*material (microblades only)*	*materials (tools only)*	*Tools missing / total tools*
C1	15	6	9	-	1	60%
C2a	42	12	36	7	4	75%
C2b	15	2	13	4	1	87%
C2c	61	16	49	19	1	75%
C3	18	3	15	-	0	83%
C4	17	5	16	6	1	76%
C5a	10	1	11	2	0	92%
C5b	9	0	9	3	0	100%
C6a	22	3	20	1	1	87%
C6b	4	0	4		0	100%
C7a	19	3	16		0	84%
C7b	3	1	3		1	75%
C8a	21	11	16		6	59%
C8b	43	5	38		0	88%

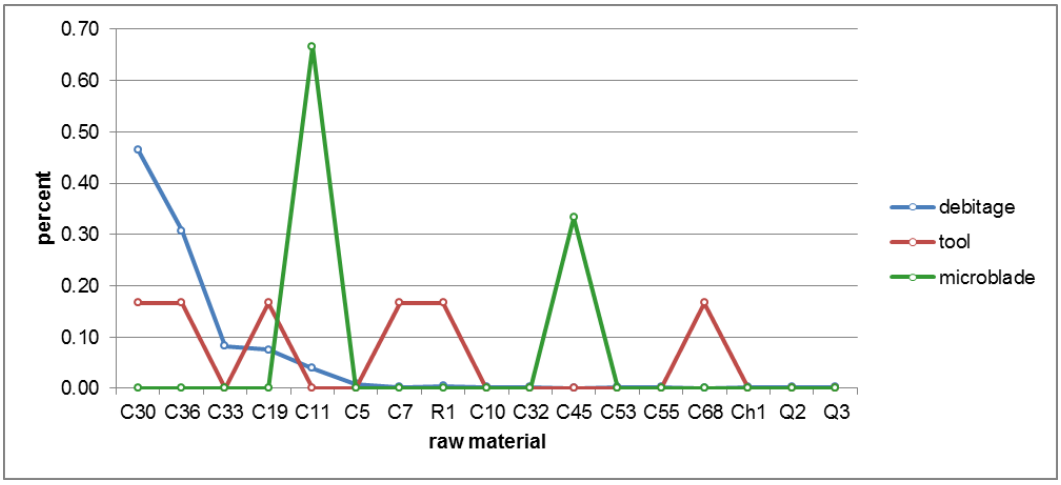

Figure 7.25 Component 1 tool, debitage, and microblade percents by material type.

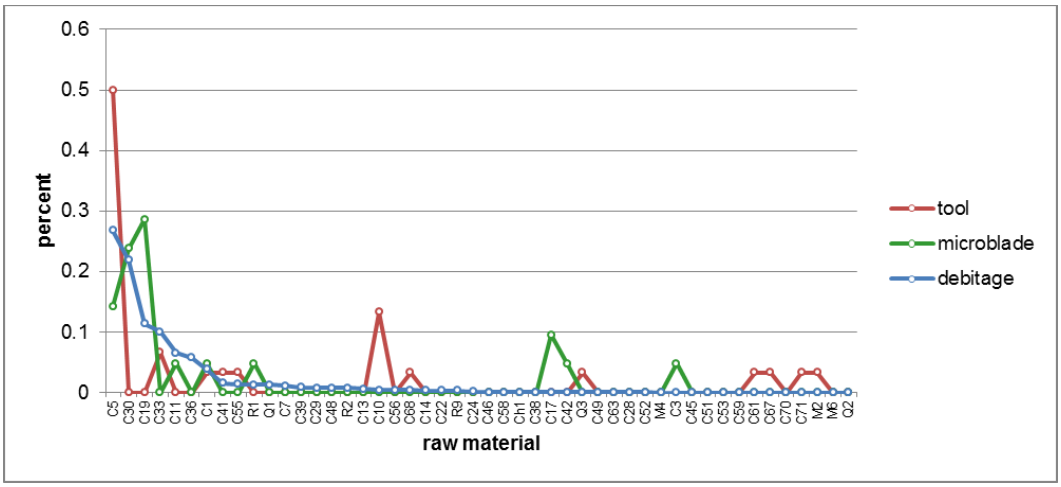

Figure 7.26 Component 2a tool, debitage, and microblade percents by material type.

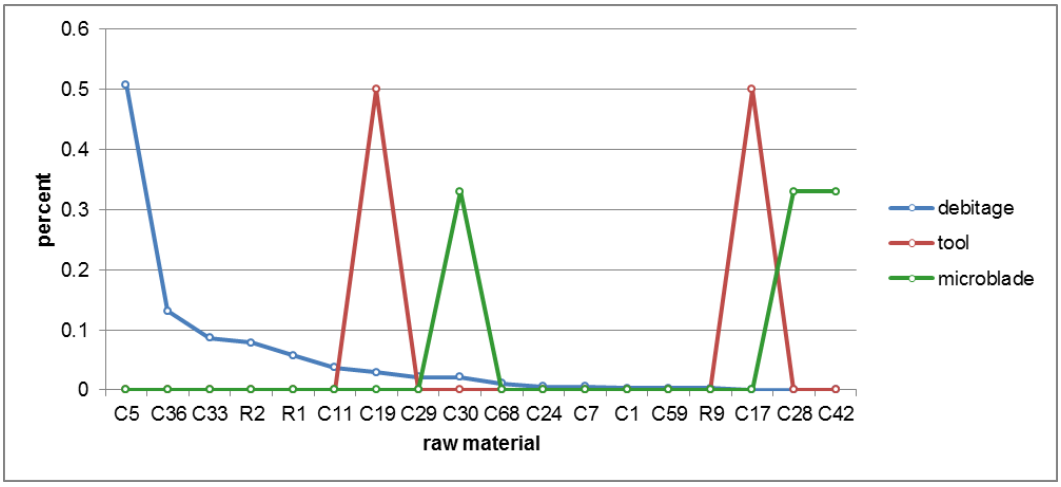

Figure 7.27 Component 2b tool, debitage, and microblade percents by material type.

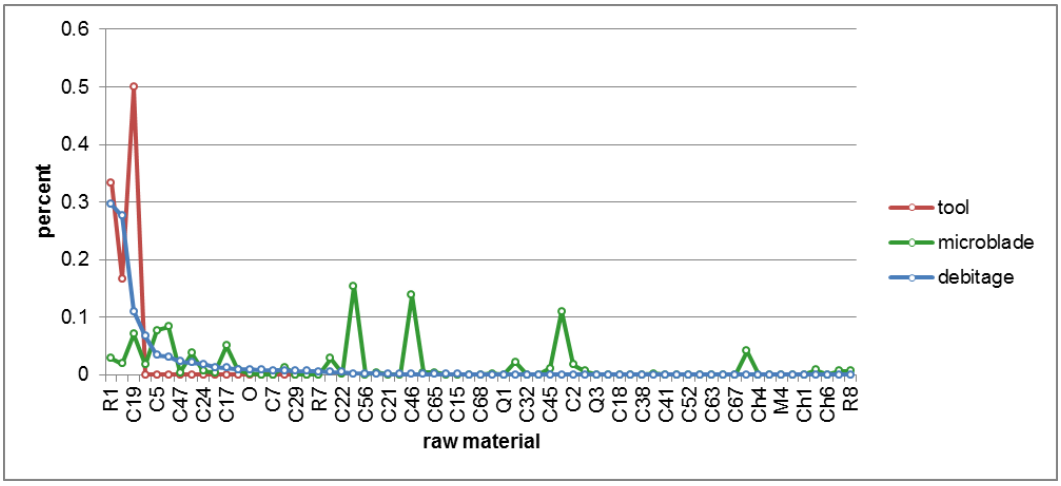

Figure 7.28 Component 2c tool, debitage, and microblade percents by material type.

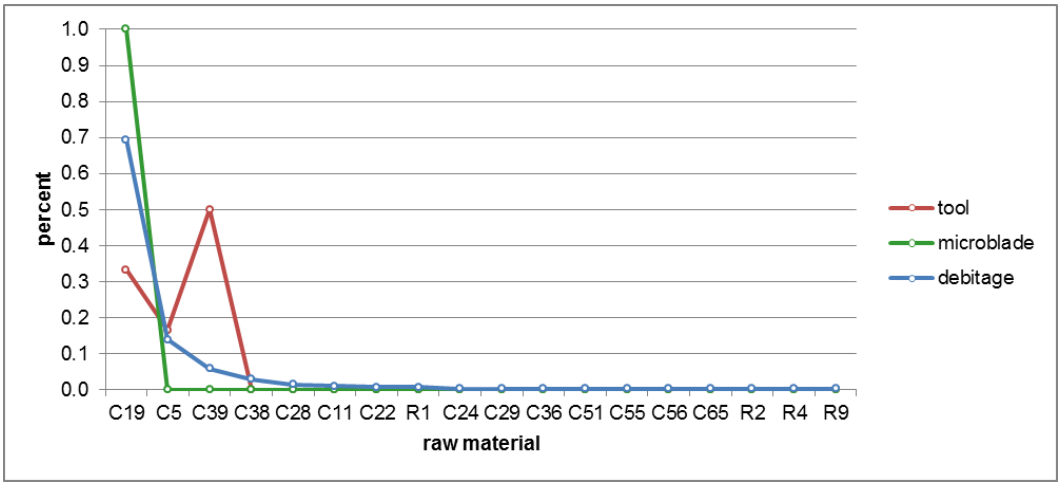

Figure 7.29 Component 3 tool, debitage, and microblade percents by material type.

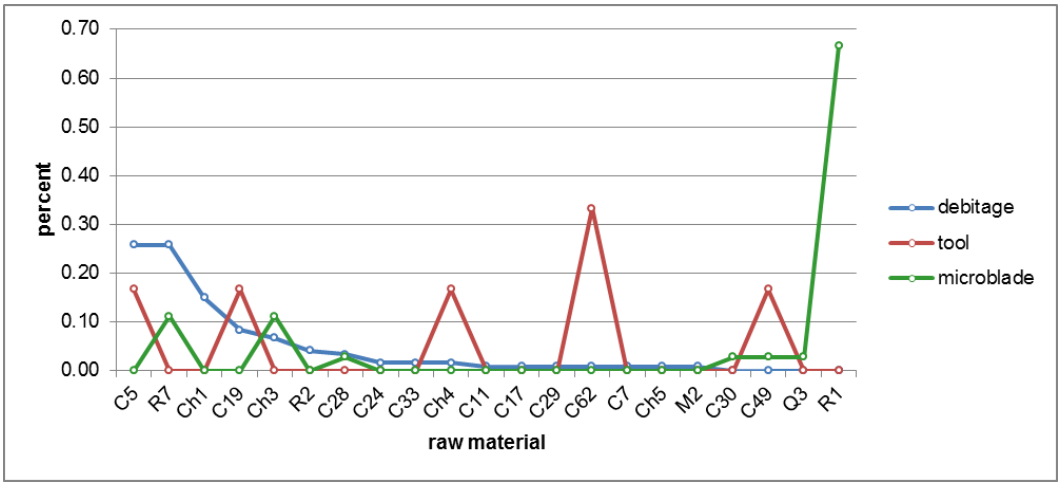

Figure 7.30 Component 4 tool, debitage, and microblade percents by material type.

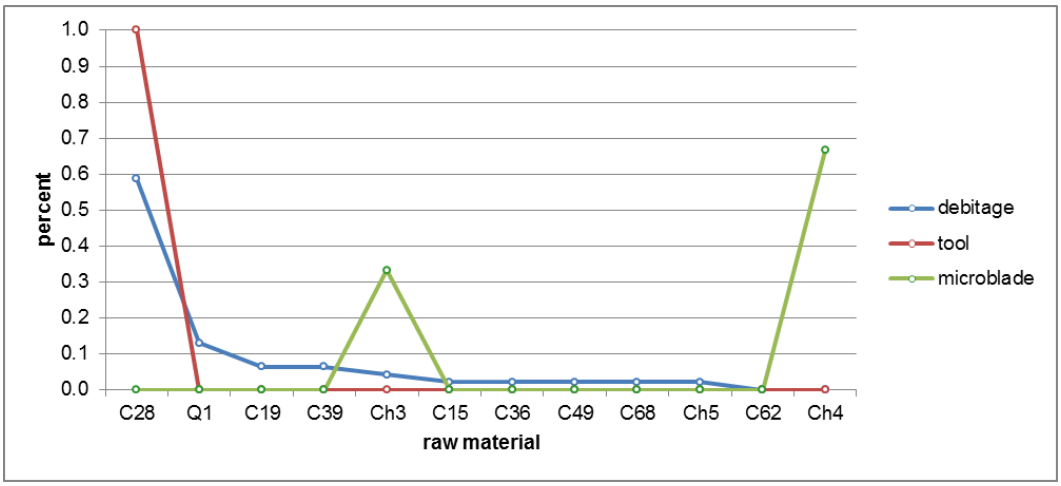

Figure 7.31 Component 5a tool, debitage, and microblade percents by material type.

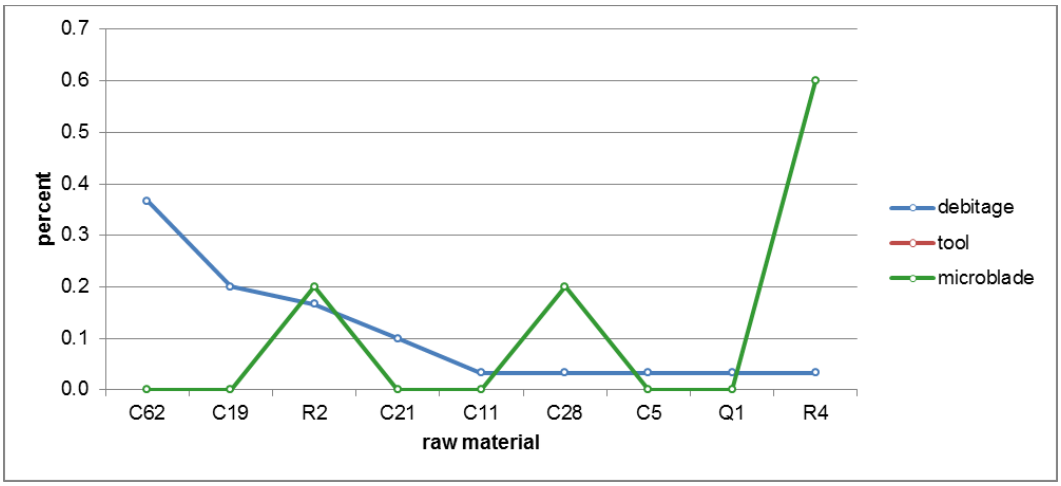

Figure 7.32 Component 5b tool, debitage, and microblade percents by material type.

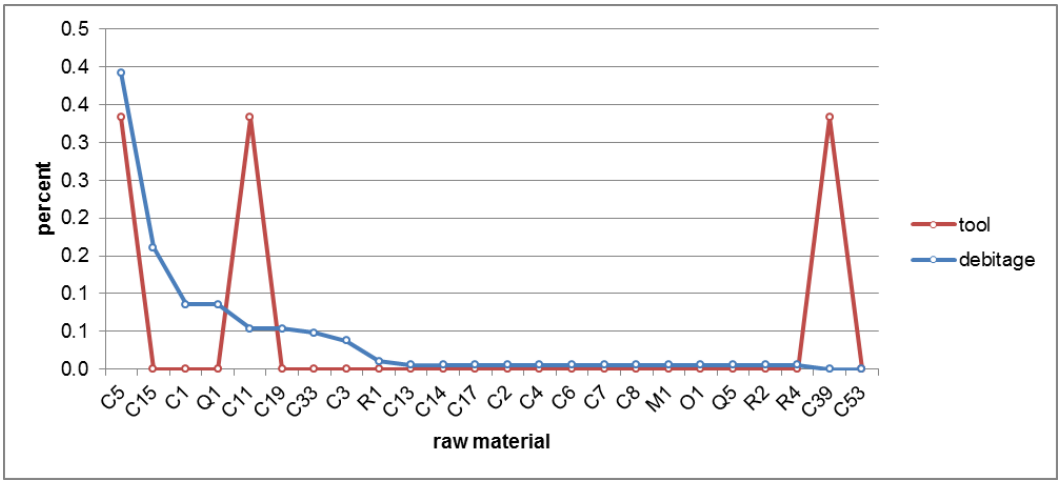

Figure 7.33 Component 6a tool, debitage, and microblade percents by material type.

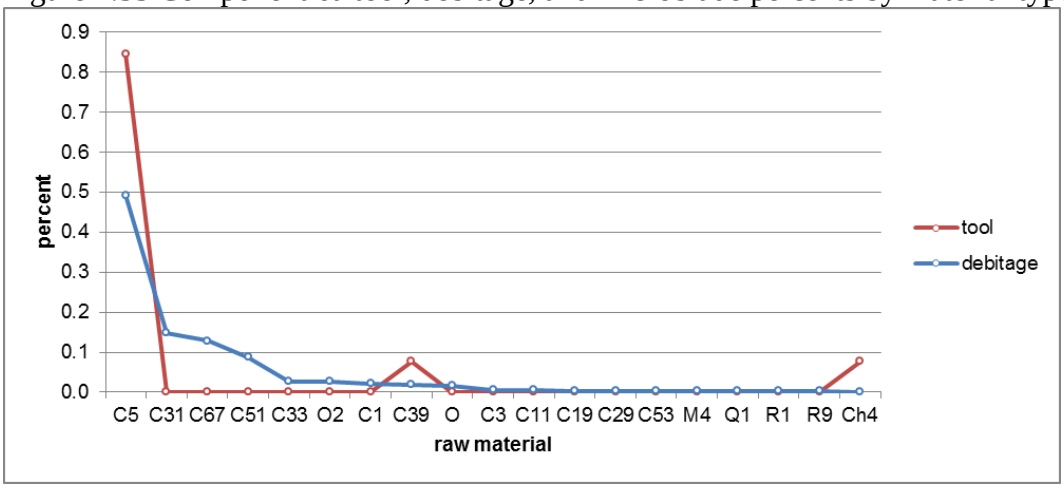

Figure 7.34 Component 7b (and 7) tool, debitage, and microblade percents by material type.

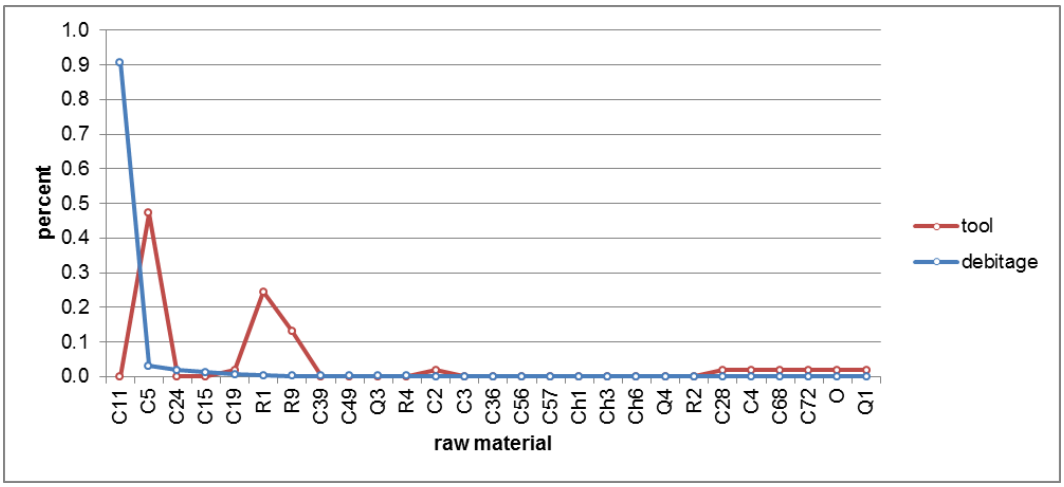

Figure 7.35 Component 8a tool, debitage, and microblade percents by material type.

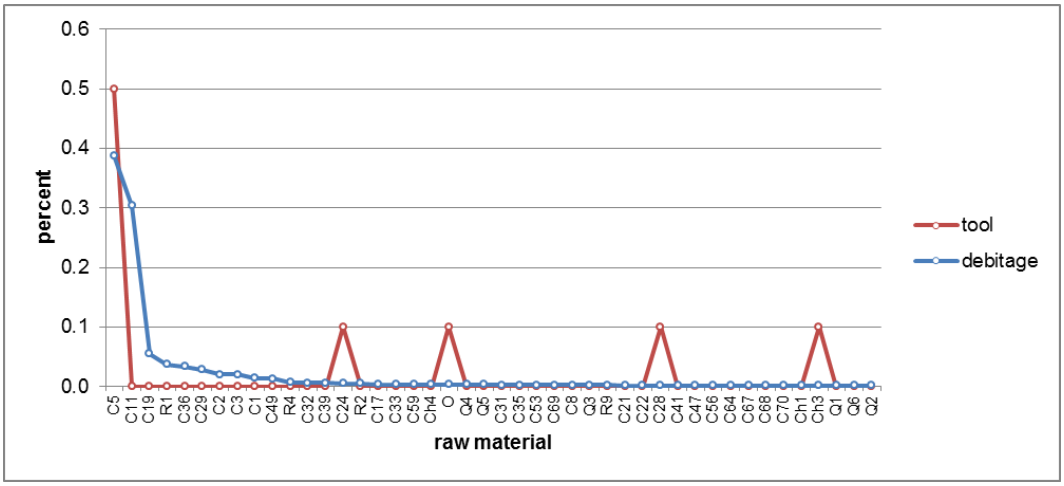

Figure 7.36 Component 8b (and 8) tool, debitage, and microblade percents by material type.

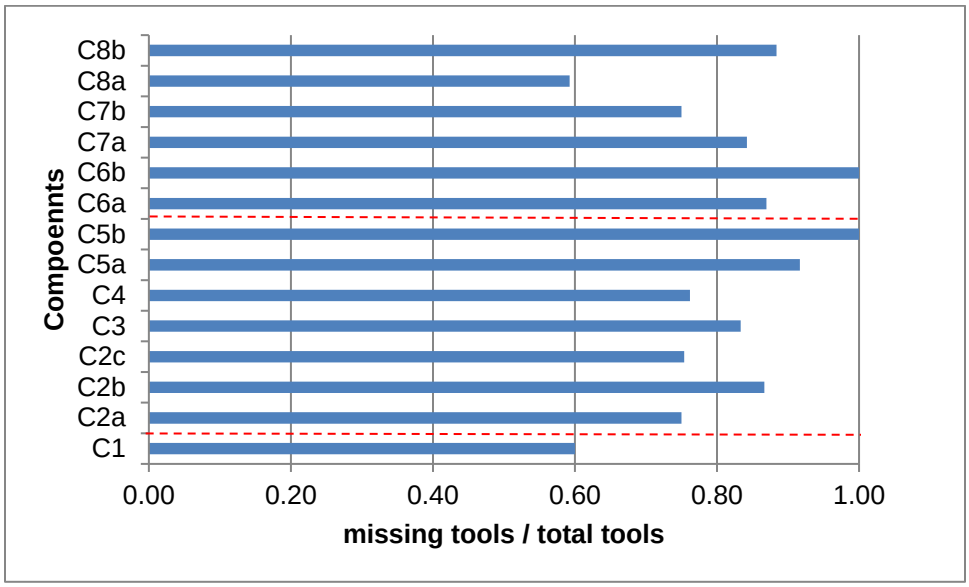

Figure 7.37 Missing tools as a percentage of total tools

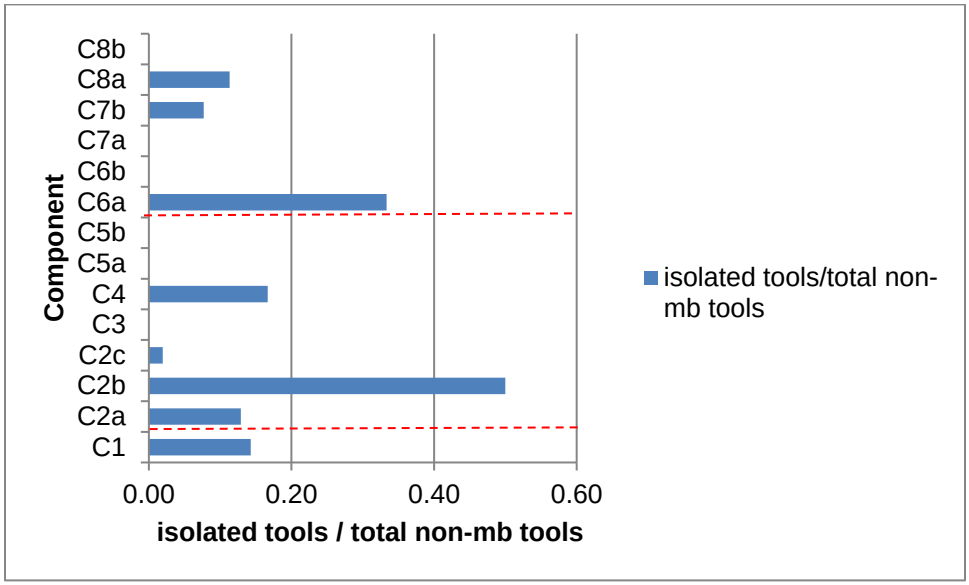

Figure 7.38 Isolated non-microblade tools (by material) / total non-microblade tools.

7.4.4 Flake Size Distributions

Size class data for each component are illustrated in Figures 7.39 and 7.40. Two additional Denali components reflecting very different behaviors are included for comparison, Gerstle River Component 3 and XBD-167 Component 2 (Potter 2005, Potter et al. 2007). Gerstle River Component 3 lithic behaviors were exclusively microblade production and bifacial tool maintenance in the context of a short-term logistical hunting camp. XBD-167 Component 2 is a lithic workshop where river cobbles were brought to the site and tested, and the primary lithic behaviors related to the production of biface roughouts (stage 2 edged bifaces). The size class

differences include far more SC 1-2 flakes at Gerstle River and more SC 3-5+ at XBD-167. All three sites were excavated by the primary author (Potter), and screen size and collection methods are similar.

Figure 7.39 shows Chindadn and Denali component size class distributions along with Gerstle River and XBD-167. Collectively, the size class distributions matched Gerstle River (late-stage maintenance) rather than XBD-167 (early stage biface production). DRO Chindadn (C1) is characterized by much smaller flakes, with very high proportions of SC1 than any of the other groups, suggesting primarily tool maintenance. Denali Components C2a, C2b, C2c, and C3 are similar, with similar distributions to Gerstle River data, consistent also wit0h the microblade technologies in these components. Denali Component C4 appears somewhat divergent, with higher SC5+ debitage

Figure 7.40 shows Northern Archaic component size class distributions along with the comparanda. They are broadly comparable to the tool maintenance distribution reflected in the Gerstle River pattern rather than the early stage reduction at XBD-167. There is some variation, with C7a and C8b broadly similar with fewer SC1 flakes and relatively more larger-sized flakes. C7b and C8a are also broadly similar, with even fewer SC3-SC5+ flakes than Gerstle River, suggesting predominantly late stage tool maintenance.

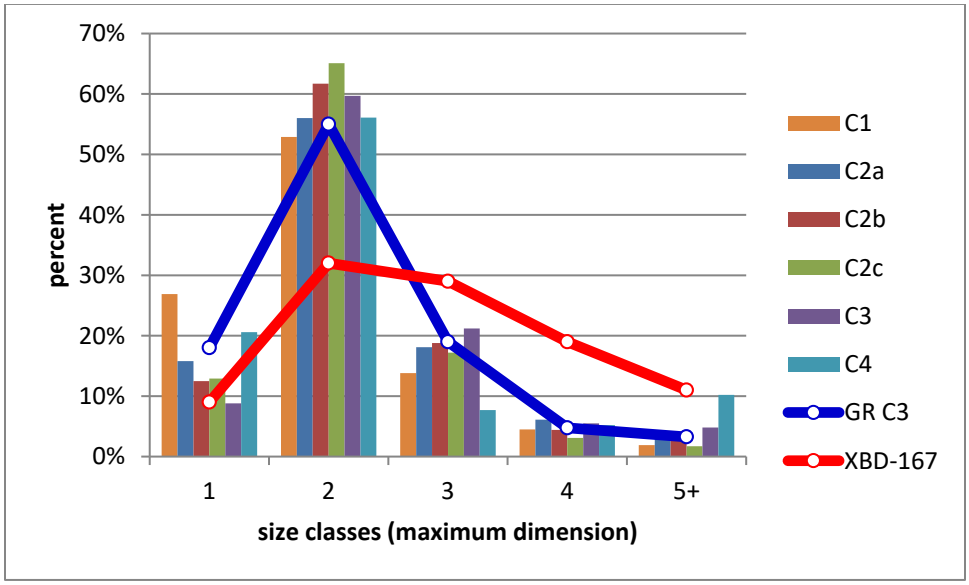

Figure 7.39 Size classes among Chindadn and Denali components, compared to a microblade production assemblage (GR C3) and an early reduction/lithic workshop assemblage (XBD-167) where cobble testing and early stage bifacial tool production occurred.

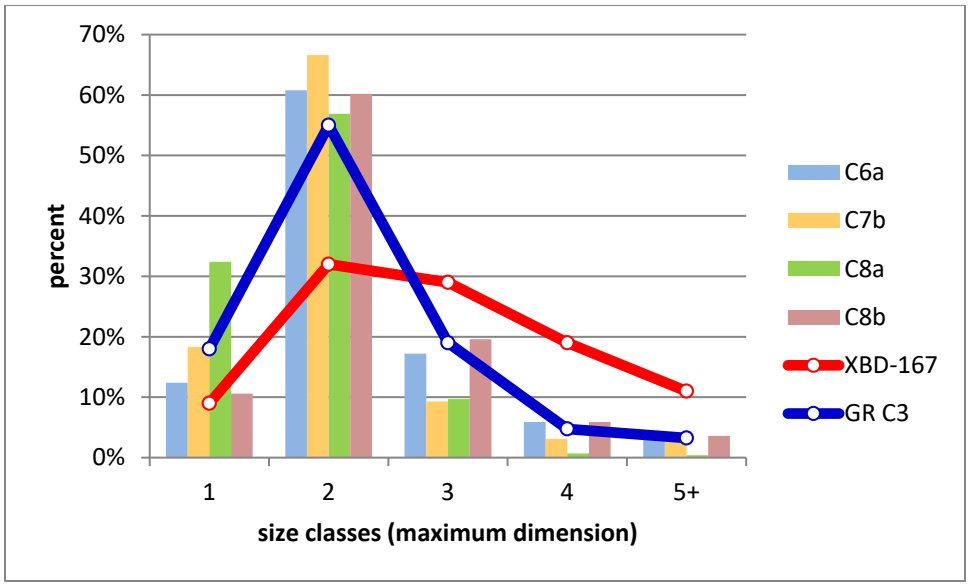

Figure 7.40 Size classes among Northern Archaic components, compared to a microblade production assemblage (GR C3) and an early reduction/lithic workshop assemblage (XBD-167) where cobble testing and early stage bifacial tool production occurred.

7.5 Spatial Analysis

7.5.1 Introduction

Using spatial distributions (clustering and gaps between clusters), 32 lithic clusters or areas of concentration were defined (Table 7.9). These include 3 for C1, 6 for C2a, 3 for C2c, 2 for C3, 4 for C4, 2 for C7b, 3 for C8a, and 3 for C8b. Other components were concentrated into a single area or had very few artifacts: C2b, C5a, C5b, C6a, C6b, and C7a. Spatial maps for each component illustrate lithic cluster boundaries in relation to 3-pointed artifacts, cultural features, and debitage count isopleths, created in Surfer 3d using a geometric scale (1, 2, 4, 8, 16, 32, etc.).

Table 7.9 Spatial clusters, associated blocks and n debitage (flakes and microblades).

Component	*Cluster (group)*	*Blocks*	*N debitage*	*N PRB flakes*	*N microblades*	*N tools*
C1	C1g1	5, 25	450	152	-	5
	C1g2	4, 6, 20, 21	9	4	-	1
	C1g3	15	3	1	3	1
C2a	C2ag1	5, 6, 7, 8, 9, 13, 21, 25	5670	1583	5	25
	C2ag2	1	286	106	4	-
	C2ag3	20	283	114	-	1
	C2ag4	4	240	88	4	2
	C2ag5	11, 15, 22, 24	208	89	1	8
	C2ag6	9, 13	285	122	7	-
C2b	C2bg1	All	384	142	3	2
C2c	C2cg1	4, 5, 6, 7, 8, 20, 21	3453	1324	87	54
	C2cg2	9, 11, 12, 15, 22, 24	4127	1371	335	87
	C2cg3	1, 2, 3, 25	86	52	55	9
C3	C3g1	1, 2, 3, 25	34	14	-	1
	C3g2	7, 9, 13, 14	231	104	2	5
C4	C4g1	4, 6, 8, 20, 21	90	51	32	9
	C4g2	2, 3	32	13	-	2
	C4g3	10, 12, 14	15	6	1	2
	C4g4	9	18	10	2	1
C5a	C5ag1	All	49	28	3	2
C5b	C5bg1	All	35	10	5	1
C6a	C6ag1	All	186	80	1	5
C6b	C6bg1	All	7	4	-	-
C7a	C7ag1	All	6	4	-	3
C7b	C7bg1	6, 7, 8, 13, 20	118	69	-	4
	C7bg2	19, 23	231	142	-	9
C8a	C8ag1	11, 12, 15, 24	1011	200	-	2
	C8ag2	22	34	13	-	48
	C8ag3	10, 14, 19	98	30	-	3
C8b	C8bg1	9, 11, 15, 21, 22, 24, B	549	217	-	9
	C8bg2	10, 12, 13, 16, 19, 23, 26	214	67	-	3
	C8bg3	5, 6, 7, 8, 25 (includes Japanese), A	20	7	-	-

7.5.2 Component 1

Component 1 contains three clusters, C1g1, a dense cluster of debitage (n=152) and two smaller clusters of 9 flakes (C1g2) and 3 microblades (C1g3) (Figure 7.41). C1g1 tools include 1 modified flake and 4 bifaces, 1 stage 3 thinned biface, and 2 stage 5 (finished bifaces), two projectile points. A single projectile point (stage 5 finished biface) was associated with C1g2 and one modified microblade was associated with C1g3.

Debitage summaries are provided in Table 7.10. Raw materials distributions are generally different for each Component 1 cluster. C1g1 is dominated by C30 and C36 (89%) with 8 materials comprising the remaining 11%. C1g2 is equally distributed between 7 raw materials. C1g3 comprises 3 microblades from 2 raw materials.

Flake types are also different among groups. C1g1 is dominated by biface thinning flakes (8.2%) with no other diagnostic flake types. C1g1 has relatively high amounts of shatter (5.8%). No cortex was observed. Dorsal scar counts are generally low (76% have 1-2), and terminations have a relatively high portion of feathered (47%). Flake sizes are generally small (95% are 1-3). Overall, size classes suggest tool production and maintenance rather than core reduction. Lipping is very common (43%), and few of the bulbs are salient (3%). Platforms have a high amount of preparation (12%) or are crushed (24%). Platform edge angle averages 59º ±12º.

C1g2 contains 11% decortication flakes and 11% of the debitage contains cortex (generally 50-99% cortex). It has a relatively high amount of complete flakes (33%). Dorsal scar counts are all between 1-3, terminations are mainly step (67%) with only 33% feathered. The flakes are considerably larger than C1g1, with 33% over Size Class 5. Many flakes have salient bulbs of force (50%) and 75% have crushed platforms. Platform edge angles are steeper than C1g1 (67º).

Collectively, these data suggest different lithic behaviors in each of the three Component 1 areas, though overall most flakes are very small, suggesting later stage lithic maintenance. C1g1 can be characterized as biface (projectile point) production and finishing, with soft hammer percussion commonly employed. C1g2 is a small concentration of earlier stage lithic reduction of a variety of materials, characterized by hard hammer percussion. An unrelated finished projectile point (material type C68, found nowhere else in Component 1) was located within this concentration. C1g3 is a small cluster of microblades, two refit, and the third is modified.

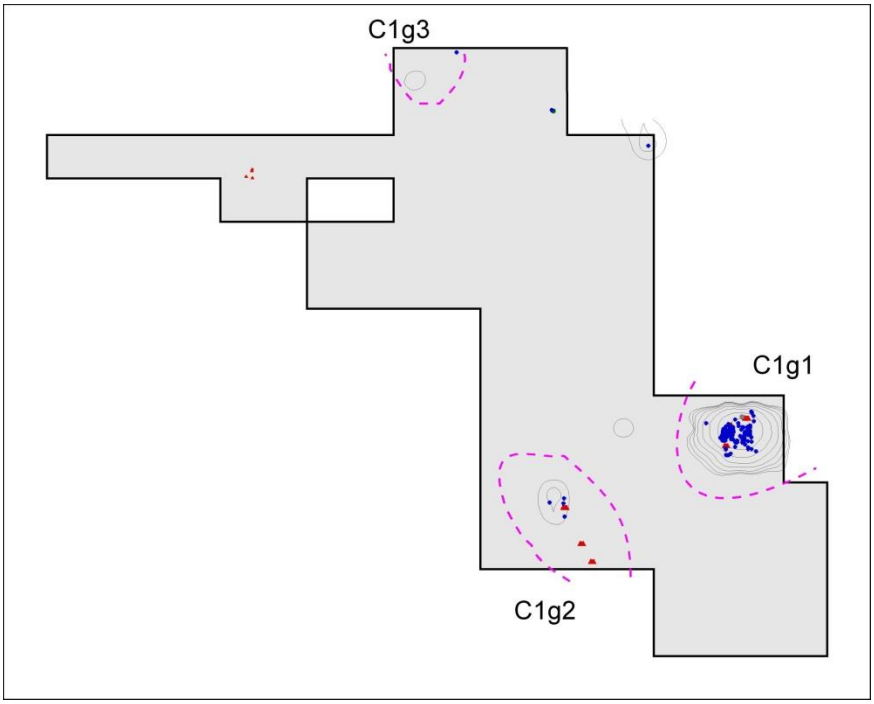

Figure 7.41 C1 spatial clusters. Blue represents lithics, red represents tools.

Table 7.10a Component 1 raw materials

Material	*C1g1*	*C1g2*	*C1g3*
C10		11.1%	
C11	3.8%	11.1%	66.7%
C19	7.8%		
C30	47.6%	11.1%	
C32	0.2%		
C33	8.2%	11.1%	
C36	31.6%		
C45			33.3%
C5	0.2%	33.3%	
C53	0.2%		
C55	0.2%		
C7		11.1%	
Ch1		11.1%	
Q3	0.2%		

Table 7.10b Component 1 debitage technical summary

	C1g1	*C1g2*	*C1g3*
N	450	9	3
Flake type			
bifacial thinning	8.2%	0.0%	0.0%
bipolar			
decortication	0.0%	11.1%	0.0%
microblade	0.0%	0.0%	100.0%
shatter	5.8%	0.0%	0.0%
simple	86.0%	88.9%	0.0%
unifacial thinning	0.0%	0.0%	0.0%
Sullivan-Rozen typology			
broken	16%	33%	33%
complete	18%	11%	
fragment	60%	56%	67%
shatter	6%		
split	0%		
Cortex			
0	100%	89%	100%
1-3		11%	
Dorsal scar count			
0	5%		
1	42%	22%	
2	34%	33%	
3	13%	44%	67%
4+	7%		33%
%≥3	20%	44%	100%
Termination			
feathered	47%	33%	
hinge	3%		
N/A	6%		
overshot			33%
step	45%	67%	67%
Thermal			
0	100%	100%	100%
1	0%		
Material quality			
Low			
Moderate	8.4%	22.2%	
High	91.6%	77.8%	100.0%

Table 7.10c Component 1 size class distributions

SC	*C1g1*	*C1g2*	*C1g3*
1	28%		
2	53%	44%	
3	14%	22%	
4	4%		100%
5	1%	11%	
6			
7+		22%	

Table 7.10d Component 1 platform remnant bearing flake summary data

	C1g1	*C1g2*	*C1g3*
N	152	4	1
Eraillure scars	1%		
Lipping	43%	25%	0%
Salient bulbs	3%	50%	100%
Platform type			
abraded	1%		
complex	11%	25%	
cortical			
crushed	24%	75%	
N/A	1%		
simple	64%		100%
platform edge angle			
N	88	1	
Mean	59º	67º	
Stdev	12º		
platform measurements			
platform width	3.57±1.94	40.4	2.39
platform thickness	1.14±0.65	14.45	0.29
Pressure, soft, hard (%)	97, 3, 0	0, 0, 100	100, 0, 0
Termination			
Feathered	51%	25%	
Hinged	6%		
Overshot			
Step	43%	75%	100%

7.5.3 Component 2a

Component 2a contains six clusters, C2ag1 is dense concentration associated with a hearth feature (F2015-8), C2ag2, 3, 4, and 6 are four satellite concentrations around the feature area (Figure 7.42). C2ag5 is an artifact cluster several meters to the north. All of these latter groups have debitage frequencies (generally 200-300 items). C2ag1 tools include 7 bifaces, 3 unifaces, 1 burin spall, 1 cobble spall tool, 10 modified flakes, and 1 modified microblade. The bifaces are from a variety of stages, including 1 stage 2 edged biface, 1 stage 3 thinned biface, and 5 bifacial preforms. The unifaces include 1 side scraper and 1 double side scraper). C2ag2 and C2ag6 contain no tools. C2ag3 tools include 1 uniface (end scraper). C2ag4 tools include 1 modified flake and 1 modified microblade. C2ag5 tools include 6 bifaces and 2 modified flakes. The bifaces include 2 stage 3 thinned bifaces, and 4 stage 5 preforms (one of which is a projectile point preform).

Debitage summaries are provided in Table 7.11. Raw material distributions are generally similar, dominated by C5, C33, C11, though there are some differences. C2ag5 has relatively few materials dominated by very high proportions of C5 (54%), C36 (14%) (absent except in C2ag1), and R9 (10%) (absent elsewhere in C2a). C2ag5 distributions are most similar to C2ag2, with high C5 and C11 proportions. The other clusters have different proportions, though all have high C5 proportions, with C2ag3 dominated by C33 (81%) and C2ag4 dominated by C41 (45%), and C2ag6 dominated by C33 and C39.

Debitage characteristics are also different among groups. C2ag3 has 18% decortication flakes and no bifacial thinning flakes, while C2ag1, C2ag2, C2ag4, and C2ag5 have moderate

values (3-8%) of bifacial thinning flakes and 0-1% decortication flakes, and low proportions of microblades (0-2%). C2ag6 contains 5% decortication flakes and 3% microblades. Microblade core parts are absent, and only relatively few microblades are present across all groups. Sullivan-Rozen typology proportions vary among groups with C2ag5 and C2ag6 with fewer flake fragments and C2ag1 with more shatter and fewer complete flakes, suggesting core reduction for the latter, though the high proportions of flake fragments suggests tool production/reduction. Cortex is present only in low levels in C2ag1, C2ag4, and C2ag6, absent in C2ag2 and C2ag5, and present at very high levels (18%) in C2ag3. C2ag1, C2ag5 and C2ag6 have similar amounts of 4+ dorsal scars (15-17%) while C2ag2, C2ag3 and C2ag4 have lower proportions (4-8%). Average dorsal scar count for C1g1 is 1.8±1.1, for C1g2 I is 2.2±0.8, and for C1g3 is 3.3±0.6. Flake terminations are similar across groups. Size class distributions are also relatively similar, except for C2ag1 and C2ag2 with higher levels of the smallest size class (17-18% vs. 6-9%) and fewer SC3-4 flakes (17-22% vs. 27-34%). Overall, size classes suggest tool production and maintenance rather than core reduction. Eraillure occurrence was similar across groups, but was elevated in C2ag3 (13% vs. 1-4%) and to a lesser extent, C2ag6 (6%). Salient bulbs were relatively similar across groups (2-5%), while lipping varied between 21-39%. Simple (unprepared) platforms were most common across groups except for C2ag3 (only 39%) where 44% of the PRB-flakes had cortical platforms. Complex platforms were most common in C2ag4 and C2ag5. Platform edge angles were relatively similar for each group (56-60º), though C2ag5 is slightly more acute (average of 51º).

Collectively, these data suggest somewhat similar lithic reduction behaviors in the various clusters of Component 2a, except C2ag3. C2ag1 likely consists of multiple lithic reduction episodes, including bifacial reduction (probably later stages). C2ag2, C2ag4, C2ag5, and C2ag6 likely consists of later stage bifacial thinning and bifacial tool maintenance. C2ag3 is the most distinct, and may represent earlier stages of lithic reduction, possibly hard hammer percussion of flake cores. C2ag6 shares some similarities with C2ag3 and may represent an amalgam of both activity sets. Microblade industries are represented in each cluster (except C2ag3), but at very low frequencies (<7), particularly compared with Component 2c. While bifaces are only found in C2ag1 and C2ag5, the debitage similarities described here suggest that bifaces were reduced and/or maintained and removed from C2ag2, C2ag4, and C2ag6.

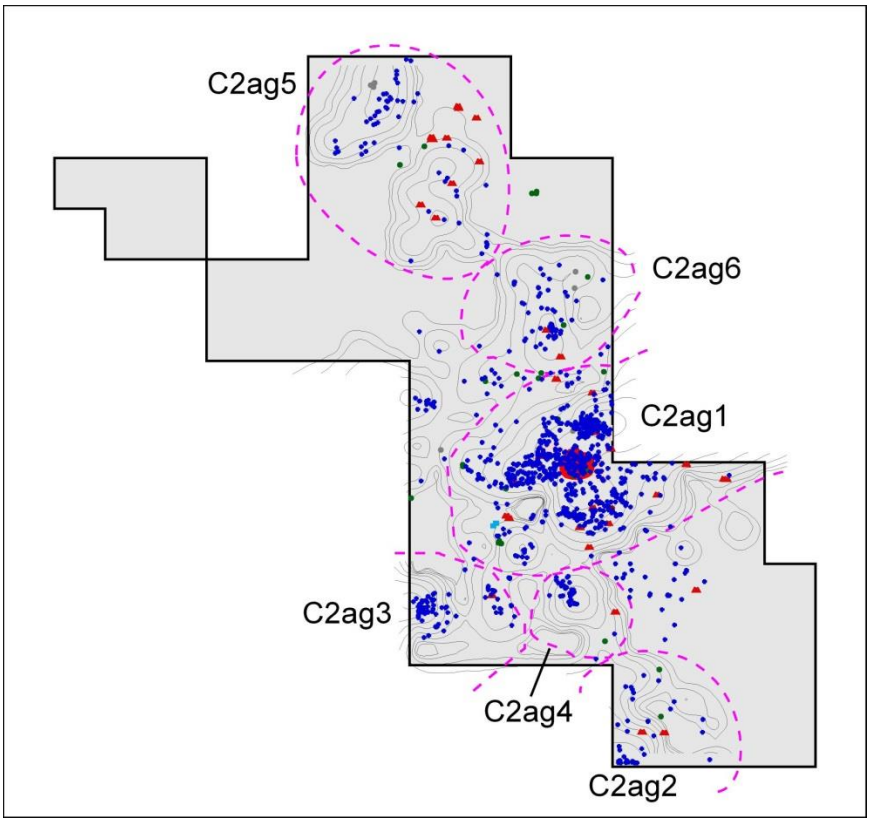

Figure 7.42 Component 2a spatial clusters. Blue represents flakes, red represents tools, and green represent bones. Red polygon represents a hearth feature.

Table 7.11a Component 2a raw materials

material	*C2ag1*	*C2ag2*	*C2ag3*	*C2ag4*	*C2ag5*	*C2ag6*
C1	4.3%	6.6%			1.0%	
C10	0.3%	3.8%				0.7%
C11	5.7%	29.7%	1.1%	5.8%	13.0%	1.1%
C13	0.6%	1.7%				
C14	0.4%					
C17	0.1%		0.4%	0.8%		
C19	13.4%	0.3%	0.4%	2.5%		11.9%
C22	0.4%					
C24	0.1%			1.7%		
C28	0.0%			0.4%		0.4%
C29	0.7%					6.3%
C3						0.4%
C30	26.6%			1.3%	2.4%	4.2%
C33	6.7%	0.3%	80.9%		2.4%	31.2%
C35						0.4%
C36	6.5%				13.9%	
C38						2.5%
C39	0.4%					11.9%
C41	0.0%			45.4%		
C42	0.1%					
C45	0.0%					
C46	0.0%					2.1%
C48	0.9%					
C49	0.1%					
C5	26.0%	52.4%	9.5%	40.0%	53.8%	3.5%

C51						0.4%
C52	0.1%					
C53	0.0%					
C55	1.6%					1.1%
C56	0.4%		1.4%			
C58	0.1%					
C59	0.0%					
C63	0.1%					
C68	0.2%		5.7%			
C7	1.0%	4.9%		0.4%		2.8%
C70	0.0%					
Ch1	0.1%					
M2						0.4%
M4	0.0%					
Q1	1.6%					
Q2	0.0%					
Q3	0.0%					0.7%
R1	1.1%		0.4%		0.5%	10.2%
R2	0.3%		0.4%	1.7%	2.9%	8.1%
R9					10.1%	

Table 7.11b Component 2a debitage technical summary

	C2ag1	C2ag2	C2ag3	C2ag4	C2ag5	C2ag6
N	5670	286	283	240	208	285
Flake type						
bifacial thinning	7.9%	5.6%	0.0%	2.9%	4.8%	1.4%
bipolar						
decortication	1.2%	0.0%	17.7%	0.4%	0.0%	5.3%
microblade	0.1%	1.4%	0.0%	1.7%	0.5%	2.5%
shatter	4.1%	0.7%	0.0%	0.0%	0.5%	1.4%
simple	86.7%	92.3%	82.3%	95.0%	94.2%	89.5%
unifacial thinning	0.0%	0.0%	0.0%	0.0%	0.0%	0.0%
Sullivan-Rozen typology						
broken	21%	26%	29%	21%	25%	33%
complete	7%	12%	11%	16%	18%	10%
fragment	68%	62%	60%	63%	57%	55%
shatter	4%	1%			0%	1%
split	0%			0%		1%
Cortex						
0	98%	100%	82%	100%	100%	95%
1-3	2%		18%	1%		5%
Dorsal scar count						
0	0%				1%	4%
1	27%	37%	10%	27%	8%	19%
2	41%	46%	62%	50%	51%	48%
3	22%	15%	25%	19%	29%	21%
4+	15%	4%	6%	8%	17%	15%
%≥3	32%	17%	28%	23%	40%	30%
Termination						
feathered	29%	33%	33%	43%	44%	24%
hinge	5%	2%	2%	3%	1%	3%
N/A	4%	1%			0%	1%
overshot	0%	0%		0%		
step	63%	64%	66%	54%	54%	72%
Thermal						
0	100%	100%	100%	100%	100%	100%
1	0%					

Material quality						
Low	0.1%					0.4%
Moderate	7.8%	3.8%	80.9%		2.4%	32.3%
High	92.1%	96.2%	19.1%	100%	97.6%	67.4%

Table 7.11c Component 2a size class distributions

SC	*C2ag1*	*C2ag2*	*C2ag3*	*C2ag4*	*C2ag5*	*C2ag6*
1	17%	18%	7%	9%	8%	6%
2	56%	63%	55%	59%	57%	53%
3	17%	13%	25%	20%	24%	26%
4	6%	4%	8%	7%	7%	8%
5	2%	1%	2%	3%	3%	4%
6	1%		1%	2%	0%	0%
7+	1%	1%	1%	1%	0%	2%

Table 7.11d Component 2a platform remnant bearing flake summary data

	C2ag1	*C2ag2*	*C2ag3*	*C2ag4*	*C2ag5*	*C2ag6*
N	1583	106	114	88	89	122
Eraillure	4%	2%	13%	1%	2%	6%
Lipping	39%	28%	37%	36%	38%	21%
Salient	3%	4%	5%	2%	4%	2%
Platform type						
abraded	1%	4%		7%		2%
complex	7%	6%	3%	11%	9%	6%
cortical	1%		44%			
crushed	35%	25%	15%	22%	43%	40%
N/A	2%					
simple	55%	65%	39%	60%	48%	52%
Platform edge angle						
n	1007	78		67	14	80
mean	56º	58º		60º	51º	60º
stdev	12º	9º		8º	10º	10º
Platform measurements						
platform width	4.05/-2.8	4.13±5.01	4.54±3.20	3.38±1.45	3.33±2.45	4.53±3.04
platform thickness	1.20±0.97	1.08±1.02	1.49±1.16	1.03±0.47	1.01±0.76	1.23±0.83
Pressure, soft, hard (%)	91, 8, 1	90, 6, 4	89, 10, 1	99, 1, 0	98, 0, 2	91, 7, 3
Termination						
Feathered	24%	28%	26%	39%	40%	24%
Hinge	6%	3%	3%	2%	1%	2%
Overshot						
Step	70%	69%	71%	58%	58%	74%

7.5.4 Component 2b

Component 2b consists of a relatively compact lithic concentration associated with concentrations of charcoal, perhaps hearths (F2015-7 and F2017-6) (Figure 7.43). Tools include 1 modified flake and 1 burin spall. Raw materials are dominated by C5 (50%), C36 (13%), with four other raw materials >3% each, including R1 and R2 (14% collectively).

Debitage summaries are provided in Table 7.12. Flake types are dominated by undiagnostic simple flakes, though there are very low levels of bifacial thinning (1%), decortication (1%), and microbaldes (1%). Sullivan-Rozen typology suggests tool production rather than core reduction. Very limited cortex was observed (1%). Average dorsal scar count is 2.3±0.8. Termination includes 25% feathered and 68% step. Flake size distributions are more similar to C2c than C2a. Overall, size classes suggest tool production and maintenance rather than core reduction. Lipping is relatively common (18%) while eraillures and salient bulbs are uncommon (2-4%), suggesting soft-hammer reduction and little hard-hammer percussion. Platform preparation suggests relatively few prepared platforms. Platform edge angle averages 54º, slightly more acute than most C2a and C2c groups, suggesting later stages of reduction.

Collectively, these data suggest later stage lithic maintenance using soft-hammer percussion and pressure flaking, perhaps of unifaces or flake tools and relatively few bifaces. A few microblades were recovered, but debitage analyses do not suggest microblade production in C2b. These tools were removed, and the relative lack of discarded tools and low density suggests a very short term occupation.

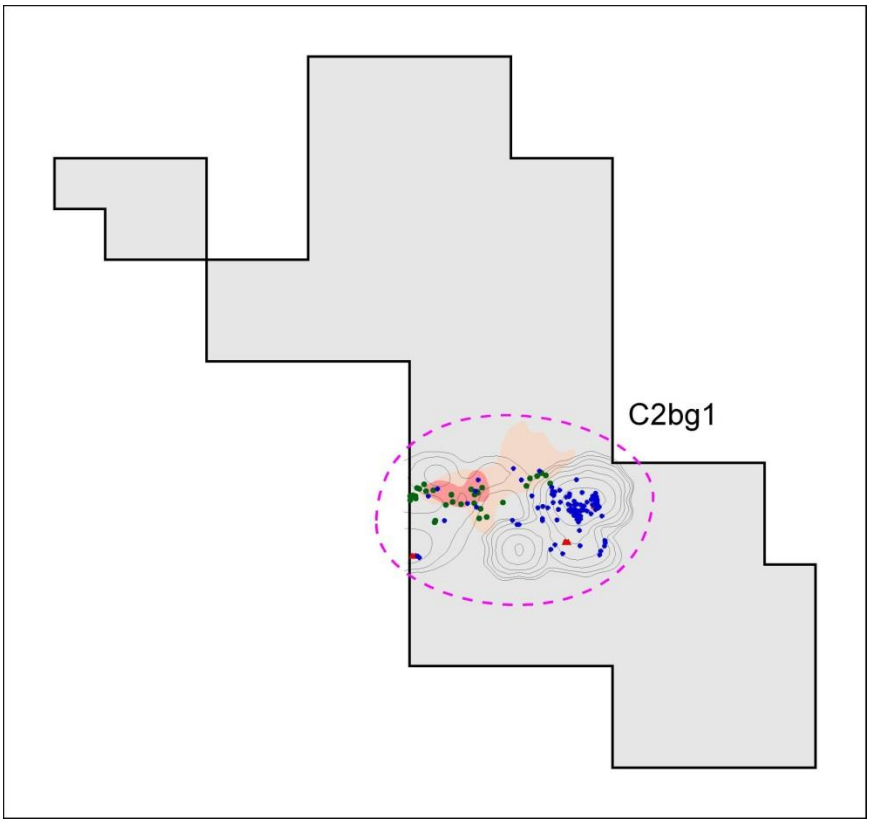

Figure 7.43 Component 2b spatial cluster. Blue represents flakes, red represents tools, and green represent bones. Red polygon represents a hearth feature, and pink polygon represents a charcoal scatter associated with the hearth feature.

Table 7.12a Component 2b raw materials

material	*C2bg1*
C1	0.3%
C11	3.6%
C19	2.9%
C24	0.5%
C28	0.5%
C29	2.1%
C30	2.3%
C33	8.6%
C36	13.0%
C42	0.3%
C5	50.3%
C59	0.3%
C68	1.0%
C7	0.5%
R1	5.7%
R2	7.8%
R9	0.3%

Table 7.12b Component 2b debitage technical summary

	C2bg1
N	384
Flake type	
bifacial thinning	0.5%
bipolar	
decortication	1.0%
microblade	0.8%
shatter	0.5%
simple	97.1%
unifacial thinning	0.0%
Sullivan-Rozen typology	
broken	29%
complete	8%
fragment	62%
shatter	1%
split	1%
Cortex	
0	99%
1-3	1%
Dorsal scar count	
1	12%
2	54%
3	28%
4	5%
%≥3	33%
Termination	
feathered	25%
hinge	5%
N/A	1%
overshot	0%
step	68%
Thermal	
0	100%
1	
Material quality	
Low	0.3%
Moderate	8.6%

High	91.1%

Table 7.12c Component 2b size class distributions

SC	*C2bg1*
1	13%
2	62%
3	19%
4	4%
5	2%
6	1%
7	1%

Table 7.12d Component 2b platform remnant bearing flake summary data

	C2bg1
N	142
Eraillure scars	4%
Lipping	18%
Salient bulbs	2%
platform type	
abraded	2%
complex	4%
cortical	
crushed	52%
N/A	
simple	42%
Platform edge angle	
mean	54º
stdev	7º
n	68
platform measurements	
platform width	4.06±2.92
platform thickness	1.05±0.62
Pressure, soft, hard (%)	92, 6, 1
Termination	
Feathered	19%
Hinge	6%
Overshot	1%
Step	74%

7.5.5 Component 2c

Component 2c contains three lithic clusters, two large groups associated with hearth features (C2cg1 with Feature F2015-5 and C2cg2 with Feature F2015-9) and a small cluster a few meters east of C2cg2 (C2cg3) (Figure 7.44). Subclusters are likely within these two broad clusters. C2cg1 tools include 4 bifaces, 1 burin, 9 burin spalls, 4 cobble spall tools, 7 modified flakes, and 5 unifaces. The bifaces consist of 1 stage 3 thinned biface, 1 stage 4 preform, and 2 stage 5 finished bifaces (one is a projectile point), and the unifaces consist of 4 side scrapers and 1 double side scraper). Microblade-related materials include 23 modified microblades and 1 microblade core tablet. C2cg2 tools include 2 bifaces, 6 burin spalls, 8 modified flakes, and 4

unifaces (4 end scrapers). The bifaces consist 1 stage 3 thinned biface and 1 stage 4 preform. Microblade-related materials include 63 modified microblades, 2 microblade cores and 2 microblade core tablets. Thus, C2cg1 and C2cg2 toolsets are very similar with respect to microblade and biface technologies, but the uniface forms are different. C2cg3 tools include 1 burin, 2 burin spalls, 1 cobble spall tool, 2 modified flakes, and 3 modified microblades.

Debitage summaries are provided in Table 7.13. Raw material distributions among the C2cg1 and C2cg2 clusters are remarkable similar, which are dominated by a few types: R1, R2, C19, C5, and R9. Figure 7.45 shows this close relationship between C2g1 and C2g2. C2cg3 is very different, dominated by C70 (42%), C5 (14%), and C46 (7%). Materials shared between all three at moderate levels include C19, C5, and R1.

Debitage characteristics vary between the groups. Bifacial thinning is present at higher levels in C2cg2 (14%) vs. 4% in the other clusters. Microblades and related debitage are present at 2.5% in C2cg1, 8.1% in C2cg2 and 64% in C2cg3. Decortication is present in all three but at low levels (0.2-2.7%). Sullivan-Rozen typology distributions are nearly identical in C2cg1 and C2cg2, but different in C2cg3, with relatively more broken flakes and less flake fragments in the latter.

Cortex is present at similar low levels across groups, at 3-5%. Dorsal counts again are broadly similar between C2cg1 and C2cg2 (averaging 2.1-2.3), but different in C2cg3 (average of 2.7), with higher proportions of 3+ dorsal scars. Terminations are roughly similar across all groups. Size class distributions are nearly identical between C2cg1 and C2cg2, with mostly SC2-3 (10-20 mm) (82-83%), while C2cg3 has far fewer in this range (68%) and larger debitage (16% vs. 4-5% for the other two clusters). Eraillure and lipping occurrences were relatively similar across groups, though salient bulbs were more common in C2cg3 (23% vs. 6-11%). Platform preparation was considerably varied across groups. C2cg2 had more complex platforms and fewer crushed platforms than C2cg1, but other platform types were similar. C2cg3 had far less platform preparation than the other two groups. Platform edge angles were similar between C2cg1 and C2cg2 while C2cg3 platforms were less acute (77 º vs. 57-63º). Platform measurements were similar between C2cg1 and C2cg22, while C2cg3 platforms were typically narrower and thinner.

Collectively, these data suggest very similar lithic reduction behaviors in the two hearth-centered activity areas (C2cg1 and C2cg2), the more remarkable given the quantity of debitage and wide variety of raw materials. While microblades are found in both of these areas at relatively low proportions, later stage biface reduction (likely with soft-hammer percussion) from thinning bifaces to tool maintenance was common. The differences between the two areas are more subtle. C2cg2 has more bifacial thinning flakes (14% vs. 4%) and relatively more microblade materials include cores and core parts, suggesting more intensive microblade production, and perhaps microblade core reduction, and rejuventation (and possibly production). The burin spalls in C2cg1 suggests perhaps organic tool fabrication. The differences in unifaces (side scrapers in C2cg1 and endscrapers in C2cg2) also suggest different activities, but unifacial and bifacial tools were likely maintained in both areas. In contrast, cluster C2cg3 is dominated by microblade materials (64% of all debitage). The burin and burin spalls also suggest organic tool fabrication or repair, likely slotted implements.

Microblade segments are differentially represented for the three groups (Table 7.14). C2cg1 and C2cg2 have low complete (1-2%) and high medial portions (48%) while C2cg3 has higher complete (6%) and depleted medial portions (22%). Modified microblades were discarded in similar proportions in C2cg1 and C2cg2 (19-26%), but there are far fewer modified

microblades in C2cg3 (6%). This suggests relatively similar onsite microblade production in C2cg1 and C2cg2 along with nonlocal damaged microblade discards. In contrast, C2cg3 is likely a microblade production zone in association with related organic (slotted) tool manufacture or repair.

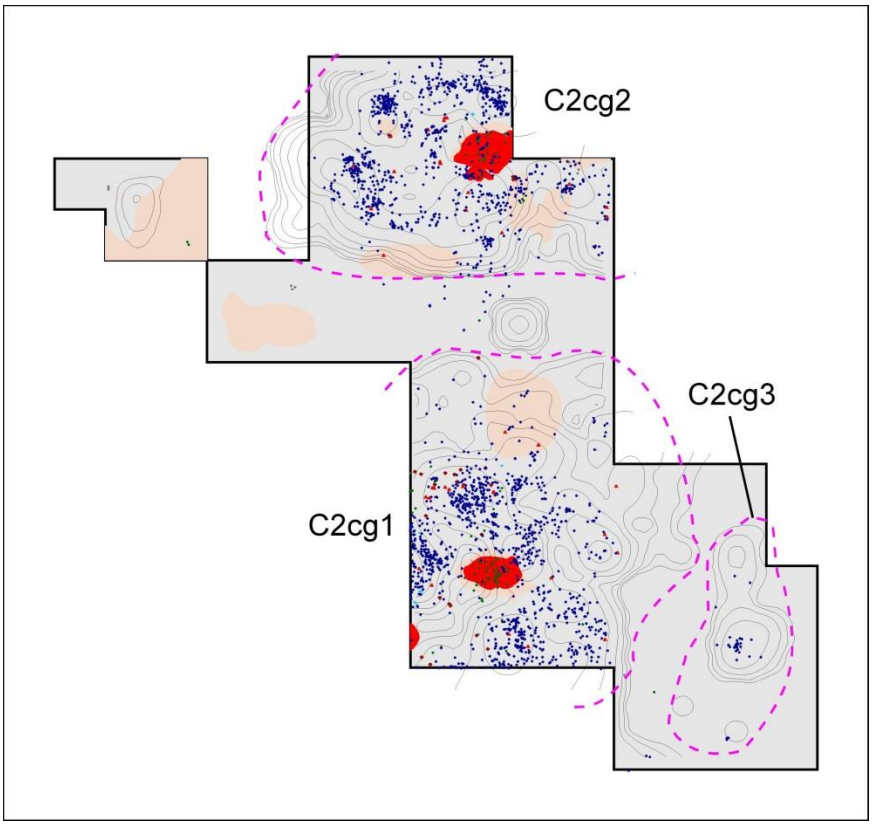

Figure 7.44 Component 2c spatial clusters. Blue represents flakes, red represents tools, and green represent bones. Red polygons represent hearth features and pink polygons represent red ochre concentrations.

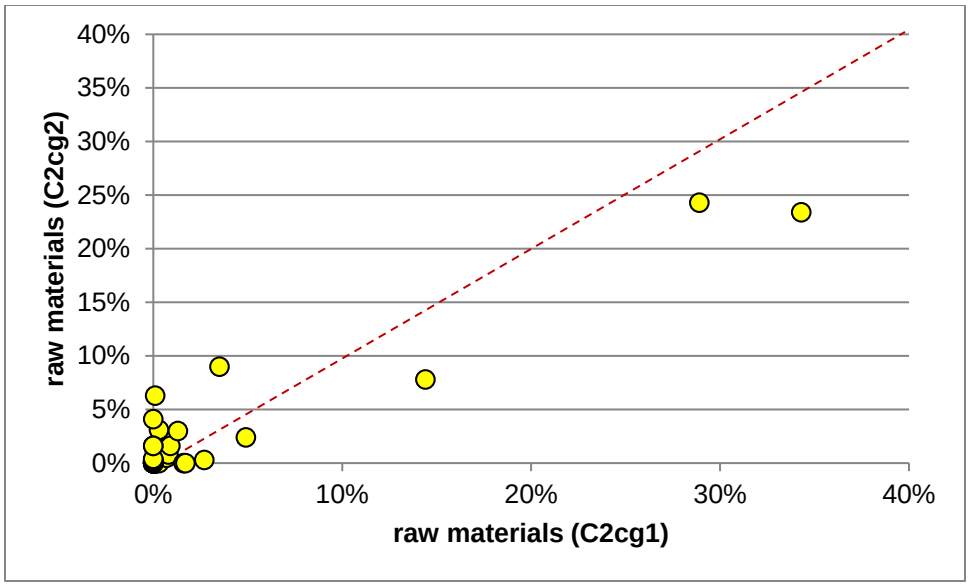

Figure 7.45 Comparison of C2cg1 and C2cg2 raw material proportions.

Table 7.13a Component 2c raw materials

material	*C2cg1*	*C2cg2*	*C2cg3*
C1	1.7%	0.0%	2.3%
C10	0.0%		
C11	0.9%	1.6%	
C13	0.0%	0.3%	
C14	0.1%	0.3%	3.5%
C15		0.1%	
C17	2.7%	0.3%	2.3%
C18			1.2%
C19	14.4%	7.8%	8.1%
C2	0.1%		7.0%
C21	0.3%	0.0%	
C22	0.3%	0.6%	
C24	0.3%	3.1%	
C28	1.3%	3.0%	
C29	0.1%	1.1%	
C30	0.4%	0.9%	
C32	0.1%		
C33	0.8%	0.8%	
C35	0.0%		
C36	0.1%	6.3%	2.3%
C38	0.0%		
C39	0.3%	1.8%	
C4		0.0%	
C41	0.0%		
C42	0.1%		1.2%
C45	0.1%	0.1%	
C46		1.6%	7.0%
C47		4.1%	
C49	0.0%	0.1%	
C5	4.9%	2.4%	14.0%
C51	0.0%		
C52		0.0%	
C55		0.0%	
C56		0.4%	

C57		0.3%	
C62		0.3%	
C63		0.0%	
C65		0.2%	2.3%
C66		0.0%	
C67	0.0%		
C68	0.1%	0.0%	
C69	0.2%	0.3%	
C7	1.6%	0.0%	2.3%
C70	0.1%	0.3%	41.9%
C72		0.2%	
C8	0.1%	0.0%	
Ch1	0.0%		
Ch3	0.5%	1.3%	
Ch4	0.0%		
Ch5	0.1%	0.0%	
M1		0.0%	
M4	0.0%		
O	0.1%	1.6%	
Q1	0.1%	0.0%	
Q2	0.1%	0.0%	
Q3	0.1%		
Q6		0.0%	
R1	34.3%	23.4%	4.7%
R10		0.1%	
R2	28.9%	24.3%	
R4	0.1%	1.0%	
R7	0.7%	0.5%	
R8	0.1%	0.0%	
R9	3.5%	9.0%	

Table 7.13b Component 2c debitage technical summary

	C2cg1	*C2cg2*	*C2cg3*
N	3453	4127	86
Flake type			
bifacial thinning	4.4%	14.3%	3.5%
bipolar			
decortication	2.7%	0.2%	1.2%
microblade	2.5%	8.1%	64.0%
microblade core tablet	0.0%	0.0%	
shatter	0.9%	3.1%	0.0%
simple	89.4%	74.3%	31.4%
unifacial thinning	0.0%	0.0%	0.0%
Sullivan-Rozen typology			
broken	25%	22%	44%
complete	14%	11%	16%
fragment	60%	62%	40%
shatter	1%	3%	
split	1%	1%	
Cortex			
0	97%	99%	97%
1-3	3%	5%	4%
Dorsal scar count			
0	1%	2%	2%
1	20%	20%	6%
2	51%	38%	33%
3	23%	27%	43%

4	5%	13%	16%
%≥3	28%	40%	59%
Termination			
feathered	32%	29%	29%
hinge	4%	1%	2%
N/A	1%	6%	
overshot	0%	0%	5%
step	63%	63%	64%
Thermal			
0	100%	100%	100%
1	0%	0%	
Material quality			
Low	0.2%	0.4%	
Moderate	1.8%	5.5%	
High	98.0%	94.1%	100%

Table 7.13c Component 2c size class distributions

SC	*C2cg1*	*C2cg2*	*C2cg3*
1	12%	14%	16%
2	66%	64%	47%
3	17%	18%	21%
4	3%	3%	7%
5	1%	1%	6%
6	1%	0%	1%
7	0%	0%	2%
8+	0%	0%	0%

Table 7.13d Component 2c platform remnant bearing flake summary data

	C2cg1	*C2cg2*	*C2cg3*
N	1324	1371	52
Eraillure scars	5%	6%	6%
Lipping	20%	28%	17%
Salient bulbs	6%	11%	23%
Platform type			
abraded	2%	1%	
complex	6%	17%	10%
cortical	1%	0%	
crushed	30%	21%	4%
N/A	1%	1%	2%
simple	59%	61%	85%
Platform edge angle			
n	473	419	15
mean	63º	57º	77º
stdev	12º	18º	15º
Platform measurements			
platform width	3.13±3.59	2.71±1.63	1.98±1.04
platform thickness	0.95±0.74	0.88±0.44	0.81±0.35
Pressure, soft, hard (%)	97, 3, 1	99, 1, 0	100, 0, 0
Termination			
Feathered	35%	31%	25%
Hinge	3%	1%	2%
Overshot		0%	
Step	62%	67%	73%

Considering microblades within the entire C2c component, it is clear that the modified microblades are generally nonlocally manufactured (and perhaps used) and discarded at DRO. Modified microblades are typically on medial segments (79% vs. 38%) (Table 7.14). Unmodified microblades are interpreted to generally represent debitage associated with the production of microblades to insert (or reinsert) into organic hafts. Almost all microblade modification occurred on lateral edges suggesting use as slicing/cutting implements within organic hafts as groups of insets, rather than distally modified singly hafted tools. Unmodified microblades are typically depleted in medial counts, given the numbers of proximal segments (38% vs. 47%), suggesting many microblades were manufactured, and some were split to desired length and removed from the site. Figure 7.46 shows proximal width differences in the groups, Where C2g1 and C2g2 have relatively normal distributions while C2g3 appears bimodal, consistent with microblade production and removal of selected segments.

Table 7.14 Component 2 microblade summary data

	C2cg1	*C2cg2*	*C2cg3*
N	87	335	55
Segments			
Complete	1%	2%	6%
Proximal	44%	38%	56%
Medial	48%	48%	22%
Distal	7%	12%	16%
Modification			
Unmodified	26%	19%	6%
Modified	74%	81%	95%

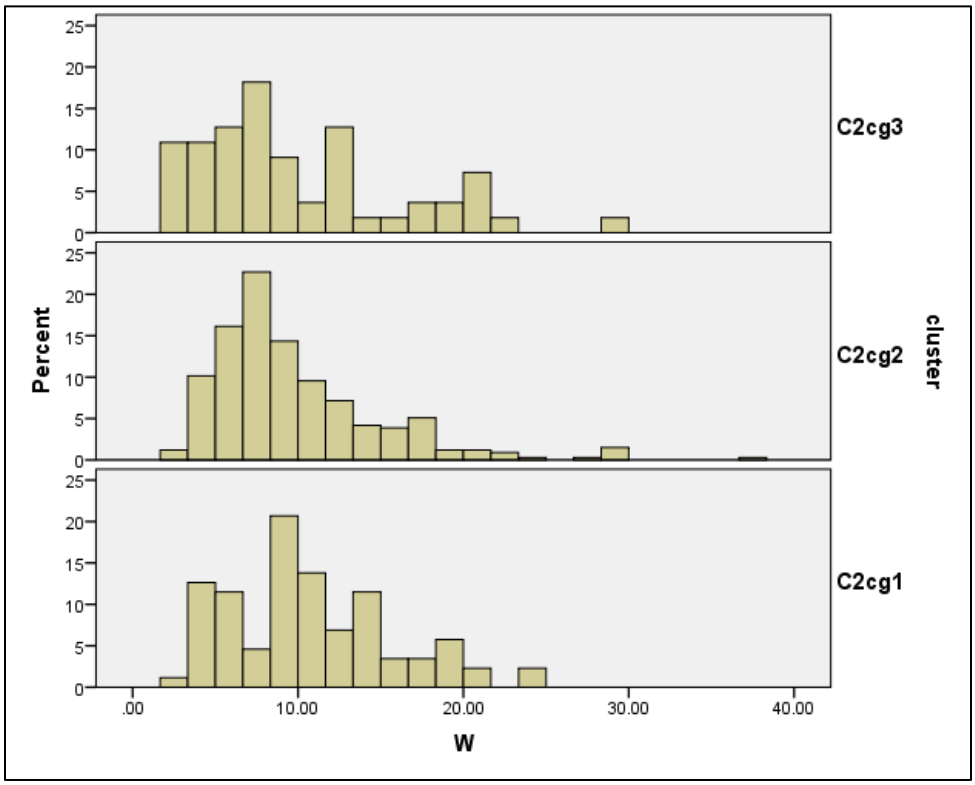

Figure 7.46 Proximal Width of C2c microblade clusters.

7.5.6 Component 3

Component 3 comprises two lithic concentrations located about 7 meters apart, C3g1 (34 debitage) and C3g2 (231 debitage) (Figure 7.47). C3g1 tools include 1 modified flake, and C3g2 tools include 1 very small biface fragment (0.17 g) and 4 modified flakes. Raw material distributions are very distinct. C3g1 is dominated by a single material type, C5 (97%) and only one other material type (R1, 3%), while C3g2 is dominated by another, C19 (82%), though the latter contains a number of other raw materials at very low proportions, including C39 (7%), C38 (4%).

Debitage summaries are provided in Table 7.15. Debitage characteristics are also different between the groups. C3g1 has 12% bifacial thinning flakes, while C3g2 has mainly simple flakes (97%), with 1.7% bifacial thinning and 1.7% decortication flakes and 0.9% microblades. Sullivan-Rozen types are roughly similar, though C3g2 has slightly more complete flakes (14% vs. 9%). Cortex is entirely absent in C3g1 and present at very low levels (<1%) at C3g2. C3g1 has more relatively more feathered terminations and less step terminations than C3g2. Dorsal scar counts are similar, averaging 2.0-2.4. Overall, size classes suggest tool production and maintenance rather than core reduction. Eraillure scars were similar between groups (7-9%), but lipping was more common in C3g1 (43%) than in C3g2 (16%). Platform preparation was similar between groups, and platform edge angle was almost identical between groups. Platform widths and thicknesses were also similar.

Collectively, these data suggest some differences and similarities between the groups. C3g1 is associated with relatively low variability in lithic behaviors, with bifacial reduction (likely late stage, perhaps bifacial tool maintenance) within a single raw material type, though the biface fragment was made on C39, which was only present in C3g2. This may suggest contemporaneity between the clusters. A wider range of lithic behaviors were present in C3g2, including microblade use and discard and tool maintenance.

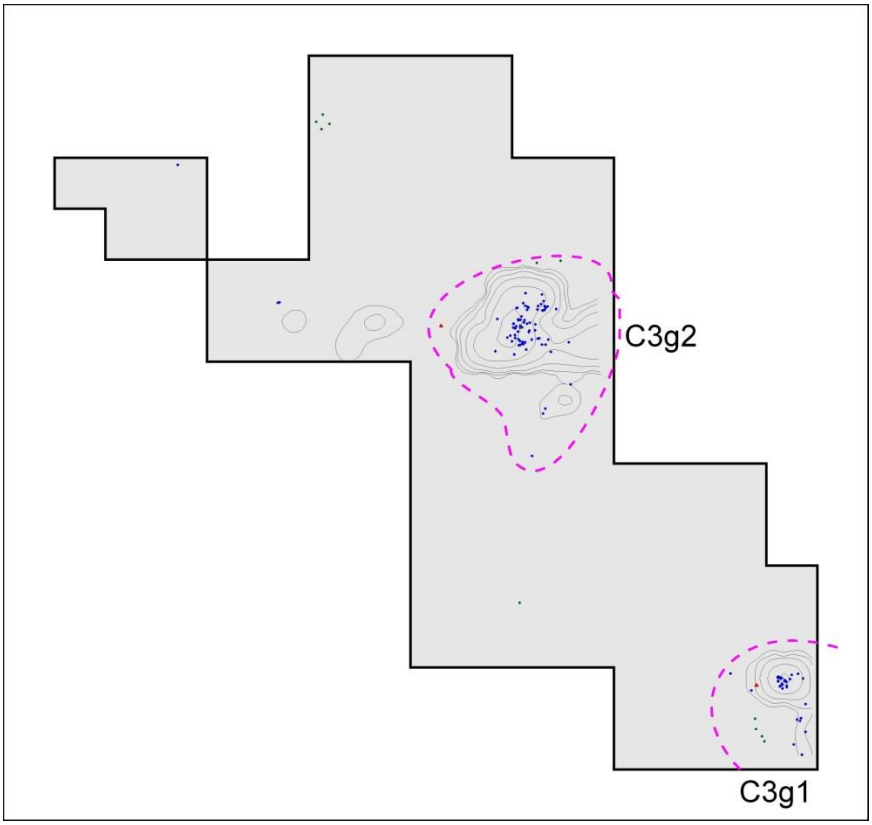

Figure 7.47 Component 3 spatial clusters. Blue represents flakes, red represents tools, and green represent bones.

Table 7.15a Component 3 raw materials

material	*C3g1*	*C3g2*
C11		0.9%
C19		81.8%
C22		0.9%
C28		1.3%
C29		0.4%
C36		0.4%
C38		3.5%
C39		6.5%
C5	97.1%	2.2%
C51		0.4%
C55		0.4%
C56		0.4%
R1	2.9%	0.4%
R2		0.4%

Table 7.15b Component 3 debitage technical summary

	C3g1	C3g2
N	34	231
Flake type		
bifacial thinning	11.8%	1.7%
bipolar		
decortication	0.0%	0.4%
microblade	0.0%	0.9%
shatter	0.0%	0.0%

simple	88.2%	97.0%
unifacial thinning	0.0%	0.0%
Sullivan-Rozen typology		
broken	32%	31%
complete	9%	14%
fragment	59%	55%
shatter		
split		
Cortex		
0	100%	100%
1-3		0%
Dorsal scar count		
0	3%	
1	35%	17%
2	35%	42%
3	15%	31%
4+	12%	10%
%≥3	26%	40%
Termination		
feathered	41%	27%
hinge		6%
overshot		
step	59%	67%
Thermal		
0	100%	100%
1		
Material quality		
Low		
Moderate		0.4%
High	100%	99.6%

Table 7.15c Component 3 size class distributions

SC	*C3g1*	*C3g2*
1		10%
2	65%	58%
3	21%	22%
4	12%	5%
5	3%	4%
6		0%

Table 7.15d Component 3 platform remnant bearing flake summary data

	C3g1	*C3g2*
N	14	104
Eraillure scars	7%	9%
Lipping	43%	16%
Salient bulbs		3%
Platform type		
abraded	7%	3%
complex	7%	7%
cortical	7%	1%
crushed	21%	37%
simple	57%	53%
Platform edge angle		
n	12	73
Mean	63º	60º
Stdev	12º	9º
Platform measurements		

platform width	4.33±2.85	3.83±1.87
platform thickness	1.24±0.86	1.15±0.61
Pressure, soft, hard (%)	83, 17, 0	97, 3, 0
Termination		
Feathered	21%	31%
Hinge		5%
Overshot		
Step	79%	64%

7.5.7 Component 4

Component 4 comprises four small lithic concentrations, C4g1 (90 debitage), C4g2 (32 debitage), C4g3 (15 debitage), and C4g4 (18 debitage) generally about 4-6 meters apart (Figure 7.48). C4g1 tools include 3 modified flakes, 5 modified microblades, and one microblade core. C4g2 includes 2 modified flakes. C4g3 includes 1 modified flake and 1 modified microblade. C4g4 includes 1 modified microblade. Raw material distributions are very dissimilar for each group, dominated by different raw materials per group. C4g1 is the most even, with R7, R1, and Ch1 most common (82%), C4g2 is dominant by a single material, C5 (97%), C4g3 is dominated by Ch3 and C28 (60%) and C4g4 is dominated by C19, C24, and C33 (78%).

Debitage summaries are provided in Table 7.16. Debitage characteristics vary, with bifacial thinning present at high levels in C4g1 and C4g3 (20-22%), and absent in C4g4 (0%). Microblades range from 0% in C4g2, 7-11% in C4g3 and C4g4, to 36% in C4g1. Sullivan and Rozen typology varies, with C4g4 most divergent, with fewer complete flakes and flake fragments, and more broken flakes, though C4g2 contains more shatter and split flakes. Cortex is absent in all groups except for 1% in C4g1. Dorsal scar counts are similar between C4g1 and C4g3 (averaging 2.6-2.8), with fewer flakes with 4+ scars in C4g4 and particularly C4g2 (averaging 1.8). Termination is most dissimilar with C4g1, with fewer feathered, more hinge, and fewer step fractures, and C4g4 have more step terminations. Size classes suggest tool production and maintenance rather than core reduction or early stage bifacial reduction. Eraillure scars are common in C4g3 and C4g4 (17-20%), along with lipping (17-30%), while C4g1 and C4g2 have more salient bulbs (14-15% vs. 0%). Platform preparation include more complex platforms in C4g1 and C4g2 (12-15% vs. 0%). Platform edge angles vary. Platform width and thickness are different, with C4g2 and C4g4 similar, C4g3 larger (and more variable) and C4g1 smaller.

Microblade data are summarized in Table 7.17. A total of 32 microblades are found in C4g1, most (84%) are unretouched, with depleted medial segments (34%). In contrast, the microblades in the other two clusters are all medial segments, and 2 of the 3 are modified. This suggests microblade production in C4g1 and nonlocal microblade discards in C4g2 and C4g3.

Collectively, these data suggest differences in raw materials, but some similarities in lithic behaviors in Component 4. C4g1 lithic behaviors include both late stage bifacial reduction and microblade production (particularly R1). C4g2 may reflect later-stage biface and/or flake tool maintenance (of C5). C4g3 have nondiagnostic debitage, with low microblade proportions. Given the small flake sizes, C4g3 likely represents tool maintenance. C4g1 and C4g4 also included some earlier stage hard-hammer reduction.

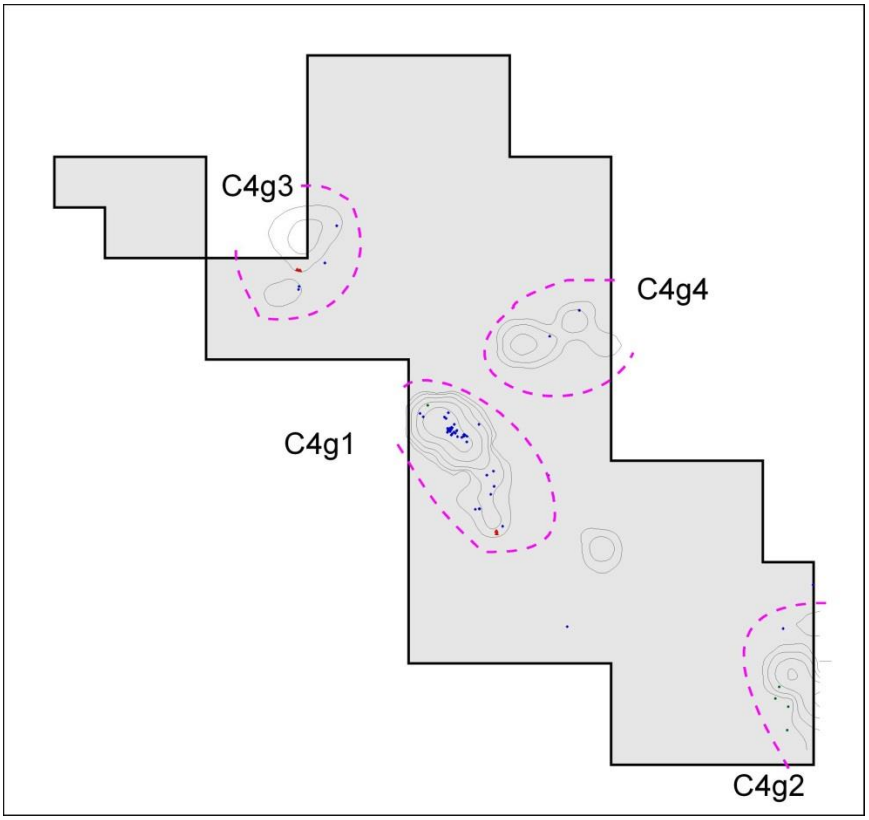

Figure 7.48 Component 4 spatial clusters. Blue represents flakes, red represents tools, and green represent bones.

Table 7.16a Component 4 raw materials

material	*C4g1*	*C4g2*	*C4g3*	*C4g4*
C11			6.7%	
C17		3.1%		
C19				55.6%
C24				11.1%
C28	3.3%		13.3%	5.6%
C29				5.6%
C30			6.7%	
C33				11.1%
C49	1.1%			
C5		96.9%		
C62			6.7%	
C7	1.1%			
Ch1	20.0%			
Ch3	5.6%		46.7%	
Ch4	1.1%		6.7%	
Ch5			6.7%	
Q3	1.1%			
R1	24.4%			5.6%
R2	4.4%		6.7%	
R7	37.8%			5.6%

Table 7.16b Component 4 debitage technical summary

	C4g1	*C4g2*	*C4g3*	*C4g4*
N	90	32	15	18
Flake type				
bifacial thinning	22.2%	3.1%	20.0%	0.0%
bipolar				
decortication	1.1%	0.0%	0.0%	0.0%
microblade	35.6%	0.0%	6.7%	11.1%
shatter	0.0%	3.1%	0.0%	0.0%
simple	41.1%	93.8%	73.3%	88.9%
unifacial thinning	0.0%	0.0%	0.0%	0.0%
Sullivan-Rozen typology				
broken	29%	22%	20%	44%
complete	28%	19%	20%	11%
fragment	43%	53%	60%	44%
shatter		3%		
split		3%		
Cortex				
0	99%	100%	100%	100%
1-3	1%			
Dorsal scar count				
1	12%	39%	13%	6%
2	30%	45%	40%	44%
3	34%	13%	33%	39%
4+	23%	3%	13%	11%
%≥3	58%	16%	47%	50%
Termination				
Feathered	32%	47%	40%	22%
Hinge	51%			6%
N/A		3%		
Overshot				
step	17%	50%	60%	72%
Thermal				
0	100%	100%	100%	100%
1				
Material quality				
Low				
Moderate	37.8%			16.7%
High	62.2%	100%	100%	83.3%

Table 7.16c Component 4 size class distributions

SC	*C4g1*	*C4g2*	*C4g3*	*C4g4*
1	25%	22%		17%
2	58%	47%	60%	56%
3	3%	16%	13%	11%
4	3%	6%	13%	6%
5	6%	3%	7%	11%
6	2%	3%		
7	1%	3%		
8+	1%		7%	

Table 7.16d Component 4 platform remnant bearing flake summary data

	C4g1	*C4g2*	*C4g3*	*C4g4*
N	51	13	6	10
Eraillure scar	4%		17%	20%
Lipping	10%	15%	17%	30%
Salient bulbs	14%	15%		
Platform type				
abraded		8%		10%
complex	12%	15%		
cortical				
crushed	10%	23%		20%
N/A	2%			
simple	76%	54%	100%	70%
Platform edge angle				
n	40	10	5	8
mean	78º	62º	64º	60º
Stdev	18º	7º	9º	4º
platform measurements				
platform width	1.94±1.65	3.26±2.21	5.80±9.48	3.54±1.83
platform thickness	0.81±0.57	0.84±0.52	1.62±1.89	1.00±0.28
Pressure, soft, hard (%)	100, 0, 0	100, 0, 0	83, 0, 17	100, 0, 0
Termination				
Feathered	41%	38%	50%	20%
Hinge	37%			10%
Overshot				
Step	22%	62%	50%	70%

Table 7.17 Component 4 microblade summary data

	C4g1	*C4g3*	*C4g4*
N	32	1	2
Segments			
Complete	9%		
Proximal	50%		
Medial	34%	100%	100%
Distal	6%		
Modification			
Modified	16%	100%	50%
Unmodified	84%	0%	50%

7.5.8 Component 5a

Component 5a consists of a relatively diffuse spread of lithics (totaling 51), primarily in the central part of the excavation area (Figure 7.49). Tools and cores consist of 1 uniface and 1 microblade core. Microblade technology is represented by the core and 3 microblades.

Debitage summaries are provided in Table 7.18. Raw materials are dominated by C28 (55%) with the rest relatively evenly distributed among a dozen other raw materials. Flake types are dominated by undiagnostic simple flakes, though there are moderate levels of bifacial thinning flakes, decortication flakes and microblades (each at 6%). Sullivan-Rozen typology has relatively few flake fragments and more complete and broken flakes, suggesting tool reduction. Cortex is present in relatively high amounts (6%). Dorsal scar count average (2.7) is relatively

high compared with most C2a and C2c groups. Almost half of the debitage have feathered terminations. Thermal alteration is relatively high in this component compared with others (12%). No hearth was identified in this stratum, and 100% of the thermally alteration was within C28 (29% of total C28 flakes), suggesting that this could reflect heat treatment.

Overall, size classes are relatively small, similar to other Denali components, suggesting later stage reduction (tool production and maintenance rather than initial core reduction). Lipping (21%), eraillures (11%), and salient bulbs (29%) are relatively common, suggesting multiple lithic reduction techniques, soft-hammer, hard-hammer, and pressure. Platforms are generally unprepared (79%), suggesting early stage reduction. Platform edge angle is relatively high, averaging 66º, again suggesting earlier stages of lithic reduction. Platform width and thickness measures are relatively small, suggesting soft-hammer reduction and pressure flaking.

Collectively, these data suggest an unusual mix of small flake sizes and unprepared platforms, yet with multiple lithic reduction techniques, including heat treatment. The data are consistent with later stages of tool production and maintenance. Given the spatial diffuseness of the materials, it is entirely possible that these represent multiple different very short-term reduction episodes, perhaps by different site occupants.

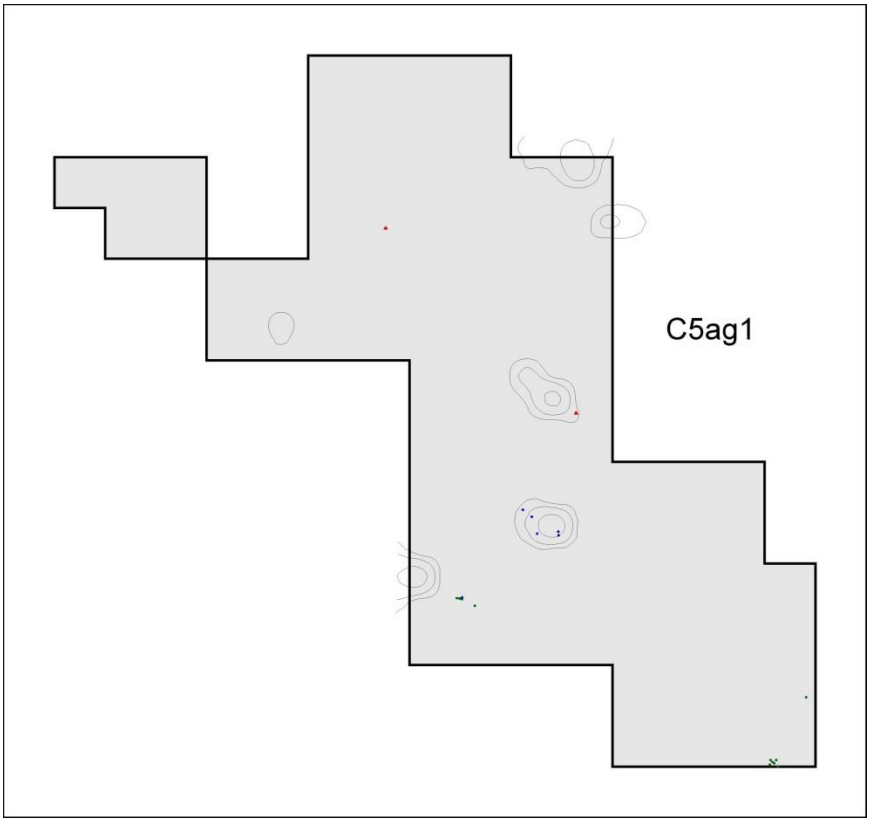

Figure 7.49 Component 5a spatial cluster. Blue represents flakes, red represents tools.

Table 7.18a Component 5a raw materials

Material	*C5ag1*
C15	2.0%
C19	6.1%
C28	55.1%
C36	2.0%
C39	6.1%
C49	2.0%
C68	2.0%
Ch3	6.1%
Ch4	2.0%
CH4	2.0%
Ch5	2.0%
Q1	12.2%

Table 7.18b Component 5a debitage technical summary

	C5ag1
N	49
Flake type	
bifacial thinning	6.1%
bipolar	
decortication	6.1%
microblade	6.1%
shatter	0.0%
simple	81.6%
unifacial thinning	0.0%
Sullivan-Rozen typology	
broken	29%
complete	29%
fragment	43%
shatter	
split	
Cortex	
0	94%
1-3	6%
Dorsal scar count	
0	2%
1	14%
2	37%
3	18%
4+	28%
%≥3	47%
Termination	
feathered	49%
hinge	
N/A	
overshot	2%
step	49%
Thermal	
0	88%
1	12%
Material quality	
Low	
Moderate	
High	100%

Table 7.18c Component 5a size class distributions

SC	*C5ag1*
1	14%
2	53%
3	24%
4	4%
5	2%
6	2%

Table 7.18d Component 5a platform remnant bearing flake summary data

	C5ag1
N	28
Eraillure scar	11%
Lipping	21%
Salient bulb	29%
platform type	
abraded	
complex	11%
cortical	
crushed	11%
N/A	
simple	79%
Platform edge angle	
mean	66º
stdev	10º
n	11
platform measurements	
platform width	2.49±0.80
platform thickness	0.77±0.35
Pressure, soft, hard (%)	100, 0, 0
Termination	
Feathered	46%
Hinge	
Overshot	4%
Step	50%

7.5.9 Component 5b

Component 5b consists of a relatively small cluster of lithics (totaling 35 artifacts), primarily in the northern part of the excavation (Figure 7.50). Besides unmodified flakes, 1 microblade core and 5 microblades were recovered.

Debitage summaries are provided in Table 7.19. Raw materials are relatively even, with C62 (31%) the most common. Flake types are dominated by bifacial thinning (23%) and microblades (14%). Sullivan-Rozen typology shows mostly flake fragments (66%) followed by broken flakes, with some shatter (6%), more consistent with bifacial reduction than microblade core production. Cortex is present in low quantities (3%). Dorsal scar counts are evenly split between 2, 3, and 4. A relatively large portion (9%) of debitage is thermally altered.

Overall, size classes are relatively small, similar to other Denali components, suggesting later stage reduction (tool production and maintenance rather than initial core reduction). Lipping is absent, while eraillure scars (10%) and salient bulbs (20%) are relatively common, suggesting hard hammer percussion as well as pressure flaking techniques. Platforms are generally unprepared (80%), suggesting early stage reduction. Platform edge angle is relatively high, averaging 68º, again suggesting earlier stages of lithic reduction. Platform width and thickness measures are relatively small.

The microblade core and 3 of the 5 microblades (all unretouched) are made from R4, as is 1 flake. This suggests a small amount of microblade production prior to discard of the core.

Collectively, these data suggest hard hammer percussion and pressure flaking relating to tool production, with some microblade production. The assemblage characteristics also suggest a very short term occupation.

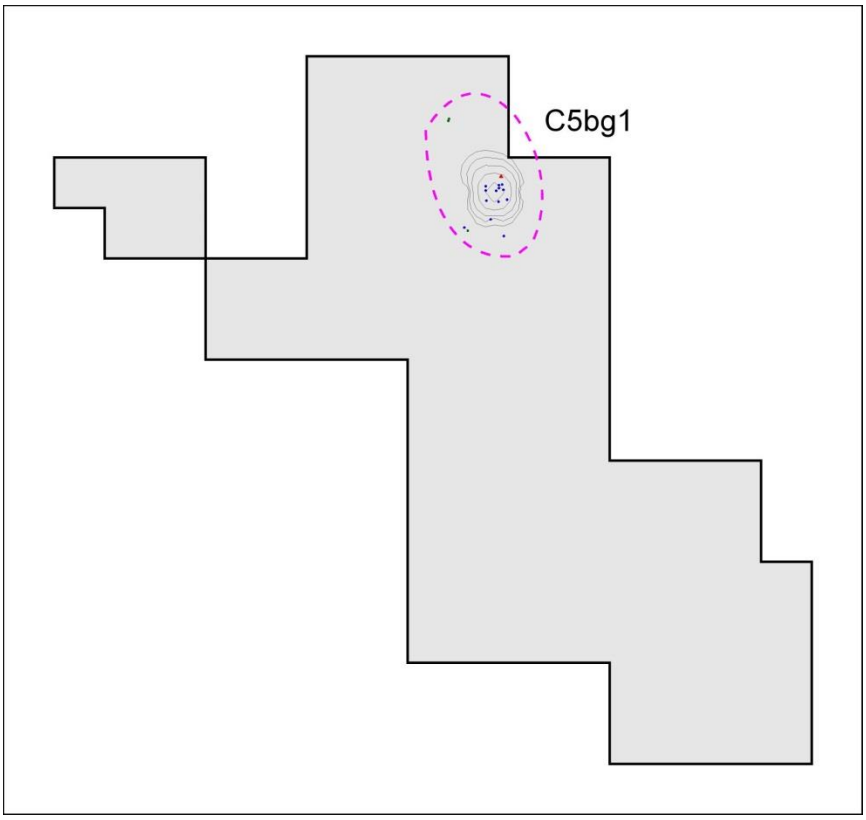

Figure 7.50 Component 5b spatial clusters. Blue represents flakes, red represents tools, and green represent bones.

Table 7.19a Component 5b raw materials

Material	*C5bg1*
C11	2.9%
C19	17.1%
C21	8.6%
C28	5.7%
C5	2.9%
C62	31.4%
Q1	2.9%
R2	17.1%
R4	11.4%

Table 7.19b Component 5b debitage technical summary

	C5bg1
N	35
Flake type	
bifacial thinning	22.9%
bipolar	
decortication	0.0%
microblade	14.3%
shatter	5.7%
simple	57.1%
unifacial thinning	0.0%
Sullivan-Rozen typology	
broken	20%
complete	9%
fragment	66%
shatter	6%
split	
Cortex	
0	97%
1-3	3%
Dorsal scar count	
1	24%
2	27%
3	30%
4+	18%
%≥3	48%
Termination	
feathered	17%
hinge	11%
N/A	6%
overshot	
step	66%
Thermal	
0	91%
1	9%
Material quality	
Low	
Moderate	
High	100%

Table 7.19c Component 5b size class distributions

SC	*C5bg1*
1	26%
2	37%
3	31%
4	3%
5	3%
6+	

Table 7.19d Component 5b platform remnant bearing flake summary data

	C5bg1
N	10
Eraillure	10%
Lipping	
Salient	20%
platform type	
abraded	
complex	10%
cortical	
crushed	10%
N/A	
simple	80%
Platform edge angle	
mean	68º
stdev	15º
n	8
platform measurements	
platform width	2.74±1.53
platform thickness	1.05±0.46
Pressure, soft, hard (%)	100, 0, 0
Termination	
Feathered	10%
Hinge	40%
Overshot	
Step	50%

7.5.10 Component 6a

Component 6a consists of three concentrations of lithics in the southern part of the excavation area (totaling 191 artifacts) (Figure 7.51). Tools include 1 biface (stage 5 finished biface – projectile point), 2 modified flakes, and one flake core. A single microblade was recorded for this component. A hearth was associated (F2017-2) and large cobbles were associated with this component.

Debitage summaries are provided in Table 7.20. Raw materials are relatively evenly distributed, with C5 (39%) and C15 (16%) the most common. Flake types include bifacial thinning (8%) and decortication (3%). Sullivan-Rozen typology shows relatively high amounts of broken and complete flakes. Cortex is present on 4% of the materials, including 2% with 100% cortex. Dorsal scar count averages are relatively low (1.9), compared with other Northern Archaic assemblages at DRO. Many flakes have feathered terminations (42%). Overall, size classes are relatively small, though there are 10% greater than size class 4, generally higher than other Northern Archaic components, but still suggesting later stage reduction (tool production and maintenance rather than initial core reduction). Lipping is common (38%) while eraillure scars and salient bulbs are rare (4% each). Platform preparation is relatively high, suggesting later stage reduction. Platform edge angles are relatively acute (averaging 59º), suggesting later stage bifacial reduction. Platform width and thickness values are relatively high, suggesting soft-hammer bifacial reduction.

Collectively, these data suggest soft hammer percussion in the context of later stage bifacial reduction. The projectile point is C39, not represented by any debitage in Component 6a, suggesting the bifacial implements made or maintained were removed from the site.

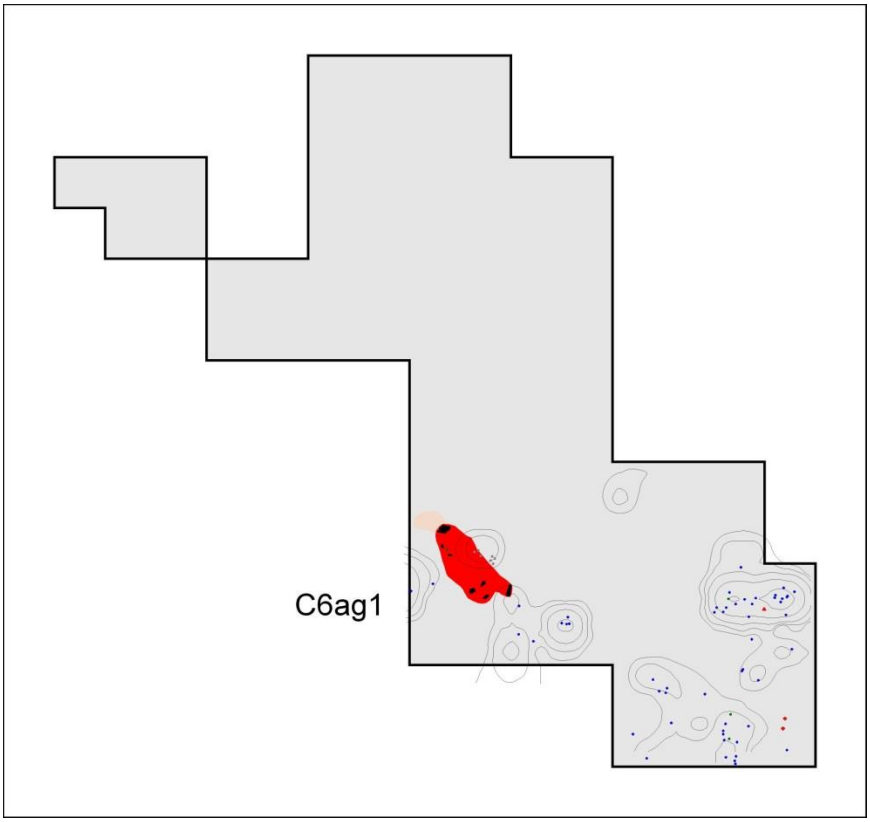

Figure 7.51 Component 6a spatial cluster. Blue represents flakes, red represents tools, green represent bones, and red polygon represents hearth feature.

Table 7.20a Component 6a raw materials

Material	*C6ag1*
C1	8.6%
C11	5.4%
C13	0.5%
C14	0.5%
C15	16.1%
C17	0.5%
C19	5.4%
C2	1.1%
C3	3.8%
C33	4.8%
C4	0.5%
C5	39.2%
C6	0.5%
C7	0.5%
C8	0.5%
M1	0.5%
O1	0.5%
Q1	8.1%
Q5	0.5%
R1	1.1%

R2	0.5%
R4	0.5%

Table 7.20b Component 6a debitage technical summary

	C6ag1
N	186
Flake type	
bifacial thinning	8.0%
bipolar	
decortication	3.2%
microblade	0.5%
shatter	1.1%
simple	87.1%
unifacial thinning	0.0%
Sullivan-Rozen typology	
broken	20%
complete	23%
fragment	55%
shatter	1%
split	1%
Cortex	
0	96%
1-3	4%
Dorsal scar count	
0	2%
1	33%
2	48%
3	15%
4+	3%
%≥3	18%
Termination	
feathered	42%
hinge	2%
N/A	1%
overshot	
step	54%
Thermal	
0	99%
1	1%
Material quality	
Low	0.5%
Moderate	6.5%
High	93.0%

Table 7.20c Component 6a size class distributions

SC	*C6ag1*
1	12%
2	61%
3	17%
4	6%
5	2%
6	1%
7+	1%

Table 7.20d Component 6a platform remnant bearing flake summary data

	C6ag1
N	80
Eraillure scars	4%
Lipping	38%
Salient bulbs	4%
platform type	
abraded	9%
complex	9%
cortical	4%
crushed	15%
N/A	
simple	64%
Platform edge angle	
Mean	59º
stdev	8º
n	59
platform measurements	
platform width	4.92±5.34
platform thickness	1.55±1.97
Pressure, soft, hard (%)	89, 6, 6
termination	
Feathered	50%
Hinge	3%
Overshot	
Step	48%

7.5.11 Component 6b

Component 6b consists of only 7 unmodified flakes from 4 raw material types. Debitage summaries are provided in Table 7.21. None of the flakes are diagnostic. All are small tertiary flakes. Salient bulbs and lipping are both present, and platforms are generally prepared. Platform measurements are relatively large, suggesting soft-hammer percussion, but given the small sample size, relatively little can be generalized. However, the data suggest a very short term occupation.

Table 7.21a Component 6b raw materials

material	*C6bg1*
C24	14.3%
C28	14.3%
C5	57.1%
Q1	14.3%

Table 7.21b Component 6b debitage technical summary

	C6bg1
N	7
Flake type	
bifacial thinning	0.0%
bipolar	0.0%
decortication	0.0%
microblade	0.0%
shatter	0.0%
simple	100.0%
unifacial thinning	0.0%
Sullivan-Rozen typology	
broken	43%
complete	14%
fragment	43%
shatter	
split	
Cortex	
0	100%
1-3	
Dorsal scar count	
1	
2	14%
3	71%
4+	14%
%≥3	86%
Termination	
feathered	29%
hinge	
N/A	
overshot	
step	71%
Thermal	
0	100%
1	
Material quality	
Low	
Moderate	
High	100%

Table 7.21c Component 6b size class distributions

SC	*C6bg1*
1	
2	14%
3	43%
4	29%
5	14%
6+	

Table 7.21d Component 6b platform remnant bearing flake summary data

	C6bg1
N	4
Eraillure scar	
Lipping	25%
Salient bulb	50%
platform type	
abraded	
complex	25%
cortical	
crushed	50%
N/A	
Simple	25%
platform measurements	
platform width	5.33+/0.81
platform thickness	1.39±0.98
Pressure, soft, hard (%)	100, 0, 0
Termination	
Feathered	25%
Hinge	
Overshot	
Step	75%

7.5.12 Component 7a

Component 7a consists of 6 flakes and 1 uniface from 3 raw material types, from the northwestern part of the excavated area. Debitage summaries are provided in Table 7.22. The flakes are undiagnostic, and little can be said about this component other than it represents a very short-term occupation.

Table 7.22a Component 7a raw materials

material	*C7ag1*
C11	50.0%
C19	16.7%
C5	33.3%

Table 7.22b Component 7a debitage technical summary

	C7ag1
N	6
Flake type	
bifacial thinning	0.0%
bipolar	0.0%
decortication	0.0%
microblade	0.0%
shatter	0.0%
simple	100.0%
unifacial thinning	0.0%
Sullivan-Rozen typology	
broken	67%

complete	
fragment	33%
shatter	
split	
Cortex	
0	100%
1-3	
Dorsal scar count	
1	33%
2	33%
3	17%
4+	17%
%≥3	33%
Termination	
feathered	17%
hinge	
N/A	
overshot	
step	83%
Thermal	
0	100%
1	
Material quality	
Low	
Moderate	
High	100%

Table 7.22c Component 7a size class distributions

SC	*C7ag1*
1	
2	83%
3	17%
4+	

Table 7.22d Component 7a platform remnant bearing flake summary data

	C7ag1
N	4
Eraillure scars	
Lipping	
Salient bulbs	
platform type	
abraded	
complex	
cortical	
crushed	100%
N/A	
simple	
platform measurements	
platform width	2.9
platform thickness	0.39
Pressure, soft, hard (%)	100, 0, 0
Termination	
Feathered	

Hinge	
Overshot	
Step	100%

7.5.13 Component 7b

Component 7b consists of two concentrations of lithics,about 8 meters apart (Figure 7.52). C7bg1 (n=118) and C7bg2 (n=231) appears in the northwestern and central-eastern part of the excavated area respectively. C7bg1 tools include 4 unifaces (all are end scrapers) and C7bg2 tools include 7 modified flakes and 2 unifaces (both end scrapers).

Debitage summaries are provided in Table 7.23. Raw materials are very different for these groups, with C7bg1 more evenly distributed with C31 (46%) and C51 (27%) most common (both do not appear in C7bg2). The most common raw material in C7bg2 is C5 (73%) followed by C67 (20%), the latter does not appear in C7bg1. Flake types are also different, with C7bg1 having more bifacial thinning flakes (10% vs. 3%). Sullivan-Rozen typology is somewhat dissimilar, with fewer broken flakes and more complete flakes in C7bg2. Cortex is absent in both groups. Dorsal scar counts are distinctly different, with C7bg1 averaging 1.8 and C7bg2 averaging 2.5. Since size class distributions are roughly similar, this suggests later stages of reduction for C7bg2 than for C7bg1, all things being equal. C7bg2 flakes also have higher feathered terminations (53% vs. 39%). Eraillures are relatively uncommon, but lipping is more common in C7bg2 (46% vs. 13%), suggesting soft-hammer reduction. Platform edge angles for C7bg1 are acute (averaging 51º) suggesting later stages of reduction. Platform width and thickness measurements are relatively similar for the two groups.

Collectively, these data suggest later stages of lithic reduction, likely bifacial and other tool production and maintenance, with C7bg1 more associated with bifacial maintenance and C7bg2 with later stages of bifacial and other tool maintenance.

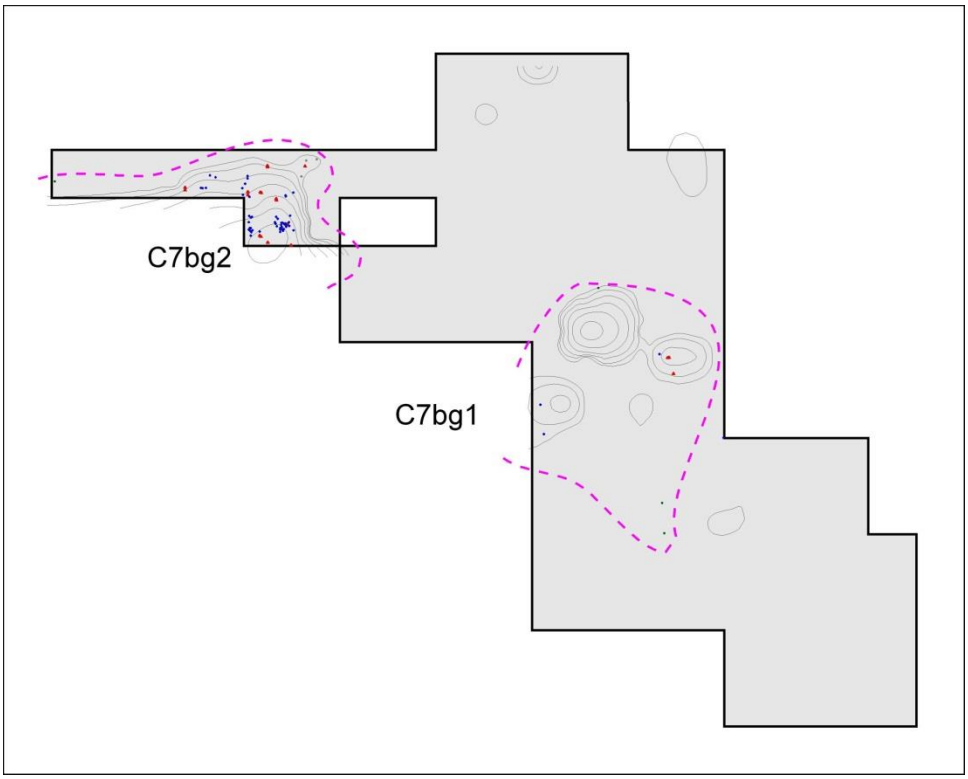

Figure 7.52 Component 7b spatial clusters. Blue represents flakes, red represents tools.

Table 7.23a Component 7b raw materials

material	*C7bg1*	*C7bg2*
C1	6.8%	
C11		0.9%
C19	0.8%	
C28	0.8%	
C29	0.8%	
C3	1.7%	
C31	45.8%	
C33	0.8%	3.9%
C39	5.9%	
C5	3.4%	73.2%
C51	27.1%	
C53	0.8%	
C67		20.3%
M4	0.8%	
O1		1.7%
O2	1.7%	
Q1	0.8%	
R1	0.8%	
R9	0.8%	

Table 7.23b Component 7b debitage technical summary

	C7bg1	*C7bg2*
N	118	231
Flake type		
bifacial thinning	10.2%	3.0%
bipolar	0.0%	0.0%
decortication	0.0%	0.4%
microblade	0.0%	0.0%
shatter	0.8%	0.4%
simple	89.0%	94.8%
unifacial thinning	0.0%	1.3%
Sullivan-Rozen typology		
broken	36%	21%
complete	23%	40%
fragment	41%	38%
shatter	1%	0%
split		
Cortex		
0	100%	100%
1-3		0%
Dorsal scar count		
1	47%	10%
2	35%	49%
3	11%	33%
4+	7%	8%
%≥3	18%	41%
Termination		
feathered	39%	53%
hinge	4%	3%
N/A	1%	0%
overshot		
step	56%	44%
Thermal		
0	99%	100%
1	1%	
Material quality		
Low	0.8%	
Moderate	28%	3.9%
High	71.2%	96.1%

Table 7.23c Component 7b size class distributions

SC	*C7bg1*	*C7bg2*
1	13%	22%
2	77%	62%
3	7%	9%
4	3%	3%
5	1%	2%
6		1%
7		
8+		0%

Table 7.23d Component 7b platform remnant bearing flake summary data

	C7bg1	*C7bg2*
N	69	142
Eraillure scars	1%	2%
Lipping	13%	46%
Salient bulbs		4%
Platform type		
abraded	4%	
complex	9%	6%
cortical		
crushed	39%	13%
N/A		1%
simple	48%	79%
Platform edge angle		
N	49	
Mean	51º	
Stdev	14º	
Platform measurements		
platform width	3.23±1.94	3.00±3.00
platform thickness	1.00±0.91	0.88±0.71
Pressure, soft, hard (%)	98, 2, 0	98, 2, 1
Termination		
Feathered	41%	65%
Hinge	4%	2%
Overshot		
Step	55%	33%

7.5.14 Component 8a

Component 8a consists of three concentrations (Figure 7.53), one dense concentration of generally unretouched flakes (C8ag1, n=1011), a very dense lithic blank cache (C8ag2, n=34 debitage), and a diffuse scatter in the northeastern part of the excavation area (C8ag3, n=98). C8ag1 tools consist of a single modified flake. C8ag2 tools include 5 bifaces, 40 modified flakes, and 3 unifaces. The bifaces include 5 stage 2 edged bifaces and the unifaces include 1 side scraper and 1 double side scraper and a uniface fragment). C8ag3 tools consist of 2 modified flakes and 1 uniface (end scraper).

Debitage summaries are provided in Table 7.24. Raw materials are distinctly different for each C8a group. C8ag1 is almost exclusively (99.5%) comprised of C11, which appears in moderate portions in C8ag3 (33%) but is absent in C8ag2. C8ag2 debitage is dominated by a few types, C14 (41%), C5 (44%), R1 (9%), and R9 (6%). The tools from the cache roughly match this, with C5 (49%), R1 (28%) and R9 (13%). Flake types are also different between groups, with C8ag1 dominated by bifacial thinning (20% vs. 0-2%). C8ag3 is generally undiagnostic, though there are 2% bifacial thinning and 3% decortication flakes. C8ag2 contains no bifacial thinning flakes but 9% decortication and 3% shatter, suggesting early stage core/blank reduction, consistent with the cache blanks.

Sullivan-Rozen typology shows high numbers of fragments and very few complete flakes in C8ag1, with more complete flakes in the other groups, particularly in C8ag2. Cortex was prominent in C8ag2, with 9% of specimens with cortex, including 3% primary flakes. C8ag3 contained 4% of cortex. Dorsal scar counts were relatively similar (averaging 2 for all groups),

though C8ag1 contained many flakes with fewer scar counts. Terminations varied, but C8ag2 exhibited more feathered terminations. Size classes were different, with C8ag1 dominated by smaller flakes (91% less than 10 mm compared with 71-73%), and C8ag2 contained 6% over size class 8. Eraillure scars and salient bulbs were more common in C8ag2 and to a lesser extent C8ag3, while lipping was more common in C8ag1. C8ag1 flakes also exhibited more platform preparation. Platform edge angles were more acute in C8ag1 than in C8ag3. Platform width and thickness values were larger for C8ag2 than for either of the other groups.

Collectively, these data suggest different lithic behaviors in the three C8a clusters. C8ag1 likely represents late stage bifacial tool maintenance, while C8ag3 reflects earlier stages of reduction, including some decortication. C8ag2 reflects early stage reduction of bifacial, unifacial and flake blanks of roughly similar dimensions.

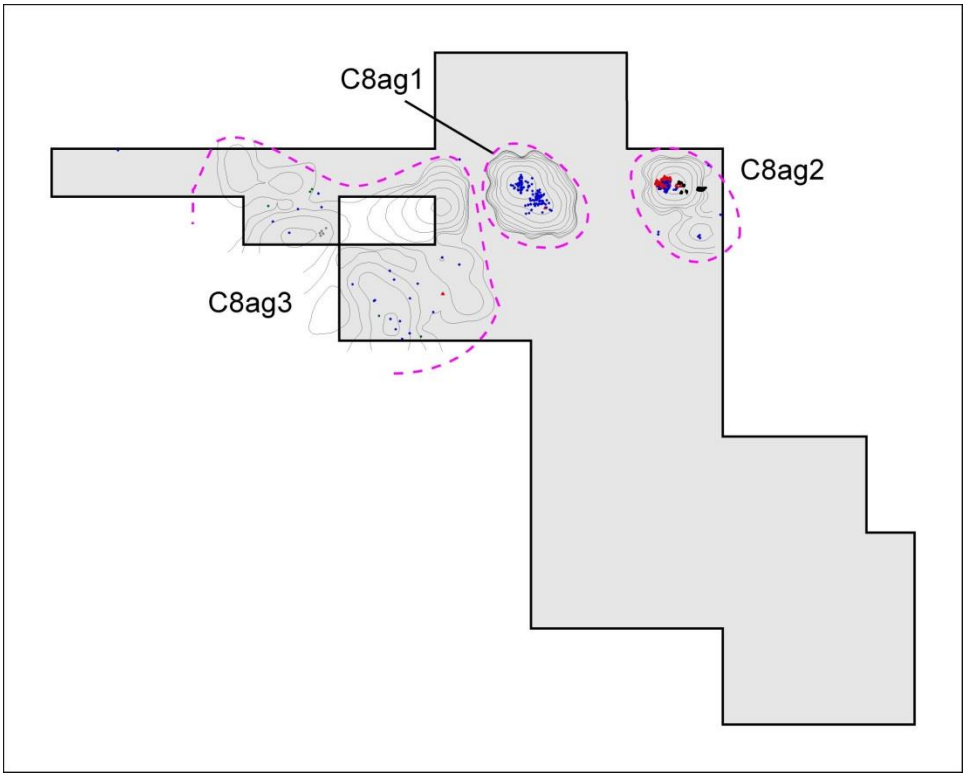

Figure 7.53 Component 8a spatial clusters. Blue represents flakes, red represents tools.

Table 7.24a Component 8a raw materials

material	*C8ag1*	*C8ag2 Debitage*	*C8ag2 Tools*	*C8ag3*
C11	99.5%			32.7%
C15		41.2%		
C19			2.1%	7.1%
C2				1.0%
C24				22.4%
C3				1.0%
C36				1.0%
C39				2.0%
C49	0.1%			1.0%
C4			2.1%	
C5	0.1%	44.1%	48.9%	20.4%
C56				1.0%

C57				1.0%
C68			2.1%	
Ch1				1.0%
Ch3				1.0%
Ch6				1.0%
O			2.1%	
Q1			2.1%	
Q3				2.0%
Q4				1.0%
R1	0.2%	8.8%	27.7%	
R2				1.0%
R4	0.1%			1.0%
R9		5.9%	12.8%	1.0%

Table 7.24b Component 8a debitage technical summary

	C8ag1	C8ag2	C8ag3
N	1011	34	98
Flake type			
bifacial thinning	20.3%	0.0%	2.0%
bipolar	0.0%	0.0%	0.0%
decortication	0.0%	8.8%	3.1%
microblade	0.0%	0.0%	0.0%
shatter	1.7%	2.9%	0.0%
simple	78.0%	88.2%	94.9%
unifacial thinning	0.0%	0.0%	0.0%
Sullivan-Rozen typology			
broken	16%	18%	20%
complete	4%	21%	10%
fragment	78%	59%	69%
shatter	2%	3%	
split	0%		
Cortex			
0	100%	91%	96%
1-3		9%	4%
Dorsal scar count			
0		3%	1%
1	44%	21%	24%
2	29%	55%	50%
3	20%	15%	21%
4+	8%	6%	3%
%≥3	28%	21%	24%
Termination			
feathered	25%	38%	17%
hinge	0%	6%	5%
N/A	2%	3%	
overshot			
step	73%	53%	78%
Thermal			
0	100%	100%	99%
1	0%		1%
Material quality			
Low			
Moderate			
High	100%	100%	100%

Table 7.24c Component 8a size class distributions

SC	*C8ag1*	*C8ag2*	*C8ag3*
1	35%	3%	13%
2	56%	68%	60%
3	8%	24%	21%
4	0%		4%
5			
6			1%
7			
8+	0%	6%	

Table 7.24d Component 8a platform remnant bearing flake summary data

	C8ag1	*C8ag2*	*C8ag3*
N	200	13	30
Eraillure scars	4%	8%	7%
Lipping	36%	15%	23%
Salient bulbs	2%	8%	3%
Platform type			
abraded			
complex	17%		
cortical		8%	
crushed	15%	15%	50%
simple	69%	77%	50%
Platform edge angle			
n	170		12
mean	48º		57º
Stdev	12º		7º
platform measurements			
platform width	3.05±2.02	4.46±4.97	3.45±2.03
platform thickness	0.87±0.43	1.44±1.49	0.89±0.43
Pressure, soft, hard (%)	99, 1, 1	82, 9, 9	95, 5, 0
Termination			
Feathered	22%	54%	30%
Hinge	1%		3%
Overshot			
Step	78%	46%	67%

7.5.15 Component 8b

Component 8b consists of three concentrations (Figure 7.54), one dense scatter associated with a hearth features (F2017-1) in the northern part of the excavation area (C8bg1, n=549), another associated with a hearth feature (F2015-1) to the east (C8bg2, n=214), and smaller cluster to the south (C8bg3, n=20). C8bg1 tools consist of 2 bifaces, 3 modified flakes, and 2 unifaces. The bifaces include 1 stage 4 preform and 1 stage 5 finished biface (projectile point), and the unifaces include 1 end scraper and 1 side scraper). C8bg2 tools consist of 1 modified flake and 2 unifaces (1 end scraper and 1 side scraper). No tools are associated with C8bg3.

Debitage summaries are provided in Table 7.25. Raw materials are generally relatively similar for each C8b group, with C5 (15-42%) and C11 (20-53%) the most common. Flake types are different among the groups, with bifacial thinning flakes varying between 25% in C8bg3, 11% in C8bg2 and 6% in C8bg1. Decortication flakes are only present in C8bg1, along with higher amounts of shatter (4% vs. 0-1%). Sullivan-Rozen typology indicates much fewer broken

and more complete flakes in C8bg3 while C8bg1 and C8bg2 are roughly similar. Cortex is only found in C8bg1 (on 5% of debitage). Dorsal scar count averages are similar among the groups (2.3). C8bg3 has many more feathered terminations (65% vs. 22-28%). Size classes were generally similar, though C8bg1 had relatively more large flakes. Eraillure scars were present in C8bg1 and C8bg2 and absent in C8bg3, while lipiping was most common in C8bg2. Salient bulbs were more common in C8bg1 and C8bg3. Prepared (complex) platforms were relatively common among all groups, suggesting some later stage reduction. Platform edge angles were roughly similar between the groups. Platform width and thickness measurements are similar, though C8bg2 had narrower platforms than the other two.

Collectively, these data suggest that C8bg1 reflects a wider range of lithic behaviors, including decortication and earlier stage reduction as well as some bifacial thinning and tool maintenance. C8bg2 reflects more bifacial thinning, predominantly soft hammer bifacial reduction. C8bg3 reflects predominantly late stage controlled bifacial reduction.

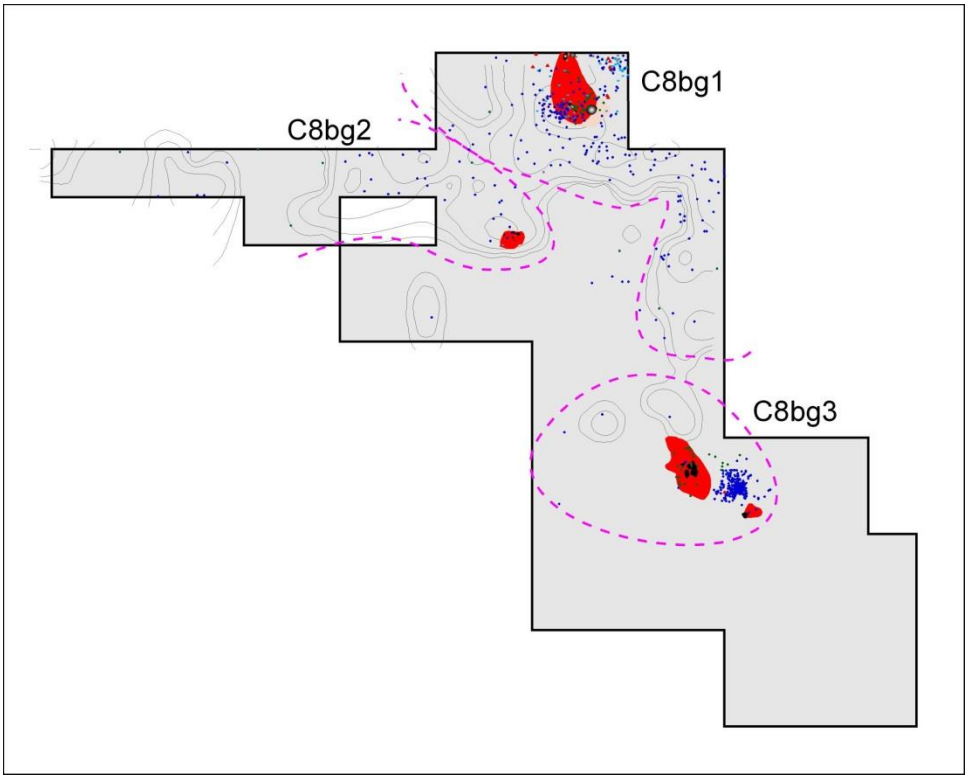

Figure 7.54 Component 8b spatial clusters. Note, C8bg3 (Kotani excavation) is not available for study. Blue represents lithics, red represents tools, and red polygons represent hearth features.

Table 7.25a Component 8b raw materials

material	*C8bg1*	*C8bg2*	*C8bg3*
C1	0.7%	0.9%	25.0%
C11	22.0%	52.8%	20.0%
C13		0.5%	
C14			5.0%
C15	1.1%		
C17	0.5%		
C19	6.4%	3.3%	
C2	3.0%	0.5%	
C21	0.2%		
C22		0.5%	
C24	0.4%	0.9%	
C28	0.2%		
C29	4.2%		
C3	2.0%	0.9%	
C31	0.4%		
C32	0.6%	0.5%	
C33	0.5%		
C35	0.2%		5.0%
C36	4.4%	1.4%	5.0%
C39		0.9%	15.0%
C41		0.5%	
C47	0.2%		
C49	1.3%	1.9%	
C5	41.7%	28.0%	15.0%
C53		0.9%	
C56		0.5%	
C59	0.2%	0.9%	
C64			5.0%
C67		0.5%	
C68		0.5%	
C69	0.4%		
C70		0.5%	
C8	0.2%	0.5%	
Ch1	0.2%		
Ch3	0.2%		
Ch4	0.5%		
O		1.0%	5.0%
Q1	0.2%		
Q3	0.2%	0.5%	
Q4	0.2%	0.9%	
Q5	0.4%		
Q6	0.2%		
R1	5.7%		
R2	0.5%		
R4	1.1%		
R9	0.2%		

Table 7.25b Component 8b debitage technical summary

	C8bg1	*C8bg2*	*C8bg3*
N	549	214	20
Flake type			
bifacial thinning	5.5%	11.2%	25.0%
bipolar	0.0%	0.0%	0.0%
decortication	3.6%	0.0%	0.0%
microblade	0.0%	0.0%	0.0%
shatter	4.2%	1.4%	0.0%
simple	86.7%	86.0%	75.0%
unifacial thinning	0.0%	1.4%	0.0%
Sullivan-Rozen typology			
broken	26%	21%	5%
complete	14%	10%	30%
fragment	56%	67%	65%
shatter	4%	1%	
split	0%		
Cortex			
0	95%	100%	100%
1-3	5%		
Dorsal scar count			
0	1%	1%	
1	21%	23%	45%
2	38%	42%	25%
3	27%	20%	5%
4+	12%	13%	25%
%≥3	39%	34%	30%
Termination			
feathered	28%	22%	65%
hinge	2%	4%	
N/A	11%	2%	
overshot	0%		
step	59%	72%	35%
Thermal			
0	100%	98%	100%
1	0%	2%	
Material quality			
Low	0.5%	0.9%	
Moderate	1.8%	0.5%	
High	98.6%	100%	93.1%

Table 7.25c Component 8b size class distributions

SC	*C8bg1*	*C8bg2*	*C8bg3*
1	11%	11%	20%
2	58%	64%	50%
3	20%	16%	25%
4	5%	7%	5%
5	3%		
6	2%	1%	
7	0%		
8+	0%	0%	

Table 7.25d Component 8b platform remnant bearing flake summary data

	C8bg1	*C8bg2*	*C8bg3*
N	217	67	7
Eraillure scars	6%	9%	
Lipping	28%	52%	29%
Salient bulbs	12%	4%	14%
Platform type			
abraded			
complex	46%	21%	14%
cortical	2%		
crushed	15%	19%	
N/A	1%		
simple	36%	60%	86%
platform edge angle			
N	31	22	7
mean	58º	54º	61º
Stdev	12º	13º	16º
platform measurements			
platform width	3.95±3.11	3.09±1.37	4.50±3.94
platform thickness	0.90±0.96	0.96±0.50	1.78±1.27
Pressure, soft, hard (%)	94, 4, 2	100, 0, 0	71, 29, 0
Termination			
Feathered	34%	22%	86%
Hinge	1%	10%	
Overshot	0%		
Step	60%	67%	14%

7.6 Tool Analysis

7.6.1 Chindadn tradition (C1) tools

Component 1 has a narrow range of tools and cores, consisting of 4 bifaces, 2 modified flakes and 1 large flake core/chopper. Biface data are summarized in Table 7.26. All four bifaces are made from different raw materials. Three of the bifaces are finished projectile point bases (Figure 7.55), two with concave bases and one with a straight to slightly concave base, consistent with other Chindadn bifaces recovered at Healy Lake Chindadn, Mead, Swan Point, and Erodaway (Cook 1969; Potter et al. 2013). Edge grinding was observed on two of the points, and the overall context and debitage analyses, we infer that broken projectile points in hafts were transported to the site, discarded, and replacement projectile points were manufactured onsite to be rehafted.

Three microblades were recovered from clear Component 1 contexts directly above glacial till (Figure 7.56). All were found in close association with each other in Block 15. One was a medial fragment of C45 chert and the other two refit into a complete microblade of C11 chert with distal edge damage. Average metric values are 17.47±2.63 mm long, 5.29±0.30 mm wide, and 1.33±0.40 mm thick and 0.22±0.13 g weight. The widths are similar to Denali microblade widths (averaging 4.86±1.93 mm).

The single large (1041 g) flake core/chopper of material C7 was located at some distance from other C1 materials, in the northwest part of the excavated area (Table 7.27, Figure 7.57). A

total of 18 large flake scars were on the core, removed from multiple directions, and average flake scar width is 21.49 mm, suggesting relatively large flakes were removed from the core. Only one tool (modified flake) and one unmodified flake were of the same material, suggesting that this core was not reduced onsite (at least not in the areas of excavation).Crushing and chipping damage along two edges (121.12 and 126.72 mm long) suggests use of the core/tool as a heavy-duty chopper or scraper.

Modified flake data are summarized in Table 7.28. The two modified flakes were made on different materials, but both have numerous debitage of those same materials, suggesting that these were manufactured and/or maintained onsite prior to discard. Edge angles are generally acute (19-42 degrees) suggesting similar light cutting/slicing uses for both. Percent of retouched margins is relatively low, 25-33%, suggesting lower levels of curation.

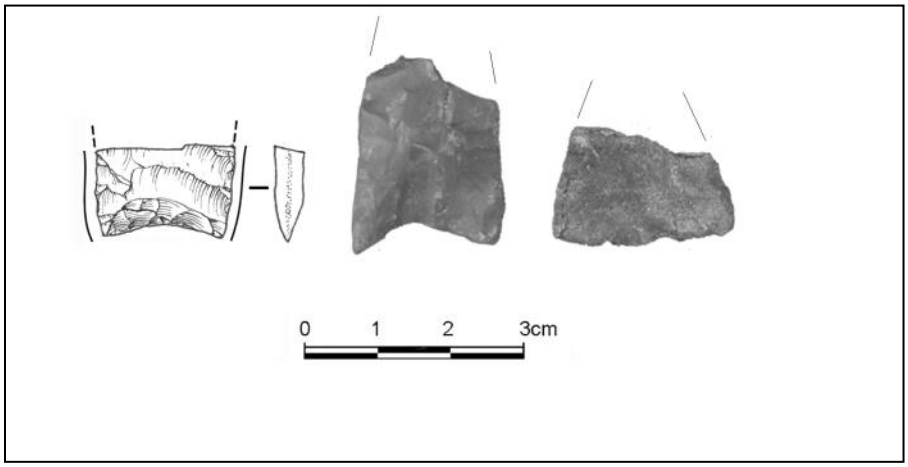

Figure 7.55 Chindadn complex projectile point bases (Component 1).

Figure 7.56 Chindadn complex microblades.

Figure 7.57 Chindadn complex flake core/chopper.

Table 7.26a. Chindadn biface metric attributes

Block	*FS*	*Mat.*	*maxL*	*maxW*	*maxT*	*L/W*	*W/T*	*Area*	*Wt.*	*Edge angle*
5	178	C30	12.76	11.6	4.89	1.10	2.37	148	0.62	45-50
5	109	R9	11.23	18.55	3.35	0.61	5.54	208	0.88	28-36
20	452	C68	14.02	22.06	2.51	0.64	8.79	309	0.95	31-35
25	55	C19	24.77	19.15	3.93	1.29	4.87	474	1.83	25-33

Table 7.26b. Chindadn biface non-metric attributes

Block	*FS*	*flaking pattern*	*dfse**	*condition*	*hafted*	*modification*	*stage*
5	178	comedial	<	medial	indet.	N/A	3 thinned biface
5	109	random	>	base	yes	edge grinding + polish	5 finished proj pt
20	452	comedial	<	base	no	N/A	5 finished proj pt
25	55	comedial	<	base	yes	edge grinding + polish	5 finished proj pt

*dorsal flake scar extent (< = less than half, > = more than half)

Table 7.27 Chindadn flake core attributes

Block	*FS*	*Mat.*	*max L*	*max W*	*max T*	*wt.*	*N flake scars*	*Avg. scar width*	*Type*
19	119	C7	149.46	77.5	63.76	1041.46	18	21.49	multidirectional

Table 7.28. Chindadn modified flake attributes

Bl.	*FS*	*Mat.*	*wt.*	*maxL*	*maxW*	*maxT*	*blank*	*Mod.*	*position*	*edge angle*	*retouch L (mm)*	*edge shape*	*Mod_type*	*Edge shape*	*%ret margins*
5	124	C36	18.41	58.28	33.84	8.77	flake	Retouch	R dorsal	42L, 75R-retouch	42.38	concave	moderate	concave	0.33
7	450	C7	6.31	55.05	27.22	5.53	flake	Damage	R edge	22LR	18.75	convex	light	convex	0.25

7.6.2 Denali tradition (C2a-C5b) tools

7.6.2.1 Denali tradition formal tools

Denali components contain 195 tools and 10 cores and core parts. Selected tools and cores are illustrated in Figures 7.58, 7.59, and Appendix B. Tools include 42 modified flakes, 20 bifaces, 14 unifaces, 2 burins, and 19 burin spalls. Cores include 2 flake cores. Microblade technology includes 448 unmodified microblades, 98 modified microblades, 4 microblade cores and 4 microblade core tablets. Six cobble tools are also present.

The 20 bifaces comprise 1 edged biface, 5 thinned bifaces, 11 preforms, 2 finished bifaces, and one indeterminate biface fragment (Table 7.29). The edged biface is complete, while all of the thinned bifaces are fragments, including 2 distal, 1 proximal (base), and 2 medial fragments. Three of these are split longitudinally, suggesting manufacturing errors. Only one stage 4 (preform) is complete (Block 11, FS 369), though polish is present, suggesting some use prior to discard. The two finished bifaces are projectile point bases, likely made offsite, broken during use, and discarded onsite. Both are near each other in Component 2c, suggesting hunting weapon discards. The bulk of the bifaces in all Denali components, primarily C2a and C2c, are earlier stage manufacturing discards, in contrast with Northern Archaic bifaces (see below). Basal shapes of early stage bifaces and preforms are biconvex, though two are straight-based. Both projectile points have convex bases with edge grinding and polish, typical for the Denali tradition (e.g., Upward Sun River, Healy Lake Village, and Mead) (West 1981).

Denali uniface data are provided in Table 7.30. Of the 14 Denali unifaces, three of the C2c specimens are broken and refit. Specimen 24-547 to 553 was an end scraper broken into 7 pieces within a hearth, and are analyzed in Table 7.30 together. Specimens 21-510 and 21-540 refit and Specimens 20-97 and 20-143 refit. Of these 12 unifaces, five (42%) are classed as end scrapers and six (59%) are classed as side scrapers (two are double side scrapers). Four of the five end scrapers (80%) are limited to Component 2c, suggesting different domestic activities between C2a and C2c. All but one of the unifaces are made on flake blanks (one is on a blade). All are retouched. Edge angles for end scrapers are steeper (61±11 degrees) than for side scrapers (42±16 degrees). Edge thickness also differs, with end scrapers averaging 11±8 mm and side scrapers averaging 3±2 mm. None of the unifaces were burinated.

All four C2a unifaces are made on raw materials with numerous debitage, consistent with onsite production. Five of the seven C2c unifaces are made on materials with numerous debitage, consistent with onsite production, though two are from materials with 66 and 9 debitage (8.15 g and 0.43 g) that could suggest transport as tools with higher curation. The single C5a specimen (9.63 g) is made on the highest frequency material (C28), but total debitage weighs 0.98 g, suggesting that this tool was made offsite, brought onsite and used/resharpened and ultimately discarded onsite. Interestingly, unifaces are completely absent in most Denali assemblages (C2b, C3, C4, and C5b), which contrasts with Northern Archaic components where unifaces are more prominent.

7.6.2.2 Denali tradition microblade and burin technology

Overall microblade and burin technology are directly proportional for the Denali components. Component 2c contains the most, including two microblade cores (50% of total), two microblade core tablets (50% of total), 90% of the modified microblades, both burins, and

89% of burin spalls, as well as 86% of all unmodified microblades. Component 2a contained far fewer of all classes of material. All of this suggests the close relationship between microblade production and burin use (see Guthrie 1983).

Microblade core and core tablet data are provided in Table 7.31. A total of 8 microblade cores and core parts were recovered from Denali components, mostly with C2c (63%). Components 2a, 2b and 3 contain no microblade core or core parts. Component 2c microblade cores are both wedge shaped. Overall they have similar morphology and size. Core diameter is 7-12 mm and platform edge angle is 81-85 degrees. Flute widths average 4.8±0.6 mm. Complete microblade widths for C2c average 5.7±1.3 mm, suggesting the microblade cores are exhausted. Microblade cores and core tablets represent 5 distinct material types. All of these raw materials include microblades (2-38), suggesting onsite microblade production prior to discard. However, 27 additional microblade raw materials are present, suggesting the presence of additional microblade cores that were removed. Some microblades may reflect nonlocal discards (i.e., not produced onsite). A number of other raw materials contain substantial numbers of microblades: C39, C46, C70, C5, and C17 have 23-70 microblades each, suggesting at least 5 additional microblade cores were used to produce microblades onsite and removed offsite. With the five recovered cores and core tablets, we can infer 10 microblade cores were transported to the site and used onsite, and only 2 were discarded (20%), suggesting microblade cores were highly curated.

Microblade cores were recovered from Components 5a and 5b. The Component 5a specimen is atypical, but does exhibit unidirectional blade and flake scars from a single platform. The platform is mostly removed, and a number of hinges are on the fluting face suggesting failure of material (defects) that prevented more systematic microblade removal. The Component 5b specimen is a semi-conical core common in the later Denali period, with similar examples at Healy Lake and Gerstle River Component 3 (Potter 2005). The weight of these later cores are substantially higher than those of Component 2c (12-14 g vs. 7-8 g), and the morphologies are different; C5a and C5b cores are semi-conical and have flat backs rather than bifacial keels.

A total of 451 unmodified and 99 modified microblades are present in Denali components (Tables 7.32 and 7.33). There are few differences in weight, width, length, and thickness between modified and unmodified microblades. However, there are substantial differences in segment distribution. Modified microblades are on 16% proximal and 76% medial segments compared with 47% proximal and 37% medial segments for unmodified specimens. Medial fragments were selected differentially to modify. Figure 7.60 shows segment percentages for the seven largest C2c microblade assemblages by material type (all >20 microblades per material type). These are compared with nonlocal discards vs. onsite production of microblades from Gerstle River Component 3 (Potter 2005). Of DRO C2c material types, C5, C17, C36, and C39 appear consistent with nonlocal discards (except material C36 also includes a core tablet) while C19, C46, and C70 are consistent with onsite production. These classifications are supported by percent modified microblades. C5 and C17 are 57-59% modified, with C36 and C39 are 13-21% modified. In contrast, microblade production materials (C19, C46, and C70) are only 2-10% modified, consistent with Gerstle River Component 3 microblade production, which yielded <10% modified microblades (Potter 2005). The overall wide range of microblade material types in C2c (32 materials, 49% of total) and the high number of materials with low numbers of microblades (20 with <10 microblades) suggest a relatively high number of microblades brought onsite in tool hafts rather than produced onsite. Other nonlocal discards by low numbers per raw material and high percent modified (25-100%) for C2c are made on

materials C4, C24, C28, C47, C62, C65, C69, Ch5, O, R1, and R9. This suggests 165 C2c microblades were brought to the site and discarded while a minimum of 183 microblades were produced onsite.

Component 4 is the only other Denali component with substantial numbers of microblades (n=36, 23% of total debitage). All materials comprise <4 microblades, while R1 comprise 23 microblades. R1 materials segment percentages have depressed medial (39%) and high complete and proximal (13% and 44% respectively), and are consistent with onsite microblade production rather than nonlocal discards (Figure 7.60). The other raw materials may represent nonlocal discards. Supporting this interpretation is that the only microblade core part is from R1 material.

Other Denali components have fewer microblades (n=2 to 19) suggesting lesser importance of microblade technology to onsite activities.

Two burins were recovered, both within Component 2c (Table 7.34). Both specimens are made on nonlocal materials (C21, Ch6). One material (Ch6) contains no debitage, and the other (C21) contains only 12 specimens (weighing 0.62 g, compared with 7.31 g for the burin). Five burin spalls of the same material refit with the burin, suggesting both burins were manufactured onsite and used/maintained onsite, and discarded onsite. Both are characteristic of high curation. Burin facet lengths and widths were similar and working edge angles are similar, and damage depth (a measure of intensity of use) were similar (6.69±1.10 mm). Both specimens were classed as Donnelly burins, as both had a small unifacial notch to isolate the striking platform for burin spall removal, and one (4-131) is a dihedral burin (two facets).

Burin spalls are well represented in Component 2c (16 of total 18), and the following analysis will be on the C2c specimens (Table 7.35). Most burin spalls are secondary (62%) and fewer are primary (38%). Damage depths are roughly similar (averaging 1.62±0.83 mm), less than damage depth on burins (see above). Damage length varies, averaging 11.88±8.57 mm, ranging from 1.23 to 23.58 mm. Edge angles are similar, averaging 74±16 degrees. One of the burin spalls saw additional use as a retouched flake, with retouch along one lateral edge (15.74 mm long at a 69 degree edge angle).

While burins are absent in Components 2a and 2b, burin spall data suggest at least one burin was used at these components. The raw material diversity of C2c burin spalls suggests that five spalls were derived from burin 4-131, four spalls were derived from a missing burin (C22), 2 spalls were derived from a missing burin (C28), and five other burin spalls from other material types suggest five missing burins. Total C2c burin spall data suggest the use of a minimum of 9 burins, only two of which were discarded onsite. This is consistent with expectations of high curation of burins.

7.6.2.3 Denali tradition expedient tools

Denali cobble spall tools are most common in Component 2c (n=5), with one specimen in Component 2a (Table 7.36). All are made on coarse-grained cobbles, and three of the five C2c specimens are damaged/retouched with relatively steep edge angles. Overall morphology and weights suggest functions as choppers, perhaps for early stage faunal processing (e.g., dismemberment, bone breakage for marrow extraction).

A number of large cobble manuports were found in Denali components 2a (n=9) and 2c (n=7) (Table 7.37). A number of C2a cobbles have heat damage, but none of them have obvious lithic damage. They may have functioned as anvils for bone fracturing.

Two (non-standardized) flake cores were recovered, both in C2a, but they have different characteristics (Table 7.38). One (6-372) was a 549 g core of C24 with 12 flake removals, with an average scar width of 13 mm. This core was split in half, then worked unidirectionally to form a chopping/cutting edge, and it was possibly also utilized as a hammer. The second flake core (8-169) was considerably larger (885 g) with 4 flake scars, averaging 50 mm wide. This core was multidirectional, likely for the purpose of removing large flakes.

Modified flakes make up the second largest category of tools (after modified microblades) in Denali components (Table 7.39). C2a modified flakes have relatively low percent retouched (as opposed to damaged) (8% vs. 24% of C2c modified flakes). Table 7.40 provides component averages for Denali modified flakes. There is no standardized sizes or shapes for modified flakes in these components, and there are high standard deviations for all metric variables. There are some component differences (Figure 7.61-7.62). Utilized edge angles have a wide distribution, from ~15 to 80 degrees, but there are clusters of low edge angles in C2a, C2c, and C3, likely cutting implements. In contrast, C4 modified flakes do not have these items. C2a modified flakes tend to be smaller and are more retouched, and retouch length tends to be shorter. In general, percent of modified margins increases through time, from 36% in C2c to 64% in C4, suggesting increasing use intensity of the modified flakes.

Table 7.29a. Denali biface metric attributes

Block	*FS*	*Mat.*	*maxL*	*maxW*	*maxT*	*L/W*	*W/T*	*Area*	*Wt.*	*Edge angle*
Component 2a										
6	469	C5	66.25	23.89	8.54	2.77	2.80	1583	15.21	43-50
6	645	C61	10.86	13.54	4.12	0.80	3.29	147	0.48	38-46
7	368	C10	28.17	67.49	11.26	0.42	5.99	1901	18.42	40-57
7	202	C5	24.00	26.06	6.82	0.92	3.82	625	4.76	33-40
7	216	C5	24.72	19.21	6.13	1.29	3.13	475	3.09	41-56
7	311	C55	5.32	10.52	2.1	0.51	5.01	56	0.11	38
11	343	C5	17.62	17.46	4.4	1.01	3.97	308	1.13	43-54
11	369	C5	15.88	26.38	5.52	0.60	4.78	419	2.77	29-31
11	369	C5	26.62	15.38	5.53	1.73	2.78	409	2.74	46-58
21	681	C5	76.93	27.19	10.98	2.83	2.48	2092	22.09	35-55
24	640	C5	12.97	11.74	4.49	1.10	2.61	152	0.62	35-49
24	644	C5	11.63	21.29	5.48	0.55	3.89	248	1.57	37-44
24	647	C5	54.29	29.12	9.81	1.86	2.97	1581	17.3	43-58
Component 2c										
5	181	R1	34.74	9.34	6.9	3.72	1.35	324	1.5	47-58
15	115	R9	19.05	29.78	9.71	0.64	3.07	567	4.83	35-55
20	95	R1	6.24	7.87	2.13	0.79	3.69	49	0.06	35-45
20	435	R1	10.63	21.18	3.21	0.50	6.60	225	0.77	32-40
21	175	R1	23.98	26.66	5.87	0.90	4.54	639	4.4	41-58
22	169	R1	31.17	9.73	4.97	3.20	1.96	303	1.46	34-40
Component 3										
9	57	C39	7.12	12.58	2.94	0.57	4.28	90	0.17	47

Table 7.29b. Denali biface non-metric attributes

Block	*FS*	*flaking pattern*	*dfse**	*condition*	*hafted*	*Modification*	*stage*
Component 2a							
6	469	comedial	<	Tip (split)	Yes	edge grinding + polish	3 thinned biface
6	645	comedial	<	Indet.	Indet.	edge grinding	4 preform
7	368	comedial	<	Complete	No	Polish	4 preform
7	202	random	>	Medial	Yes	edge grinding + polish	4 preform
7	216	comedial	<	Medial	Yes	edge grinding + polish	4 preform
7	311	comedial	<	Medial	Indet.	N/A	4 preform
11	343	random	>	Medial	Yes	edge grinding	3 thinned biface
11	369	random	<	Base (split)	Yes	edge grinding	4 preform
11	369	random	<	Base (split)	Yes	edge grinding	3 thinned biface
21	681	comedial	<	Complete	No	N/A	2 edged biface
24	640	random	>	tip/distal	Indet.	edge grinding	4 preform
24	644	comedial	<	Base	Yes	edge grinding + polish	4 preform
24	647	comedial	<	Tip	Indet.	N/A	4 preform
Component 2c							
5	181	comedial	<	Medial (split)	Indet.	edge grinding	3 thinned biface
15	115	comedial	>	Tip	Indet.	N/A	3 thinned biface
20	95	comedial	<	Tip	Indet.	N/A	4 preform
20	435	comedial	<	Base	Yes	edge grinding + polish	5 finished proj pt
21	175	comedial	>	Base	Yes	edge grinding + polish	5 finished proj pt
22	169	random	NA	Medial (split)	Indet.	edge grinding	4 preform
Component 3							
9	57	comedial	<	Indet.	Indt.	edge grinding + polish	

*dorsal flake scar extent (< = less than half, > = more than half)

Table 7.30a. Denali uniface attributes

Block	*FS*	*mat.*	*wt.*	*maxL*	*maxW*	*maxT*	*blank*	*mod.*	*Edge shape*	*% ret margins*
Component 2a										
6	349	C5	8.48	52.8	30.91	5.13	flake	retouch, damage, polish	convex	75
7	406	C5	25.65	44.59	43.57	16.17	flake	damage, polish	convex	66
20	321	C5	3.1	21.89	28.35	5.44	flake	retouch, damage	multiple	66
25	17	C1	53.19	63.93	41.37	16.34	flake	retouch, damage	multiple	50
Component 2c										
4	236	C5	6.81	35.21	35.81	6.85	flake	retouch, polish	convex	75
11	130	O2	0.47	6.81	14.38	6.65	indet			
12	116	R2	19.39	52.78	35.08	11.52	flake	retouch	convex	100
12	200	C19	11.06	42.47	25.95	8.89	flake	retouch	multiple	100
20	97	C19	0.07	8.47	5.54	0.98	indet			
20	143	C19	0.1	7.57	5.77	1.23	indet			
21	510	C62	4.36	30.83	30.46	5.25	flake	retouch, damage	convex	25
21	514	C62	16.24	44.9	31.27	12.82	flake	retouch, damage	multiple	25
24	547-553	C19	18.47	38.78	39.35	12.9	flake	retouch, damage	convex	75
Component 5a										
7	29	C28	9.63	76.22	20.52	5.52	blade	retouch, damage	multiple	66

Table 7.30b. Denali uniface attributes

Block	*FS*	*edge angle*	*retouch L (mm)*	*Sum retouch L*	*edge diam*	*edge thickness*	*type*
Component 2a							
6	349	52L, 25D, 20R	LD77.77, R51.54	129.31	53.5	2.24	Side
7	406	65R, 47L	73.37	73.37			
20	321	40R, 48L-retouch	46.29	46.29	28.35	8.38	End
25	17	47LR-retouch, 64-72 general	L16.24, R22.8	39.04	L14.92, R20.9	L1.17, R2.02	Double Side
Component 2c							
4	236	50L, 67R	L53.87, R20.44	74.31	L34.86, R17.54	L2.53, R2.88	Double side
11	130		14.11	14.11	13.35	2.19	End
12	116	40-75	137.71, ventral 39.32	137.71	35.09-52.99, ventral 22.63	9.38-17.98, ventral 5.93	End (graver)
12	200	38-64	LRD103.58, P12.47	116.05	LRD42.62, P12.47	LRD2.4-17.39, P5.29	End
20	97		8.45	8.45	8.45	0.85	Side
20	143		7.4	7.4	7.4	1.1	Side
21	510	20R, 51L-retouch	38.52	38.52	37.73	2.13-5.54	Side
21	514	20R, 26L, 53-retouch	28.74	28.74	28.81	2.61	Side
24	547-553	L43L, 45R, 68D	86.59	86.59	38.96	L21.98, R15.02	End
Component 5a							
7	29	41L, 40-60R	L86.51, RM retouch 6.39, RP retouch 7.93, RD 34.16, RM19.58	154.57	L74.49, RM6.39, RP7.17	L6.13, RM0.81, RP3.19	Side

Table 7.31 Denali microblade cores and core tablet attributes

Block	*FS*	*Mat.*	*Wt.*	*Max L*	*Max W*	*Max H*	*N flutes*	*Flute width*	*Core circum.*	*Core diam.*	*Platform angle*
Component 2c											
12	284	C45	6.59	12.03	11.70	32.44	6	4.38	27.98	11.7	81
24	300	C69	8.37	22.68	10.41	28.66	8	5.22	44.19	7.24	85
8	88	C11	0.93	15.53	11.68	4.46	5	3.11	Core tablet		
12	220	C36	0.12	8.96	9.05	1.76	3	1.92	Core tablet		
12	335	C24	0.26	13.88	9.30	1.72	2	2.59	Core tablet		
Component 4											
8	26	R1	0.08	7.50	5.70	2.10			Core tablet		
Component 5a											
12	106	C62	11.98	15.53	19.85	36.33	5	5.16	20.66	20.17	78
Component 5b											
11	127	R4	13.58	15.31	23.95	30.62	8	4.26	28.43	22.55	81

Table 7.32 Denali microblade metric summary data

Comp.	*N*	*Wt*	*Max L*	*Max W*	*Max T*	*% retouched*
C2a	21	0.13±0.13	11.74±6.40	6.10±3.55	1.27±0.72	9.5%
C2b	3	0.34±0.29	18.27±10.86	7.50±2.05	2.33±1.62	0.0%
C2c	477	0.08±0.11	10.02±5.27	4.65±1.63	1.12±0.43	18.7%
C3	2	0.18±0.18	13.84±5.14	8.36±4.41	01.29±0.70	0.0%
C4	35	0.14±0.24	10.57±7.74	6.09±2.52	1.22±0.50	20.0%
C5a	3	0.39±0.16	19.60±6.12	9.72±1.28	1.82±0.36	0.0%
C5b	5	0.10±0.07	12.10±4.78	6.01±1.17	1.17±0.32	0.0%
Total		**0.09±0.13**	**10.28±5.60**	**4.86±1.93**	**1.14±0.47**	**18.0%**

Table 7.33 Denali microblade modified and unmodified summary data

Variable	*Unmodified*	*Modified*	*Total*
N	451	99	550
Segment			
Complete	2.9%	2.0%	2.7%
Proximal	47.0%	16.2%	41.5%
Medial	36.6%	75.8%	43.6%
Distal	13.3%	6.1%	12.0%
Split	0.2%	0.0%	0.2%
Dorsal scar	2.77±0.69	2.83±0.66	2.78±0.68
Weight	0.09±0.12	0.09±0.15	0.09±0.13
Width	4.88±1.91	4.81±1.90	4.86±1.91
Length	10.28±5.68	10.31±5.27	10.28±5.60
Thickness	1.16±0.48	1.09±0.42	1.14±0.47

Table 7.34 Denali burin attributes.

Block	*FS*	*mat.*	*wt.*	*max L*	*max W*	*max T*	*burin facet L*	*burin facet W*	*damage edge angle*	*damage depth*
1	24	Ch6	1.77	17.97	3.99	16.34	14.16	3.62	>90, 43	5.42/7.38
4	131	C21	6.28	24.81	8.36	28.08	13.97	6.74	47	7.26

Table 7.35 Denali burin spall attributes

Block	*FS*	*mat*	*wt*	*maxL*	*maxW*	*maxT*	*Type*	*Damage*	*Damage depth*	*Damage L*	*edge angle*
Component 2a											
13	38	C42	0.17	15.1	5	1.5					
Component 2b											
6	174	C17	0.11	9.4	6.34	1.38	secondary	none			
Component 2c											
1	22	C21	0.32	14.28	7.42	3.77	secondary	crushing	1.45	2.96	84
3	85	C70	0.48	27.39	5.77	3.99	secondary	crushing	0.53	1.23	82
4	31	C21	0.09	5.97	6.64	2.22	secondary	crushing	0.4	6.3	98
4	212	C36	0.32	25.85	4.36	1.81	secondary	crushing	0.95	19.1	67
6	35.1	C45	0.4	23.57	4.9	2.18	secondary	crushing	2.14	22.00	72
7	82	C22	0.14	17.97	3.04	2.31	primary	crushing		16.27	71
12	145	C17	0.13	17.29	2.68	1.38					
12	153	C22	0.16	15.55	3.93	3.73	primary	none			
12	197	C28	0.07	10.53	3.87	1.09					
12	336	C28	0.03	7.67	2.23	1.46					
12	337	C22	0.07	9.75	3.19	2.4	primary	crushing		8.84	71
15	185	C22	0.14	23.59	3.67	2.35	primary	crushing		23.58	75
20	90	C21	0.17	15.78	5.53	2.35	secondary	crushing, retouch	2.34	Dor 2.69, L 15.74	Dor 30, L 69
20	110	C21	0.27	14.02	6.3	4.13	secondary	crushing	2.68	6.75	72
20	261	C21	0.13	9.46	5.43	1.97	secondary	crushing	1.87	8.93	84
20	424	R2	0.51	26.74	5.7	3.2	primary	crushing	2.23	23.91	84

*Material type C21 refit with burin (FS 4-131)

Table 7.36 Denali cobble spall tool attributes

Block	***FS***	*Mat.*	*maxL*	*maxW*	*maxT*	*Wt.*	*retouch/damage*	*edge angle*
Component 2a								
6	555	M5	86.02	47.19	7.32	36.63	no	
Component 2c								
1	25	M7	140.27	99.57	27.42	504.04	Yes (distal/ventral edge)	39
5	196	M7	56.12	55.84	11.52	44.19	No	
6	73	M7	108.93	53.73	12.6	105.08	No	
8	190	M6	93.75	53.29	16.33	93.36	Yes (distal edge) (crushing/chopping)	91
21	508	M3	76.55	47.84	14.65	64.02	Yes (proximal edge)	92

Table 7.37 Denali cobble attributes

Block	***FS***	*mat.*	*max L*	*max W*	*max T*	*wt.*	*Notes*
Component 2a							
5	66	M8	55.69	36.14	21.91	39.04	
5	76	M4	55.04	54.11	15.83	44.75	heat damaged
5	92	C5	82.41	41.2	25.16	75.77	
7	168	M9	94.11	46.43	16.86	77.78	Material fragmenting
7	308	M9	83.82	55.54	12.66	66.35	Material fragmenting, measures on largest intact piece
9	162	M8	133.21	122.76	46.5	1188.88	
9	196	Q2	49.07	43.65	31.45	80.71	
15	326	M8	72.79	63.15	49.95	315.72	
21	682	M5	106.08	25.72	24.78	144.2	heat damaged
Component 2c							
3	95	Q2	42.43	31.9	24.26	43.81	
4	274	M7	54.52	49.35	24.87	16.11	
7	117	Q6	99.77	37.89	26.82	116.79	
8	72	M7	44.76	32.33	23.19	52.57	
19	117	Q2	93.05	65.31	12.44	94.49	
22	312	M8	105.13	55.72	19.25	137.33	
22	313	M8	63.3	44.76	19.62	61.98	

Table 7.38 Denali (C2a) flake core attributes

Block	***FS***	*Mat.*	*max L*	*max W*	*max T*	*wt.*	*N flake scars*	*Avg. scar width*	*Type*
6	372	C24	110.05	38.09	48.92	549.39	12	13.23	unidirectional
8	169	M6	111.39	89.83	54.06	884.79	4	49.88	multidirectional

Table 7.39 Denali modified flake attributes

Bl.	*FS*	*Mat.*	*wt.*	*maxL*	*maxW*	*maxT*	*blank*	*Mod.*	*position*	*edge angle*	*retouch L (mm)*	*edge shape*	*Mod_type*	*Edge shape*	*%ret margins*
Component 2a															
4	345	C41	2.53	15.6	25.02	6.45	flake	Damage	LD edge	47RD, 33L	RD29.71, L4.73	convex, straight	moderate	multiple	0.66
5	89	C33	299.77	109.92	72.13	48.46	cobble	Retouch	RD dorsal, R edge	50R, 23L	D97.27, R30.16	convex	moderate	convex	0.66
6	545	C5	0.71	15.89	20.75	1.96	flake	Damage	L edge	42L, 20R	17.06	straight-convex	moderate	multiple	0.33
7	141	C71	2.05	21.23	25.29	2.98	flake	Damage	D edge	24	41.33	convex	moderate	convex	
7	156	C5	9.08	32.07	39.55	7.88	flake	Damage	RD edge	30RD, 45LD	17.81	concave	moderate	concave	0.2
7	167	C33	18.47	64.8	49.08	4.97	flake	Damage	LR edge	19LR	R73.13, L45.32	convex, convex-straight	light	multiple	0.5
7	370	C10	3.8	27.5	25.43	5.79	flake	Damage	LD edge	43RDL	16.38	straight	light	straight	0.25
7	400	C10	3.68	31.75	25.79	4.58	flake	Damage	L edge	22LR, 54D	8.77	straight	light	straight	0.25
7	407	C10	8.54	40.58	47.54	4.29	flake	Damage	D edge	20LD, 35R	18.86	straight	moderate	straight	0.25
9	170	C47	12.25	39.52	23.89	10.58	flake	Damage	D edge	50R, 34D, 62L	19.69	straight	moderate	straight	0.25
9	181	C67	1.01	18.13	18.73	3.08	flake	Polish	P edge	40	9.44	convex-straight	moderate	multiple	0.25
11	357	C68	15.38	31.21	55.77	10.14	flake	Damage	D edge	20D	42.82	convex	light	convex	0.33
24	650	Q3	25.55	50.59	39.37	13.6	flake	Damage							
Component 2b															
21	632	C19	0.09	8.27	6.48	1.52	flake	Retouch	R dorsal	72	7.42	convex	moderate	convex	0.33
Component 2c															
1	30	R1	1.14	13.53	22.11	4	flake	Damage	LR edge	29L, 42R	L5.96, R12.85	straight, concave	moderate	multiple	0.5
2	80, 81	C33	22.2	78.34	44.12	9.65	flake	Damage	R edge	35R	51.62	concave-straight	light	multiple	0.33
4	97	C19	0.23	15.3	7.51	1.56	flake	damage, polish	L edge	20	16.11	convex-concave	moderate	multiple	
4	141	R2	0.12	7.16	5.28	2.31	flake	Damage	LD edge	57R, 37L	8.14	concave-straight	moderate	multiple	0.33
4	203	C21	0.05	5.74	9.24	1.41	flake	Damage	D edge	18	8.89	straight	light	straight	0.33
4	217	R1	1.36	19.19	18.35	7.04	flake	Damage	L edge	37	16.86	straight	light	straight	
4	231	C19	0.1	12.21	6.94	1.09	flake	Damage	D edge	20LR	4.99	straight	light	straight	0.25
4	251	C19	0.14	5.94	15.8	1.26	flake	Damage	PD edge	N/A	P2.66, D2.7	straight	light	straight	
6	297	R1	6.56	58.92	31.88	4.02	BLF	Damage	RP edge	22RP	31.79	convex	moderate	convex	0.25
11	167	R1	1.59	21.77	28.36	3.51	flake	Damage	L edge	18L, 21R	6.61	straight	light	straight	0.25
11	231	C17	1.19	20.24	12.22	6.14	flake	Retouch	R edge, L distal	43R, 48R	R6.35, L19.74	convex	light, heavy	convex	0.66

11	274-275	R2	8.12	62.39	36.21	4.18	flake	Retouch	L dorsal, R edge	40R, 50L	R13.93, L59.06	convex-straight	moderate	multiple	0.66
15	56	C36	0.17	8.8	9.12	2.38	flake	Retouch	R: dorsal D: dorsal	R63.9 D76.1	R9.01 D7.36	R: convex D: straight	light on both damaged edges	convex	0.5
22	303	R1	1.43	22.08	16.23	6	flake	Damage	L edge	55R, 24L	24.48	convex	light	convex	0.33
22	307	C30	1.26	13.43	23.59	3.95	flake	Damage	P edge	53	24.56	convex	moderate	convex	
24	341	R9	16.93	61.56	54.34	8.99	flake	damage, polish	RDL edge	30L, 19D, 36R	71.66, D52.97, R47.83	concave-straight	light	multiple	1
24	494	R7	0.71	13.5	17.37	4.2	flake	Retouch	dorsal	74.7	11.47	convex	light retouch	convex	0.33
Component 3															
2	25	C5	56.64	72.63	85.31	15.26	flake	Damage	LD edge	47L, 23-55D	L65.76, D16.03, RD44.36	convex-concave	moderate	multiple	0.66
9	65	C19	0.92	22.31	15.39	3.54	flake	Damage	LD edge	23	10.61	convex	moderate	convex	
9	227	C39	0.4	13.07	17.48	2.25	flake	Damage	D dorsal/edge	19	17.7	convex	moderate	convex	
9	80-81	C19	0.25	16.95	8.18	2.13	flake	Damage	D dorsal/edge	18	7.96	straight	moderate	straight	
13	20	C39	5.36	11.63	51.65	10.95	flake	damage, polish	RD edge	47D, 50R	D52.7, R9.06	convex-straight	moderate	multiple	
Component 4															
3	52	C19	7.14	34.62	36.23	4.95	flake	Damage	LR edge	22R, 25L	R10.6, L23.08	convex-straight, concave-straight	light	multiple	0.5
3	53	C62	17.69	57.42	40.66	7.68	flake	Damage	LR edge	32L, 23-35R	R63.69, L61.56	convex-concave, convex-straight	light	multiple	0.66
4	18	Ch4	123.17	99.5	58.81	24.06	flake	damage, polish	RLD edge, dorsal ridge	42R, 52L	R109.86, L98.06, P ridge8.3, D ridge 3.89	convex-concave	moderate	multiple	0.75
14	21	C5	7.91	58.52	19.08	4.71	blade	damage, polish	LR edge	46R, 35L	R53.5, L53.51	straight	light	straight	0.5
21	24	C62	7.77	61.67	13.5	10.4	blade	Retouch	R edge, dorsal ridge	55R, 76 dorsal ridge/retouch	R33.39, ridge 62.04	convex-straight	moderate	multiple	0.66
21	32	C49	15.35	99.72	26.7	7.97	blade	damage, polish	LRD edge	29R, 42D, 45L	R65.89, RD7.45, D20.35,	straight-convex	light	multiple	0.75

											L66.79				

Table 7.40 Denali modified flake summary by components

Comp.	*N*	*Wt*	*L*	*W*	*T*	*% retouched*	*Edge angle*	*Retouch length*	*% retouched margins*
C2a	13	30.99±81.12	38.37±25.75	36.03±16.21	9.60±12.16	8%	36±13	31.50±24.66	36±17
C2c	17	3.72±6.44	25.89±23.40	21.10±13.94	4.22±2.60	24%	39±18	21.57±20.10	44±22
C3	5	12.71±24.65	27.32±25.67	35.60±32.47	6.83±5.96	0%	34±15	28.02±22.73	66
C4	6	29.84±45.94	68.58±25.89	32.50±16.42	9.96±7.22	17%	41±15	46.37±32.47	64±11
All Denali	41*	16.88±49.26	35.60±27.95	28.73±18.69	6.95±7.94	15%	38±15	31.05±26.59	45±20

Excluding the single C2b specimen

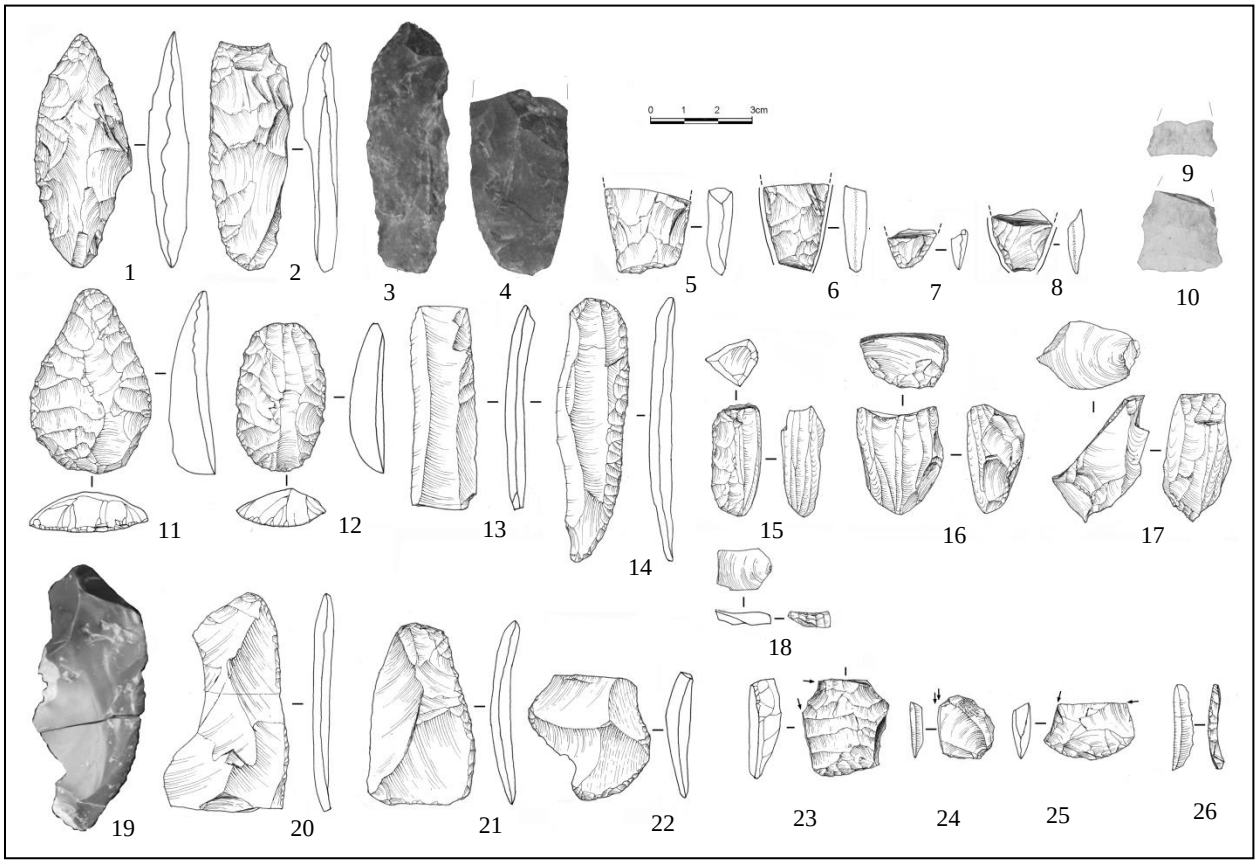

Figure 7.58 Denali complex materials (Components 2-5). Bifaces (1-5, 9, 10, 25), projectile points (6-8), unifaces (11-14, 19-22), microblade cores (15-17), microblade core tablet (18), burins (23-25), burin spall (26). Component 2a (1-8, 21, 25), Component 2c (9-12, 15, 18-20, 22-23, 26), Component 4 (13, 24), Component 5a (14, 17), Component 5b (16).

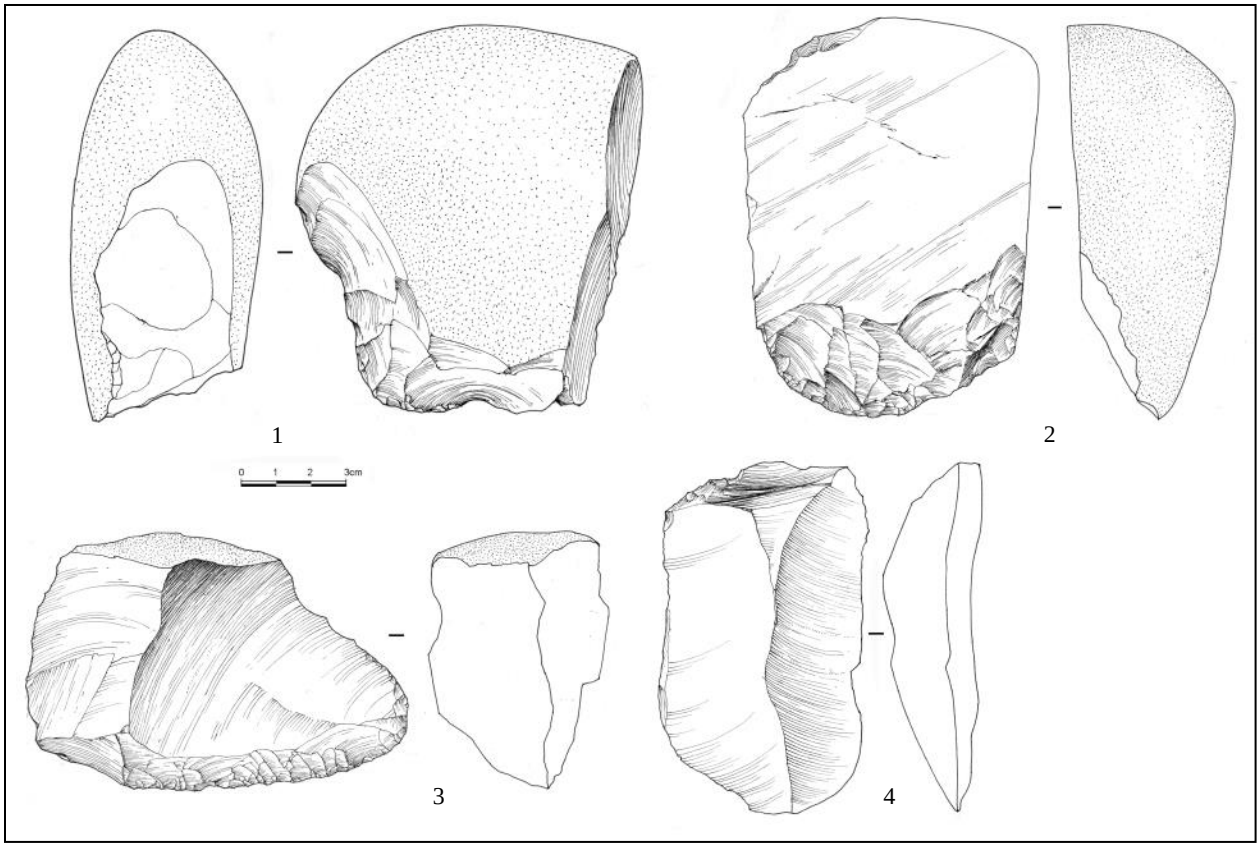

Figure 7.59 Denali complex materials (Components 2-5). Choppers (1-2), flake core/uniface (3), modified blade (4). Component 2a (1, 2, 3), Component 4 (4).

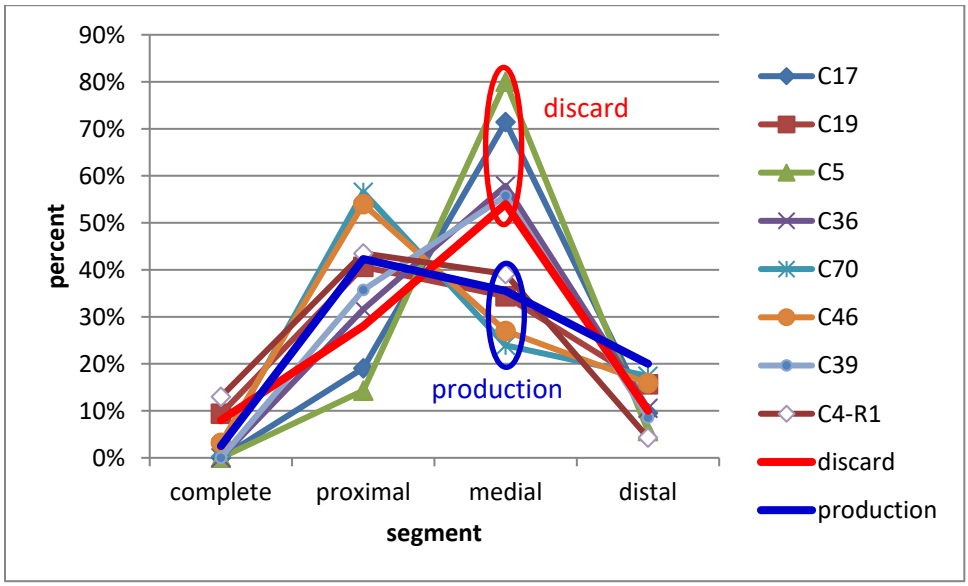

Figure 7.60 Material types (>20 microblades) by segment representation (all from C2a except for R1, from C4)

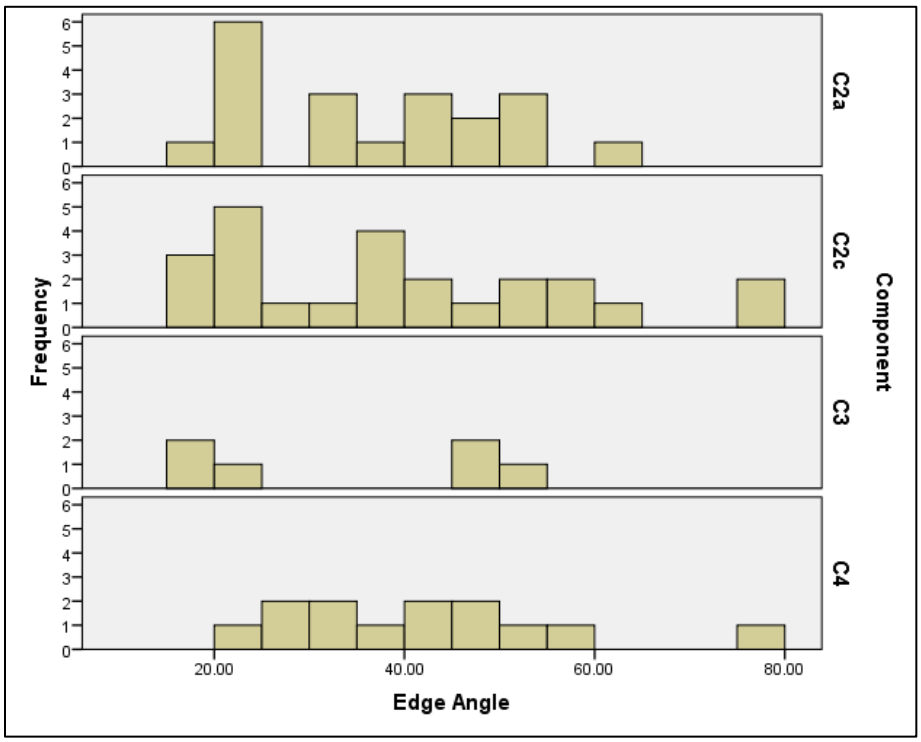

Figure 7.61 Denali modified flake utilized edge angles

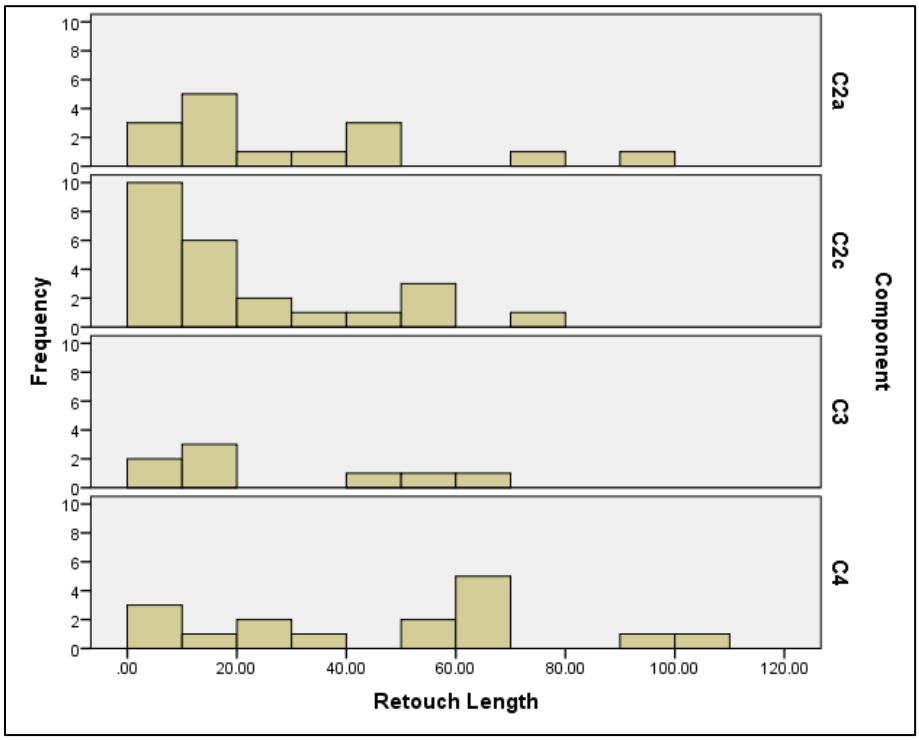

Figure 7.62 Denali modified flake utilized edge lengths

7.6.3 Northern Archaic (C6a-C8b) tools

7.6.3.1 Northern Archaic tradition formal tools

Northern Archaic components contain 80 tools and 1 flake core. Selected tools are illustrated in Figure 7.63 and Appendix B. Tools include 56 modified flakes, 9 bifaces, and 15 unifaces. No microblade cores or core parts, modified microblades, burins, or burin spalls are present in the Northern Archaic at DRO. A single microblade was recovered from the earliest Northern Archaic component, C6a.

The 9 bifaces comprise 5 edged bifaces, 1 preform, and 3 finished projectile points (Table 7.41). Finished projectile points are found in all 3 of the biface-containing Northern Archaic components, in contrast with the Denali biface assemblages. The edged bifaces are all from the blank cache in Component 8a. Because of the dichotomy, the cache bifaces will be considered first. All five are complete, with flake scars extending over halfway across the biface surface. All had some modification, including 3 with edge grinding, while all 5 exhibited polish on the edges. All were roughly similar in dimension, 67±10 mm long, 42±9 mm wide, and 14±2 mm thick. Areas and weights were also similar (2813±684 area and 40±17 g). Edge angles were relatively steep, generally between 44-76 degrees.

Of the remaining four bifaces, three were finished projectile points. The C6a and C8b points are remarkably similar in form and dimension, straight based, about 41 mm long, 24 mm wide, and 6 mm thick with edge angles of ~30-45 degrees. Both are edge ground. These straight-based lanceolate forms are common in the Northern Archaic (Esdale 2009). Both also appear to have been resharpened near the tip. The third projectile point is somewhat different, it is a basal fragment with concave-straight form and slightly expanding stem. It is also edge ground.

Northern Archaic uniface data are provided in Table 7.42. In addition to the 15 unifaces analyzed here, 3 additional C8b unifaces were illustrated by Kotani (n.d.), bringing the endscraper total up to 13 (or 72% of Northern Archaic unifaces). This contrasts with the even distribution of end and side scrapers among Denali components. None of the Northern Archaic unifaces were broken. All unifaces are made on flake blanks. End scrapers are relatively similar in size and shape, averaging 24.53±8.37 mm long, 23.98±5.14 mm wide, 5.61±2.26 mm thick, and weighing an average of 4.02±3.12 g. The lengths and widths are similar, contrasting with Denali end scrapers which tend to be elongated as well as larger in size (averaging 39 mm long, 32 mm wide, 10 mm thick and weighing 13 g). Northern Archaic side scrapers (n=4) tend to be more elongate, averaging 38.75±11.81 mm long, 26.13±8.64 mm wide, and 7.83±4.82 mm thick, weighing 10.44±9.46 g. Edge angles for end scrapers are steeper and more standardized (63 ±9 degrees) than for side scrapers, which also range more widely (57±16). Edge thickness also differs (4.80±2.24 mm for end scrapers and 3.64±1.24 mm for side scrapers). Edge diameter (23.34±6.19 mm) and edge length (33.54±13.68 mm) are also relatively standardized for end scrapers. Two unifaces come from the C8a cache (22-96 and 22-118) and are relatively similar in overall size with the bifaces and modified flakes (44-49 mm long x 30-35 mm wide x 11-13 mm thick).

The C7a uniface is the sole representative of Ch4 material, suggesting it was made offsite. The six C7b unifaces are from 3 raw materials: the Ch4 and C39 unifaces may have been made offsite, while some/all of the 4 C5 unifaces may have been manufactured or maintained onsite (there are 180 C5 debitage weighing 19.47 g). The 4 C8a unifaces are on two different raw materials, both with large debitage quantities, suggesting some onsite manufacture and/or

maintenance. The 4 C8b unifaces are on 2 different raw materials, both with large debitage quantities, suggesting some onsite manufacture and/or maintenance.

7.6.3.2 Northern Archaic tradition expedient tools

Northern Archaic cobble spall tools are found in three components (C6a, C7a, and C8b) (Table 7.43). The C6a and C7a spall tools are generally larger than the C8b spall tools (averaging 131 L x 104 W x 45 T mm vs. 72 x 52 x 16 mm). Two of the four have retouch/damage, one edge angles are generally high (72-87 degrees).

A number of large cobble manuports were found in Northern Archaic components C6a (n=1), C7a (n=1), C7b (n=4), C8a (n=1), and C8b (n=3) (Table 7.44). Most have heat damage (n=6, 60%) and some were found associated with hearths. They may have functioned as hearthstones for cooking or other tasks.

A single flake core was recovered from C6a, from material C53 (Table 7.45). There were 9 flake scars averaging 44 mm wide. There was multidirectional flake removal from three sides. The material was heat treated, likely due to original poor quality. Interestingly, no flakes were recovered at C6a from the excavation, suggesting that it may have been flaked in other unexcavated parts of the site.

Modified flakes make up the largest category of tools in Northern Archaic components (Table 7.46). They are present in C6a, C7b, C8a and C8b. Because modified flakes from the C8a cache dominate the record (n=40, 71% of modified flakes), they are separated for some of the analyses. However, other Northern Archaic modified flakes (n=16) are generally similar in overall dimension to the cached flakes (see Figure 7.64), though the latter are larger. Average dimensions of other modified flakes are 34.55±19.35 L, 26.54±9.67 W, and 5.22±2.94 T in mm. In comparison, average dimensions for C8a cached modified flakes are 44.48±17.73 L, 31.05±15.77 W, and 8.59±3.81 T in mm). Blank types are generally flakes (79%) but also include blade like flakes (20%) and blade (2%) All but one of blade-like flakes are from the cache. Most modified flakes are elongate, and some have blade-like dimensions, though this may be accidental (Figure 7.65).

Modified flakes per component are compared in Table 7.47. Edge angles vary widely, but have the least variability in C8a. Retouch length (summed) also varies, with C7b and C8b similar (averaging 45-49 mm) whereas C8a are considerably longer (averaging 78 mm). Percent retouched margins generally increase through time, from 25% in C6a to 48% in C8b, with C8a much higher, at 57%. Figure 7.65 illustrates edge angles for each Northern Archaic component. Two modes are apparent, one around 30 degrees and the other around 60 degrees, suggesting perhaps cutting/slicing vs. scraping/grinding functions.

Table 7.41a. Northern Archaic metric biface attributes

Block	*FS*	*Mat.*	*maxL*	*maxW*	*maxT*	*L/W*	*W/T*	*Area*	*Wt.*	*Edge angle*
Component 6a										
3	16	C39	37.27	23.82	6.02	1.56	3.96	888	7	26-46
Component 8a										
11	45	C2	15.24	19.46	6.42	0.78	3.03	297	1.82	39-48
22	89	C19	53.32	34.01	13.59	1.57	2.50	1813	22.12	53-65
22	93	C5	72.61	43.55	14.66	1.67	2.97	3162	57.25	45-76
22	101	C5	78.14	41.55	14.38	1.88	2.89	3247	45.5	48-74
22	134	C5	61.34	56.1	15.34	1.09	3.66	3441	55.2	59-75
22	98	C68	67.82	35.47	11.24	1.91	3.16	2406	22.06	44-65
Component 8b										
24	195	C5	12.47	15.27	2.78	0.82	5.49	190	0.56	25
24	190	O2	43.82	23.59	5.55	1.86	4.25	1034	6.46	33-45

Table 7.41b. Northern Archaic non-metric biface attributes

Block	*FS*	*flaking pattern*	*dfse**	*condition*	*hafted*	*modification*	*stage*
Component 6a							
3	16	comedial	<	Base	y	edge grinding	5 finished proj pt
Component 8b							
11	45	comedial	<	Base	y	edge grinding	5 finished proj pt
22	89	random	>	complete	n	polish	2 edged biface
22	93	random	>	complete	n	edge grinding + polish	2 edged biface
22	101	random	>	complete	n	edge grinding + polish	2 edged biface
22	134	random	>	complete	n	Polish	2 edged biface
22	98	comedial	>	complete	n	edge grinding + polish	2 edged biface
Component 8b							
24	195	comedial	NA	Indet.	Indet.	polish	4 preform
24	190	comedial	>	complete	y	edge grinding	5 finished proj pt

*dorsal flake scar extent (< = less than half, > = more than half)

Table 7.42a. Northern Archaic uniface attributes

Block	*FS*	*mat.*	*wt.*	*maxL*	*maxW*	*maxT*	*blank*	*mod.*	*Edge shape*	*% ret margins*
Component 7a										
24	277	Ch4	3.27	25.03	20.33	6.42	flake	retouch, damage	convex	25
Component 7b										
7	13	C5	2.3	17.68	21.79	4.85	flake	retouch, damage, polish	convex	
7	14	C5	1.59	21.04	20.18	3.1	flake	retouch, damage, polish	convex	75
7	15	Ch4	6.24	24.77	25.58	10.3	flake	retouch, damage	convex	75
8	9	C39	0.81	12.76	15.37	3.49	flake	retouch, damage	convex	
19	78	C5	6.37	36.39	31.88	5.66	flake	retouch, damage, polish	convex	33
19	104	C5	3.11	27.29	22.92	4.24	flake	retouch, polish	convex	25
Component 8a										
14	3	C5	11.24	40.09	31.73	8.56	flake	retouch, polish	convex	50
22	96	R1	21.77	48.5	35.08	11.48	flake	retouch, polish	multiple	33
22	118	R1	14.56	43.52	29.93	12.49	flake	retouch, polish	multiple	66
22	133	Q1	0.08	4.16	13.46	1.18	indet			
Component 8b										
9	32	R1	2.03	18.81	26.09	4.69	flake	retouch, damage	convex	
19	2	C5	1.31	21.6	14.84	3.81	flake	retouch, damage, polish	multiple	33
23	2	C5	3.26	21.4	23.97	4.79	flake	retouch, damage	convex	25
24	135	C5	4.12	41.36	24.67	3.53	flake	damage, retouch	multiple	50

Table 7.42b. Northern Archaic uniface attributes

Block	*FS*	*edge angle*	*retouch L (mm)*	*Sum retouch L*	*edge diam*	*edge thickness*	*Uniface type*
Component 7a							
24	277	30R, 47L, 62D-retouch	27.05	27.05	20.92	7.39	End
Component 7b							
7	13	53L, 62D retouch	39.24	39.24	23.52	5.46	End
7	14	54-70	51.79	51.79	22.2	3.56	End
7	15	43L, 67 retouch	L10.81, retouch27.41, R13.99	52.21	24.04	6.74	End
8	9	69 retouch	16.93	16.93	15.37	3.66	End
19	78	50D-retouch	43.32	43.32	29.77	8.3	End
19	104	57D	24.63	24.63	22.92	4.24	End
Component 8a							
14	3	47L, 80D, 60R	54.37	54.37	33.46	2.36	End
22	96	69L	43.19	43.19	37.1	5.15	Side
22	118	62R, 73L	R35.97, L39.76	75.73	R 34.21, L 37.52	R 1.91, L 4.45	Double side
22	133		12.99	12.99	12.99	1.09	Indet
Component 8b							
9	32	retouch 54	43.06	43.06	30.73	6.43	End
19	2	63R-retouch	19.74	19.74	19.53	3.35	Side
23	2	30L, 23R, 59D-retouch	28.11	28.11	20.81	3.55	End
24	135	40L, 35R	L25.9, R14.46	40.36	25.54	3.32	Side

Table 7.43 Northern Archaic cobble spall tools

Block	***FS***	*Mat.*	*maxL*	*maxW*	*maxT*	*Wt.*	*retouch/damage*	*edge angle*
Component 6a								
21	11	Q1	156.34	104.95	54.35	825.75	Yes (distal/ventral edge)	72
Component 7a								
19	16	M7	106.49	103.68	35.53	761.18	Yes (left edge) (flaking/crushing), heated	
Component 8b								
9	10	M5	69.83	46.92	8.00	34.54	No	
24	140	M4	73.64	56.94	24.51	126.87	Yes (flaking)	87

Table 7.44 Northern Archaic cobble attributes

Block	***FS***	*mat.*	*max L*	*max W*	*max T*	*wt.*	*Notes*
Component 6a							
6	22	Q2	39.37	39.08	17.91	41.92	
Compoennt 7a							
19	16		106.49	103.68	35.53	761.18	heat treated. Modification along one edge (L=103.88) with flaking and some crushing damage
Component 7b							
6	12	M7	43.08	32.38	25.8	69.31	
19	12		104.03	79.01	73.44	805.78	heat damaged
19	13	M10	114.07	83.19	15.07	262.99	heat damaged
19	14	M5	154.75	21.32	16.58	81.13	Perhaps rounded
Component 8a							
10	20	M9	100.31	76.52	29.36	300.07	
Component 8b							
24	141	M7	129.14	74.55	57.95	731.86	heat damaged
24	242						Material fragmenting
24	269	M8	150.5	90.49	48.85	858.25	heat damaged

Table 7.45 Northern Archaic (C6a) flake core attributes

Block	*FS*	*Mat.*	*max L*	*max W*	*max T*	*wt.*	*N flake scars*	*Avg. scar width*	*Type*
21	10	C53	153.47	101.02	68.49	1404.84	9	43.97	multidirectional

Table 7.46 Northern Archaic modified flake attributes

Bl.	*FS*	*Mat.*	*wt.*	*maxL*	*maxW*	*maxT*	*blank*	*Mod.*	*position*	*edge angle*	*retouch L (mm)*	*edge shape*	*Mod_type*	*Edge shape*	*%ret margins*
Component 6a															
1	17	C11	1.52	18.65	15.48	5.66	flake	Retouch	R edge	39	19.78	convex	moderate	convex	
3	47	C5	1.38	12.75	24.24	3.52	flake	Damage	P: edge	84.3	20.98	straight	heavy	straight	0.25
Component 7b															
19	77	C5	1.94	22.14	26.83	3.41	flake	Damage	D edge	35D	39.53	convex	moderate	convex	0.25
19	79	C5	6.01	26.66	34.33	6.97	flake	damage, polish	LD edge	31D, 52L	D34.84, L7.59	convex-straight	moderate	multiple	0.66
19	80	C5	4.48	46.06	24.75	3.72	flake	Retouch	LRD edge, LR dorsal	17L, 58L retouch, 20R	90.62	convex	moderate	convex	0.75
19	85	C5	0.31	8.15	24.03	1.24	flake	Retouch	D edge	17	29.1	convex	moderate	convex	
19	93	C5	2.73	44.8	18.21	4.12	BLF	Polish	LD edge	30	39.61	convex-straight	light	multiple	0.33
19	103	C5	0.76	18.4	17.75	2.33	flake	damage, polish	D edge	27R, 18L	9.49	straight	moderate	straight	0.25
23	30	C5	6.71	63.87	24.52	4.9	flake	Damage	R edge	45R, 57D	63.79	convex	moderate	convex	0.33
Component 8a															
10	13	C28	14.7	55.93	41.44	6.78	flake	Damage	L edge	34L, 28R	L9.39, LD6.06	concave, straight	light	multiple	0.25
10	16	C5	12.74	49.13	44	6.51	flake	damage, polish	LRD edge	40L, 32D, 22R	L28.72, D38.04, R47.4	convex, concave	moderate	multiple	0.75
12	59	C72	2.69	21.46	29.94	7.02	flake	Retouch	D edge	28	13.56	convex	moderate	convex	0.33
22	79	R9	16.37	51.71	36.05	11	flake	damage, polish	LRD edge	38R, 35L	R46.99, L67.55	convex, straight	moderate	multiple	0.75
22	80	C5	10.05	41.07	32.34	8.91	flake	damage, polish	LR edge	39R, 44-68L	L39.89,R25.85	Lconcave, Rstraight	light	multiple	0.5
22	81	R9	19.04	44.53	37.83	9.45	flake	damage, polish	D edge	26D	22.21	convex-straight	moderate	multiple	0.25
22	82	R1	1.58	17.3	13.97	6.68	flake	Polish	LR edge	60	R16.25, L13.64	convex	light	convex	0.66
22	83	C5	4.26	45.82	21	6.29	BLF	Damage	LR edge	23R, 45-50L	LP 16.06, LD 21.92, R36.39	convex-straight	light	multiple	0.66
22	84	C5	7.66	47.07	21.45	7.89	BLF	damage	R edge	30-60R, 37-70L	43.69	convex-concave	light	multiple	0.25
22	85	C5	4.15	48.53	16.47	4.81	BLF	Retouch	L edge-dorsal, D edge, R edge-ventral	36R, 20D, 27L	L39.3, LD5.85, D11.79, RD16.98, R13.67, RP14.16	convex-straight	light	multiple	0.75

22	86	O2	3.08	34.31	17.92	4.64	flake	Damage	edge	63L, 32R	L9.14, D29.81, R28.81, P17.94	straight	light	straight	1
22	87	C5	5.18	42.25	17.5	7.05	BLF	damage, polish	LR edge	65L, 32R	L37.14, R43.52	convex, straight	light	multiple	0.5
22	88	C5	2.15	24.47	19.59	5.76	flake	damage, polish	L edge	55L, 32R	11.53	straight	light	straight	0.25
22	90	R1	46.73	53.63	79.73	15.95	flake	damage, polish	LRD edge	40R, 31D, 66L	R22.79, D33.88, LD22.39, L35.63	concave	moderate	concave	0.75
22	91	R1	19.74	56.8	37.79	10.41	BLF	damage, polish	LR edge	39L, 40-52R	L54.07, R44.68	straight, convex-concave	moderate	multiple	0.5
22	92	C5	3.51	38.68	18.84	6.68	BLF	damage, polish	LR edge	27L, 29-40R	L24.46, 37.33R	convex-straight	light	multiple	0.33
22	94	C4	11.75	44.46	31.43	11.9	flake	damage, polish	LRD edge	57L, 35-45R	R44.67, L42.15, D19.26	convex-straight	light	multiple	0.75
22	95	R1	18.82	57.66	41.84	10.58	flake	Retouch	LRD edge	35R, 32L, 65 retouch	R57.69, D33.11, L33.06	convex-straight	moderate	multiple	0.75
22	97	R9	21.48	58.19	45.79	9.1	flake	Retouch	L dorsal, R edge	25R, 50-81L, 71 retouch	R23.21, L52.4	concave-convex	moderate	multiple	0.5
22	99	R1	42.04	73.54	49.85	13.45	flake	Retouch	LR dorsal, edge	35R, 63R-retouch, 52LP, 58LD	R46.71, LP23.51, LD16.37, L18.55	convex, straight	moderate	multiple	0.5
22	100	R1	24.45	56.33	56.45	9.27	flake	damage, polish	LRD edge	38R, 54D, 40L	R54.32, D41.12, L58.25	convex-straight, concave-straight	moderate	multiple	0.75
22	102	R1	37.89	88.64	30.12	15.98	BLF	damage, polish	LRD edge	55RDL	R63.16, D26.07, 73.74	convex, straight	moderate	multiple	0.75
22	103	C5	15.8	52.63	36.02	10	flake	damage, polish	LR edge	29L, 34R	L45.56, R24.05	convex-straight, concave-straight	light	multiple	0.5
22	104	R1	12.51	62.04	27.08	8.24	BLF	damage, polish	LRD edge	31L, 37D, 62R	R25.47, D35.21, L63.16	concave, straight	moderate	multiple	0.75

22	105	R1	11.92	44.41	34.55	6.12	flake	damage, polish	LR edge	23L, 45R	L40.73, R25.43	convex, straight	moderate	multiple	0.5
22	106	C5	6.21	35.4	23.4	8.48	flake	damage, polish	LDR edge	44-57R, 40-60L	D44.42, RP16	convex, straight	light	multiple	0.75
22	108	C5	0.74	15.31	10.05	7.45	flake	damage, polish	LR edge, dorsal ridge	58L, 78R	L17.59, R12.41, ridge 16.62	convex	light	convex	0.75
22	111	C5	0.89	15.52	13.3	5.26	flake	Damage	edge	35	R14.84, D9.76	concave	light	concave	0.5
22	112	R1	20.94	49.03	48.42	10.53	flake	damage, polish	LRD edge	57-78R, 21D, 30L	R30.35, D30.7, L41.6	convex-straight	moderate	multiple	0.75
22	113	R9	43.81	60.6	55.64	21.75	flake	damage, polish	LRD edge	61L, 55R, 20RD	R35.24, D61.04, L72.91	convex-straight, concave	moderate	multiple	0.75
22	114	R9	0.44	9.89	17.18	3.64	flake	damage, polish	LD edge	20L	D13.62, L6.97	straight	moderate	straight	0.66
22	116	R1	40.45	78.22	58.55	11.09	flake	damage, polish	LRD edge	28R, 30D, 59L	R38.86, D46.19, L73.66	convex, straight, concave	moderate	multiple	0.75
22	117	R9	23.38	56.59	43.92	12.23	flake	damage, polish	LRD edge	21-31L, 34D, 45-50R	L59.83, D42.95, R46.94	convex-straight	moderate	multiple	0.75
22	119	C5	14.88	44.7	41.77	7.85	flake	damage, polish	RV edge	39R, 52L	31.49	convex	light	convex	0.33
22	120	C5	3.65	43.16	19.19	5.91	BLF	damage, polish	LR edge	26-33L, 37-44R	L35.17, R41.58	concave-straight	light	multiple	0.5
22	121	C5	2.13	35.14	17.13	4.42	flake	Retouch	LR edge, R ventral	22R, 34-45L	L37.46, 38.83, retouch 15.34	convex-straight, concave-straight	moderate	multiple	0.33
22	122	C5	5.92	41.72	25.04	7.16	flake	damage, polish	LRD edge	55L, 32R	R12.22, L36.48	convex-straight, concave-straight	light	multiple	0.66
22	123	R9	14.72	53.26	42.03	8.51	flake	damage, polish	LR edge	25R, 20L	L56.01, R73.4	convex, concave	moderate	multiple	0.66
22	124	C5	0.52	16.05	12.02	3.19	flake	Damage	LD edge	41R, 25D	R19.97, D3.74	convex, straight	light	multiple	0.5
22	126	C5	9.53	48.7	22.66	10.92	BLF	damage, polish	LR edge	45-79L, 36R	L33.46, R41.25	convex-straight	light	multiple	0.5
22	127	C5	0.76	20.35	16.2	3.86	flake	damage	edge	20	22.38	straight-convex	light	multiple	0.33
22	130	C5	0.63	16.94	12.84	3.18	flake	damage	edge	52	13.84	straight	light	straight	0.25
22	135	C5	12.98	54.7	39.21	8.18	flake	damage, polish	LR edge	33-62L, 60-83R	L53.45, R54.41	convex-straight	light	multiple	0.66

Component 8b															
24	231	Ch3	29.27	58.22	43.67	13.97	flake	damage	PR edge	54R, 65L	P10.62, R54.07	convex-straight	light	multiple	0.5
24	234	C28	6.79	63.2	19.38	6.13	blade	Retouch	LR edge	54 retouch, 35L, 70R	L62.04, R33.39	convex, straight	moderate	multiple	0.66
24	281	C24	2.79	27.35	21.69	4.67	flake	Damage	RD edge	17R, 20DL	R13.48, D5.13	straight	light	straight	0.5
26	3	C5	0.57	16.04	14.38	2.56	flake	Damage	D edge	20D	16.28	convex	moderate	convex	0.25

Table 7.47 Northern Archaic modified flake summary by components

Comp.	*n*	*wt*	*L*	*W*	*T*	*edge angle*	*Sum retouch length*	*%ret margins*
C6a	2	1.45±0.10	15.70±4.17	19.86±6.19	4.59±1.51	62±32	20.38±0.86	25
C7b	7	3.28±2.51	32.87±19.37	24.35±5.59	3.81±1.84	35±16	44.94±25.86	43+-/22
C8a	43	13.32±12.76	44.32±17.55	31.57±15.40	8.47±3.70	40±14	78.45±45.83	57±19
C8b	4	9.86±13.20	41.20±23.08	24.78±12.96	6.83±4.98	42±22	48.75±38.29	48±17

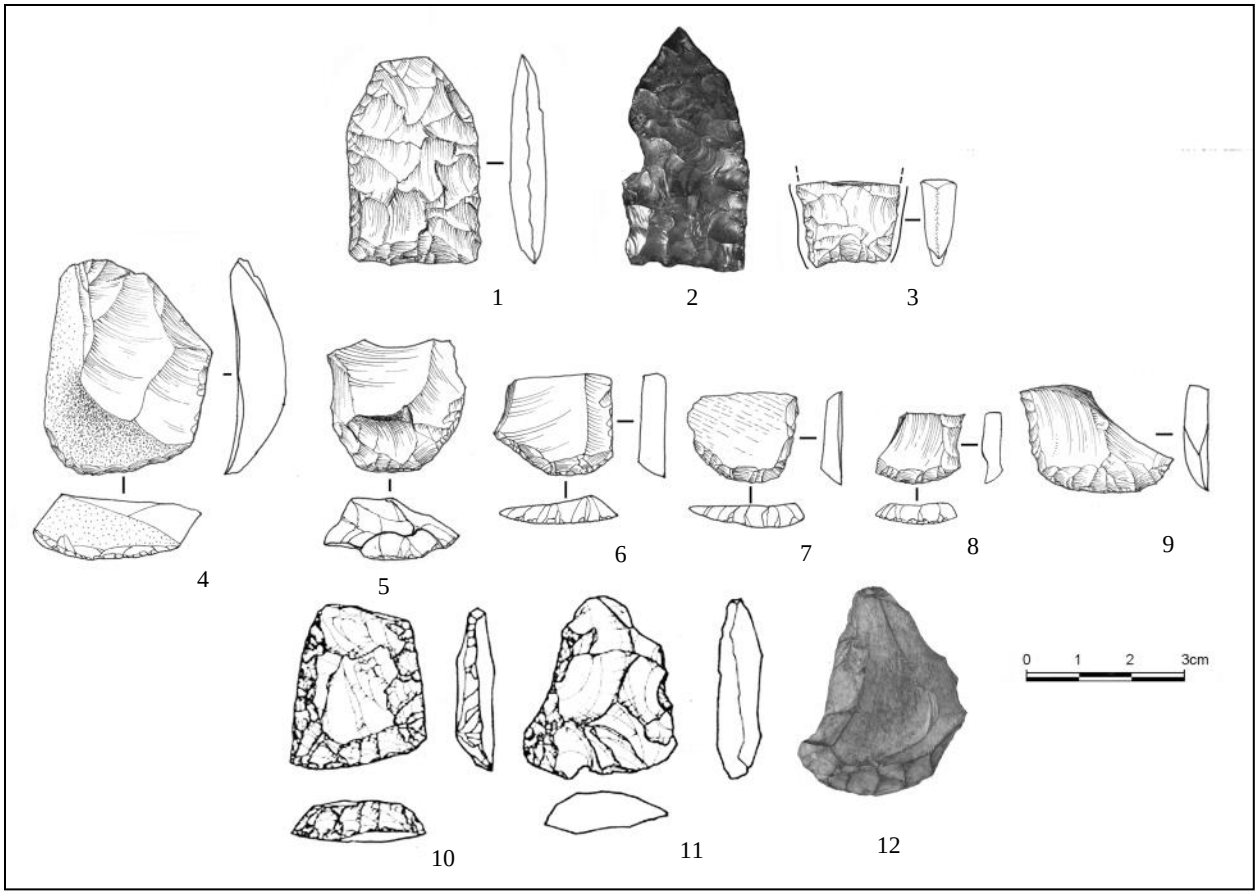

Figure 7.63 Northern Archaic tradition (Components 6-8). Projectile points (1-3), unifaces (4-12). Component 6a (1), Component 7b (5-8, 12), Component 8a (3-4), Component 8b (9), 1985 excavation, likely Component 8b (10-11).

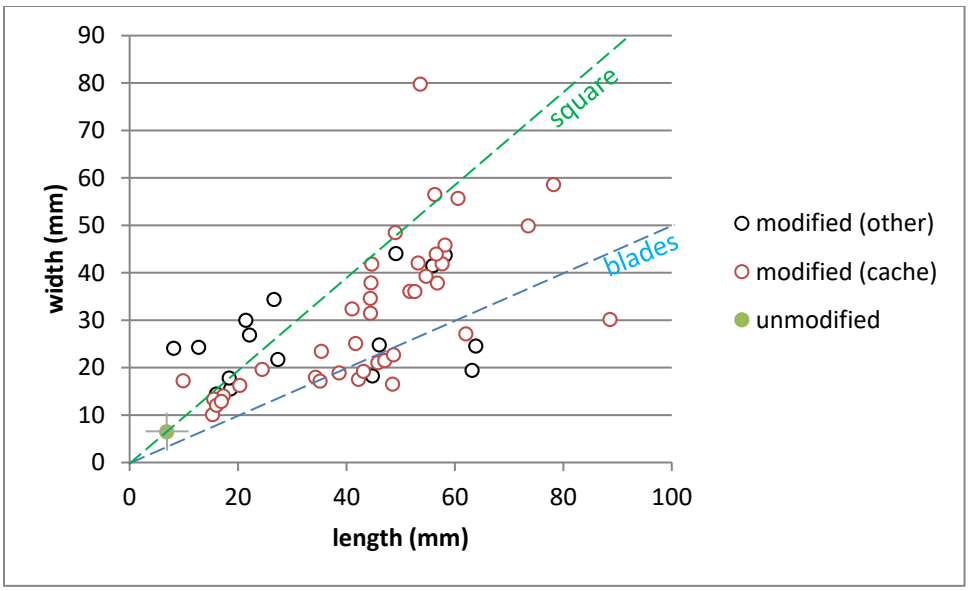

Figure 7.64 Northern Archaic modified weight lengths and widths.

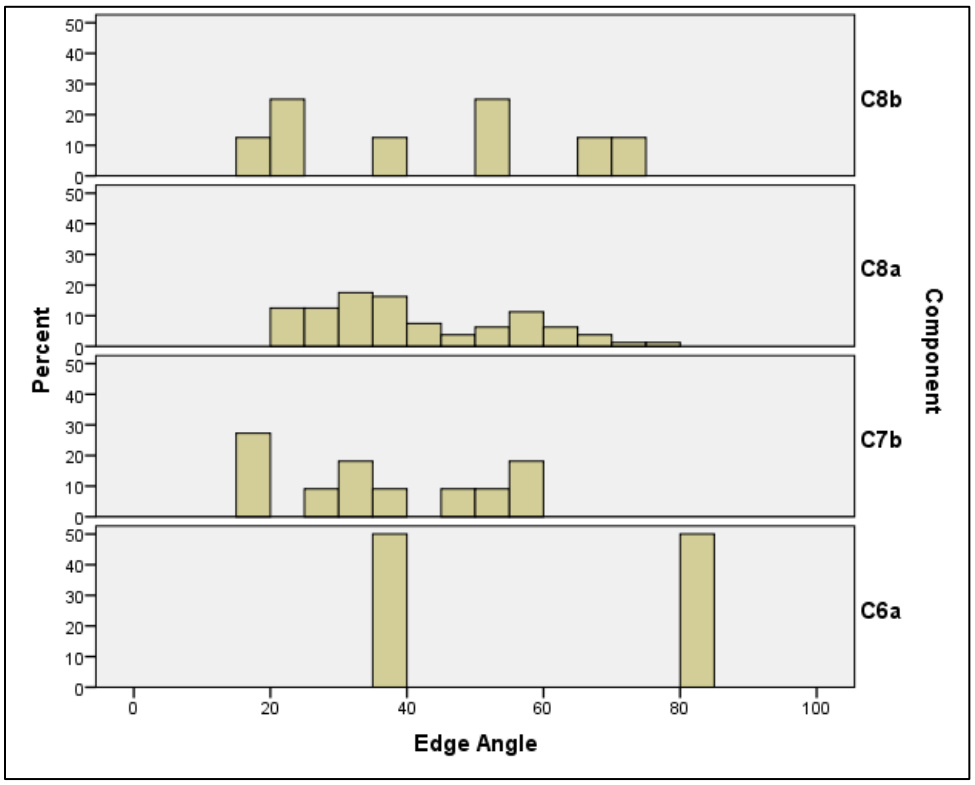

Figure 7.65 Northern Archaic modified flake utilized edge angles

7.7 Component 8a Lithic Cache Analysis

A very dense concentration of large lithic items was discovered in 2017 in close proximity in Block 22 (Figures 7.66-7.68). The stratigraphic position of the materials was within Paleosol 7a, directly above the upper tephra (T2), which corresponds with Component 8a across the site. The feature was labeled F2017-3. This paleosol has been dated to 3330±30 BP (3637-3477 cal yr BP), and there are bracketing ages of 3600-2870 BP. This firmly places the cache within the Northern Archaic tradition, regionally.

Within an area of 40 cm in diameter, we recovered 63 lithics, including 47 retouched pieces. Given their position stacked up against one another, we suspect they were originally deposited within a bag which later deteriorated. This group of materials allows us a window into lithic procurement, planning, and technological reduction strategies of the Northern Archaic tradition.

The 63 lithic items included 47 tools, totaling 781.2 g (or 99.8% of total weight) and 16 smaller debitage (1.72 g, or 0.2% of total weight). The material type distribution is uneven, with a few materials predominating, C5 (56%), R1 (21%) and R9 (14%) (Table 7.48). The few small debitage pieces associated with the cache are primarily from the most common materials (C5, R9), suggesting that they may have been accidentally included in the cache, either as part of earlier reduction events in the bag, or perhaps fragmentation peri- or post-depositionally.

To explore the cache, we compared the cache materials (n=82, the 63 items in the cache and a few debitage pieces within Block 22) with all other C8a lithics (n=1114). Table 7.49a compares cache and other C8a flakes (unmodified flakes, modified flakes, and unifaces) and Table 7.49b compares PRB flake attributes. As per debitage analyses in Section 7.5, the two non-cache clusters within C8a reflect different lithic behaviors: C1ag1 represents soft hammer, later stage bifacial tool manufacture and maintenance and Cga3 represents soft hammer bifacial reduction as well smaller amounts of earlier stages of reduction, including some decortication. Collectively, these two clusters are dominated by late stage tool manufacture and/or maintenance, primarily bifacial. The raw materials among all three groups differ (see Section 7.5), and this difference, in addition to those discussed below, indicate that the cached tools were not manufactured onsite were made elsewhere and transported to the site and deliberately cached.

Flake types are different, with 17% cortex in cached items (vs 0%) and total absence of bifacial thinning flakes (0% vs. 19%). Sullivan-Rozen typology proportions are also different, with cached items dominated by complete and broken flakes (45% vs. 21% of other C8a items). Cached items retain more cortex (18% vs. 0%). Considering PRB flakes, cached items have more eraillure scars and salient bulbs and fewer lipping, indicating hard hammer percussion compared with other C8a lithics. Cached items also have fewer complex platforms and more cortical platforms. Cached items also exhibited more feathered and hinge terminations and fewer step terminations. Size class distributions are also different (Table 7.50), with the majority of other C8a items less than 1 cm maximum dimension (89.4% vs. 29.2% of cached items). Only 0.5% of other C8a items are larger than 20 mm maximum dimension compared with 52.4% of cached items.

Collectively, these data indicate substantial differences between cached items and the rest of Component 8a. These data suggest primarily early stage reduction, large platform dimensions and other characteristics of hard hammer percussion, with limited evidence of soft hammer reduction (18% lipping). The cortex on the rhyolites and overall larger sizes also suggests the materials may have traveled some distance in blank form (relatively unretouched) unless the source is located nearby, a possibility.

These large cached items, unifaces, bifaces, modified and unmodified flakes, are all of roughly of similar size (average length = 44.48±16.93, width = 31.75±15.33, thickness = 8.78±3.79) (Figure 7.69). We interpret these items to be blanks, transportable for situational tool production. This exemplifies provisioning of place, consistent with Northern Archaic mapping-on strategies and overall collector-like behaviors (Potter 2008).

The most common Northern Archaic formal tools are notched bifaces and small endscrapers (Dixon 1985; Esdale 2008). Figure 7.70a and 7.70b show blank measurements compared with a large sample of Northern Archaic notched bifaces (Potter, n.d.) Given the size of the C8a blanks, most of these can be easily reduced into the most common tool forms of the cultural tradition.

Table 7.48 F2017-3 cache lithic raw material types

Material	*Debitage*	*Modified flake*	*Uniface*	*Biface*	*Total*
C5	12	20		3	35
R1		11	2		13
R9	2	7			9
C19				1	1
C4		1			1
C68				1	1
C15	1				1
C16	1				1
C2		1			1
O		1			1
Totals	16	41	2	4	63

Table 7.49a Cache and other C8a materials flake summary.

	Cache	*Other*
N	82	1114
Flake type		
bifacial thinning	0%	19%
bipolar	0%	0%
decortication	17%	0%
microblade	0%	0%
shatter	1%	2%
simple	76%	79%
unifacial thinning	0%	0%
Sullivan-Rozen typology		
Broken	22%	16%
complete	23%	5%
fragment	48%	77%
shatter	1%	2%
split	0%	0%
Cortex		
0	82%	100%
1-3	18%	0%
Dorsal scar count		
0	3%	0%
1	21%	42%
2	55%	31%
3	15%	20%
4+	6%	7%
%≥3	21%	27%
Thermal		
0	100%	100%
1		
Material quality		
Low		
Moderate		0.4%
High	100%	99.6%

Table 7.49b Platform remnant bearing flake and modified flake summary data

	Cache	*Other*
N	40	254
Eraillure scars	32%	4%
Lipping	18%	32%
Salient bulbs	18%	2%
Platform type		
Abraded	0%	0%
Complex	10%	15%
Cortical	5%	0%
Crushed	30%	19%
Simple	53%	66%
Platform edge angle		
N		184
Mean		49
Stdev		12
Platform measurements		
platform width	8.54±7.30	3.07±2.01
platform thickness	2.77±2.01	1.44±0.88
Termination		
Feathered	37%	24%
Hinge	10%	1%
Overshot		
Step	46%	74%

Table 7.49c Component 8a size class distributions

SC	*Cache*	*Other*
1	1.2%	33.1%
2	28.0%	56.3%
3	11.0%	9.2%
4	7.3%	0.8%
5	2.4%	
6		0.2%
7	1.2%	
8+	48.8%	0.3%

Figure 7.66 F2017-3 lithic cache overview, Block 22.

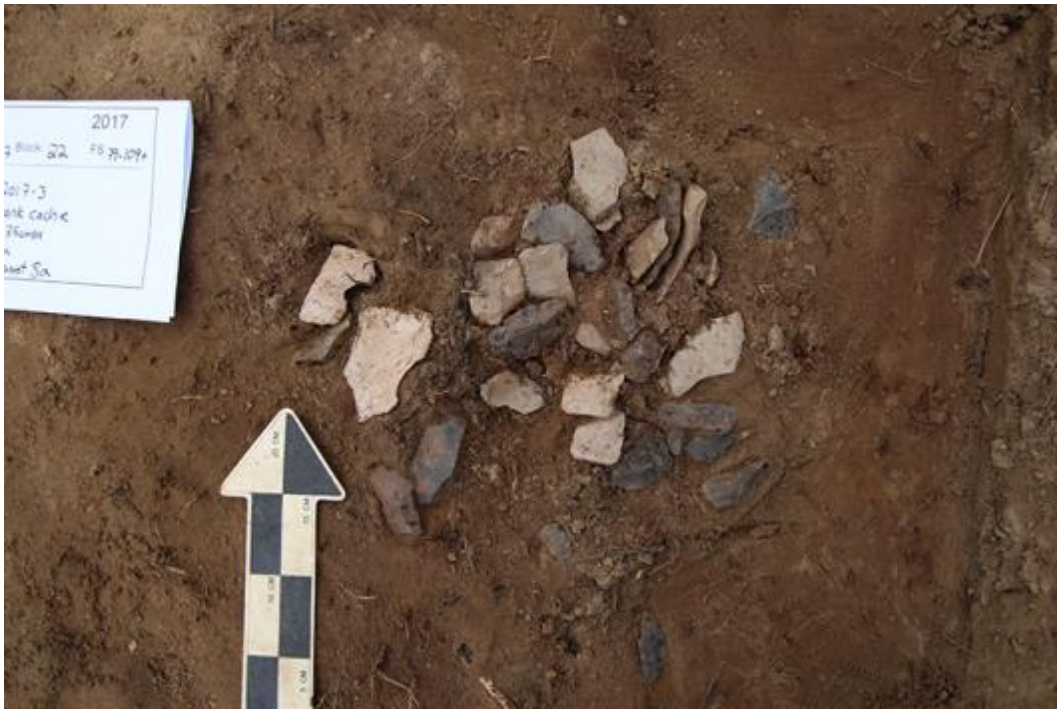

Figure 7.67 F2017-3 lithic cache during excavation.


Figure 7.68 Component 8a blank cache

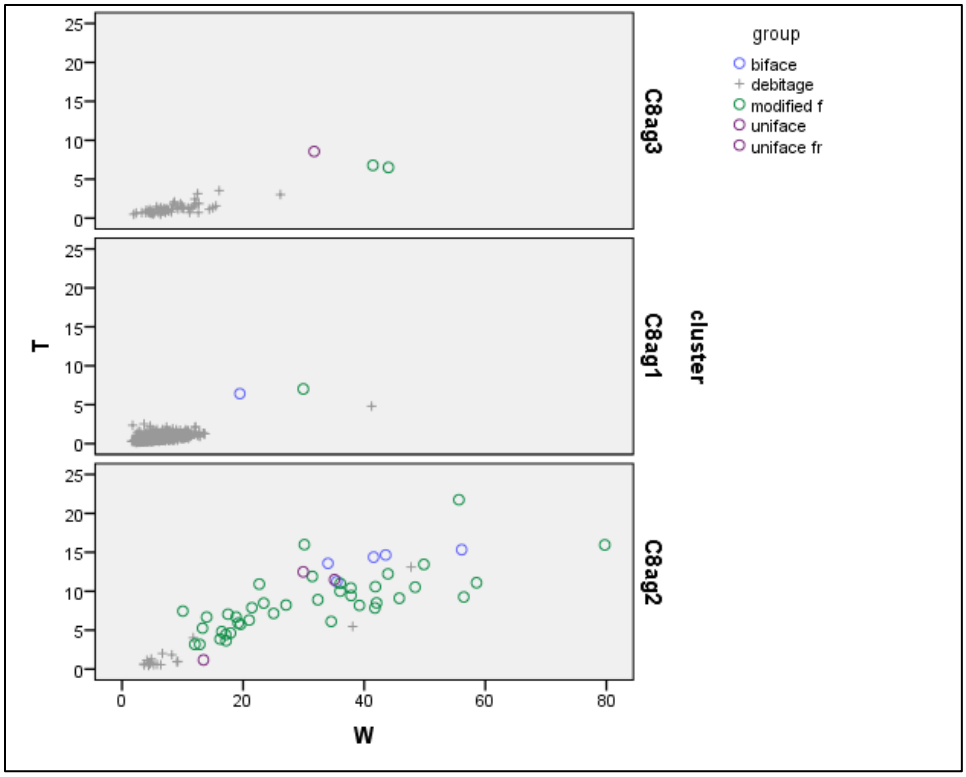

Figure 7.69 Maximum width and thickness by cluster and artifact type.

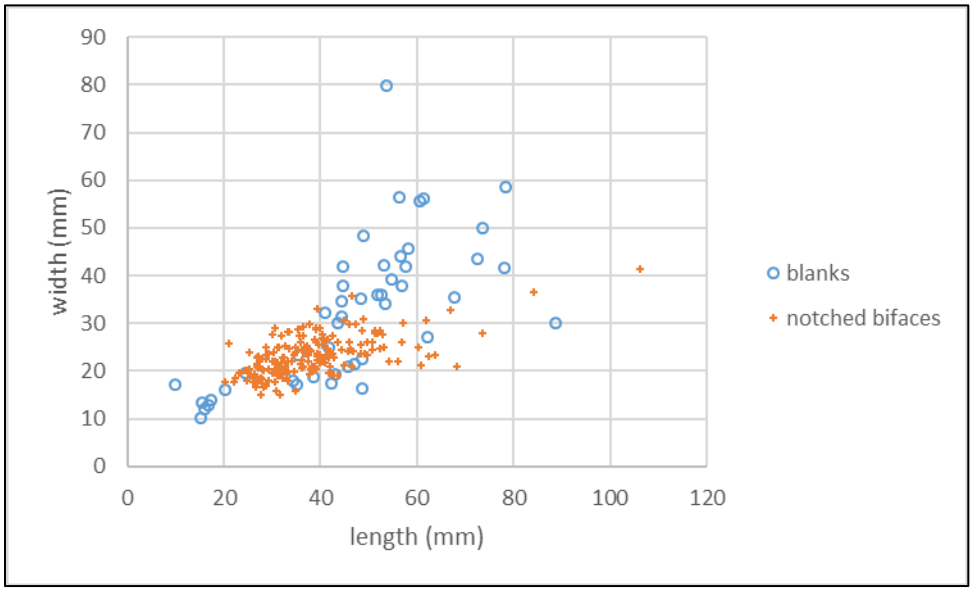

Figure 7.70a Length and Width of C8a blanks and Northern Archaic notched bifaces

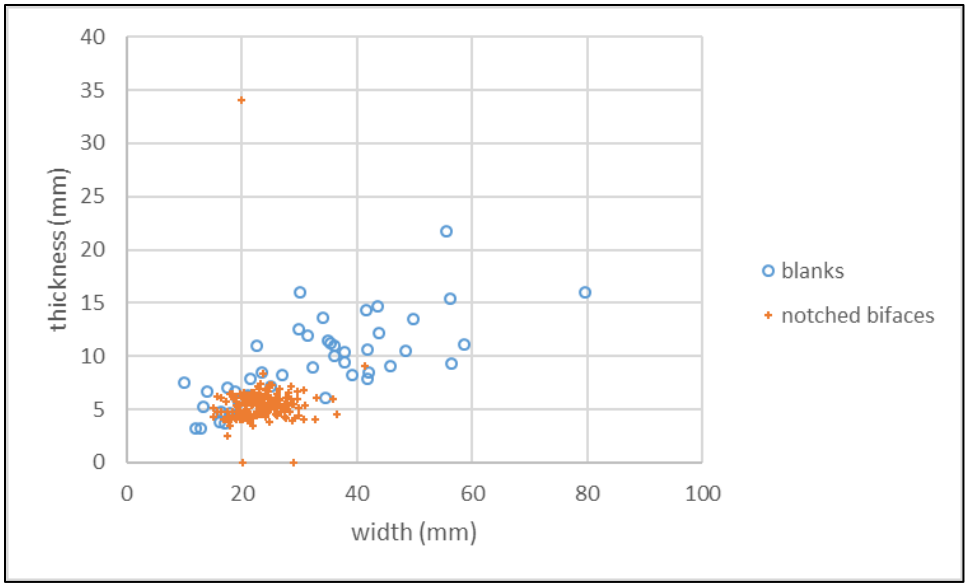

Figure 7.70b Width and Thickness of C8a blanks and Northern Archaic notched bifaces

7.8 Intersite Comparisons

Comparative data are available in Denali components from Gerstle River and Dry Creek. Artifact covariation at Delta River Overlook can be compared with Dry Creek and Gerstle River early activity areas. Hierarchical cluster analysis was used to classify assemblages into groups on a co-similarity matrix, using the Ward method and squared binary Euclidean measure for presence-absence tool classes for DRO, Gerstle River, and Dry Creek components and activity areas. Data from Dry Creek were derived from Hoffecker (1983) and Gerstle River from Potter (2005). Assemblages were clustered at Component levels (illustrated in Figure 7.71) and assemblage levels (illustrated in Figure 7.72).

When clustered at the component level, as expected, the components with microblade technology were clearly differentiated from those without (Figure 7.71). Chindadn and Denali components without substantial microblades are clustered together. Note there is no clear separation of the two, while there is a lot of variation within both complexes. DRO C1 is clustered with Gerstle River C4 (Denali), then with DRO C2b, C5a and C3. DRO C2c is most closely similar to Gerstle River C3 and C4 and Dry Creek C2 (all Denali). DRO C2a is most similar to DRO C4. Interestingly, bison is present in most of these Denali components, even within different clusters, suggesting that other factors like seasonality and raw material availability may play a role in structuring the assemblages.

When clustered at the level of activity area, there is again substantial variation in both the 2 Chindadn and 11 Denali components (Figure 7.72). Two major groups (1 and 2) emerged, composed of five sub-groups. The most divergent clusters include groups 1a, 1b, and 1c with microblades, microblade cores, and burins, and groups 2a and 2b without these artifact classes. Within the microblade group, Group 1a also contains bifaces, burins, flake core-scrapers, denticulates, and modified flakes. Group 1b contains bifaces, burins, flake core-scrapers, denticulates, modified flakes, and half contain utilized

cobbles. Group 1c contains bifaces, burin spalls, chopping tools, hammerstones, modified flakes, and unifaces, and half contain burins. Previous analyses (Potter 2005) indicate Groups 1a and 1b are distinguished by microblade core production in the former and microblade core maintenance in the latter. Later stages of core reduction are evident in Group 1b.

Within the non-microblade group, Group 2a contains bifaces, chopping tools, flake cores, flake corescraper, core-biface, and unifaces (and some contain microblades). Group 2b contains a wide variety of tools but at varying levels. Most common are bifaces, projectile points, and modified flakes, other classes include burin spalls, chopping tools, modified flakes and unifaces. Clearly, Denali tradition components and activity areas, while superficially similar in tool typology, exhibit considerable patterned diversity, likely related to technological organization. Therefore, we should not expect a simplistic binary microblade presence:absence to be demonstrative of any behavioral characteristic.

Group 1b components include the later Denali components DRO C3, C4, and C5a, as well as C2b, most similar to Gerstle River C2e, C3a, C4h, and Dry Creek C2a, C2b, C2n. Group 1c components include DRO C2c, most similar to Gerstle River C3d. Group 2b components include DRO C2a, most similar to Dry Creek C1y and C2j. There appear to be modal Denali configurations with respect to lithic tool classes with DRO C2a being most divergent with relatively few microblades and more bifacial reduction and projectile point manufacture and maintenance, and most similarities in microblade production and composite tool maintenance in the other DRO Denali assemblages.

To explore the artifact covariation that is driving these patterns, artifact classes themselves were clustered (Figure 7.73). Two main groups are apparent, one associated with microblade technology, but also fabricators associated with organic tool manufacture (burins, burin spalls), domestic tools (unifaces), and processing tools (modified flakes, choppers). The second group is composed of two subgroups, one associated with bifaces, bifacial projectile points and utilized cobbles, and the other associated with flake cores, percussion tools, denticulates, and other tool classes. Interestingly, the Denali components considered here vary in specific patterned ways, suggesting multiple toolkits or toolkit configurations, as well as complexity in systematic tool use and discard.

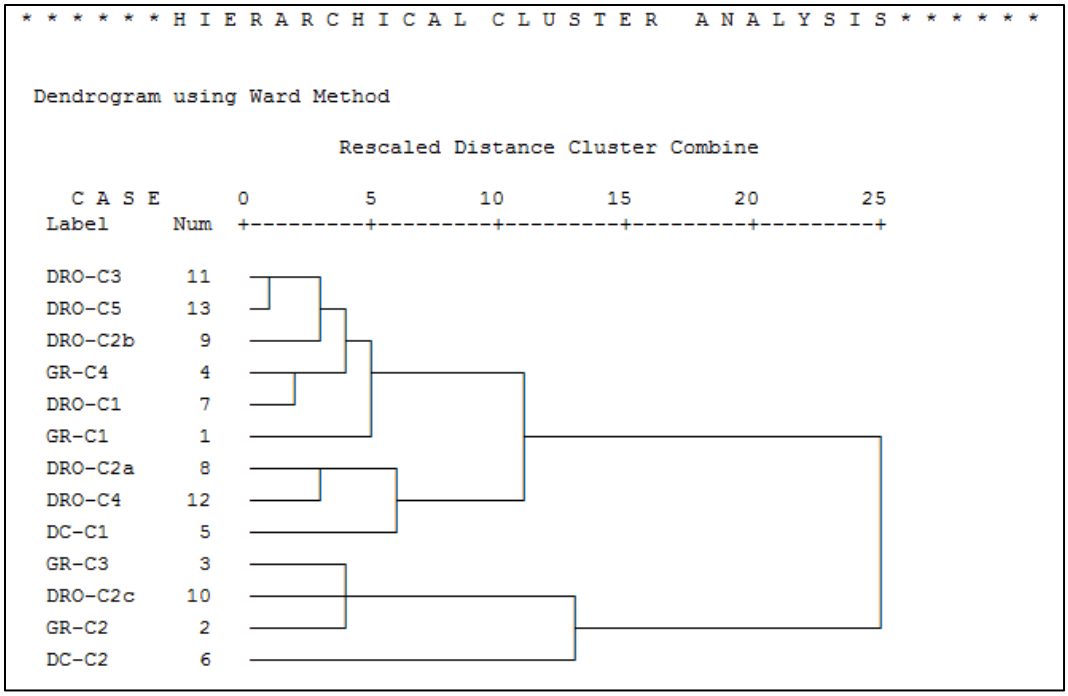

Figure 7.71 Hierarchical cluster results of DRO, Gerstle River and Dry Creek

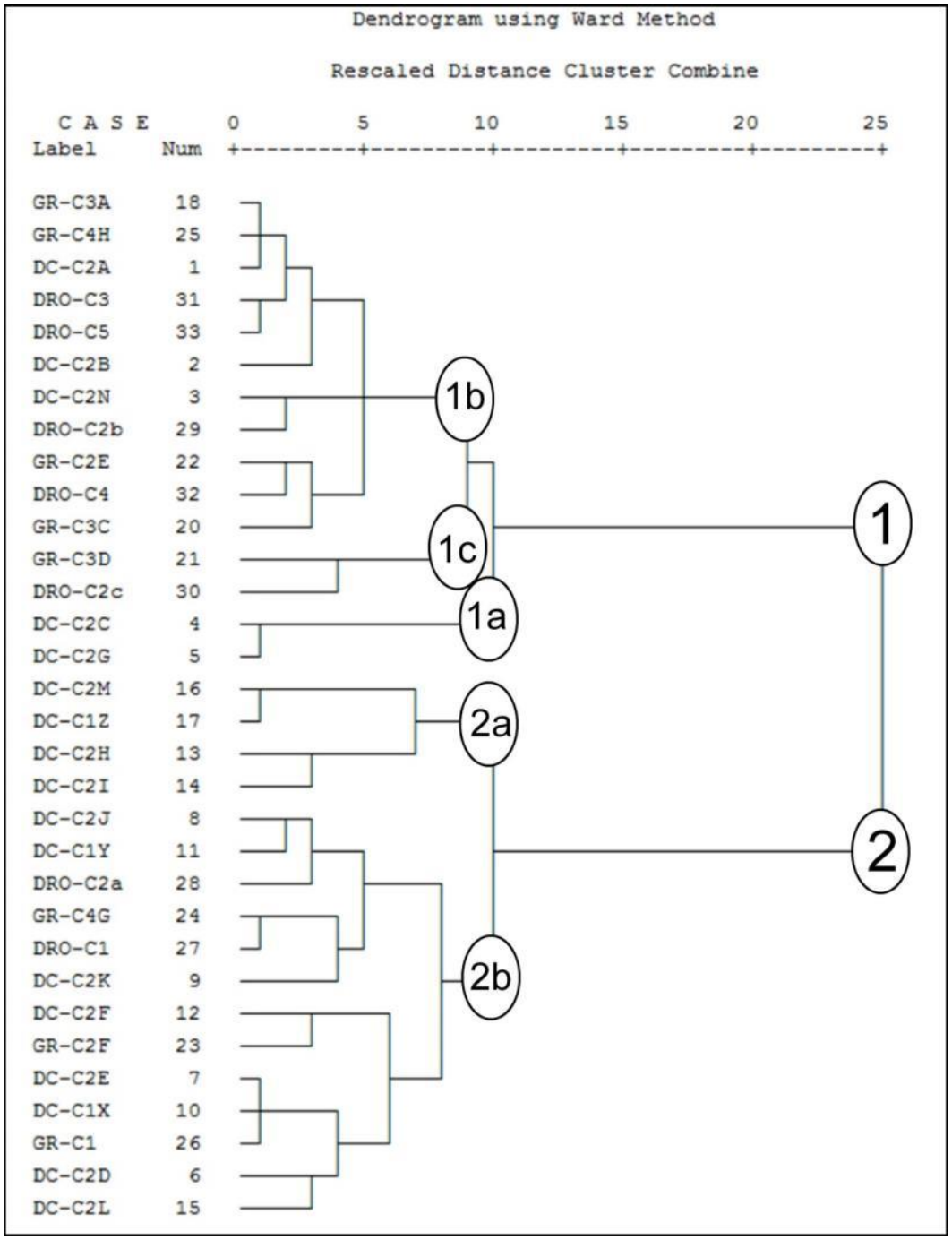

Figure 7.72 Hierarchical cluster results of DRO, Gerstle River, and Dry Creek lithic concentrations.

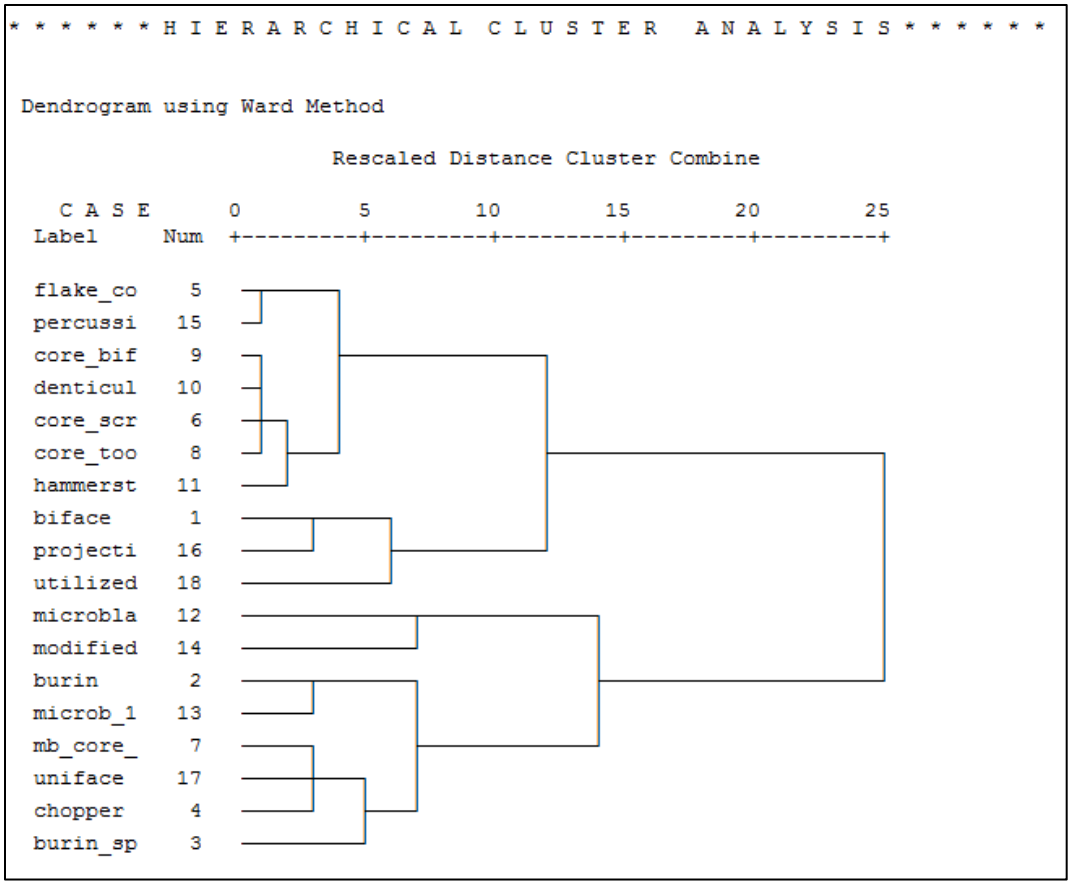

Figure 7.73 Hierarchical cluster results for implement classes

CHAPTER 8. FAUNAL ANALYSES

Holly J. McKinney and Ben A. Potter

8.1 Introduction

The presence of well-preserved faunal remains in close association with cultural features and lithic artifacts are rare in Beringia. A number of distinct faunal assemblages are present at DRO, allowing for evaluation of changing economic strategies through time. This present study focuses on assemblage composition, skeletal element presence/absence, and taxonomic richness and diversity, and implications for site functions and prehistoric faunal use.

8.2 Methods

8.2.1 Faunal Catalog and Attributes

An Excel spreadsheet was established to record the following contextual information for bags containing faunal materials recovered from the DRO site: excavation block, field specimen number (FS#), northing (N), easting (E), depth (Z-CMBS), recovery method (3pt or screen), cultural component, and stratum. Identifications were made using modern synoptic comparative collections belonging to the UAF Department of Anthropology, the University of Alaska Museum of the North, and one of us (McKinney). Faunal materials were separated from other material classes (e.g. lithics, flora, etc.) and re-housed in bags containing the previously mentioned contextual information.

Faunal materials that were identifiable to the genus or species level were handled differently from those faunal remains that were too fragmentary to identify beyond the class level (e.g. Mammalia, Aves, and Osteoichthyes). For those faunal materials that were too fragmentary to identify beyond the class level, the following zooarchaeological identification information was recorded within an Excel spreadsheet: notes (a description of the number of fragments present within the bag), size class (VL=very large, L=large, M=medium, S=small), burning (1=white charred, 2=black charred, 3=brown/tan charred, 4=gray charred, 5=possibly charred, 6=not burned, 7=reddened, 9=indeterminate), weathering (1=bleached, 2=surface flaking, 3=mosaic cracking, 4=longitudinal cracking, 5=erosion, 6=vegetation, 7=root etching, 8=mineral deposits, 9=indeterminate), notes (weight is of all fragments), weight (g), notes (dimensions are of the largest fragment), length (cm), width (cm), and thickness (cm).

Faunal materials that were identifiable to the genus or species level had the following zooarchaeological information recorded: notes (a description of the bone), size class (VL=very large, L=large, M=medium, S=small), class, order, family, genus, species, skeletal element, side (right, left, N/A), breakage (yes, no), fusion (1=unfused, 2=partially fused, 3=fused, 4=indeterminate), burning (1=white charred, 2=black charred, 3=brown/tan charred, 4=gray charred, 5=possibly charred, 6=not burned, 7=reddened, 9=indeterminate), weathering (1=bleached, 2=surface flaking, 3=mosaic cracking, 4=longitudinal cracking, 5=erosion, 6=vegetation, 7=root etching, 8=mineral deposits,

9=indeterminate), weight notes, weight (g), dimension notes, length (cm), width (cm), thickness (cm), completeness (C=complete, MC=mostly complete, U=unspecified or unknown, D#=distal end and % of diaphysis, P#=proximal end and % of diaphysis, DE=distal epiphysis, PE=proximal epiphysis), shape (1=indeterminate bone fragment, 2=indeterminate long bone fragment, 3=unidentified flat bone fragment, 4=unidentified epiphysis fragment, 5=tooth/enamel, 6=long bone, 7=flat bone, 8=short/irregular bone), fragment notes (fragment number defined as those pieces > 1/8 inch), number of fragments (NISP), minimum number of skeletal elements (MNE), long bone circumference (100%=closed, 75%=mostly closed, 50%=halfway closed, 25%=mostly open, <25%=nearly flat).

8.2.2 Analytical Methods

8.2.2.1 Number of Identified Specimens (NISP)

NISP consists of a count of the total number of identifiable fragments per taxon (species, genus, family, or higher taxonomic category) in a given faunal sample (Grayson, 1984; Lyman, 1994, 2008). NISP measures abundance within the recovered faunal assemblage (Grayson, 1984; Lyman, 1982, 2008). Inferences about temporal and spatial changes in deposited archaeological assemblages may be made using NISP (Grayson, 1984; Lyman, 1982, 2008). NISP may be transformed into MNI or MNE counts, be used to estimate the size of the death population, or be used to estimate animal weights (Grayson, 1984).

While NISP is simple to calculate, it is plagued by several biases that affect values (Klein and Cruz-Uribe, 1984). The NISP technique does not account for differential bone preservation (Bunn *et al.*, 1988; Gilbert and Singer, 1982; Grayson, 1984; Holtzman, 1979; Kent, 1993), nor does it account for differential identifiability of specific taxa and skeletal elements (Grayson, 1984; Reitz and Wing, 1999). Additionally, there is a lack of agreement as to what constitutes a countable specimen (Casteel, 1972; Grayson, 1984; Lyman, 1994, 2008). Therefore, differing methods result in different NISP counts, which often prevent the direct comparison of multiple assemblages (Klein and Cruz-Uribe, 1984). This problem of differential fragmentation may be overcome by comparing %MNE, %MNI, and %MAU values with %NISP values. Significant differences in values between the abundance measures may indicate differential fragmentation (Lyman, 1994).

When compiling NISP values for the DRO faunal assemblage, only those faunal remains that were identified to family-level taxonomic grouping and skeletal element were counted. If a skeletal element was too fragmentary to identify beyond class, it was not included in NISP counts.

8.2.2.2 Minimum Number of Elements (MNE)

MNE is the “minimum number of complete skeletal elements necessary to account for all observed specimens” (Lyman, 1994: 290). MNE is essentially a modification of NISP values that estimates the number of skeletal elements represented in fragmented bone assemblages (Marean *et al.*, 2001; Lyman, 2008). MNE estimates are

the foundation for MNI and MAU calculations (Marean *et al.*, 2001). MNE aids researchers in determining why some of the skeletal elements that make up a complete animal skeleton are not recovered from archaeological contexts (Lyman 1994, 2008).

There are a number of ways to calculate MNE values, which include estimates based on whole elements, shaft fragments, articular ends, and diagnostic zones (Bartram, 1993; Bunn, 1986; Bunn and Kroll, 1986; Klein and Cruz-Uribe, 1984; Lyman, 1994; Marean *et al.*, 2001; Watson, 1979). Each method varies in its degree of accuracy and applicability. Watson's (1979) method, which uses small diagnostic zones (e.g. areas on bones that possess species-specific morphology, are free of age bias, and are rarely broken), was used for this research.

8.2.2.3 Minimum Number of Individuals (MNI)

MNI is a measure of the smallest number of individuals necessary to account for all of the specimens (skeletal elements) of a particular taxon in a given archaeological assemblage (Shotwell, 1955, 1958). MNI has been calculated several different ways since the 1950's, when it was first used by American Archaeologists (Grayson, 1973; Lyman, 2008). White's (1953) method, which uses the most abundant sided (right or left) skeletal element from a particular taxon, was used for this research.

Problems associated with calculating MNI values are numerous, and may prohibit the effective use of this abundance measure (Payne, 1972b). When sample size is inadequate, rare taxa may be over-estimated (Payne, 1972b). Additionally, different aggregation units for the same archaeological assemblage will provide different MNI values (Grayson, 1978). MNI, therefore, simply reflects the differing sample sizes from which values have been derived (Grayson, 1982).

8.2.2.4 Minimum Animal Units (MAU)

MAU is a count of the minimum number of animal units necessary to account for all of the observed specimens (Binford, 1978, 1984; Binford and Bertram, 1977). MAU is calculated by determining the minimum number of particular skeletal parts (e.g. proximal femur or distal humerus) in a faunal collection (MNE), and dividing by the number of times the element is present in a complete skeleton of the animal (Binford, 1978, 1984). After deriving the MAU for each skeletal element, the largest MAU value is used as the standard for the entire assemblage (Binford, 1978). Binford (1978, 1984) developed MAU because he did not believe that the entire animal (as expressed in MNI counts) was the most appropriate unit of analysis. Binford noted that meat was utilized in segments (e.g. cranial or post-cranial portions for fish); MNI values obscure the existence of these segments (Binford, 1978).

MAU calculations may be problematic; bone fragmentation often obscures the number of animal units present in the assemblage (Grayson, 1984). Fragmentation may be overcome by using MNE values as the basis for MAU calculations. Therefore, MAU calculations are subjected to the same aggregation problems associated with MNE counts (Grayson, 1984).

MAU estimates derived from fish bone assemblages may identify butchery practices and can aid in deciphering subsistence strategies (e.g. storage) (Partlow, 2000,

2006). If a fishbone assemblage is primarily composed of post-cranial elements, it may indicate a village context. Conversely, if the fishbone assemblage is primarily comprised of cranial elements, it may indicate a fish-processing context (e.g. salmon stream) (Hoffman *et al.,* 2000; Partlow, 2000, 2006).

8.2.2.5 Rank Order

Because NISP, MNE, MNI, and MAU estimates bear an unknown relationship to the actual abundances of individual taxa, animal units, or skeletal elements recovered from archaeological contexts, they are ordinal-scale measures (ranked) (Grayson, 1984; Lyman, 2008). With an ordinal-scale, those taxa, animal units, or skeletal elements with the largest number are ranked #1, and those with the next largest are ranked #2, and so on. NISP estimates represent the maximum number of individual taxa, animal units, or skeletal elements whereas MNI, MAU, MNE estimates represent the minimum number of individual taxa, animal units, or skeletal elements, respectively, that are recovered from an archaeological site (Grayson, 1984). In reality, actual individual taxa, animal units, or skeletal elements are most often somewhere between those measures.

NISP, MNI, MAU, and MNE estimates may provide acceptable estimates of the Rank Order of some common taxa, but may be affected by calculation problems. Differing aggregation strategies may result in differing Rank Orders even when analyzing a single faunal assemblage. The stability of Rank Order between the different measures is closely linked with sample size and the degree of separation of the number of individual taxa, animal units, or skeletal elements (Cannon, 1995; Grayson, 1984). Differences in Rank-Order are largely because of differing aggregation strategies and inter-observer identification ability differences (Grayson, 1984; Lyman, 2008).

Some differences in Rank Order may be overcome by completing taphonomic analysis before completing zooarchaeological analyses (Cannon, 1995; Gifford *et al.,* 1980; Grayson, 1984). If the Rank Orders from NISP, MNI, MAU, and MNE measures are the same, it is clear that all of the measures are providing an accurate assessment of the Rank Order. If there are differences in Rank Order between the different measures, those taxa whose Rank Order is the most divergent from NISP as compared to MNI, MAU, and MNE should be used as the measuring unit (Grayson, 1984).

8.3 Results

A total of 1433 g of faunal remains representing 2398 fragments and 1150 NISP were recovered from all components (Table 8.1). These NISP comprise 78 MNE of various taxa. In general, there is a decreasing trend of faunal assemblage size and total weight through time, from early to late (Figures 8.1-8.2). Denali components (C2a through C5b) comprise 82% of NISP and 87% of bone weight compared with Northern Archaic (C6a through C8b), with 22% and 13% respectively. All components had associated fauna except for C6b and C7a, while C5b contained a single specimen. Denali averaged 135+/-122 NISP/component, twice as high as Northern Archaic, with 64+/-70 NISP/component. Denali averaged 177+/-212 g/component, much higher than Northern Archaic with 47+/-52 g/component. These differences in faunal abundance appear to reflect different site functions between the cultural traditions. Because this faunal

abundance variation is not correlated with lithic abundance across all components (though it follows a logarithmic pattern), it is unlikely that faunal abundance is due primarily to occupation duration or overall assemblage size (Figure 8.3). Interestingly, two distinct patterns are represented: Denali components have a positive logarithmic trend between fauna and lithic abundance ($y = 0.0272 Ln(x)+74.171$ with high correlation, $R^2 = 0.837$) while Northern Archaic components have a negative logarithmic trend ($y = -0.1015Ln(x)+130.46$ with high correlation, $R^2 = 0.547$). This suggests a distinctive trend of a single specific relationship of faunal abundance related to occupation duration/intensity within Denali, implying similar faunal procurement patterns throughout the Denali occupations. For Northern Archaic, a more complex relationship is inferred, that is independent of occupation duration/intensity. In sum, Northern Archaic components appear to reflect distinctively different faunal accumulation processes, perhaps relating to season, resource scheduling, site function, or other social variables.

Taxonomic richness also differed between components (Figure 8.4), ranging from 1 to 6 taxa, with Chindadn taxa = 2, Denali averaging 1.9+/-0.9, and Northern Archaic averaging 4.3+/-1.7. Many of these additional Northern Archaic taxa are small mammals (see below). This suggests a broader economic exploitation strategy for the DRO occupations during the Northern Archaic. The differences in standard deviation suggest more variability within Northern Archaic components. Mammal size class summaries are illustrated in Figure 8.5. Denali components are dominated by large and very large mammals (e.g., caribou, bison) while Northern Archaic components contain proportionally more small and medium mammals (e.g, hare, beaver).

Specific identified taxa summaries are provided in Table 8.2. In the 1979 excavation, a bison tibia was recovered from strata associated with Component 7, and probably Component 7a, but is not included here. VL mammals are present in almost every component, and individual taxa include *Bison* sp., probably *Bison priscus* (steppe bison) in components C2b and C3 and *Cervus canadensis* (wapiti) in components C3, C5a, C6a, and C8b. L mammals are also present in C2a, C2c, C6a and C7b, and individual taxa include *Rangifer tarandus* (caribou) in C6a and *Ovis dalli* (sheep) in C2a. Small/medium mammals are present in 7 of the 12 components, and most common are *Urocitellus parryi* (ground squirrel) and *Lepus americanus* (snowshoe hare). When comparing Denali assemblages (n=6) and Northern Archaic assemblages (n=4) there are striking contrasts. Large and very large mammals, primarily Artiodactyla (bison, wapiti, caribou, sheep) are much more common in Denali, while small mammals are much less common, compared with Northern Archaic. Northern Archaic contain a wider variety of small game, including carnivores (e.g., Lynx, mink) that may reflect non-food resources (i.e., furs). Overall, these distributions suggest broader foraging spectrum by Northern Archaic peoples compared with a more directed megafauna exploitation strategy of Denali peoples. Interestingly, the small Chindadn occupation, while associated with bifacial weapon maintenance, contains grouse and ground squirrel, possibly reflecting a failed hunt or deposition of faunal remains in unexcavated areas.

Fragmentation also varies by component (Table 8.1), with NISP/MNE values between 1 and 32.9. Chindadn NISP/MNE = 2.7, while Denali averages 17.0+/-13.3 and Northern Archaic averages 5.3+/-5.8, suggesting much more faunal processing of Denali vs. Northern Archaic. The coefficients of variation differences (0.78 for Denali and 1.09

for Northern Archaic) again indicate more variation within Northern Archaic components. NISP/MNE ratios are good proxies for taphonomic preservation. Clearly, there is no increasing fragmentation trend from later to earlier occupations. In addition, the presence of small mammals and birds in early and later contexts are independent evidence that the assemblages are not substantially altered by density-mediated attrition due to taphonomy.

Each component is analyzed separately in the succeeding sections.

Table 8.1 DRO faunal summary.

Comp.	*Age (cal yr BP)*	*fragments (count)*	*fragments (weight, g)*	*NISP*	*MNE*	*Richness*	*NISP/MNE*
C1	12908	8	1.52	8	3	2	2.7
C2a	11596	838	132.30	263	8	3	32.9
C2b	11496	219	127.89	150	7	1	21.4
C2c	10736	602	72.72	280	12	3	23.3
C3	9683	259	672.74	213	7	2	30.4
C4	8422	25	50.94	25	3	1	8.3
C5a	7560	65	183.76	13	8	2	1.6
C5b	7252*	1	0.96	1	1	1	1.0
C6a	6824	182	82.10	159	12	6	13.3
C6b	5940*	-	-	-	-	-	-
C7a	4472	-	-	-	-	-	-
C7b	4153	45	3.98	23	4	4	5.8
C8a	3560	13	2.39	2	2	2	1.0
C8b	2239	141	101.52	72	67	5	1.1
Total	**N/A**	**2398**	**1432.82**	**1150**	**78**	**N/A**	**N/A**

*estimate

Table 8.2 Taxonomic summary by component (NISP).

Taxon	*C1*	*C2a*	*C2b*	*C2c*	*C3*	*C4*	*C5a*	*C5b*	*C6a*	*C7b*	*C8a*	*C8b*
Bison sp. (bison)	-	-	22	-	47	-	-	-	-	-	-	-
Cervus canadensis (wapiti)	-	-	-	-	1	-	1	-	1	-	-	1
VL Artiodactyla	-	141	128	175	165	25	9	1	121	1	1	5
Rangifer tarandus (caribou)	-	-	-	-	-	-	-	-	1	-	-	-
Ovis dalli (sheep)	-	20	-	-	-	-	-	-	-	-	-	-
L Artiodactyla	-	100		100	-	-	-	-	-	2	-	-
Canis sp. (wolf/dog)	-	-	-	-	-	-	-	-	2	-	-	-
Lynx canadensis (lynx)	-	-	-	-	-	-	-	-	-	-	-	39
Castor canadensis (beaver)	-	-	-	-	-	-	-	-	2	-	-	-
Urocitellus parryi (g. squirrel)	2	-	-	2	-	-	-	-	-	-	-	2
Lepus americanus (hare)	-	-	-	-	-	-	3	-	-	-	-	20
Neovision vision (mink)	-	-	-	-	-	-	-	-	2	-	-	-
S/M mammal	-	2	-	3	-	-	-	-	28	-	1	4
Cricitidae (microtine)	-	-	-	-	-	-	-	-	-	20	-	1
Tetraoninae (grouse)	6	-	-	-	-	-	-	-	2	-	-	-
Total	**8**	**263**	**150**	**280**	**213**	**25**	**13**	**1**	**159**	**23**	**2**	**72**

Table 8.3 Taxonomic Summary by cultural tradition (NISP).

Taxon	*Chindadn*	*Denali*	*Northern Archaic*
Bison sp. (bison)	-	69	1*
Cervus canadensis (wapiti)	-	2	2
VL Artiodactyla	-	644	128
Rangifer tarandus (caribou)	-	-	1
Ovis dalli (sheep)	-	20	-
L Artiodactyla	-	200	2
Canis sp. (wolf/dog)	-	-	2
Lynx canadensis (lynx)	-	-	39
Castor canadensis (beaver)	-	-	2
Urocitellus parryi (ground squirrel)	2	2	2
Lepus americanus (hare)	-	3	20
Neovision vision (mink)	-	-	2
S/M mammal	-	5	33
Cricitidae (microtine)	-	-	21
Tetraoninae (grouse)	6	-	2
Total	**8**	**263**	**150**

* 1979 bison tibia

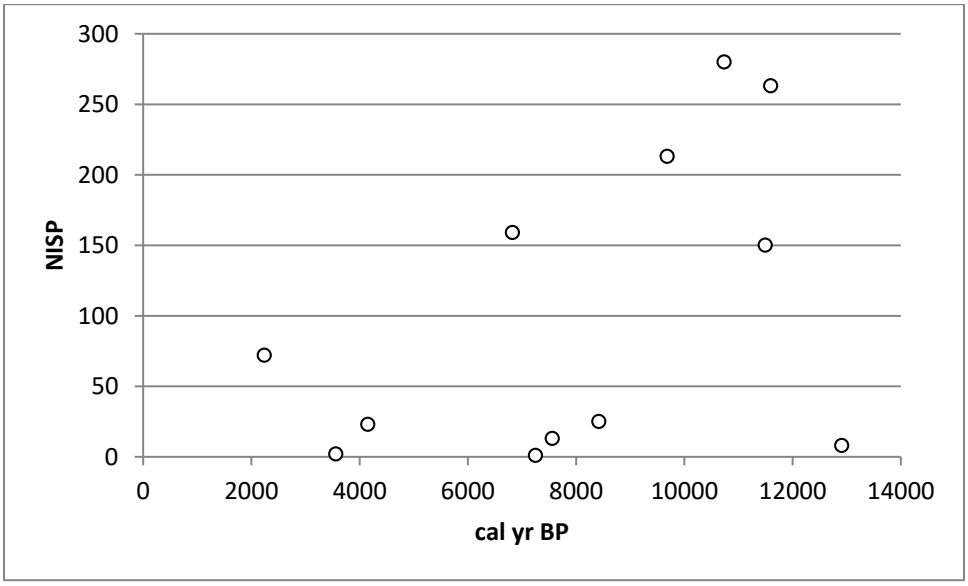

Figure 8.1 Faunal NISP by component age.

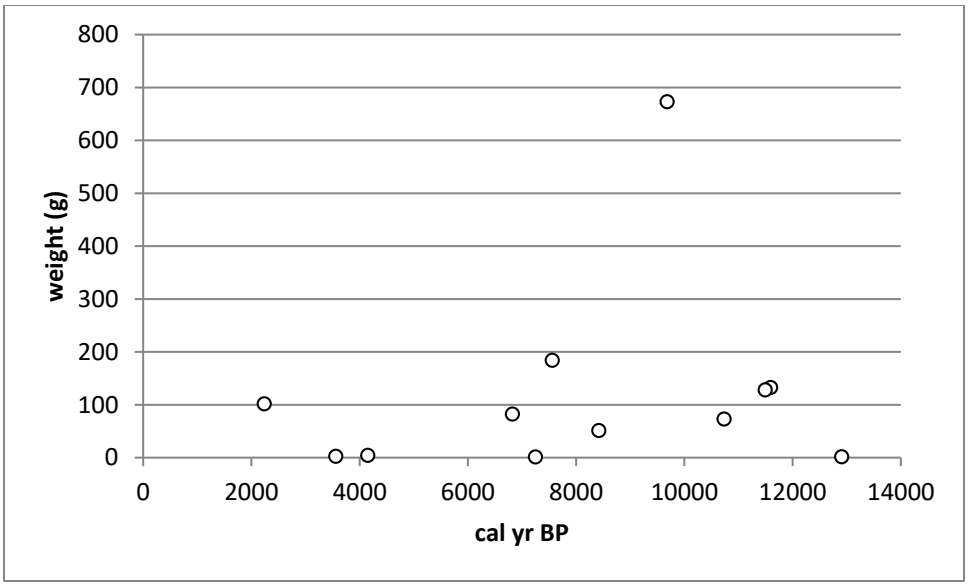

Figure 8.2 Faunal weight by component age.

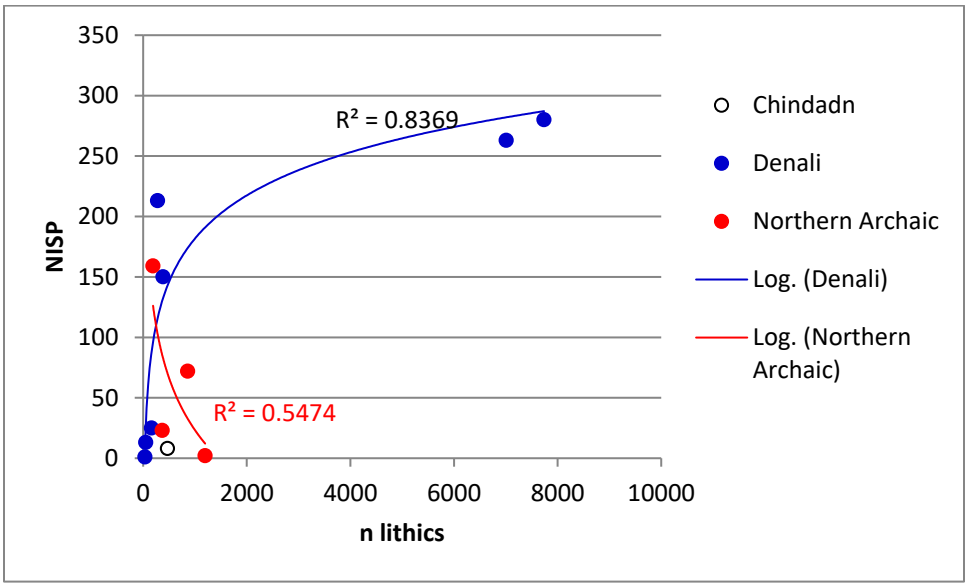

Figure 8.3 Faunal NISP and n lithics by component and logarithmic trendlines.

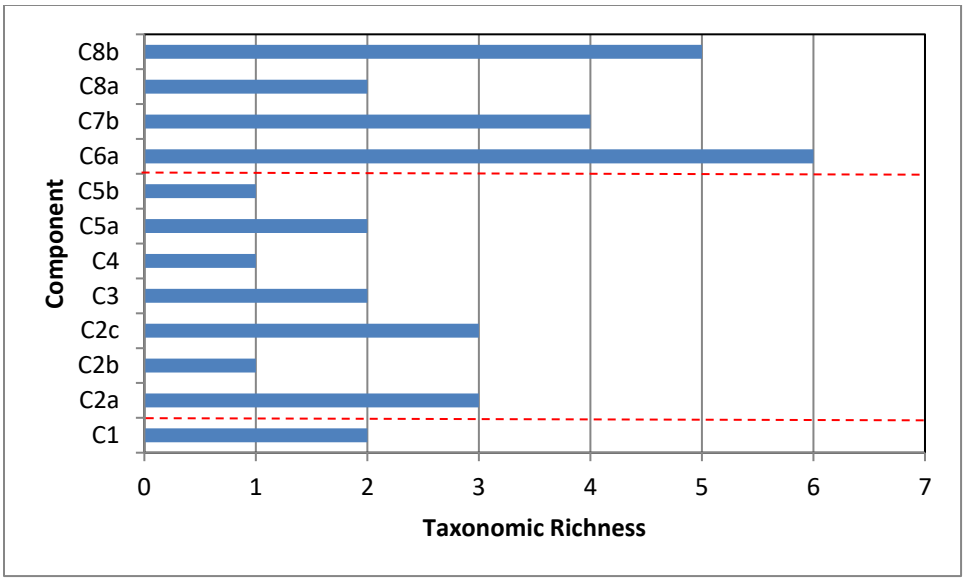

Figure 8.4 Taxonomic richness (Σ taxa) by component.

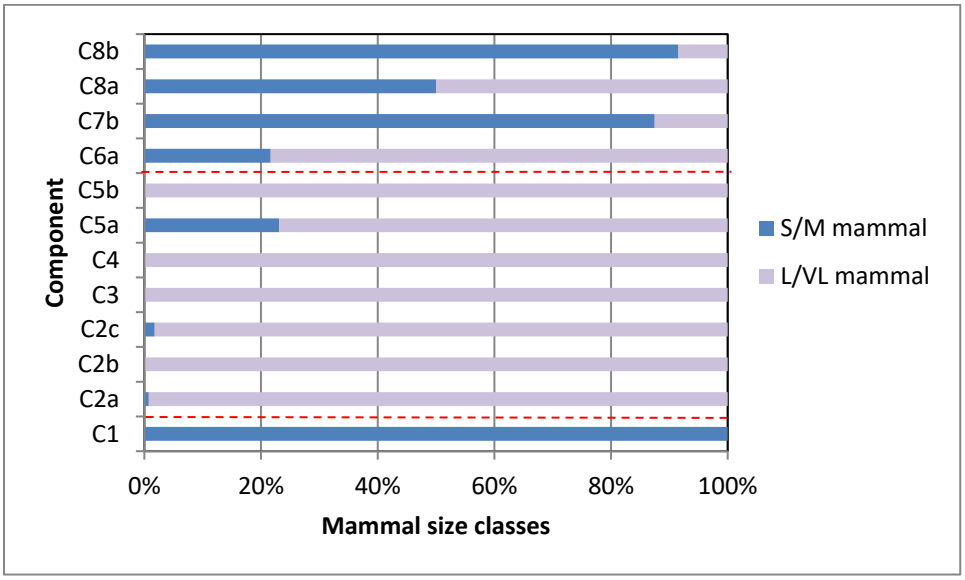

Figure 8.5 Mammal size classes by component.

8.3.1 Component 1 Fauna

Component 1fauna is comprised of two ground squirrel specimens and one grouse specimen (Table 8.4). No large or very large mammals were recovered, making this assemblage unique at DRO. The meager fauna and lithic abundances make it difficult to draw conclusions about overall Chindadn economic strategies. However, the presence of birds is consistent with avian exploitation evident at Mead, Upward Sun River, and Broken Mammoth (Potter 2008; Potter et al. 2013).

Table 8.4 C1 faunal summary.

Taxon	Skeletal element	Side	NISP	MNE	MNI
Urocitellus parryi (Ground squirrel)	Mandible	L	1	1	1
Urocitellus parryi (Ground squirrel)	Humerus	L	1	1	
Tetraoninae (Grouse)	Femur	R	6	1	1

8.3.2 Component 2a Fauna

Component 2a fauna is dominated by L/VL artiodactyls, with many bison-sized fragments (Table 8.5). However, the only identifiable taxon was a sheep mandible. Two long bone fragments of a medium-sized mammal were also recovered. Identified elements are limited to highly fragmented long bones (mainly diaphysis) and tooth enamel fragments. Three faunal clusters were identified, C2a-F1 in Block 1, C2a-F2, associated with hearth F2015-8, and C2a-F3, in the northern part of the main excavation area. Both C2a-F1 and F2 have long bone fragments and tooth enamel fragments. C2a-F3 contains a long bone fragment and a sheep mandible. The presence of teeth suggest the kills occurred relatively near to DRO, and that this reflects an early processing site, with axial elements like vertebra and ribs absent from the site. High meat yield elements were likely transported from the site to a residential base camp elsewhere. From the faunal patterns, C2a likely represents a short-term hunting camp, where early processing of large mammals took place.

Table 8.5 C2a faunal summary.

Taxon	Skeletal element	Side	NISP	MNE	MNI
C2a-F1 (Block 1)					
VL Artiodactyla	Long bone fragment	N/A	1	1	1
L/VL Artiodactyla	Tooth enamel	N/A	33	1	
C2a-F2 (F2015-8)					
L Mammal	Long bone fragments	N/A	100+	1	1
M Mammal	Long bone fragments	N/A	2	1	1
L/VL Artiodactyla	Tooth enamel	N/A	16	1	1
VL Artiodactyla	Long bone fragments	N/A	90	1	
C2a-F3 (Blocks 12, 22, 24)					
VL Artiodactyla	Long bone fragment	N/A	1	1	1
Ovis dalli (Dall sheep)	Mandible	L	20+	1	1

8.3.3 Component 2b Fauna

Component 2b fauna is dominated by L/VL artiodactyl remains, including 22 NISP of bison (Table 8.6). The remains are concentrated in one small area adjacent to the main lithic concentration. The bison remains are entirely mandible or teeth, suggesting a kill relatively close to DRO, and deposition of the other low yield remains outside the excavation area. No long bones were found, nor any high yield elements, suggesting removal of meat-bearing portions for transport elsewhere, likely to a residential base camp. From the faunal patterning, C2b likely represents a short-term hunting camp, where early processing of bison took place.

Table 8.6 C2b faunal summary.

Taxon	Skeletal element	Side	NISP	MNE	MNI
Bison priscus (Steppe bison)	Mandible	R	1	1	1
Bison priscus (Steppe bison)	Tooth enamel	N/A	20+	2 teeth	
Bison priscus (Steppe bison)	Molar	R	1	1 tooth	
L/VL Artiodactyla	Tooth enamel	N/A	128	Several teeth	

8.3.4 Component 2c Fauna

Component 2c fauna is dominated by L/VL artiodactyl remains, but five small/medium sized mammal NISP were also recovered (Table 8.7). Identified elements are limited to highly fragmented long bones (mainly diaphysis) and tooth enamel fragments. Two faunal clusters were identified, C2c-F1 associated with hearth F2015-5 and C2c-F2 associated with hearth F2015-9. Both clusters are very similar to each other, and both have VL artiodactyl long bones and tooth enamel as well as ground squirrel vertebra remains. The presence of teeth suggest the kills occurred relatively near to DRO, and that this reflects an early processing site, with axial elements like vertebra and ribs absent from the site. High meat yield elements were likely transported from the site to a residential base camp elsewhere. From the faunal patterns, C2c likely represents a short-term hunting camp, where early processing of large mammals took place.

Table 8.7 C2c faunal summary.

Taxon	Skeletal element	Side	NISP	MNE	MNI
C2c-F1 (F2015-5) (Blocks 1, 4, 6, 7, 8, 20, 21					
Urocitellus parryi (Ground squirrel)	Lumbar vertebra	N/A	1	1	1
S/M Mammal	Fragments	N/A	3	N/A	
L/VL Artioodactyla	Tooth enamel	N/A	2	1	1
L/VL Artiodactyla	Tooth enamel	N/A	12	1	
L/VL Artiodactyla	Tooth enamel	N/A	27	1	
L/VL Artiodactyla	Tooth enamel	N/A	9	1	
VL Mammal	Tooth enamel	N/A	15	1	
VL Mammal	Long bone fragment	N/A	100+	1	
VL Artiodactyla	Long bone fragment	N/A	1	1	
C2c-F2 (F2015-9) (Blocks 11, 19, 22, 24)					
Urocitellus parryi (Ground squirrel)	Lumbar vertebra	N/A	1	1	1
VL Artiodactyla	Tooth enamel	N/A	2	1 tooth	
VL Artiodactyla	Long bone fragments	N/A	7	1	
L Mammal	Long bone fragments	N/A	100+	1	1

8.3.5 Component 3 Fauna

Component C3 fauna is dominated by L/VL artiodactyl remains, with 47 bison NISP and 1 wapiti (Table 8.8). Identified elements are limited to long bone fragments and mandible/teeth fragments except for the single wapiti antler. Two faunal clusters were identified, C3-F1 associated with the southern part of the excavation area and C3-F2 associated with the central/northern part of the area. Both clusters are similar, dominated by tooth and long bone fragments and both lacking any axial elements beyond a mandible

and tooth enamel fragments. A nearly complete wapiti antler was found in isolation at the northern edge of this area. The presence of teeth suggest the kills occurred relatively near to DRO, and that this reflects an early processing site, with axial elements like vertebra and ribs absent from the site. High meat yield elements were likely transported from the site to a residential base camp elsewhere. From the faunal patterns, C3 likely represents a short-term hunting camp, where early processing of large mammals took place.

The bison R mandible includes an erupting M3 without wear, intermediate between Group III (2.3 years old) and Group IV (3.3 years old). Taking a midpoint of 2.8 years old, and assuming a May birth (ranging from April to August), this yields an estimated death date of late February (ranging from January to May). Thus, Component C3 may reflect a winter to early spring occupation.

Table 8.8 C3 faunal summary.

Taxon	Skeletal element	Side	NISP	MNE	MNI
C3-F1 (Blocks 2, 4)					
Bison priscus (steppe bison)	Mandible	R	47	1	1
VL Artiodactyla	Long bone fragments	N/A	2	1	
C3-F2 (Blocks 9, 13, 14, 15)					
L/VL Artiodactyla	Long bone fragments	N/A	6	1	1
VL Artiodactyla	Tooth enamel	N/A	31	1	
L/VL Artiodactyla	Tooth enamel	N/A	29	1	
VL Artiodactyla	Long bone fragments	N/A	97	1	
Cervus canadensis (wapiti)	Antler	N/A	1	1	1

8.3.6 Component 4 Fauna

Component 4 fauna is dominated by L/VL artiodactyl remains, with 25 NISP (Table 8.9). Identified elements include long bone fragments, rib fragments, and tooth enamel, all representing 3 MNE. Two faunal clusters were identified: C4-F1 in the southern part of the main excavation area associated with long bone fragments, and C4-F2 in the central part of the area associated with VL artiodactyl rib and tooth enamel fragments. The presence of teeth suggests the kills occurred relatively near to DRO, and that this may reflect an early processing site. However, some axial high meat-yield elements are present, perhaps suggesting some later processing or on-site consumption.

Table 8.9 C4 faunal summary.

Taxon	Skeletal element	Side	NISP	MNE	MNI
C4-F1 (Block 2)					
VL Artiodactyla	Long bone fragments	N/A	5	1	1
C4-F2 (Block 8)					
VL Artiodactyla	Rib	N/A	14	1	1
L/VL Artiodactyla	Tooth enamel	N/A	6	1	

8.3.7 Component 5a Fauna

Component 5a fauna is dominated by L/VL artiodactyl remains, with 13 NISP (Table 8.10). Identified elements include long bone fragments, tooth enamel, ribs, and a first phalanx. Three faunal clusters were identified: C5a-F1 in the southern part of the

excavation area, C5a-F2 in the northwest part of the area, and C5a-F3 in the northern part of the area. C5a-F1 contains VL artiodactyl long bones and tooth enamel along with 3 snowshoe hare NISP. C5a-F2 contains a wapiti phalanx, and VL artiodactyl rib and long bone fragments. C5a-F3 contains two rib specimens. The presence of teeth suggests the kills occurred relatively near to DRO, and that this may reflect an early processing site. However, some axial high meat-yield elements are present, perhaps suggesting some later processing or on-site consumption.

Table 8.10 C5a faunal summary.

Taxon	Skeletal element	Side	NISP	MNE	MNI
C5a-F1 (Blocks 8, 20, 21)					
VL Artiodactyla	Long bone fragments	N/A	1	1	1
VL Artiodactyla	Tooth enamel	N/A	3	1 tooth	
L/VL Mammal	Long bone fragment	N/A	1	1	
Lepus americanus (Snowshoe hare)	Tooth enamel	N/A	3	1 tooth	1
C5a-F2 (Blocks 10, 14, 19)					
Cervus canadensis (Wapiti)	1st phalanx	L	1	1	1
VL Artiodactyla	Rib	N/A	1	1	
VL Artiodactyla	Long bone fragment	N/A	1	1	
C5a-F3 (Block 22, 24)					
VL Mammal	Rib	N/A	2	1	1

8.3.8 Component 5b Fauna

Component 5b fauna consists of a single VL artiodactyl thoracic vertebra (Table 8.11). The presence of an axial high meat yield element suggests some on-site consumption or later processing.

Table 8.11 C5b faunal summary.

Taxon	Skeletal element	Side	NISP	MNE	MNI
VL Artiodactyla	Thoracic vertebra	N/A	1	1	1

8.3.9 Component 6a Fauna

Component C6a fauna comprises a range of specimens, from L/VL artiodactyl to small and medium mammals and terrestrial birds (Table 8.12). Three faunal clusters were identified, C6a-F1 in the southeast part of the main excavation area, C6a-F2 in the far eastern extension of the area (Block 16), and C6a-F3, associated with a hearth feature in the southwestern part of the area. C6a-F1 contains a caribou radius, a canid (likely wolf or dog) molar, two mink vertebra, 2 beaver specimens, and 2 grouse limb specimens. The concentration of fur-bearers in this area is intriguing, suggesting a specialized activity area relating to processing of carcasses for matériel. C6a-F2 contains a wapiti antler fragment and VL artiodactyl long bone fragments (i.e., larger than caribou-sized). C6a-F3 contains both VL artiodactyl and small/medium sized mammal long bones and tooth enamel. The suite of elements suggests possible organic tool production or maintenance as well as a specialized fur-bearer processing area.

Table 8.12 C6a faunal summary.

Taxon	Skeletal element	Side	NISP	MNE	MNI
C6a-F1 (Blocks 5, 7)					
Rangifer tarandus (Caribou)	Radius	R	1	1	1
Canis sp. (wolf/dog)	Molar	N/A	2	1	1
Neovision vision (Mink)	Atlas vertebra	N/A	1	1	1
Neovision vision (Mink)	Axis vertebra	N/A	1	1	
Castor canadensis (Beaver)	Tarsal	N/A	1	1	1
Castor canadensis (Beaver)	Sesmoid	N/A	1		
Tetraoninae (Grouse)	Radius	L	1	1	1
Tetraoninae (Grouse)	Carpometacarpus	L	1	1	
C6a-F2 (Block 16)					
Cervus canadensis (Wapiti)	Antler	N/A	1	1	1
VL Artiodactyla	Long bone fragments	N/A	119	1	
C6a-F3 (F2017-2, Blocks 20, 21)					
VL Artiodactyla	Long bone fragments	N/A	2	1	1
S/M mammal	Tooth enamel	N/A	10	1	1
S/M mammal	Long bone fragment	N/A	18	1	

8.3.10 Component 7b Fauna

Component 7b fauna consists of VL artiodactyl, small/medium sized mammals, and microtine specimens (Table 8.13). Three faunal clusters were identified, C7b-F1 in the central part of the main excavation area, C7b-F2 in the northwest and C7b-F3 in the north. The sample size is very small, but S/M mammals, L mammals, and VL artiodactyl are represented. In addition, the bison tibia fragment recovered in 1979 at ~60-65 cmbs, is associated with either C7a or C7b, and given that no C7a fauna were recovered, it is tentatively assigned to the Component 7b.

Table 8.13 C7b faunal summary.

Taxon	Skeletal element	Side	NISP	MNE	MNI
C7b-F1 (Block 6)					
VL Artiodactyla	Cranium	N/A	1	1	1
C7b-F2 (Block 19)					
S/M Mammal	Too frag. To identify	N/A	0	1	1
C7b-F3 (Blocks 22, 24)					
Cricetidae (Microtine)	Cranium	N/A	20	1	1
L Mammal	Too frag. To identify	N/A	N/A	N/A	N/A

8.3.11 Component 8a Fauna

Component 8a fauna consists of a VL artiodactyl long bone fragment and a M mammal limb element (Table 8.14) in the eastern part of the excavation area. The sample size is small, but medium and VL mammals are represented.

Table 8.14 C8a faunal summary.

Taxon	Skeletal element	Side	NISP	MNE	MNI
M Mammal (Snowshoe hare?)	Metacarpal	R	1	1	1
VL Artiodactyla	Long bone fragment	N/A	1	1	1

8.3.12 Component 8b Fauna

Component 8b fauna consist of a wide range of specimens, from L/VL artiodactyl to small and medium mammals (Table 8.15). Three faunal clusters were identified, C8b-F1 in the western part of the excavation area, C8b-F2 associated with hearth F2017-1, and C8b-F3 associated with hearth F2015-1.C8b-F1 is a scatter of fauna including VL artiodactyl axial elements (3 MNE: rib, molar, mandible) as well as axial and appendicular elements from snowshoe hare (16 MNE), lynx (39 MNE) both likely representing single individuals. The concentration of fur-bearers in this area is interesting, suggesting a specialized activity area relating to processing of small mammals for material. C8b-F2 is associated with a hearth, and contains wapiti and L/VL artiodactyl remains, a single ground squirrel element and S/M mammals most likely representing snowshoe hare (6 MNE). C8b-F3 contains a single VL artiodactyl tooth. Collectively, these materials suggest early (and possibly later) processing and possibly consumption of large ungulates as well as a specialized fur-bearer processing area.

Table 8.15 C8b faunal summary.

Taxon	Skeletal element	Side	NISP	MNE	MNI
C8b-F1 (Blocks 10, 16, 19, 23, 26)					
L/VL Artiodactyla	Rib	N/A	1	1	1
VL Artiodactyla	Molar	N/A	1	1	
L/VL Artiodactyla	Mandible	N/A	1	1	
Lepus americanus (Snowshoe hare)	Femur	L	3	1	1
Lepus americanus (Snowshoe hare)	Lumbar vertebrae	N/A	4	4	
Lepus americanus (Snowshoe hare)	Thoracic vertebrae	N/A	3	3	
Lepus americanus (Snowshoe hare)	Cervical vertebra	N/A	1	1	
Lepus americanus (Snowshoe hare)	Incisor	N/A	1	1	
Lepus americanus (Snowshoe hare)	Rib	N/A	1	1	
Lepus americanus (Snowshoe hare)	Cranium	N/A	1	1	
Lepus americanus (Snowshoe hare)	Humerus	L	1	1	
Lepus americanus (Snowshoe hare)	Tibia	L	1	1	
Lepus americanus (Snowshoe hare)	Ulna	R	1	1	
Lepus americanus (Snowshoe hare)	1st phalanx	N/A	1	1	
Lynx canadensis (Lynx)	Thoracic vertebrae	N/A	16	16	1
Lynx canadensis (Lynx)	Lumbar vertebrae	N/A	9	9	
Lynx canadensis (Lynx)	Caudal vertebra	N/A	1	1	
Lynx canadensis (Lynx)	Vertebra fragment	N/A	2	N/A	
Lynx canadensis (Lynx)	Rib	N/A	7	7	
Lynx canadensis (Lynx)	1st phalanx	L	1	1	
Lynx canadensis (Lynx)	Tooth enamel	N/A	1	1	
Lynx canadensis (Lynx)	Femur	L	1	1	
Lynx canadensis (Lynx)	Tibia	N/A	1	1	
Cricetidae (Microtine)	Incisor	N/A	1	1	1
C8b-F2 (F2017-1, Blocks 9, 11, 15, 24)					
L/VL Artiodactyla	Long bone fragment	N/A	1	1	1
Cervus canadensis (Wapiti)	Tibia	R	1	1	
Urocitellus parryi (Ground squirrel)	Incisor	N/A	2	1	1
Lepus americanus (Snowshoe hare)	Humerus	L	1	1	1
Lepus americanus (Snowshoe hare)	Humerus	R	1	1	
M mammal (likely Snowshoe hare)	Cervical vertebra	N/A	1	1	
M mammal (likely Snowshoe hare)	Rib	N/A	1	1	
M mammal (likely Snowshoe hare)	Tibia	R	1	1	
S/M mammal (likely Snowshoe hare)	Tooth enamel	N/A	1	1 tooth	
C8b-F3 (F2015-1, Block 12)					
VL Artiodactyla	Premolar	R	1	1	1

8.4 Discussion

There are trends in faunal patterning among the DRO components. The L/VL ungulate record is dominated by long bones and teeth. These are generally the densest bones and may suggest density-mediated attrition has severely affected the DRO record. However, the concurrent preservation of small mammals and birds in all levels, including the upper strata, where we may expect more differential destruction due to humic acids from Bwb horizons suggests this patterning results from human decisions. Specifically, for the 7 Denali components, there was recurrent use of the site to process bison and wapiti, probably killed locally, but probably not onsite, as no bison crania were recovered, only mandibles and related mandibular teeth. Importantly, this is the only known site (except Dry Creek C2) with bison teeth, allowing us to examine seasonal movements of the animals, particularly with respect to seasonal bison migration. These problems are analyzed in Chapter 11.

Seasonality was identified for one component, Component 3, representing the first documented case of a winter occupation in eastern Beringia. This furthermore provides evidence for year-round occupation of central Alaska, since summer occupations [e.g., Carlo Creek and Upward Sun River (Bowers 1980; Potter et al. 2010)], fall occupations [e.g., Dry Creek and Gerstle River (Powers et al. 1983; Potter 2007)], and spring occupations [e.g., Broken Mammoth CZ4 (Yesner 1996)] are all documented in the local region.

The presence of bison teeth also suggest site occupants killed the animals in relatively close proximity, bringing selected portions back to the site during the Denali period. High meat yield animal portions (e.g., meat associated with ribs and vertebrae) were likely removed from the site and transported to residential base camps like Upward Sun River or Mead. Mass marrow processing of long bones probably occurred onsite, very similar to the faunal assemblage expressed at Gerstle River (Potter 2007). However, there are some differences in within the Denali complex. Early Denali occupations (C2a, C2b, C2c, C3) (12,908-9683 cal yr BP) are characterized as above, with early stage processing, discard of primarily long bones and teeth with no high meat yield elements. This suggests site function for these components as a short-term hunting/processing camp within a logistical mobility system. Later Denali occupations (C4, C5a, and C5b) (8422-7252 cal yr BP) contain more ribs and vertebrae, suggesting later stage processing and possibly consumption. This may indicate shifts in Denali residential mobility in the early/mid Holocene, and changes in how the DRO landform was used.

In contrast to Denali, the two Northern Archaic components with substantial materials, C6a and C8b, contain very different assemblages, with a much wider range (and proportionality) of fauna, including beaver, mink, canid, grouse, lynx, hare, and ground squirrel. Denali staple ungulates (bison and wapiti) are well represented at multiple Northern Archaic components, as is the first presence of caribou, a typical Northern Archaic food resource (Potter 2008). Overall, these data suggest increasing diet breadth, consistent with models of Northern Archaic adaptive strategies (Potter 2008). Each Northern Archaic component is also more distinct from each other than the Denali components, which share many elements (see above). This suggests a more generalized hunting strategy focused on bison and wapiti in the Denali tradition and a mapping-on

strategy employed in the Northern Archaic tradition, the latter a form of intensive local land use. This interpretation is independently supported using relationships of abundance and occupation duration/intensity (see Figure 8.3) where Denali strategies tend to directly vary relative to the latter, whereas Northern Archaic strategies appear more complex, reflecting distinctly different faunal accumulation processes.

Of particular interest is the continuing occurrence of bison and wapiti extending well into the later Holocene, suggesting abundant megafauna present in these regions long after their extirpation/extinction in surrounding areas of Beringia. Wapiti are well represented, reinforcing the contention that wapiti were significant resources throughout the early to middle Holocene (Potter 2005). The co-occurrence of bison and wapiti, likely hunted/captured in similar areas using similar technology, replicates the relationships found at Gerstle River (Potter 2007), Broken Mammoth (Yesner 1996), and Mead (Potter et al. 2011) where bison and wapiti co-occur as the two dominant ungulate taxa.

The paucity of birds indicates that this was not a major prey species in the immediate DRO environs, though the absence of waterfowl, common in pre-Younger Dryas occupations in the area (Potter et al. 2013), is interesting, and may reflect local paleoecology. Notably absent are fish remains, which have become more commonly identified throughout the Tanana River basin record (Potter et al. 2011; Halffman et al. 2015).

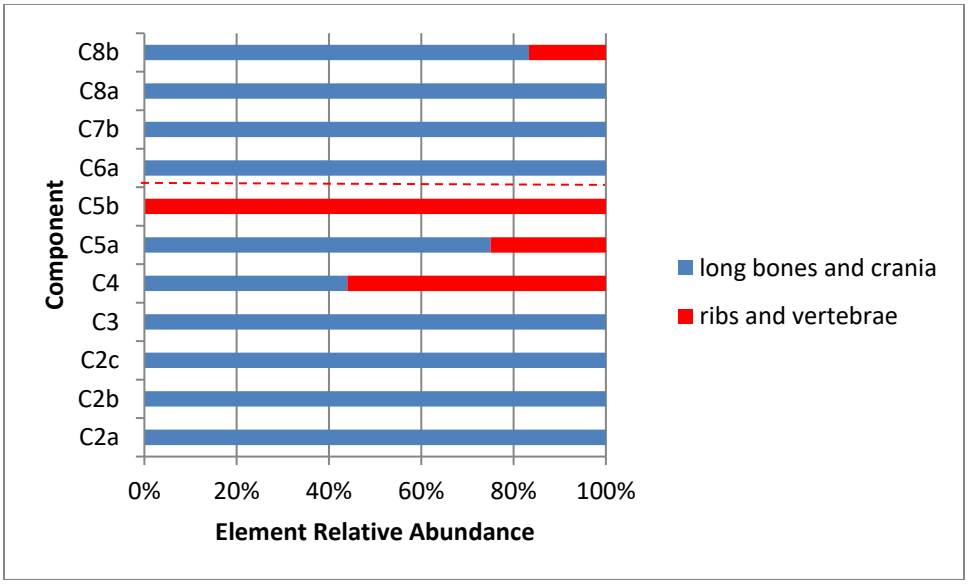

Figure 8.6 L/VL artiodactyl high meat yield (ribs, vertebrae) and low meat yield (long bones, crania, teeth) proportions by component.

CHAPTER 9. ARCHAEOBOTANICAL ANALYSES

Caitlin R. Holloway

9.1 Introduction and Methods

To evaluate seasonality and floral resource use by site occupants, we selected two well-preserved features in the lower components most likely to preserve organic remains for archaeobotanical analyses. These were hearths F2015-5 and F2015-9, both in Component 2c. They are illustrated in the process of excavation in Figures 9.1 and 9.2. Both hearths are dated and overlap at two standard deviations (see Chapter 4). F2015-5 dates to 9510+/-30 BP (11,069-10,685) and F2015-9 dates to 9470+/-30 BP (11,047-10,588 cal yr BP).

Samples were weighed (g) and volume was measured with water displacement (ml). To separate organic remains from feature matrix, we processed the bulk sediment samples with a standard manual buck flotation system to retrieve the light fraction, then sieved the heavy fraction with 425, 250, and 125 micron (µm) geological sieves (Figure 9.3). Procedures followed those outlined in Pearsall (2000).

For each sample, we examined the light organic fraction, the 425 µm, and the 250 µm fraction. The 125 µm fraction from one field specimen number was picked, but no identifiable organic remains were recovered. We determined that the time required to process the smallest fraction would not be worth the yield of identifiable organic remains.

Organic remains were placed in a petri-dish and examined with a stereo-microscope (up to 20x magnification) to search for charcoal and plant remains with distinguishing characteristics (such as morphology and surface texture). Robust charcoal samples were picked from the light and 425 µm organic fractions. We also collected lithics greater than approximately 2 mm and classified sample characteristics (such as inclusions, sand and gravel content, and charcoal abundance) on a qualitative scale from 0 to 5, with 5 the highest mark.

The plant macroremains (including seeds, buds, needles, and charcoal) were identified to the most specific taxonomic level possible through comparison with modern reference collections at the UA Alaska Quaternary Center, reference books, and online databases. Although identifiable uncarbonized plant remains were collected, we excluded these remains as modern contamination in the final analysis. We separated unknown and identifiable taxa into “Types” based on differences in morphology, size, and surface texture. Identifiable taxa include those that can be identified (given time) based on distinguishing characteristics.

For analysis, discussion, and comparison of the XMH-000297 features, we calculated diversity, evenness, and ubiquity of the archaeobotanical assemblage. First, the raw counts were standardized at the feature-scale to account for differences in subsample size. For each feature, the raw count of each taxon was divided by the volume of feature matrix processed and the resulting value was multiplied by the volume of the smallest feature included in the analysis, which yielded the standardized concentration of a particular taxon per unit of matrix processed.

The Shannon Weaver Index (Shannon and Weaver 1949) considers the richness (number of taxa per sample) and evenness (abundance of taxa) of a sample. The resulting

value is a measure of diversity (*H'*) ranging between zero (a community with only one species) and a maximum value dependent on the number of taxa present in a sample. Evenness accounts for the relative abundance of different species in a community and values fall between zero and one, with one representing a completely even distribution of species. Ubiquity is a percentage measure of the number of units that contain a taxon. These measures are often applied in paleoethnobotany as a means of hypothesis testing and inter-assemblage comparison (Marston et al. 2014).

A total of 14 features features were included for inter-site comparison:

- Delta River Overlook (DRO) Features 2015-5 and 2015-9 (10,800 cal yr BP).
- Keystone Dune Site (KDS) Feature 1 (13,410-13,190 cal yr BP).
- Upward Sun River (USRS) Component 1 (13,300-13,120 cal. BP) Features 2010-2 and 2014-5.
- Upward Sun River Component (USRS) 3 (11,610-11,280 cal yr BP) Features 2010-5, 2013-9, 2010-2, 2014-5, 2013-20, 2014-6, and 2011-6A.
- Gerstle River (GR) Component 3 (10,160-9,910 cal. BP) Features 5, 10, 12, and 14.

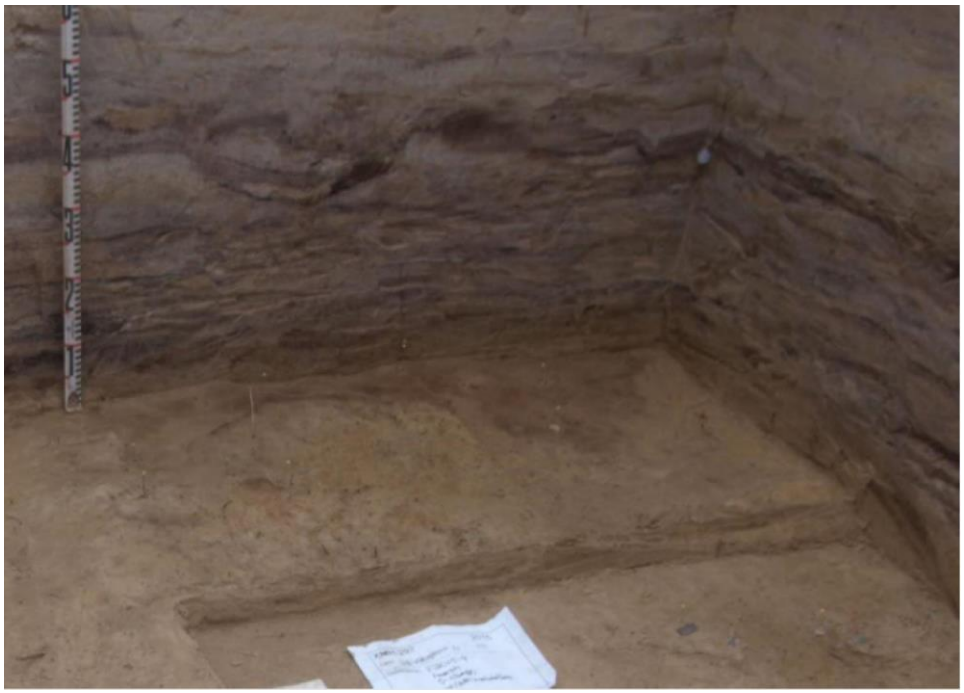

Figure 9.1. Hearth F2015-9, 10,880 cal yr BP

Figure 9.2. Hearth F2015-5, 10,820 cal yr BP

Figure 9.3. Bulk sample of feature matrix and wet-sieving system.

9.2 Hearth F2015-5 Results

Feature 2015-5 is a hearth feature that was collected as six separate field specimens consisting of a total of 10 bags. The combined weight of the matrix totaled 14,675.38 grams, 9,506.80 grams (3.45 liters) of which we subsampled for archaeobotanical remains. The processed subsamples contained a total of 58 distinct carbonized plant macroremains (57 seeds and one bud; Table 9.1). A Rosaceae species (cf. *Rubus* sp.) dominates the F2015-5 archaeobotanical assemblage at 47%, followed by *Arctostaphylos uva-ursi* at 31%. The remainder of the assemblage consists of a few *Carex* sp. seeds (5%), two Rosaceae species seeds that resemble *Fragaria* or *Potentilla* (3%), a small component of five distinct Types of unidentified seeds (12%), and one unidentified bud (1%).

A total of 246 charcoal fragments were picked from the light fraction and 425 micron fraction. A total of 4 lithics and 78 fragments of calcined bone greater than approximately 2 mm were also picked from the feature matrix. The calcined bone was highly fragmented and unidentifiable. A qualitative comparative scale is provided in Table 9.2.

Sample Description: F2015-5 (10 bags) Provenience: N201.5-202.5 E495496
Sample Depth: 10-15 cmbP1 Processed Date: 3/30 – 4/4/2018
Sample Date: 8/1 and 8/8/2017 Subsample Weight (g): 9506.80
Bulk Sample Weight (g): 14675.38 Subsample Volume (ml): 3450

Table 9.1. F2015-5 Macroremains and other materials

Description	*Count*
Carbonized plant macroremains	
Arctostaphylos uva-ursi (Bearberry; Kinnikinnick)	18
cf. *Rubus* sp. (cf. Raspberry sp.)	27
Carex sp. (Sedge sp.) seed	3
Fragaria/Potentilla-type (identifiable; Strawberry/Cinquefoil-type) seeds	2
Unknown (identifiable) seed - Type 14	1
Unknown (identifiable) seed – Type 15	1
Unknown (identifiable) seed - Type 16	3
Unknown (identifiable) seed - Type 17	1
Unknown (identifiable) seed - Type 18	1
Unknown (identifiable) bud - Type 3	1
Total	58
Other macroremains	
Flakes (picked)	4
Fauna (picked)	78
Insect (modern)	0

Table 9.2 F2015-5 Qualitative (Scale 0-5)

Description	*Count*
Wood fragments	2
Moss	0
Sand and gravel	1
Leaf fragments	1
Charcoal	2
Roots	2

9.3 Hearth F2015-9 Results

Feature 2015-9 is a hearth feature that was collected as four separate field specimens consisting of a total of 10 bags. The combined weight of the matrix totaled 15,027.58 grams, 8,722.90 grams (3.90 liters) of which we subsampled for archaeobotanical remains (Table 9.3). The processed subsamples contained a total of 32 distinct carbonized plant remains and two uncarbonized plant macroremains that are likely recent contamination and are excluded from the final analysis. *Arctostaphylos uva-ursi* dominates the F2015-9 archaeobotanical assemblage at 59%, followed by a *Carex* species at 16%. A Rosaceae species (cf. *Rubus* sp.), a Rosaceae species seeds that resembles *Fragaria* or *Potentilla*, an unknown Rosaceae species, and a distinct but unidentified Type species each comprise 6% of the archaeobotanical assemblage.

In addition, we picked a total of 304 charcoal fragments from the light fractions and 425 micron fractions. A total of 36 lithics and 98 fragments of calcined bone greater than approximately 2 mm were also picked from the feature matrix. The calcined bone was highly fragmented and unidentifiable. A qualitative comparative scale is provided in Table 9.4.

Sample Description: F2015-9 (9 bags)
Sample Depth: 0-5 cmbP1
Sample Date: 8/7/2017
Bulk Sample Weight (g): 15,027.58
Provenience: N210-211 E494.5-496
Processed Date: 2/15 – 3/29/2018
Subsample Weight (g): 8,722.9
Subsample Volume (ml): 3900

Table 9.3 F2015-9 Macroremains and other materials

Description	*Count*
Carbonized plant macroremains	
Arctostaphylos uva-ursi (Bearberry; Kinnikinnick)	19
Carex sp. (Sedge sp.) seed	5
cf. *Rubus* sp. (cf. Raspberry sp.)	2
Fragaria/Potentilla-type (identifiable; Strawberry/Cinquefoil-type) seeds	2
Rosaceae sp. seed (identifiable)	2
Unknown (identifiable) seed - Type 19	2
Total	32
Uncarbonized plant remains	
Carex sp. (Sedge sp.) seed	1
Picea sp. (Spruce sp.) needle	1
Total	2
Other macroremains	
Flakes (picked)	36
Fauna (picked)	98
Insect (modern)	1

Table 9.4 F2015-9 Qualitative (Scale 0-5)

Description	*Count*
Wood fragments	2
Moss	0
Sand and gravel	2
Leaf fragments	2
Charcoal	3
Roots	1

9.4 Analysis

When considering the archaeobotanical remains from DRO, the combined assemblage from F2015-5 and F2015-9 contains a total of 90 carbonized plant macroremains and is dominated by common bearberry (*Arctostaphylos uva-ursi*) at 41%, followed by a Rosaceae species (cf. *Rubus* sp.) at 32%. Sedge (*Carex* sp.) comprises a smaller component of the assemblage (9%), followed by an unknown Rosaceae species (2%). A total of six unknown but distinguishable "Types" constitute 10% of the overall assemblage, in addition to one unknown but distinct bud Type (1%).

We calculated the diversity and evenness of the Delta River Overlook archaeobotanical assemblage and additional assemblages from three interior Alaskan sites for inter-site comparison, including: Upward Sun River Components 1 and 3 (Holloway 2016; Potter et al. 2008; Potter et al. 2011), Gerstle River Component 3 (Potter 2005), and the Keystone Dune Site (Lanoe et al. 2018). We standardized the raw counts from the four sites based on the volume of the smallest feature analyzed (Upward Sun River, Component 1, Feature 2010-2 at 1.8 liters). To simplify the comparison, we grouped identifications at the genus level and combined macroremain types into the same category (for example, if one genus was represented by seeds and leaves, the counts were combined into a single category).

The diversity DRO F2015-5 is slightly higher than DRO F2015-9 due to the presence of five distinct (but unidentified) "Type" species in F2015-5 (Table 9.5). DRO F2015-5 is the second-most diverse of the Features included in this analysis, preceded by USRS F2013-9. USRS F2010-5 had the highest diversity (*H'*= 2.02), but this value is likely inflated due to the large amount of matrix processed (16.28 L) and the feature is excluded as an outlier. Overall, the features with the lowest diversity (less than 0.3) included those with few taxa and a relatively uneven distribution in terms of taxa abundance (KDS F1, USRS F2010-2 and F2014-5, and GR F12).

Table 9.5 Shannon Weaver diversity values (*H*) and sample evenness (E) when calculated for inter-site comparison. Delta River Overlook (DRO), the Keystone Dune Site (KDS), the Upward Sun River Site (USRS), and Gerstle River (GR).

	DRO		*KDS*	*USRS*						*GR*		
	2015-5	*2015-9*	*1*	*2013-9*	*2010-2*	*2014-5*	*2013-20*	*2014-6*	*2011-6A*	*10*	*12*	*14*
H'	1.49	1.29	0.26	1.84	0.25	0.29	1.10	1.36	1.27	1.47	0.24	1.21
E	0.65	0.72	0.12	0.89	0.35	0.15	1.00	0.76	0.65	0.92	0.17	0.88

When considering the ubiquity of plant taxa identified at the four sites compared here, common bearberry (*Arctostaphylos uva-ursi*) is the most common and appears in 64% of the features analyzed, followed by sedge (*Carex* spp.) in 50% of the features analyzed. A Rosaceae species (cf. *Rubus*) and a *Vaccinium* species (low-bush cranberry/blueberry genus) both occur in 35% of the features analyzed. Approximately 36 additional plant taxa have been identified in archaeobotanical assemblages at the four sites described here, though these taxa only appear in one or two features at most.

9.5 Discussion

Although the preferred habitat of the taxa identified at the Delta River Overlook site varies, the range of environments could have occurred at or around the site during the time of human occupation (Table 9.6). Common bearberry prefers well-drained settings and could have comprised a portion of the vegetation mat during the time that the site was occupied. Both Rosaceae species can tolerate dry to moist soil habitats, ranging from disturbed areas to forest borders, open areas, and clearings. Sedge has a highly variable habitat, though the genus generally prefers moist habitats.

In terms of plant availability and seasonality, common bearberry ripens in August, though the berry can remain on the plant under snow-cover throughout the winter. Species belonging to the *Rubus* genus (such as wild raspberry, cloudberry, and nagoonberry) ripen between July and September (Table 9.6). The additional Roaceae species identified in the Delta River Overlook features is tentatively described as a *Fragaria* or *Potentilla* type (wild strawberry or brush cinquefoil). The July-September seasonality of *Potentilla* is consistent with the seasonality assigned by common bearberry and the *Rubus* species. If the additional Roseaceae species more closely resembles *Fragaria*, the presence of this taxon would expand the seasonality to include early summer (June).

Overall, the similarities between C2c features F2015-5 and F2015-9 are striking (Table 9.7). The similarities in taxa, dates, and location in the center of possible tent features suggests multiple consumer groups cohabiting at a single site. Overall, the plant resources suggest opportunistic foraging for seasonally available plants in addition to hunting activities. These data also indicate that plant resource availability likely impacted forager subsistence strategies, even at sites that primarily preserve evidence of faunal exploitation activities.

Table 9.6 Seasonality and habitat preference for taxa identified at DRO.

Taxon	*Common Name*	*Availability/ Seasonality**	*Habitat**
Arctostaphylos uva-ursi	Common bearberry	August	Coarse, well to excessively drained soils of forests, sand dunes, bald or barren areas. Does not tolerate moist settings.
Rosaceae sp. cf. *Rubus* sp.	Rose family sp.	July-September (*Rubus* sp.)	Forest borders, clearings, and disturbed areas.
Carex sp.	Sedge sp.	-	Variable; generally prefer moist habitats such as marshes, bogs, peatlands, pond and stream banks, and riparian zones.
Rosaceae sp. cf. *Fragaria/Potentilla*-type	Wild strawberry or brush cinquefoil	June (*Fragaria* sp.); July-September (*Potentilla* sp.)	Dry to moist open woodlands and clearings, meadows, disturbed areas (*Fragaria* sp.); Moist soils along borders of lakes and streams, dry rocky hillsides (*Potentilla* sp.).

*Hultén 1968; Viereck and Little 2007

Table 9.7 Comparison of F2015-9 and F2015-5 macrofossil remains

Hearth F2015-9	*Macroremains taxa*	*Hearth F2015-5*
304	Charcoal	246
32	Macroremains	58
1	Bearberry (*Arctostaphylos uva-ursi*)	18
1	Arctic raspberry (*Rubus arcticus*)	27
2	Strawberry (*Fragaria*-type)	2
6	Sedge (*Carex* sp.)	3
1	Spruce (*Picea* sp.)	-

CHAPTER 10. OBSIDIAN ARTIFACT GEOCHEMICAL SOURCING

Joshua D. Reuther

10.1 Introduction

Obsidian (volcanic glass) is a very useful material to use to track its distribution across geographic space as past peoples moved across landscapes, and traded materials with other peoples, sometimes very far distances (~1000 km) from an obsidian's geological origin or source. Obsidian tends to have relatively homogenous structural and chemical properties when compared to other rocks (Glascock et al. 1998; Shackley 2005). As a fast cooling igneous material it had little time to incorporate external chemical constituents beyond its internal chemical concentrations that were developed in the magma chamber and as it was extruded through vents. Its cryptocrystalline structure makes it an excellent medium for knapping stone tools and was used widely throughout prehistory in Alaska (Rasic 2015). For these reasons, obsidian has been widely used in prehistoric studies concerned with the distribution and movement of materials across landscapes through direct procurement by groups or through trade with outside groups.

Trace element concentrations were measured on a total of 73 obsidian artifacts from the DRO collection with the goal to understand any potential changes in obsidian source material use throughout time and between components. Obsidian artifacts were found in at least four DRO components: C2c, C7b, C8a, and C8b.

10.2 Methods

A select range of trace elements was measured in the DRO obsidian artifacts using a portable Bruker Tracer III-SD X–ray florescence (pXRF) spectrometer at the University of Alaska Museum of the North (UAMN). The Bruker Tracer III-SD has a rhodium (Rh) tube and silicon drift detector, and a 10 mm diameter window that the X-rays pass through to a target. The selected trace elements measured by pXRF that are generally used to discriminate obsidian from Alaska and the Yukon, Canada, include manganese (Mn), iron (Fe), zinc (Zn), rubidium (Rb), strontium (Sr), yttrium (Y), zirconium (Zr), niobium (Nb), and thorium (Th).

Each sample was analyzed for 200 seconds at 40kV and 15μA. A filter composed of 0.006" Cu, 0.001" Ti, 0.012" Al was used to maximize the amount of X-rays between 17 and 40 keV to reach a target and provides more sensitivity in counting the mid-Z elements between Fe and Nb.

A calibration (RJS Obsid Cal 4-30-09.CFZ) developed specifically for converting x-ray counts (or pulses) to parts per million (ppm) when measuring the targeted elements in obsidian with the UAMN Bruker Tracer III-SD. The peak heights of the selected elements were calculated as ratios to the Compton peak of Rh and converted into parts per million (ppm) using a linear regression of elemental concentrations of international rock reference materials measured by neutron activation analysis (NAA) and XRF (Coffman and Rasic 2015). We measured a piece of obsidian from an Oregon source as a standard reference to ensure that the UAMN Bruker Tracer III-SD machine was performing properly throughout each set of measurements on the DRO samples. This

Oregon obsidian reference has measurements on the targeted elements derived from NAA and XRF analyses. Each of the measurements of the California obsidian standard for each set of DRO analyses was comparable to the standard's accepted values and the counting variation generally documented by the use of pXRFs (Speakman and Shackley 2013). When the standard's measurements were within one standard deviation (68% probability) or within 2-4% of the percent relative standard deviation (%RSD), the measurements were considered accurate and reliable and the UAMN Bruker Tracer III-SD to be working properly (Table 1).

The Alaska Obsidian Database [AOD] contains measurements and XRF spectra from a wide variety of obsidian geological sources and obsidian artifacts from sites across Alaska, western Canada, and the Russian Far East (Rasic et al. 2009; Reuther et al. 2012). Each artifact or geological obsidian sample that have their trace elements measured are assigned unique numbers for the AOD. These numbers begin with the prefix "AOD" (Table 2).

We have used a few ways to discriminate among element measurements on DRO obsidian artifacts themselves, and between measurements on geological source materials and obsidian artifacts from archaeological sites throughout Alaska and western Canada. Rb, Sr, and Zr tend to be trace elements that can be reliably used with pXRF machines to distinguish between the majority of Alaska obsidian sources and groups. We have compared the variation among these specific elements within that DRO obsidian artifacts to the AOD with measurements from a wide variety of obsidian geological sources and obsidian artifacts from sites across Alaska, western Canada, and the Russian Far East.

We have also compared the ratios of Sr and Zr graphically through the use of biplots to discriminate between AOD obsidian sources and groups and DRO samples (Figure 10.1). Major obsidian source and groups in the AOD discriminated from one and another on bivariate plots based on cluster and discriminant classification analyses with a 95% or greater probability (Glascock et al. 1998; Reuther et al. 2012).

Our analyses have made a distinction between quantitative and non-quantitative results. Quantitative results are from pieces that ≥2 mm in maximum diameter and cover the pXRF's aperture and are ≥1 cm in thickness. These samples have higher count rates that accurately reflect the elemental concentrations in the materials. Non-quantitative results are from artifacts that are <2 mm in maximum diameter and are <1 cm in thickness. The measurements on this size of artifacts generally have lower counts and elemental concentrations that do not necessarily accurately reflect the elemental concentrations in the materials (Davis 2011; Lundblad et al. 2008). We have generally assigned those "unassigned" to a specific source. However, we were able to assign a few samples that were slightly under, but near, the maximum dimension and thickness thresholds for quantitative results to sources or group designations from the AOD. The measurements from these samples fell within the range of AOD obsidian source and group measurements even with the samples being slightly under the size and thickness thresholds.

Lastly, we qualitatively compared the spectra peak intensities (or heights) of elements from DRO artifacts and representative spectra of AOD obsidian source and groups. The relative peak heights of Rb, Sr and Zr also generally show variation between sources and groups (Figure 10.2).

10.3 Results

Trace element concentrations were measured on a total of 73 obsidian artifacts from the DRO collection (Table 10.2). Of the 73 DRO artifacts, the elemental concentrations of 64 artifacts (87.67%) were similar to source materials from the Wiki Peak obsidian source (also referred to as Group A obsidian; Cook 1995; Reuther et al. 2011). Wiki Peak materials were recognized in 2 of the 4 DRO components (C2c and C8b). The Wiki Peak source is located in the Nutzotin Mountains in Wrangell-St. Elias National Parks, approximately 280 km southeast of the DRO site (Figure 10.3).

Two samples (AOD-22360 and AOD-22361) from component C7b have elemental concentrations similar to Group A' obsidian. Group A' has also been referred to as the "Ringling source" (Goebel et al. 2008; Reuther et al. 2011) based on the large quantity of obsidian artifacts at the Ringling site (GUL-00077) that are similar to this obsidian group; however, referring to this group as the "Ringling source" is misleading because the physical location of the geological source is not at the Ringling site itself, and the Group A' source location away from this site that has yet to be identified. Group A' obsidian has been found at archaeological sites mostly in interior Alaska with the largest distribution found near Gulkana and the Wrangell-St. Elias National Park in the eastern part of the state (Goebel et al. 2008; Reuther et al. 2011), which is likely the region where the geological source is also located. The trace element concentrations for the Wiki Peak source and Group A' are roughly similar; however, Group A' generally has higher concentrations of Zr and Sr and lower Rb values that Wiki Peak. Variation in the concentrations within the source and group are also different. Wiki Peak obsidian has higher concentrations of Zr and Rb when compared to Sr, while Group A' has high Zr and Sr when compared to Rb. These patterns within the Rb, Sr and Zr concentrations allow us to easily distinguish between the two types of obsidian materials.

One artifact (AOD-22357), the sole obsidian artifact from C8a, has elemental concentrations similar to the Batza Tena obsidian source, located near the Indian River in the Koyukuk River region southeast of the village of Hughes (Clark and Clark 1993). The Batza Tena source is located roughly 470 km northwest of the DRO site (Figure 10.3). The Batza Tena source has concentrations of Zr and Sr that are much lower and Rb values higher than measurements for those elements from Wiki Peak and Group A' obsidians.

Five DRO obsidian artifacts (less than 7% of the DRO obsidian analyzed) could not be assigned to a particular obsidian source or group. Each of these artifacts are smaller and under the size and thickness thresholds of quantitative results. Three of these artifacts (AOD-12674, AOD-12675, and AOD-12723) were recovered from similar proveniences as other DRO obsidian artifacts that we assigned to the Wiki Peak source, which is most likely the source material but the thinness and small size of these artifacts made the elemental concentrations too low to confidently assign them to Wiki Peak. The other two unassigned samples (AOD-12697 and AOD-22359) that do not occur directly near other obsidian materials show similar patterns in the Rb, Sr and Zr concentrations to Wiki Peak obsidian, but with lower values, again, likely due to the thinness and small size of these artifacts. AOD-12697 and AOD-22359 do occur in stratigraphic contexts at DRO where other Wiki Peak materials were found at other locations of the excavation.

The behavioral implications of the use of Wiki Peak, Group A', and Batza Tena obsidians at DRO will be more below in the detailed lithic analysis section of this report.

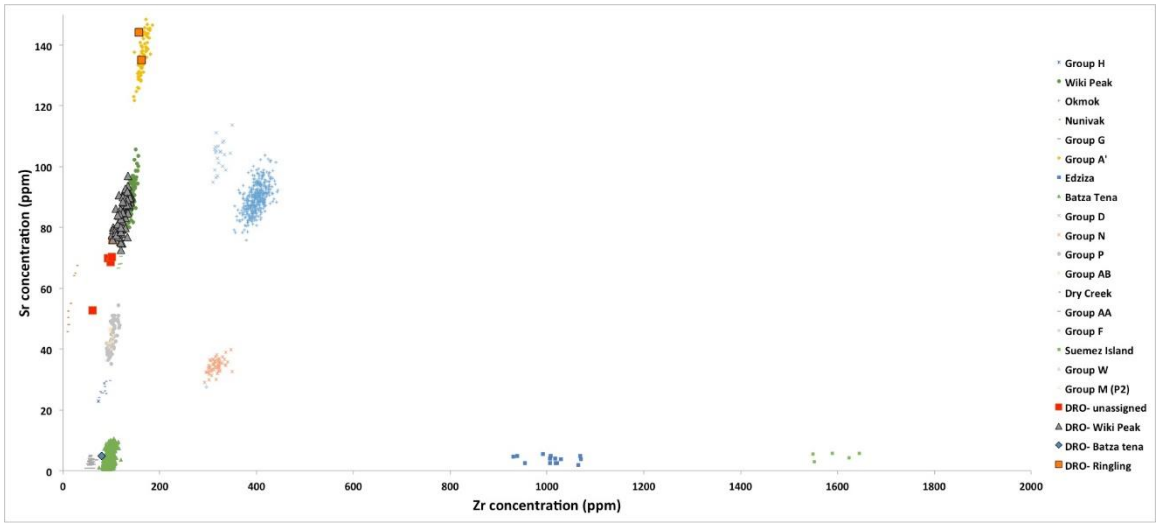

Figure 10.1. Biplot of Sr and Zr concentrations (ppm) of source materials and obsidian groups from the AOD and concentrations of DRO obsidian artifacts.

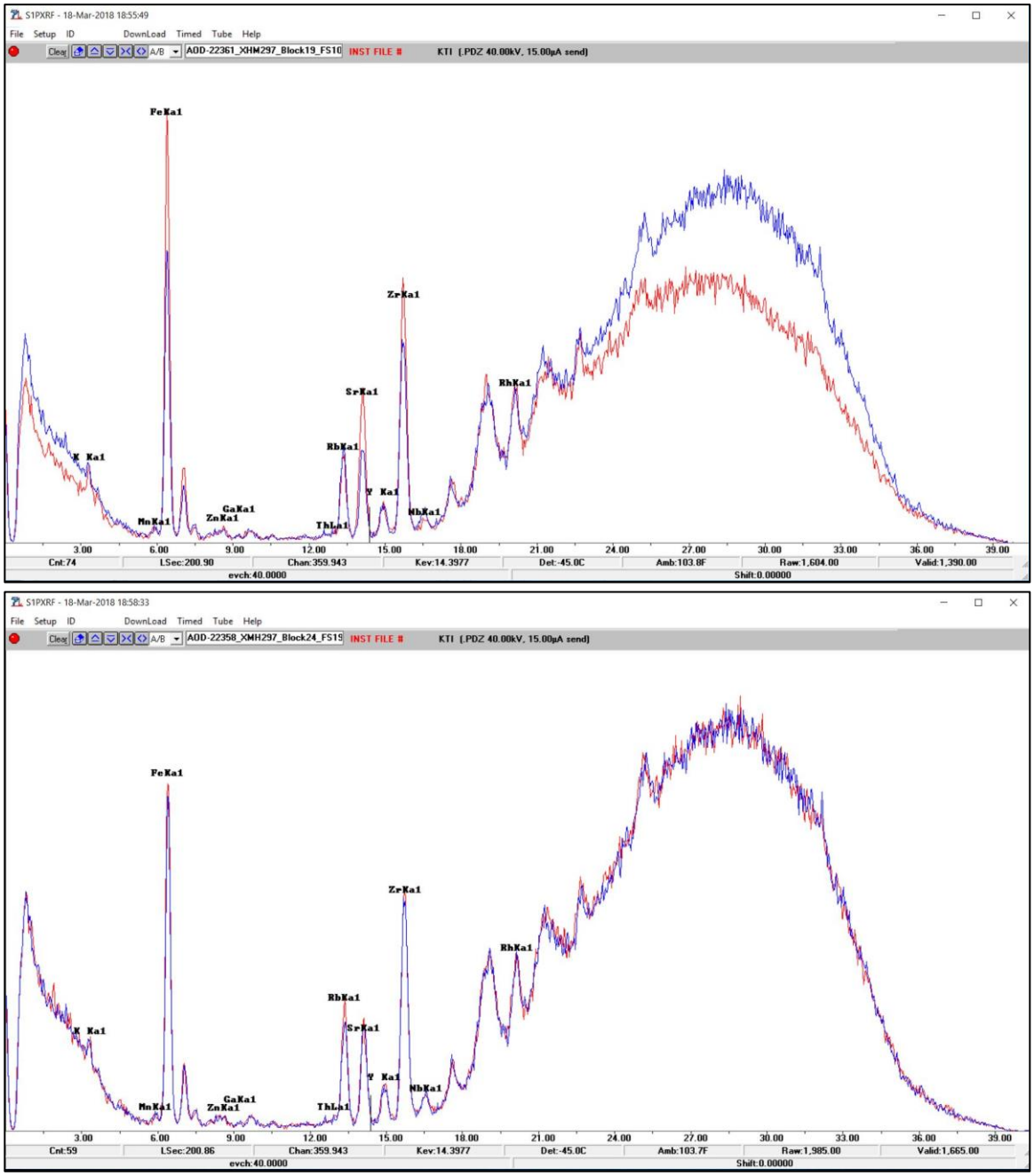

Figure 10.2. Bruker Tracer SD-II spectra comparisons. Above: spectra comparison between Wiki Peak source material (blue) and Group A' artifact (red) from DRO. Below: spectra comparison between Wiki Peak source material (blue) and Wiki Peak artifact (red) from DRO.

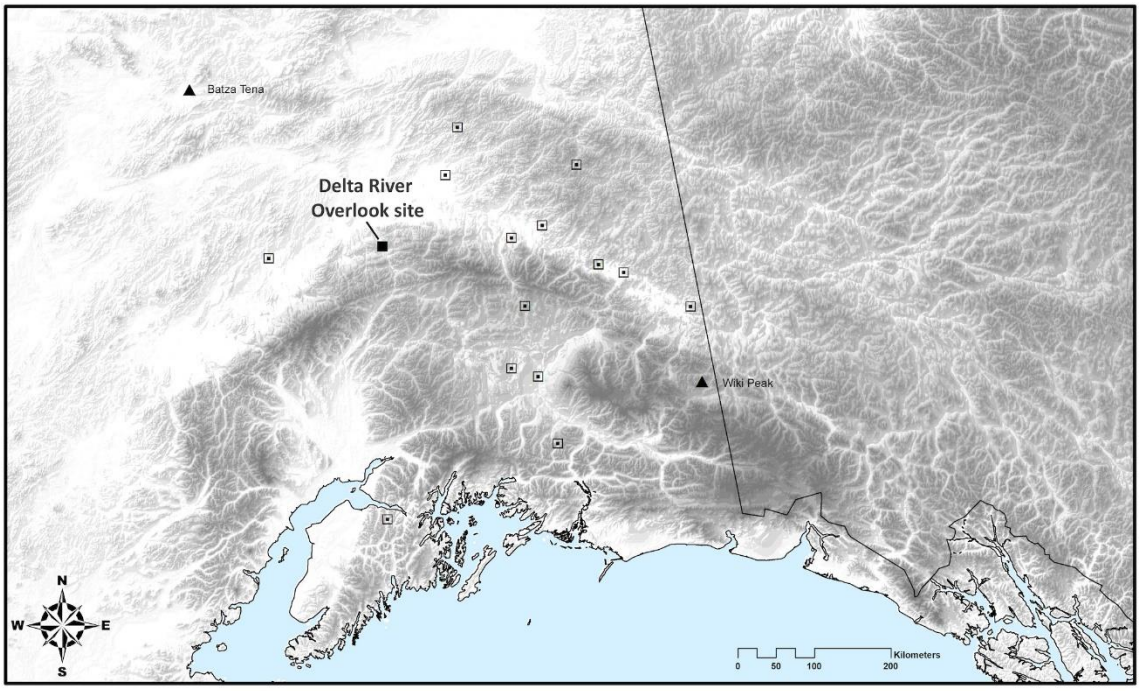

Figure 10.3. Map showing the Wiki Peak and Batza Tena obsidian sources, the distribution of archaeological sites with Group A' obsidian (open squares), and the location of the DRO.

Table 10.1. Trace element concentrations (ppm) of the Coral obsidian standard during the DRO obsidian analyses.

Standard[1] Analysis #	*K*	*Mn*	*Fe*	*Zn*	*Ga*	*Th*	*Rb*	*Sr[3]*	*Y*	*Zr*	*Nb*
20151012_Control_Run1	35469	342	15369	93	20	15	103	2	75	581	33
20151012_Control_Run2	37429	342	15571	106	20	15	100	3	73	593	34
20151020_Control_Run1	34079	418	15049	104	20	13	98	3	74	575	33
20151020_Control_Run2	34658	522	16225	110	20	13	99	3	77	605	34
20180118_Control_Run1	34948	398	15031	110	21	15	98	3	71	565	34
20180118_Control_Run2	35267	421	15712	108	20	14	98	4	72	581	32
Mean[2]	35786	415	15447	100	20	14	100	3	76	589	34
Standard deviation (1 σ)	1001	57	540	10	1	1	4	1	2	12	2
% relative standard deviation (%RSD)	3	14	3	10	3	10	4	23	3	2	5

[1]Coral Source, OR obsidian sample used as an internal standard to check machine setup and proper functioning.
[2]The mean element values presented here are based on 192 analyses of the Coral standard with the UAMN Bruker Tracer SD-III from 2009 to 2018.
[3]Because this obsidian has an extremely low concentration of Sr, any deviation will make a substantial impact on the %RSD values. Therefore, we do not consider high %RSD values in this standard for Sr to reflect issues in the machine's performance or instrument error (Speakman and Shackley 2013).

Table 10.2. Trace element concentrations (ppm) of DRO obsidian artifacts and their source assignments.

AOD_Number	*Block*	*FS*	*Component*	*K*	*Mn*	*Fe*	*Zn*	*Ga*	*Th*	*Rb*	*Sr*	*Y*	*Zr*	*Nb*	*Source_Name*	*Source_Group*
AOD-12664	8	2	C8?	56261	281	8244	55	18	11	89	78	17	118	9	Wiki Peak	Group A
AOD-12665	8	9	C7?	47106	274	8487	12	15	15	106	88	19	139	9	Wiki Peak	Group A
AOD-12666	8	9	C7?	52902	383	8987	24	15	13	104	87	19	137	11	Wiki Peak	Group A
AOD-12667	11	130	C2c	41267	300	8240	23	15	14	103	90	19	141	11	Wiki Peak	Group A
AOD-12668	11	130	C2c	44481	460	11227	63	18	14	111	92	16	127	9	Wiki Peak	Group A
AOD-12669	11	130	C2c	54747	350	10696	51	17	13	108	87	17	124	9	Wiki Peak	Group A
AOD-12670	11	130	C2c	62251	334	9881	44	17	11	103	83	17	124	9	Wiki Peak	Group A
AOD-12671	11	130	C2c	57607	355	10659	70	18	14	104	75	16	118	7	Wiki Peak	Group A
AOD-12672	11	130	C2c	40882	274	10472	110	21	14	100	80	14	104	7	Wiki Peak	Group A
AOD-12673	11	130	C2c	40803	382	11794	163	25	14	107	78	16	101	8	Wiki Peak	Group A
AOD-12674	11	130	C2c	42433	279	11374	102	21	14	93	70	17	93	6	unassigned	unassigned
AOD-12675	11	130	C2c	41579	405	8559	134	23	11	72	53	18	61	6	unassigned	unassigned
AOD-12676	11	133	C2c	52651	387	10882	49	18	15	114	92	17	128	9	Wiki Peak	Group A
AOD-12677	11	133	C2c	56941	346	10114	46	17	13	103	93	19	132	9	Wiki Peak	Group A
AOD-12678	11	133	C2c	58403	364	12087	68	18	12	108	85	18	133	9	Wiki Peak	Group A
AOD-12679	11	133	C2c	51127	255	11108	44	17	12	99	91	15	115	7	Wiki Peak	Group A
AOD-12680	11	133	C2c	49845	302	10764	69	18	12	100	83	18	124	8	Wiki Peak	Group A
AOD-12681	11	133	C2c	40880	535	12673	74	20	14	105	79	16	109	7	Wiki Peak	Group A
AOD-12682	11	136	C2c	59340	374	9869	20	16	13	109	91	18	139	9	Wiki Peak	Group A
AOD-12683	11	136	C2c	42492	471	12456	53	17	13	102	81	16	118	8	Wiki Peak	Group A
AOD-12684	11	136	C2c	50543	401	11384	63	17	12	107	85	17	124	10	Wiki Peak	Group A
AOD-12685	11	136	C2c	38689	651	14071	97	19	14	111	84	14	115	8	Wiki Peak	Group A
AOD-12686	11	136	C2c	56975	414	8890	63	17	11	91	79	16	112	6	Wiki Peak	Group A
AOD-12687	11	136	C2c	40624	373	12120	55	18	13	99	78	16	116	9	Wiki Peak	Group A
AOD-12688	11	136	C2c	56986	287	9785	42	17	12	102	79	15	116	7	Wiki Peak	Group A
AOD-12689	11	174	C2c	50940	314	7739	29	15	11	93	75	18	123	9	Wiki Peak	Group A
AOD-12690	11	180	C2c	44941	308	8069	36	16	14	96	79	21	122	9	Wiki Peak	Group A
AOD-12691	11	193	C2c	35995	540	14196	92	20	15	103	86	15	110	8	Wiki Peak	Group A
AOD-12692	11	198	C2c	49153	180	7458	6	15	13	88	75	21	120	8	Wiki Peak	Group A
AOD-12693	11	348	C2c	55860	298	9550	28	16	15	104	88	19	135	9	Wiki Peak	Group A
AOD-12694	11	256	C2c	57992	245	9323	31	16	14	109	90	19	139	11	Wiki Peak	Group A
AOD-12695	11	257	C2c	52746	266	9088	30	15	14	104	87	18	136	9	Wiki Peak	Group A
AOD-12696	11	320	C2c	54823	285	9564	32	14	11	106	90	17	139	10	Wiki Peak	Group A
AOD-12697	12	11	C8b	40109	497	13449	117	20	11	97	69	14	99	6	unassigned	unassigned
AOD-12698	12	122	C2c	50156	285	11076	33	16	14	111	87	15	122	8	Wiki Peak	Group A
AOD-12699	12	124	C2c	47977	353	9826	33	17	14	104	84	19	124	9	Wiki Peak	Group A
AOD-12700	12	125	C2c	48272	302	11403	48	16	14	109	89	17	132	10	Wiki Peak	Group A
AOD-12701	12	126	C2c	45434	458	12069	53	18	16	120	94	17	134	11	Wiki Peak	Group A
AOD-12702	12	193	C2c	56649	291	8999	225	31	12	101	80	18	124	8	Wiki Peak	Group A

AOD-12703	12	198	C2c	39868	388	12967	94	21	16	103	79	17	104	7	Wiki Peak	Group A
AOD-12704	12	254	C2c	44926	397	11426	80	19	16	111	93	17	130	9	Wiki Peak	Group A
AOD-12705	12	356	C2c	59783	230	8355	14	15	15	106	83	18	130	9	Wiki Peak	Group A
AOD-12706	12	357	C2c	56360	248	7870	17	16	13	97	78	19	122	8	Wiki Peak	Group A
AOD-12707	12	358	C2c	58793	407	9958	40	16	14	107	85	18	134	9	Wiki Peak	Group A
AOD-12708	12	358	C2c	60949	297	8101	25	15	11	94	73	16	120	9	Wiki Peak	Group A
AOD-12709	12	359	C2c	47213	530	12233	63	17	13	99	80	16	109	7	Wiki Peak	Group A
AOD-12710	12	360	C2c	55729	370	8312	42	17	12	89	77	17	117	8	Wiki Peak	Group A
AOD-12711	12	361	C2c	52654	422	11121	59	18	13	111	82	15	123	8	Wiki Peak	Group A
AOD-12712	12	350	C2c	40724	429	11677	64	18	15	112	86	16	118	7	Wiki Peak	Group A
AOD-12713	12	350	C2c	60218	246	9934	45	17	15	99	81	19	113	8	Wiki Peak	Group A
AOD-12714	12	350	C2c	49868	320	10472	55	18	12	95	77	20	114	10	Wiki Peak	Group A
AOD-12715	12	366	C2c	56140	332	10018	36	16	13	109	92	17	133	10	Wiki Peak	Group A
AOD-12716	12	366	C2c	56775	234	8857	24	16	13	104	80	19	129	9	Wiki Peak	Group A
AOD-12717	12	366	C2c	65714	332	9378	28	15	12	108	88	18	132	8	Wiki Peak	Group A
AOD-12718	12	366	C2c	56753	285	10356	40	17	14	110	97	17	134	9	Wiki Peak	Group A
AOD-12719	12	366	C2c	60485	409	11060	49	17	14	108	85	18	123	8	Wiki Peak	Group A
AOD-12720	12	366	C2c	53645	388	12609	63	17	13	110	90	14	124	8	Wiki Peak	Group A
AOD-12721	12	366	C2c	50854	394	10688	43	16	11	106	88	14	124	9	Wiki Peak	Group A
AOD-12722	12	366	C2c	52847	332	9473	48	17	13	101	83	16	120	8	Wiki Peak	Group A
AOD-12723	12	366	C2c	41422	481	13499	69	18	11	91	70	16	102	7	unassigned	unassigned
AOD-12724	12	366	C2c	53068	434	11148	74	19	13	97	76	17	103	7	Wiki Peak	Group A
AOD-12725	12	366	C2c	49694	406	11596	79	18	12	102	85	17	117	9	Wiki Peak	Group A
AOD-12726	12	366	C2c	57973	352	9695	30	17	15	99	78	18	109	8	Wiki Peak	Group A
AOD-12727	12	113	C2c	49126	272	10909	38	17	16	113	88	19	124	9	Wiki Peak	Group A
AOD-12728	12	113	C2c	57961	513	11959	79	17	10	89	77	17	111	8	Wiki Peak	Group A
AOD-12729	12	113	C2c	56319	237	9858	38	16	14	102	79	18	119	9	Wiki Peak	Group A
AOD-12730	12	113	C2c	49177	327	10060	48	16	13	98	80	17	120	7	Wiki Peak	Group A
AOD-12731	12	113	C2c	56080	487	12172	53	17	12	96	84	14	113	7	Wiki Peak	Group A
AOD-22357	22	86	C8a	41168	535	4879	36	20	26	170	5	37	80	20	Batza Tena	Group B
AOD-22358	24	190	C8b	33803	326	7849	19	16	15	111	77	20	134	10	Wiki peak	Group A
AOD-22359	20	29	C2c	37966	436	13539	85	18	14	98	76	16	102	8	unassigned	unassigned
AOD-22360	19	105	C7b	46089	235	10803	12	15	13	81	144	17	157	7	Ringling	Group A'
AOD-22361	19	106	C7b	41603	325	9728	28	15	12	79	135	17	163	6	Ringling	Group A'

CHAPTER 11. BISON SEASONAL MOBILITY: ISOTOPIC ANALYSES ON FOUR BISON TEETH FROM XMH-297

Crystal L. Glassburn

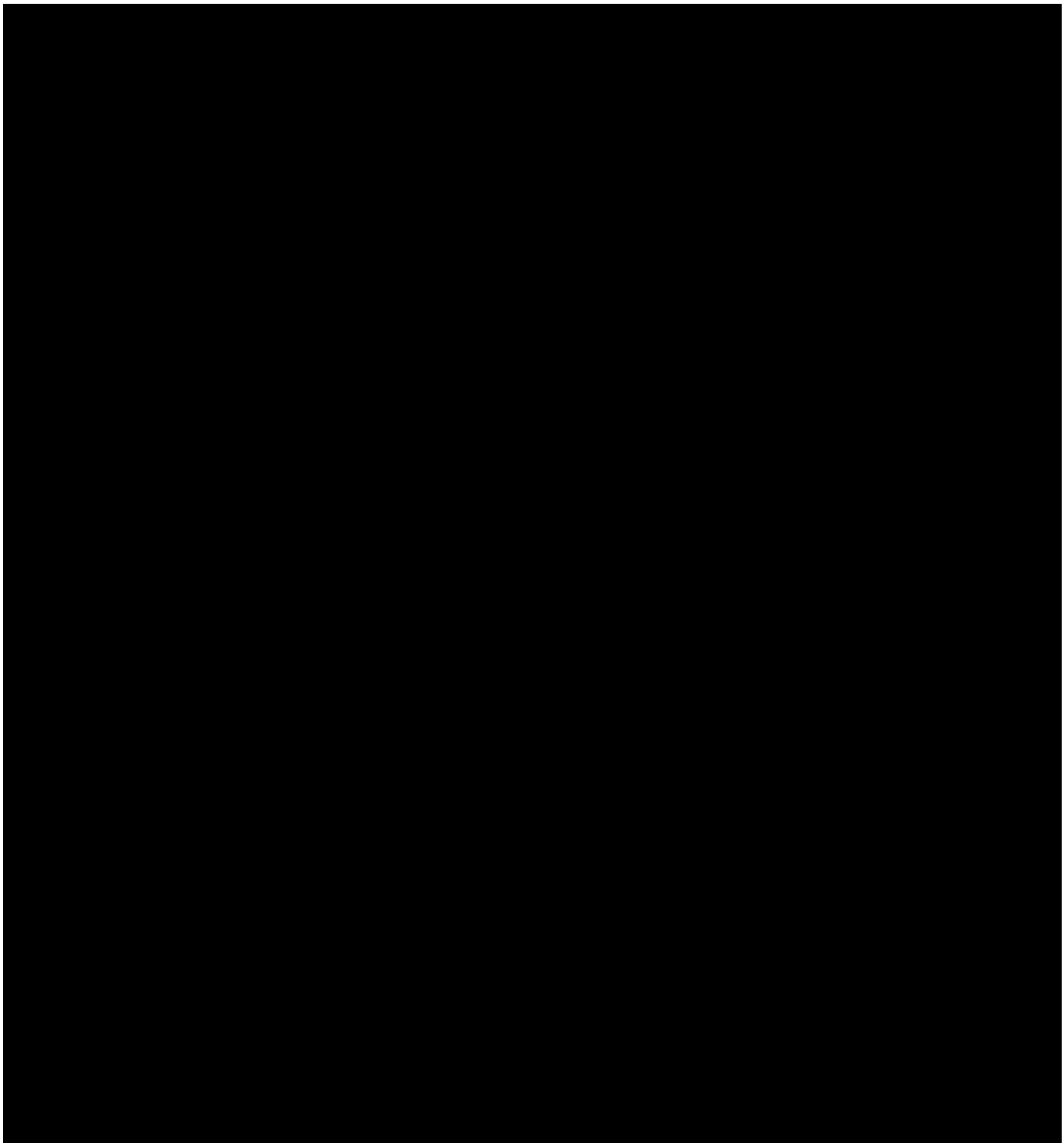

CHAPTER 12. FEATURE AND SPATIAL ANALYSIS

Ben A. Potter

12.1 Introduction and Methods

Features were identified through localized sediment-staining, concentrations of charcoal and calcined bones, or sharp breaks with surrounding undisturbed sediments, and other evidence. A total of 19 features were recorded in 2015 and 2017 (Table 12.1). Most features discovered at DRO were *hearths*, or unlined firepits, defined through the presence of locally oxidized sediments, localized concentrations of abundant charcoal, and generally calcined and burnt faunal fragments. Other features were classified as *charcoal scatters*, which are similar to hearths except without oxidized (reddened) sediments. Several bright reddish stains were discovered ~5 cm below Paleosol 1 directly associated with cultural material from Component 2c. These may be areas of ochre staining.

Two hearths were discovered in plan view drawings obtained from the Japanese excavation at DRO in 1985. These were likely related to Component 8b given the depth of their excavation, and are labeled F1985-1 and F1985-2.

In addition to ancient cultural features, a number of other features were discovered at DRO. F2015-2 was the original 1978 test pit, found within Block 5. F2015-3 and F2015-4 are small clay deposits, each about 10 cm in diameter, and neither are associated with cultural material. F2015-10 was a very narrow (~10 cm wide), 25 cm deep trench, excavated by Holmes in 1979 to connect stratigraphy Blocks A and B.

Feature descriptions and analyses are provided in the context of spatial analyses that follow, by component. Spatial summaries of fauna and lithic assemblages (Chapter 7 and 8) are combined to infer site function and specific onsite activities.

Table 12.1 Feature summary data

Feature ID	*Block*	*Depth*	*Strat*	*Component*	*Description*
F2015-1	12	3-8 cmbs	L6	C8b	FCR, charcoal, flakes directly associated. No bone, but abundant charcoal and oxidized sediment. (53 x 37 x 8 cm)
F2015-2	5	35 cmbs to till	NA	NA	1978 test pit
F2015-3	3		L1	NA	Clay deposit (natural)
F2015-4	3		L1	NA	Clay deposit (natural)
F2015-5	6	10 cmbP1	L1	C2c	Hearth (9470±30 BP) (115 x 65 x 5 cm)
F2015-6	19	60-65cmbs	Just above T1		Cobble cluster
F2015-7	6, 7	17 cmbP1	L1	C2b	Charcoal scatter (10,060±40 BP) (317 x 233 x 0.5 cm)
F2015-8	6, 7	27 cmbP1	L1	C2a	Hearth (10,000±40 BP) (89 x 65 x 7.5 cm)
F2015-9	11	0-5cmbP1	L1	C2c	Hearth (9510±30 BP) (115 x 93 x 5 cm)
F2015-10	Multiple	0-25 cmbs	NA	NA	1985 mini-trench excavated by Japanese connecting Blocks A and B
F2017-1	24	5-10cmbs	Loess above P7b	C8b	Hearth (2210±20 BP) (150 x 95 x 8 cm)
F2017-2	20, 21	50-55cmbs	P3	C6a	Hearth (5980±30 BP) (195 x 87 x 3 cm)
F2017-3	22	30-40cmbs	P7a	C8a	Blank cache (~3330±30 BP)
F2017-4	10	5-10cmbP1	L1	C2c	Red layer (ochre?) (97 x 32 x 2 cm)
F2017-5	20	8-13cmbP1	L1	C2c	Red layer (ochre?) (55 x 17 x 7 cm)

F2017-6	21	15cmbP1	L1	C2b	Hearth (charcoal concentration with calcined bone) (1227 x 70 x 1 cm)
F2017-7	15	0-5cmbP1	L1	C2c	Red layer (ochre?) (97 x 32 x 2 cm)
F2017-8	22	0-5cmbP1	L1	C2c	Red layer (ochre?) (147 x 130 cm x 2 cm)
F2017-9	19	0-5cmbP1	L1	C2c	Red layer (ochre?) (200+ x 200+ cm x 2 cm)
F1985-1		? upper strat	?	C8b	Hearth? (153 x 75 cm)
F1985-2		? upper strat	?	C8b	Hearth? (30 x 40 cm)

12.2 Component 1 Activity Areas

No cultural features were identified for Component 1. Three activity areas were identified within Component 1: C1g1, C1g2, and C1g3 (Figure 12.1). Area C1g1 contains the largest proportion of C1 materials, 152 flakes, 1 modified flake, and 4 bifaces. Debitage analyses indicate biface (projectile point) production and finishing, with soft hammer percussion commonly employed. A minimum of two points were likely produced, material types C30 and C36, as they comprise 89% of the debitage. Tool maintenance of at least 8 additional tools (based on raw materials) also occurred.

Area C1g2 is a small concentration of slightly earlier stage lithic reduction of a variety of materials, characterized by hard hammer percussion (with some cortical flakes). An unrelated finished projectile point was also located in this area. This area has more even distribution of 7 raw materials, suggesting maintenance of various tools.

Area C1g3 is a small cluster of microblades, one of which was modified. The only fauna at this component are associated with this activity area: ground squirrels and grouse. This suggests the microblades may have been used for faunal processing and that the bifacial projectile point replacement in the other areas may be unrelated to recent hunting episodes.

Collectively, Component 1 bifaces indicate broken projectile points in hafts were transported to the site, discarded, and replacement projectile points were manufactured onsite to be rehafted and taken offsite. Modified flakes were likely made onsite and used as expedient tools (with low levels of curation), possibly for processing fauna. Compared to Denali components, this component is relatively small, indicating short-term occupation. Site function is inferred to be bifacial weapon maintenance and limited production, and this site can be classed as a weapon maintenance station.

Fauna include ground squirrel and grouse, with no large or very large artiodactyl, different than most other DRO components. This suggests opportunistically and locally acquired animals were processed onsite.

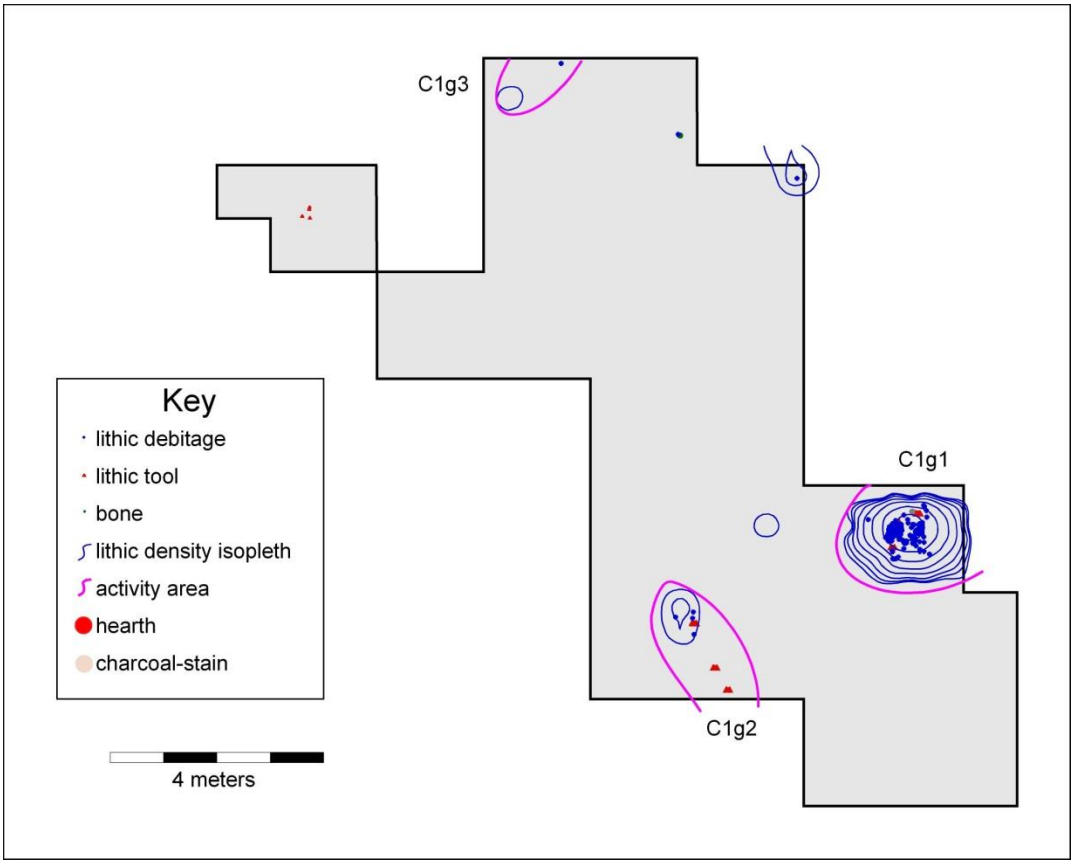

Figure 12.1 Component 1 activity areas.

12.2 Component 2a Activity Areas

Six activity areas were identified within Component 2a (Figure 12.2), a large, dense lithic concentration centered around a central hearth feature, F2015-8, labeled C2ag1, and four smaller lithic concentrations surrounding this area: C2ag2, -3, -4, and -6. Each of these areas have similar lithic quantities (200-300 items) suggesting modal occupations around each hearth. An additional activity area, C2ag5, is located a few meters to the north.

C2ag1 is a ~4 x 6 m area centered on hearth F2015-8, dating to 10,000±40 BP. The hearth is 89 x 65 cm at the widest extent and 7.5 cm deep. Most of the lithics are within the drop zone of this hearth (i.e., <2.5 m from hearth centroid). Lithic debitage analyses indicate multiple lithic reduction episodes including later stage bifacial reduction. Recovered tools include 7 bifaces, 3 unifaces, 1 burin spall, 3 cobble spall tools, 10 modified flakes and 1 modified microblades. The bifaces are from a variety of stages, including an edged biface (stage 2), thinned biface (stage 3), and 5 bifacial preforms (stage 4). Collectively the lithic analyses suggest later stages of bifacial tool production (3-5, with finished points removed from the site), probably geared towards projectile point manufacture. Some of these bifaces may have produced from satellite area C2ag3 given the debitage patterning (see below). Associated faunal materials (C2a-F1) include many L/VL (bison-sized) artiodactyl fragments.

The four satellite areas surrounding this hearth area reflect similar lithic behaviors: later stage bifacial reduction. C2ag3 (and to a lesser extent, C2ag6) is distinct, and reflects earlier

stages of lithic reduction, probably hard hammer percussion of flake cores. Microblade technology is also absent from C2ag3, and is present at all other activity areas at low frequencies.

Area C2ag5 reflects similar lithic behaviors as C2ag1, later stage bifacial reduction, though with different raw materials, including C36 and R9 (24% of area total), and both of these are absent in other C2a areas. Associated tools include 2 modified flakes and 6 bifaces (2 thinned bifaces [Stage 3], and 4 preforms [Stage 4], one of which is a projectile point preform. Again, later-stages of biface production, most likely projectile points, is the primary activity. Associated faunal cluster C2a-F3 contains long bone fragment and sheep mandible.

The faunal remains are relatively similar for each of the three faunal clusters, primarily L/VL artiodactyl long bones and tooth fragments. One sheep mandible (L artiodactyl) was the only element identified to species. High meat yield elements were probably removed from the site. Collectively, Component 2a likely represents a short-term hunting camp, where early processing of large ungulates and weapon production took place.

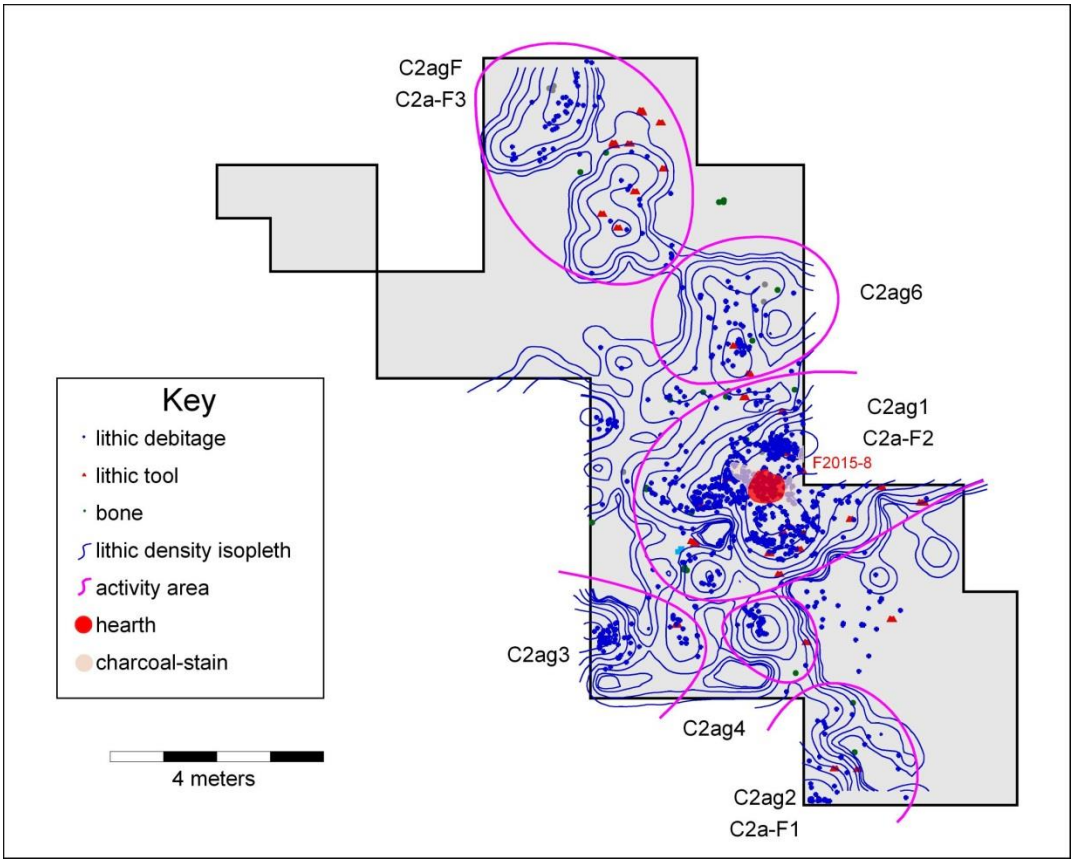

Figure 12.2 Component 2a activity areas.

12.3 Component 2b Activity Areas

Component 2b reflects a single concentrated activity area, composed of a faunal concentration to the west of the hearth, Feature F2017-6 and associated charcoal scatter, Feature F2015-7, and a lithic concentration to the east of the hearth (Figure 12.3). Hearth F2017-6 is a 1 cm thick concentration of charcoal and calcined bone measuring 127 x 70 cm in dimension. A

directly associated charcoal scatter (F2015-7) (without calcined bone) measuring 317 x 233 cm wide and 0.5 cm thick extends to the east of the hearth. The top of both features are 15-17 cm below Paleosol 1. Most of the lithics are within the drop zone of hearth F2017-6. Lithic debitage analysis indicates later stage lithic tool maintenance using soft-hammer percussion and pressure flaking, perhaps of unifaces or flake tools with relatively few bifaces. A few microblades were recovered, but debitage analysis does not indicate substantial microblade production. Lithic tools include 1 modified flake and 1 burin spall, with no unifaces or bifaces recovered. These data suggest very short term occupation where tools were transported to the site, maintained briefly onsite, and largely transported offsite.

Fauna are dominated by L/VL artiodactyl remains, including 22 NISP of bison. The remains are concentrated, consisting of mandible and teeth, suggesting kill relatively close to DRO, and deposition of low yield remains outside of the excavation area. Associated bison remains may occur in the unexcavated area to the west. No long bones were found, nor any high yield elements, suggesting removal of meat-bearing portions for transport elsewhere, likely to a residential base camp. From the faunal and lithic data, Component 2b likely represents a short-term hunting camp, where early stage processing of recently killed bison took place.

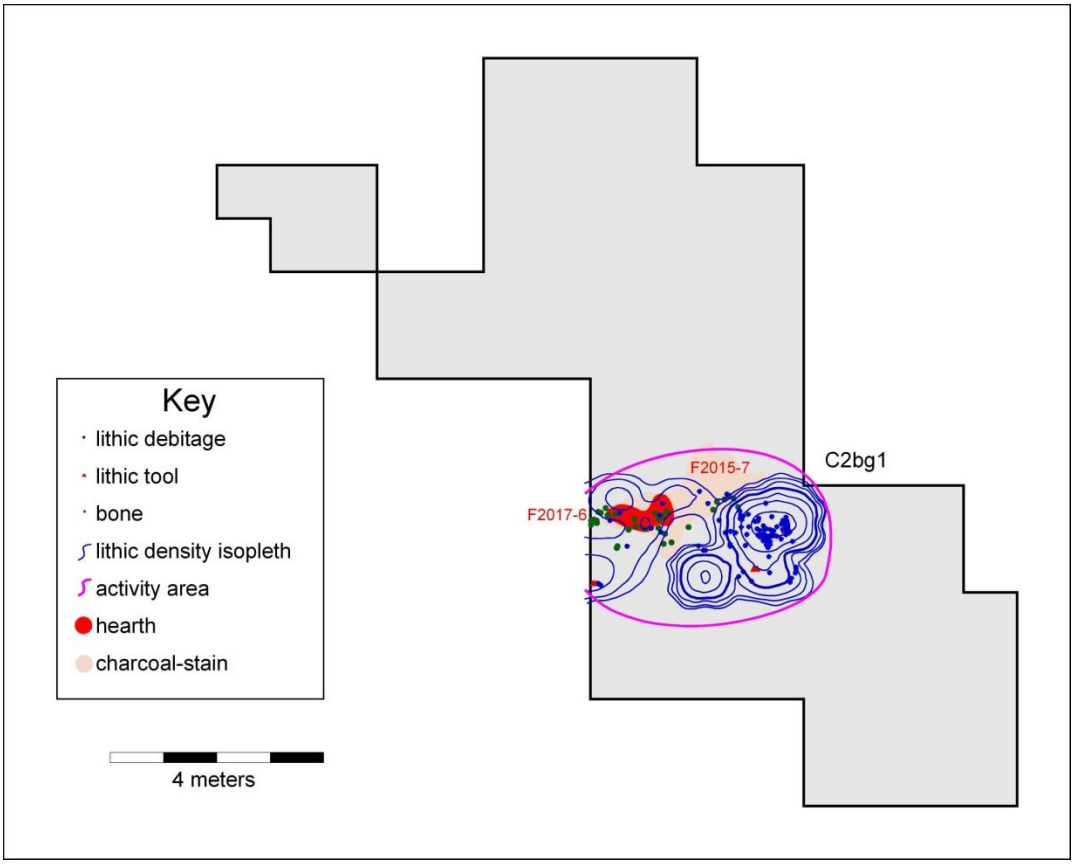

Figure 12.3 Component 2b activity areas.

12.4 Component 2c Activity Area

Component 2c consists of two activity areas, both centered on hearth features (Figure 12.4). Activity area C2cg1 is centered on hearth F2015-5, dating to 9470+/-30 BP. This hearth measures 115 by 65 cm at the surface and is 5 cm thick. Another possible hearth, F2017-5 is located ~2 m to the southwest, truncated by the excavation area, measuring a minimum of 55 by 17 cm wide and is ~5 cm thick. Almost all of the lithic concentrations are within the drop zone of the F2015-5 hearth, within ~2.5 m. Tools include 4 bifaces, 1 burin, 9 burin spalls, 4 cobble spall tools, 7 modified flakes, and 5 unifaces. The bifaces consist of 1 thinned biface (stage 3), 1 preform (stage 4), and 2 finished bifaces (stage 5) (a projectile point and a possible knife). Microblade technology includes 23 modified microblades, 64 unmodified microblades, and 1 microblade core tablet.

Activity area C2cg2 is located to the north of C2cg1, and is centered on hearth F2015-9, located 8 meters from the other central hearth. Hearth F2015-9 measures 115 by 93 cm at the surface and is 5 cm thick. Almost all of the lithic concentrations are within the drop zone of F2015-9, within ~2.5 m. Tools include 2 bifaces, 6 burin spalls, 8 modified flakes, and 4 unifaces (all end scrapers). The bifaces consist of 1 thinned biface (stage 3) and 1 preform (stage 4). Microblade materials include 63 modified microblades, 272 unmodified microblades, 2 microblade cores, and 2 microblade core tablets.

A smaller activity area, C2cg3, was located about 2 meters to the east of C2cg1, comprising 87 flakes, 1 burin, 2 burin spalls, 1 cobble spall tool, 2 modified flakes and 3 modified microblades.

The two major activity areas are very similar in debitage characteristics and raw material proportions, indicating redundant (and similar) behaviors, suggesting they are part of logistically organized settlement systems. Overall, the debitage data suggest very similar lithic reduction behaviors in the two hearth-centered activity areas, remarkable given the large subassemblage sizes (both over 3,000 artifacts). Microblade production was present, but the majority of the debitage relates to later stage biface reduction (likely with soft hammer percussion) from thinning bifaces to maintaining finished tools. C2cg2 has more bifacial thinning flakes than C2cg1 and relatively more microblade materials, suggesting more intensive microblade production there. The differences in unifaces (sidescrapers in C2cg1 and endscrapers in C2cg2) suggest different activities, but unifacial and bifacial tools were likely maintained in both areas. In contrast, cluster C2cg3 is dominated by microblade materials (64%) and the burin and burin spalls suggest organic tool fabrication/repair, likely slotted implements to receive microblades. Damaged organic composite tools were repaired in C2cg1 and C2cg2, given the high number of modified microblades (19-26%), contrasting with C2cg3 where microblades were likely produced. The presence of microblade/composite and bifacial projectile point technology is intriguing, suggesting both systems were used within the same contexts, at least at this fall hunting site.

The Component 2c faunal record is dominated by L/VL artiodactyl remains, mainly diaphysis fragments of long bones and tooth enamel fragments. The two main faunal clusters correspond to the hearth-centered activity areas described above. Both clusters are very similar to each other, and both have VL artiodactyl long bones and teeth as well as ground squirrel vertebra remains. The macrofossil remains from two hearths in this component indicate a fall season of occupation. This component is very similar to another fall hunting camp at Gerstle River, dominated by composite implement repair, microblade production, and bifacial tool maintenance

(Potter 2005). There, bison and wapiti were killed nearby, early stage processing occurred onsite, including marrow consumption and removal/transport of high meat yield portions to a base camp. The similarities in DRO C2c and Gerstle River C3 assemblages are striking, dominated by hunting-related tools like microblades, weapon fabricators like burins, and expedient processing implements like cobble tool artifacts (tci-thos) and modified flakes. In sum, Component 2c likely represents a short term hunting camp, where early processing of large mammals took place.

Content analysis and overall morphology of the two activity areas suggest tent-like structures, supported by clear positive and negative arcs of debris surrounding the hearths in a circular manner. Overall dimensions suggest 4 to 5 meter diameter circular structures, perhaps short-term tents centered on the hearths. The central hearths are ~8 meters apart and the edges are ~5 meters apart. Immediately outside the dense lithic concentrations are five ochre-stained areas, F2017-4, F2017-8, F2017-9, and two unnumbered features encountered in 2015. These are all similar in dimension, about 150 by 120 cm (ranging between 32 and 200+ cm) and between 0.5 and 2 cm thick. These features are very different from observed soil horizons, are spatially delimited at the exact same stratigraphic location as the other C2c materials (~0-10 cm below Paleosol 1), and are generally in voids where lithics are absent. It is possible these features represent hide processing areas.

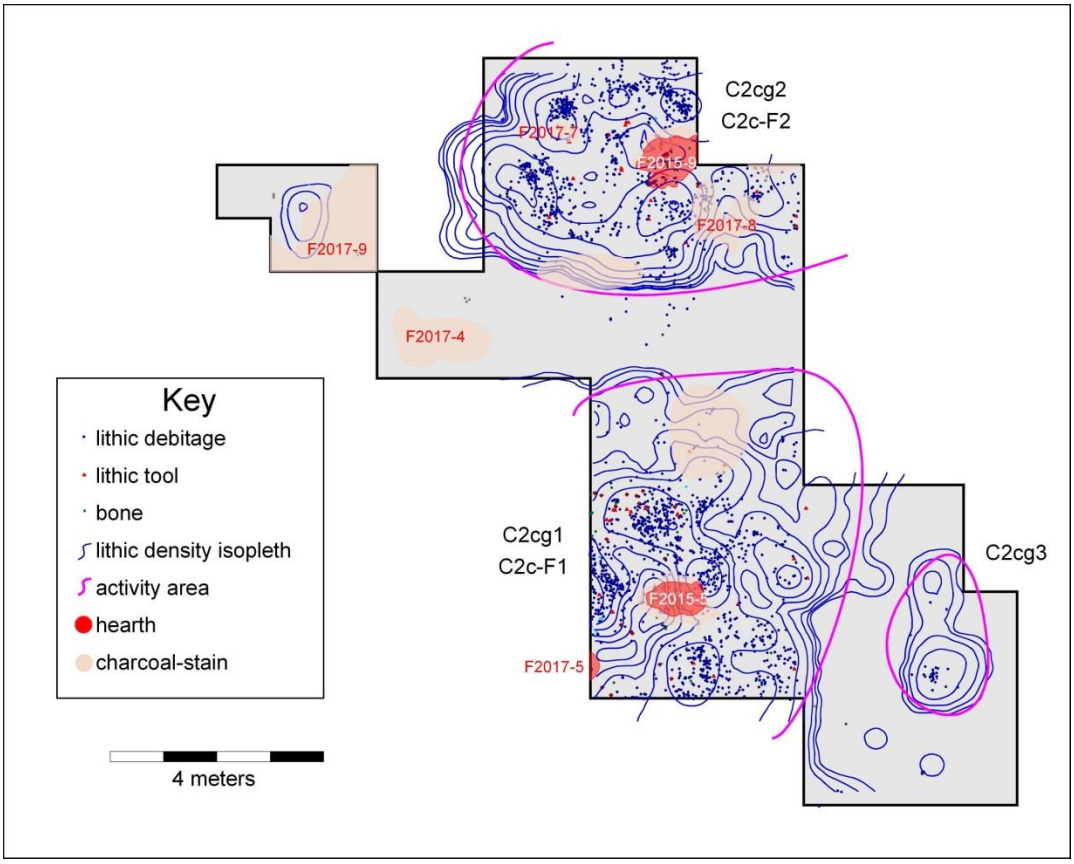

Figure 12.4 Component 2c activity areas.

12.5 Component 3 Activity Areas

Component 3 consists of two activity areas C3cg1 and C3cg2, located ~6 meters apart (Figure 12.5). C3cg1 contains 34 pieces of debitage and 1 modified flake and C3cg2 contains 231 flakes, 2 microblades, and 5 tools: 1 small biface fragment and 4 modified flakes. The two activity areas are dominated by different raw material types, C5 and C19 respectively. Debitage patterns are dissimilar between the areas, with C3g1 characterized by late stage bifacial reduction (likely bifacial tool maintenance) within a single raw material type. A wider range of behaviors are apparent in C3g2, including microblade use, discard, and tool maintenance. The dominance of single lithic raw materials, low artifact density, and absence of hearth features all suggest a very short term occupation.

The faunal record of Component 3 is dominated by L/VL artiodactyl remains, including 47 bison NISP and 1 wapiti, generally long bone diaphysis fragments and mandible/teeth fragments, along with a single wapiti antler. C3-F1 is associated with the southern part of the excavation and C3-F2 is associated with the central/northern part of the site. Both clusters are similar, dominated by teeth and broken long bone shafts. The faunal data suggests that this is an early processing site, with high meat yield elements removed from the site and transported to a residential base camp elsewhere. Most importantly, a bison right mandible includes an erupting M3, suggesting a death date of late February (January to May), reflecting a winter/early spring occupation, the first of its kind in Beringia. Compared to Components C2a, C2b, and C2c, the Component 3 occupation is more ephemeral, suggesting higher mobility and shorter occupation duration during winter months.

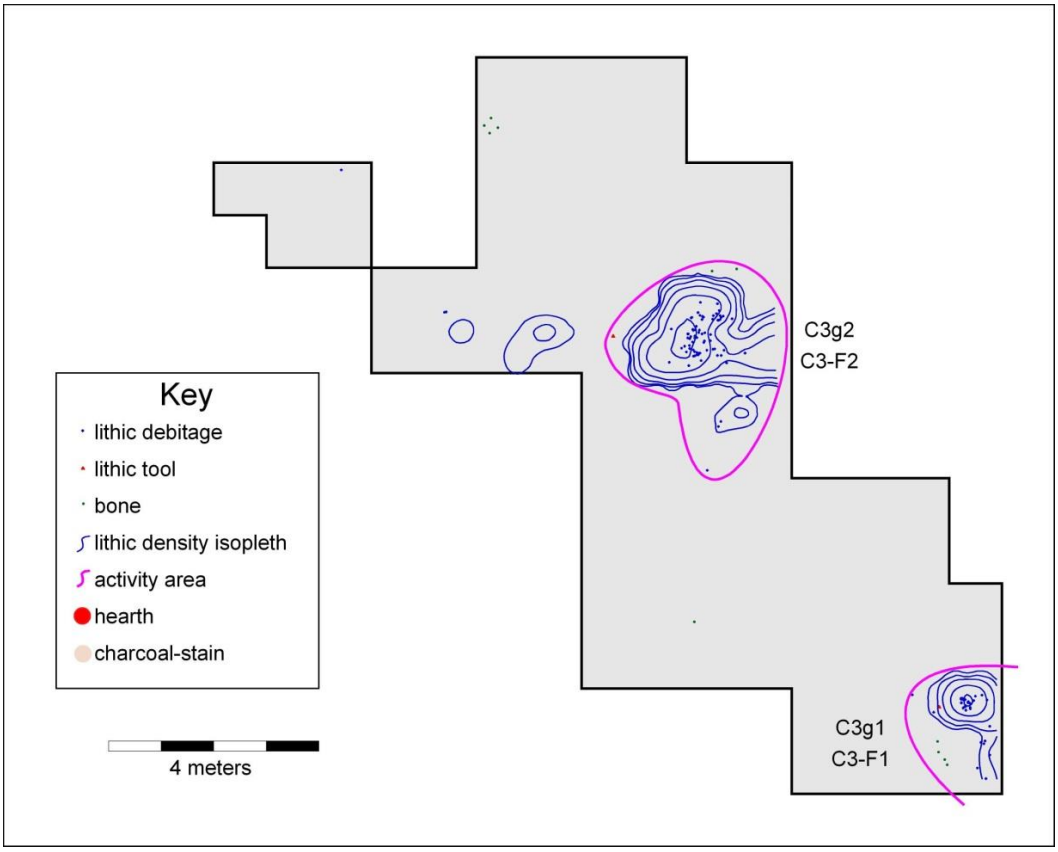

Figure 12.5 Component 3 activity areas.

12.6 Component 4 Activity Areas

Component 4 consists of four small activity areas, all 2-3 meters in diameter with between 18 and 131 lithic artifacts (Figure 12.6). No cultural features were discovered in Component 4. Tools include 6 modified flakes, 7 modified microblades, and a microblade core. Lithic raw materials are all different for each group, each dominated by a different material (between 60-97% of each subassemblage). While raw material differences exist, overall lithic behaviors overlap among the groups. C4g1 reflects late stage biface reduction and microblade production, with 90 flakes and 32 microblades). C4g2 reflects late stage biface and/or flake tool maintenance (with 32 flakes). C4g3 and C4g4 reflect tool maintenance and nonlocal microblade discard (with 15 flakes and 1 microblade). C4g1 and C4g4 also included some evidence of earlier stages of (hard-hammer) reduction. Collectively, these data suggest overall late stage biface and flake-tool maintenance of tools produced offsite and taken offsite, also suggesting a very short term occupation.

Component 4 fauna is dominated by L/VL artiodactyl remains, mainly long bone diaphysis fragments, tooth enamel, and rib fragments. The presence of teeth and long bone fragments suggests early processing; however, some high meat yield elements are present, perhaps suggesting some later stage processing or onsite consumption.

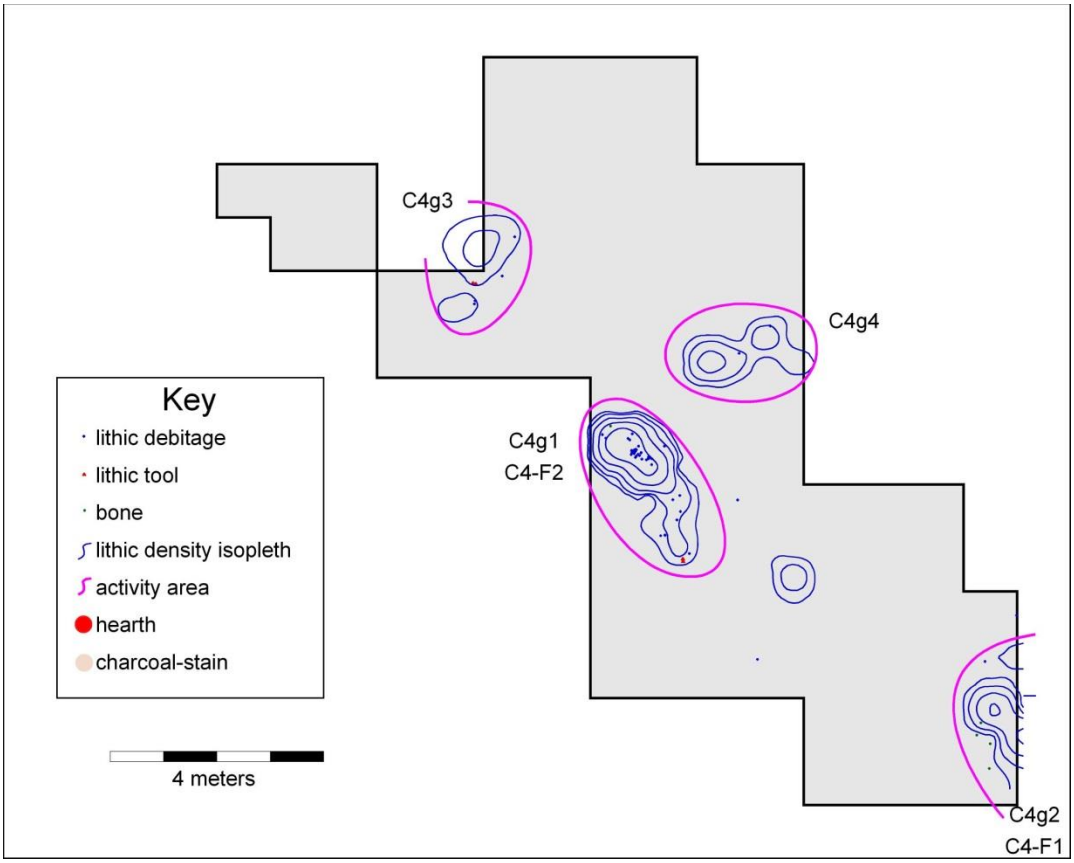

Figure 12.6 Component 4 activity areas.

12.7 Component 5a Activity Areas

Component 5a consists of a relatively diffuse spread of lithics, including 51 flakes, 3 microblades, 1 uniface, and 1 microblade core (Figure 12.7). Overall size classes are relatively small, suggesting later stage reduction (later stages of tool production and maintenance), however other debitage characteristics suggest earlier stages of reduction. Collectively, there is an unusual mix of small flake sizes and unprepared platforms with multiple lithic reduction techniques, including heat treatment. It is entirely possible that this assemblage represents multiple different very short-term reduction episodes, perhaps by different occupations.

Component 5a fauna is dominated by L/VL artiodactyl remains (including 1 wapiti NISP), including long bone diaphysis fragments, tooth enamel, and ribs. Snowshoe hare was also identified. Like Component 4, the overall assemblage suggests an early faunal processing, but the presence of ribs suggests some later processing or onsite consumption.

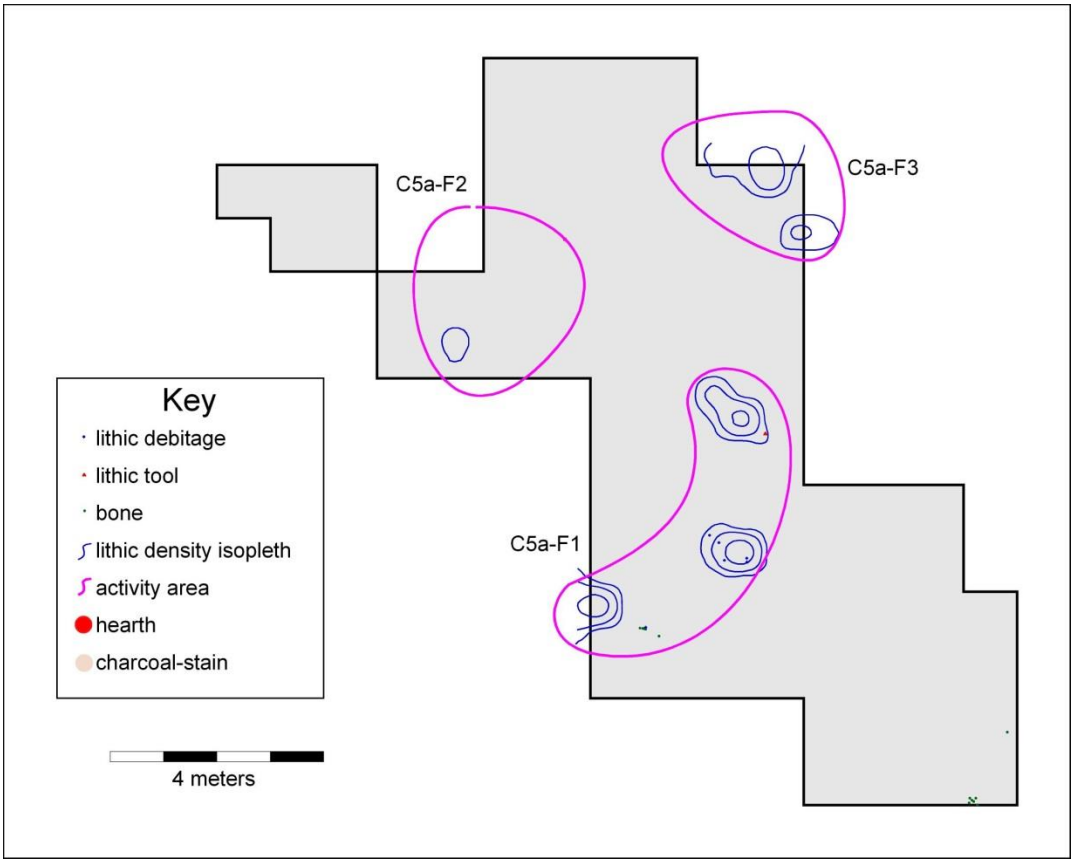

Figure 12.7 Component 5a activity areas.

12.8 Component 5b Activity Area

Component 5b consists of a single cluster of lithics, including 35 flakes, 5 microblades, and 1 microblade core (Figure 12.8). Debitage analyses suggest hard hammer percussion and pressure flaking relating to non-bifacial tool production (e.g. expedient flake tools) with some microblade production prior to discard of the microblade core. The assemblage characteristics

also suggest a very short term occupation. Component 5b fauna consists of a single VL artiodactyl thoracic vertebra, suggesting later processing or onsite consumption.

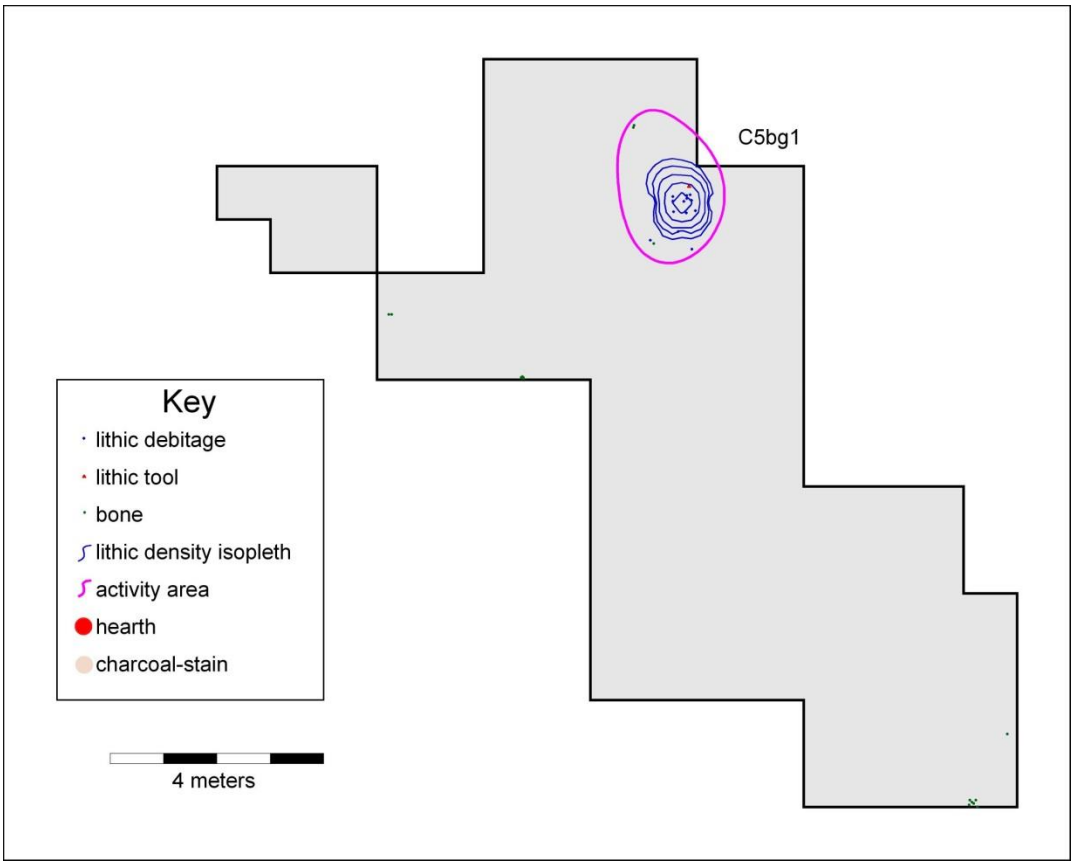

Figure 12.8 Component 5b activity area.

12.9 Component 6a Activity Area

Component 6a consists of three concentrations of lithics in close proximity to each other, all associated with a hearth feature, F2017-2 (Figure 12.9). The hearth feature measures 195 x 87 cm at the surface and is 3 cm thick. A number of cobbles are associated with the hearth. Lithic artifacts include 186 flakes, 1 projectile point (stage 5), 2 modified flakes, and 1 flake core. A single microblade was recovered from this component. Raw materials are evenly distributed suggesting embedded procurement. Debitage characteristics suggest late stage soft-hammer bifacial reduction. The projectile point is square based and shouldered complete except for the tip and is made on a raw material with no associated debitage, suggesting a hunting site where a damaged weapon was discarded and a replacement projectile points were prepared.

Component 6a fauna comprises a wide range of specimens, from L/VL artiodactyl to small and medium mammals and terrestrial birds (grouse family). Three faunal clusters were identified, C6a-F1 associated with caribou, canid, mink, beaver, and grouse remains, C6a-F2 associated with wapiti and other VL artiodactyl remains, and C6a-F3 associated with the hearth feature with VL artiodactyl and S/M sized mammal long bones and tooth enamel. Early stage processing of large game at the hearth area and elsewhere contrasts with processing of small

furbearers. The antler fragment was fashioned into a ladle-like instrument. This unique faunal assemblage suggests a specialized fur-bearer processing area, where organic tools/matériel were fabricated.

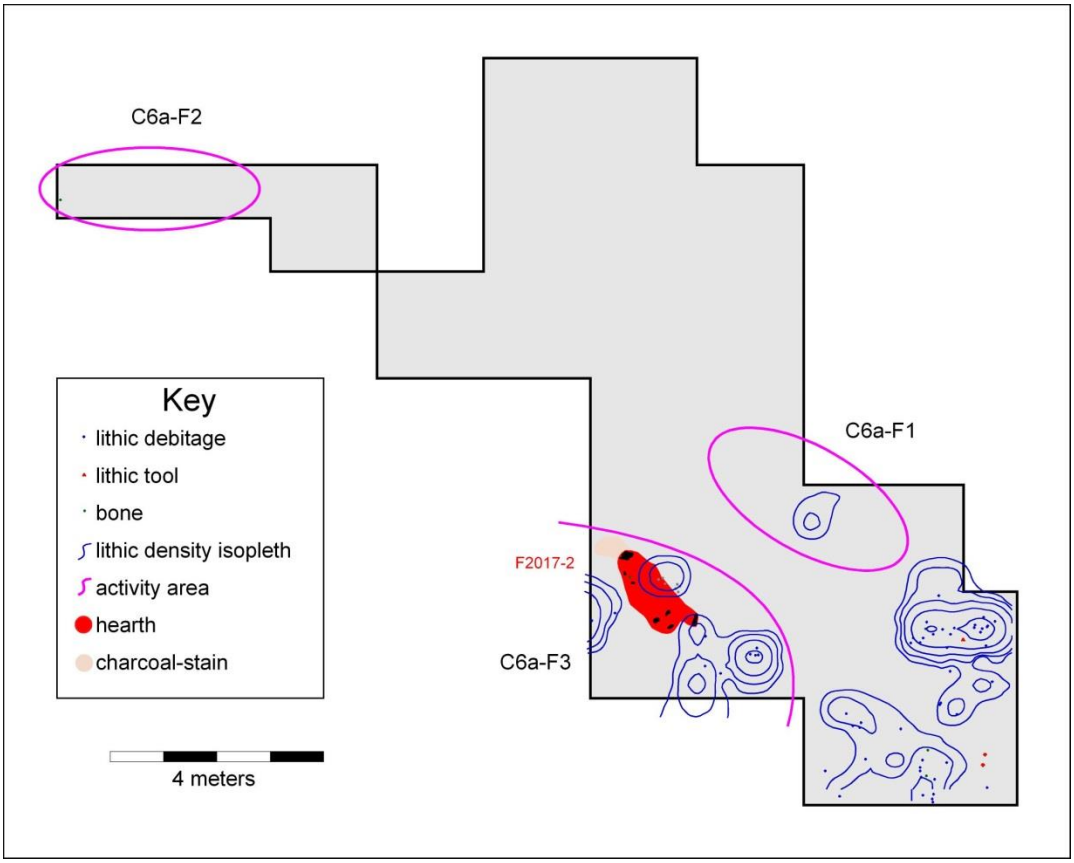

Figure 12.9 Component 6a activity areas.

12.10 Component 6b Activities

Component 6b consists of only 7 unmodified flakes, and all are small tertiary flakes. The data suggest a very short term (perhaps transient) occupation. No fauna was recovered.

12.11 Component 7a Activities

Component 7a consists of 6 flakes and 1 uniface. The data suggest a very short term (perhaps transient) occupation. No fauna was recovered.

12.12 Component 7b Activity Areas

Component 7b consists of four activity areas, two lithic concentrations, C7bg1 and C7bg2, and 4 faunal concentration, two aligning with the lithic clusters (Figure 12.10). C7bg1

contains 118 flakes and 4 end scrapers and C7bg2 contains 231 flakes, 7 modified flakes, and 2 end scrapers. A cobble cluster comprised of 3 cobbles and 1 modified (battered) cobble was found at an outer edge of the C7bg1 cluster. The two lithic clusters exhibit some different debitage characteristics, though the tool types are identical. Collectively, debitage analyses indicate later stages of lithic reduction, likely bifacial and other tool production and maintenance, with C7bg1 more associated with bifacial maintenance and C7bg2 with later stages of bifacial and flake tool maintenance.

Component 7b fauna include VL artiodactyl and small/medium sized mammals. A bison tibia recovered in 1979 likely belongs to this component. The fauna were highly fragmented and no firm conclusions can be drawn, other than multiple size classes of mammal are present. This represents one of the latest occurrences of bison in archaeological contexts in Alaska. This component likely represents a short term hunting site.

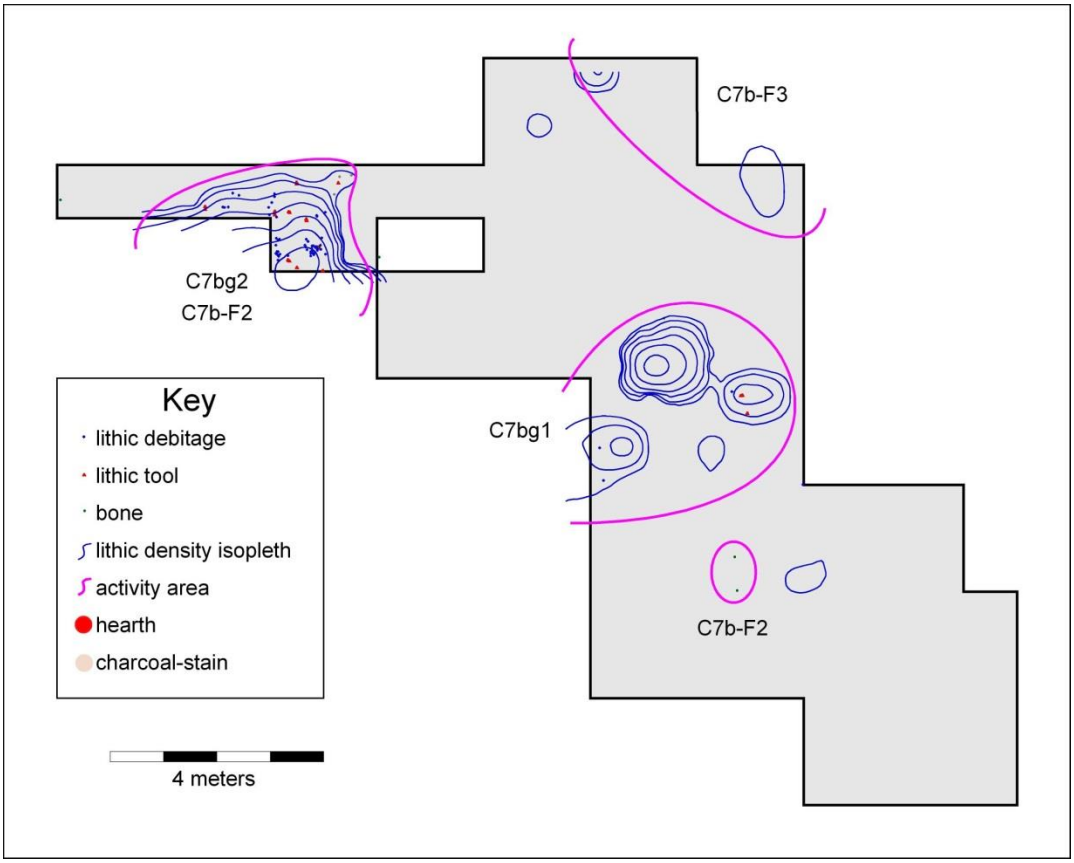

Figure 12.10 Component 7b activity areas.

12.13 Component 8a Activity Areas

Component 8a consists of three activity areas (Figure 12.11). C8ag1 is a dense concentration of 1011 unretouched flakes and a modified flake. C8ag2 is a blank cache designated F2017-3 with 34 flakes and 48 tools, including 5 edged bifaces (stage 2), 3 unifaces (1 sidescraper, 1 double side scraper, and 1 uniface fragment), and 40 modified flakes. C8ag3

consists of 98 flakes, 2 modified flakes, and 1 unifacial end scraper. Raw materials are distinctly different for each group, with C8ag1 comprised of 99.5% chert 11. Debitage analyses indicate C8ag1 represents late stage bifacial tool maintenance of a single raw material, perhaps even a single tool, C8ag3 reflects earlier stages of reduction, including some decortication. Detailed analysis of the cache (C8ag2) reflects early stage reduction of bifaces, unifaces, and modified flakes of roughly similar dimensions of primarily two raw material types. This reduction took place elsewhere and the 5 stage 2 edged bifaces were deposited along with the modified flakes and unifaces into a small area. These material were likely contained in a bag that deteriorated with relatively little postdepositional disturbance.

Component 8a fauna consists of two elements, a VL artiodactyl long bone diaphysis fragment and a medium mammal limb bone, all associated with the C8ag3 concentration. Assuming all three areas were occupied at the same time, middle to late stage biface reduction occurred in C8ag3 along with faunal processing of multiple sizes of mammals. Nearby at C8ag1, very late stage bifacial tool maintenance occurred in a delimited area. Neither of these clusters provided the source of the blanks found in the lithic cache (C8ag2). The presence of the intact cache suggests a Northern Archaic system of provisioning places rather than provisioning people, consistent with a "mapping on" system requiring more intensive local landscape knowledge than that exhibited by Denali components at DRO. The site may be a short-term hunting camp within a logistically organized settlement system where site occupants may have expected to return seasonally to use the site.

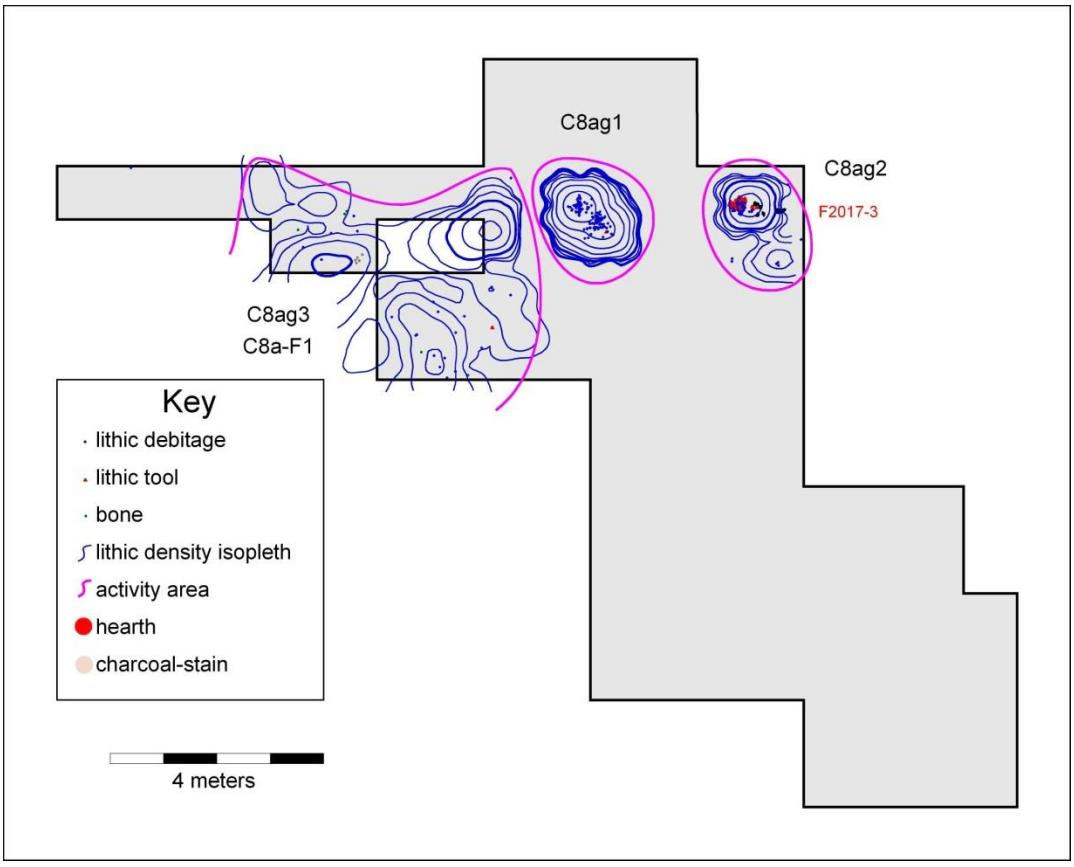

Figure 12.11 Component 8a

12.14 Component 8b Activity Areas

Component 8b consists of 3 activity areas, two associated with hearth features (Figure 12.12). C8bg1 contains 549 flakes, 2 bifaces (1 preform (stage 4), and projectile point (stage 5)), 3 modified flakes, and 2 unifaces (1 end scraper and 1 side scraper). This cluster is associated with hearth F2017-1, which measures 150 x 95 cm along the surface and is 8 cm thick. C8bg2 contains 214 flakes, 2 unifaces (1 end scraper and 1 side scraper), and 1 modified flake. This cluster is associated with hearth F2015-1, a dense concentration of charcoal, burned sediment, and thermally altered rocks (no bone was present), measuring 53 x 37 cm at the surface with a depth between 3-8 cm. A third activity area is mainly associated with the 1985 Japanese excavation, with numerous lithics and bone as well as two hearths present on plan views. F1985-1 measures 153 x 75 cm and F1985-2 measures 40 x 30 cm in maximum dimension. Two unifaces (end scrapers) were associated with this component in 1985. Only 20 flakes and no tools were recovered during our investigation of DRO, and are associated with this activity area. Lithic raw materials were relatively similar for each activity area. Debitage analyses indicate a wide range of lithic behaviors were present in C8b, including decortication and earlier to later stage reduction as well as some bifacial thinning and tool maintenance within C8bg1. C8bg2 reflects more bifacial thinning and C8bg3 reflects late stage controlled bifacial thinning. Compared with other Northern Archaic assemblages, this component reflects a wider range of lithic behaviors. The large amount of processing tools (end and side scrapers) suggests this may not be primarily a hunting site, and may reflect a wider range of non-lithic behaviors.

Component 8b fauna consist of a wide range of species, from L/VL artiodactyl to small mammals. Faunal clusters C8b-F1 and F3 are associated with the western part of the site, including snowshoe hare and lynx as well as a VL artiodactyl tooth. Cluster C8b-F2 is associated with hearth F2017-1 contains wapiti and L/VL artiodactyl remains as well as ground squirrel and snowshoe hare. Collectively, these fauna suggest a wide range of early and later stage processing and consumption of large ungulates and small mammals. The lynx (and possibly snowshoe hare) also may reflect local capture and processing for matériel (e.g., clothing). This wide range of fauna may indicate that C8b functioned as a base camp with a larger range of individuals present, including women and children.

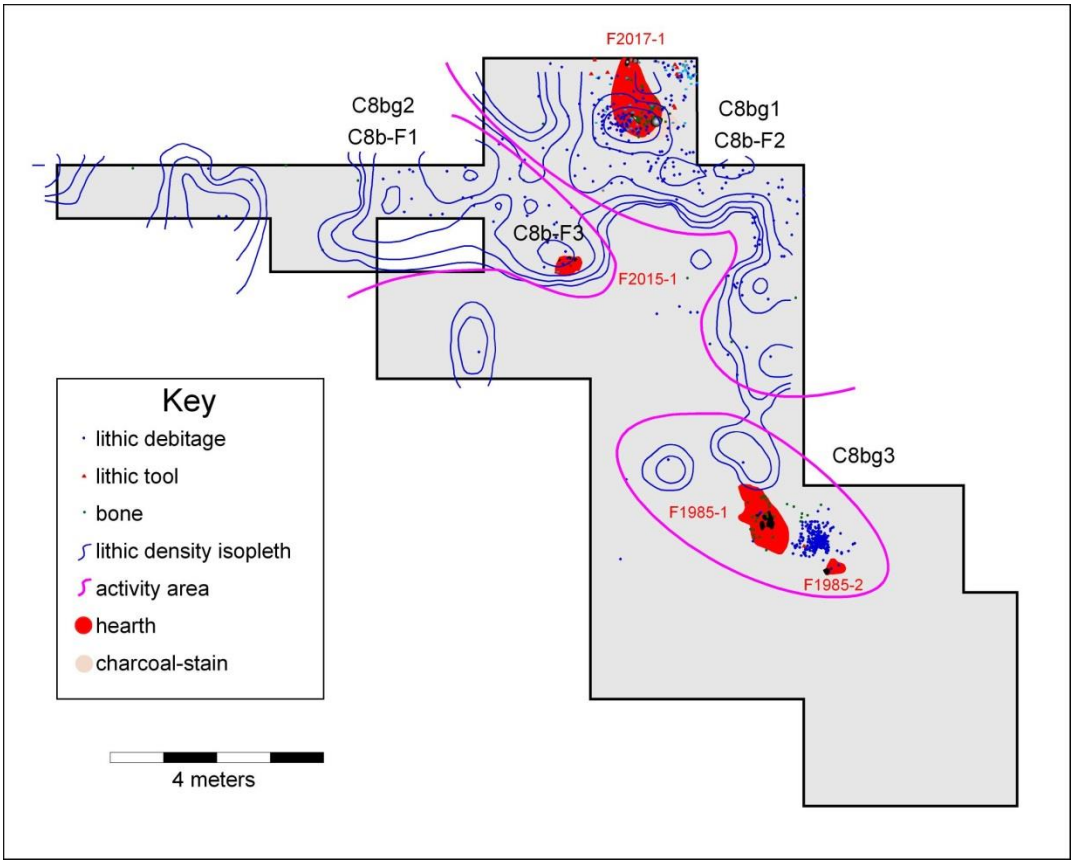

Figure 12.12 Component 8b activity areas.

CHAPTER 13. INTERPRETATIONS

Ben A. Potter

This chapter summarizes interpretations of cultural occupations at Delta River Overlook and evaluates trends in lithic raw material use, lithic technology, and faunal exploitation through components and cultural traditions. These interpretations draw on the analyses presented in earlier chapters of this monograph. Table 13.1 summarizes interpretations for each component. Site significance of DRO is evaluated in light of these findings.

13.1 Component Interpretations

13.1.1 Chindadn Complex (Component 1)

The only Chindadn Complex occupation at DRO is Component 1. The site was occupied around 13,000 cal yr BP, after the cessation of aeolian sand deposition and the onset of loess deposition and the initial formation of the earliest stabilized surfaces (Paleosol 0). The occupation was relatively ephemeral, with no cultural features and three well-defined activity areas with no blurring between them suggesting trampling or reoccupation. Lithic behaviors include transport to the site at least 17 tools or preforms, and onsite discard of 6 tools and one flake core. Onsite behaviors include later stages of projectile point production and finishing. Two small clusters indicate earlier stage lithic reduction (along with a finished projectile point) and 2 microblades respectively. The narrow range of tools suggests this is a weapon (bifacial projectile point) maintenance station, where opportunistically and locally acquired ground squirrel and grouse were processed. Other gear was maintained in an ad hoc manner, consistent with a high residential mobility strategy (Bousman 2005).

13.1.2 Denali Complex (Components 2a, 2b, 2c, 3, 4, 5a, 5b)

A series of seven components assigned to the Denali Complex were present at DRO, from 11,600 to 7250 cal yr BP. Two of the occupations correlate with stabilized surfaces represented by paleosols: C3 with P1 and C5a with P2. Most occupations are not directly associated with prominent paleosols, though they may be associated with very thin discontinuous Ab horizon stringers: C2a, C2b, C2c, C4, and C5b. This suggests a relationship between site occupation during episodes of loess deposition reflecting colder, more arid conditions. Mason et al. (2001) suggested a similar pattern reflects Denali complex dependence on caribou. Later faunal analyses (Potter 2008) indicate that caribou were uncommon and that Denali subsistence depended more on bison and wapiti. This pattern may suggest increases in local abundance of large ungulates during these periods.

Denali components vary considerably in form and activity area content, though not as much as Northern Archaic components. Overall tool types are and proportions are relatively similar, though microblade technology varies in proportion of overall assemblages. Component 2a (11,600 cal yr BP) consists of a very large hearth-centered activity area surrounded by several smaller activity areas. In the central area, projectile points were manufactured (stage 3-4) and removed (stage 4-5) from the site. The satellite areas vary, but overall indicate later stage bifacial reduction. A total of 48 raw materials are present, suggesting at least 36 additional tools were

brought to the site and removed from the site. The faunal record is relatively similar, primarily large (including sheep) and very large artiodactyl long bone diaphysis and teeth fragments. C2a represents a short-term hunting site where early processing of large ungulates and projectile point production took place. The presence of sheep in C2a may suggest a summer occupation, given ethnographic data on sheep hunting strategies in the region (reviewed in Potter 2005).

Component 2b (11,500 cal yr BP) is a single concentrated hearth-centered activity area representing a short-term hunting camp where early stage processing of bison occurred. At least 18 tools were transported to the site, maintained briefly onsite, and most were transported offsite.

Component 2c (10,740 cal yr BP) consists of two hearth-centered (possibly tents) activity areas, both with very similar lithic and faunal characteristics. Microblade production was present, but the majority of lithic behaviors relate to later stage biface reduction (stage 3-5) and maintenance. These bifaces likely include both projectile points and bifacial knives. At least 66 tools were brought to the site and worked in some fashion, while 46 tools were discarded onsite (and a minimum of 50 removed from the site). Microblade technology is common, including nonlocal microblade discard, microblade production, and probably organic composite tool manufacture or maintenance. This component is a fall hunting site within a logistical mobility strategy, dominated by hunting weapon production and maintenance. Bison and wapiti were processed onsite, with high meat yield elements transported to a residential base camp elsewhere. Denali processing tools like end scrapers are limited to C2c, suggesting (along with several ochre concentrations) a longer-term occupation, including perhaps hide processing activities.

Component 3 (9680 cal yr BP) consists of two activity areas reflecting bifacial tool maintenance of a single raw material type in one, and microblade use, discard, and tool maintenance in the other. No cultural features were present. The dominance of single lithic raw materials, low artifact density, and absence of hearth features all suggest a very short term occupation. At least 18 tools were brought to the site, and 6 were discarded onsite, and when considering raw material distributions, at least 15 tools were removed from the site. A bison mandible indicates a winter/early spring occupation. Overall, C3 represents a very short term winter hunting camp.

Component 4 (8420 cal yr BP) consists of several very small activity areas and no cultural features. Lithic behaviors include late stage biface and flake tool maintenance. At least 21 tools were brought onsite, and only 6 were discarded onsite (suggesting at least 16 tools were removed from the site). Fauna are dominated by L/VL artiodactyl remains, mainly long bones and teeth fragments. Overall, C4 represents a very short term hunting camp.

Component 5a (7560 cal yr BP) and Component 5b (7250 cal yr BP) consist of relatively few lithics (n = 56 and 41 respectively). C5a lithic behaviors include later stages of tool production and maintenance, including heat treatment. C5b lithic behaviors include hard hammer percussion and pressure flaking relating to expedient flake tool production and use. A minimum of 12 and 9 tools (respectively) were brought to C5a and C5b, while only 1 tool was discarded in C5a and no tools were discarded in C5b. Semiconical microblade cores were found in both components, along with a few microblades. Both components contain L/VL artiodactyl high meat yield elements like ribs and vertebra, though C5a also contained snowshoe hare. This suggests a different type of faunal processing, perhaps onsite consumption. It is difficult to characterize site function, but C5a and C5b may represent short term transient camps (long distance travel stops) where tools were maintained associated with meat consumption.

Microblade technology varies in proportion throughout the Denali occupations, though it is present in every assemblage. The relative lack of microblades in C2a may reflect movement

associated with montane areas to the south associated with sheep hunting (the only sheep at the site occurs in this component) compared with VL artiodactyl (bison, wapiti) hunting in other Denali components, probably hunted in the surrounding lowlands (see Potter 2007, 2008). Fall and winter occupations contain higher proportions of microblade materials, suggesting differential use of composite and bifacial projectile points may be functions of seasonal land use and embedded procurement of differentially available high quality toolstone.

13.1.3 Northern Archaic Tradition (Components 6a, 6b, 7a, 7b, 8a, 8b)

A series of six components assigned to the Northern Archaic tradition were present at DRO, from 6820 to 2240 cal yr BP. In contrast with the Denali components, almost all of the Northern Archaic components are directly associated with distinct paleosols: C6a with P3, C6b with P4, C7a with P6a, C7b with P6b, and C8a with P7a. C8b was the only one not directly associated with a paleosol. This suggests occupation of the DRO site during periods of soil formation, perhaps linked with faunal abundance including a variety of small and medium mammals like hare and ground squirrel. This very different land use pattern is one way Northern Archaic components are differentiated from Denali components at DRO.

Northern Archaic components vary in form and activity area content, more than Denali components. However, overall tool types are relatively similar, primarily finished bifacial points and fragments, modified flakes, and end scrapers. Component 6a (6820 cal yr BP) consists of materials around a hearth feature. A minimum of 23 tools were brought to the site, only 3 were discarded onsite, with a minimum of 23 tools transported offsite. Lithic behaviors include late stage bifacial reduction, likely the production of projectile points (one was discarded). A wide range of fauna include caribou, wapiti, canid, mink, beaver, and grouse were recovered, suggesting early stage processing of large ungulates and onsite processing of small/medium mammals, possibly for fur and other matériel. The site could be characterized as a specialized hunting camp for fur bearers. In the local ethnographic record, furbearers (particularly beaver) were hunted in the spring (see review in Potter 2005).

Component 6b (5940 cal yr BP) and 7a (4470 cal yr BP) consist of a few flakes and no fauna or features, suggesting very short term (perhaps transient) occupations.

Component 7b (4150 cal yr BP) consists of four activity areas, two concentrations of lithics and fauna and two faunal-only concentrations. At least 5 raw materials are present at the site, 9 tools are discarded, with a minimum of 4 additional tools transported offsite. Lithic behaviors include late stages of lithic reduction, likely bifacial and unifacial tool production and maintenance. End scrapers are the most common tool type, suggesting domestic activities. Faunal data include highly fragmented small, medium, and very large sized mammals, including bison. This component could be characterized as a short term hunting – processing site.

Component 8a (3560 cal yr BP) consists of three disparate activity areas, all with different characteristics. One area represents late stage bifacial tool maintenance of a single raw material, another consists of earlier stages of reduction. A third is a blank cache comprised of 48 tools (edged bifaces, unifaces, and modified flakes). Reduction of these tools took place in an unexcavated area or offsite, and the tools were left in a bag. A minimum of 26 material types are present, 53 tools are discarded onsite (mostly from the cache), suggesting at least 16 tools were transported offsite. Besides the cache, tools include 3 modified flakes and an end scraper. The small faunal assemblage includes VL artiodactyl and medium mammal. C8a may reflect a short term hunting camp within a logistically organized settlement pattern.

Component 8b (2240 cal yr BP) consists of 3 activity areas, two associated with hearth features. Tools include 2 bifaces, 4 modified flakes, 4 end scrapers, and 2 side scrapers. The bifaces include a preform and a projectile point, similar to the point in Component 6a. A minimum of 43 tools were brought onsite, 9 were discarded onsite, and at least 38 were transported offsite. Lithic behaviors include a wide range of reduction, from decortication to later stage reduction, mainly reflecting bifacial thinning and tool maintenance. Faunal remains consist of a wide range of species, from small to very large mammals, including wapiti, ground squirrel, hare, and lynx. Overall, the diversity of lithic and fauna and the presence of many domestic tools (end scrapers) may indicate that C8b was a residential base camp.

Table 13.1 Component interpretation summary

Comp.	*Age*	*Season*	*Occupation span*	*Lithics*	*Fauna*	*Function*
C1	Chindadn	?	Short	Bifacial weapon maintenance	Opportunistic consumption	Weapon maintenance station
C2a	Denali	Summer?	Short	Bifacial weapon production	VL artiodactyl early processing	Hunting camp
C2b		?	Short	Tool maintenance	VL artiodactyl early processing	Hunting camp
C2c		Fall	Short/ medium	Bifacial weapon production / maintenance and microblade production	VL artiodactyl early processing	Hunting camp (tents)
C3		Winter	Very short	Bifacial tool maintenance	VL artiodactyl early processing	Hunting station
C4		?	Very short	Biface/flake tool maintenance, microblade production	VL artiodactyl early + late processing	Hunting station
C5a		?	Very short	Tool maintenance	VL artiodactyl early + late processing	Unknown
C5b		?	Very short	Flake tool maintenance	VL artiodactyl late processing	Transient flaking station?
C6a	Northern Archaic	Spring	Short	Bifacial tool production/ maintenance	VL artiodactyl early processing, furbearer processing	Hunting camp
C6b		?	Very short	Limited tool maintenance	No fauna	Transient flaking station?
C7a		?	Very short	Limited tool maintenance	No fauna	Transient flaking station?
C7b		?	Short	Bifacial tool maintenance	Processing of S/M and VL mammals	Hunting camp
C8a		?	Short	Bifacial tool maintenance / blank cache	Processing of M and VL mammals	Hunting camp/ lithic cache
C8b		?	Long	Core reduction and bifacial tool production/ maintenance	early + late stage processing/ consumption of S, M, L, VL mammals	Residential base camp?

13.1.4 Discussion

DRO data from these 14 components can be used to explore changing technological and land use strategies for eastern Beringia (and interior Subarctic) from the earliest inhabitants in the late Pleistocene to the later Holocene. The site and topographical location can be held constant, while many other variables like lithic raw materials, exploited fauna, formal tool types, and seasonality vary. Importantly, the presence of multiple components within cultural

complexes and traditions provides a hitherto unprecedented window into variation within cultures for this region.

13.1.4.1 Lithic Raw Material Use

In terms of lithic raw material use, there is greater diversity in Denali components than in Northern Archaic components. Denali material type richness is higher, including rhyolite types common in Denali components and absent or nearly absent in Chindadn and Northern Archaic. Chindadn and later Denali components are quite dissimilar, with almost all common Denali raw materials absent in the Chindadn component and vice versa. This suggests different overall procurement strategies for Chindadn and Denali, at least in terms of suites of lithic sources utilized. Similar differences are found between Denali and later Northern Archaic components. A few materials are shared, but most are different. Interestingly, many Denali components share appreciable amounts of raw material suites (45% shared), whereas Northern Archaic components have individually dissimilar raw materials (5%), suggesting Denali components shared some procurement strategies while Northern Archaic components exhibited more individualistic uses of the site and regional lithic landscape.

Lithic raw material diversity measures are different between the cultural traditions. Denali components exhibit more even distributions of material types than Northern Archaic or Chindadn. Denali assemblages exhibit both more evenness and diversity in raw material types than Northern Archaic assemblages. This suggests more similar lithic procurement and recurrent seasonal uses of the location by Denali populations and multiple and/or different lithic procurement and/or seasonal use of the location by Northern Archaic populations. Chindadn values are intermediate.

Artifact density values are much higher for Denali (40 items/m^2) than Northern Archaic (6 items/m^2) and Chindadn (6 items/m^2), suggesting relatively intensive occupations during the Denali period bracketed by lower artifact densities and perhaps shorter occupations.

Within the seven Denali components, there are several differences. Early Denali (C2a, C2b, C2c, C3) share more raw materials, whereas later Denali components have higher diversity measures, suggesting more embedded procurement in early Denali and less embedded in later Denali. Northern Archaic have more uneven distributions, suggesting direct procurement and/or reduced mobility in relation to Denali.

Component 1 exhibits very high local:nonlocal ratio (147:1) whereas early Denali components are relatively high (12-82:1), later Denali components have lower ratios (0.6-5:1). Northern Archaic components have low ratios throughout (3-10:1). This general trend is independent of assemblage size, and suggests primarily local toolstone use during the Chindadn occupation, relatively high but decreasing local use during the Denali period, and relatively low local toolstone use during the Northern Archaic. While this is unexpected given overall lower residential mobility, it may be explained by different procurement strategies, perhaps more direct procurement, as well as increasing exchange.

Obsidian use is also different among cultures (Table 13.2). No obsidian was found in the Chindadn component. Of the Denali components, only one (C2c, n = 65) contained obsidian, and almost all of it (94%) was assigned to Wiki Peak (A). In contrast, four of the six Northern Archaic components contain obsidian, but at lower numbers (n = 8) utilizing more sources, including Batza Tena, Ringling, and Wiki Peak. Wiki Peak obsidian is the closest known source to DRO, and the uneven distribution in C2c suggests direct procurement. The wider range of

obsidian in smaller frequencies suggests a different procurement system for obsidian, perhaps facilitated by long distance trading systems.

Table 13.2 Obsidian source by component and cultural tradition.

Component	*Wiki Peak (A)*	*Ringling (A')*	*Batza Tena (B)*	*Unassigned*	*Total*
C2c (Denali)	61 (93.8%)	-	-	4 (6.2%)	65 (100%)
C7a	2 (100%)	-	-	-	2 (100%
C7b	-	2 (100%)	-	-	2 (100%)
C8a	-	-	1 (100%)	-	1 (100%)
C8b	2 (66.7%)	-	-	1 (33.3%)	3 (100%)
All Northern Archaic	4 (66.7%)	2 (33.3%)	1 (16.7%)	1 (16.7%)	8 (100%)

13.1.4.2 Lithic Technology

Chindadn (Component 1) has a narrow range of tools and cores. Three bifaces are finished projectile point bases with concave to straight bases similar to other Chindadn materials at Healy Lake, Mead, Swan Point, and Erodaway (Cook 1969; Potter et al. 2013). Microblades were recovered and though the core form is unknown, the microblade widths are similar to Denali widths. A large flake core/chopper that was not reduced onsite, and this along with the lack of heat treatment, lack of bipolar reduction, and predominance of high quality raw materials (>90%) suggests little or no lithic resource stress. Modified flake data suggest light use in cutting/slicing soft materials. Percent of retouched margins is low (25-33%) suggesting lower levels of curation.

Denali components have a wide range of tools (n = 195) and cores (n = 10), including modified flakes and microblades, bifaces (points and knives), unifaces (both end and side scrapers), burins, burin spalls, microblade cores, and core tablets. Six cobble tools were also present. Bifaces include the entire range of bifacial reduction stages, 1 edged biface, 5 thinned bifaces, 11 preforms, and 2 finished bifaces (point bases), suggesting a wider range of biface production than in Chindadn or most Northern Archaic components. The bulk of Denali bifaces are early stage manufacturing discards/rejects, contrasting with Northern Archaic bifaces (see below). Of the 12 unifaces, five are end scrapers and 6 are side scrapers (2 are double side scrapers). Side scrapers cluster in C2a while end scrapers cluster in C2c, suggesting different domestic activities. Cobble spall artifacts probably functioned in early stage processing of large artiodactyls (see Potter 2005). Modified flakes are common and are varied in form, with no standardized sizes or shapes. Utilized edge angles have a wide distribution, but there are clusters of low edge angles suggesting expedient cutting implements. In general, percent modified margins increases through time from 36% in C2c to 64% in C4, suggesting increased use intensity of the modified flakes.

There are some significant differences between early Denali components (C2a, C2b, C2c) and later Denali components (C3, C4, C5a, C5b). Early Denali components tend to exhibit more early reduction and tool production, along with more processing tools (scrapers). In contrast, later Denali components contain more tools relative to debitage, fewer overall artifacts, lower artifact densities, and almost entire absence of unifaces. These data suggest that the later Denali

components may reflect shorter term occupations where fewer lithic items were maintained or refurbished, while the earlier Denali components reflect longer term occupations. This interpretation is further supported by the presence of hearths in all early Denali components and the lack of hearths in all later Denali components.

Northern Archaic components contain 80 tools and 1 flake core. Tools include modified flakes, bifaces, and unifaces. No microblade cores or core parts were present in Northern Archaic components at this site, though they are common in other assemblages (Esdale 2008, Potter 2008). Bifaces comprise 5 edged bifaces, 1 preform, and 3 finished projectile points. Finished projectile points are found in all 3 of the biface-containing Northern Archaic components, in contrast with Denali biface assemblages. The edged bifaces are all from the blank cache in C8a. Thus, Northern Archaic bifaces were generally brought to the site as finished points, and were not manufactured onsite. Northern Archaic unifaces are mainly end scrapers (72%), contrasting with more even distribution of end and sidescrapers among Denali components. Northern Archaic modified flakes make up the largest category of tools, present in four components. Percent retouched margins generally increase through time, from 25% in C6a to 48% in C8b, with C8a much higher, at 57%, likely related to the blank cache. Two modes of edge angles are apparent, one around 30 degrees and the other around 60 degrees, suggesting cutting/slicing vs. scraping/grinding functions.

Microblade and burin technologies are only associated with Chindadn and Denali components, but at various proportional levels. Nonlocal microblade discards and onsite microblade production clusters are discernible for C2c and C4. C2a, C2b, and C3 contain no microblade cores or core parts, and have relatively few microblades. Microblade core forms change from wedge shaped forms in C2c to semi-conical forms in C5a and C5b. C2c data suggest 10 microblade cores were transported offsite, with only 2 discarded onsite, suggesting cores were highly curated. Burins and burin spalls are directly proportional to microblade frequencies, suggesting a close relationship of slotted organic implement production/ maintenance and microblade insets (Guthrie 1983). At least 1 burin was used in C2a and C2b each, and a minimum of 9 burins were used in C2c, suggesting high levels of curation of burins.

A wide range of data suggests that these populations did not suffer from lithic resource stress. Each component had a relatively high percentage of high quality raw materials, generally over 90%. No evidence of bipolar reduction was observed. Heat treatment was very rare, and absent in most components. Percent modified edges on modified flakes were generally low, and retouch intensity was relatively low. Projectile points do not show evidence of reworking or resharpening. Except for C1, the presence of large unmodified flakes (potential blanks) suggests low lithic resource stress.

Debitage:tool ratios are different among components. The Chindadn debitage: tool ratio is 34+/-49. In contrast, early Denali (C2a, C2b, C2c) are nearly four times as high, averaging 121+/-102, suggesting increased occupation duration and/or relatively earlier stages of reduction represented. The debitage: tool ratios for later Denali decline, averaging 24+/-14. Even though the culture, technology, and exploited fauna are the same, site structural differences suggest different (but recurrent) land use strategies in the later Denali period. Northern Archaic debitage: tool ratio values average 85+/-159, an intermediate value. Importantly, the coefficient of variation is high (1.87 compared with 0.84 and 0.58 for Denali components), indicating more intra-tradition variation within the Northern Archaic.

13.1.4.3 Activity Areas and Features

Activity area sizes vary among components. The three major Denali activity areas centered on hearths are much higher in artifact frequencies and tool class richness, with total sample sizes of 3594-5700 items. Other (possibly ancillary) Denali activity areas are relatively similar, averaging 152+/-123 lithic items per area. In contrast, Northern Archaic activity areas vary more, averaging 225+/-304 lithic items, ranging from 7 to 1013 items. The Chindadn complex contains one activity area with 455 lithic items and two areas with 7 and 10 items respectively. This suggests two modes of activity areas within Denali, a longer-term mode associated with hearth features, and perhaps tent structures, and a shorter-term mode not associated with cultural features. In contrast, Northern Archaic components have no single mode of lithic activity areas, varying by site function, seasonal land use, or other factors.

13.1.4.4 Faunal Comparisons

The faunal data indicate trends in faunal exploitation and processing among the components and cultural traditions. For the Denali occupations, there was recurrent use of the site to process locally killed bison and wapiti. Selected portions of the carcasses were brought on site, marrow extraction from long bones occurred onsite and high meat yield elements were likely processed for transport offsite to residential base camps. There are some differences in faunal treatment within the Denali occupations. Early Denali occupations (C2a through C3) are associated with early faunal processing and removal of high meat yield elements, suggesting the sites functioned as logistically organized hunting camps, at least for fall and winter seasons. In contrast, later Denali occupations (C4 through C5bb) contain more ribs and vertebrae, suggesting later stage processing and possibly consumption. This may indicate shifts in Denali residential mobility after 9680 cal yr BP and changes in how the DRO landform was used.

In contrast, the two Northern Archaic components with substantial materials contain very different assemblages, with a much wider range of fauna, including many medium and small mammals: beaver, mink, canid, lynx, hare, and ground squirrel, as well as large and very large ungulates like caribou, wapiti, and bison. Denali staple ungulates (bison and wapiti) are well represented at multiple Northern Archaic components. Overall, these data suggest increasing diet breadth, consistent with models of Northern Archaic adaptive strategies (Potter 2008). Each Northern Archaic component is also more distinctive from each other than the Denali components, which are very similar. This suggests a generalized hunting strategy focused on bison and wapiti in the Denali tradition versus a mapping-on strategy employed during the Northern Archaic tradition, the latter a form of intensive local land use.

The continuing occurrence of bison and wapiti extending into the later Holocene demonstrates abundant megafauna in the region long after their extinction in surrounding areas of Beringia and the western Subarctic. This suggests the presence of suitable habitat for large gregarious herbivores well into the Holocene and raises new questions about the final late extirpation of bison in the region. Notably absent are waterfowl and fish, which may reflect local paleoecology of the region.

13.2 Site Significance

We have collected and analyzed a substantial amount of data at DRO. The site is more significant than previously thought, and easily could be listed on the National Register of Historic Places (NRHP) under Criterion D. DRO was found eligible (NRE) on 8/30/1979 and Hurricane Bluff was found eligible (NRE) on 12/19/2013. We briefly summarize here the salient conclusions. Items 1, 2, 3, and 4 make DRO unique among archaeological sites in Alaska.

1) The most significant aspect of DRO is the *number of distinct cultural occupations*, fourteen (14) episodes of human occupation have occurred at the site over 13,000 years, including multiple occupations of individual traditions (Chindadn, Denali, and Northern Archaic). This is unprecedented in interior Alaska, allowing us for the first time to address variation *within* cultural traditions as well as *among* traditions, controlling for site location.

2) *Ancient animal and plant remains are very well preserved*, allowing us to directly evaluate human use of plants and animals from the last Ice Age to the recent past. This allows us a unique window to understand effects of climate change directly on exploited faunal resources accessible from the site. Significant new discoveries (so far) include very late human exploitation of bison (long after they disappeared in other regions) and the first evidence (through bison teeth geochemical analyses) of bison migration patterns.

3) *Stratigraphy at DRO (layering of sediments and soils) is very highly resolved*, and we have identified and dated 11 major paleosol complexes, representing at least 32 buried soils. This provides a significant window into tracking regional and local environmental changes for 13,000 years in very precise intervals. No other interior Alaskan site has a similar high-resolution stratigraphic record allowing this quality of detailed analyses.

4) *New ancient Alaskan human behaviors* have been inferred at DRO, including (a) presence of multiple ochre-stained areas that probably served as hide processing areas and (b) the first known winter occupation in all of Beringia (east or west). There is also evidence of tent structures that would represent some of the earliest habitation structures in Alaska.

5) *Artifact density is much higher* than previously thought, and we have recovered 18,760 stone artifacts, including 283 stone tools, making this one of the most productive sites in the interior of Alaska (Potter 2008).

6) *DRO site extent is very large*; we estimate total area with preserved cultural remains to be 4,037 m^2. All excavations to date have sampled approximately 2.5% of the overall estimated site area.

REFERENCES CITED

Allen, TE
2018 Testing debitage typologies with statistical analysis: experimental inferences upon archaeological materials from FaPx-1, a sub-alpine hunting camp in the Alberta Rockies. *Archaeological Survey of Alberta Occasional* Paper No. 38: 25-33.

Andrefsky, W, Jr.
2001 Emerging directions in debitage analysis. In *Lithic Debitage: context, form, meaning*, edited by W Andrefsky, Jr., pp 2-14. University of Utah Press, Salt Lake City.
2008 *Lithic Technology: Measures of production, use, and curation*. Cambridge University Press, Cambridge, UK.

Ball, DF
1964 Loss-on-ignition as an estimate of organic matter and organic carbon in non-calcareous soils. *Journal of Soil Science* **15**, 84-92.

Bacon, G and CE Holmes
1980 Archaeological Survey and Inventory of Cultural Resources at Fort Greely, Alaska 1979. Report prepared by ALASKARCTIC for Alaska District, Corps of Engineers under contract DACA85-78-C-0045, May, 1980.

Bartram, LE, Jr.
1993 Perspectives on Skeletal Part Profiles and Utility Curves from Eastern Kalahari Ethnoarchaeology. In *From Bones to Behavior: Ethnoarchaeological and Experimental Contributions to the Interpretation of Faunal Remains*, edited by J Hudson, pp 115-137. Southern Illinois University at Carbondale Center for Archaeological Investigations Occasional Paper 21.

Bataille, C., Brennan, S., Hartmann, J., Moosdorf, N., Wooller, M., and G Bowen
2014 A geostatistical framework for predicting variations in strontium concentrations and isotope ratios in Alaskan rivers. *Chemical Geology* 389:1-15

Begét, J, Reger, RD, Pinney, D, Gillespie, T, and K Campbell
1991 Correlation of the Holocene Jarvis Creek, Tangle Lakes, Cantwell, and Hayes Tephras in South-Central and Central Alaska. Quaternary Research 35, 174–189.

Binford, LR
1978 *Nunamiut Ethnoarchaeology*. Academic Press, New York.

Binford, LR
1984 Butchering, sharing, and the archaeological record. *Journal of Anthropological Archaeology* 3, 235-257.

Binford, LR, and JB Bertram
1977 Bone Frequencies and Attritional Processes. In *For Theory Building in Archaeology: Essays on faunal Remains, Aquatic Resources, Spatial-Analysis, and Systematic Modeling*, edited by LR Binford, pp 77-153. Academic Press, New York.

Blott, SJ, and K Pye
2001 GRADISTAT: A Grain Size Distribution and Statistics Package for the Analysis of Unconsolidated Sediments. *Earth Surface Processes and Landforms* 26:1237-1248.

Brennan, S., Fernandez, D., Mackey, G., Cerling, T., Bataille, C., Bowen, G., and M Wooller
2014 Strontium isotope variation and carbonate versus silicate weathering in rivers from across Alaska: Implications for provenance studies. *Chemical Geology* 389:167-181.

Briner, JP, JP Tulenko, DS Kaufman, NE Young, JF Baichtal, and A Lesnek
2017 The Last Deglaciation of Alaska. Geographical Research Letters. *Cuadernos de Investigación Geográfica* 43(2):429-448.

Britton, K., Grimes, V., Niven, L., Steele, T., McPherron, S., Soressi, M., Kelly, T., Jaubert, J., Hublin, J.J., and Richards M.P.
2011 Strontium isotope evidence for migration in late Pleistocene Rangifer: Implications for Neanderthal hunting strategies at the middle Paleolithic site of Jonzac, France. *Journal of Human Evolution* 61(2):176-185.

Brochardt, GA
1974 The SIMAN Coefficient for Similarity Analysis. *The Classification Society Bulletin* 3(2):2–8.

Bunn, HT
1986 Patterns of skeletal representation and Hominid subsistence activities at Olduvai Gorge, Tanzania, and Koobi Fora, Kenya. *Journal of Human Evolution* 15, 670-90.

Bunn, HT, LE Bartram, and EM Kroll
1988 Variability in bone assemblage formation from Hadza hunting, scavenging, and carcass processing. *Journal of Anthropological Archaeology* 7, 412-57.

Bunn, HT, and EM Kroll
1986 Systematic butchery by Plio/Pleistocene Hominids at Olduvai Gorge, Tanzania. *Current Anthropology* 27, 431-52.

Burr, DB
1980 The relationships among physical, geometrical and mechanical properties of bone, with a note on the properties of nonhuman primate bone. *Yearbook of Physical Anthropology* 23, 109-146.

Cannon, A
1995 The ratfish and marine resource deficiencies on the Northwest Coast. *Canadian Journal of Archaeology* 19, 49-60.

Casteel, RW
1972 Some biases in the recovery of archaeological faunal remains. *Proceedings of the Prehistoric Society* 38, 382-388.

Clark, DW, and A McFadyen Clark
1993 *Batza Téna: Trail to Obsidian.* Archaeological Survey of Canada Mercury Series Paper 147. Canadian Museum of Civilization, Ottawa.

Coffman, S and JT Rasic
2015 Rhyolite Characterization and Distribution in Central Alaska. *Journal of Archaeological Science* 57:142-157.

Cook, JP
1969 The Early Prehistory of Healy Lake, Alaska. PhD Dissertation, Department of Anthropology, University of Wisconsin, Madison.
1995 Characterization and Distribution of Obsidian in Alaska. *Arctic Anthropology* 32(1):92-100.

Davies, BE
1974 Loss-on-ignition as an Estimate of Soil Organic Matter. *Soil Science Society of America Proceedings* 38:150-151.

Davis, MK, TL Jackson, MS Shackley, T Teague, and JH Hampel
2011 Factors Affecting the Energy-Dispersive X-Ray Fluorescence Analysis of Archaeological Obsidian. In *X-Ray Fluorescence Spectrometry (XRF) in Geoarchaeology*, edited by MS Shackley, pp. 45–64. Springer, New York.

Dean, WE
1974 Determination of Carbonate and Organic Matter in Calcareous Sediments and Sedimentary Rocks by Loss on Ignition: Comparison with Other Methods. *Journal of Sedimentary Petrology* 44:242-248.

Dilley, TE
1988 Holocene Tephra Stratigraphy and Pedogenesis in the Middle Susitna River Valley. M.S. Thesis, University of Alaska, Fairbanks
1998 Late Quaternary Loess Stratigraphy, Soils, and Environments of the Shaw Creek Flats Paleoindian Sites, Tanana Valley, Alaska. Ph.D. dissertation, Department of Geosciences, University of Tucson, Tucson.

Dixon, EJ, Jr.
1985 Cultural chronology of central interior Alaska. *Arctic Anthropology* 22(1):47-66.

Dixon, E.J., Smith, GS
1990 *A regional application of tephrochronology in* Alaska. Archaeological Geology of North America. Geological Society of America, Centennial Special Volume 4, Boulder, Colorado.
Donovan, JJ
2015 Probe for EPMA [computer software]. Probe Software, Inc.

Esdale, JA
2008 A Current synthesis of the Northern Archaic. *Arctic Anthropology* 45(2):3-38.
2009 Lithic production sequences and toolkit variability: examples from the middle Holocene, northwest Alaska. PhD dissertation, Brown University.

Folk, RL, and WC Ward
1957 Brazos River Bar: A Study in the Significance of Grain Size Parameters. *Journal of Sedimentary Petrology* 27:3–26.

Gilbert, AS, Singer, BH
1982 Reassessing zooarchaeological quantification. *World Archaeology* 14, 21-40.

Glascock, MD, GE Braswell, and RH Cobean
1992 A Systematic Approach to Obsidian Source Characteristics. In *Archaeological Obsidian Studies: Method and Theory*, edited by MS Shackley, pp. 15-66. Plenum Press, New York.

Glassburn, CL
2015 A reconstruction of steppe bison mobility in the Yukon-Tanana uplands and implications for prehistoric human behavior. M.A. thesis. University of Alaska, Fairbanks Alaska.

Glassburn, CL, BA Potter, JL Clark, JD Reuther, DL Bruning, and MJ Wooller
2018 Strontium and oxygen isotope analyses of sequentially-sampled modern bison (*Bison bison bison*) teeth from Interior Alaska as a proxy of seasonal mobility. *Arctic* 71(2): 183-200.

Goebel, TE, RJ Speakman, and JD Reuther
2008 Results of Geochemical Analysis of Obsidian Artifacts from the Walker Road Site, Alaska. *Current Research in the Pleistocene* 25:88-90.

Grayson, DK
1973 On the methodology of faunal analysis. *American Antiquity* 38, 432-439.

Grayson, DK
1978 Minimum numbers and sample size in vertebrate faunal analysis. *American Antiquity* 43, 53-65.

Grayson, DK
1982 Toward a history of Great Basin mammals during the Past 15,000 Years. In *Man and Environment in the Great Basin*, edited by DB Madsen and JF O'Connell, pp 82-101. Society forAmerican Archaeology Papers 2.

Grayson, DK
1984 *Quantitative Zooarchaeology: Topics in the analysis of Archaeological Faunas.* Academic Press, Orlando, Florida.

Guthrie, RD
1983 Osseous projectile points; biological considerations affecting raw material selection and design among Paleolithic and Paleoindian peoples. In Ani*mals and Archaeology: hunters and their prey*, edited by J Clutton and C Grigson, pp 273-294. BAR International Series 163. British Archaeological Reports, London.

Higgs, AS, BA Potter, PM Bowers and OK Mason
1999 Cultural Resource Survey of the Yukon Training Area and Fort Greely Army Lands Withdrawal, Alaska. NLUR Technical Report 66. Report prepared for ABR, Inc. and U.S. Army Cold Regions Research and Engineering Laboratory by Northern Land Use Research, Inc., Fairbanks.

Hoffecker, JF
1983 A description and analysis of artifact clusters in Components I and II at the Dry Creek Site. Appendix A in *Dry Creek: archaeology and paleoecology of a Late Pleistocene Alaskan hunting camp*, edited by WR Powers, RD Guthrie, and JF Hoffecker, pp 307-347. Report submitted to the National Park Service.

Hoffman, BW, JMC Czederpiltz, and MA Partlow
2000 Heads or tails: The zooarchaeology of Aleut salmon storage on Unimak Island, Alaska. *Journal of Archaeological Science* 27, 699-708.

Holliday, VT
2004 *Soils and Archaeological Research*. Oxford University Press, Oxford.

Holliday, VT, and JK Stein
1989 Variability of Laboratory Procedures and Results in Geoarchaeology. *Geoarchaeology* 4(4):347-358.

Holloway, CR
2016 Paleoethnobotany in Interior Alaska. M.A. Thesis, Department of Anthropology, University of Alaska Fairbanks.

Holmes, CE
1979 Archaeological Reconnaissance Report for Fort Wainwright, Fort Greely, and Fort Richardson Withdrawal Lands, Alaska. Report prepared for U.S. Army Corps of Engineers under contract DACA85-79-M-0001, April, 1979.

Holtzman, RC
1979 Maximum likelihood estimation of fossil assemblage composition. *Paleobiology* 5, 77-89.

Janitzky, P
1986 Particle-size Analysis. In *Field and Laboratory Procedures Used in a Soil Chronosequence Study*, edited by M.J. Singer and P. Janitsky, pp. 11-16. USGS Bulletin 1648. United States Government Printing Office, Washington D.C.

Julien, AM, H Bocherens, A Burke, D Drucker, M Patou-Mathis, O Krotova, and S Pean
2012 Were European steppe bison migratory: ^{18}O, ^{13}C and Sr intra-tooth isotopic variations applied to a palaeoethological reconstruction. *Quaternary International* 271:106-119.

Kenneth Pye Associates Ltd
2010 GRADISTAT software package, available at http://www.kpal.co.uk/gradistat.html. Accessed August 2018.

Kent, S
1993 Variability in faunal assemblages: The influence of hunting skill, sharing, dogs, and mode of cooking on faunal remains at a sedentary Kalahari community. *Journal of Anthropological Archaeology* 12, 323-85.

Klein, RG, and K Cruz-Uribe
1984 *The Analysis of Animal Bones from Archaeological Sites*. University of Chicago Press, Chicago.

Koch, PL, N Tuross, and ML Fogel
1997 The effects of sample treatment and diagenesis on the isotopic integrity of carbonate in biogenic hydroxylapatite. *Journal of Archaeological Science* 24:417- 430.

Larson, ML
2004 Chipped stone aggregate analysis in archaeology. In *Aggregate analysis in chipped stone*, edited by CT Hall and ML Larson, pp 3-17. University of Utah Press, Salt Lake City.

Larson, ML, and M Kornfeld
1997 Chipped stone nodules: theory, method, and examples. *Lithic Technology* 22:4-18.

Leehan, KD
1981 A Sedimentological Analysis of Three Archaeological Sites in the Delta Junction Area, Alaska. M.A. thesis, Department of Anthropology, Washington State University, Pullman.

Lundbland, SP, PR Mills, and K Hon
2008 Analysing archaeological basalt using Non-Destructive Energy-Dispersive X-Ray Fluorescence (EDXRF): Effects of Post-Depositional chemical weathering and sample

size on analytical precision. *Archaeometry* 50:1–11.

Lyman, RL
1982 Archaeofaunas and Subsistence Studies. In: Schiffer, M.B. (Ed.), *Advances in Archaeological Method and Theory, vol. 5*. Academic Press, New York, pp. 331-393.
1994 *Vertebrate Taphonomy*. Cambridge University Press, Cambridge.
2008 *Quantitative Paleozoology*. Cambridge University Press, New York.

Machette, M
1986 Calcium and Magnesium Carbonates. In *Field and Laboratory Procedures Used in a Soil Chronosequence Study*, edited by M. J. Singer and P. Janitsky, pp. 30-33. USGS Bulletin 1648. United States Government Printing Office, Washington D.C.

Mackey, GN, and DP Fernandez
2011 High throughput Sr isotope analysis using an automated column chemistry system. American Geophysical Union, San Francisco, California. AGU Fall Meeting Abstracts, 1:2525.

Marean, CW, Y Abe, PJ Nilssen, and EC Stone
2001 Estimating the minimum number of skeletal elements (MNE) in zooarchaeology: A review and a new image-analysis GIS approach. *American Antiquity* 66, 333-348.

Marston, JM, JD Gudes, and C Warinner (editors)
2014 *Method and Theory in Paleoethnobotany*. University of Colorado Press, Boulder.

Matmon, A, JP Briner, G Carver, P Bierman and RC Finkel
2010 Moraine chronosequence of the Donnelly Dome region, Alaska. *Quaternary Research* 74:63-72.

Muhs, DR, TA Ager, JM Been, JG Rosenbaum, and RL Reynolds
2000 An Evaluation of Methods for Identifying and Interpreting Buried Soils in Late Quaternary Loess in Alaska. In *Geological Studies in Alaska by the U.S. Geological Survey, 1998*, edited by K.D. Kelley and L.P. Gough, pp. 127- 146. U.S. Geological Survey Professional Paper 1615. U.S. Geological Survey, Denver.

Muhs, DR, TA Ager, EA Bettis III, J McGeehin, JM Been, JE Begét, MJ Pavich, TW Stafford, Jr., and DSP Stevens
2003 Stratigraphy and Palaeoclimatic Significance of Late Quaternary Loess-Palaeosol Sequences of the Last Interglacial-Glacial Cycle in Central Alaska. *Quaternary Science Reviews* 22:1947-1986.

Mulliken, K
2016 Holocene volcanism and human occupation in the middle Susitna River, Alaska. MA Thesis, Department of Anthropology, University of Alaska Fairbanks.

Natural Resources Conservation Service (NRCS)
2010 *Keys to Soil Taxonomy*. 11th edition. United States Department of Agriculture, Washington D.C.

Nettleton, WD, CG Olson, and DA Wysocki
2000 Paleosol Classification: Problems and Solutions. *Catena* 41:61-92.

Nokleberg, WJ, NRD Albert, GC Bond, PL Herzon, RT Miyaoka, WH Nelson, DH Richter, TE Smith, JH Stout, W Yeend and RE Zehner
1982 Geologic Map of the Southern Part of the Mount Hayes Quadrangle, Alaska. United States Geological Survey, Open File Report 82-52

Nokleberg, WJ, JN Alienikoff, IM Lange, SR Silva, RT Miyaoka, CE Schwab and RE Zehner
1992 Preliminary geologic map of the Mount Hayes quadrangle, eastern Alaska Range, Alaska. In U.S. Geological Survey, Open-File Report OF-92-594.

Palmer, AS
2007 Pedostratigraphy. In *Encyclopedia of Quaternary Science*, edited by S.A, Elias, pp. 2847-2856. Elsevier Ltd.

Partlow, MA
2000 Salmon Intensification and Changing Household Organization in the Kodiak Archipelago. Ph.D. Dissertation. Madison: University of Wisconsin.

Partlow, MA
2006 Sampling fish bones: A consideration of the importance of screen size and disposal context in the North Pacific. *Arctic Anthropology* 43, 67-79.

Payne, S
1972 Partial Recovery and Sample Bias: The Results of Some Sieving Experiments. In: Higgs, ES (Ed.), *Papers in Economic Prehistory*. Cambridge University Press, Cambridge, pp. 49-64.

Pearsall, DM
2000 *Paleoethnobotany: A Handbook of Procedures*, 2nd ed. Academic Press, San Diego, CA.

Péwé, TL
1968 Loess Deposits in Alaska. In *Genesis and Classification of Sedimentary Rocks, Proceedings Section 8. Report of the Twenty-third Session of the International Geological Congress,* pp. 297-*309. International Geological Congress, Czechoslovakia*.

Péwé, TL, and GW Holmes
1964 Geology of the Mt. Hayes D-4 Quadrangle, Alaska. U.S. Geological Survey. Miscellaneous Geological Investigations Map I-394. U.S. Government Printing Office, Washington D.C.

Pinney, DS
1991 Laboratory Procedures for Processing Tephra Samples: Alaska Division of Geological and Geophysical Surveys Public-data file 91-31, 12 p.

Potter, BA
2005 Site Structure and Organization in Central Alaska: Archaeological Investigations at Gerstle River. PhD Dissertation, Department of Anthropology, University of Alaska Fairbanks.
2008 Radiocarbon chronology of central Alaska: Technological continuity and economic change. *Radiocarbon* 50 (2): 181-204.

Potter, BA, PM Bowers, JD Reuther, and OK Mason
2007 Holocene assemblage variability in the Tanana Basin: NLUR archaeological research, 1994-2004. *Alaska Journal of Anthropology* 5(1):23-42.

Potter, BA, CE Holmes, and DR Yesner
2013 Technology and Economy among the earliest prehistoric foragers in interior Eastern Beringia. In *Paleoamerican Odyssey*, edited by KE Graf, C Ketron, and M Waters, pp 81-103. Texas A&M University Press, College Station.

Potter, BA, JD Irish, JD Reuther, C Gelvin-Reymiller, and VT Holliday
2011 A Terminal Pleistocene Child Cremation and Residential Structure from Eastern Beringia. *Science* 331: 1058–1062.

Potter, BA, JD Irish, JD Reuther, and HJ McKinney
2014 New insights into Eastern Beringian mortuary behavior: A terminal Pleistocene double infant burial at Upward Sun River. *Proceedings of the National Academy of Sciences* 111(48): 17060-17065.

Potter, BA, JD Reuther, PM Bowers, and C Gelvin-Reymiller
2008 Little Delta Dune Site: A Late-Pleistocene Multicomponent Site in Central Alaska. *Current Research in the Pleistocene* 25: 132-135.

Prentiss, WC
1998 The reliability and validity of a lithic debitage typology: implications for archaeological interpretation. *American Antiquity* 63:635-650.

Rasic, JT
2011 Functional variability in the late Pleistocene archaeological record of eastern Beringia: a model of late Pleistocene land use and technology from northwest Alaska. In *From the Yenisei to the Yukon: interpreting lithic assemblage variability in Late Pleistocene/Early Holocene Beringia* (2011): 128-164.
2015 Archaeological Evidence for Transport, Trade, and Exchange in the North American Arctic. In *The Oxford Handbook of the Prehistoric Arctic*, edited by Max Friesen and Owen Mason, pp. 131-152. Oxford University Press, New York.

Rasic, JT, C Houlette, N Slobodina, JD Reuther, V Florey, and R Speakman
2009 A Twelve Thousand Year History of Obsidian Prospecting in Eastern Beringia. *Geological Society of America Abstracts and Programs* 41(7):679.

Reger, RD, DSP Stevems and DN Solie
2008 Surficial Geology of the Alaska Highway Corridor, Delta Junction to Dot Lake, Alaska. Alaska Division of Geological and Geophysical Surveys, State of Alaska, Department of Natural Resources.

Reitz, EJ, and ES Wing
1999 *Zooarchaeology*. Cambridge University Press, Cambridge.

Reuther J.D.
2013 Late Glacial and Early Holocene Geoarchaeology and Terrestrial Paleoecology in the Lowlands of the Middle Tanana Valley, Subarctic Alaska. PhD Thesis, University of Arizona.

Reuther, JD, N Slobodina, JT Rasic, JP Cook, and RJ Speakman
2011 Gaining Momentum – Late Pleistocene and Early Holocene Archaeological Obsidian Source Studies in Interior and Northern Eastern Beringia. In *From the Yensei to the Yukon: Interpreting Lithic Assemblage Variability in Late Pleistocene/Early Holocene Beringia*, edited by TE Goebel and I Buvit, pp. 270-286. Texas A&M Press, College Station.

Reuther, JD, C Gelvin-Reymiller, L Cwynar, B Gaglioti, MJ Wooller, NH Bigelow, DR Klein, J Kurek, JP Smol, and A Lopez
2010 A 13,000 year record of human-environment interactions at Quartz Lake, Interior Alaska. Abstracts of the Geological Society of America, 2010 Annual Meeting.

Reimer PJ, Bard E, Bayliss A, Beck JW, Blackwell PG, Bronk Ramsey C, Buck CE, Cheng H, Edwards RL, Friedrich M, Grootes PM, Guilderson TP, Haflidason H, Hajdas I, Hatté C, Heaton TJ, Hoffmann DL, Hogg AG, HughenKA, Kaiser KF, Kromer B, Manning SW, Niu M, Reimer RW, Richards DA, Scott EM, Southon JR, Staff RA, Turney CSM, van der Plicht J.
2013 IntCal13 andMarine13 radiocarbon age calibration curves 0–50,000 years cal BP. *Radiocarbon* 55(4):1869–87.

Riehle, JR
1994 Heterogeneity, Correlatives, and Proposed Stratigraphic Nomeclature of Hayes Tephra Set H, Alaska. *Quaternary Research* 41:285-288.

Riehle, JR, PM Bowers, and TA Ager
1990 The Hayes Tephra Deposits, and Upper Holocene Marker Horizon in South-Central Alaska. *Quaternary Research* 33(3), 276–290.

Shackley, MS
2005 *Obsidian: Geology and Archaeology in the North American Southwest.* University of

Arizona Press, Tucson.

Shott, MJ
1992 Radioocarbon dating as a probabilistic technique: the Childers Site and Late Woodland occupation in the Ohio Valley. *American Antiquity* 57(2):202-230.

Shotwell, JA
1955 An approach to the paleoecology of mammals. *Ecology* 36, 327-37.
1958 Inter-community relationships in hemphillian (mid-Pliocene) mammals. *Ecology* 39, 271-282.

Soil Survey Staff
2015 *Illustrated Guide to Soil Taxonomy, Version 2*. U.S. Department of Agriculture, Natural Resources Conservation Service, National Soil Survey Center, Lincoln, Nebraska.

Speakman, RJ, and MS Shackley
2013 Silo and portable XRF in archaeology: a response to Frahm. *Journal of Archaeological Science* 40:1435-1443.

Stein, JK
1984 Organic Matter and Carbonates in Archaeological Sites. *Journal of Field Archaeology* 11:239-246.

Stein, JK, JN, Deo, and LS Phillips
2003 Big Sites-Short Time: Accumulation Rates in Archaeological Sites. *Journal of Archaeological Science* 30:297-316.

Sullivan III, AP, and KC Rozen
1985 Debitage analysis and archaeological interpretation. *American Antiquity* 50:755-779.

United States Department of Agriculture (USDA)
1993 *Soil Survey Manual*. USDA Handbook 18. Washington, D.C.: Soil Conservation Service, USDA Soil Survey Division.

Wallace, KL, ML Coombs, LA Hayden, and CF Waythomas
2014 Significance of a near-source tephra-stratigraphic sequence to the eruptive history of Hayes volcano, south-central Alaska. U.S. Geological Survey Scientific Investigations Report 2014-5133, 32p.

Ward, GK, and SR Wilson
1978 Procedures for comparing and combining radiocarbon age determination: a critique. *Archaeometry* 20:19-31.

Watson, JPN
1979 The estimation of the relative frequencies of mammalian species: Khirokitia, 1972. *Journal of Archaeological Science* 6, 127-137.

West, FH
1981 *The Archaeology of Beringia*. Columbia University Press, New York.

White, TE
1953 A method of calculating the dietary percentage of various food animals utilized by Aboriginal peoples. *American Antiquity* 18, 396-398.

Widga, C, D Walker, and L Stockli
2010 Middle Holocene bison diet and mobility in the eastern Great Plains (USA) based on δ13C, δ18O, and 87Sr/86 Sr analyses of tooth enamel carbonate. *Quaternary Research* 73(3):449–463.

Wilson, FH, CP Hults, CG Mull and SM Karl
2015 Geologic map of Alaska. Scientific Investigations Map, U. S. Geological Survey, Reston, VA.

APPENDIX A. LITHIC RAW MATERIALS

Ben A. Potter

A1. Lithic Raw Material Descriptions

Chert C1 is fine-grained (high flaking quality), moderately translucent, of a dark gray color (5Y 4/1) field characterized as dark gray. Color texture is uniform, and there are large light colored crystals. Cortex was present as river-worn cobble. A total of 366 specimens weighing 62.42 g are represented at the site, 330 from Denali and 36 from Northern Archaic components. It is found in 6 components (43%). Cortex is present in low quantities (5, 1.4%) and a few larger artifacts have been recovered (9, 2.5%).

Chert C2 is fine-grained (high flaking quality), moderately translucent, of a gray color (10 YR 6/1) field characterized as light gray chert. Color texture is uniform, and there are widely spaced large black crystals. No cortex was observed. A total of 30 specimens weighing 2.02 g are represented at the site, 10 from Denali and 20 from Northern Archaic components. It is found in 4 components (29%). No larger artifacts have been recovered.

Chert C3 is fine-grained (high flaking quality), moderately translucent of a dark gray color (Gley 1 4/N) field characterized as medium gray. Color texture is uniform with widely spaced large tan crystals. No cortex was observed. A total of 28 specimens weighing 7.79 g are represented at the site, 1 from Denali and 27 from Northern Archaic components. It is found in 5 components (36%). No larger artifacts have been recovered.

Chert C4 is medium-grained (moderate flaking quality), opaque of a very dark brown color (2.5 Y 3/2) field characterized as dull reddish brown. Color texture is uniform with widely spaced dark crystals. No cortex was observed. A total of 3 specimens weighing 0.19 g are represented at the site, 2 from Denali and 1 from Northern Archaic components. It is rare, found in 2 components (14%). Only 1 larger artifact (33%) was recovered.

Chert C5 is fine-grained (high flaking quality), opaque of a black color (gley 1 2.5/N) field characterized as black. Some specimens ranged in color from very dark gray (3/N) to dusky red (10R 3/3). Color texture ranges between uniform and some areas of lighter gray banding. Inclusions include moderately spaced small light-colored crystals. No cortex was observed. A total of 3,038 specimens weighing 366.58 g are represented at the site, 4 from Chindadn, 2,412 from Denali, and 622 from Northern Archaic components. It is very common, found in 13 components (93%). Cortex is present in low quantities (20, 0.7%) and a few larger artifacts have been recovered (64, 2.1%).

Chert C6 is medium-grained (moderate flaking quality), opaque of a reddish black color (2.5 YR 2.5/1) field characterized as mottled purplish brown. Color texture is mottled mixture of purple, black and white. There are closely spaced light colored crystals. No cortex was observed. Only 1 specimen weighing 0.15 g from one Northern Archaic component was recovered.

Chert C7 is fine to medium-grained (high-moderate flaking quality), moderately opaque of a dark greenish gray color (Gley 1 4/10Y to 3/1) field characterized as medium grayish green. Color texture consists of thin dark brown banding and there are closely spaced light colored crystals. Cortex is dark greenish gray. A total of 140 artifacts weighing 76.92 g are represented at the site, 139 from Denali and 1 from Northern Archaic components. It is found in 5 components (36%). A relatively high amount of cortex was present (25, 17.9%) and many larger specimens were observed (15, 10.7%).

Chert C8 is fine-grained, with the appearance of polish (high flaking quality), opaque with a color of dark brown (7.5 YR 3/3) field characterized as medium brown. Color texture is uniform and there are no inclusions. No cortex was observed. A total of 8 artifacts weighing 0.4 g are represented at the site, 5 from Denali and 3 from Northern Archaic components. It is found in 3 components (21%). No larger specimens were observed.

Chert C10 is medium-grained (moderate flaking quality), moderately opaque with a color of greenish gray (Gley 1 6/10 GY) field characterized as light greenish gray. Color texture includes rust colored inclusions and there are light colored crystal inclusions. No cortex was observed. A total of 30 artifacts weighing 157.65 g are represented at the site, 1 from Chindadn and 29 from Denali components. It is found in 3 components (21%). Cortex (3, 10%) and larger artifacts (15, 23.3%) were observed at relatively high levels.

Chert C11 is fine-grained (high flaking quality), translucent with a color of light yellowish brown (2.5Y 6/3) field characterized as light tan, though color ranged to olive gray (5Y 5/2) and very dark gray (Gley1 3/N). Color texture is uniform, though some pieces had widely spaced darker gray banding, and there are moderately spaced small light or dark colored crystal inclusions. Cortex was observed. A total of 865 artifacts weighing 91.72 g are represented at the site, 20 from Chindadn, 574 from Denali, and 271 from Northern Archaic components. It is found in 11 components (79%). Cortex (2, 0.2%) and larger flakes (9, 1%) were relatively rare.

Chert C12 is fine-grained (high flaking quality), moderately translucent with a color of olive gray (5Y 5/2) field characterized as olive gray. Color texture consists of widely spaced banding and there are no inclusions. No cortex was observed. A total of 1,038 artifacts weighing 43.13 g are represented at the site, all from a single Northern Archaic component. No larger flakes were observed.

Chert C13 is fine-grained (high flaking quality), moderately translucent with a color of very dark gray (5Y 3/1) with some dark gray (Gley1 4/N) field characterized as very dark brownish gray. Color texture includes mottling, generally light gray splotches with some light brownish areas. No inclusions were observed on some specimens, others had small clear crystals. No cortex was observed. A total of 53 artifacts weighing 3.81 g are represented at the site, 52 from Denali components, and 1 from Northern Archaic components. It is found in 3 components (21%). No larger flakes were observed.

Chert C14 is fine-grained with the appearance of polish (high flaking quality), moderately translucent with a color of black (Gley 1 2.5/N) field characterized as glossy black. Color texture is uniform with small clear crystals. No cortex was observed. A total of 39 artifacts weighing

15.62 g are represented at the site, 38 from Denali components and 1 from Northern Archaic components. It is found in 3 components (21%). A few larger flakes (3, 7.7%) were recovered.

Chert C15 is fine-grained and glossy (high flaking quality), moderately translucent with a color of light gray (2.5Y 7/1 to N7) field characterized as very light gray. Color texture is uniform and there are small clear crystals. No cortex was observed. A total of 51 artifacts weighing 1.76 g are represented at the site, 7 from Denali components and 44 from Northern Archaic components. It is found in 4 components (29%). No larger flakes were recovered.

Chert C17 is fine-grained with a polished appearance (high flaking quality), moderately translucent with a color of dark yellowish brown (10YR 3/6) field characterized as reddish brown. Color texture is uniform with linear crystalline inclusions. No cortex was observed. A total of 120 artifacts weighing 8.64 g are represented at the site, 116 from Denali components and 4 from Northern Archaic components. It is found in 5 components (36%). No larger flakes were recovered.

Chert C18 is fine-grained with a polished appearance (high flaking quality), moderately translucent with a color of gray (5Y 5/1) field characterized as shiny light gray. Color texture is uniform with small clear crystals. No cortex was observed. A total of 1 artifact weighing 0.02 g is represented at the site, from a Denali component.

Chert C19 is fine-grained with a polished appearance (high flaking quality), moderately translucent with a color of dark gray (including Gley1 4/N to 5N, 5Y 5/1, 2.5Y 5/1, 5Y 4/2) field characterized as steel gray. Color texture has lighter colored banding, with no inclusions observed on some specimens and small widely spaced crystals on others. A total of 1,947 artifacts weighing 147.62 g are represented at the site, 35 from Chindadn, 1,847 from Denali, and 65 from Northern Archaic components. It is common, found in 12 components (86%). Relatively few pieces with cortex (8, 0.4%) and larger flakes (11, 0.6%) were recovered.

Chert C21 is fine-grained with a polished appearance (high flaking quality), opaque with a color of dark brown (7.5YR 3/3) field characterized as mottled brownish red. Color texture is mottled, with dark brown dendritic inclusions/mottling. No cortex was observed. A total of 16 artifacts weighing 0.76 g are represented at the site, 15 from Denali components and 1 from a Northern Archaic component. It is found in 3 components (21%). No larger flakes were recovered.

Chert C22 is fine-grained (high flaking quality), opaque with a color of gray (5Y 5/1) field characterized as opaque gray. Color texture includes dark reddish brown banding, and there are no inclusions. No cortex was observed. A total of 61 artifacts weighing 8.96 g are represented at the site, 60 from Denali components and 1 from a Northern Archaic component. It is found in 4 components (29%). A few larger flakes (2, 3.3%) were recovered.

Chert C24 is fine-grained (high flaking quality), moderately opaque with a color of very dark gray (Gley1 3/N, Gley1 4/10Y) field characterized as medium gray banded. Color texture includes light gray banding and there are sometimes black dendritic inclusions. A total of 181 artifacts weighing 15.42 g are represented at the site, 154 from Denali components and 27 from

Northern Archaic components. It is found in 8 components (57%). Relatively few cortical pieces (2, 1.1%) and larger flakes (2, 1.1%) were recovered.

Chert C28 is fine-grained (high flaking quality), moderately translucent to opaque with a color of dark reddish brown (2.5YR 3/3 to 10R 2.5/1) field characterized as mottled red. Color texture includes brown and red mottling, and there are moderately spaced clear crystals in some specimens. No cortex was observed. A total of 217 artifacts weighing 42.85 g are represented at the site, 214 from Denali components and 3 from Northern Archaic components. It is found in 9 components (64%). A few larger flakes (5, 2.3%) were recovered.

Chert C29 is fine-grained (high flaking quality), moderately opaque with a color of gray (N6) field characterized as light brownish gray chert. Color texture is uniform and there are scattered crystal inclusions. No cortex was observed. A total of 142 artifacts weighing 13.98 g are represented at the site, 117 from Denali components and 25 from Northern Archaic components. It is found in 7 components (50%). No larger flakes were recovered.

Chert C30 is fine-grained (high flaking quality), moderately translucent with a color of dark greenish gray (Gley1 4/10Y) field characterized as grass green. Color texture is uniform and there are widely spaced black inclusions. A total of 1,800 artifacts weighing 263.68 g are represented at the site, 117 from Denali components and 25 from Northern Archaic components. It is found in 5 components (36%). Relatively few cortical pieces (2, 0.1%) and larger flakes (24, 1.3%) were recovered.

Chert C31 is fine-grained (high flaking quality), moderately translucent with a color of very dark gray (2.5Y 3/1) to grayish brown (10YR 5/2) field characterized as brown. Color texture is mottled to uniform, and there are moderately spaced dark brown or clear crystal inclusions. No cortex was observed. A total of 56 artifacts weighing 2.22 g are represented at the site, all from two Northern Archaic components (36% of all components). No larger flakes were recovered.

Chert C32 is medium-grained with the appearance of polish (moderate flaking quality), opaque with a color of black (Gley1 2.5/N) field characterized as brownish black macrocrystalline. Color texture is uniform and there are widely spaced white crystal inclusions. A total of 9 artifacts weighing 3.38 g are represented at the site, 1 from Chindadn, 3 from Denali, and 5 from Northern Archaic components. It is found in 3 components (21%). Two pieces (22.2%) retained cortex. No larger flakes were found.

Chert C33 is medium-grained (moderate flaking quality), opaque with a color of gray (Gley1 5/N) to dark greenish gray (Gley1 4/10Y) field characterized as dull gray. Color texture is uniform, with a flaky surface texture and moderately spaced clear crystals. A total of 861 artifacts weighing 315.29 g are represented at the site, 38 from Chindadn, 801 from Denali, and 22 from Northern Archaic components. It is found in 8 components (57%). High amounts of cortical pieces (112, 13%) and larger pieces (45, 5.2%) were recovered.

Chert C35 is fine-grained (high flaking quality), opaque with a color of reddish black (2.5YR 2.5/1) field characterized as dark purple. Color texture is uniform, and there are closely spaced clear crystal inclusions. No cortex was observed. A total of 3 artifacts weighing 13.72 g are

represented at the site, 1 from Denali and 2 from Northern Archaic components. It is represented in 2 components (14%). One larger piece (33.3%) was recovered.

Chert C36 is medium-grained (high-medium flaking quality), moderately opaque with a color of very dark gray (Gley1 3/N) field characterized as chalkboard gray. Color texture was uniform with closely spaced clear crystals. A total of 894 artifacts weighing 116.62 g are represented at the site, 142 in Chindadn, 723 in Denali, and 29 in Northern Archaic components. It is represented in 8 components (57%). Relatively few cortical pieces (4, 0.4%) and larger pieces (15, 1.7%) were recovered.

Chert C38 is fine-grained (high flaking quality), moderately translucent with a color of dark brown (7.5YR 3/2) field characterized as speckled brown. Color texture is uniform with closely spaced black crystals. No cortex was observed. A total of 16 artifacts weighing 0.22 g are represented at the site, all from 4 Denali components (29% of total components). No larger pieces were recovered.

Chert C39 is fine-grained (high flaking quality), opaque with a color of black (7.5YR 2.5/1) field characterized as purplish black. Color texture included mottling with small uniform color blocks, and no inclusions were observed. A total of 180 artifacts weighing 13.79 g are represented at the site, 166 from Denali and 14 from Northern Archaic components. It is present in 7 components (50%). Relatively few cortical pieces (1, 0.6%) or larger pieces (2, 1.1%) were recovered.

Chert C41 is fine-grained (high flaking quality), moderately opaque with a color of very dark greenish gray (Gley1 3/10Y) field characterized as dark brownish gray. Color texture is uniform and there were widely spaced light-tan colored crystal inclusions. No cortex was observed. A total of 113 artifacts weighing 12.99 g are represented at the site, 112 from Denali and 1 from Northern Archaic components. It is present in 3 components (21%). A few larger pieces (3, 2.7%) were recovered.

Chert C42 is fine-grained (high flaking quality), opaque with a color of reddish black (5R 2.5/1) field characterized as reddish black. Color texture was uniform and there were closely spaced clear crystal inclusions. No cortex was observed. A total of 10 artifacts weighing 1.51 g are represented at the site, all from 3 Denali components (21% of total components). No larger pieces were observed.

Chert C45 is fine-grained (high flaking quality), moderately opaque with a color of greenish black (Gley2 10G 2.5/1) field characterized as greenish black. Color texture is uniform and there were widely spaced white crystal inclusions. No cortex was present. A total of 10 artifacts weighing 1.62 g are represented at the site, 1 from Chindadn and 9 from Denali components. It is found in 3 components (21%). No larger pieces were observed.

Chert C46 is fine-grained (high flaking quality), moderately translucent with a color of very dark greenish gray (Gley1 3/10Y) field characterized as dark greenish gray banded. Color texture is banded, and there are widely spaced white crystals. No cortex was observed. A total of 80 artifacts weighing 6.06 g are represented at the site, all from 2 Denali components (14% of total components). No larger pieces were observed.

Chert C47 is medium-grained (moderate flaking quality), moderately opaque with a color of light greenish gray (Gley1 8/1) field characterized as white speckled. Color texture is uniform with closely spaced large white crystals. No cortex was present. A total of 171 artifacts weighing 5.73 g are represented at the site, 170 from Denali and 1 from Northern Archaic components. It is found in 2 components (14%). Only 1 (0.6%) larger piece was recovered.

Chert C48 is medium-grained (moderate flaking quality), moderately opaque with a color of olive gray (5Y 4/2) field characterized as medium brownish gray. Color texture is mottled with lighter colored areas and a flaky surface, and there were widely spaced light-colored crystal inclusions. No cortex was observed. A total of 53 artifacts weighing 3.67 g are represented at the site, all from a single Denali component (7% of total components). No larger pieces were recovered.

Chert C49 is fine-grained (high flaking quality), opaque with a color of olive gray (5Y 4/2) field characterized as gray banded opaque. Color texture is banded and there are closely spaced clear crystal inclusions. A total of 24 artifacts weighing 4.6 g are represented at the site, 11 from Denali and 13 from Northern Archaic components. It is found in 6 components (43%). Relatively high amounts of cortical flakes (1, 4.2%) and larger pieces (4, 16.7%) were recovered.

Chert C51 is medium-grained (moderate flaking quality), opaque with a color of dark greenish gray (Gley1 4/10Y) field characterized as dark tree green. Color texture is uniform, and there are closely spaced clear crystal inclusions. No cortex was observed. A total of 35 artifacts weighing 1.61 g are represented at the site, 3 from Denali and 32 from Northern Archaic components. It is found in 4 components (29%). No larger pieces were recovered.

Chert C52 is medium-grained (moderately flaking quality), opaque with a color of dark gray (N4) field characterized as dark gray speckled. Color texture is mottled with large, light greenish-gray (10Y 7/1) crystalline inclusions. No cortex was observed. A total of 4 artifacts weighing 2.69 g are represented at the site, all from 2 Denali components (14% of total components). No larger pieces were recovered.

Chert C53 is medium-grained (high flaking quality), moderately opaque with a color of dark greenish gray (10Y 4/1) field characterized as dark greenish gray. Color texture is uniform with scattered black inclusions. No cortex was observed. A total of 5 artifacts weighing 0.18 g are represented at the site, 1 from Chindadn, 1 from Denali, and 3 from Northern Archaic components. It was found in 4 components (29%). No larger pieces were recovered.

Chert C55 is fine-grained (high flaking quality), moderately opaque with a color of very dark gray (5Y 3/1) field characterized as coffee bean brown. Color texture is uniform with linear inclusions/cleavage planes. A total of 99 artifacts weighing 6.63 g are represented at the site, 1 from Chindadn and 98 from Denali components. It was found in 4 components (29%). A few cortical pieces (2, 2.0%) and no larger pieces were recovered.

Chert C56 is fine-grained (high flaking quality), moderately opaque with a color of greenish gray (5BG 3/1) field characterized as dark green. Color texture is uniform with scattered black

inclusions. No cortex was present. A total of 48 artifacts weighing 2.14 g are represented at the site, 46 from Denali and 2 from Northern Archaic components. It is found in 5 components (36%). No larger pieces were recovered.

Chert C57 is medium-grained (high flaking quality), opaque with a color of green (5G 4/1) field characterized as opaque green. Color texture includes mottling with scattered inclusions. A total of 13 artifacts weighing 1.0 g are represented at the site, 12 from Denali and 1 from Northern Archaic components. It is found in 2 components (14%). Relatively high numbers of cortical pieces (7, 53.8%) were recovered.

Chert C58 is fine-grained (high flaking quality), opaque with a color of brown (2.5Y 3/1) field characterized as banded brown. Color texture includes banding of a lighter yellowish brown (2.5Y 6/3). No cortex was observed. A total of 8 artifacts weighing 2.38 g are represented at the site, all from one Denali component (7%). One larger flake (12.5%) was recovered.

Chert C59 is medium-grained (low flaking quality), opaque with a color of brown (10YR 4/3) field characterized as chocolate brown. Color texture is uniform with dark round inclusions. A total of 5 artifacts weighing 1.39 g are represented at the site, 2 from Denali and 3 from Northern Archaic components. It is found in 3 components (21%). A relatively high number of cortical pieces (2, 40%) were recovered.

Chert C62 (jasper) is fine-grained (high flaking quality), opaque with a color of yellowish brown (10YR 5/4) field characterized as “sugar-daddy”. Color texture includes mottling and banding, and there were no inclusions. A total of 23 artifacts weighing 1.75 g were recovered, all from 3 Denali components (21% of total). Relatively high numbers of cortical pieces (1, 4.3%) and larger pieces (4, 17.4%) were recovered.

Chert C63 (chert or quartzite?) is coarse-grained (low flaking quality), opaque with a color of black (2.5Y 2.5/1) field characterized as dark brown. Color texture varies and there are large dark and light crystals in voids. No cortex was observed. A total of 5 artifacts weighing 2.62 g is represented at the site, all from 2 Denali components (14% of total). Two (40%) larger flakes were recovered.

Chert C64 is a fine-grained and glassy (high flaking quality), moderately opaque with a color of red (10R 3/3) field characterized as dusky red. Color texture is uniform with tightly spaced crystals. No cortex was observed. A total of 1 artifact weighing 0.46 g is represented at the site, from a Denali component (7%).

Chert C65 is fine-grained and glassy (high flaking quality), moderately translucent with a color of black (10YR 2/1) field characterized as glossy dark brown. Color texture is uniform and there are no inclusions. No cortex was observed. A total of 12 artifacts weighing 0.87 g are represented at the site, all from 2 Denali components (14%). No larger artifacts were recovered.

Chert C66 is fine-grained (high flaking quality), opaque with a color of purple (10R 2.5/2) field characterized as glossy eggplant. Color texture is mottled and there are no inclusions. No cortex

was observed. A total of 1 artifact weighing 0.03 g is represented at the site, from a Denali component (7%).

Chert C67 is fine-grained (high flaking quality), moderately opaque with a color of brown (10YR 3/1) field characterized as very dark brown. Color texture is uniform and there are brown crystalline inclusions. No cortex was observed. A total of 49 artifacts weighing 3.28 g are represented at the site, 1 from Denali and 48 from Northern Archaic components. It is found in 3 components (21%). A single larger flake (2.0%) was recovered.

Chert C68 is fine-grained (high flaking quality), opaque with a color of gray (Gley1 4/N) field characterized as speckled blue gray. Color texture is uniform with a mixture of dark and light grains, and there are no inclusions. A total of 38 artifacts weighing 16.19 g are represented at the site, 1 from Chindadn, 36 from Denali, and 1 from Northern Archaic components. It is found in 6 components (43%). Relatively few cortical pieces (1, 2.6%) and larger pieces (1, 2.6%) were recovered.

Chert C69 (chert or macrocrystalline) is coarse-grained (low flaking quality), opaque with a color of dark gray (Gley1 3/N) field characterized as black macrocrystalline. Color texture is uniform and there are no inclusions. No cortex was observed. A total of 22 artifacts weighing 3.01 g are represented at the site, 20 from Denali and 2 from Northern Archaic components. It is found in 2 components (14%). No larger pieces were recovered.

Chert C70 is fine-grained (high flaking quality), moderately opaque with a color of very dark gray (Gley1 3/N) field characterized as black “swamp.” Color texture is uniform and there are no inclusions. No cortex was observed. A total of 55 artifacts weighing 3.7 g are represented at the site, 54 from Denali and 1 from Northern Archaic components. It is found in 3 components (21%). A few larger pieces (2, 3.6%) were recovered.

Chert C72 is fine-grained (high flaking quality), moderately opaque with a color of brown (2.5YR 1/3) field characterized as lavender brown. Color texture is uniform and there are no inclusions. No cortex was observed. A total of 7 artifacts weighing 0.13 g are represented at the site, all from a single Denali component (7%). A single larger flake (14.3%) was recovered.

Chalcedony Ch1 is fine-grained (high flaking quality), translucent with a color of clear/white and black (Gley1 2.5/N) field characterized as clear with black inclusions. Color texture is mixture of clear/white and black with dendritic inclusions. No cortex was observed. A total of 30 artifacts weighing 0.66 g are represented at the site, 1 from Chindadn, 27 from Denali, and 2 from Northern Archaic components. It is found in 6 components (43%). No larger pieces were recovered.

Chalcedony Ch3 is fine-grained (high flaking quality), moderately translucent with a color of brown (7.5YR 4/4) field characterized as mottled brown. Color texture is mottled with a mixture of medium reddish brown and clear/white, and no inclusions were observed. No cortex was observed. A total of 87 artifacts weighing 4.55 g are represented at the site, 85 from Denali and 2 from Northern Archaic components. It is found in 5 components (36%). A single larger piece (1.1%) was recovered.

Chalcedony Ch4 is fine-grained (high flaking quality), translucent with a color of light gray (2.5Y 7/1) field characterized as translucent clear. Color texture is uniform, with dendritic yellow inclusions. No cortex was observed. A total of 8 artifacts weighing 1.45 g are represented at the site, 5 from Denali and 3 from Northern Archaic components. It is found in 4 components (29%). A relatively large amount of larger pieces (7, 87.5%) were recovered.

Chalcedony Ch5 is medium-grained and glassy (high flaking quality), translucent to opaque with a variable color (5G 8/2 to 2.5Y 5/6) field characterized as pale green to yellowish brown. Color texture varies, with mottling and multi-colored banding, and there are pale green volumetric and dark reddish brown linear inclusions. No cortex was observed. A total of 6 artifacts weighing 0.74 g are represented at the site, all from 3 Denali components (21%). No larger artifacts were recovered.

Chalcedony Ch6 is fine-grained (high flaking quality), moderately translucent with a color of black (N 2.5/1) field characterized as smoky. Color texture includes mottling (opaque black to smoky clear) and there are black inclusions. No cortex was observed. A total of 1 artifact weighing 0.01 g is represented at the site, from one Northern Archaic component (7%).

Macrocrystalline M1 is medium-grained (low flaking quality), opaque with a color of brown (10YR 4/3) field characterized as dull reddish brown. Color texture includes mottling, and there are no inclusions. No cortex was observed. A total of 3 artifacts weighing 0.18 g are represented at the site, 2 from Denali and 1 from Northern Archaic components. It is found in 3 components (21%). No larger pieces were recovered.

Macrocrystalline M4 is coarse-grained (low flaking quality), opaque with a color of olive gray (5Y 5/2) field characterized as olive gray. Color texture includes mottling. No cortex was observed. A total of 4 artifacts weighing 2.93 g are represented at the site, 3 from Denali and 1 from Northern Archaic components. It is found in 3 components (21%). A single larger piece (25%) was recovered.

Obsidian (O) is fine-grained and glassy (high flaking quality), translucent to moderately translucent. They are grouped together for this analysis, as all are considered non-local (Wiki Peak, Batza Tena, and Ringling). pXRF analysis differentiated different types (see Chapter 10). A total of 78 artifacts weighing 12.89 g are represented at the site, 67 from Denali and 11 from Northern Archaic components. It is found in 4 components (29%). A total of 4 artifacts (5.3%) have cortex and 1 larger piece (1.3%) was recovered. Of the 78 obsidian artifacts, 64 were assigned to Wiki Peak, 2 were assigned to Group A' (Ringling), 1 was assigned to Batza Tena, and 5 could not be assigned to a particular source or group (likely due to their small size). The remaining 6 have not yet been isotopically analyzed.

Quartzite Q1 is fine-grained with a polished appearance (high flaking quality), translucent with a color of white (5Y 8/1) field characterized as white. Color texture is uniform, and there are small widely spaced dark crystal inclusions. A total of 118 artifacts weighing 30.76 g are represented at the site, 99 from Denali and 19 from Northern Archaic components. It is found in 8

components (57%). Relatively large amounts of cortical pieces (20, 16.9%) and larger pieces (5, 4.2%) were recovered.

Quartz Q2 is fine-grained (moderate flaking quality), opaque with a color of pale yellow (2.5Y 8/2) field characterized as cream. Color texture is uniform and there are no inclusions. No cortex was observed. A total of 8 artifacts weighing 0.24 g are represented at the site, 1 from Chindadn, 6 from Denali, and 1 from Northern Archaic components. It is found in 4 components (29%). No larger pieces were recovered.

Quartz Q3 is fine-grained with a polished appearance (high flaking quality), translucent and clear, field characterized as translucent. Color texture is uniform and there is internal fracturing visible. A total of 13 artifacts weighing 3.24 g are represented at the site, 1 from Chindadn, 8 from Denali, and 4 from Northern Archaic components. It is found in 6 components (43%). Relatively high amounts of cortical pieces (1, 7.7%) and larger pieces (2, 15.4%) were recovered.

Quartzite Q4 (quartzite or chert) is medium-grained and glassy (high flaking quality), moderately translucent with a color of black (N2.5) field characterized as black glassy. Color texture is uniform, and there are regular gas bubble and crystal inclusions. No cortex was observed. A total of 4 artifacts weighing 0.13 g are represented at the site, all from 2 Northern Archaic components (14%). No larger pieces were recovered.

Quartzite Q5 is medium-grained (moderate flaking quality), moderately translucent with a color of light gray (5Y 7/1) field characterized as speckled white. Color texture is uniform, and there are large reddish brown crystal inclusions. No cortex was present. A total of 4 artifacts weighing 4.46 g are represented at the site, all from 2 Northern Archaic components (14%). No larger pieces were recovered.

Quartzite Q6 is medium-grained (moderate flaking quality), moderately opaque with a color of green (5BG 7/2) field characterized as green-white. Color texture includes banding (green), and there are green crystal inclusions. No cortex was observed. A total of 2 artifacts weighing 3.67 g are represented at the site, one from Denali and one from Northern Archaic components (14%). No larger pieces were recovered.

Rhyolite R1 is fine-grained (high flaking quality), opaque with a color of light gray (2.5Y 8/1 to 10YR 7/1) field characterized as white/light gray. Color texture is uniform, but some specimens show gray banding with black phenocrysts. Cortex is gray. A total of 2,338 artifacts weighing 254.51 g are represented at the site, 2 from Chindadn, 2,297 from Denali, and 39 from Northern Archaic components. It is found in 10 components (71%). Relatively low numbers of cortical pieces (68, 2.9%) and large pieces (49, 2.1%) were recovered.

Rhyolite R2 is medium to fine-grained (medium to high flaking quality), opaque with a color of dark gray (2.5Y 4/1 to 5YR 4/1) field characterized as gray/maroon. Color texture is uniform with some banding, and phenocrysts are apparent. Cortex is light red (10R 6/6). A total of 2,106 artifacts weighing 160.77 g are represented at the site, 2100 from Denali, and 6 from Northern

Archaic components. It is found in 9 components (64%). Relatively low numbers of cortical pieces (59, 2.8%) and large pieces (10, 0.5%) were recovered.

Rhyolite R4 is fine-grained (high flaking quality), opaque with a color of brown (10YR 5/3 to 7.5YR 5/3) field characterized as tan/light brown. Color texture includes black and brown lines and some mottling. Inclusions include closely spaced light colored crystals and scattered black crystals. A total of 63 artifacts weighing 5.39 g are represented at the site, 54 from Denali and 9 from Northern Archaic components. It is found in 6 components (43%). A single cortical piece (1.6%) and no larger pieces were recovered.

Rhyolite R7 is medium-grained (moderate flaking quality), opaque with a color of pink (5YR 6/1) field characterized as rose. Color texture ranges from blue to white on a single flake, and there are scattered crystal inclusions. No cortex was observed. A total of 77 artifacts weighing 5.32 g are represented at the site, all from 2 Denali components (14%). A single larger piece (1.3%) was recovered.

Rhyolite R8 is fine-grained (high flaking quality), opaque with a color of pale blue (5PB 5/1) field characterized as pale blue. Color texture includes banding. No cortex was observed. A total of 3 artifacts weighing 0.45 g are represented at the site, all from a single Denali component (7%). No larger pieces were recovered.

Rhyolite R9 is fine-grained (high flaking quality), opaque with a variable color (Gley 5/- to 5Y 7/1) field characterized as gray banded. Color texture includes gray banding with some gray speckling. A total of 522 artifacts weighing 38.76 g are represented at the site, 516 from Denali and 6 from Northern Archaic components. It is found in 7 components (50%). Relatively low numbers of cortical pieces (4, 0.8%) and larger pieces (9, 1.7%) were recovered.

A2. Lithic Raw Materials per component

Table A1. Component 1 raw materials

counts

material	*debitage*	*mb*	*tool*	*core*	*total*
C30	215		1		216
C36	142		1		143
C33	38				38
C19	35		1		36
C11	18	2			20
C5	4				4
C7	1		1	1	3
R1	2		1		3
C10	1				1
C32	1				1
C45		1			1
C53	1				1
C55	1				1
C68			1		1
Ch1	1				1

weights

debitage	*mb*	*tool*	*core*	*total*
23.05		0.62		23.67
9.06		18.41		27.47
1.74				1.74
1.45		1.83		3.28
1.10	0.31			1.41
0.34				0.34
12.16		6.31	1045.10	1063.57
0.06		0.88		0.94
15.13				15.13
0.05				0.05
	0.12			0.12
0.03				0.03
0.08				0.08
		0.95		0.95
0.04				0.04

Q2	1				1	0.02				0.02
Q3	1				1	0.19				0.19
total	462	3	6	1	472	64.50	0.43	29.00	1045.10	1139.03

Table A2. Component 2a raw materials

	counts					weights				
material	*debitage*	*mb*	*tool*	*core*	*total*	*debitage*	*mb*	*tool*	*core*	*total*
C5	1865	3	15		1883	209.77	0.16	118.30		328.23
C30	1521	5			1526	230.92	1.10			232.02
C19	793	6			799	72.31	0.99			73.30
C33	702		2		704	284.16		318.24		602.40
C11	454	1			455	47.93	0.23			48.16
C36	402				402	77.04				77.04
C1	266	1	1		268	43.07	0.02	53.19		96.28
C41	111		1		112	12.89		2.53		15.42
C55	96		1		97	5.50		0.11		5.61
R1	93	1			94	16.90	0.04			16.94
Q1	88				88	9.03				9.03
C7	79				79	47.68				47.68
C39	59				59	3.10				3.10
C29	57				57	7.70				7.70
C48	53				53	3.67				3.67
R2	52				52	9.89				9.89
C13	39				39	1.86				1.86
C10	28		4		32	46.54		34.44		80.98
C56	28				28	0.91				0.91
C68	27		1		28	1.92		15.38		17.30
C14	22				22	13.82				13.82
C22	22				22	2.89				2.89
R9	21				21	0.51				0.51
C24	11			1	12	2.64			549.39	552.03
C46	8				8	2.52				2.52
C58	8				8	2.38				2.38
Ch1	8				8	0.17				0.17
C38	7				7	0.11				0.11
C17	4	2			6	0.10	0.11			0.21
C42	5	1			6	0.60	0.17			0.77
Q3	5		1		6	1.39		25.55		26.94
C49	4				4	1.27				1.27
C63	4				4	2.12				2.12
C28	3				3	0.14				0.14
C52	3				3	2.43				2.43
M4	2				2	2.08				2.08
C3		1			1		0.04			0.04
C45	1				1	0.01				0.01
C51	1				1	0.12				0.12
C53	1				1	0.01				0.01
C59	1				1	1.20				1.20
C61			1		1			0.48		0.48
C67			1		1			1.01		1.01

C70	1				1	0.25				0.25
C71			1		1			2.05		2.05
M2			1		1		0.09			0.09
M6				1	1				884.79	884.79
Q2	1				1	0.02				0.02
total	6956	21	30	2	7009	1169.57	2.95	571.28	1434.18	3177.98

Table A3. Component 2b raw materials.

	counts					weights				
material	*debitage*	*mb*	*tool*	*core*	*total*	*debitage*	*mb*	*tool*	*core*	*total*
C5	193				193	28.71				28.71
C36	50				50	4.39				4.39
C33	33				33	6.70				6.70
R2	30				30	1.54				1.54
R1	22				22	1.90				1.90
C11	14				14	2.06				2.06
C19	11		1		12	1.63		0.09		1.72
C30	8	1			9	0.53	0.27			0.80
C29	8				8	0.49				0.49
C68	4				4	1.31				1.31
C24	2				2	0.37				0.37
C7	2				2	0.19				0.19
C1	1				1	0.29				0.29
C17			1		1			0.11		0.11
C28		1			1		0.10			0.10
C42		1			1		0.66			0.66
C59	1				1	0.03				0.03
R9	1				1	0.01				0.01
total	380	3	2	0	385	50.15	1.03	0.20	0.00	51.38

Table A4. Component 2c raw materials.

	counts					weights				
material	*debitage*	*mb*	*tool*	*core*	*total*	*debitage*	*mb*	*tool*	*core*	*total*
R1	2142	13	10		2165	206.58	0.74	20.27		227.59
R2	1997	9	4		2010	144.87	1.19	28.14		174.20
C19	796	32	7		835	43.18	2.24	30.17		75.59
R9	485	8	2		495	36.94	1.06	21.76		59.76
C5	246	35	1		282	39.85	1.08	6.81		47.74
C36	231	38	2	1	272	16.98	1.65	0.49	0.12	19.24
C28	154	17			171	6.66	3.05			9.71
C47	168	2			170	5.50	0.16			5.66
C24	135	3		1	139	7.97	1.01		0.26	9.24
O	63		1		64	4.39	0.47			4.86
C17	86	23	1		110	4.91	1.79	1.19		7.89
C11	98	2		1	101	6.19	0.20		0.93	7.32
C39	18	70			88	1.00	4.36			5.36
C46	9	63			72	1.12	2.42			3.54
Ch3	66	4			70	2.37	0.14			2.51
C33	64		1		65	19.46		22.20		41.66
C1	56	6			62	5.00	1.06			6.06
C7	57				57	25.88				25.88
C70	3	50	1		54	0.36	3.05	0.48		3.89
C29	50				50	2.30				2.30
C30	36	13	1		50	5.77	1.97	1.26		9.00
R4	49				49	3.80				3.80
R7	42				42	3.97				3.97
C22	35	1	4		40	4.47	0.02	0.51		5.00
C69	1	19		1	21	0.09	2.48		8.37	10.94
C21	12		7		19	0.62		7.31		7.93
C56	17				17	1.19				1.19
C14	14	2			16	1.69	0.07			1.76
C13	3	10			13	0.36	1.49			1.85
C62	9	2	2		13	0.43	0.15	20.60		21.18
C57	12				12	0.92				0.92
C65	9	2			11	0.43	0.41			0.84
C2	2	8			10	0.05	0.71			0.76
C45	3	5		1	9	0.23	1.26		6.59	8.08
C72	7				7	0.13				0.13
C15	6				6	0.22				0.22
C49	2	3			5	0.26	0.14			0.40
C8	4	1			5	0.11	0.07			0.18
Q2	5				5	0.15				0.15
C68	4				4	0.45				0.45
Ch5		4			4		0.41			0.41
Q1	4				4	1.71				1.71
C32	3				3	0.14				0.14
C42	3				3	0.08				0.08
R10		3			3		0.27			0.27
R8		3			3		0.45			0.45
C35	1		1		2	0.02		0.08		0.10
C4	1	1			2	0.06	0.03			0.09

O3	1	1			2	0.01	0.17			0.18
Q3	2				2	0.30				0.30
C10	1				1	95.98				95.98
C18	1				1	0.02				0.02
C38	1				1	0.01				0.01
C41	1				1	0.07				0.07
C51	1				1	0.43				0.43
C52	1				1	0.26				0.26
C55	1				1	0.07				0.07
C63	1				1	0.50				0.50
C66	1				1	0.03				0.03
C67	1				1	0.06				0.06
Ch4	1				1	0.04				0.04
Ch6			1		1			1.77		1.77
M1	1				1	0.02				0.02
M4	1				1	0.01				0.01
Q6	1				1	0.07				0.07
Ch1	1				1	0.02				0.02
total	7226	453	46	5	7730	706.76	35.77	163.04	16.27	921.80

Table A5. Component 3 raw materials.

	counts					weights				
material	*debitage*	*mb*	*tool*	*core*	*total*	*debitage*	*mb*	*tool*	*core*	*total*
C19	188	2	2		192	18.40	0.36	1.17		19.93
C5	38		1		39	4.78		56.64		61.42
C39	16		3		19	4.48		5.93		10.41
C38	8				8	0.10				0.10
C28	4				4	0.16				0.16
C11	3				3	0.14				0.14
C22	2				2	1.56				1.56
R1	2				2	0.05				0.05
C24	1				1	0.06				0.06
C29	1				1	0.01				0.01
C36	1				1	0.01				0.01
C51	1				1	0.01				0.01
C55	1				1	0.98				0.98
C56	1				1	0.01				0.01
C65	1				1	0.03				0.03
R2	1				1	0.02				0.02
R4	1				1	0.03				0.03
R9	1				1	0.05				0.05
Total	271	2	6	0	279	30.88	0.36	63.74	0.00	94.98

Table A6. Component 4 raw materials.

counts

material	*debitage*	*mb*	*tool*	*core*	*total*
R7	31	4			35
C5	31		1		32
R1		24			24
Ch1	18				18
Ch3	8	4			12
C19	10		1		11
C28	4	1			5
R2	5				5
C62	1		2		3
Ch4	2		1		3
C24	2				2
C33	2				2
C49		1	1		2
C11	1				1
C17	1				1
C29	1				1
C30		1			1
C7	1				1
Ch5	1				1
M2	1				1
Q3		1			1
total	120	36	6	0	162

weights

debitage	*mb*	*tool*	*core*	*total*
1.05	0.30			1.35
6.95		7.91		14.86
	1.39			1.39
0.40				0.40
0.67	0.97			1.64
1.51		7.14		8.65
0.32	0.31			0.63
2.37				2.37
0.19		25.46		25.65
0.48		123.17		123.65
0.86				0.86
0.59				0.59
	0.61	15.35		15.96
0.01				0.01
0.02				0.02
0.01				0.01
	0.07			0.07
3.11				3.11
0.02				0.02
0.08				0.08
	1.28			1.28
18.64	4.93	179.03	0.00	202.60

Table A7. Component 5 raw materials.

counts

material	*debitage*	*mb*	*tool*	*core*	*total*
C28	27		1		28
Q1	6				6
C19	3				3
C39	3				3
Ch3	2	1			3
Ch4		2			2
C15	1				1
C36	1				1
C49	1				1
C62				1	1
C68	1				1
Ch5	1				1
total	46	3	1	1	51

weights

debitage	*mb*	*tool*	*core*	*total*
0.98		9.63		10.61
0.32				0.32
0.28				0.28
0.03				0.03
0.20	0.26			0.46
	0.90			0.90
0.06				0.06
0.02				0.02
0.14				0.14
			11.98	11.98
0.21				0.21
0.31				0.31
2.55	1.16	9.63	11.98	25.32

Table A8. Component 5b raw materials.

counts

material	*debitage*	*mb*	*tool*	*core*	*total*
C62	11				11
C19	6				6
R2	5	1			6
R4	1	3		1	5
C21	3				3
C28	1	1			2
C11	1				1
C5	1				1
Q1	1				1
total	30	5	0	1	36

weights

debitage	*mb*	*tool*	*core*	*total*
0.98				0.98
0.21				0.21
0.40	0.16			0.56
0.15	0.32		13.58	14.05
0.06				0.06
0.03	0.03			0.06
0.01				0.01
0.12				0.12
0.25				0.25
2.21	0.51	0.00	13.58	16.30

Table A9. Component 6 raw materials.

counts

material	*debitage*	*mb*	*tool*	*core*	*total*
C5	73		1		74
C15	30				30
C1	16				16
Q1	16				16
C11	10		1		11
C19	10				10
C33	9				9
C3	7				7
C2	1	1			2
R1	2				2
C13	1				1
C14	1				1
C17	1				1
C39			1		1
C4	1				1
C53				1	1
C6	1				1
C7	1				1
C8	1				1
M1	1				1
O	1				1
Q5	1				1
R2	1				1
R4	1				1
total	186	1	3	1	191

weights

debitage	*mb*	*tool*	*core*	*total*
7.76		1.38		9.14
1.11				1.11
5.52				5.52
16.43				16.43
1.50		1.52		3.02
0.61				0.61
1.91				1.91
5.34				5.34
0.03	0.06			0.09
0.36				0.36
0.10				0.10
0.04				0.04
0.01				0.01
		7.00		7.00
0.10				0.10
			1404.80	1404.80
0.15				0.15
0.06				0.06
0.10				0.10
0.08				0.08
0.06				0.06
4.30				4.30
0.06				0.06
0.15				0.15
45.78	0.06	9.90	1404.80	1460.54

Table A10. Component 6b raw materials.

	counts					weights				
material	*debitage*	*mb*	*tool*	*core*	*total*	*debitage*	*mb*	*tool*	*core*	*total*
C5	4				4	1.02				1.02
C28	2				2	0.03				0.03
C24	1				1	0.12				0.12
Q1	1				1	2.96				2.96
total	8	0	0	0	8	4.13	0.00	0.00	0.00	4.13

Table A11. Component 7 raw materials.

	counts					weights				
material	*debitage*	*mb*	*tool*	*core*	*total*	*debitage*	*mb*	*tool*	*core*	*total*
C31	54				54	2.17				2.17
C51	32				32	1.05				1.05
C5	9		2		11	1.24		3.89		5.13
C1	8				8	0.26				0.26
C39	7		1		8	0.22		0.81		1.03
O	2				2	0.82				0.82
C3	2				2	0.41				0.41
C19	1				1	0.93				0.93
C29	1				1	0.49				0.49
C33	1				1	0.03				0.03
C53	1				1	0.02				0.02
Ch4			1		1			6.24		6.24
M4	1				1	0.84				0.84
Q1	1				1	0.04				0.04
R1	1				1	0.04				0.04
R9	1				1	0.09				0.09
Total	122	0	4	0	126	8.65	0.00	10.94	0.00	19.59

Table A12. Component 7a raw materials.

	counts					weights				
material	*debitage*	*mb*	*tool*	*core*	*total*	*debitage*	*mb*	*tool*	*core*	*total*
C11	3				3	0.11				0.11
C5	2				2	0.25				0.25
C19	1				1	0.09				0.09
Ch4			1		1			3.27		3.27
total	6	0	1	0	7	0.45	0.00	3.27	0.00	3.72

Table A13. Component 7b raw materials.

	Counts					weights				
material	*debitage*	*mb*	*tool*	*core*	*total*	*debitage*	*mb*	*tool*	*core*	*total*
C5	171		9		180	18.23		32.42		50.65
C67	47				47	3.21				3.21
C33	9				9	0.13				0.13
O	2				2	0.52				0.52
C11	2				2	0.03				0.03
total	231	0	9	0	240	22.12	0.00	32.42	0.00	54.54

Table A14. Component 8 raw materials.

	counts					weights				
material	*debitage*	*mb*	*tool*	*core*	*total*	*debitage*	*mb*	*tool*	*core*	*total*
C11	5				5	1.03				1.03
C5	4				4	0.40				0.40
Q2	1				1	0.05				0.05
Q3	1				1	0.02				0.02
Q4	1				1	0.01				0.01
R1			1		1			2.03		2.03
total	12	0	1	0	13	1.51	0.00	2.03	0.00	3.54

Table A15. Component 8a raw materials.

	counts					weights				
material	*debitage*	*mb*	*tool*	*core*	*total*	*debitage*	*mb*	*tool*	*core*	*total*
C11	1038				1038	43.13				43.13
C5	36		25		61	4.75		293.53		298.28
C24	22				22	2.11				2.11
R1	5		13		18	18.96		313.40		332.36
C15	14				14	0.37				0.37
R9	3		7		10	0.08		139.24		139.32
C19	7		1		8	1.11		22.12		23.23
C2	1		1		2	0.04		1.82		1.86
C39	2				2	0.04				0.04
C49	2				2	0.21				0.21
Q3	2				2	0.03				0.03
R4	2				2	0.07				0.07
C28			1		1			14.70		14.70
C3	1				1	0.03				0.03
C36	1				1	0.03				0.03
C4			1		1			11.75		11.75
C56	1				1	0.02				0.02
C57	1				1	0.08				0.08
C68			1		1			22.06		22.06
C72			1		1			2.69		2.69
Ch1	1				1	0.02				0.02
Ch3	1				1	0.03				0.03
Ch6	1				1	0.01				0.01
O			1		1			3.08		3.08
Q1			1		1			0.08		0.08
Q4	1				1	0.02				0.02
R2	1				1	0.01				0.01
total	1143	0	53	0	1196	71.15	0.00	824.47	0.00	895.62

Table A16. Component 8b raw materials.

	counts					weights				
material	*debitage*	*mb*	*tool*	*core*	*total*	*debitage*	*mb*	*tool*	*core*	*total*
C5	323		5		328	41.10		9.82		50.92
C11	251				251	30.45				30.45
C19	46				46	2.32				2.32
R1	31				31	7.49				7.49
C36	28				28	7.44				7.44
C29	24				24	2.98				2.98
C2	17				17	1.13				1.13
C3	17				17	1.97				1.97
C1	12				12	2.81				2.81
C49	11				11	1.97				1.97
R4	6				6	0.87				0.87
C24	4		1		5	0.28		2.79		3.07
C32	5				5	3.19				3.19
C39	5				5	0.56				0.56
O	3		1		4	0.07		6.46		6.52
R2	4				4	0.26				0.26
C17	3				3	1.70				1.70
C33	3				3	0.19				0.19
C59	3				3	0.16				0.16
Ch4	3				3	0.03				0.03
Q5	3				3	0.16				0.16
C28	1		1		2	0.04		6.79		6.83
C31	2				2	0.05				0.05
C35	2				2	13.70				13.70
C53	2				2	0.12				0.12
C69	2				2	0.44				0.44
C8	2				2	0.12				0.12
Ch3	1		1		2	0.17		29.27		29.44
Q4	2				2	0.10				0.10
R9	2				2	0.02				0.02
C21	1				1	0.08				0.08
C22	1				1	0.02				0.02
C41	1				1	0.03				0.03
C47	1				1	0.07				0.07
C56	1				1	0.01				0.01
C64	1				1	0.46				0.46
C67	1				1	0.01				0.01
C68	1				1	0.14				0.14
C70	1				1	0.04				0.04
Ch1	1				1	0.01				0.01
Q1	1				1	0.02				0.02
Q3	1				1	0.03				0.03
Q6	1				1	3.60				3.60
total	831	0	9	0	840	126.40	0.00	55.13	0.00	181.53

Table A17. Unknown raw materials.

counts

Material	*debitage*	*mb*	*tool*	*core*	*total*
C1	4				4
C11	3				3
Q1			3		3
C33	2				2
R1			2		2
C5	1				1
C7			1		1
R2			1		1
Total	10	0	7	0	17

weights

debitage	*mb*	*tool*	*core*	*total*
4.39				4.39
0.42				0.42
		27.30		27.30
0.38				0.38
		5.98		5.98
0.07				0.07
		0.92		0.92
		19.22		19.22
5.26	0.00	53.42	0.00	58.68

A3. Debitage Summaries Per Component

Table A.18 Debitage summary data by component

	C1	C2a	C2b	C2c	C3	C4	C5a	C5b	C6a	C6b	C7a	C7b	C8a	C8b
N	465	6974	384	7588	273	149	49	35	186	7	6	356	1143	850
Flake type														
bifacial thinning	8%	7%	1%	10%	3%	15%	6%	23%	9%	0%	0%	6%	18%	7%
bipolar	0%	0%	0%	0%	0%	0%	0%	0%	0%	0%	0%	0%	0%	0%
decortication	0%	2%	1%	1%	0%	1%	6%	0%	3%	0%	0%	0%	1%	3%
microblade	1%	0%	1%	6%	1%	22%	6%	14%	1%	0%	0%	0%	0%	0%
shatter	6%	3%	1%	2%	0%	1%	0%	6%	1%	0%	0%	1%	2%	3%
simple	85%	87%	97%	81%	96%	61%	82%	57%	87%	100%	100%	93%	80%	87%
unifacial thinning	0%	0%	0%	0%	0%	0%	0%	0%	0%	0%	0%	1%	0%	0%
Sullivan-Rozen Typology														
broken	16%	22%	29%	24%	32%	28%	29%	20%	20%	43%	67%	26%	16%	24%
complete	18%	8%	8%	12%	14%	23%	29%	9%	23%	14%	0%	34%	5%	13%
fragment	60%	66%	62%	61%	54%	47%	43%	66%	55%	43%	33%	39%	77%	60%
shatter	6%	3%	1%	2%	0%	1%	0%	6%	1%	0%	0%	1%	2%	3%
split	0%	0%	1%	1%	0%	1%	0%	0%	1%	0%	0%	0%	0%	0%
Cortex														
0	100%	98%	99%	98%	100%	99%	94%	97%	96%	100%	100%	100%	99%	97%
1-3	0%	2%	1%	2%	0%	1%	6%	3%	4%	0%	0%	0%	1%	3%
Dorsal scar count														
Avg.	1.83	2.17	2.29	2.25	2.33	2.57	2.71	2.55	1.85	3.00	2.33	2.25	1.95	2.30
Stdev	1.11	1.03	0.80	0.99	1.00	1.13	1.14	1.28	0.81	0.58	1.51	1.02	1.03	1.06
%≥3	21%	31%	33%	34%	39%	48%	46%	48%	18%	85%	34%	33%	27%	38%
Material quality														
Low		0.1%	0.3%	0.3%		0.6%			0.5%			0.3%		0.6%
Mod.	8.8%	11.2%	8.6%	3.8%	0.4%	23.7%			6.5%			11.8%		1.5%
High	91.2%	88.7%	91.1%	95.9%	99.6%	75.6%	100%	100%	93.0%	100%	100%	87.9%	100%	97.9%
Heating	0.2%	0.2%		0.2%	0.4%		12.2%	8.6%	0.5%			0.3%	0.3%	0.6%

Table A.19 Size class summary data by component (percentages)

size	C1	C2a	C2b	C2c	C3	C4	C5a	C5b	C6a	C6b	C7a	C7b	C8a	C8b
0-5 mm	26.9	15.8	12.5	12.9	8.8	20.6	14.3	25.7	12.4			18.3	32.4	10.6
5-10 mm	52.9	56.0	61.7	65.1	59.7	56.1	53.1	37.1	60.8	14.3	83.3	66.6	56.9	60.2
10-15 mm	13.8	18.1	18.8	17.2	21.2	7.7	24.5	31.4	17.2	42.9	16.7	9.3	9.7	19.6
15-20 mm	4.5	6.1	4.4	3.1	5.5	5.2	4.1	2.9	5.9	28.6		3.1	0.7	5.9
20-25 mm	1.5	2.3	1.6	1.0	4.0	5.8	2.0	2.9	2.2	14.3		1.7		1.9
25-30 mm		0.9	0.5	0.4	0.4	1.9	2.0		1.1			0.8	0.1	1.3
>30 mm	0.4	0.8	0.5	0.3	0.4	2.6			0.5					0.5

Table A.20 Platform remnant bearing flake summary data by component

	C1	C2a	C2b	C2c	C3	C4	C5a	C5b	C6a	C6b	C7a	C7b	C8a	C8b
N														
Eraillure scars	2%	4%	4%	6%	10%	6%	11%	10%	4%	0%	0%	2%	5%	7%
Lipping	5%	3%	2%	9%	2%	11%	29%	20%	4%	50%	0%	3%	2%	10%
Salient bulbs	43%	37%	18%	25%	18%	15%	21%	0%	38%	25%	0%	35%	34%	33%
Platform type														
abraded	1%	1%	2%	1%	3%	4%	0%	0%	9%	0%	0%	2%	0%	0%
complex	13%	7%	3%	12%	7%	10%	11%	10%	9%	25%	0%	8%	14%	37%
cortical	0%	3%	0%	1%	2%	0%	0%	0%	4%	0%	0%	0%	0%	2%
crushed	25%	34%	52%	25%	36%	13%	11%	10%	15%	50%	100%	22%	19%	19%
N/A	62%	55%	42%	61%	52%	74%	79%	80%	64%	25%	0%	69%	67%	42%
Simple														
Platform edge angle														
N	89	1252	68	914	86	64	11	8	60			49	184	60
Mean	59	57	54	60	60	72	66	68	59			51	49	57
Stdev	12	12	7	15	8	17	10	15	8			14	12	13
Platform measurements (mean)														
platform width	3.80	4.05	4.06	2.88	3.84	2.64	2.49	2.74	4.92	5.33	2.90	3.05	3.15	3.77
platform thickness	1.22	1.20	1.05	0.91	1.14	0.90	0.77	1.05	1.55	1.39	0.39	0.90	0.90	1.10
Terminations														
Feather-ed	50.3%	25.9%	19.0%	32.9%	30.4%	38.8%	46.4%	10.0%	50.0%	25.0%		56.3%	24.7%	31.4%
Hinged	5.7%	4.8%	6.3%	2.1%	4.0%	25.0%		40.0%	2.5%			2.8%	0.8%	3.5%
Over-shot		0.1%	0.7%	0.2%			3.6%						0.3%	
Step	44.0%	69.2%	73.9%	64.7%	65.6%	36.3%	50.0%	50.0%	47.5%	75.0%	100%	40.9%	74.5%	61.6%

APPENDIX B. ARTIFACT PHOTOGRAPHS

Ben A. Potter

Figure B1. Component 1 projectile point bases.

Figure B2. Component 1 microblades.

Figure B3. Component 1 flake core/chopper.

Figure B4. Component 2a bifaces (1-11, 10 is burinated), unifaces (12-17).

Figure B5. Component 2c bifaces (1-7), unifaces (8-12), microblade cores (13-14), burin (15).

Figure B6. Component 4 modified blades (1-2).

Figure B7. Component 5a (1, 3) and 5b (2) microblade cores (1-2), unifacially retouched blade (3).

Figure B8. Component 6a projectile point.

Figure B9. Component 7a and 7b unifaces (1-6).

Figure B10. Component 8a projectile point base (1) and uniface (2)

Figure B11. Component 8a blank cache, bifaces, unifaces, and modified flakes

Figure B12. Component 8b projectile point (1), biface fragment (2), unifaces (3-5).

APPENDIX C. HURRICANE BLUFF INVESTIGATION

Julie A. Esdale, Ben A. Potter, Joshua D. Reuther

C1. Introduction

The Hurricane Bluff site (XMH-838) is situated 45 m above the Delta River floodplain at the southwestern edge of a partially deflated bluff, approximately 200 m south of DRO (see Chapter 3). Sediments at the edge of the bluff stand in 1-3 m cliffs where they are actively eroded horizontally by wind and bison. Artifacts are found on the ground surface at the base of the cliffs every time the site is visited. Lithics form the majority of cultural material discovered, and they are primarily from a surficial context. Much of the original site has already been lost to erosion. Although the stratigraphic profile represents the same duration and resolution as DRO, it is much more difficult to place the artifacts in stratigraphic sequence.

Goals of the investigations at Hurricane Bluff were to:

1) correlate the stratigraphic sequences, paleosols, volcanic ashes, and cultural sequences with DRO;

2) understand the age of cultural materials eroding out of the bluff edge; and

3) determine the extent of erosion and the potential for intact cultural deposits.

C2. Previous Work

Hurricane Bluff was located in 1998 by Northern Land Use Research, Inc. (NLUR) archaeologists after inspecting DRO (Higgs et al. 1999, Potter et al. 2007). A surface inspection was made of the bluff face, and upon finding eroding artifacts and bone (Figure C1), NLUR archaeologists excavated a test trench in order to record site stratigraphy (Figure C2). The site was gridded with total station and a 1 x 1 meter test (EU 1) was excavated adjacent to the test trench (Figure C3). Two additional Excavation Units (EU) were started (EU 2-3). A few weeks later, two additional test units (EU 4-5) were excavated adjacent to the bluff edge and the trench (Figure C4). Excavation methods included skim shoveling and troweling in arbitrary 10 cm levels below surface. Diagnostic artifacts and material types were collected from the surface because of possible loss due to further erosion.

Surface artifacts were distributed over 408 m^2 on the eroded surface of the blowout. One cluster consisted of three flakes and a bone fragment. A second cluster consisted of six flakes, 20 bone fragments and burned wood fragments. Other surface materials included a obsidian flake core, chert flake core, chert biface, chert bifacial preform, three flakes, and one *Canis* sp. molar (M1) (Figure C5, Table C1).

Two distinct cultural components were identified. The first, found in (EU 4 and 5), was approximately 130 cm below surface, contained flakes, and was associated with Paleosol Complex 3. The second cultural component was found in EU1, had forty chert flakes, was found approximately 140 cm below surface, and was associated with Paleosol Complex 5.

Test Trench 1 produced no artifacts, but did uncover faunal remains. However, at least two stratigraphically distinct cultural components were discerned at the site, based on flakes found during controlled excavations. The upper component was found in EU 5, with 2 additional flakes found in EU 4 at a depth between 129-133 cmbs. All flakes from EU 4 and 5 are

associated with the lower section of Paleosol Complex 3. A sample of organics from this complex returned a radiocarbon date of 1750+/-40 yr BP (Beta-123338). The lower cultural component was found during the excavation of EU 1. Forty chert flakes were found associated with one of the upper paleosol stringers of Paleosol complex 5. Units 2 and 3 produced no artifacts or faunal material. No formal tools or diagnostic artifacts were found in the controlled excavation of these units.

The large trench that was excavated demonstrated the site had a 4 m thick section of loess, sand, and paleosols spanning the entire Holocene (Potter et al. 2007) (Figure C2, Figure C6). In 1998, the top 1.5 m of bluff sediments stood in a vertical profile but the remainder of the deposits were eroded into a gentle 45° slope. Most of the slope was exposed however, although alders and grassland vegetation grew in some areas (Figure C2).

The excavations and surface artifacts demonstrated a multi-millennial and fine-grained stratigraphic section, at least two cultural components, potential for precise dating of occupations, exotic raw materials, and multiple lithic technologies. Although the NLUR report recommended that the site be found eligible for the NRHP, a formal DOE was never completed (Higgs et al. 1999).

In August of 2012 a CEMML crew visited the site to complete fieldwork in order to recommend the site for eligibility for inclusion on the NRHP, determine site boundaries, and to document and monitor any impacts to the site since its discovery in 1998. The 1998 test areas were relocated and mapped. Next surface artifacts were mapped relative to the datum using their angle and distance, and collected (Figure C7). A series of eight shovel tests were excavated behind the eroding bluff edge to a depth of 140-180 cmbs. No artifacts were found in any of these units suggesting that the cultural occupations were likely located in the eroded section of the bluff. One excavation unit (EU1), located just 0.5 m from the edge of the bluff at its southernmost point, was also excavated to 180 cmbs. No artifacts were found in the excavation unit. The bluff edge wall was also cleaned and profiled. Flakes were found eroding out of Paleosol Complex 3 (as defined in 1998). On the surface, a total of 37 artifacts were recovered including a chert scraper, a net sinker, an obsidian flake and two tabular cores (Figure C8, Table C2).

Although much of the site is clearly eroded, CEMML recommended that Hurricane Bluff was eligible for the NRHP under Criterion D because it contained well stratified aeolian deposits with volcanic ash layers, well developed paleosols, and cultural horizons, buried artifacts, obsidian, and intact deposits with future research potential. The SHPO concurred with this finding on 19 December, 2013.

C3. Current Excavation

In 2015 CEMML again revisited the site to attempt to locate intact cultural deposits in association with the DRO mitigation. Artifacts were again found eroding out of the bluff edge downslope toward the river. A new datum was set on a flat area at the highest elevation in the area and given the coordinates N500, E500, Z500 (Figure C7). A total station was used to map the location of surface artifacts, excavation unit corners, and the location of previous tests. The 1998 rebar locations marked Datum and Grid Rebar (Figure C3) were located at N475.421 E507.045, Z496.790, and N463.880 E514.120, Z494.797 respectively. Near the new mapping datum, a 1 x 2 m and 1 x 3 m trench were excavated in an attempt to recover artifacts in situ (Figure C7). Excavation in N484 E500-502 and N500 E495-496 proceeded by skim shovel at 10

cm intervals. Excavations continued from 0-210 cm below surface, when time constraints concluded excavation for the season. Although the excavations were not complete, the paleosols containing artifacts elsewhere in the site were excavated, and not cultural material was found in this location. A possible hearth feature was located in the southern trench (N484 E501). Bone and burnt wood fragments were found within a charcoal-rich stain at 60 cmbd (Figure C9).

An additional 1 x 2 unit was dug at the southern end of the site, at the base of the bluff face, for a geological sampling. No artifacts were located but soil samples were taken for radocarbon dating by Josh Reuther and for OSL dating by Laurence Forget Brisson (University of Quebec at Montreal) (Figure C10).

C3.1 Site Stratigraphy and Dating

The site stratigraphy and dating was previously described in Chapter 4 (see Figure 4.2). The field paleosol sequence prior to correlation with DRO is given in Figure C11. At least nine well developed paleosols representing ancient periods of relative surface stability span the Holocene period. During correlation, paleosol numbers at Hurricane Bluff were reversed, and several paleosols that were clear at DRO appeared are not represented at Hurricane Bluff. The geological trench was not excavated to glacial deposits in this location. Paleosol 7a (correlated to P1 at DRO) provided a date of 8590+/-30 BP (Beta-420651, 9602-9505 cal yr BP) and was the lowest paleosol in the section. A loess layer separates this paleosol from the paleosol complex above. Hurricane Bluff paleosols 7b and 6a correlate to P2 at DRO and provided ages of 6990+/30 BP (Beta-389635, 7930-7736 cal yr BP) (7b) and 6230+30 BP (Beta-396693, 7251-7019 cal yr BP) (6a). P3 and P4 are not found at Hurricane Bluff. The next paleosol represented at Hurricane Bluff, located above another thick loess deposit, is paleosol 5. This correlates to P5 at DRO although dates between the paleosols in each location do not overlap at two standard deviations. Paleosol 5 at Hurricane Bluff dates to 3980±30 BP (Beta-38634, 4526-4406 cal yr BP). P6 at DRO may correlate with a paleosol between paleosol 5 and paleosol 4 at Hurricane Bluff dating to 3670±30 BP (Beta-386246, 4087-3907 cal yr BP). Paleosol 4 at Hurricane Bluff correlates with P7b at DRO and dates to 3210±30 BP (Beta-386245 3543-3368 cal yr BP). Dating to 1800±30 BP (Beta-386244, 1894-1548 cal yr BP), paleosol 3 is younger than P8 at DRO by 400-1000 years and is difficult to correlate. Paleosol 2 at Hurricane Bluff was renamed P9 and has a date of 340±30 BP (Beta-386243, 480-311 cal yr BP). At least one tephra was visible between paleosols 4 and 5 at Hurricane Bluff and may result from an event of the Hayes Volcano (Mulliken 2016).

C3.2 Component Delineation

Only two cultural components were identified at Hurricane Bluff. The lower component, C1, dates to 1750±40 BP and is found in paleosol 3 (DRO P8). This component is represented by 32 flakes and some FCR found in the 1998 excavation units EU4 and EU5. The upper component, C2, contained 42 flakes and bone fragments in EU1 and EU2. The possible hearth feature in the 2015 excavation unit N484 E501 appears to correlate with paleosol 3 (DRO P8) and not paleosol 2 (P9) and may relate to the C1 occupation. Many artifacts are found eroding from the bluff. Unfortunately, there is no way to tell which occupation these artifacts may have come from. Raw materials of surface finds include quartzite, gray chert, black chert, beige chert,

striped gray and black chert, black basalt, light beige rhyolite, and obsidian. The majority of buried flakes in both components are chert, and at the moment there is no way to assign cultural affiliation on raw material or technology.

C3.3 Lithic Analysis

All of the artifacts collected in during the 2015 investigations are part of the surface collection. They are located all along the bluff edge from the 2015 excavation units to the base of the landform (Figure C7). Artifacts include flaked and ground stone tools, bone fragments, and FCR. One ground stone tool was found on the surface. It is a 13 cm long igneous cobble with battering along the long ends and in the center of the cobble to create an indent around the circumference. It has been labelled as a netsinker based on its similarity to those tools found in other sites, but the actual function of the tool is unknown. Three bifaces were found in the collection. Two are small blanks made from basalt and black chert. The third is a large (15 cm long and 4 cm wide) piece of slate or argillite that is bifacially flaked. The tool is curved and resembles a boomerang. One gray chert end scraper and a basalt retouched flake are among the unifacial tools. Of the flaking debris, there is one complete microblade made from gray chert, and 30 waste flakes (Table C4). Forty percent (n=12) of these are undiagnostic flake fragments. Secondary decortication flakes make up 7% of the assemblage (N=2) and interior flakes make up 4% (n=1). Three linear flakes were discovered (10%) that may reflect early stages of microblade production. The remainder of the flakes (n=12, 40%) relate to late stage bifacial thinning and pressure flaking.

When the artifacts are considered spatially, few patterns emerge (Figure C12). Flakes are distributed across the site with no sub patterning by technology or stage of tool production. There are also no patterns in the distribution of tools. There is a cluster of FCR in and adjacent to the excavation unit that contained the possible hearth feature (N484 E501). Moreover, downslope from this feather is a small cluster of bone and flakes. This may signify that the charcoal rich stain is indeed a cultural feature although no artifacts were found in situ in the excavation. Raw material types are also scattered across the site with little clustering (Figure C.13) giving few clues to the location of activity areas that have been eroded over time.

C.4 Interpretation and Summary

Hurricane Bluff serves as a cautionary tale for sites located in fragile bluff environments. The site has been significantly impacted by wind erosion, wildlife, and possibly recreation and training in the intervening 17 years since original discovery. Comparison of the present bluff edge location to the 1998 site map and photographs demonstrate that at least 1 m of sediment has eroded back from the bluff face (Figure 3.15). The exposed bluff edge continues to undergo wind erosion and bison trails along the bluff edge (and bison hair caught in roots along the bluff face) indicate that bison are also contributing to physical weathering of the site. People also commonly used this corridor in the recent past for access between military operation points no longer in use. The lack of artifacts in the shovel tests north of the bluff edge, the new test units and the general infrequency of artifacts elsewhere across the site suggests that either the site has a low density of cultural material or much of the prehistoric campsite has already been eroded during the past. A significant amount of erosion of cultural material is indicated by abundant downslope surface finds, lack of artifacts back from the edge of the bluff, and flakes, FCR, and bone found

immediately downslope of a potential hearth in an excavation unit. Although there are still large areas of intact deposits at the site, it is our interpretation that the main concentrations of cultural activity have already been destroyed.

Two cultural components have been identified at the site dating to the late Holocene period. Artifacts found on slope demonstrate unifacial, bifacial, and core and blade technology consistent with any time period. No diagnostic projectile points have been discovered to make any further chronological interpretations. Bone is small and fragmented but further analyses may indicate the size of animals being processed at this site. Because of the lack of context of artifacts and faunal material found at the site, few interpretations can be made about cultural affiliation or activities pending more extensive investigation.

Table C1 Summary of artifacts and fauna recovered in 1998.

Area	*Component*	*N lithics*	*N tools*	*Microblades*	*Proj. pt.*	*Tools*	*N fauna*	*Fauna*
Surface	N/A	7	4	No	No	2 flake cores, 2 bifaces, 3 flakes	1	1 tooth
EU1	C2	40	0	No	No	40 flakes	4	Bone frags
EU2	C2	2	0	No	No	2 flakes	0	
EU4	C1	2	0	No	No	2 flakes	0	
EU5	C1	30	0	No	No	30 flakes, FCR	0	

Table C2 Summary of artifacts recovered in 2012.

Area	*Component*	*N lithics*	*N tools*	*Microblades*	*Proj. pt.*	*Tools*
Surface	N/A	37	3	Yes	No	1 scraper, 1 flake core, 1 net sinker, 1 core tablet, 1 microblade, 32 flakes

Table C3 Summary of artifacts and fauna recovered in 2015.

Area	*Component*	*N lithics*	*N tools*	*Microblades*	*Proj. pt.*	*Tools*	*N fauna*	*Fauna*
Surface		38	6	Yes	o	4 bifaces, 31 flakes, 1 microblade, 1 retouched flake, 1 scraper, FCR	7	Bone frags
N484E501	C2? 50-60 cmbs	0	0	No	No	FCR	1	Bone frags

Table C4 Lithic artifact types from surface assemblage.

Raw Material	Biface	Scraper	Retouched flake	Microblade	Net sinker	Flake fragment	Decortication flake	Interior flake	Bifacial thinning flake	Edge preparation flake	Bifacial pressure flake	Linear flake
quartz						1						
gray chert		1		1		5	1		1	1	1	2
striped chert						4				1	2	1
basalt	1		1			1		1	1	1	2	
rhyolite							1				2	
beige chert						1						
black chert	1											
slate	1											
ground stone					1							
Total	3	1	1	1	1	12	2	1	2	3	5	3

Table C5 Trace element concentrations (ppm) of the Hurricane Bluff obsidian artifact and its source assignment.

AOD_Number	*K*	*Mn*	*Fe*	*Zn*	*Ga*	*Th*	*Rb*	*Sr*	*Y*	*Zr*	*Nb*	*Source_Name*	*Source_Group*
AOD-12269	36581	580	5172		19	25	161	9	37	95	21	Batza Tena	Group B

Figure C1 Overview of XMH-838 in 1998, view north.

Figure C2 Test trench (left) and other excavations (facing south) from original investigations.

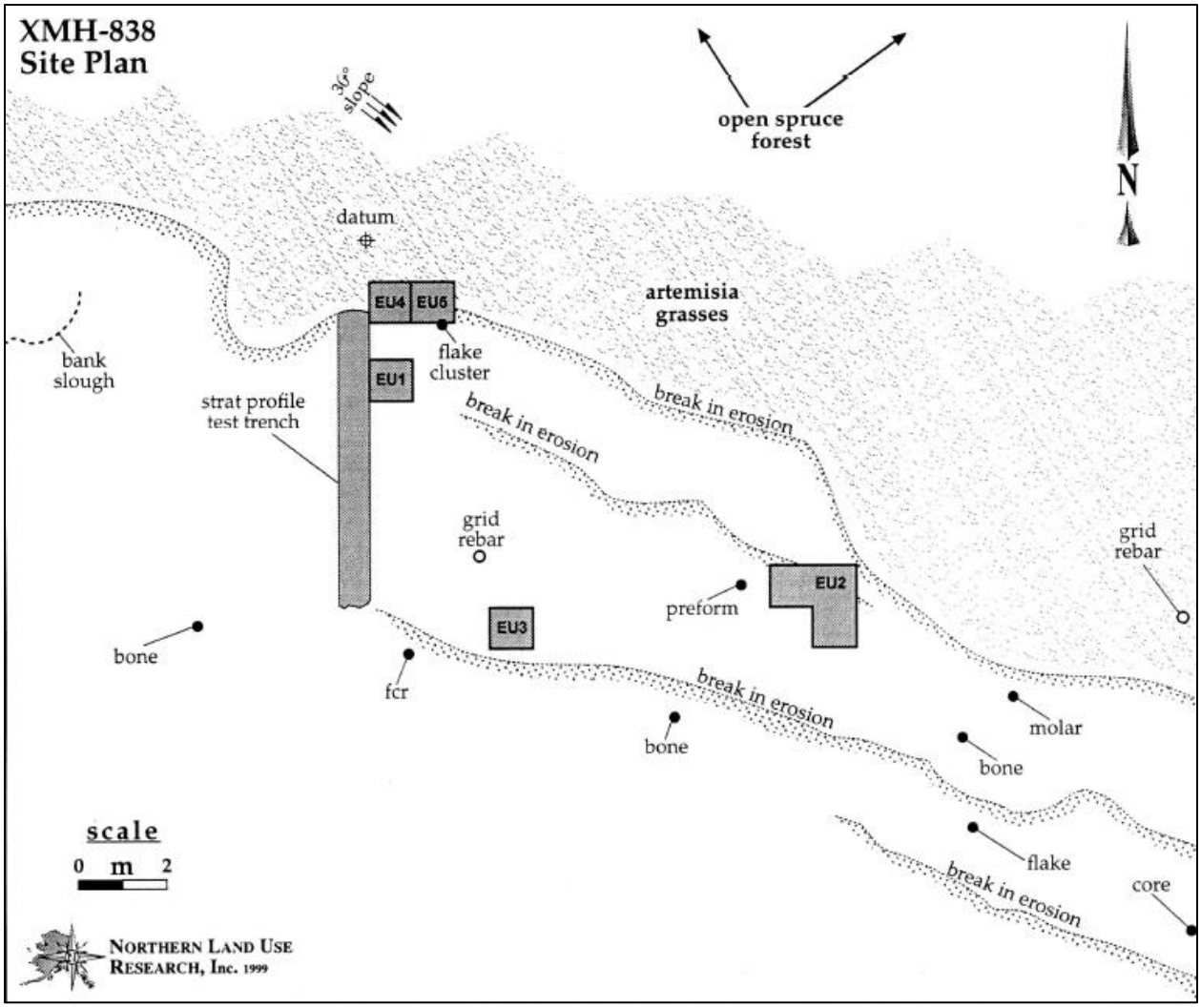

Figure C3 NLUR site map, 1998 excavations (from Higgs et al. 1999).

Figure C4 Overview of 1998 excavation at bluff edge.

Figure C5 Artifacts recovered from deflated surface: chert and obsidian flake cores, and chert biface and preform.

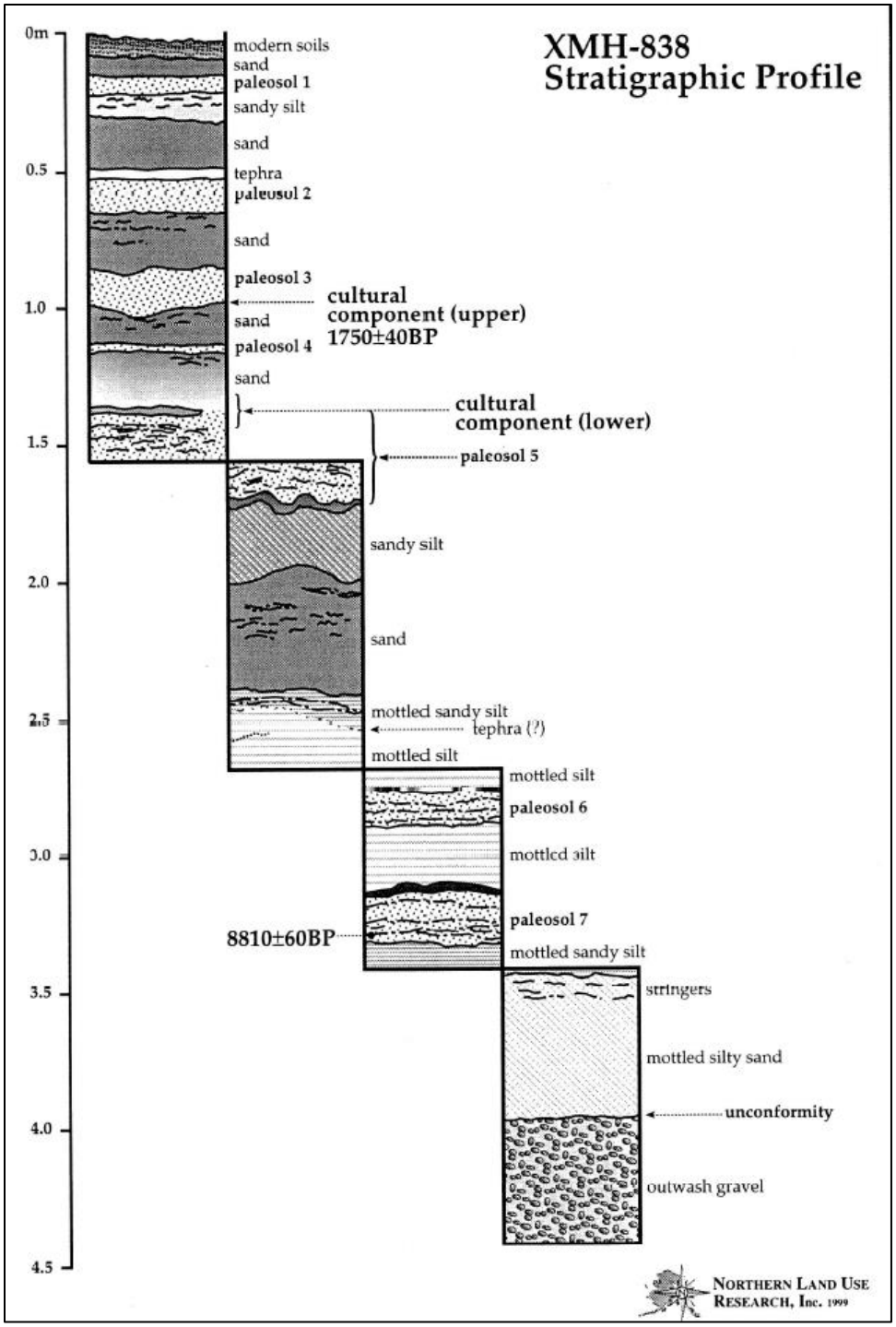

Figure C6 1998 excavation trench stratigraphic profile.

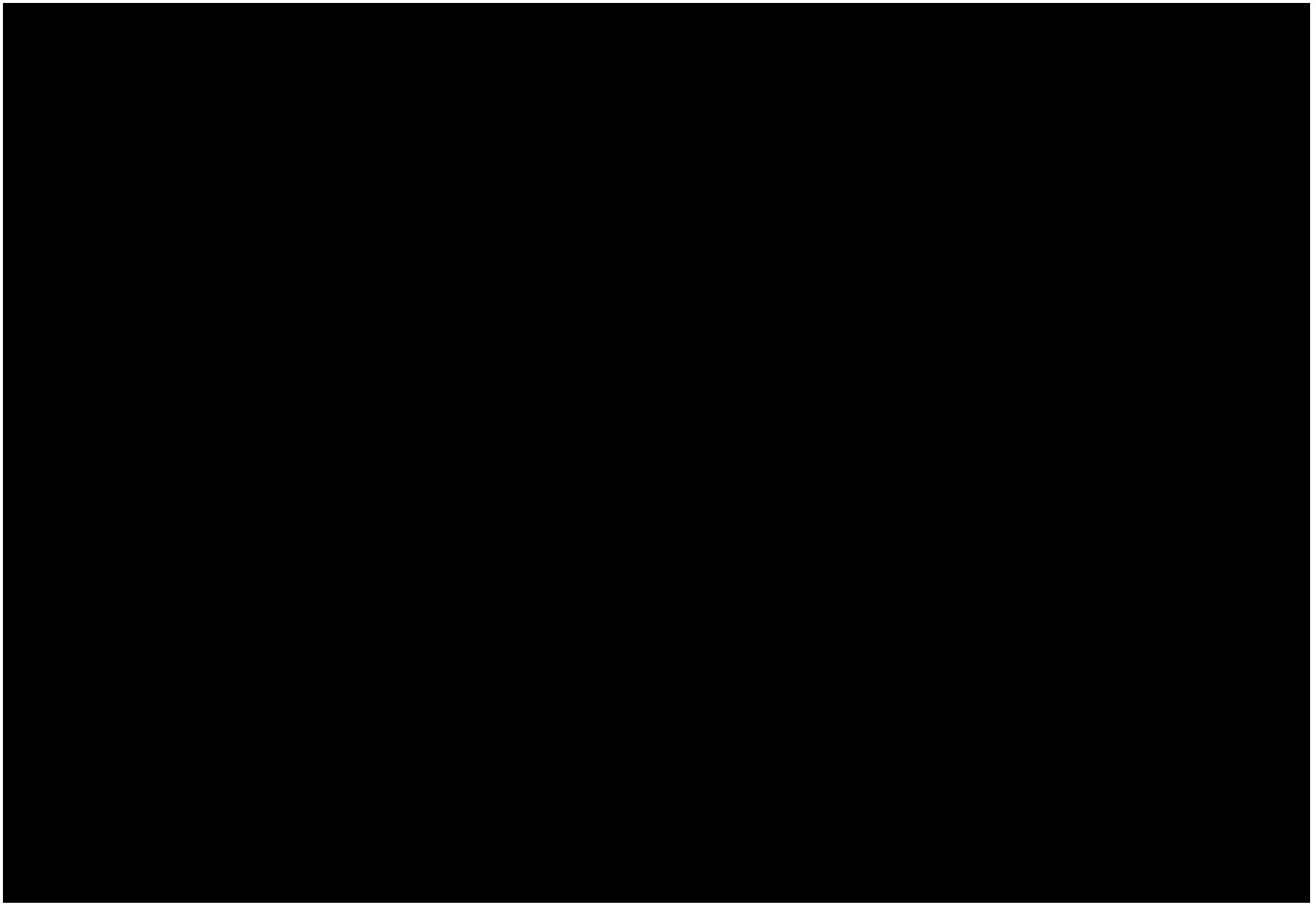

Figure C7 Field map with 1998, 2012, and 2015 shovel tests, excavation units, and surface artifacts.

Figure C8 Artifacts from 2012 investigations, all found on surface (chert microblade, chert scraper, net sinker).


Figure C9 Possible hearth feature in N484 E501.

Figure C10 Laurence Forget Brisson sampling for OSL dating.

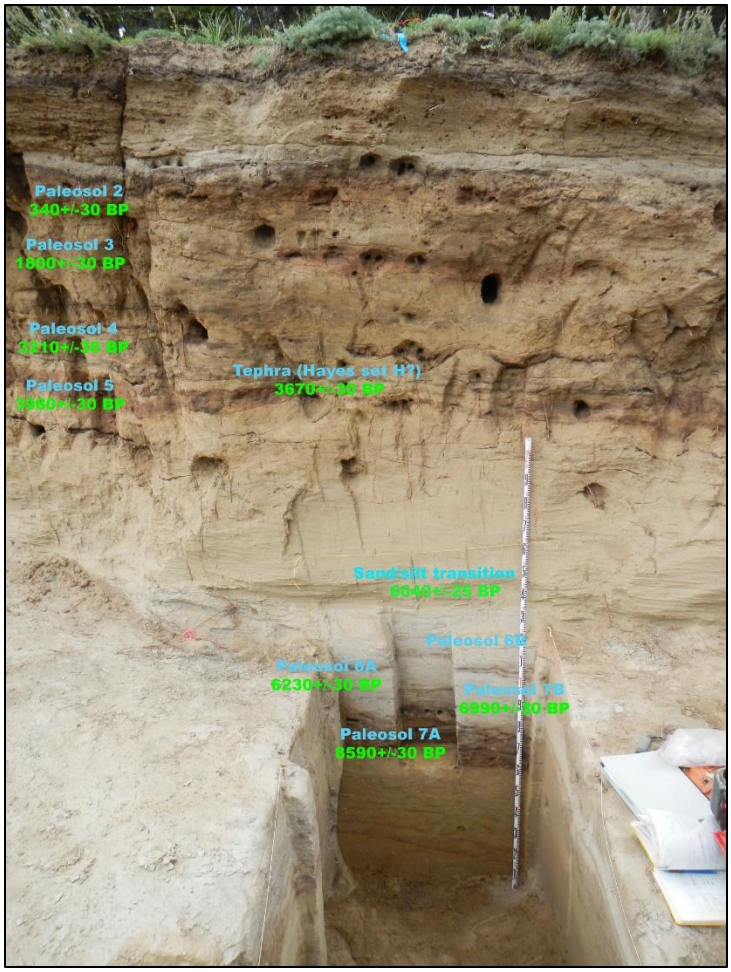

Figure C11 Hurricane Bluff paleosol sequence with radiocarbon dates prior to correlation with DRO.

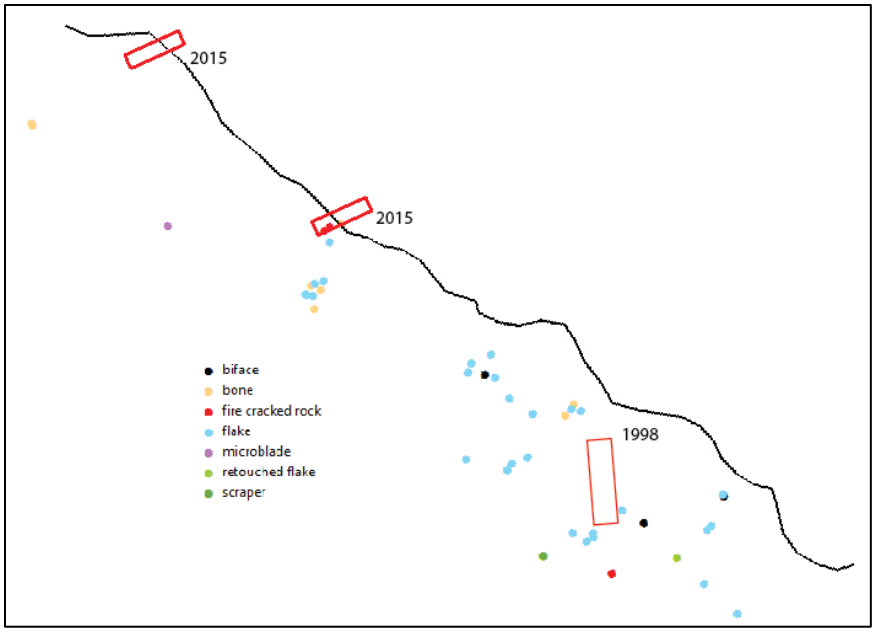

Figure C12 Distribution of surface finds across the site by artifact type.

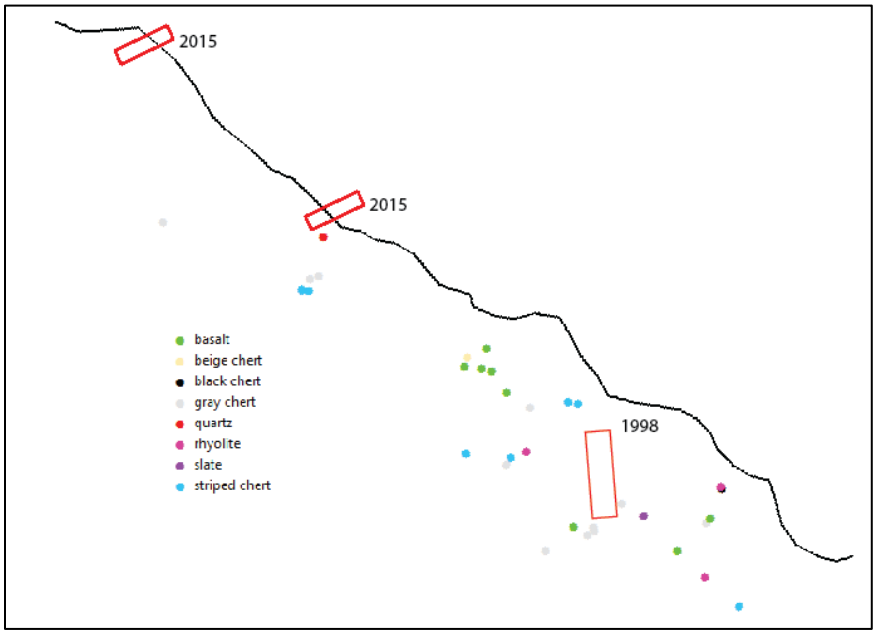

Figure C13 Distribution of surface finds across the site by raw material.

APPENDIX D. AHRS SITE CARDS FOR XMH-297 AND XMH-838

Ben A. Potter and Julie A. Esdale

D1 XMH-297 Card

Reset Form

ALASKA OFFICE OF HISTORY AND ARCHAEOLOGY

AHRS SITE CARD Page 1 of 1

AHRS #: XMH-00297 **Site Name:** Delta River Overlook

Site Description

This multicomponent site is located in stratified deposits on a high bluff overlooking the Delta River floodplain. At least 14 separate occupations were discovered within 5 m deep deposits of aeolian sands, silts, and tephras. This stratified sites has well developed paleosols and an excellent radiocarbon chronology dating from 10,990 to 2,210 radiocarbon years ago. Three multicomponent cultural complexes were identified during excavations of 164 square meters of deposits during the 2015 and 2017 field seasons. The Chindadn Complex has one component dating to 13,000 years ago and includes bifacial tools, microblades, and the remains of small game. The Denali Complex is comprised of 7 components dating from 11,600 to 7,250 years ago. Hearth centered activities demonstrate bifacial tool production and maintenance and small amounts of microblade production. Fauna remains are mainly bison and wapiti, although later components include snowshoe hare. Seasonal indicators demonstrate the site was used as a winter camp in at least one Denali occupation. The Northern Archaic Tradition has six complexes dating from 6,280 to 2,240 years ago. These components feature bifacial technology including the production and maintenance of projectile points and the discard of scrapers indicating animal processing. The Northern Archaic diet was much more varied than earlier complexes and included large game, bison and wapiti, as well as caribou, mink, beaver, and grouse. A flake blank cache was discovered in the latest Northern Archaic component. Delta River Overlook is an extremely significant site for its excellent faunal preservation, well delineated activity areas, amazing stratigraphic sequence, and unprecedented cultural chronology.

Location Description:

[redacted]

Pertinent Dates:

Component 1 10,990+/-50, C2a 10,000+/-40, C2c 9510+/-30, C3 8555+/-380, C4 7630+/-30, C5 6675+/-170, C6a 5980+/-30, C7a 4010+/-30, C8a 3330+/-30, C8a 2210+/-20

Significance Statement: (for DOE or NRHP)

[DOE] Site had potential to yield information important in understanding of the prehistory of interior Alaska.

Present Condition:

Partially excavated (C5)

Cultural Affiliation: Chindadn, Denali, Northern Archaic

Property Owner: USARAK (managed by Army in association with US

Acres:

BIA/BLM #::

Other # (Specify):

Repository: Univeristy of Alaska Museum of the North

Accession #: UA79-153, UA2015-137, UA2017-275

Danger of Destruction:

Military Activities Erosion

Comments or Additional Information

References to add to AHRS Card: Potter et al. 2018

Prepared By: Julie Esdale

Date Prepared: 09/06/18

form updated on 4/3/14

D2. XMH-838 Card

Reset Form

ALASKA OFFICE OF HISTORY AND ARCHAEOLOGY

AHRS SITE CARD Page 1 of 1

AHRS #: XMH-00838 **Site Name:** Hurricane Bluff

Site Description

Hurricane Bluff is a multicomponent archaeological site found on the edge of an eroding bluff. Two cultural components dating to the late Holocene were discovered during tests when the site was discovered in 1998. These date to 1,750 and 340 radiocarbon years BP. Most of the artifacts found at the site are found scattered across a 400 square meter area of the surface. Artifacts, bone, and fire-cracked rock are eroding out of the bluff and moving downslope, dozens of flakes, microblades, and tools (including bifaces, scrapers, and flake cores) have been discovered out of context. Animal bone includes one Canid molar. Two obsidian artifacts were sourced to Wiki Peak and Batza Tena. This site is significant for its buried cultural components, excellent stratigraphy, and correlations with XMH-00297 a few hundred meters to the north. Unfortunately, much of the site has already been lost to erosion and the deposits are eroding at a rapid rate.

Location Description:

[redacted]

Prehistoric

Pertinent Dates:

Component 1 1,750+/-40

Significance Statement: (for DOE or NRHP)

Determined eligible for the NRHP for potential to provide important information about the prehistory of interior Alaska.

Present Condition:

Partially destroyed (B1)

Cultural Affiliation: Athabaskan

Property Owner: USARAK (managed by Army in association with US

Acres:

BIA/BLM #::

Other # (Specify):

Repository: University of Alaska Museum of the North

Accession #: UA99-59, UA2012-92, UA2015-154

Danger of Destruction:

Erosion Military Activities

Comments or Additional Information

Reference to add: Potter et al. 2018

Prepared By: Julie Esdale

Date Prepared: 09/06/2018

form updated on 4/3/14